New anion receptors for molecular recognition and organocatalysis

Arseni Borissov

Wadham College, University of Oxford

A dissertation presented in partial fulfilment of the requirements for the award of the degree of Doctor of Philosophy







Declaration

This dissertation describes work carried out in the Chemistry Research Laboratory at the University of Oxford between February 2015 and October 2018. This dissertation is a product of my own work and includes no results obtained through collaboration, except where specifically indicated in the text. This dissertation has not been previously submitted for a degree, diploma or any other qualification at the University of Oxford or elsewhere.

Arseni Borissov

Acknowledgements

I would like to thank several people who have made my life and work in Oxford such a good experience. First of all, many thanks to both of my DPhil supervisors, Professors Martin D. Smith and Paul D. Beer. Your guidance was very important in developing my ability to discover new knowledge. On top of that, I have always enjoyed the atmosphere that both of you were creating in your research groups. Thank you for the opportunity to realise an unusual joint project with both of you and for tolerating my eccentric character along the way.

I am also grateful to my colleagues who made my life in the CRL so enjoyable. First I should mention those with whom I have occasionally cooperated: Robert the electrochemistry specialist, Jason the prolific author, Valentine, Alex, and Asha. Apart from that, cheers to the SBM buddies Minh and Alison, fellow metalheads Luiza, Ben J, and Harry, fellow night workers Yao, Hasanain, and Hena, and the weird music enthusiasts Ben Ra, Phil, and Liz. John and Antti, you two were the perfect matches for my rotten sense of humour. Somewhat more refined humour could always be shared with Nick, Tudor, Jack, or Andrew. I should also mention the wise and experienced postdocs Niels, Craig, Jamie, Matt, Jessica, and Bryony, as well as the young and uncontaminated Part IIs Pearse, Terry, Annie, Hugo, and Seb. And all the rest of you: George, Jane, Jessica, Andrew, TJ, Tim, Stuart, Tanya, Kat, Shuyu, Owen, Mihai, Zac, Ben D, Richard, Lucia, and anyone I forgot here but certainly not in the grand scheme of things.

Finally, thanks to my wonderful family and to Ira, the rare being from my home planet.

I would like to dedicate this work to my grandfather Sergei Shalnev who was the first to awaken my curiosity for the workings of the physical world.

Abstract

This thesis describes the investigation of anion binding molecules in application to molecular recognition and organocatalysis. A focus is made on exploring the properties of σ-hole interactions: halogen and chalcogen bonding which are scarcely studied in the context of anion sensing, especially in an aqueous environment.

Chapter 2 describes the preliminary design of a tetradentate XB anion receptor (Figure I a). This system is shown to be effective for anion complexation in organic solvent media, more so than the isostructural HB analogues. Fluorescent sensing and chiral discrimination capabilities are also demonstrated.

Chapter 3 discusses the water-soluble, preorganised XB and ChB anion receptors (Figure I b). This provides the first examples of charge-neutral, all-XB and all-ChB host molecules to be used for anion binding in water. In addition to the fundamental studies of anion coordination, applications in fluorescent and electrochemical anion sensing are shown.

Chapter 4 details the development of biomimetic transesterification catalysts that include an oxyanion hole function (Figure I c). The series of compounds is iterated towards high reactivity, arriving at highly effective catalysts with a modular, easily customised structure.

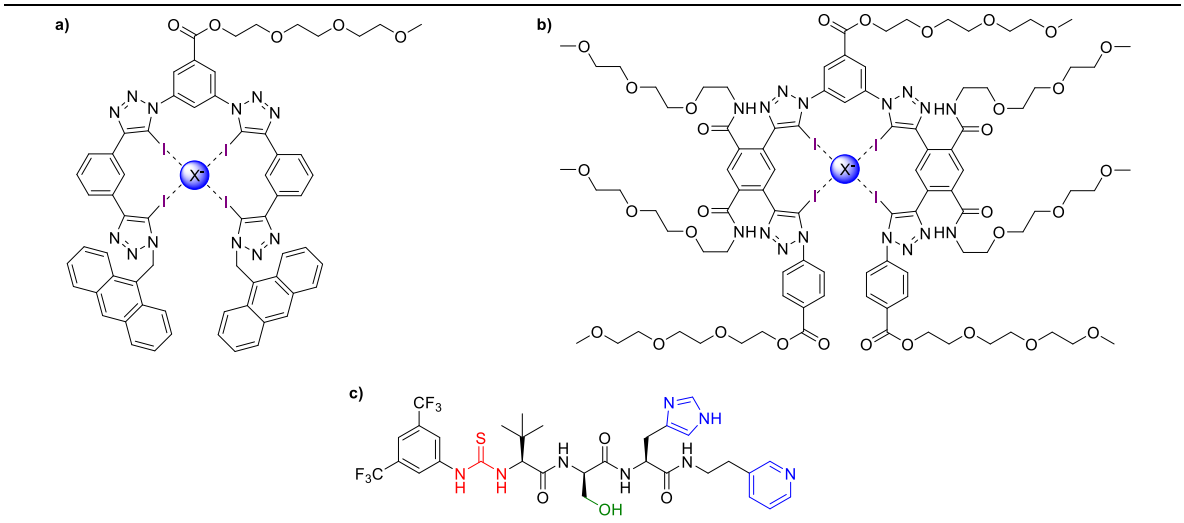

Figure I Examples of compounds presented in this work.

List of abbreviations

ABC	ATP-binding cassette
ADP	Adenosine diphosphate
AMP	Adenosine monophosphate
ATP	Adenosine triphosphate
Boc	*tert*-Butoxycarboxyl
BTA	Benzyltriazolylmethylamine
cAMP	Cyclic adenosine monophosphate
CD	Circular dichroism
CFTR	Cystic fibrosis transmembrane conductance regulator
ChB	Chalcogen bonding
COMU	(1-Cyano-2-ethoxy-2-oxoethylidenaminooxy)dimethylamino-morpholino-carbenium hexafluorophosphate
CSA	Camphorsulfonic acid
CuAAC	Copper-catalysed azide-alkyne cycloaddition
CV	Cyclic voltammetry
D	Diffusion coefficient
DBU	1,8-Diazabicyclo[5.4.0]undec-7-ene
DCC	Dicyclohexyl carbodiimide
DCE	Dichloroethane
DCM	Dichloromethane
DIBAL	Diisobutylaluminium hydride
DIPEA	*N*,*N*-Diisopropylethylamine
DMAP	*N*,*N*-Dimethyl-4-aminopyridine
DMF	Dimethylformamide
DMSO	Dimethyl sulfoxide
DOSY	Diffusion-ordered NMR spectroscopy
DPPA	Diphenyl phosphoryl azide
EC_{50}	Half maximal effective concentration
ECS	Electrochemical capacitance spectroscopy
ee	Enantiomeric excess
EIS	Electrochemical impedance spectroscopy
EPR	Electron paramagnetic resonance
eq	Equivalents

EtOH	Ethanol
GMP	Guanosine monophosphate
GTP	Guanosine triphosphate
HB	Hydrogen bonding
HBSS	Hank's Balanced Salt Solution
HSA	Human serum albumin
ITC	Isothermal titration calorimetry
K	Equilibrium constant or degree Kelvin
k	Rate constant
KHMDS	Potassium bis(trimethylsilyl)amide
LOD	Limit of detection
m	*meta*
MD	Molecular dynamics
MeCN	Acetonitrile
MeOH	Methanol
MS	Mass spectrometry
MS3Å	Molecular sieves, 3 Å pore size
M_W	Weight-average molecular weight
NDI	Naphthalenediimide
NIS	*N*-Iodosuccinimide
NMM	*N*-Methylmorpholine
NMR	Nuclear magnetic resonance
o	*ortho*
OCP	Open circuit potential
p	*para*
PBP	Phosphate binding protein
PDB	Protein data bank
PDI	Perylenediimide
PEG	Poly(ethylene glycol)
PIPES	Piperazine-N,N'-bis(2-ethanesulfonic acid)
PMDTA	*N*,*N*,*N*',*N*'',*N*''-Pentamethyldiethylenetriamine
PnB	Pnictogen bonding
PPi	Pyrophosphate
ppm	parts per million

Py	Pyridine
SAM	Self-assembled monolayer
S_NAr	Nucleophilic aromatic substitution
SWV	Square wave voltammetry
T	Temperature
t	time
TBA	Tetra-*n*-butyl-ammonium
TBDPS	*tert*-Butyldiphenylsilyl
TBTA	Tris(benzyltriazolylmethyl) amine
TBTU	O-(Benzotriazol-1-yl)-*N*,*N*,*N*′,*N*′-tetramethyluronium tetrafluoroborate
TEG	Tri(ethylene glycol)
TFA	Trifluoroacetic acid
THF	Tetrahydrofuran
TIPS	Triisopropylsilyl
TMS	Trimethylsilyl
Trt	Trityl
XB	Halogen bonding
XPS	X-ray photoelectron spectroscopy
β	Complex formation constant
δ	Chemical shift
ΔH	Change of enthalpy
ΔS	Change of entropy
Δδ	Change in NMR chemical shift
λ_{ex}	Excitation wavelength

Table of Contents

Declaration i

Acknowledgements iii

Abstract v

List of abbreviations vii

Chapter 1 Introduction 1

1.1 Background of anion supramolecular chemistry 1

1.1.1 Significance of anion binding 1

1.1.2 Properties of anions 2

1.1.3 Development of the field 3

1.2 Natural anion receptors 5

1.2.1 Anion binding proteins 5

1.2.2 Ion channels 7

1.3 Non-covalent interactions and synthetic anion receptors 8

1.3.1 Hydrogen bonding 8

1.3.2 Sigma-hole interactions 17

1.3.3 Anion-π interactions 25

1.3.4 Metal coordination 27

1.4 Relevant applications of anion receptors 30

1.4.1 Aqueous anion sensors 30

1.4.2 Transmembrane anion transport 33

1.5 Anion binding in catalysis 38

1.5.1 Anion abstraction catalysis 38

1.5.2 Activation of electrophilic substrates 39

1.5.3 Control of anionic reactants 41

1.6 Project outline and aims 43

Chapter 2 Simple tetradentate XB anion receptors 45

2.1 Background 45
2.2 Synthesis 46
2.3 Anion binding studies 49
2.3.1 ^{1}H NMR titrations 49
2.3.2 ^{1}H NMR host-host competition experiments 53
2.3.3 Results of anion affinity analysis 58
2.3.4 Solid state structure of **3b·NaI** 60
2.4 Fluorescent sensing 61
2.5 Stereoselectivity in anion binding 62
2.5.1 Chiral discrimination experiments with **2.4b** 62
2.5.2 Attempt at stereoselective anion binding catalysis 66
2.6 Conclusions 68
Chapter 3 Water-soluble XB and ChB receptors 69
3.1 Background 69
3.2 Synthesis 73
3.2.1 Initial attempts 73
3.2.2 Final synthesis of preorganised, solubilised XB receptors 76
3.2.3 Synthesis of a Te-based ChB receptor 81
3.3 Anion binding studies 86
3.3.1 ITC experiments 86
3.3.2 Investigation of the binding mode by diffusion-ordered NMR 89
3.3.3 Results and discussion 92
3.4 Fluorescent anion sensing 98
3.5 Electrochemical sensing 100
3.5.1 Synthesis 100
3.5.2 Capacitive anion sensing 102
3.5.3 Voltammetric sensing 106
3.6 Conclusions 107

Chapter 4 Biomimetic transesterification catalysis 109
4.1 Background 109
4.2 Initial advances towards higher reactivity 112
4.2.1 Synthesis 113
4.2.2 Reactivity studies 117
4.3 Final tripeptide-based design 121
4.3.1 Synthesis 122
4.3.2 Kinetic studies 125
4.4 Introduction of auxiliary base 128
4.4.1 Synthesis 128
4.4.2 Kinetic and mechanistic studies 129
4.4.3 Attempts at enantioselective transesterifications 138
4.5 Conclusions 139
Chapter 5 Summary 140
Chapter 6 Experimental 141
6.1 General information 141
6.2 Compound data for Chapter 2 143
6.3 Compound data for Chapter 3 171
6.4 Compound data for Chapter 4 228
6.4.1 First generation compounds 228
6.4.2 Second and third generation compounds 251
Appendix A Host-host competition binding 293
Appendix B Crystallographic data for **2.3b**·NaI 299
Appendix C Data for electrochemical sensing 303
References 307

Chapter 1 Introduction

1.1 Background of anion supramolecular chemistry

1.1.1 Significance of anion binding

Binding, recognition, and sensing of anions is of great interest due to the multitude of roles played by these species in living organisms, environment, and chemical processes. Phosphate, for example, is a building block of several biomolecules including nucleic acids and ATP which are themselves anionic. Additionally, phosphorylation of nucleophilic amino acid residues by kinases allows signalling, enzyme switching, and regulation of gene transcription.[1] Chloride is highly abundant with normal concentrations in human blood serum[2] of 0.096 – 0.106 M and is transported through ion channels to regulate osmotic pressure, acidity, and membrane polarisation. Impaired function of the CFTR chloride channels in epithelial cells causes cystic fibrosis[3] that manifests by accumulation of thick mucus in airways and by increased chloride concentration in sweat.[4] Bromide is oxidised to hypobromite in eosinophils as a part of their antiparasitic function[5] and by peroxidasin to induce sulfilimine cross-link formation in collagen IV.[6] Iodide is transported into follicular cells of the thyroid by the Na^+/I^- symporter[7] and incorporated into thyroxine and triiodothyronine hormones. Other biologically relevant anions include toxic CN^-, N_3^-, and HS^-, as well as a wide range of carboxylates.

Several anions are important environmental analytes that provide information about soil and water quality, and the extent of anthropogenic pollution. This is certainly true for nitrate and phosphate as they are widely used in agriculture as fertilisers and are also present in manure and sewage. Their runoff into bodies of water[8] causes eutrophication while also contributing to soil degradation. Sulfur anions: sulfate, disulfate, and sulfite form via solvation and oxidation of SO_2 in the atmosphere,[9] and together with nitrate account for acidity in atmospheric water droplets. Anionic pollutants also include the carcinogenic CrO_4^{2-}, toxic AsO_4^{3-}, and ClO_4^-.

Sensing and extraction of anionic species is also relevant to certain industrial processes. This includes $AuCl_4^-$ and $AuBr_4^-$ involved in gold recovery and refining[10] and TcO_4^- which is present in spent nuclear fuel.[11] Additionally, the binding of anionic reaction intermediates forms the basis for a wide range of organocatalysis. Overall, there is a great amount of applications for selective binding and sensing of anions. Development of anion receptors is needed for new technologies in diagnostics, environmental monitoring, water remediation, and industrial chemical processes.

1.1.2 Properties of anions

Anions are generally characterised by large size and diffuse charge caused by charge repulsion and delocalisation. For example, ionic radius of Cl^- (1.81 Å) is significantly larger than of the isoelectronic cation K^+ (1.33 Å).[12] Anions also represent a great variety of molecular geometries (Figure 1) where in most cases the negative charge is distributed over several atoms. These factors result in relatively weak electrostatic interactions, which is a challenge to effective anion binding. Additionally, anions are characterised by high enthalpies of hydration (Cl^-: −381 kJ/mol; K^+: −322 kJ/mol).[13] Compared to alkali metal cations, it is therefore more difficult to overcome the hydrogen bonding interactions of isoelectronic halides with water and other protic solvents. Some anions such as phosphates are also pH-dependent, changing their character in acid-base equilibria. All these intrinsic properties have to be taken into account in the design of selective anion receptors.

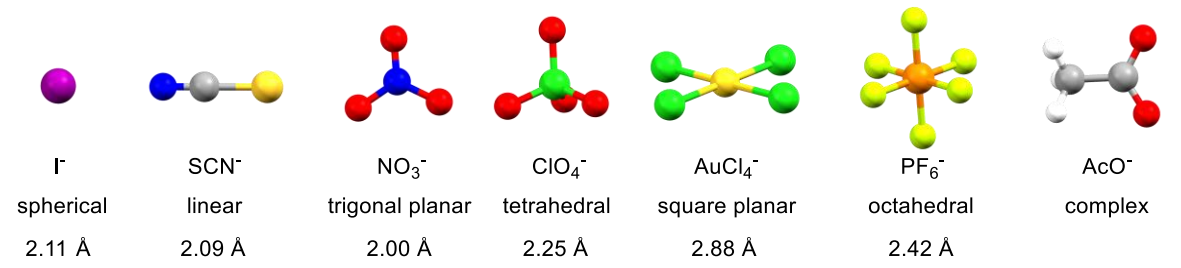

Figure 1 Shape variety of anions and the respective thermochemical radii.

Interactions of anions with dissolved organic (macro)molecules in aqueous solution are heavily governed by the anion charge density and hydration enthalpy. Strongly hydrated anions like F^- and SO_4^{2-} tend to destabilise hydrogen bonding interactions between organic solutes and water by

polarisation of adjacent water molecules, resulting in a higher tendency of the solute to aggregate (salting out). Large and soft anions such as I^- and SCN^- are more capable of direct interactions with organic solutes via dispersion forces and hydrogen bonding. This leads to increased solubility (salting in) while also causing the denaturing of folded macromolecules.[14,15] This trend is reflected by the Hofmeister series (Figure 2),[16,17] first established in the late XIX century by observing the effect of salts on protein solubility. These effects are notably stronger and more consistently observed in anions than cations.[18] This has implications for the design of aqueous anion receptors. Architectures containing a buried, hydrophobic binding site are optimal for weakly hydrated guests, while sites exposed to water are better suited for strongly hydrated anions.[19]

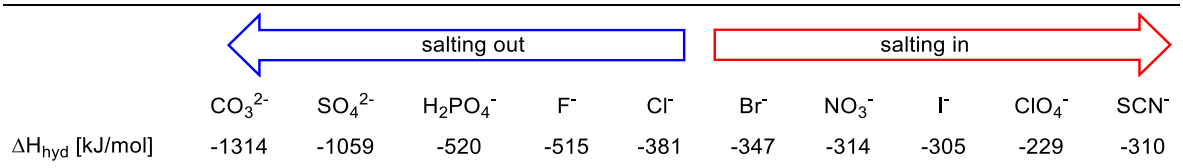

Figure 2 The Hofmeister series for anions and the respective hydration enthalpies.[13,20]

1.1.3 Development of the field

Anion receptor chemistry had its beginnings in the 1960s with the first reports of simple anion binding molecules. These include the observation of methoxide abstraction by a chelating Lewis acid bis(difluoroboryl)ethane (Figure 3a)[21] and halide encapsulation by a bis(ammonium) bicyclic cage (Figure 3b).[22] The latter is notably an early example of using NMR to monitor association phenomena. These first findings coincided with the work on crown ethers and their metal complexing properties by C. J. Pedersen,[23] thus marking the beginning of both anion and cation host-guest chemistry. These first examples were followed by polyamine macrocycles[24–26] and cages[27,28] (Figure 3c), the protonated forms of which could act as anion receptors in organic and aqueous media. Another notable class of early anion complexing agents were the simple charge-neutral tetrel bonding receptors based on silicon (Figure 3d)[29] and tin.[30]

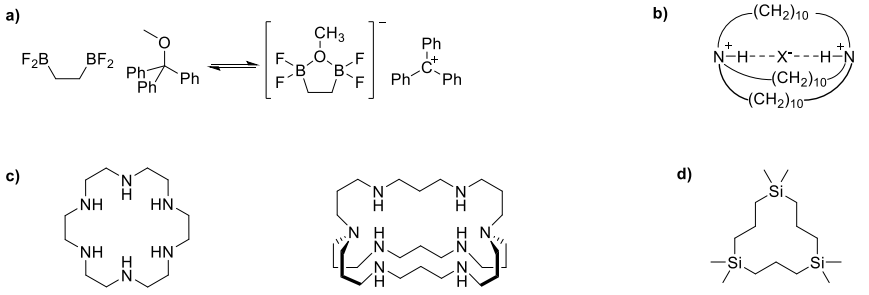

Figure 3 Early examples of anion binding molecules.

Progress in the field accelerated greatly over the last 25 years and we have seen anion receptors increase in complexity and come closer to practical applications.[31–39] In contrast to the highly charged early examples, several neutral hydrogen bonding (HB) receptors have been reported. These were typically based on acidic amide, (thio)urea and pyrrole protons as HB donors. Unusual C-H HB donors have also been described, making use of triazoles and other polarised carbon scaffolds.

In addition to that, other scarcely studied non-covalent interactions have been applied to anion binding (Figure 4). These include σ-hole interactions (most notably halogen bonding),[40,41] anion-π interactions,[42] and their various combinations with HB. As opposed to the non-directional electrostatic interactions with cationic receptors, these have a higher potential for selective binding.

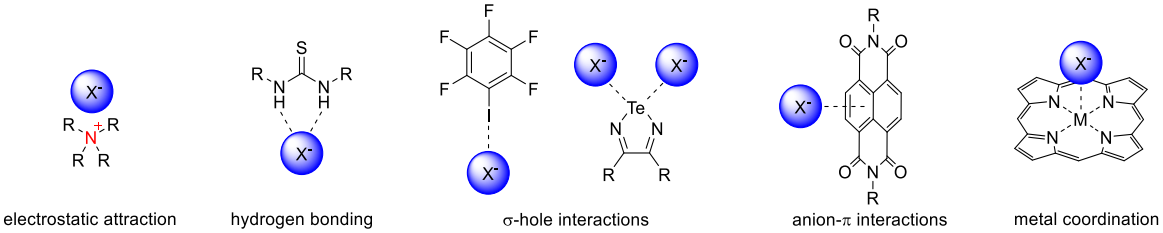

Figure 4 Anion binding toolbox – non-covalent interactions used in anion receptors.

To realise practical molecular recognition applications, receptors functioning in the highly competitive aqueous medium have been particularly sought for.[43,44] Anion binding was also used for template-directed synthesis of macrocycles and mechanically interlocked supramolecular

assemblies.[45–47] Upon removal of template these could generally act as anion receptors and be made to display sensing properties. Apart from anion binding and sensing, progress has been made in using synthetic anion receptors for transmembrane anion transport[48] and in tandem with metal complexing motifs for ion pair recognition.[49,50]

1.2 Natural anion receptors

1.2.1 Anion binding proteins

Many biomolecules possess an evolved function of strong and selective binding of biologically relevant anionic species. A classic example of this is the phosphate binding protein (PBP) of *E. coli*, which sequesters phosphate in the periplasm and transfers it to a membrane protein.[51] Its phosphate binding site (Figure 5) is a complementary pocket relying on multiple HB interactions to bind a fully desolvated HPO_4^{2-} ion.[52] The guest is bound by HB from five amide NH units, four OH groups (two Ser and two Thr residues), and a protonated Arg residue. Additionally, an Asp carboxylate group (in the back of the picture) accepts HB from the $H_2PO_4^-$ proton. A total of 12 HB contacts overcomes the strong hydration of HPO_4^{2-}, resulting in K_a of 3.3×10^7 M^{-1} (H_2O, pH = 7, 10 mM PIPES, 1 mM $MgCl_2$).[53]

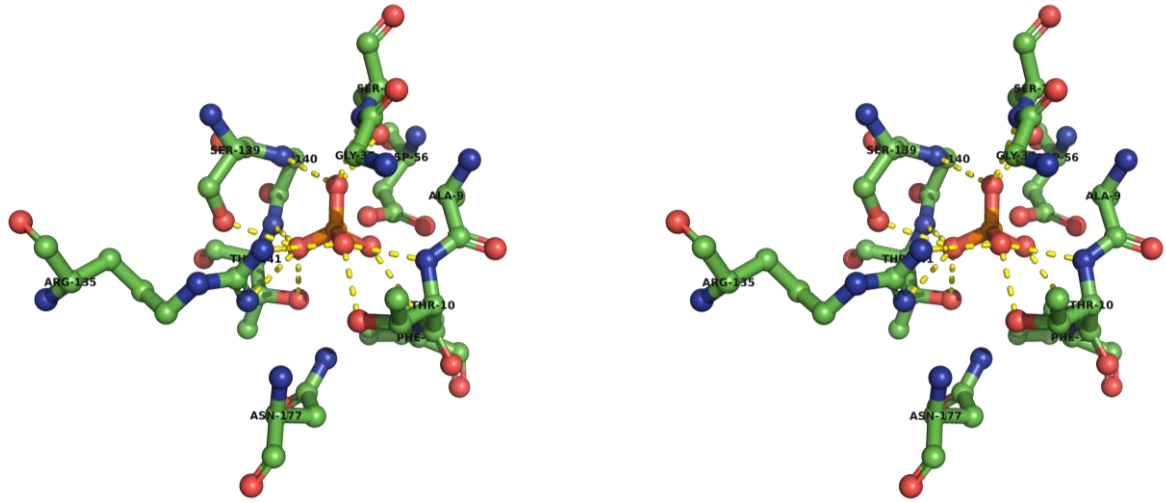

Figure 5 Cross-eye stereo view of the binding site of PBP-coumarin conjugate (PDB 1a54).[52]

1.2 Natural anion receptors

A sulfate binding protein from *Salmonella typhimurium* has an analogous mode of action to the PBP described above as it is a periplasmic SO_4^{2-} binder. The guest anion is surrounded by five amide NH, a Ser OH, and a Trp indole HB donor (Figure 6).[54] However, unlike in PBP, negative charge of SO_4^{2-} is not compensated by contacts with positively charged residues. Instead, the binding site is at the convergence point of three α-helices, all of which point towards the site with their N-termini. The complex is therefore stabilised by local dipoles originating from the first turns of each helix. This auxiliary binding force results in high ($K_a = 4.03 \times 10^6$ M^{-1}, pH = 7.2) affinity for SO_4^{2-} ion, despite its high hydration enthalpy.

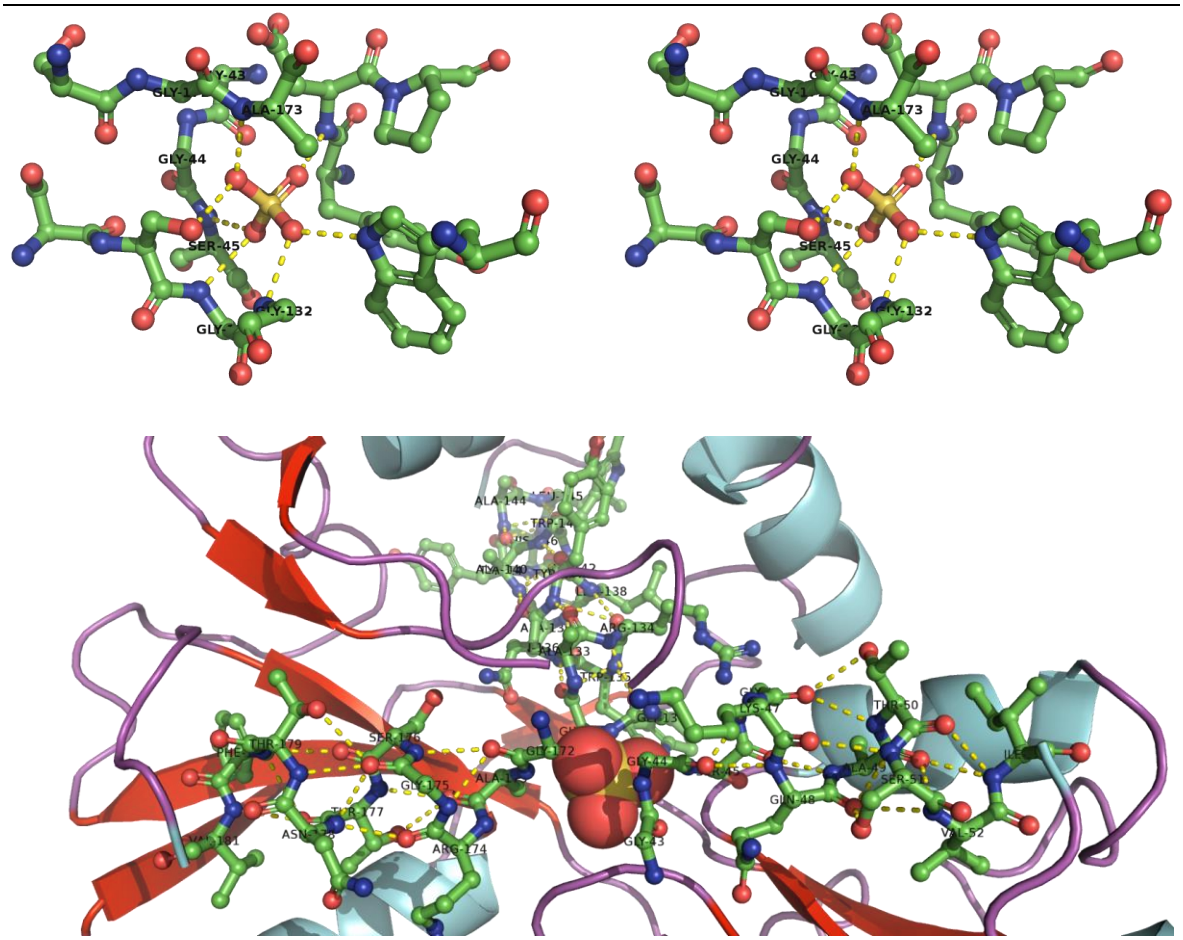

Figure 6 Top: cross-eye stereo view of the SO_4^{2-} binding site of sulfate binding protein (PDB 1spb).[54] Bottom: Binding site shown with the nearby α-helices that provide a dipole-charge interaction with SO_4^{2-}.

ATP binding structures are plentiful in proteins, they are needed to utilize ATP as chemical fuel and as a phosphorylating agent. A class of membrane proteins called ABC (ATP binding cassette)

transporters contain two ATPase subunits which provide the power for active transmembrane transport. The structure of the ATP binding subunit of histidine permease from *Salmonella typhimurium* is shown in Figure 7.[55] Contrary to the two previous examples, it has an open binding site and the triphosphate unit of bound ATP remains partially hydrated. In the ABC membrane complex this allows for ATP-induced formation of a dimer of two ATPase subunits, which is a part of the transport mechanism.[56] The triphosphate unit is bound by the amide NH and OH HB contacts from the Ser41–Gly–Ser–Gly–Lys–Ser–Thr47 motif, known as the P-loop. Additionally, there is a hydrophobic interaction between adenosine and a Tyr-16 residue. Although not present in this crystal structure, under normal conditions there is most likely a Mg^{2+} cation bridging the γ-phosphate and an Asp residue, which is necessary for ATP hydrolysis.

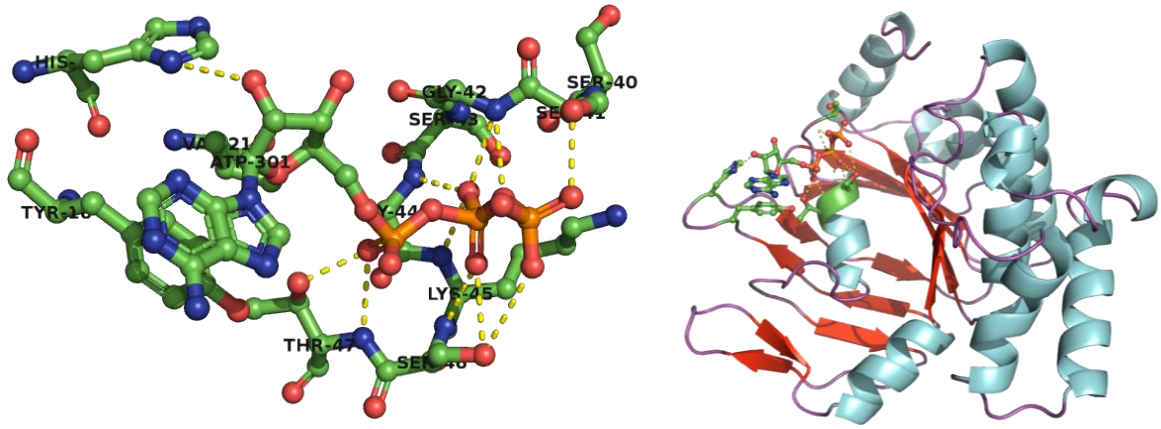

Figure 7 ATP binding site and its position within the overall structure of the ATP-binding subunit of histidine permease from Salmonella typhimurium (PDB 1b0u).

1.2.2 Ion channels

The typical architecture of a transmembrane ion channel includes a membrane-spanning assembly of hydrophobic α-helices with a passage that contains selective binding elements. This is shown on the example of *Escherichia coli* ClC channel (Figure 8), functioning as a H^+/Cl^- exchanger.[57–59] The channel is a homodimer where each subunit contains a separate transmembrane pore. The anion passage consists of three closely positioned binding sites that bridge between water-filled vestibules. The internal (open to the cytoplasm) site binds Cl^- weakly via two amide NH contacts. In

the central site, three amide NHs are reinforced by Ser107 and Tyr445 OHs, resulting in higher Cl^- affinity. The external site is shown occupied by the Glu148 side chain, which blocks the anion pore and has to be displaced by Cl^- for the transport to be enabled. This forms the basis of fast gating observed for this channel. Indeed, Glu148 ⟶ Ala mutation or protonation of Glu148 at pH 5 was observed to open the channel.

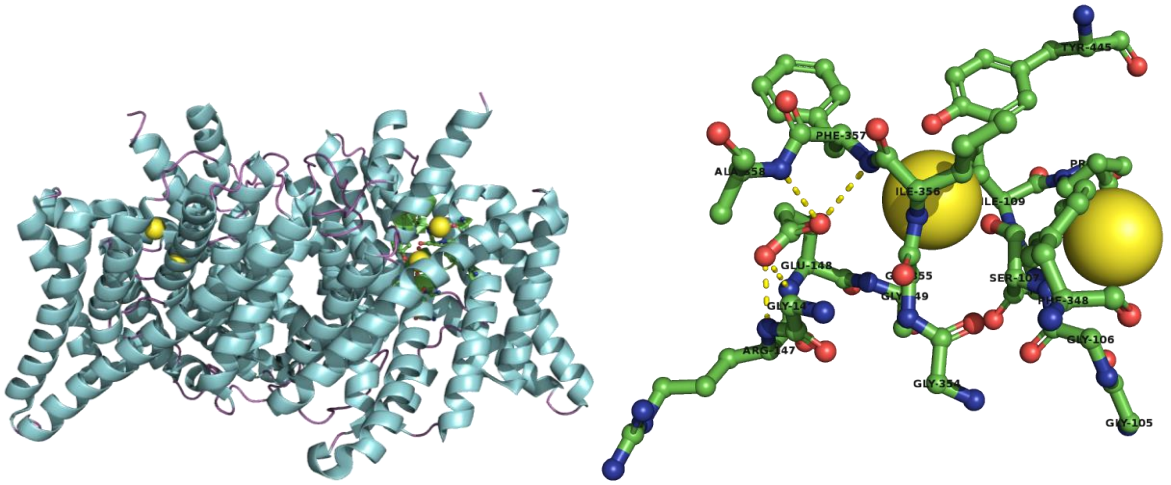

Figure 8 Left: The structure of ClC homodimer (PDB 1ots).[57] Two Cl^- ions (yellow) are shown in each channel. Right: Structure of the anion pore with Cl^- occupying the central and internal sites. The external site is occupied by the Glu148 carboxylate with polar contacts shown.

1.3 Non-covalent interactions and synthetic anion receptors

1.3.1 Hydrogen bonding

As discussed in the previous section, this interaction is the most widespread in biomolecules and synthetic receptors alike. Being responsible for the high boiling point of water, secondary structure of proteins and the double-strand assembly of nucleic acids, multiple cooperative hydrogen bonds (HB) are also useful for anion binding. Enthalpy of HB is typically in the range of 2-30 kJ/mol, although exceptionally strong examples display values up to 161.5 kJ/mol in the bifluoride (HF_2^-) ion.[60] There is a significant directionality to this interaction: the D-H···A angle observed in the solid state is ≥ 150° in most cases and computational studies show HB to be almost non-existent at ∠D-H···A < 120°.[61] Additionally, distribution of electrostatic potential around the HB acceptor determines its optimal orientation relative to the HB donor.[62]

Ammonium and guanidinium

These positively charged units form strong HB and electrostatic interactions with anions such as phosphates, sulfates, and carboxylates. The presence of these cationic units has a strong water-solubilising effect which provided some of the earliest anion receptors to be studied in water.

Comparison of simple polyammonium and polyguanidinium cations (Figure 9a) is a part of the early anion receptor work of J. M. Lehn (1979).[63] In this example, the ammonium analogue proved to be a stronger binder for phosphates. However, its guanidinium counterpart was less pH-dependent due to the lower acidity of protonated guanidines. In another example (Figure 9b),[64] a tricarboxylate-selective tris(guanidinium) was a stronger citrate receptor compared to the tris(ammonium) variant. It was then applied for sensing of citrate via displacement of fluorescein from its complex with the receptor.[65]

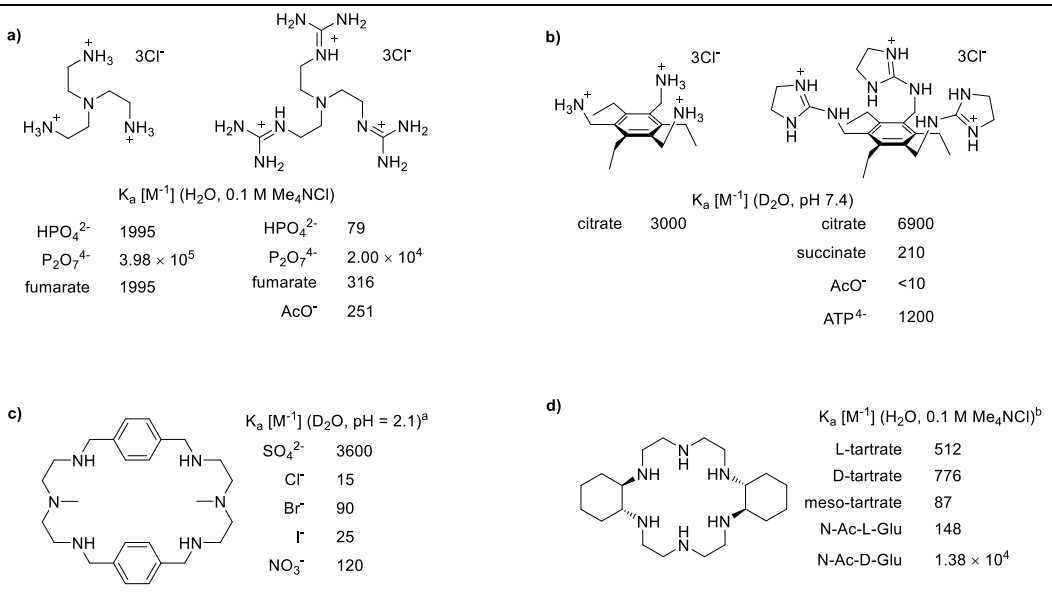

Figure 9 Examples of ammonium and guanidinium anion hosts. [a]Hexaprotonated receptor. [b]Tetraprotonated form of the receptor which is dominant at pH 5-7.

Hexaamine macrocycle (Figure 9c)[66] was shown to be selective for SO_4^{2-} under acidic conditions (pH 2.1) in water. The solid state structure of the hexaprotonated receptor complex with SO_4^{2-} shows the anion encapsulated inside the macrocycle with HB contacts from ammonium protons as well as relatively long C-H···O contacts. Another example of a hexaamine macrocycle (Figure 9d) was

described in an early study on chiral anion recognition.[67] This dicarboxylate receptor is optically active thanks to its diaminocyclohexane units. It exhibited a very strong discrimination between the enantiomers of N-acylglutamate. The binding of L- and D-tartrate was also significantly stronger than of *meso*-tartrate.

Amides and sulfonamides

Amide and sulfonamide-based anion receptors were established early on and observed to be selective for $H_2PO_4^-$ and other strong HB acceptor anions in organic media. Examples include Crabtree's bidentate receptors (Figure 10a) which displayed selectivity for Cl^-, F^-, and AcO^- over Br^- and I^-.[68,69] The sulfonamide analogue had a higher affinity for F^- but lower for Cl^- compared to its amide counterpart. A structurally related tetradentate receptor was strongly selective for $H_2PO_4^-$ owing to the auxiliary HB acceptor pyridine units (Figure 10b).[70]

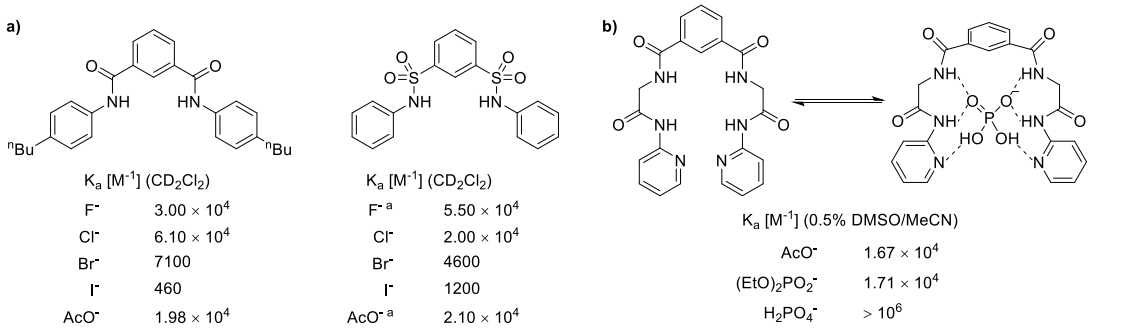

Figure 10 Simple amide and sulfonamide anion receptors. [a]Weak 1:2 binding also observed.

An interesting class of primarily amide-based receptors are the macrocyclic hexapeptides reported by S. Kubik. Constructed from alternating proline and 6-aminopicolinic acid units, these molecules bind anions via convergent hydrogen bonds.[71] The initial macrocycle (Figure 11a) bound SO_4^{2-} in 2:1 stoichiometry in highly competitive 50% D_2O/CD_3OD medium.[72] Due to this 2:1 host:guest binding mode, SO_4^{2-} affinity could be greatly enhanced by joining two macrocycles with a linker (Figure 11b)[72] or incorporating them into a cage structure (Figure 11c).[73] Anions are fully dehydrated in complexes with these receptors and the binding is entropy-driven. Very strong SO_4^{2-} binding was

also observed in a macrocycle functionalised with amine-terminated chains (Figure 11d) that contributed to anion binding in their protonated form.[74]

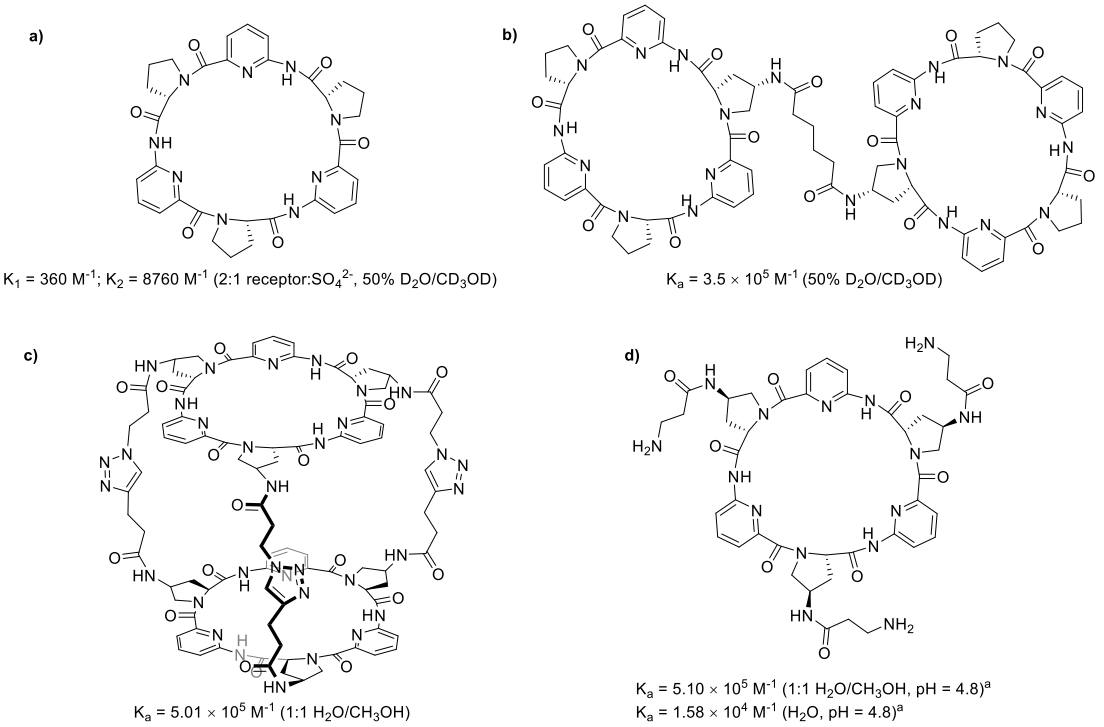

Figure 11 Kubik's macrocyclic hexapeptides and the respective SO_4^{2-} binding constants. [a]40 mM acetate buffer, binding species is $(M+3H)^{3+}$.

Ureas, thioureas, and squaramides

Ureas, thioureas, and squaramides have also been widely used for anion recognition. Due to the high acidity and parallel alignment of their N-H protons they are particularly good at associating with phosphates and carboxylates. This is visualised by the simple examples shown in Figure 12a: a bis(thiourea) receptor[75] was shown to be selective for H_2PO_4 and AcO^- over Cl^-. Likewise, the tripodal urea and thiourea[76] were primarily evaluated for PO_4^{3-} binding. A charge-assisted tris(squaramide) receptor[77] was also consistent with this trend, being selective for tricarboxylate guests such as citrate.

Examples with higher complexity include macrocycles such as a bis(thiourea) shown in Figure 12b[78] which fully showcases the same trend of anion selectivity. Another remarkable macrocycle with six urea units (Figure 12c)[79] was synthesised in the presence of chloride anions acting as template. It

also bound Cl^- in a 1:2 host-guest stoichiometry and with a very high affinity in organic medium. A solid-state structure of its complex with TBACl reveals a figure of eight conformation adopted by the macrocycle bound to two Cl^- ions. Another receptor consists of urea units appended on a lower rim calix[4]arene scaffold (Figure 12d).[80] It is a very early example of a non-metallic, charge-neutral anion receptor and yet again displays anion selectivity typical for (thio)ureas.

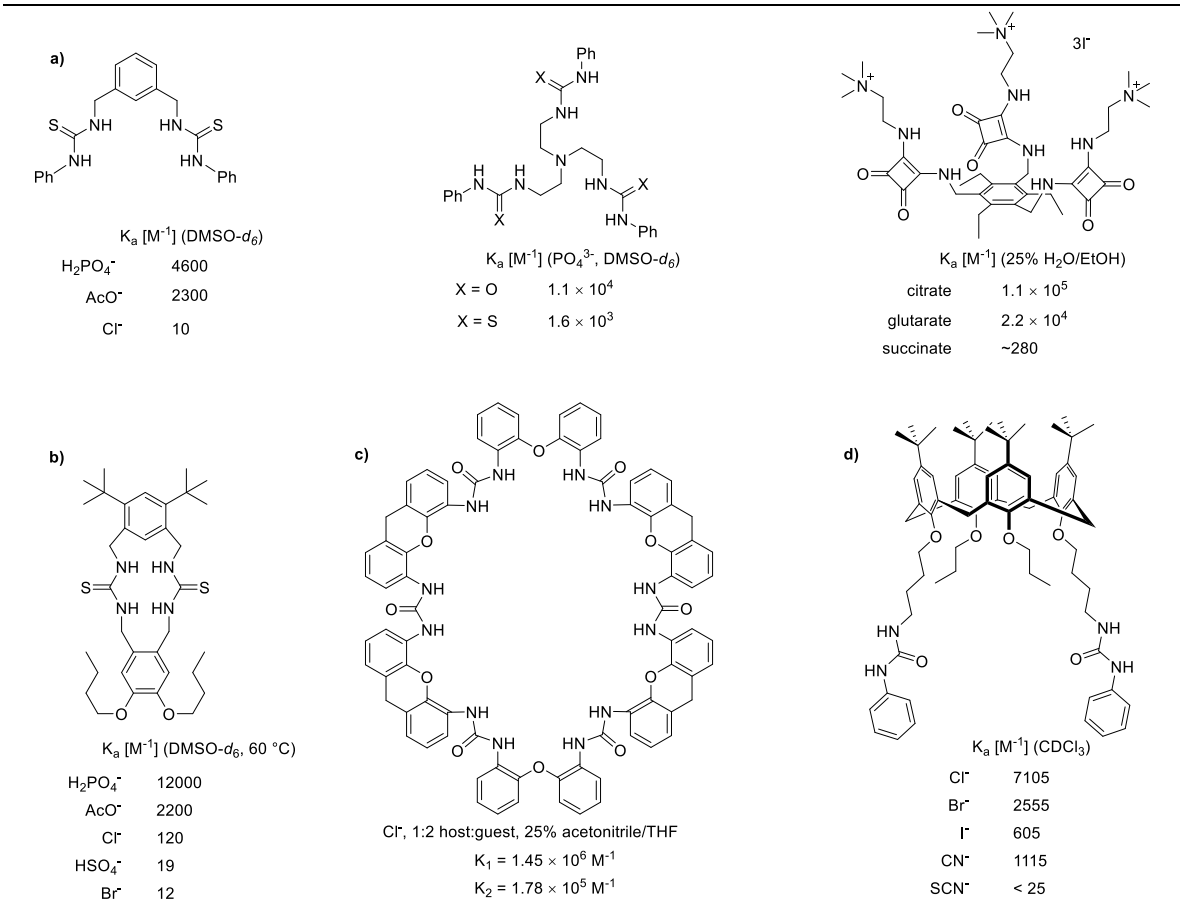

Figure 12 Examples of urea, thiourea, and squaramide-based anion receptors.

Pyrroles and indoles

Calix[4]pyrrole (Figure 13a) is a classic anion binding structure which can be easily prepared by condensation of pyrrole with aldehydes or ketones. Known since the late XIX century,[81] it was recently applied as an anion binding unit, most prominently in the work of J. L. Sessler.[82] For example, extended-cavity calix[4]pyrrole (Figure 13b) displayed an improved F^- selectivity compared to the nonfunctionalized variant.[83] A bicyclic cage consisting of calix[4]pyrrole strapped

with an additional pyrrole unit (Figure 13c) was a very strong Cl^- receptor.[84] Enhancement of Cl^- binding was lost when a furan strap was present instead. Another pyrrole-based macrocycle, cyclo[8]pyrrole (Figure 13d) can be obtained via anodic oxidation of a bipyrrole.[85] Its formation is anion-templated, with the highest yield being obtained using $TBAHSO_4$ as an electrolyte. This was attributed to size complementarity of SO_4^{2-} as the yields of electrochemical synthesis correlate with the size of electrolyte anion. Anion binding studies using cyclo[8]pyrrole iodide-triiodide salt revealed its high affinity for ReO_4^-.[86] The macrocycle was shown to extract TcO_4^- into DCE from aqueous solution of NH_4TcO_4 as well as from underground water samples collected close to lake Karachay (Chelyabinsk Oblast, Russia)* that contained nearly 10^{-5} M of TcO_4^-.

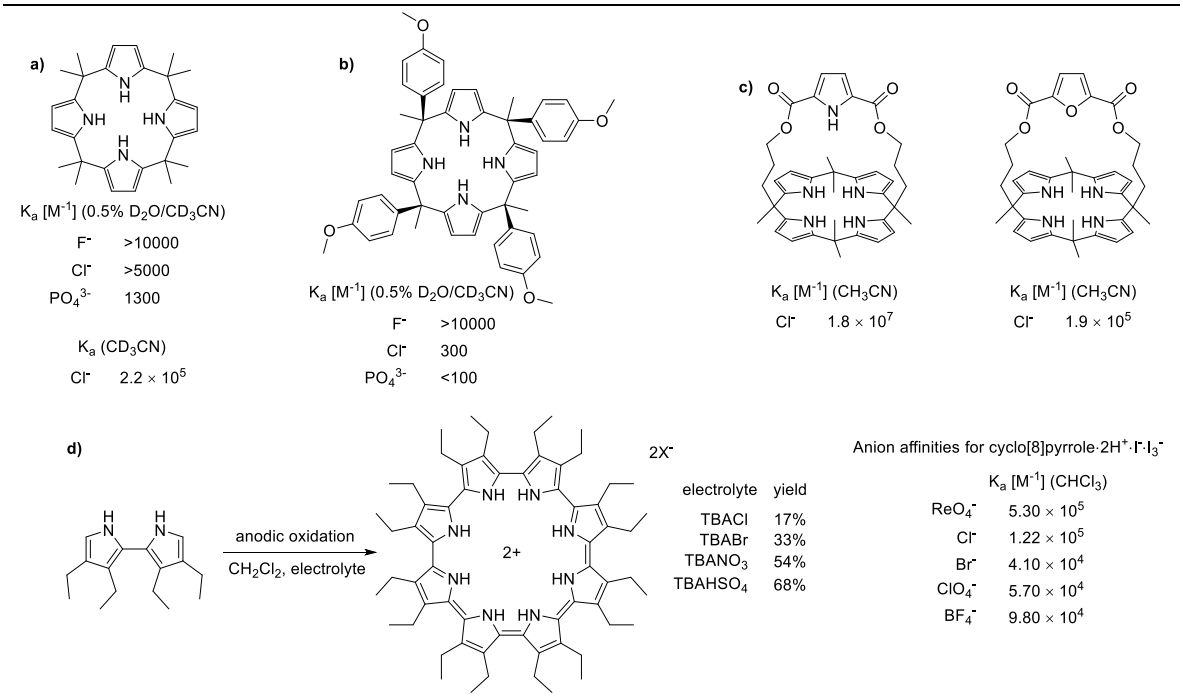

Figure 13 Examples of pyrrole-based anion receptors.

Indoles and indolocarbazoles contain a HB donor on a rigid aromatic scaffold and are therefore attractive building blocks for preorganised anion receptors. This was showcased in the work of K.-S. Jeong on anion binding macrocycles with indolocarbazole units connected via acetylene

* Former waste disposal site for the Mayak plant that produced plutonium for the Soviet nuclear weapons program.

bridges (Figure 14a).[87,88] Size of the inner cavity (distance between NH protons) was determined to be 2.6 × 2.6 Å with a single acetylene spacer and 2.6 × 5.1 Å with diacetylene. The latter is able to accommodate multi-atomic anions, resulting in greatly increased $H_2PO_4^-$, NO_3^-, and N_3^- affinity. A foldamer chain of three fused indolocarbazole units (Figure 14b) able to rotate only around its acetylene hinges was shown to wrap around SO_4^{2-} in a helical arrangement, resulting in strong and selective recognition.[89] Sulfate binding also caused attenuation of fluorescence emission and a bathochromic shift due to the excimer emission of π-stacked aromatic units. Titration with chiral organic anions (CSA and cAMP) resulted in a CD signal which was opposite with (*S*)- and (*R*)-CSA, thus confirming the helical bound state.[90]

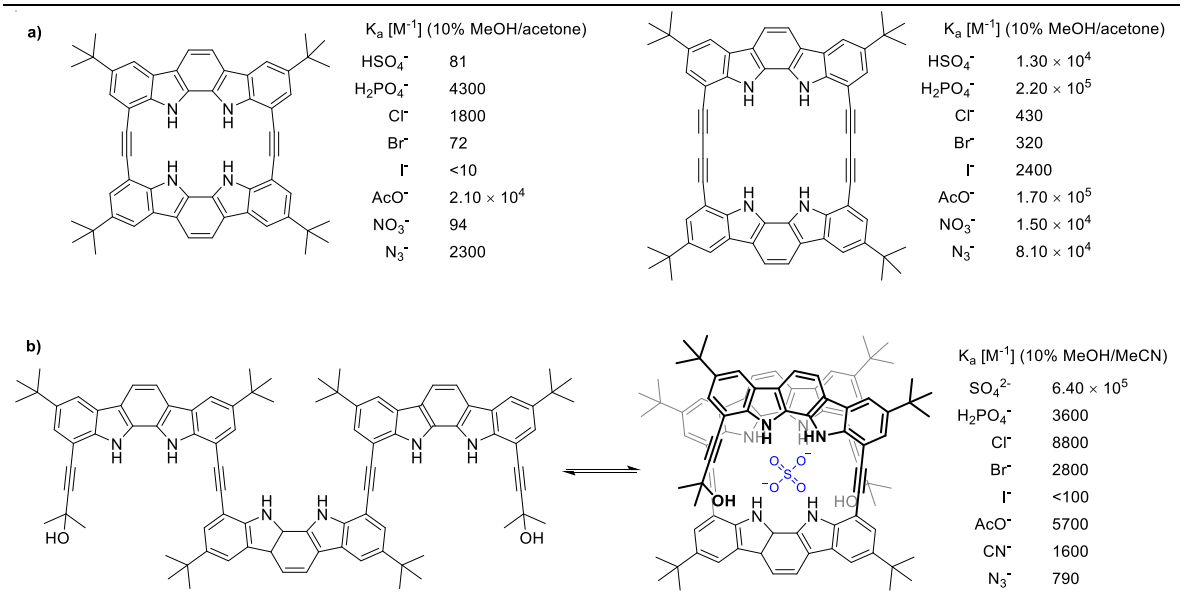

Figure 14 Indolocarbazole anion receptors from the work of K.-S. Jeong.

C-H hydrogen bond donors

Electron-deficient C-H protons are able to act as HB donors similarly to the classic N-H and O-H units. Although C-H HB donors are significantly less acidic, cooperativity of multiple weak interactions and receptor preorganization can result in high anion affinities. In water there is little interaction between C-H anion binding elements and water molecules, which is highly favourable

for binding of weakly hydrated anions such as I^-, SCN^-, and ClO_4^-.[39] This ability to combine hydrophobic effect and HB is a powerful design principle for the recognition of such anions.

Several receptors based on 1,2,3-triazole units are known.[91] With a dipole moment of > 5 D,[92] triazole has a significant positive charge on its proton. Considering its easy assembly via Cu(I)-catalysed azide-alkyne cycloaddition (CuAAC), it is a very attractive building block for anion binding molecules. Examples are the acyclic (Figure 15a)[93,94] and macrocyclic (Figure 15b)[95] tetrakis(triazole) receptors. In both cases the binding cavity formed by the folded triazole-*m*-phenylene backbone had a size complementarity with Cl^-. Anion affinity was much higher in the preoganized macrocyclic system than in the flexible acyclic one. In another example (Figure 15c),[96] a bis(triazole) unit is preorganised via intramolecular HB and combined with naphthaleneimides acting as auxiliary C-H HB donors. Similar to the two previous examples, it is complementary with Cl^-. A related anion binding unit is the imidazolium motif which is a charge-assisted HB donor. An example is the cyclic tetradentate receptor (Figure 15d),[97] demonstrated to be selective for F^- due to its small cavity size and high positive charge.

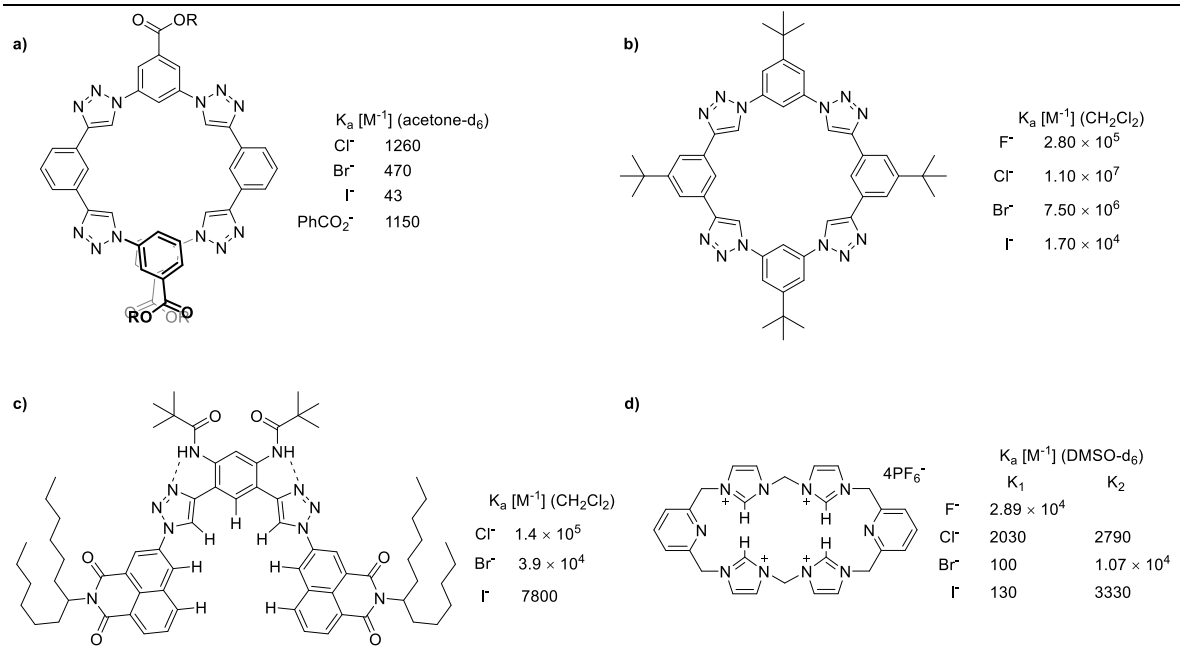

Figure 15 Examples of triazole- and imidazolium-based anion receptors.

Apart from triazole- and imidazolium-based receptors, various macrocycles containing a hydrophobic inner cavity lined with electron-deficient C-H bonds have been described (Figure 16). These receptors have been studied in water or in the presence of protic solvent and share a common selectivity for large, weakly hydrated anions. Cyanostar (Figure 16a)[98] reported by A. Flood can be easily synthesised in high yield via Knoevenagel condensation of a 3-(cyanomethyl)benzaldehyde monomer. It tends to form complexes with anions in 2:1 host:guest stoichiometry (higher complexes have also been observed),[99] stabilised by π-stacking of macrocycle backbones. It has a preference for large anions with diffuse charge such as PF_6^-, IO_4^-, ReO_4^-, SbF_6^-, and ClO_4^-. However, it can also form a 2:1 host-guest complex with a dialkyl phosphate, thus enabling the synthesis of a [3]rotaxane.

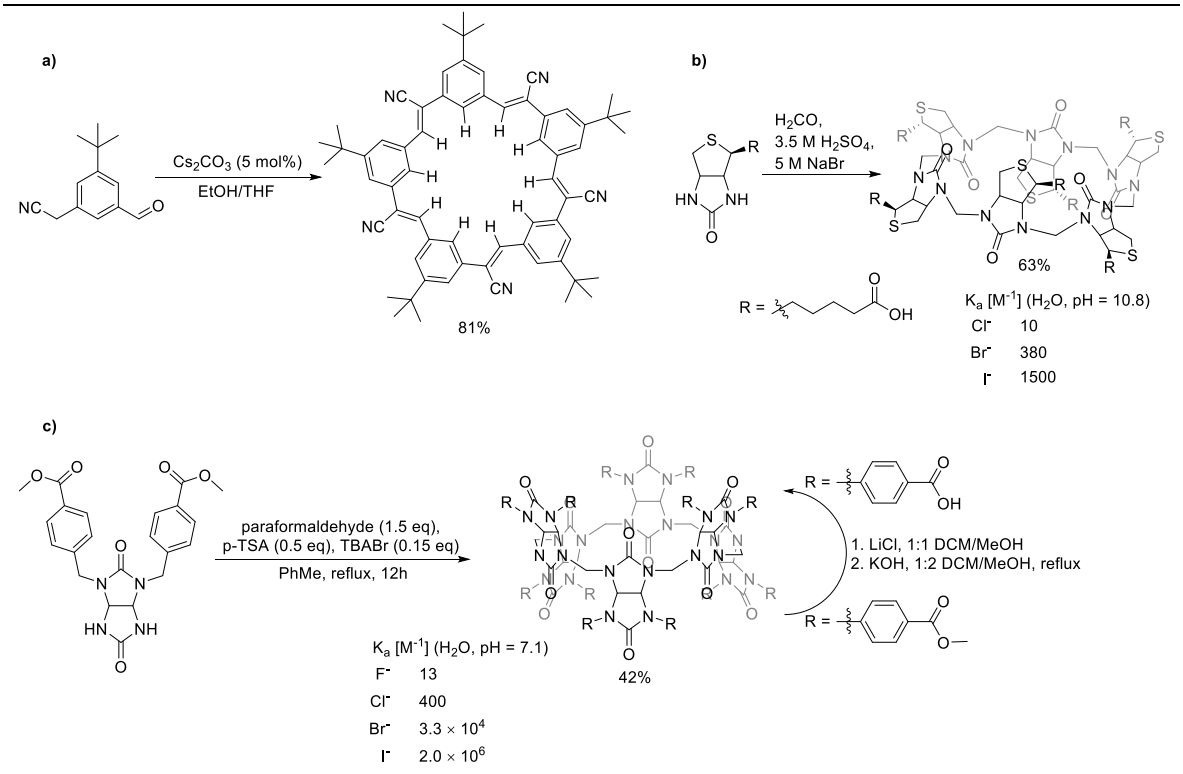

Figure 16 Cyanostar, biotin[6]uril, and bambus[6]uril: easily accessible macrocycles with hydrophobic C-H HB donor cavities.

Biotin[6]urils[100] (Figure 16b) and bambus[6]urils[101–103] (Figure 16c) are closely related macrocycles that can be synthesised via Br^-–templated condensation reactions. Similar to their simpler

congener hemicucurbit[6]uril,[104] they exhibit anion binding properties due to their arrays of inward-directed, electron deficient C-H bonds. This structural feature differentiates them from barrel-shaped cucurbiturils which bind cationic and neutral guests rather than anions. Similarly to cyanostar, biotin[6]uril and bambus[6]uril exhibit the strongest interactions with large and weakly hydrated anions. Complexation of I^- by acidic and neutral[105] bambus[6]urils is currently the strongest known host-guest interaction in 1:1 stoichiometry between an anion and a synthetic receptor in water.

1.3.2 Sigma-hole interactions

This class of non-covalent interactions arises from anisotropic distribution of electron density around electron-deficient atoms of Group 14-17 elements (Figure 17).[106,107] Regions of positive charge on such atoms develop opposite to the electron-withdrawing covalent bonds and may form attractive interactions with nucleophiles. This effect is stronger in large, more electropositive and polarizable atoms: size and positive charge of σ-holes increases down the periodic table.[108] In most publications regarding σ-hole receptors, their interaction with nucleophiles is vaguely described as attraction between regions of positive and negative charge. However, the reality is more complex as contributions from charge transfer (due to the $n \rightarrow \sigma^*$ orbital overlap), electrostatic attraction, and dispersion forces have been identified.[109,110] In particular, the significant charge transfer contribution explains the remarkable directionality and solvent independence[111] of σ-hole interactions.

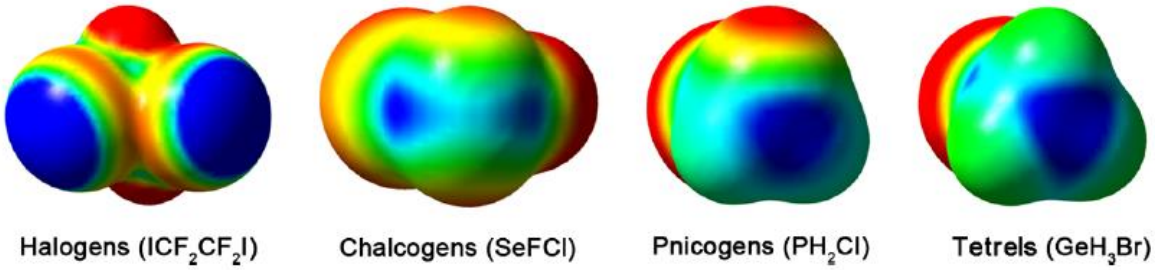

Figure 17 Calculated surface electrostatic potential maps of selected simple Group 17-14 molecules, illustrating different classes of σ-holes.[112] Regions of positive potential are marked in blue.

In addition to Group 14-17 elements, σ-hole interactions originating from Xe compounds have been identified by observation of solid-state Xe···O contacts in XeO_3 and Xe···N in $XeOF_2$·MeCN, and by computational studies.[113] What's more, HB has been theorized to be a subset of σ-hole interactions due to their manifold similarities.[114]

Halogen bonding (XB)

The σ-hole interaction originating from Group 17 elements is the most well-known. It was initially identified in solid-state structures of dihalogens and simple halogen compounds in complexes with N, O, S, and Se bases, as well as in halogen-halogen contacts.[115] XB is highly directional, especially with I as XB donor: mean ∠C-I···N observed in the solid state is 171.4°, while Br and Cl tend to form longer and less directional contacts.[116] Because of this, XB has found use in formation of liquid crystals and other self-assembled materials.[117,118] XB donor strength greatly increases down the group, culminating in At recently identified as a stronger σ-hole donor than I.[119] Anion receptors based on XB are a very recent development. These compounds generally contain I atoms (rarely Br) on electron-withdrawing organic scaffolds.

A tridentate perfluoroiodoaromatic receptor (Figure 18a)[120] was found to be highly selective for halides over oxoanions in organic medium, with halide affinity order $Cl^- > Br^- > I^-$. This order is explained by size complementarity, as this receptor was computationally shown to form a small binding site. A structurally related receptor (Figure 18b)[121] displayed a different halide preference ($Br^- > Cl^- > I^-$), due to a larger binding site as demonstrated by solid-state structures. In a charge-assisted iodopyridinium receptor (Figure 18c)[122] significant oxoanion affinities were observed alongside halide binding. Compared with the charge-neutral receptor (Figure 18a), this demonstrates that electrostatic interactions result in stronger but less specific anion binding.

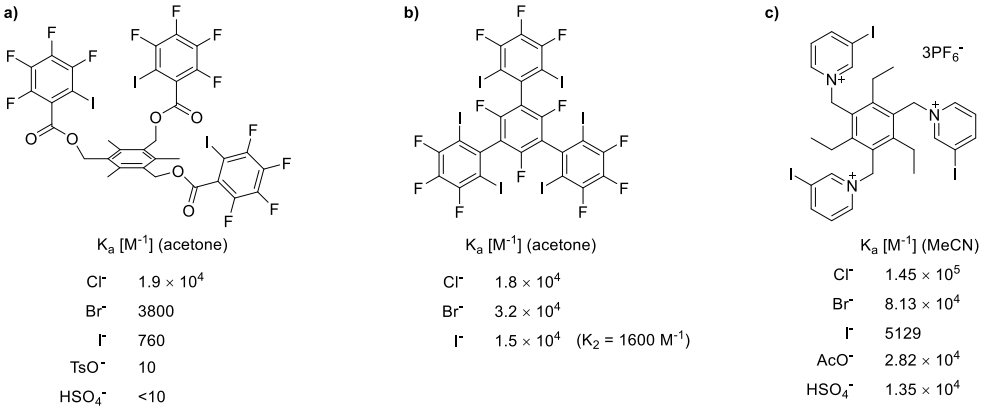

Figure 18 Perfluoroiodoaromatic and iodopyridinium receptors with tridentate binding sites.

Bromo- and iodoimidazolium XB donors were studied in several bidentate anion receptors. In simple bis(imidazolium) compounds (Figure 19a) much higher halide affinities were observed with iodoimidazolium compared to the Br counterpart.[123] This difference was largely entropy-dependent, but a smaller enthalpic contribution was also responsible. In a structurally similar example (Figure 19b), an interesting mode of receptor preorganisation was explored: the receptor is atropisomeric due to the CF_3 group clashing with the I atom as well as the benzimidazole ring.[124] Affinity for Br^- was found to be two orders of magnitude higher in the *syn* atropisomer compared to the *anti* variant.

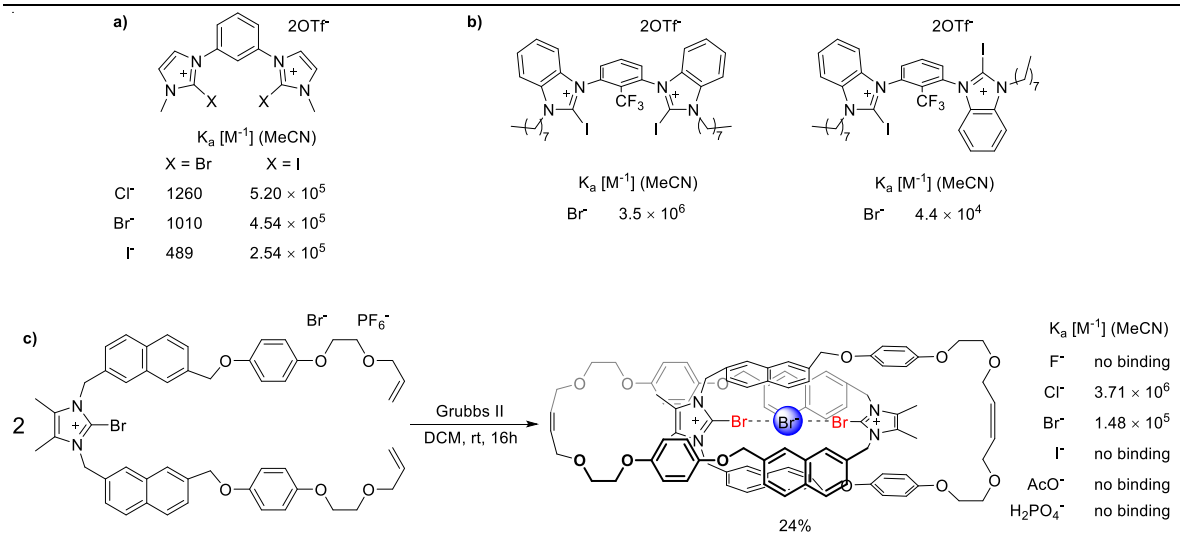

Figure 19 Examples of bromo- and iodoimidazolium XB anion receptors.

A bromoimidazolium [2]catenane (Figure 19c)[125] was synthesised in a Br^-–templated alkene metathesis reaction. The resulting interlocked structure's XB donor cavity selectively bound Cl^- and Br^- while showing no interaction with I^- and oxoanions. This shows that the catenane cavity has a precise size complementarity with Cl^-, in strong contrast with the previously described XB receptors with open binding sites.

Iodotriazoles are very convenient XB donor units due to their facile synthesis from organic azides and alkynes or iodoalkynes. In anion receptors these have mostly been used as cationic iodotriazoliums or as pyridinium-bridged bis(iodotriazole) units. A comparison of these two structures (Figure 20a) revealed very similar anion binding properties in organic medium.[126] They also displayed similar level of reactivity as catalysts in an anion abstraction-mediated reaction; it was however noted that the improved solubility of the monocationic pyridinium system might have practical benefits. Iodotriazolium XB donors were used in a bidentate receptor (Figure 20b) which provided a strong fluorescence response in the presence of dihydrogenpyrophosphate.[108] In this case the bis(iodotriazolium) receptor was found to be a better binder than the bis(bromotriazolium) counterpart. They were both superior to the HB and HB+XB analogues.

The 3,5-bis(iodotriazole) pyridinium motif was used as an axle component in a remarkable rotaxane host (Figure 20c) containing a HB donor macrocycle.[127] Solubilised by its β-cyclodextrin stoppers, this was the first XB receptor to be studied in pure water. It was selective for weakly hydrated I^- with binding being enthalpically favoured due to the formation of XB contacts. This receptor greatly outperformed its amide- and triazole- based HB analogues, which in contrast displayed entropically driven I^- binding.

Neutral iodotriazole systems were used in a pseudopeptide macrocycle (Figure 20d)[128] to create a XB analogue of the previously discussed cyclopeptides (Figure 11). Its rigid, preorganised structure provided significant anion affinities despite the lack of charge assistance. The binding cavity had a size complementarity with Cl^-, which was bound preferentially over the other halides. Another

application of neutral iodotriazoles was the tetradentate all-XB rotaxane (Figure 20e).[129] Studied in wet acetone medium, it was selective for I^-. Compared with more strongly hydrated anions, I^- binding diminished to a lesser extent when the water content was increased. The tetradentate rotaxane also outperformed its analogues with a decreased number of XB donors.

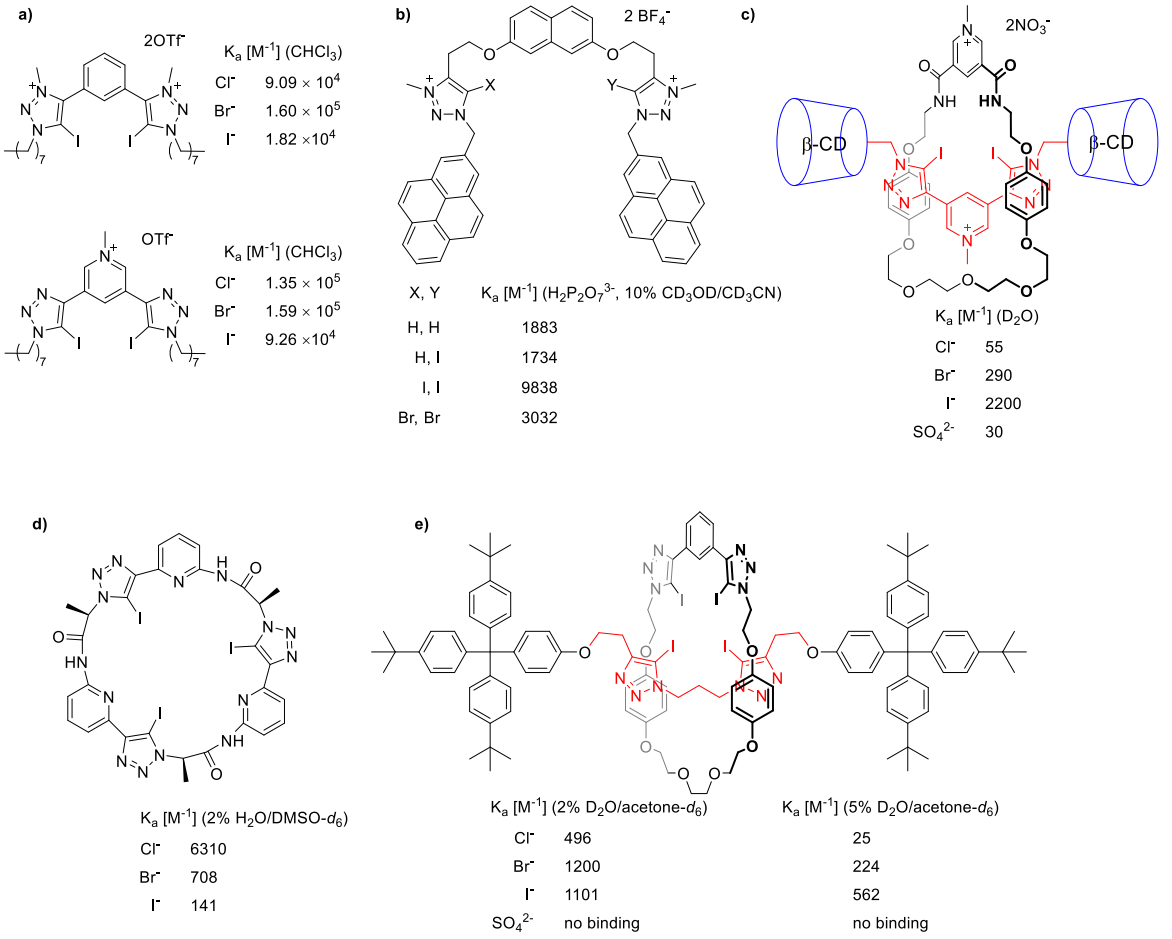

Figure 20 Examples of iodotriazole-based XB donor systems.

Chalcogen bonding

Although chalcogen bonding (ChB) is well known in weak intramolecular and solid-state intermolecular interactions,[130] it has been very scarcely used in anion receptors. In particular, strong ChB donors based on Te are often unstable to air, moisture and especially nucleophiles.[131] However, certain viable Se- and Te-based receptor structures have been identified.

ChB donor properties of tellurodiazole compounds were first identified in the solid-state structures of various complexes containing anions and N bases.[132] Anion complexation in solution was then studied in a series of compounds with increasingly electron withdrawing substituents (Figure 21a).[133] A very strong dependency on the electronic environment of the benzodiazole was observed. Additionally, stronger ChB donors decomposed in the presence of I^-; decomposition was also observed in the presence of F^-, AcO^-, $H_2PO_4^-$, HSO_4^-, and TfO^-.

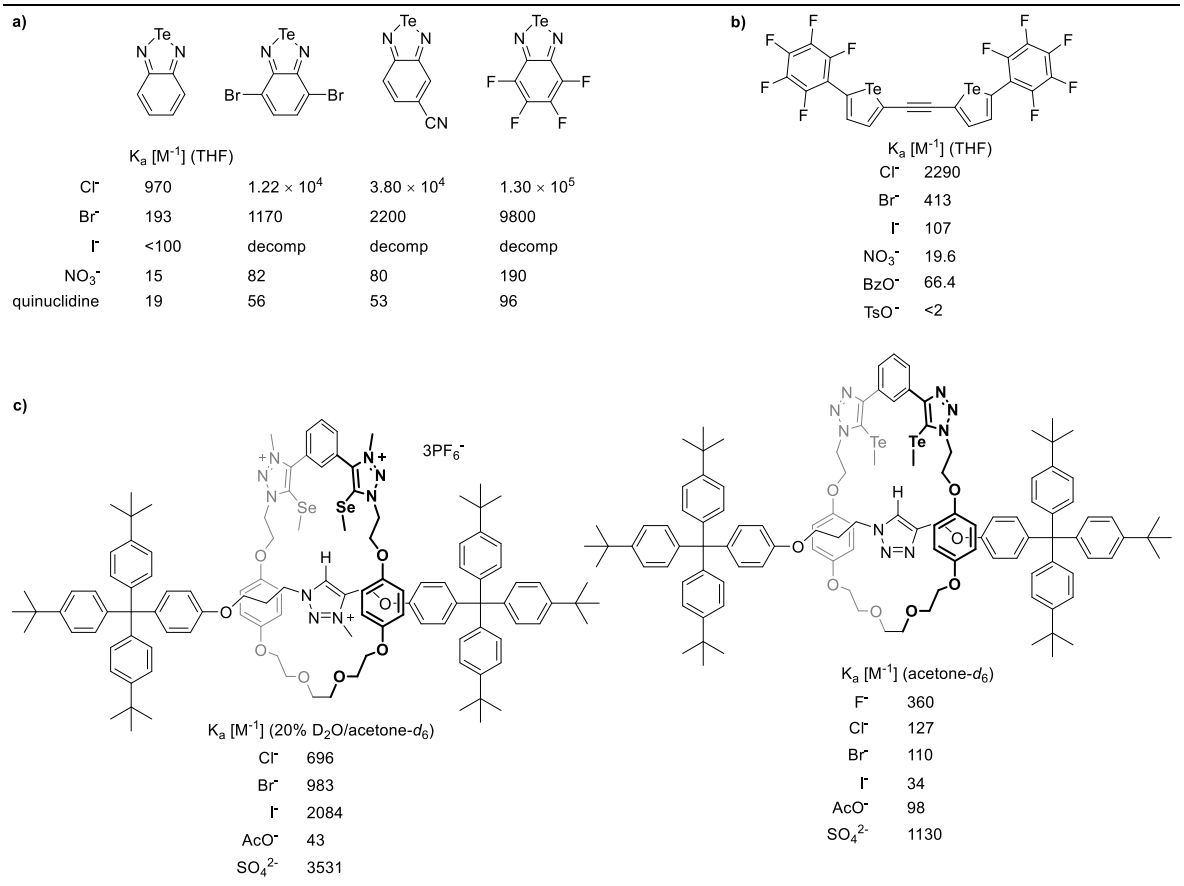

Figure 21 Examples of chalcogen bonding anion receptors.

Bidentate bis(tellurophene) receptor (Figure 21b) was observed to selectively bind Cl^- in THF.[134] The acetylene spacer between the tellurophene units allowed a bidentate coordination mode, enhancing Cl^- binding compared to the monodentate analogues. The order of anion selectivity is in favour of more charge-dense guests which is similar to what is generally observed for XB receptors in aprotic media. Another type of ChB donors, methylselenyl- and methyltellanyl triazoles were

introduced into the macrocycle component of a rotaxane (Figure 21c).[135] The chalcogen atoms assisted the active metal templated rotaxane synthesis and accounted for anion binding properties of the products, remarkably acting as both Cu^+ and anion coordinators. Neutral Te-based rotaxane was studied in acetone and displayed the expected preference for charge-dense anions. The cationic Se-based analogue was a strong enough binder to be analysed in the presence of water, where it demonstrated selectivity for heavier halides, following the trend of lower hydration enthalpy. Strong binding was however observed with SO_4^{2-}, which was attributed to the charge assistance in the tricationic host.

Pnictogen bonding

Interaction of electron-deficient Group 15 elements with anions and nucleophiles have been observed in various solid-state complexes[136] and investigated theoretically,[137,138] highlighting their similar nature and energetics to HB and XB.[139] Notable examples are the bidentate Sb(III) compounds which were characterised in solid-state complexes with pyridine (Figure 22a).[140] The bidentate binding mode as well as occupancy of two σ-holes on one Sb atom was found in these structures. Computational studies indicated strong association with halides, especially the electron-dense F^- and Cl^-.

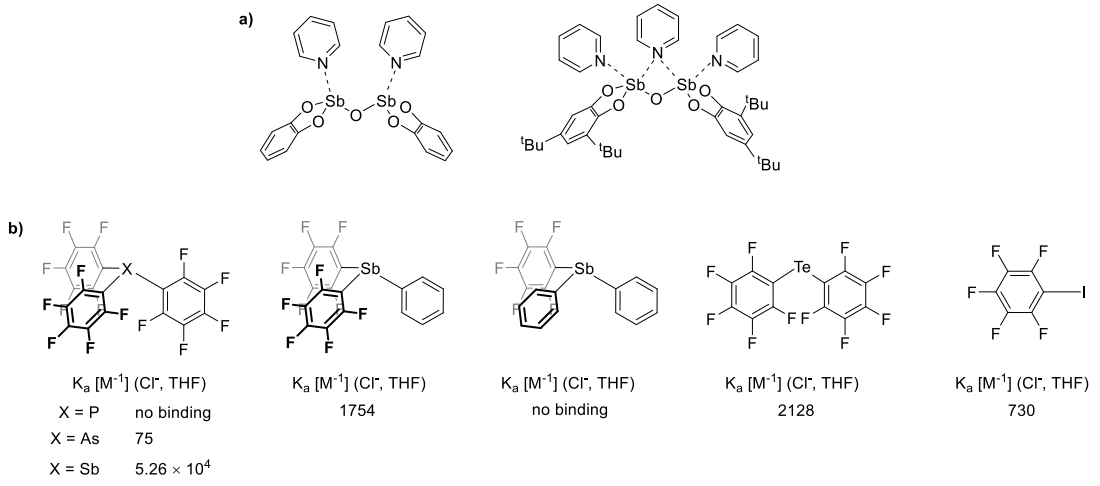

Figure 22 a) Oxygen-bridged Sb(III) catecholates and the binding modes in their pyridine adducts. b) Comparison of pentafluorophenyl-bound PnB, ChB and XB anion binding organocatalysts.

The only solution-phase PnB anion receptors reported to date are the tris(perfluoroaryl)pnictogen compounds (Figure 22b) investigated as anion abstraction catalysis and as Cl^- binders.[141] A very large increase in binding strength was found moving from P to As to Sb analogues. A similar dependency on the electron-withdrawing character of the aromatic substituents was observed. Remarkably, PnB donors proved to be stronger receptors than the structurally related ChB and XB versions. This was attributed to the more electropositive and polarisable nature of Group 15 elements as well as their ability to accommodate three electron-withdrawing substituents. Analogues based on Group 14 (Ge, Sn) elements were also tested, but proved to be too sterically crowded to accommodate the Cl^- guest. This indicates Sb-based receptors as optimal in the pentafluorophenyl-substituted σ-hole donor family.

Tetrel bonding

Similarly to PnB, this class of σ-hole interactions is scarcely studied due to the steric crowding around tetravalent Group 14 atoms, tendency for heavier Group 14 elements (Sn and Pb) to exhibit metallic coordination chemistry, and the difficulty of constructing multidentate receptors. Existing structures include the previously mentioned 12-silacrown-3 (Figure 23a) that accelerated the transport of Cl^- and Br^- (as Me_4N^+ salts) between aqueous solutions separated by DCM phase in a U-tube.[29] Other early examples were the macrocycles and bicyclic cages with Sn bridgeheads (Figure 23b).[30,142,143] A solid-state structure was reported for a macrobicycle with C_6 bridges complexed with F^-, where a bidentate binding mode was clearly shown. In the case of a Cl^--bound homolog with longer C_8 bridges, the binding was asymmetric (Sn···Cl distances 2.610 Å and 3.388 Å), indicating the presence of a strong and a weak interaction with Cl^-. Binding studies in solution revealed size complementarity effects, as Cl^- could not enter the cavity of the smallest bicyclic cage.

Triethoxysilanes were observed to form octasilsesquioxane cages in the presence of F^- (Figure 23c).[144–146] This process was enabled by anion templation via convergent tetrel bonds and the resulting F^- complexes were studied in the solid state. They were found to symmetrically bind F^-

with eight 2.65 – 2.66 Å Si···F contacts. Similar encapsulation is thought to occur in siliceous zeolites. A germanium analog is also known; in this case F^- position was found to be disordered, indicating that due to the large size of Ge atoms F^- occupies positions displaced towards a face or a vertex of the cage.[147]

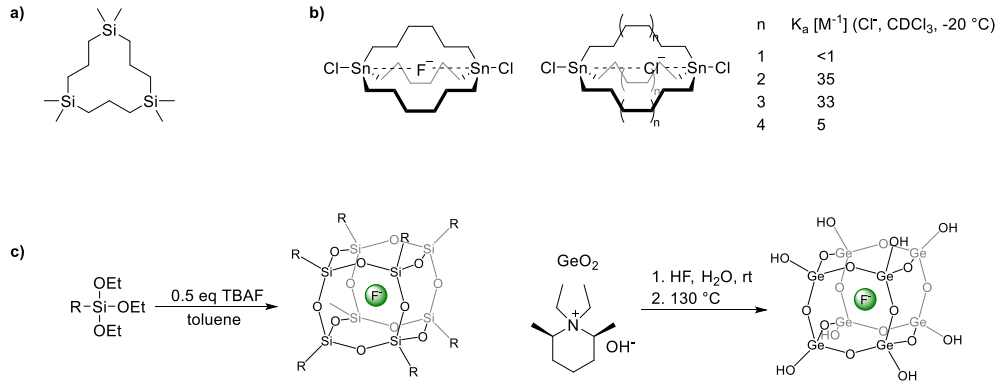

Figure 23 Some known cases of tetrel bonding to anions.

1.3.3 Anion-π interactions

Electron-deficient aromatics can be used to interact with anions. This phenomenon is more elusive compared to the related cation-π interaction due to the overall larger size and lower charge density of anions. Strongest interactions typically occur with small, hard anions such as F^-, OH^-, and Cl^-. In some cases, especially with F^-, formation of charge-transfer complexes leads to highly selective spectral responses. This occurs in the bis(triazine) macrocycle (Figure 24a), where an additional absorption band (313 nm) was observed in the presence of F^- but not any other anions.[148,149] With other guests bidentate anion-π contacts were confirmed in the solid state for SCN^- and BF_4^-. In the case of NO_3^-, one anion-π contact (2.953 Å) and two weak σ-interactions with triazine carbons (O···C = 3.243 Å) were observed.

A dendritic ligand (Figure 24b) provided one of the first clear observations of anion-π interactions.[150] In the solid-state structure of its complex with 4 equivalents of $CuCl_2$ half of the Cl^- ions were observed to be encapsulated by the pyridine rings (Cl··· ring centroid distance 3.466 – 3.697 Å). Contacts with the triazine N atoms were also present.

The combination of triazine units with a crown ether (Figure 24c)[151] or a bisimine-ether chain (Figure 24d)[152] provided ion-pair receptors. The former was able to solubilise $CaBr_2$ and CaI_2 in organic solvents. The solid state structure of its CaI_2 complex showed two I^- ions in contact with the triazine rings, with a water molecule bridging between them and the Ca^{2+} cation bound nearby. Ion pair binding was highly cooperative, as no interaction was observed upon titration with TBA halides. The bicyclic ion-pair receptor with imine units (Figure 24d) displayed increased binding of F^- in the presence of Zn^{2+} or Pb^{2+} in MeCN with a strong fluorescence enhancement.[152]

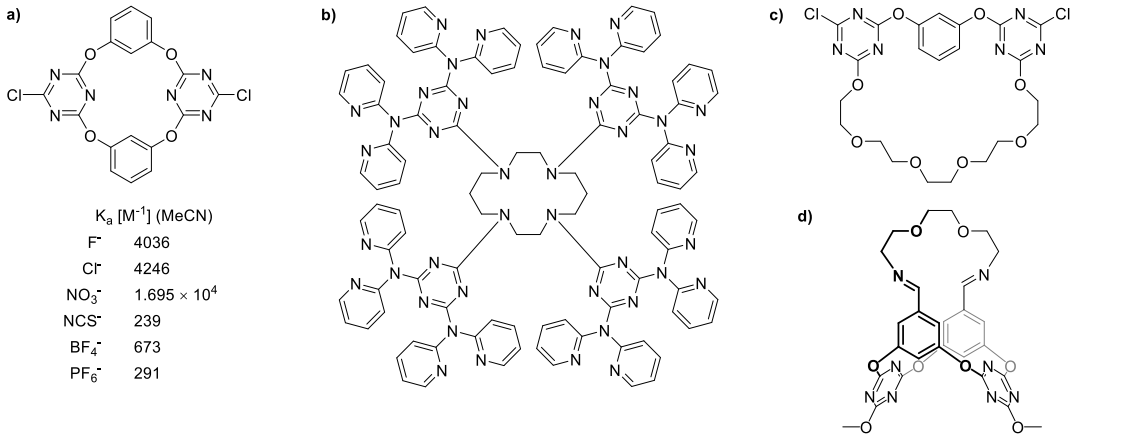

Figure 24 Triazine-based molecules that exhibit anion-π interactions.

Other highly electron-deficient aromatics, especially naphthalenediimides, have featured in anion receptors. A tripodal compound with three 3,5-dinitrobenzoate units (Figure 25a) could interact with halides in benzene solution.[153] As C-H HB contacts are prevented by the steric environment, this association was due to halides interacting with the electron deficient aromatic rings.

A "molecular triangular prism" reported by F. Stoddart (Figure 25b)[154] was found to encapsulate I_3^- as evidenced EPR and CV studies of redox-active NDI units. The resulting assembly crystallised with a helical superstructure induced by π-stacking, where the helical turn was controlled by point chirality of the macrocycle, providing right-handed helices with (*RR*)-diaminocyclohexane bridges.

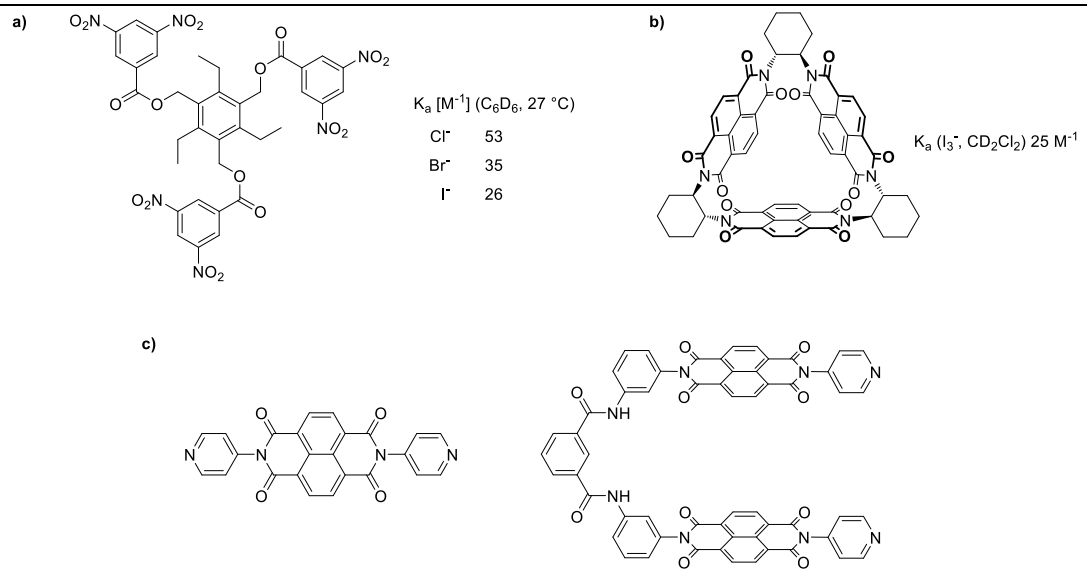

Figure 25 Examples on non-triazine anion-π receptors.

Anion to NDI charge transfer was observed in NDI-pyridine conjugates (Figure 25c) in the presence of F^- in DMSO.[155] This enabled highly selective naked-eye F^- sensing by the means of strong spectral changes. Upon titration with F^-, an absorption band at 475 nm appeared, corresponding to $NDI^{\bullet-}$. Large excess of F^- led to a broad band at 542 nm, consistent with NDI^{2-}. At the same time, no response was seen in the presence of Cl^-, Br^-, I^-, NO_2^-, NO_3^-, N_3^-, AcO^-, and $H_2PO_4^-$. Joining two NDI units together facilitated the formation of a sandwich complex. This receptor could respond to nanomolar concentrations of F^-.

1.3.4 Metal coordination

Lewis acidic metals are routinely used for anion coordination. In particular, metals are able to form stable complexes with strongly hydrated anions that are very difficult to bind with HB and other receptors in the presence of protic solvents.

Zinc complexes have been widely used for the recognition of phosphate species.[156] For example, Zn^{2+} complexes of a bis(dipicolylamine) ligands with anthracene cores (Figure 26a) were able to bind phosphate species such as ATP in aqueous buffer, providing a modest fluorescent enhancement by which the association could be monitored.[157,158] In the case of receptor with

1,8-anthryl core binding of polyanionic ATP and ADP was much stronger than that of AMP and $H_2PO_4^-$. The receptors were also able to bind negatively charged oligopeptides with a phosphorylated Tyr or Ser residue while displaying no interaction with a non-phosphorylated analogue.

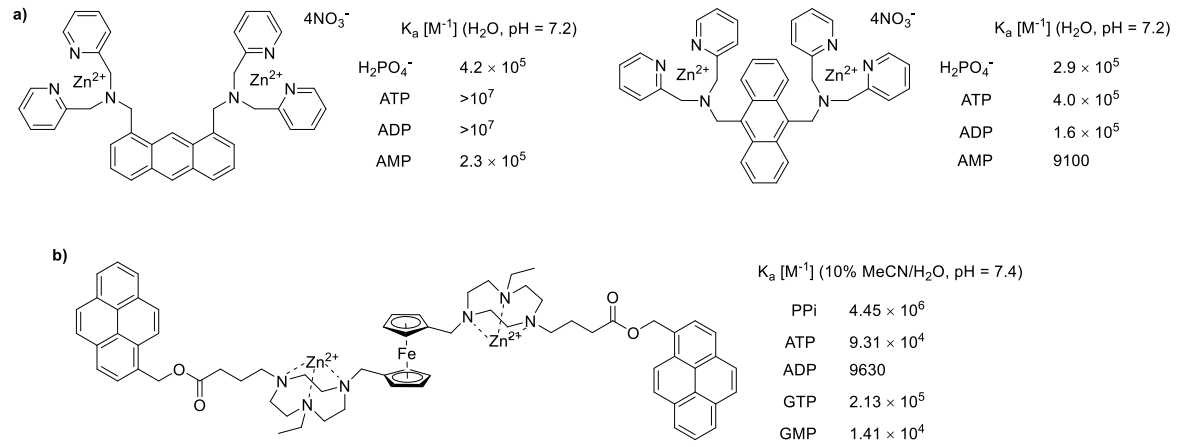

Figure 26 Examples of zinc-based receptors for molecular recognition of polyphosphate species.

A bis(triazacyclononane) Zn^{2+} complex (Figure 26b) was selective for pyrophosphate, which was attributed to its higher charge density compared to organic polyphosphates.[159] Binding of a phosphate species to both Zn centres caused the arms of the receptor to come together. This resulted in a strong enhancement of the excimer emission from the pyrene termini due to their increased π-stacking. Additionally, a change in oxidation potential of the ferrocene core was detected electrochemically, thus providing a two-channel response upon binding.

Lanthanide complexes based on a tetraazacyclododecane core (Figure 27a) were used to sense bicarbonate concentrations inside mitochondria, monitoring its production via the Krebs cycle.[160] The azaxanthone group in the ligand had the dual function of sensitization and directing the mitochondrial uptake of the probe. In the Eu^{3+} complex a reduction of emission intensity was observed in the presence of common biological anions (HPO_4^{2-}, ATP, citrate, lactate, and HSA protein), while HCO_3^- caused a strong enhancement of emission. This enhancement was much lower in the Tb^{3+} analogue, permitting ratiometric analysis of mitochondrial HCO_3^- concentration.

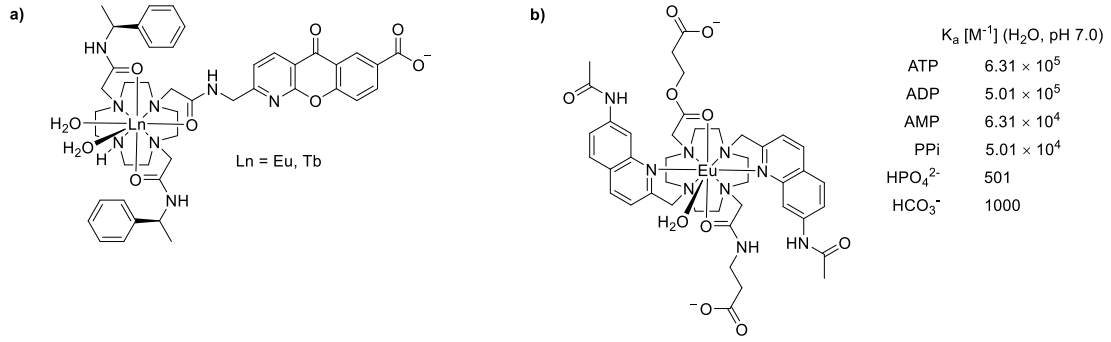

Figure 27 Examples of lanthanide-based intracellular anion sensors.

A similar Eu^{3+} complex (Figure 27b) preferentially bound polyphosphate species such as ATP, for which a bound state with auxiliary HB from the quinoline-attached amides was proposed.[161] Addition of ATP resulted in displacement of a Eu-coordinated H_2O molecule and strong enhancement of its fluorescence, which could be conveniently monitored by the intense 605-630 nm emission band. Although the ATP and ADP affinities were similar, it was found that in the presence of 5 mM Mg^{2+} (relevant as most of the cellular ATP is Mg-bound) a stronger fluorescent response was induced by ATP compared to ADP. This difference allowed monitoring of ATP build-up or depletion in live cells. In contrast to the previous example, no response to HCO_3^- concentration was observed.

Boron is a Lewis acidic entity that can be readily incorporated into organic molecules. Boron-based receptors have proved particularly useful for binding and recognition of F^-. Several simple systems are known that contain two B centres or combine a B Lewis acid with a donor of another anion binding interaction. A simple bis(borane) (Figure 28a) was described as early as 1985 in complexes with F^-, OH^-, and H^-.[162] A related compound equipped with a chromophore(Figure 28b) lost its visible absorption upon F^- binding.[163] This effect was highly selective, as other halides displayed no signs of interaction. Due to the chelating character of the receptor, its F^- affinity in THF was > 5 × 10^9 and the complex was stable in the presence of water.

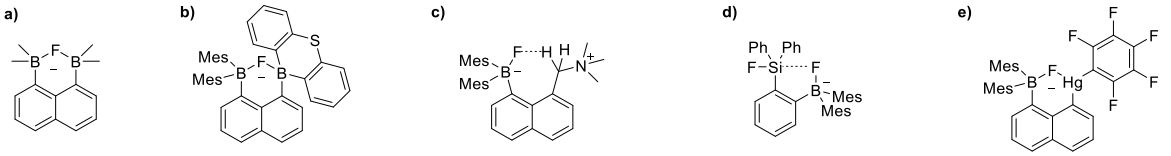

Figure 28 Bidentate F^- receptors based on boron Lewis acids and auxiliary interactions.

The boron receptor assisted by HB from a neighbouring quaternary ammonium (Figure 28c) was notable for being able to extract F^- (as TBAF) from water into a $CHCl_3$ phase, exchanging it for TfO^-. The presence of auxiliary HB was confirmed by a 2.826 Å C–H···F contact in the solid state.[164] Another interesting example is the F^- receptor assisted by tetrel bonding from an electron-deficient fluorosilyl group (Figure 28d).[165] The B–F···Si distance of 2.248 – 2.266 Å and ∠F–Si···F of 175 – 176° are both consistent with this auxiliary binding. The boron-based receptor assisted by a Hg Lewis acid (Figure 28e) formed a F^- chelate with $K_a > 10^8$ M^{-1} in THF and 2.3×10^4 M^{-1} in 10% H_2O/THF.[166] As this binding disrupts conjugation between the naphthalene and mesityl groups, the receptor's low-temperature phosphorescence was noted to change from orange-red to green.

1.4 Relevant applications of anion receptors

1.4.1 Aqueous anion sensors

Anion binding and sensing in water is particularly challenging due to the need to overcome hydration enthalpies of the desired analytes. Additionally, dissolution of organic receptors in water may be difficult, especially when hydrophobic conjugated systems are used as fluorescent or colorimetric reporters. Known aqueous sensors often contain metal complexes or multiple positive charges, which solve these problems but tend to cause non-specific binding.

Examples shown in Figure 29 contain these design elements and provide either a turn-on or a turn-off fluorescent response. A tetradentate imidazolium macrocycle (Figure 29a) responded by strong quenching of the anthracene excimer emission at 525 nm as the two anthracene units were separated upon guest inclusion.[167] The receptor bound GTP in 2:1 host/guest stoichiometry, remarkably being selective over ATP and other nucleoside triphosphates. It was also able to bind I^-

in 1:1 stoichiometry, which was attributed to good size complementarity with the macrocycle cavity. A macrocyclic dinuclear Zn^{2+} complex (Figure 29b) did not exhibit a strong excimer emission but responded by an increase in anthracene monomer emission upon binding of ATP or ADP.[168] This occurred due to the intercalation of two adenine groups between the anthracenes in a 1:2 complex. Hydrogen bonding between the bound adenines and efficient π-stacking with the anthracene units were proposed to account for the selectivity over other nucleoside polyphosphates.

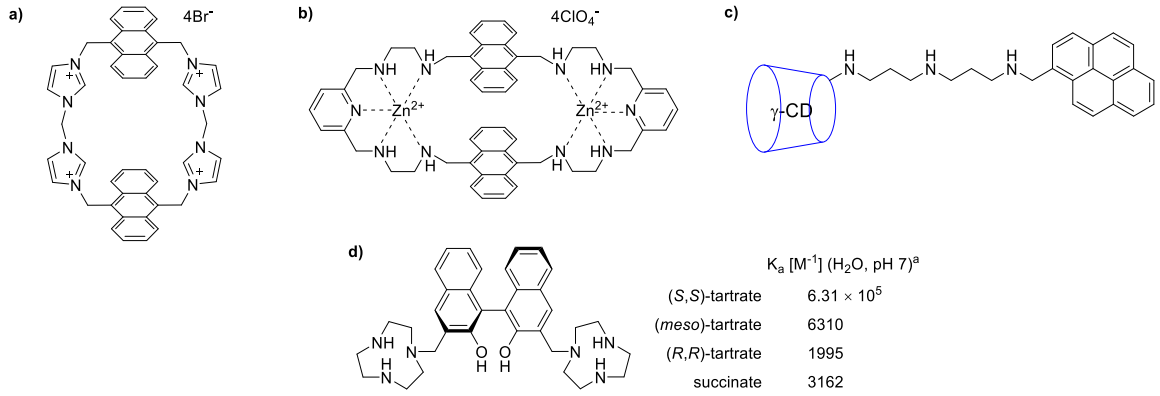

Figure 29 Examples of aqueous anion receptors with hydrophobic π-conjugated fluorophores. [a]Receptor predominantly in the diprotonated form.

A receptor constisting of γ-cyclodextrin and pyrene connected by a tris(amine) chain (Figure 29c) selectively responded to HCO_3^- over a range of other anions, including HPO_4^{2-} and AcO^-.[169] The receptor forms dimers in water where two pyrenes are π-stacked inside a barrel consisting of two γ-CD units. At pH of 6.88 – 9.81 the receptor predominantly exists as a dicationic dimer, where the two monoprotonated tris(amine) chains are well suited to bind amphoteric HCO_3^-. Binding changes the conformation of the encapsulated pyrene dimer, resulting in a new fluorescence band at 390 – 460 nm.

In a very effective example of chiral recognition a binaphthol receptor with two triazacyclononane groups was able to bind (*S*,*S*)-tartrate with a large preference over its stereoisomers and other dicarboxylic acids. Binding was accompanied by close to 8-fold increase in emission intensity at

420 nm, which was attributed to the strong hydrogen bonding between the phenol and tartrate OH groups. Differences in efficiency of this HB explain the dicarboxylate selectivity observed.

Fluoride is particularly difficult to sense in water due to its very strong hydration. However, its tendency to form strong covalent bonds with silicon has led to several sensors based on desilylation reactions. In the two examples shown in Figure 30, release of a fluorophore leads to an irreversible (chemodosimetric) response to F^-.[170,171] A TBDPS ether group was determined as appropriate as the Si atom was inaccessible to water but labile in the presence of F^-. The release of either resorufin (Figure 30a) or coumarin (Figure 30b) occurred with a strong fluorescence enhancement. The coumarin variant was used as a non-cytotoxic F^- probe in human epithelial lung carcinoma cells and their lysate.

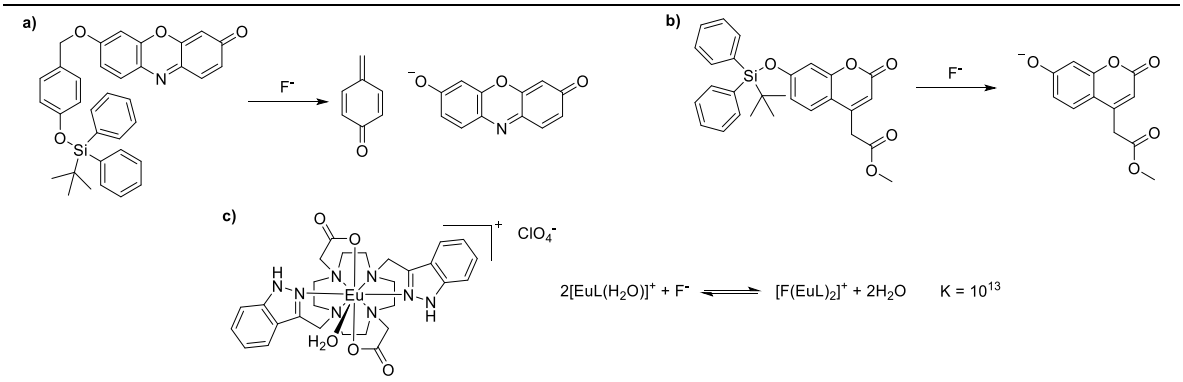

Figure 30 Fluoride sensors based on desilylation reactions and lanthanide coordination.

Europium complex of a tetraazacyclododecane derivative (Figure 30c) displayed a very strong association with F^- in 2:1 stoichiometry.[172] A crystal structure confirmed the position of F^- bridging between the two Eu centres with 2.27 Å Eu–F contacts. Additionally, the complex was stabilised by π-stacking interactions between the indazole groups. Displacement of a Eu-coordinated water molecule in the presence of F^- led to a strong (22-fold) increase in Eu emission intensity. Very high affinity for F^- led to a detection limit of 24 nM, while at the same time almost no response was seen in the presence of Cl^-, Br^-, HCO_3^-, AcO^-, and HPO_4^{2-}.

Chloride and heavier halides can be detected in water due to their ability to quench the emission of quaternary nitrogen-containing fluorophores based on quinolinium and related structures. This dynamic collisional quenching depends on formation of an excited state charge transfer complex which is not emissive.[173] Two common halide sensors based on this mechanism are SPQ[174] and lucigenin[175] which is often used to monitor Cl^- influx into liposomes (Figure 31a). A turn-on I^- sensor thought to provide response based on excited state complex formation was also reported (Figure 31b).[176] In contrast to the quinolinium sensors, this compound is selective for I^- over a wide range of anions including Cl^- and Br^-. The proposed exciplex mechanism was supported by the lack of change in absorption spectrum in the presence of I^-.

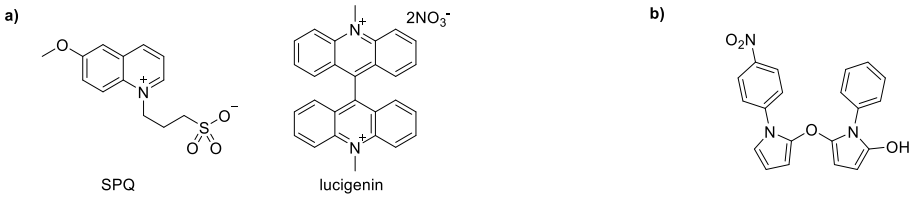

Figure 31 Fluorescent halide sensors that rely on excited state complex formation.

1.4.2 Transmembrane anion transport

As was mentioned previously, the transport of anions across lipid bilayers is ubiquitous in biology, which evokes interest in synthetic anion binding molecules that mimic the function of natural transmembrane channels and transporters. In particular, the transport of Cl^- has a potential application in the treatment of cystic fibrosis and other channelopathies, and in the manipulation of cells by inducing pH changes and membrane polarisation.[48,156]

Transport of Cl^- has been accomplished by several small molecules containing HB and other anion binding units. To enable membrane permeability, these molecules have an overall lipophilic character despite containing hydratable HB donors. This transport activity is exhibited by the tripyrrolic natural product prodigiosin (Figure 32a), a red pigment produced by *Serratia* and *Streptomyces* bacteria. Its protonated form is a tridentate HB donor, which allows it to act as a H/Cl

symporter, with effects such as uncoupling proton translocation from enzymatic catalysis.[177] Prodigiosin and its derivatives have been thoroughly studied to understand cellular ion transport mechanisms and come closer to therapeutic applications. For example, a C-ring modification of prodigiosin (Figure 32b) was found to have stronger growth inhibition properties in human cancer cells (1.0 vs 2.1 μM total growth inhibition concentration, an average of 59 cell lines).[178] At the same time it exhibited lower toxicity in mice, overall being more therapeutically promising. Reduced toxicity was also observed in the A,C-ring derivative (Figure 32c), which did not decrease the viability of healthy cell lines at 5 μM concentration.[179] It could exchange Cl^- for NO_3^- and HCO_3^- in liposomes and live cells matching the activity levels of CFTR, which makes it a promising channel prosthesis lead for the therapy of cystic fibrosis. A structurally related compound (Figure 32d) derived from a different class of natural products (tambjamines) could likewise transport Cl^- and HCO_3^-.[180]

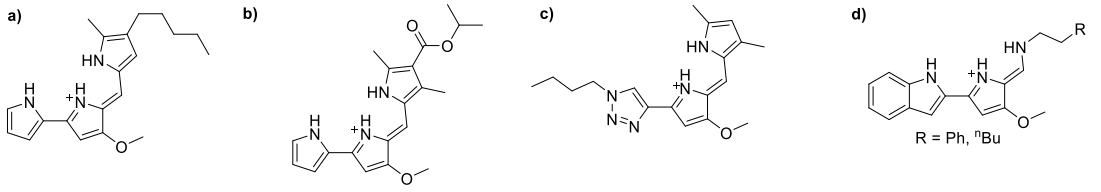

Figure 32 Prodigiosin and related compounds studied for their cytotoxic and anion transport properties.

Other synthetic transporters include various classes HB and σ-hole donors previously discussed in the context of their anion binding properties. For example, a comparison of electron-deficient ureas, thioureas, and squaramides (Figure 33a) identified the latter as particularly powerful Cl^- transporters.[181] This was attributed to their superior Cl^- affinity, although correlation between K_a and transmembrane transport is not straightforward. Additionally, being less lipophilic than the urea and thiourea analogues makes squaramide a more optimal binding unit for drug candidates. A bis(urea) with an anthracene scaffold was shown to be an exceptionally fast Cl^-/NO_3^- antiporter.[182] As of 2018 it was claimed by the authors to be the fastest known small-molecule promoter for this kind of transport, outcompeting synthetic transporters as well as prodigiosin.

A bis-amide preorganised via intramolecular HB from its resorcinol scaffold was a significantly stronger Cl^- receptor than its analogue lacking the preorganisation (Figure 33b).[183] This translated to a massively improved transport ability compared to the non-preorganised variant which displayed no detectible Cl^- transport. Preorganisation could also be disrupted by deprotonation of resorcinol at pH > 7 which inhibited Cl^- transport.

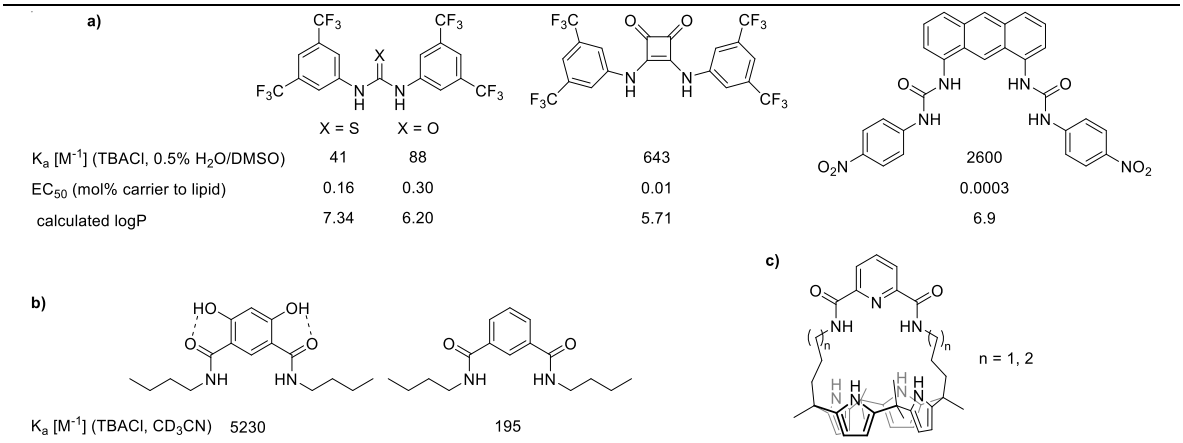

Figure 33 Examples of small molecule anion transporters.

A bis(amide)-strapped calix[4]arene (Figure 33c) promoted Cl^- influx into liposomes, which was enhanced in the presence of NO_3^- or in the presence of a cation transporter.[184] In absence of either it acted as a slow Na/Cl symporter. When tested in cells it promoted Cl^- influx which was balanced by Na^+ influx through the sodium channels. Remarkably, this induced apoptosis in HeLa and lung adenocarcinoma epithelial cells as implied by caspase activation observed after incubation of cells with transporters in HBSS buffer (containing ca 150 mM Cl^-), thus providing a novel mechanism for triggering programmed cell death.

Transmembrane anion carriers based on σ-hole interactions are also known. As the σ-hole donors are hydrophobic, such materials combine membrane permeability with anion binding capacity. Among the most notable findings, simple 1-iodoperfluoro-n-alkanes and perfluorinated iodoarenes were found to be effective halide transporters (Figure 34a).[185] As shown by the Hill coefficients measured in the Cl^- transport assay, the anion is encapsulated by multiple XB donor molecules

during transport. The optimal aliphatic homolog was 1-iodoperfluorohexane. Longer homologs were inactive, possibly due to their alignment with the lipid tails causing inability to encapsulate anions. Shorter molecules were less active, although some transport ability was seen even in iodotrifluoromethane.

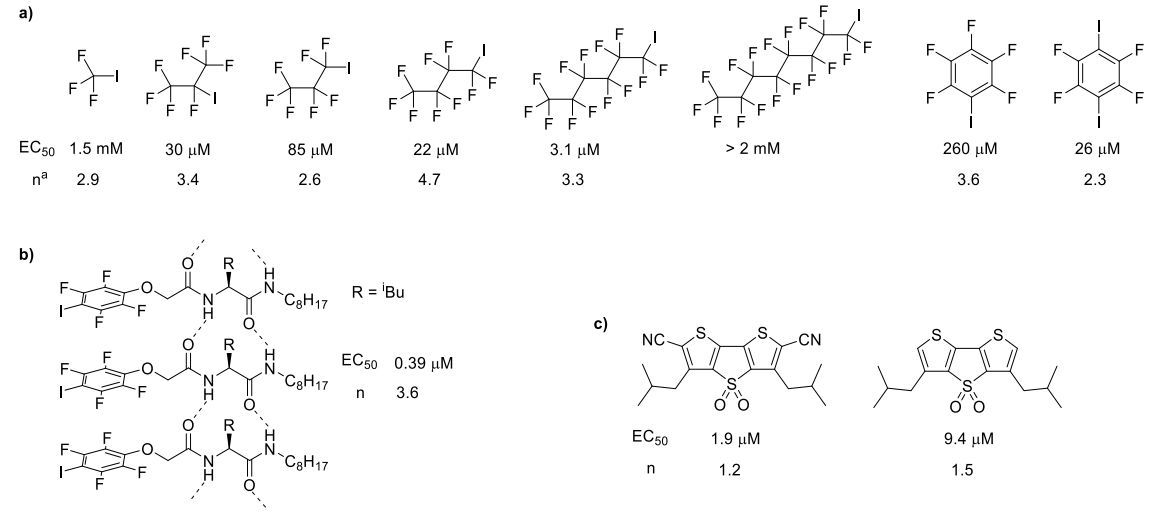

Figure 34 Examples of transmembrane transporters based on σ-hole interactions. [a]Hill coefficient.

A monopeptide carrying an XB donor structure was able to form hydrogen-bonded transmembrane assemblies (Figure 34b). These could preferentially transport Cl^- over Br^-, I^-, NO_3^-, and ClO_4^-.[186] Its activity was significantly superior to the simple XB donors in the previous example. Sulfur-based bidentate ChB donors are also known as transmembrane transporters (Figure 34c).[187] Unlike the two previous examples, these compounds showed little to no cooperativity in the dose-response dependencies. Predictably, the presence of electron-withdrawing CN groups or a sulfone bridge enhanced the transport ability.

Another class of transmembrane anion transporters are the membrane-spanning rigid molecules reported by S. Matile (Figure 35) that act as "anion slides". Remarkably, variants based on anion-π, XB, and ChB interactions are now known. The anion-π slides based on naphthalenediimides (Figure 35a)[188,189] and perylenediimides (Figure 35b)[190] displayed anti-Hofmeister preference for anion transport (Cl^- in NDI and SO_4^{2-} in PDI analogue), indicating that the strength of anion-π interaction

overrides the dehydration penalty. In the PDI rod, a light-driven active influx of electrons into the liposome occurred together with Cl^- efflux, which allowed a photosynthetic reduction of intravesicular $[Co(bpy)_3]^{3+}$.

Anion slides based on XB (Figure 35c)[191] and ChB (Figure 35d)[192] were likewise active in Cl^-/OH^- antiport. In both cases the transporter molecules were thought to assemble into transmembrane bundles where anion transmission occurs by hopping between σ-holes. Transport activity was significantly higher compared to the simple XB donors and similar to the previously mentioned XB-based peptide stacks (Figure 34b).

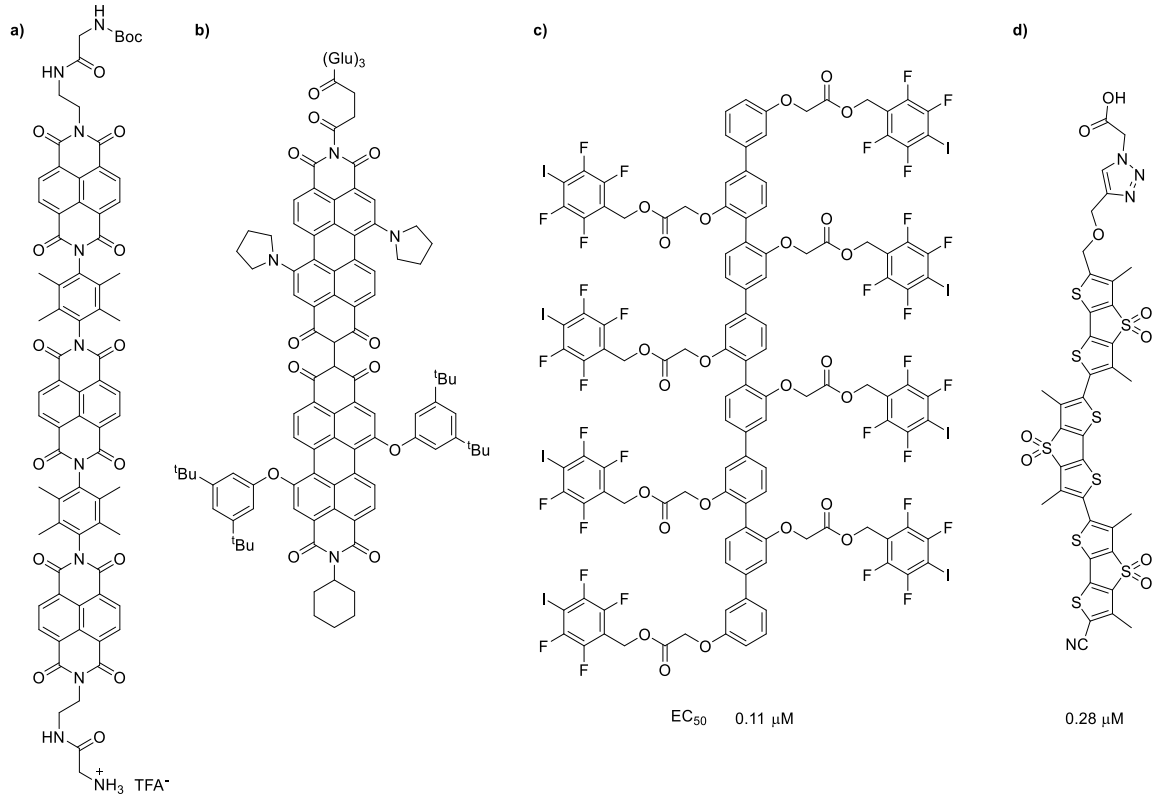

Figure 35 Transmembrane 'anion slides' from the work of S. Matile based on anion-π, XB, and ChB interactions.

1.5 Anion binding in catalysis

1.5.1 Anion abstraction catalysis

Removal of an anionic leaving group from an organic scaffold can be followed by S_N1-type reaction of the resulting cation with a nucleophile. Anion binding molecules can stabilize the intermediate ion pair, thus promoting the reaction (Scheme 1). Transformations of this type include Br^- abstraction from bromodiphenylmethane. In wet acetonitrile the resulting carbocation reacts with MeCN and H_2O molecules, providing a stable product (Scheme 1a). Various σ-hole anion receptors were reported to promote this reaction, including bis(iodoimidazolium) and bis(iodobenzimidazolium) XB donors.[193,194] Somewhat lesser reactivity was also reported for Se-based ChB analogues. In this case, the *syn* atropisomer of the conformationally restricted receptor proved to be more effective, implying that bidentate ChB is involved.

Another example is the nucleophilic substitution reaction of chloroisochroman (Scheme 1b) where the transient cation is commonly trapped with a silyl ketene acetal. Unlike in the previous case, Cl^- is sequestered by a silyl cation, thus permitting the use of catalytic amounts of activator. Stereoselective catalysis of this reaction can be effected by chiral thioureas,[195,196] which demonstrates that the reactive ion pair is bound in chiral space. This reaction was also promoted by neutral[197] and cationic[124] bidentate XB donors, the latter being effective at a very low loading (0.5 mol%).

A similar reaction involves nucleophilic addition to acylquinolinium cations (Scheme 1c). As in the previous example, a very effective thiourea catalyst has been reported.[198] The reaction could also be promoted with a modest stereoselectivity by a tetradentate triazole-based C-H HB donor.[199] In the previously mentioned study of pentafluorophenyl-substituted XB, ChB, and PnB donors this reaction was used as one of the benchmarks for comparison of test compounds.[141] A PnB receptor based on Sb was the most effective and provided 4090-fold rate enhancement over uncatalyzed reaction (−78 °C, 20 mol% cat.).

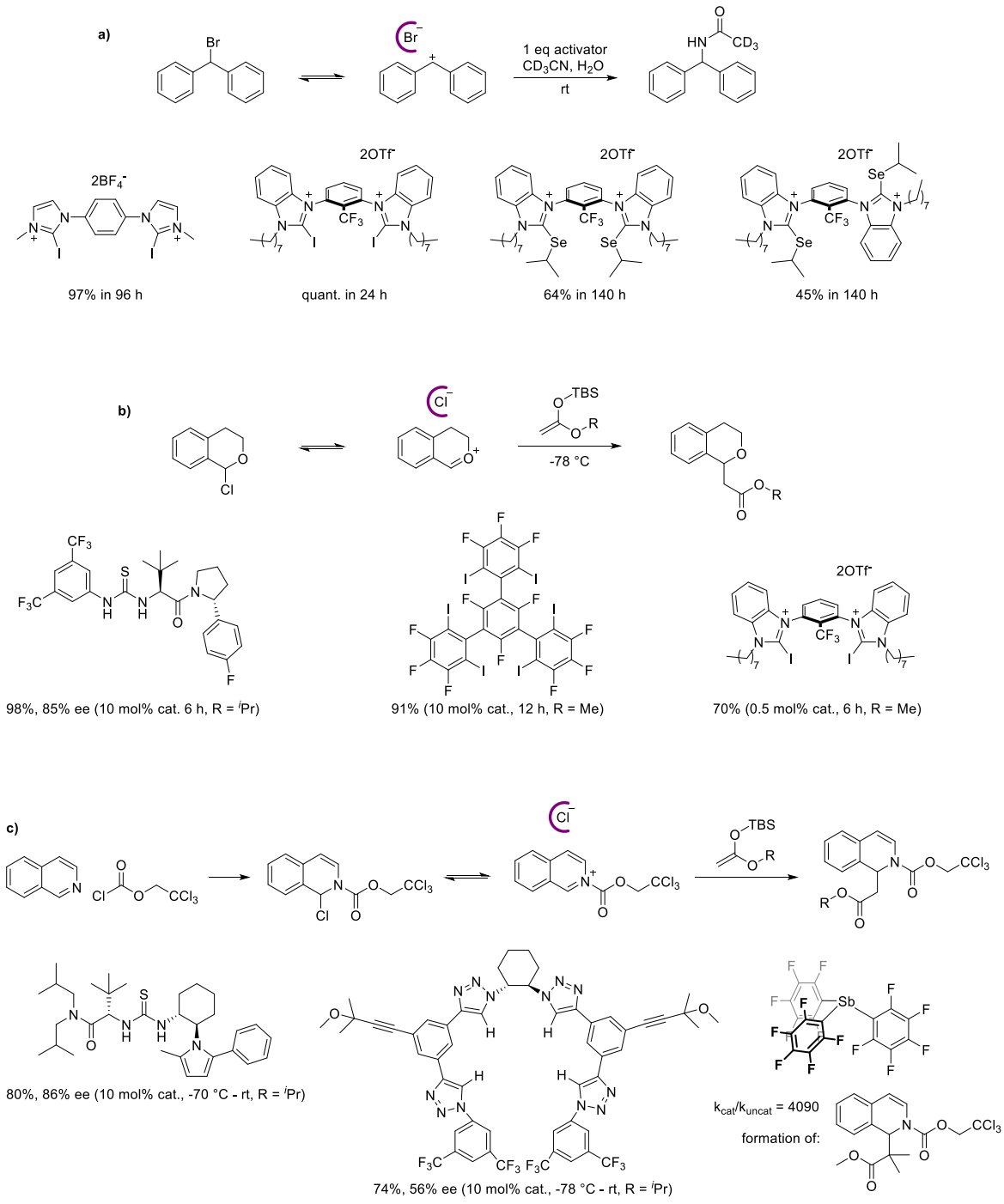

Scheme 1 Examples of reactions promoted by anion abstraction, shown together with some reported catalysts. These three reactions are commonly used to demonstrate the catalytic activity of anion receptors.

1.5.2 Activation of electrophilic substrates

A very wide range of reactions can be promoted by electrophile activation in the presence of HB donor or Lewis acidic catlalyst. These include Michael additions, Nazarov cyclizations, epoxide ring-

opening, and Diels-Alder reactions. A parallel with anion supramolecular chemistry can be drawn here, as these transformations are catalysed by binding of anionic or partially negatively charged transition states to a receptor, resulting in their stabilisation and reduction of activation energy.[200,201]

Alongside a vast number of HB, Brønsted acid and Lewis acidic metal catalysts, some σ-hole donors have been reported. A simple Diels-Alder reaction (Scheme 2a) was reported to be accelerated by bidentate XB donors based on iodoimidazolium units.[202] This σ-hole catalyst notably proved superior to Schreiner's thiourea.[203] Its catalytic activity was inhibited in the presence of TBAOTf, highlighting its anion binding properties. In a related example an aza-Diels-Alder cycloaddition (Scheme 2b) was promoted by monodentate iodoimidazolium compound.[204] An isostructural HB donor was ineffective at promoting the reaction.

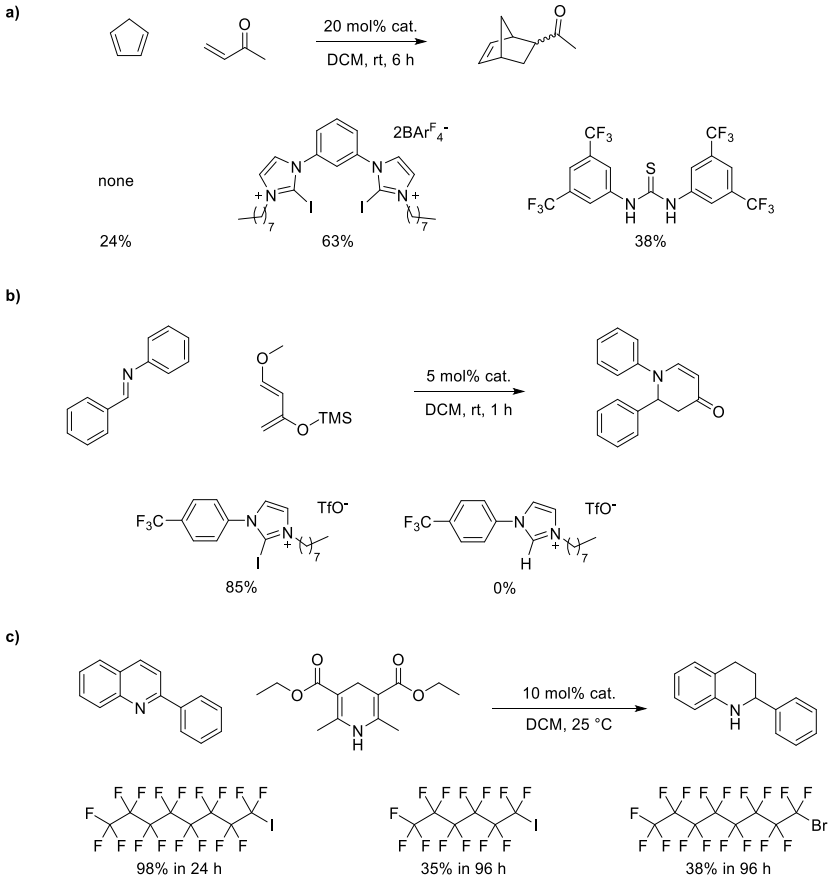

Scheme 2 Examples of reactions promoted by electrophile activation in the presence of σ-hole donors.

A biomimetic quinoline reduction with Hantzch ester (Scheme 2c) was reported to be promoted by perfluoroiodoalkanes, mirroring the ability of XB donors to bind pyridines and other nitrogen bases.[205] A Br analogue had relatively low activity, thus supporting the involvement of XB. Catalysis was also inhibited by tertiary amines known to form stable XB complexes with iodoperfluoroalkanes.[206]

1.5.3 Control of anionic reactants

Another application of anion binding is to transport anionic nucleophiles across phase boundaries to enable reactions with electrophiles. The anion receptor can also provide a chiral environment for such transformations.

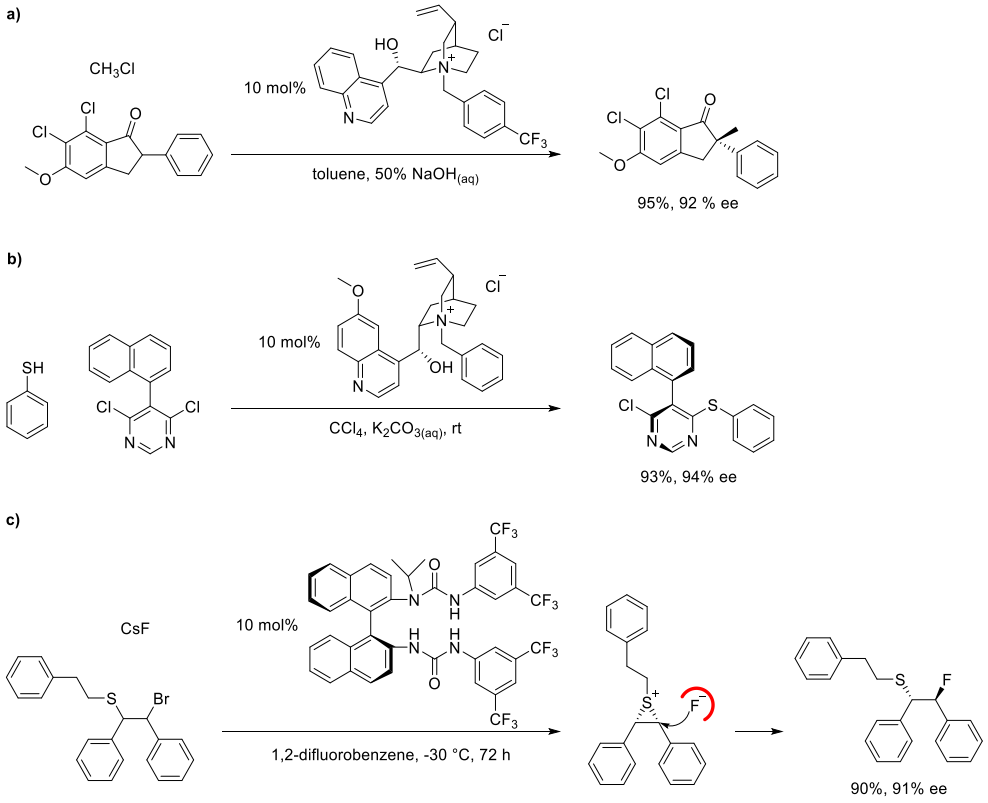

Scheme 3 Examples of enantioselective phase transfer catalysis which rely upon anion binding in a chiral environment.

Quaternary ammonium salts derived from cinchona alkaloids proved to be a particularly privileged class of chiral catalysts for such transformations.[207] A pioneering example involves alkylation of an enolate bound to the cationic catalyst (Scheme 3a).[208] The interaction relies on electrostatic

attraction, HB donated by the C–H protons surrounding the quaternary ammonium, and the stacking of aromatic rings. In a related recent study, interaction between a similar catalyst and thiophenolate anion allows the desymmetrisation of electrophilic biaryls in an S_NAr reaction (Scheme 3b).[209] Atropisomeric products were obtained with high yields and enantioselectivities.

A different catalyst class is showcased in a recent publication where a tridentate HB donor constructed on a binaphthyl scaffold was used to solubilise CsF in organic medium (Scheme 3c).[210] The bound F^- anion was delivered to a *meso* sulfonium electrophile, resulting in its enantioselective desymmetrisation.

1.6 Project outline and aims

The broadly described purpose of this work was to design new anion receptors and apply them to molecular recognition as well as organocatalysis. An especial emphasis was put on the scarcely studied σ-hole interactions: halogen and chalcogen bonding. Additionally, unusual cooperative hydrogen bond donor systems were evaluated for comparison with the isostructural σ-hole receptors and on their own as activating components of organocatalysts.

Chapter 2 presents the charge-neutral tetradentate iodotriazole XB receptor design in the simple form meant for anion binding in organic solvents. This structure is shown to be an effective anion receptor, significantly outcompeting the HB analogues. Chiral variants of XB receptors are investigated for enantioselective binding and the ability to promote stereoselective reactions.

Chapter 3 introduces an advanced σ-hole receptor design geared towards water solubility. Anion binding properties of XB and ChB variants are studied in detail, revealing their strong selectivity for I^- and ability to bind other weakly hydrated anions. These molecules are notably the first examples of charge-neutral, all-XB or all-ChB receptors to be studied in water. Additionally, applications in fluorescent and electrochemical anion sensing are demonstrated.

Chapter 4 describes a family of organocatalysts for transesterification reactions designed to work by a biomimetic mechanism analogous to that of serine esterase enzymes. This constitutes a different starting point for this work, which lies within the broader anion receptor theme due to a thiourea oxyanion hole being an important part of the catalyst design. The series of catalysts is iteratively designed towards higher reactivity. Enantioselective transformations are attempted with the final versions.

Chapter 2 Simple tetradentate XB anion receptors

2.1 Background

Anion receptor architecture based on alternating triazole and aryl (usually 1,3-phenylene) units is known and was briefly discussed in Chapter 1 in the context of C-H HB donors. These acyclic[93,94,211–213] and macrocyclic[214–216] systems (Figure 36) were assembled via CuAAC reactions and proved effective as anion receptors due to the high dipole moment of the triazole units. Fluorescent,[212,217] redox-active[218] and chiral[199] units were in some cases incorporated into these structures to effect sensing and enantioselective catalysis capabilities.

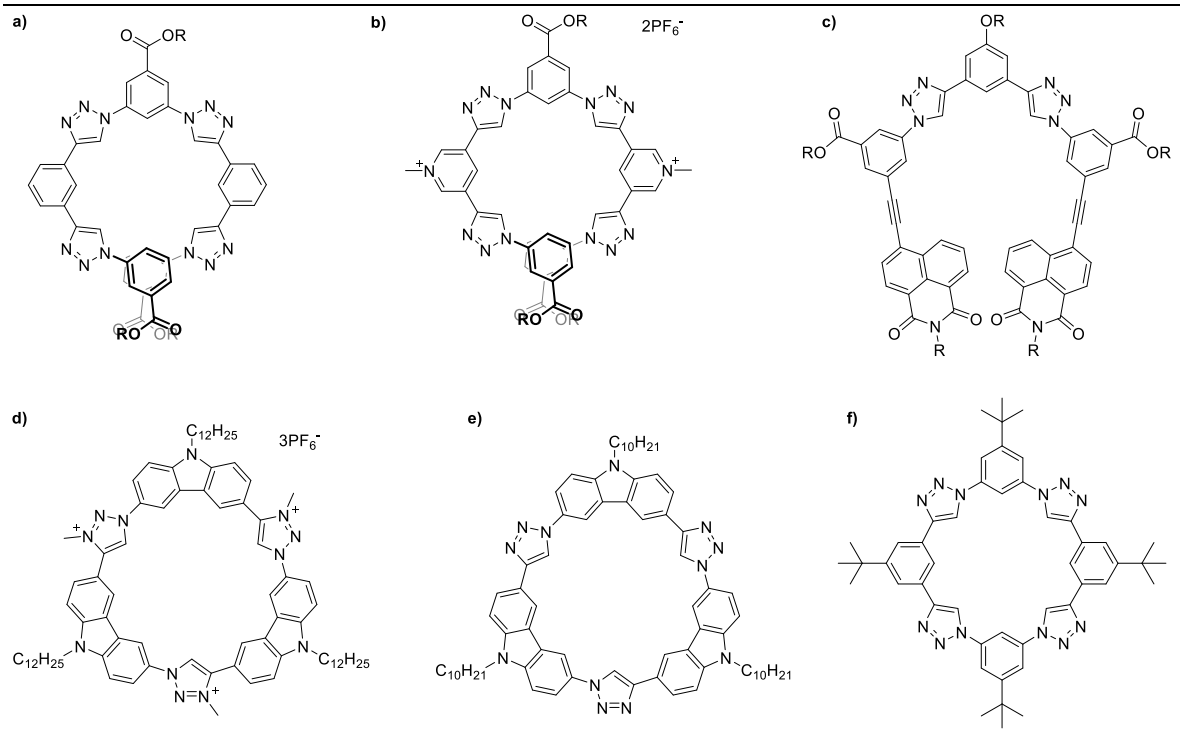

Figure 36 Examples of triazole-based anion receptors.

The objective of the work discussed in this chapter was to introduce halogen bonding into a tetradentate triazole-based framework, using the strength of this interaction to enhance anion coordination. To this end, acyclic tetradentate receptors based on the 5-iodo-1,2,3-triazole units (Figure 37) were prepared. Their anion binding properties were then probed in comparison with the respective HB analogues. The variants that were made contained the same

1,3-bis(iodotriazolyl)phenyl motifs but differed by the terminal and core groups. Compounds **2.1**, **2.2** contain triethylene glycol (TEG) chains for improved solubility. Their attachment via ether or ester linkages provides an electron-rich and an electron-deficient variant. In **2.3** and **2.4** 9-anthrylmethyl termini were introduced to provide a fluorescent response upon anion binding. System **2.4** also includes a chiral (*S*)-binaphthol core in order to investigate chiral recognition via a XB receptor, which has only previously been observed in a bidentate example.[219]

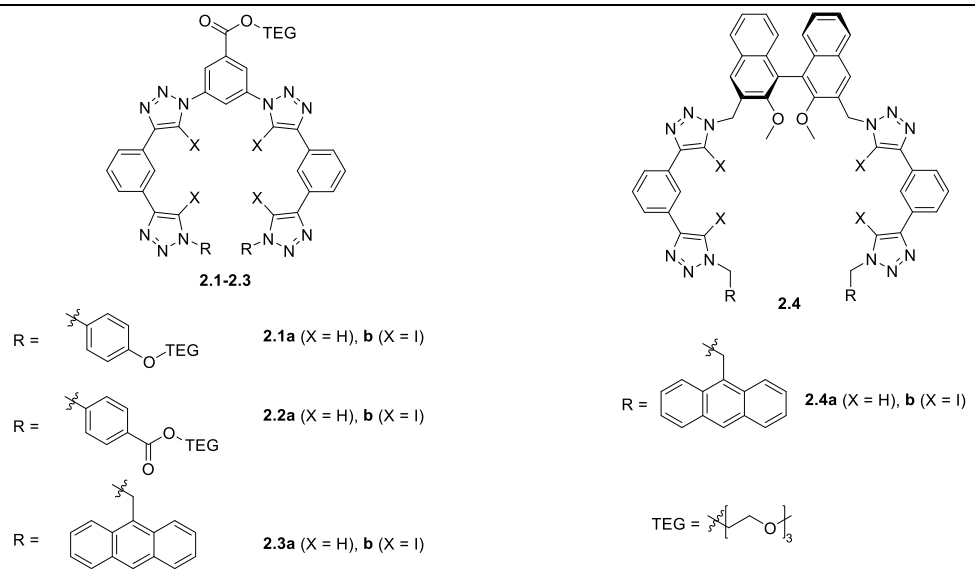

Figure 37 Halogen- and hydrogen-bond donor compounds investigated in this work.

2.2 Synthesis

Precursors to the final products **2.1**–**2.4** were prepared using generally straightforward methods (Scheme 4, Scheme 5). Aryl azides in the terminal synthons **2.8**, **2.10** and the bis-azide core **2.15** were introduced via diazotization-substitution of the respective anilines, while the benzylic azide in **2.11** was formed in a nucleophilic substitution reaction. Synthesis of the binaphthol-derived bis-azide core **2.19** was reported before[219] and here it was prepared in the same way, except for the last step where a one-pot activation and substitution of the benzylic alcohol was done using diphenyl phosphoryl azide (DPPA). The final fragment, 1,3-bis(iodoethynyl)benzene **2.12b** was synthesised by iodination of the respective lithium alkynide, or alternatively by CuI-catalysed iodination with *N*-iodomorpholine hydriodide (which was prepared from morpholine and I_2).

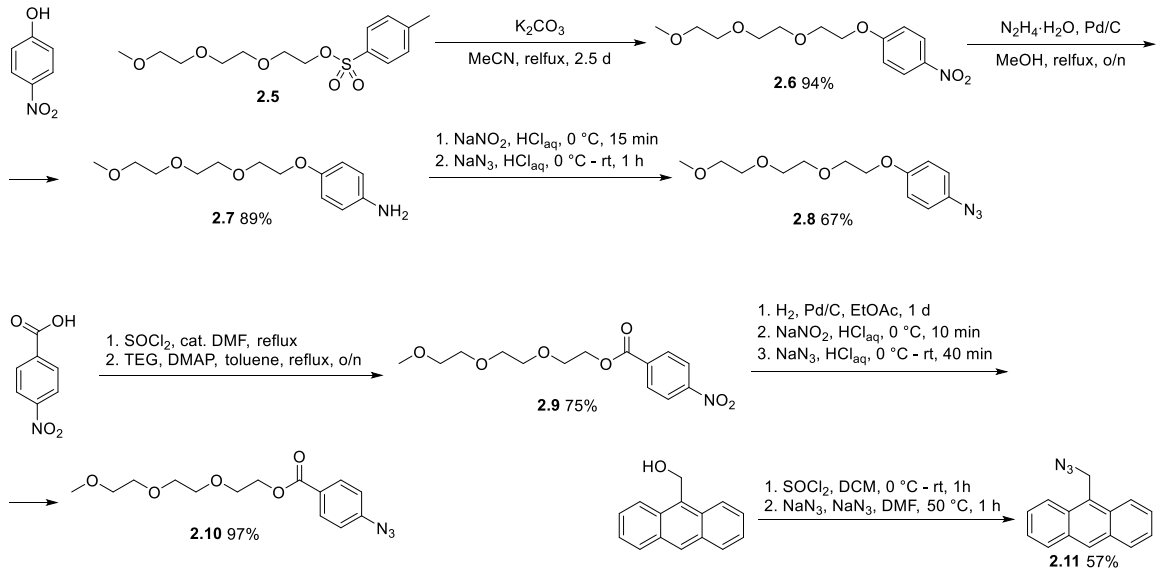

Scheme 4 Synthesis of the azide terminal receptor fragments 2.8, 2.10, 2.11.

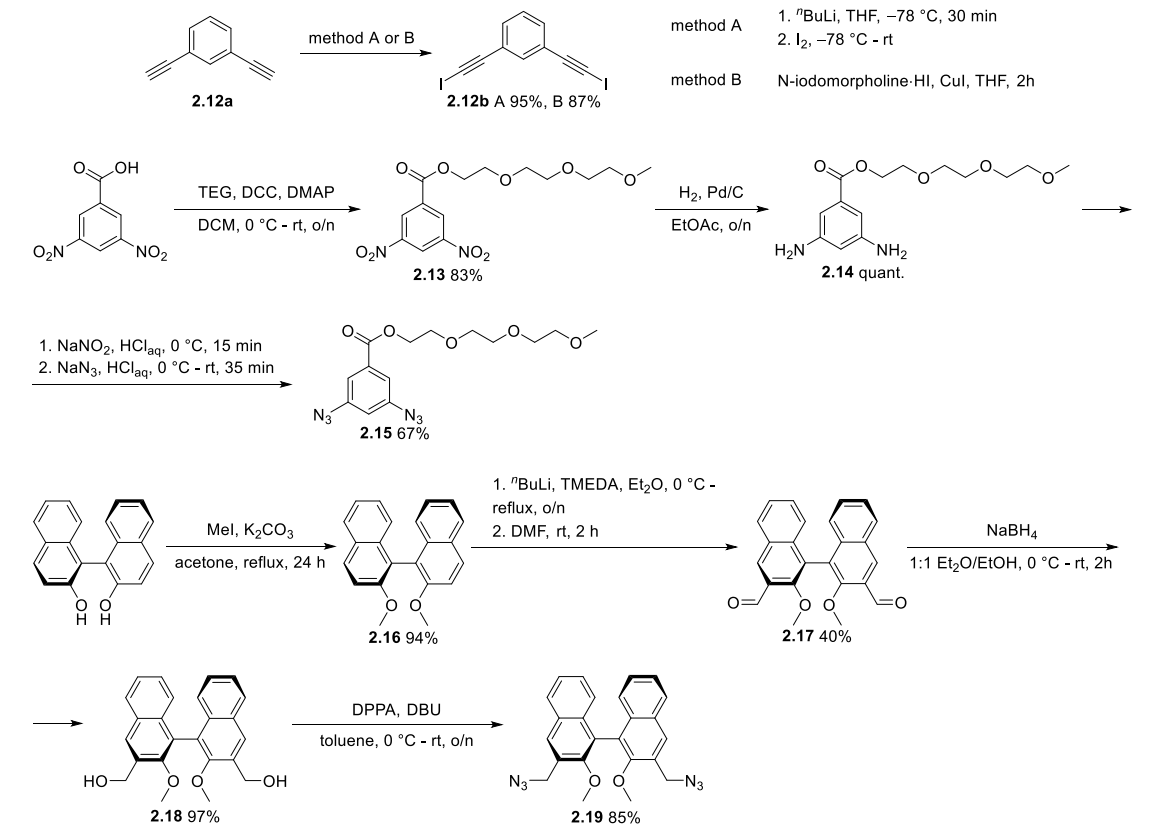

Scheme 5 Synthesis of 1,3-bis(iodoethynyl)benzene 2.12b and the the bis-azide core fragments 2.15, 2.19.

XB and HB anion receptors **2.1**–**2.4** were then assembled via Cu(I)-catalysed azide-(iodo)alkyne cycloaddition (CuAAC) reactions (Scheme 6). These were catalysed by $Cu(MeCN)_4PF_6$ in the

presence of tris(benzyltriazolylmethyl) amine (TBTA) ligand. For the preparation of **2.1a** and **2.2a** an alternative benzyltriazolylmethylamine (BTA) ligand[220] was used as these compounds co-eluted with TBTA during chromatographic purification. BTA retains the Cu(I)-activating ability of TBTA, although it lacks the function of protecting Cu(I) from oxidation by atmospheric oxygen. As it is a primary amine, it is strongly retained on a silica column and is easily separated from the reaction products.

As shown in Scheme 6, the terminal azide synthons **2.8**, **2.10**, **2.11** were reacted statistically with a slight excess (typically 1.2 eq) of bis-alkyne **2.12a** or **2.12b** to afford the arm fragments **2.20**–**2.22**. Two equivalents of **2.20**–**2.22** were then coupled under CuAAC conditions with a bis-azide core synthon **2.15** or **2.19** to give the anion receptors **2.1**–**2.4**. The cycloadditions proceeded in moderate to high yields of 46-79% for the synthesis of receptor arm fragments and 53-88% for the final CuAAC step.

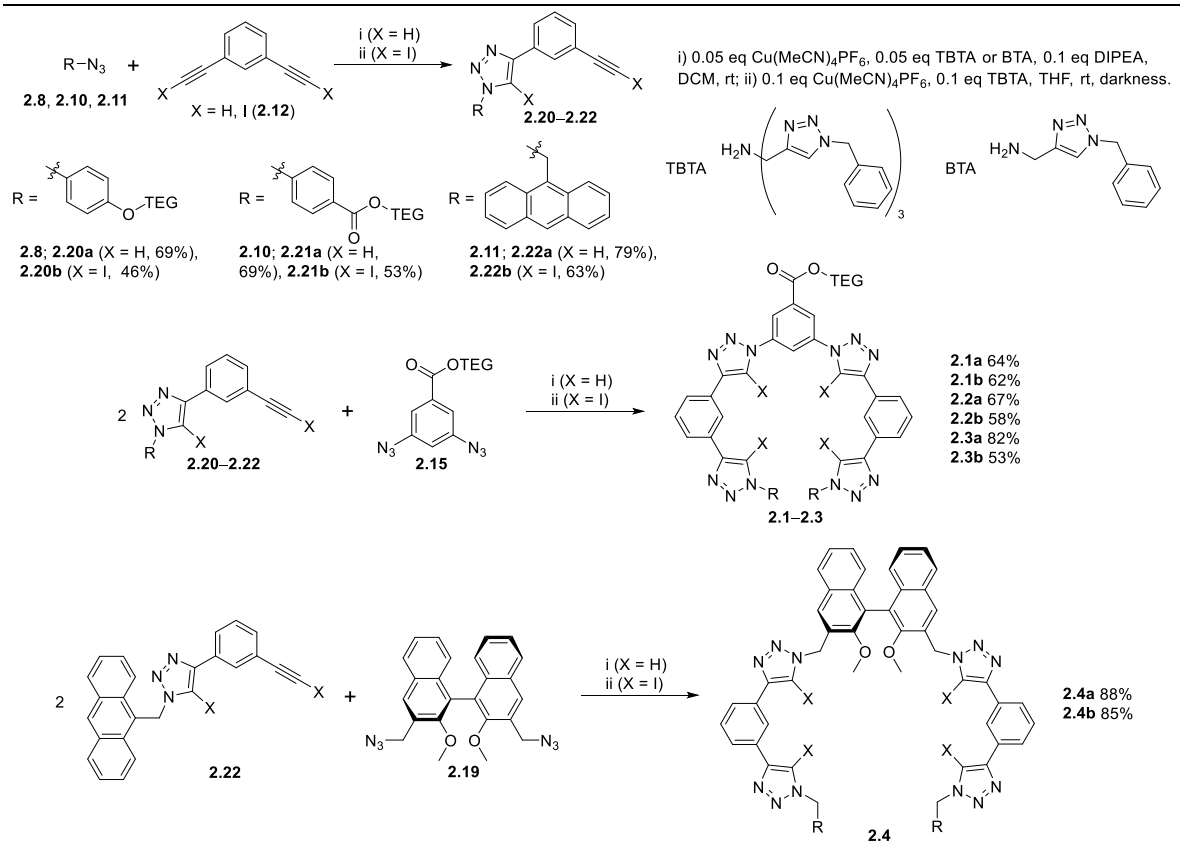

Scheme 6 CuAAC steps in the synthesis of the anion receptors 2.1–2.4.

2.3 Anion binding studies

2.3.1 ^{1}H NMR titrations

One of the standard techniques of quantifying host-guest affinities in solution relies on the observation of changes in NMR chemical shifts (Δδ) of one of the binding partners upon addition of the other. The binding isotherms can be fitted to a plot of Δδ versus the amount of titrant added, providing information about binding affinity (K_a in the case of 1:1 binding stoichiometry). This method is particularly useful for anion receptors based on HB, as protons that engage in HB interactions with anions typically exhibit large downfield Δδ.

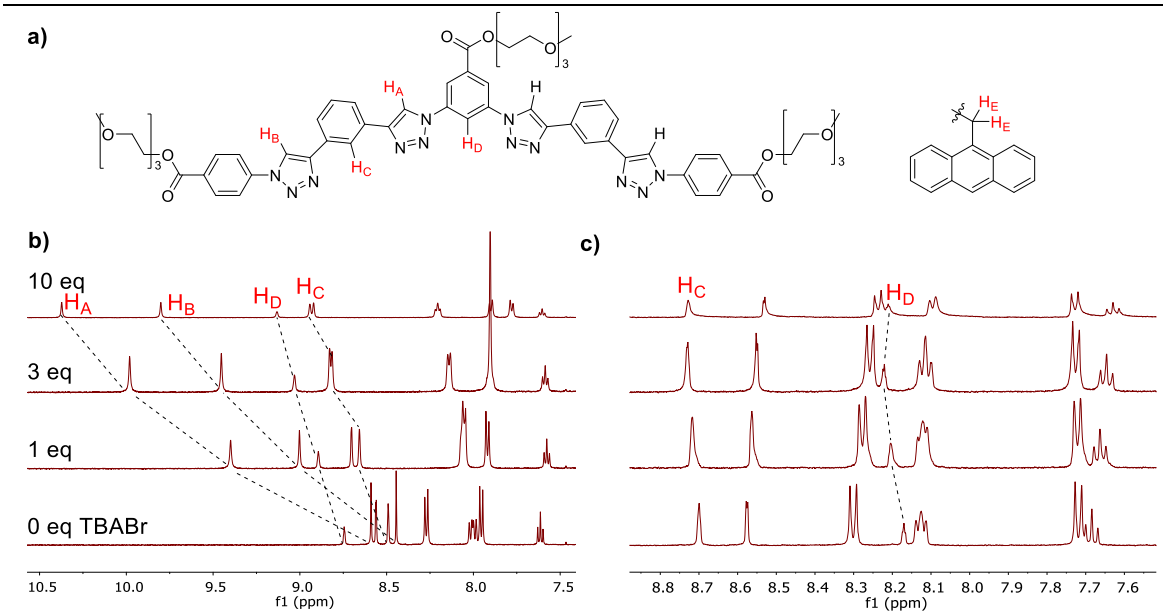

Figure 38 a) Labeling of protons monitored in ^{1}H NMR anion binding studies (consistent across 2.1–2.4). b) Partial ^{1}H NMR spectra of 2.2a titrated with TBABr (500 MHz, $CDCl_3$, 298 K). c) Partial ^{1}H NMR spectra of 2.2b titrated with TBABr.

Indeed, when the HB receptors **2.1a**–**2.4a** were titrated with $^nBu_4N^+$ (TBA) salts of various anions in $CDCl_3$ solution, large downfield movements of ^{1}H NMR signals (Δδ) of up to 2 ppm were observed for the triazole protons H_A and H_B. Smaller Δδ of 0.4-0.5 ppm were also seen for the 1,3-phenylene protons H_C and H_D (Figure 38b). This is consistent with the known binding mode of tetradentate triazole HB receptors wherein the triazole protons and the phenylene *ortho* protons all contribute to guest complexation.[93] In the case of the XB receptors **2.1b**–**2.4b** only small downfield

perturbations Δδ of 0.03-0.2 ppm were observed for the 1,3-phenylene protons H_C and H_D (Figure 38c). This can be attributed to the large size of the receptors' iodine atoms binding the guest anion at a significant distance from these protons. Due to very small Δδ values, reliable association constants could not be obtained for **2.1b**–**2.3b** using the standard ^{1}H NMR titration protocol. Therefore, **2.1b**–**2.3b** were instead analysed using a host-host competition binding method which is described in detail in section 2.3.2. The only exception was **2.4b** which displayed sufficient Δδ up to 0.17 ppm and was analysed using standard ^{1}H NMR titrations monitored at H_C or H_E.

In a typical ^{1}H NMR (500 MHz, 298 K) titration experiment, the NMR tube was loaded with 0.5 ml of 0.0015 M solution of the receptor in the solvent of choice ($CDCl_3$ for **2.1**–**2.3** and 1:1 $CDCl_3$/acetone-d_6 for **2.4**). The sample was titrated with 0.075 M solution of the appropriate anion introduced as TBA salt. The titration curves (Figure 39 – Figure 43) were built from 17 data points corresponding to 0, 0.2, 0.4, 0.6, 0.8, 1.0, 1.2, 1.4, 1.6, 2.0, 2.5, 3.0, 4.0, 5.0, 7.0, 10.0 equivalents of titrant added. Unless stated otherwise, the inner triazole proton signal (H_A) was monitored for HB receptors **2.1a**–**2.4a**. For the XB receptor **2.4b** the titration curves were derived from H_C.

The complexation of anions with all receptors was found to be fast on the NMR timescale. Binding isotherms for host-guest association in 1:1 stoichiometry were calculated by non-linear least-squares analysis to obtain the best fit between measured and calculated chemical shifts using WinEQNMR2 software.[221] Data for NMR titration experiments with **2.1a**–**2.4a** and **2.4b** is shown in Figure 39 – Figure 43.

Good fits were generally obtained using the 1:1 stoichiometric binding model. Diffusion-ordered NMR experiments done with **2.3b** revealed a slight decrease of the receptor diffusion coefficient in the presence of I^- (1.5 mM **2.3b**, 1.5 mM TBAI, $CDCl_3$). The measured values were $D = 4.53 \times 10^{-10}$ m^2/s for the free **2.3b** and $D = 4.30 \times 10^{-10}$ m^2/s after addition of TBAI. This decrease is consistent with the binding of I^- or TBA^+ I^- ion pair, but is too small to indicate the presence of more than one receptor molecule in the complex.

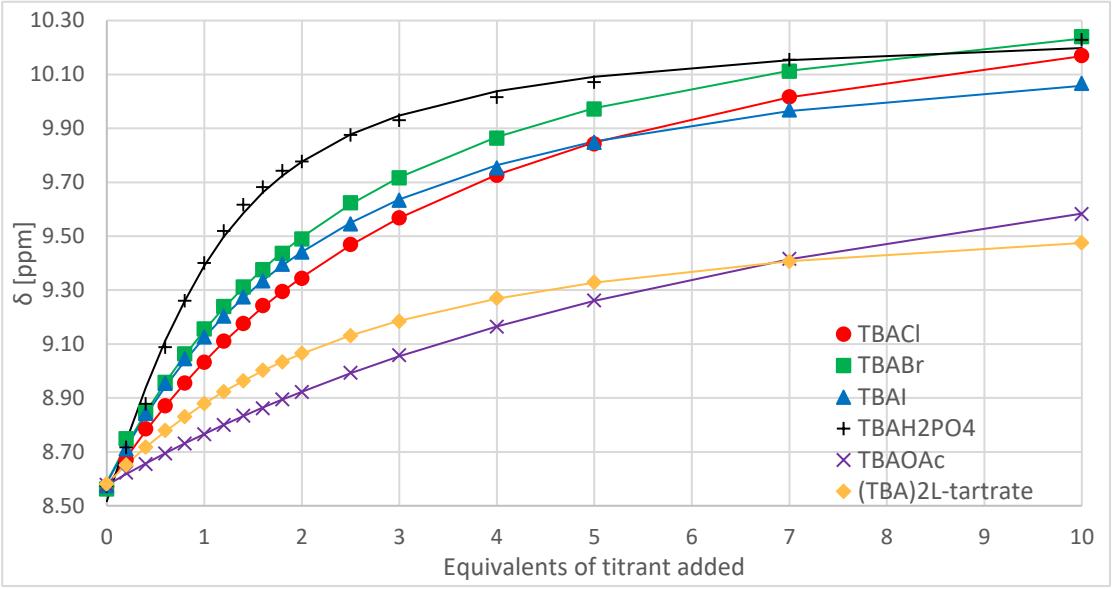

Figure 39 ^{1}H NMR titrations of 2.1a (monitored at H_A). Points: experimental data; lines: fitted binding isotherms.

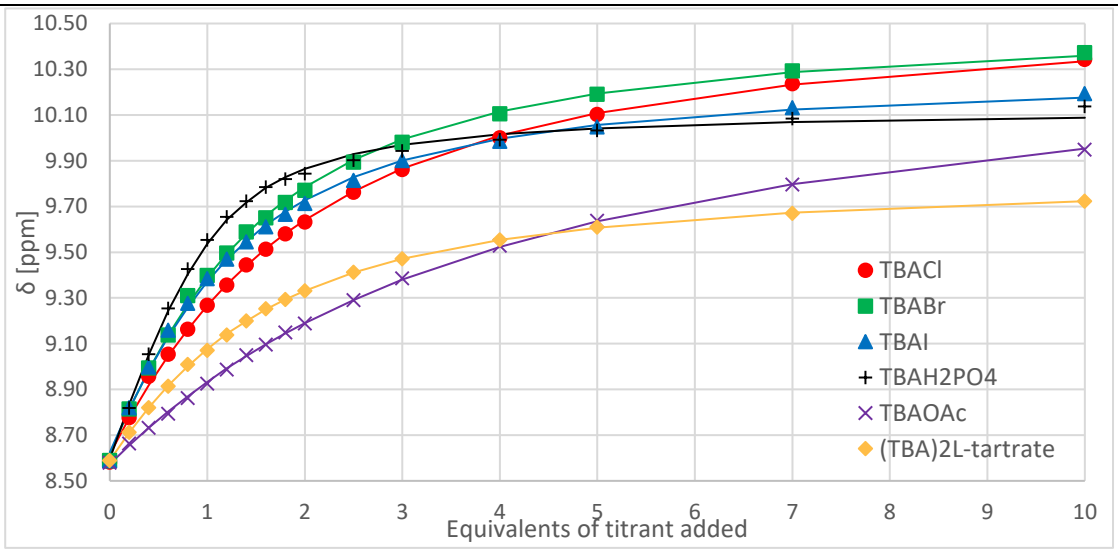

Figure 40 ^{1}H NMR titrations of 2.2a (monitored at H_A). Points: experimental data; lines: fitted binding isotherms.

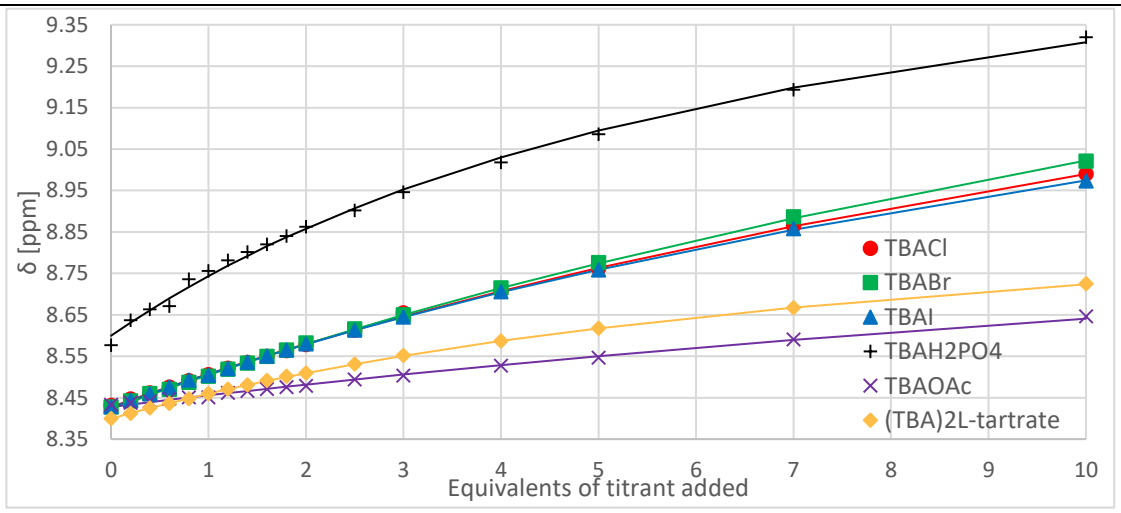

Figure 41 ^{1}H NMR titrations of 2.3a (monitored at H_A, for $TBAH_2PO_4$ monitored at H_E). Points: experimental data; lines: fitted binding isotherms.

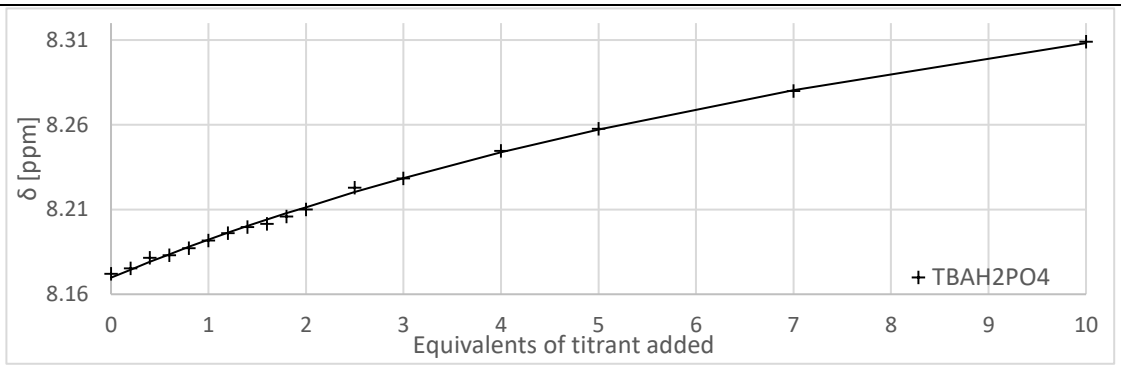

Figure 42 ^{1}H NMR titration of 2.4a with $TBAH_2PO_4$ (monitored at H_A). Points: experimental data; lines: fitted binding isotherms.

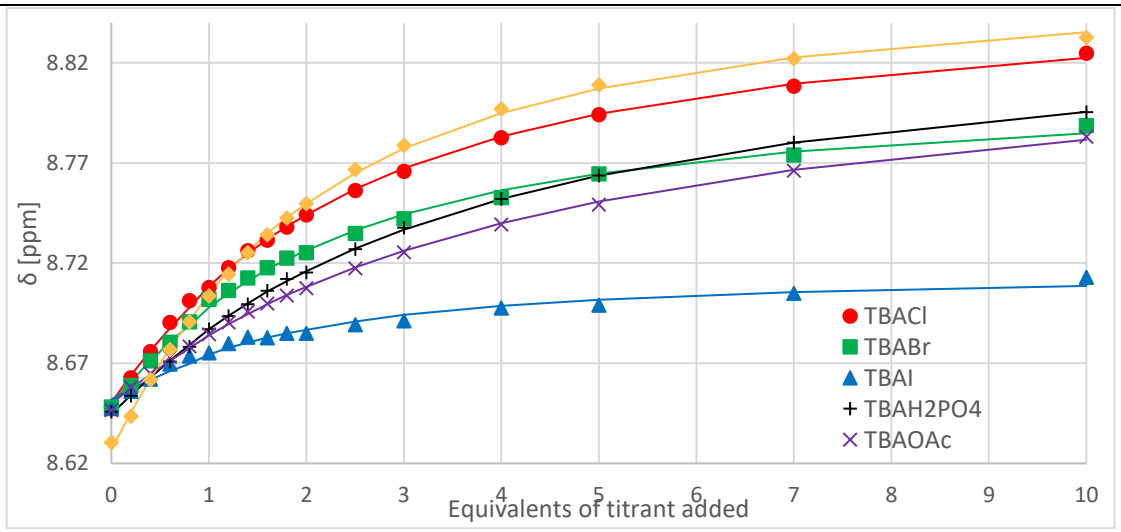

Figure 43 ^{1}H NMR titrations of 2.4b (monitored at H_C). Points: experimental data; lines: fitted binding isotherms.

2.3.2 ^{1}H NMR host-host competition experiments

As the XB receptors **2.1b**–**2.3b** contained no protons that could provide good quality titration curves, an alternative NMR-based approach was devised. Adding a small amount of the HB receptor **2.2a** to the solution of an XB receptor allowed the large Δδ of its H_A protons (Figure 44) to be monitored and information to be extracted about the anion affinity of the XB test compound. HB receptor **2.2a** effectively acts as a ^{1}H NMR-responsive anion sensor that quantifies the free anion concentration in the presence of the analysed XB receptor. No examples of this method used to quantify anion binding were found in the literature. However, a similar approach was used to analyse alkali metal complexation with crown ethers by mass spectrometry.[222]

General protocol

In a typical experiment, 0.5 ml of 0.0015 M solution of the XB receptor **2.1b**–**2.3b** was loaded into an NMR tube and combined with 0.025 ml of 0.0015 M solution of the HB reference receptor **2.2a** (5 mol% loading of **2.2a** relatively to the test compound). The resulting mixture was titrated with 0.015 M solution of anion introduced as tetrabutylammonium salt. A spectrum was recorded before titrant addition, followed by at least three data points, typically with 1, 1.5, 2 equivalents of titrant. Finally, 0.1 ml of 0.15 M titrant solution was added to a total of 22 equivalents and another spectrum recorded. The signal of the inner triazole (H_A) protons in the reference compound was monitored to extract binding constant information.

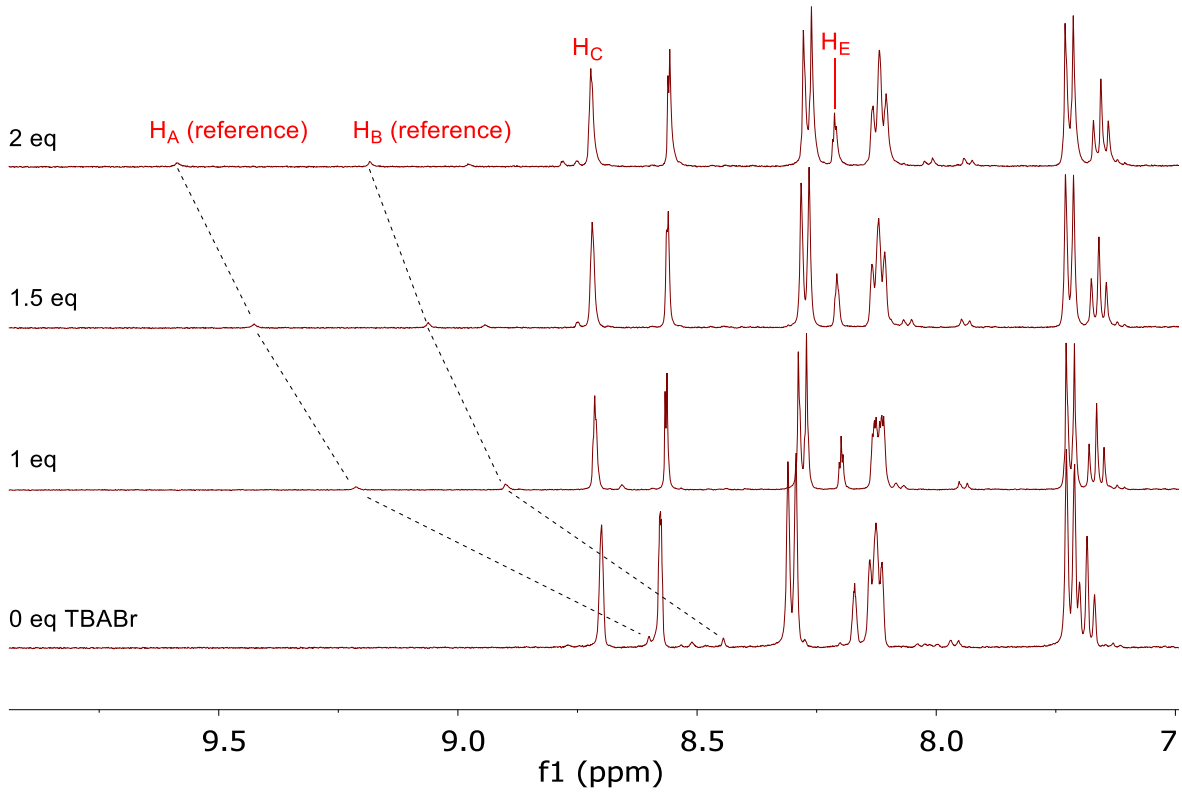

Figure 44 Partial ^{1}H NMR spectra of a host-host competition experiment where 2.2b combined with 5 mol% of 2.2a as reference is titrated with TBABr (500 MHz, $CDCl_3$, 298 K). Monitoring Δδ of the inner triazole (H_A) signals of the reference HB receptor allows to determine K_a for the XB receptor.

Data analysis

Nomenclature:

δ	observed chemical shift of the reference compound
δ_R	chemical shift of the free reference compound
δ_{RX}	chemical shift of the reference compound bound to the anion
C_R	analytical concentration of the reference compound
C_A	analytical concentration of the test compound
C_X	analytical concentration of the titrant (anion)
[R]	concentration of the free reference compound
[RX]	concentration of the reference compound bound to the anion
[A]	concentration of the free test compound
[AX]	concentration of the test compound bound to the anion
K_R	anion binding constant of the reference compound
K_A	anion binding constant of the test compound

Under fast exchange conditions the observed chemical shift of the reference compound is a weighted average of the chemical shifts of free and bound reference (1). Using this and the expression for analytical concentration of reference (2) we can derive the concentrations of free (3) and bound (4) reference.

$$\delta = \frac{\delta_R[R] + \delta_{RX}[RX]}{C_R} \qquad (1)$$

$$C_R = [R] + [RX] \qquad (2)$$

$$[R] = C_R \frac{\delta - \delta_{RX}}{\delta_R - \delta_{RX}} \qquad (3)$$

$$[RX] = C_R - [R] \qquad (4)$$

Rearranging the reference binding constant equation (5) the free anion concentration can be derived (6).

$$K_R = \frac{[RX]}{[R][X]} \qquad (5)$$

$$[X] = \frac{[RX]}{K_R[R]} \qquad (6)$$

Knowing the analytical concentrations of the anion and the test compound it is possible to obtain the concentrations of bound (7) and free (8) test compound. This gives all the components of the test compound binding constant equation (9).

$$[AX] = C_X - [\mathrm{X}] - [\mathrm{RX}] \qquad (7)$$

$$[A] = C_A - [AX] \qquad (8)$$

$$K_A = \frac{[AX]}{[A][X]} \qquad (9)$$

2.3 Anion binding studies

While δ_R can be obtained directly from a spectrum taken before addition of titrant, δ_{RX} can be calculated based on an overtitrated spectrum taken with 22 eq of the anion. As most analyte and reference is bound under these conditions, we can assume that $[X] \approx C_X - C_A - C_R$. It is then possible to derive the concentrations of bound (10) and free (11) reference from (2) and (5).

$$[RX] = \frac{K_R[X]C_R}{1 + K_R[X]} \qquad (10)$$

$$[R] = C_R - [RX] \qquad (11)$$

Knowing these, we can now rearrange (1) to subtract the contribution of the small amount of free reference from the observed chemical shift and obtain δ_{RX} (12).

$$\delta_{RX} = \frac{\delta C_R - [R]\delta_R}{[RX]} \qquad (12)$$

In practice it is necessary to simultaneously determine K_R and K_A from the competition experiment rather than use separately obtained K_R to calculate K_A. This is because binding affinity of the reference compound can be affected by the test compound and thus it is necessary to know *system-specific* K_R to determine K_A. In order to do this, we can find a relationship (13) between K_R and K_A from (6) – (9).

$$K_A = \frac{C_X - [RX] - \frac{[RX]}{K_R[R]}}{\left(C_A - C_X + [RX] + \frac{[RX]}{K_R[R]}\right)\frac{[RX]}{K_R[R]}} \qquad (13)$$

Three data points taken with different amounts of titrant provide three versions of equation (13) with different sets of concentration parameters. These equations can be arranged into three pairs of equations, where solution of each pair will provide K_A and K_R. The most convenient way of solving this system is to plot $K_A(K_R)$ for each data point as shown in Figure 45. Each intersection of two plots is a graphic solution of one of the aforementioned pairs of equations. The point of closest approach of all three plots (determined as the point of lowest standard deviation between data points) is

then found which signifies that for the respective K_R all data points are in the best agreement. The x-value of this point is then taken as the system-specific K_R.

It is necessary to note that K_R obtained from the $K_A(K_R)$ plot feeds into the calculation of δ_{RX}, and the new value of δ_{RX} feeds back into the determination of K_R. In practice this loop leads to stable values of δ_{RX} and K_R after a small number of iterations. Prior to doing the simultaneous determination of K_R and K_A an initial value of δ_{RX} can be calculated using a reasonable estimate of K_R (for example, a value from a separate NMR titration of the reference compound).

Finally, a mean value of K_A is calculated from the three data points using K_R and δ_{RX} determined as above. Data points can be omitted from inclusion into the mean if they have a high uncertainty.

Details of uncertainty analysis and the plots of $K_A(K_R)$ used to determine anion affinities for **2.1b**–**2.3b** are provided in Appendix A.

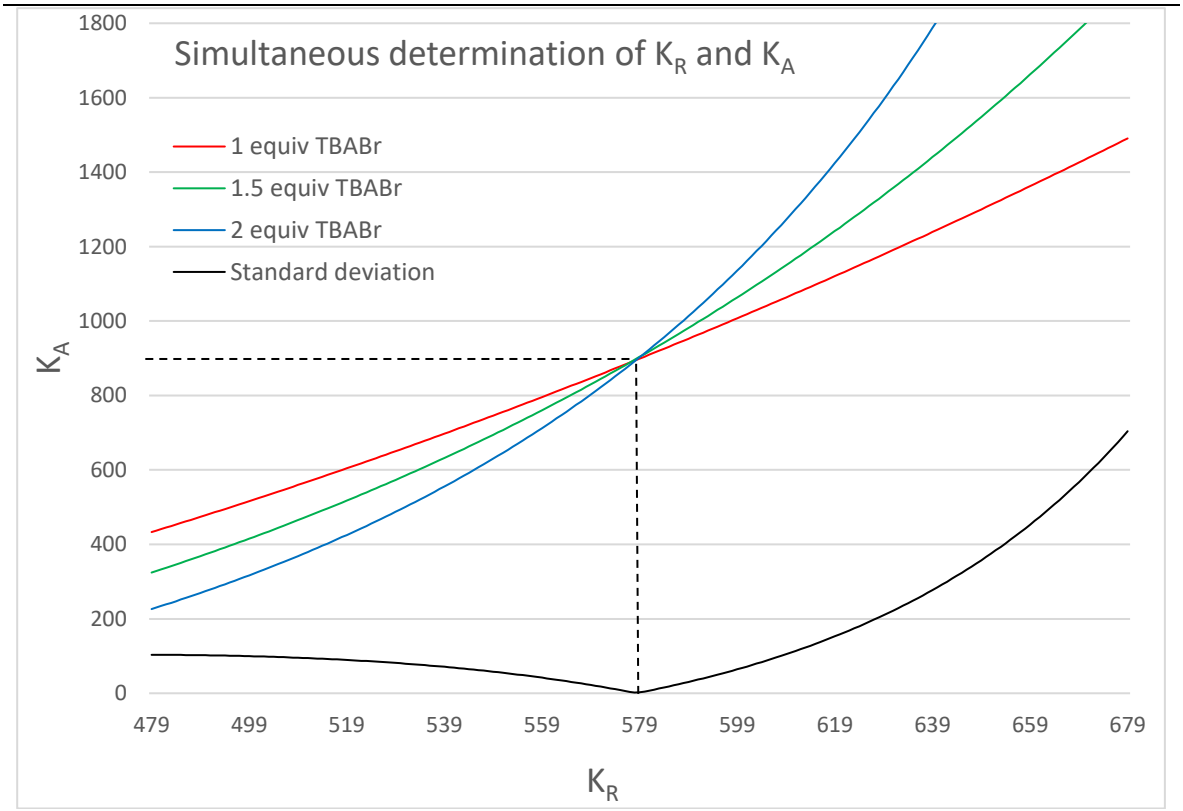

Figure 45 $K_A(K_R)$ plot for a host-host competition experiment with 2.2b as test compound and 2.2a as reference, titrated with TBABr. Lowest standard deviation of data points is for K_R = 579 M^{-1}. At this K_R, the K_A values for the three data points are: 899 M^{-1} (1 eq), 904 M^{-1} (1.5 eq), 903 M^{-1} (2 eq) which gives an average K_A = 902 M^{-1}.

2.3.3 Results of anion affinity analysis

Anion association constants for **2.1**–**2.4** determined by the two methods described above are shown in Table 1. The XB receptors **2.1b**–**2.4b** were found to be overall stronger halide and oxoanion receptors than their HB analogues. The only exception was $H_2PO_4^-$ which was strongly bound by the HB receptors **2.1a** and **2.2a**. The difference between HB and XB systems is especially prominent in systems **2.3** and **2.4**, where the HB variants **2.3a** and **2.4a** exhibit very weak binding over the entire range of anions.

Table 1 Association constants K_a [M^{-1}] for 2.1-2.4 with halides and oxoanions.[a]

	Cl^-	Br^-	I^-	$H_2PO_4^-$	AcO^-	*L*-tartrate
2.1a	232 (3)	356 (10)	427 (9)	1244 (83)	69 (1)	331 (3)
2.1b	433 (44)	600 (46)	1202 (87)	---[b]	320 (57)	281 (27)
2.2a	466 (18)	740 (29)	960 (46)	2751 (92)	174 (4)	672 (9)
2.2b	592 (59)	902 (76)	2131 (142)	---[b]	504 (88)	549 (41)
2.3a	20 (2)	15 (1)	24 (1)	87 (11)[c]	nb	64 (1)
2.3b	742 (65)	1235 (79)	2712 (187)	493 (80)[d]	753 (116)	585 (43)
2.4a	nb	nb	nb	37 (3)	nb	nb
2.4b	335 (14)	384 (28)	511 (94)	207 (4)	165 (9)	445 (16)

[a]1:1 binding stoichiometry. All anions introduced as TBA salts; **2.1**–**2.3** studied in $CDCl_3$; **2.4** in 1:1 $CDCl_3$/acetone-d_6 (500 MHz, 298 K); [receptor] = 1.5 mM. Unless stated otherwise, K_a for **2.1a**–**2.4a** were derived from H_A; for **2.4b** from H_C; for **2.1b**–**2.3b** from H_A of the reference compound **2.2a** using the host-host competition method. Uncertainties are given in parentheses. [b]Could not be determined as HB foldamers are too strong $H_2PO_4^-$ binders to be used as reference compounds. [c]Derived from H_D. [d]Derived from H_C using the standard ^{1}H NMR titration method. nb – no binding (too weak to quantify).

This significant superiority of the XB variants of systems **2.3** and **2.4** is because the XB receptors rely exclusively on the iodotriazole XB donors for anion recognition (Figure 46). HB analogues, on the other hand, benefit in part from the secondary HB donors at the phenylene rings next to the triazoles. Deletion of these binding elements as in **2.3a** and **2.4a** leads to fewer convergent HB interactions and consequently a large decrease of anion affinity. The XB receptors, on the other hand, are tolerant to these modifications. Thus, the anthryl-terminated **2.3b** displayed affinity for

Br^- and I^- that was two orders of magnitude stronger than of **2.3a**. Likewise, XB receptor **2.4b** exhibited K_a values of up to 500 M^{-1} in 1:1 $CDCl_3$/acetone-d_6, while **2.4a** displayed almost no binding (too weak to be quantified). Compounds **2.3a** and **2.4a** retained the $H_2PO_4^-$ selectivity of **2.1a** and **2.2a**, but the binding affinities were only 87 M^{-1} for **2.3a** and 37 M^{-1} for **2.4a**, an order of magnitude lower than for the XB analogues.

Comparing the XB receptors, the anion binding strength was in the order **2.3b** > **2.2b** > **2.1b** > **2.4b**. This indicates that the wider spacing of the bis-iodotriazole arms in **2.4b** leads to less effective alignment of its XB donors with halides and carboxylates. As expected, **2.2b** exhibited 1.5-2 times higher K_a values than **2.1b** due to its more electron-withdrawing termini; a similar difference was also observed in the HB analogues **2.1a** and **2.2a**.

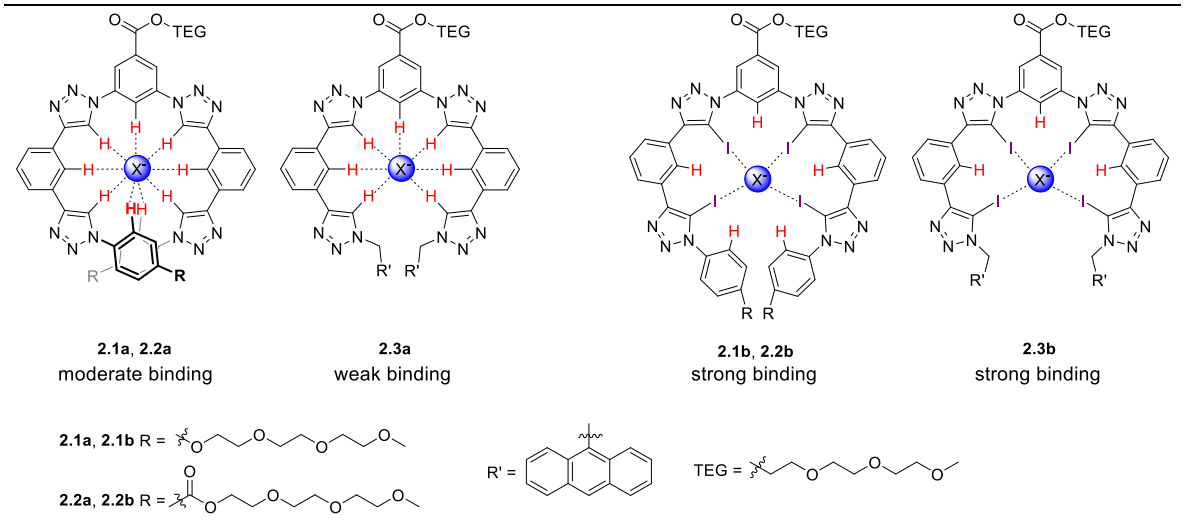

Figure 46 Proposed binding modes of HB and XB receptors 2.1–2.3.

The XB receptors displayed the order of selectivity $I^- > Br^- > Cl^- \approx AcO^- \approx H_2PO_4^-$, which suggests a better host-guest size complementarity with larger halides. Additionally, because the XB donors **2.1b**–**2.4b** are charge-neutral they do not have a charge assistance contribution that might favour binding of small, hard anions in cationic receptors. Interestingly, tartrate^{2-} > AcO^- selectivity was observed in HB receptors **2.1a**–**2.3a** and XB receptor **2.4b** but not in **2.1b**–**2.3b**. This implies that in **2.1b**–**2.3b** the anion binding site is too small to simultaneously engage both anionic groups of

tartrate due to the size of the four convergent iodine atoms. Increased spacing between the bis(iodotriazole) arms in **2.4b** allows both carboxylate groups of tartrate to be bound and induces dicarboxylate selectivity.

2.3.4 Solid state structure of **3b·NaI**

Single crystals of **3b·NaI** suitable for X-ray structural analysis* were obtained by combining **2.3b** and excess NaI in 6:4 $CHCl_3$/acetone. Vapour diffusion of acetone into the resulting supersaturated solution of **2.3b·NaI** initiated crystal growth, providing yellow needle-like crystals. The structure (Figure 47) shows the XB host encapsulating I^- via four linear halogen bonds. The guest anion is bound with C–I···I^- XB contact distances of 3.484(1) – 3.574(2) Å (88 – 90% of Σr_{vdW})[223] and C–I···I^- angles of 165.7(3) – 178.3(3)°. Due to the large size of the four iodine XB donor atoms the wrapping of the foldamer around the guest anion is less tight than in the analogous HB systems.[93,94] The iodotriazoles are tilted by 29-54° relative to the neighbouring phenylene rings and the I^- guest is situated 3.01 Å above the mean plane of the receptor backbone. The Na^+ countercation is complexed by the triethylene glycol chain, with an acetone solvate molecule and a triazole N^3 atom from an adjacent molecule competing its coordination sphere.

The sold-state structure confirms that the XB receptor scaffold of **2.1b**–**2.3b** is able to bind guest anions in a cooperative, tetradentate binding mode. Additionally, the lack of close contacts between the phenylene H atoms and the bound I^- supports the conclusions about differences in binding mode between the HB and XB variants.

* X-ray diffraction data was collected and processed with contributions from Asha Brown, Jason Y. C. Lim, Amber L. Thompson, and Kirsten E. Christensen. See Appendix B for details.

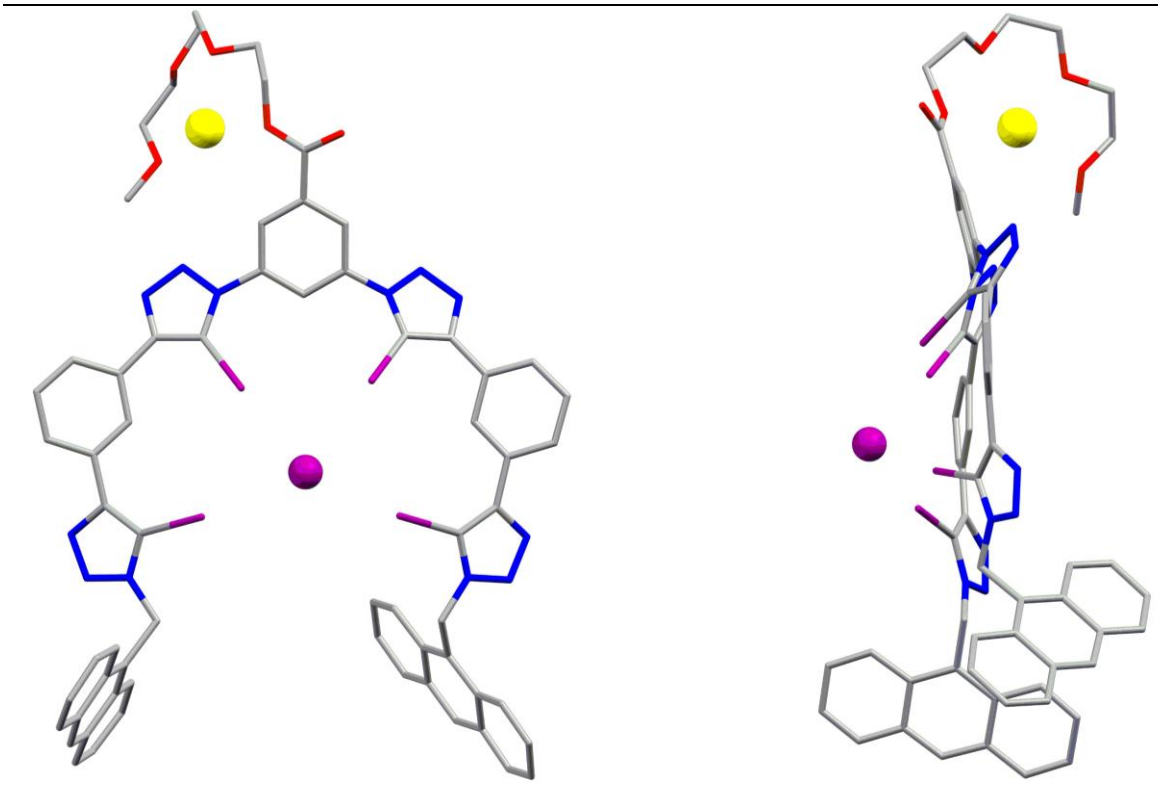

Figure 47 X-ray crystal structure of 2.3b·NaI showing the face-on (left) and side-on (right) view, visualising the folding of the receptor in a capped configuration (gray = C, blue = N, red = O, yellow = Na, purple = I).

2.4 Fluorescent sensing

The XB receptors **2.3b** and **2.4b** displayed an intense fluorescence in 375 – 525 nm region arising from the emission of anthracene termini. In **2.3b** a large increase in emission intensity, without changes in wavelength, occurred upon addition of TBABr (Figure 48). A small increase was also observed for **2.4b** (Figure 49); the most significant change occurred in the emission peak at 420 nm for both receptors. The overall increase in fluorescence intensity upon anion binding is most probably due to conformational rigidification of the receptor which suppresses non-radiative decay pathways. Thus, the larger fluorescence enhancement in **2.3b** is likely due to the receptor being less disordered in its bound state than **2.4b**. No excimer emission due to anthracene π-stacking was seen, which would have manifested itself as a broad peak close to 525 nm. As seen in the solid state structure of **2.3b·NaI**, the anthracene termini are too far from each other for effective intramolecular π-stacking, thus accounting for the absence of excimer emission.

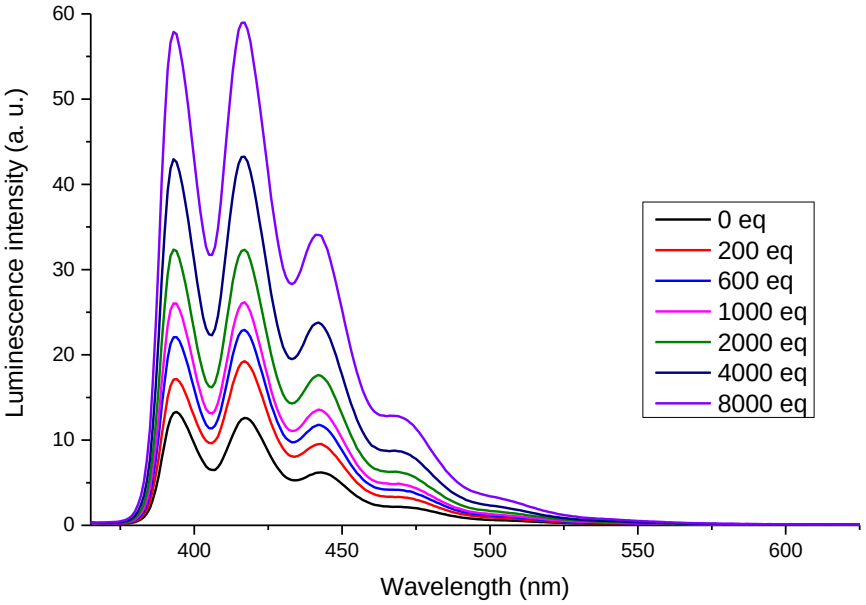

Figure 48 Compound 2.3b (1 µM in $CHCl_3$, λ_{ex} = 350 nm) titrated with TBABr.

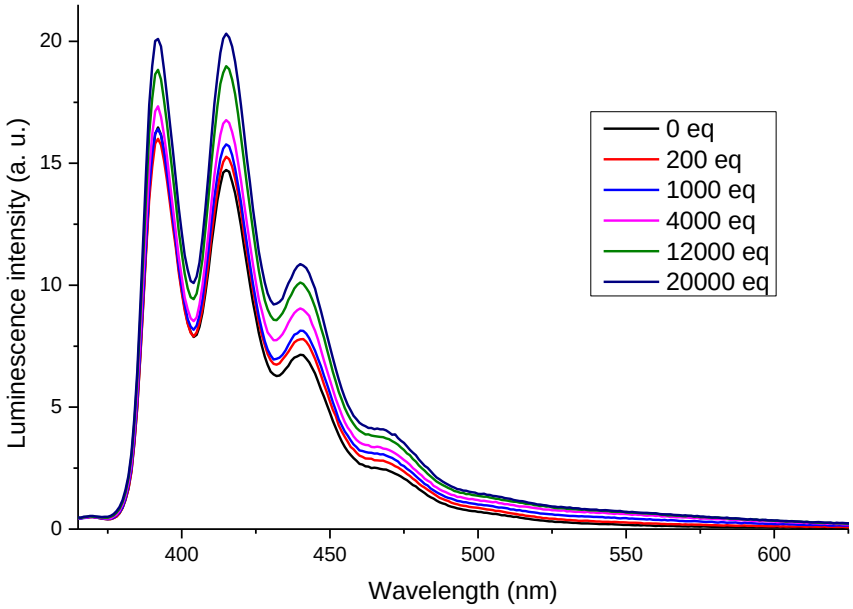

Figure 49 Compound 2.4b (1 µM in 1:1 acetone/$CHCl_3$, λ_{ex} = 350 nm) titrated with TBABr.

2.5 Stereoselectivity in anion binding

2.5.1 Chiral discrimination experiments with **2.4b**

Chiral XB **2.4b** receptor was titrated with both enantiomers of Boc-Ala, Boc-Leu, Boc-Trp, Glu and tartrate as TBA salts. Data derived from H_C as well as H_E was obtained. The resulting changes in

chemical shifts and best fits of binding isotherms are shown in Figure 50 – Figure 53. The phenylene protons H_C displayed a downfield Δδ which is typically caused by close proximity of the guest anion. In contrast, for the methylene H_E an upfield Δδ was observed. This implies that a different effect is taking place, possibly resulting from conformational changes rather than a direct interaction with an anion.

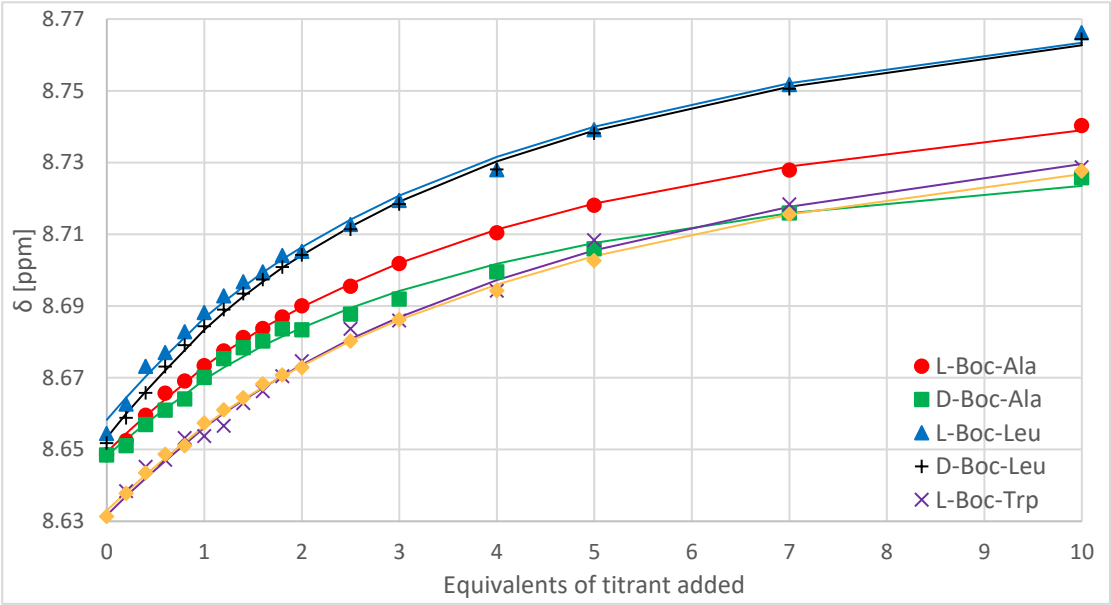

Figure 50 ^{1}H NMR titrations of 2.4b with chiral anions (monitored at H_C). All anions were introduced as tetrabutylammonium salts. Points: experimental data; lines: fitted binding isotherms.

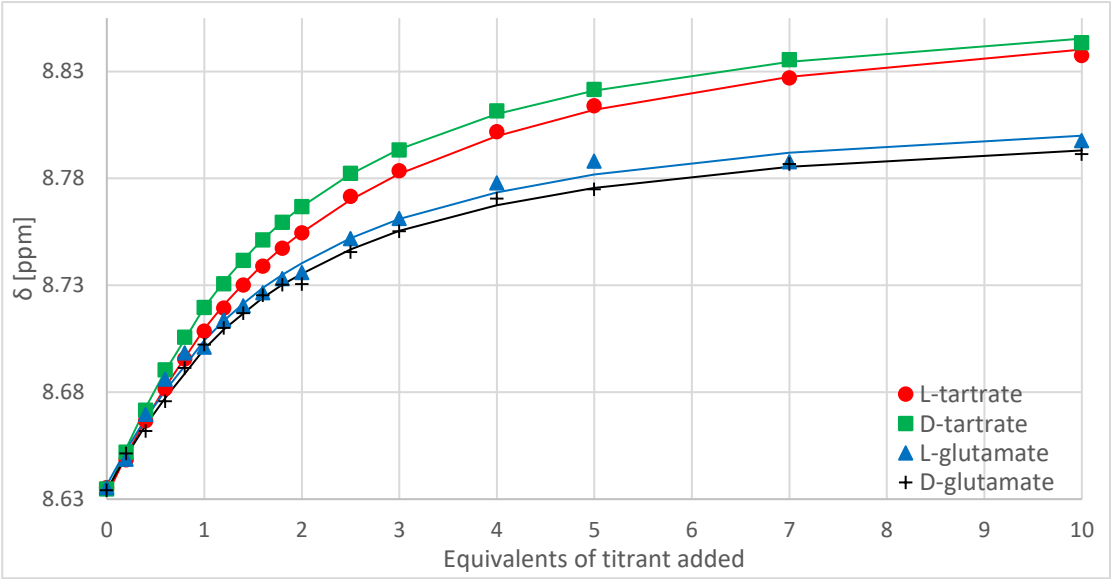

Figure 51 ^{1}H NMR titrations of 2.4b with chiral dicarboxylates (monitored at H_C). All anions were introduced as tetrabutylammonium salts. Points: experimental data; lines: fitted binding isotherms.

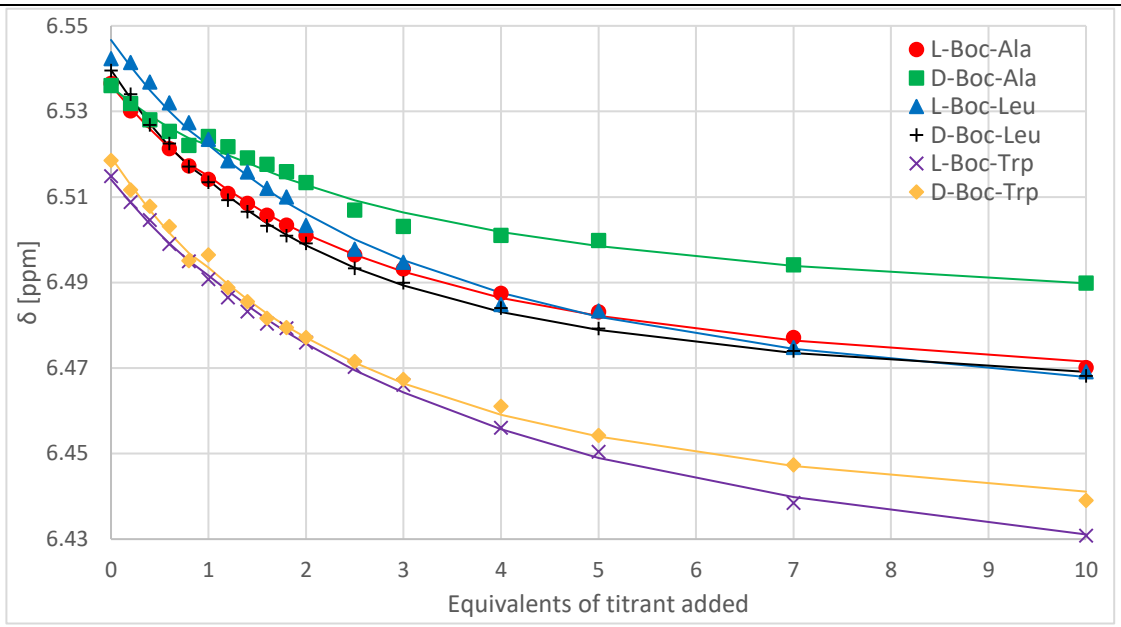

Figure 52 ^{1}H NMR titrations of 2.4b with chiral anions (monitored at H_E). All anions were introduced as tetrabutylammonium salts. Points: experimental data; lines: fitted binding isotherms.

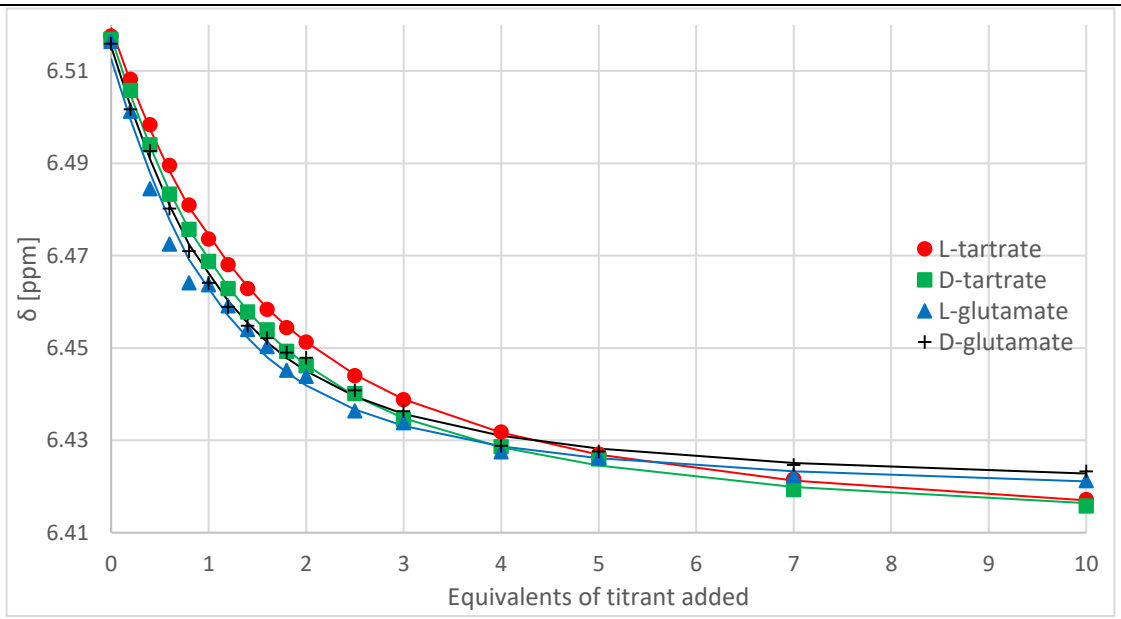

Figure 53 ^{1}H NMR titrations of 2.4b with chiral dicarboxylates (monitored at H_E). All anions are introduced as tetrabutylammonium salts. Points: experimental data; lines: fitted binding isotherms.

The association constant values K_a are shown in Table 2 along with the ratios of K_a for enantiomers (K_D/K_L). Interestingly, significantly different results were obtained by deriving data from H_C or H_E. Based on H_C little to no distinction between any enantiomers was seen. Based on H_E, however, overall weak to modest chiral discrimination was observed. The two sets of results are only in

agreement for dicarboxylates, with modest (K_D/K_L = 1.29) distinction between the enantiomers of tartrate and nearly no distinction in the case of glutamate. Binding constants derived from H_E are also higher than those derived from H_C, with up to 2.5-fold differences. Normally H_C would be the proton of choice due to the downfield Δδ consistent with direct effects of anion proximity as well as higher Δδ magnitude. However, in this case H_D is clearly more sensitive to stereochemistry of the guest anion. A possible explanation is that a non-stereoselective binding event that primarily affects H_C is accompanied by a stereoselective conformational change that affects H_E.

Table 2 Association constants K_a [M^{-1}] for 2.4b with enantiomers of chiral carboxylates.[a]

	K_a (H_C)	K_D/K_L (H_C)	K_a (H_E)	K_D/K_L (H_E)
***L*-Boc-Ala**	175 (9)	1.17 (0.14)	336 (23)	0.79 (0.16)
***D*-Boc-Ala**	204 (23)		265 (52)	
***L*-Boc-Leu**	184 (19)	1.05 (0.11)	287 (38)	1.52 (0.21)
***D*-Boc-Leu**	193 (3)		436 (21)	
***L*-Boc-Trp**	147 (18)	1.02 (0.14)	200 (14)	1.69 (0.12)
***D*-Boc-Trp**	150 (8)		337 (4)	
***L*-tartrate**	445 (16)	1.29 (0.05)	725 (6)	1.29 (0.04)
***D*-tartrate**	575 (13)		932 (28)	
***L*-glutamate**	590 (58)	1.01 (0.11)	1483 (220)	0.92 (0.15)
***D*-glutamate**	598 (32)		1363 (99)	

[a]All anions were introduced as TBA salts. All titrations were done in 1:1 $CDCl_3$/acetone-d_6 (500 MHz, 298 K). Uncertainties are given in parentheses. Determined from titration data monitoring H_C or H_E as specified.

Considering the data derived from H_E, the greatest difference in affinity was observed for tryptophan (K_D/K_L = 1.69), followed by leucine and alanine, which correlates with the steric bulk of the amino acid residue. In case of both Boc-Trp and Boc-Leu, the *D*-enantiomer was bound more strongly. The degree of chiral discrimination seen here is very close to what was observed in a related bis(iodotriazolium) receptor with the same binaphthol-derived chiral core.[219] In fact, the K_D/K_L value reported for that receptor with Boc-Leu (1.54) is almost identical to the one seen here.

Interestingly, in the case of Boc-Trp a discrimination of similar magnitude but opposite sign was reported. In the case of the dicarboxylate guests, a modest degree of discrimination was seen for tartrate while no difference was observed for glutamate. This is once again consistent with the steric factors of guest anions.

2.5.2 Attempt at stereoselective anion binding catalysis

Chiral anion receptors have a potential for the stereoselective catalysis of reactions promoted by anion abstraction, as was discussed in section 1.5.1. The chiral XB receptor **2.4b** is a candidate for such application. Additionally, a XB receptor **2.28** with a non-methylated binaphthol core was prepared as shown in Scheme 7.

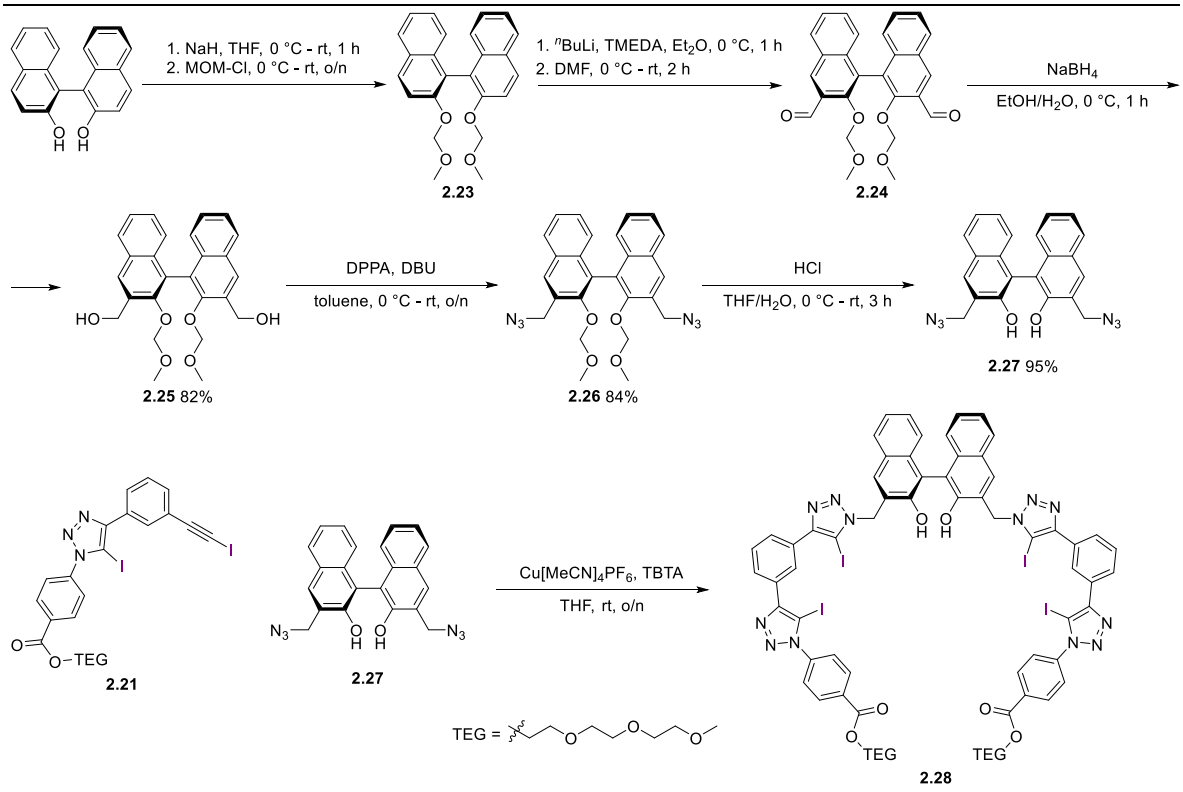

Scheme 7 Synthesis of the receptor with a non-methylated binaphthol core.

Similarly to **2.4b**, the receptor **2.28** displayed a slight preference for binding D-tartrate over the L enantiomer (Figure 54). The binding affinity was an order of magnitude higher than in **2.4b**, indicating that the binaphthol OH groups participate as HB donors. This is further confirmed by the

significant upfield Δδ of 0.25 – 0.3 ppm observed for the binaphthol protons of **2.28**. Interestingly, the level of discrimination between the tartrate enantiomers was identical to that seen in **2.4b**.

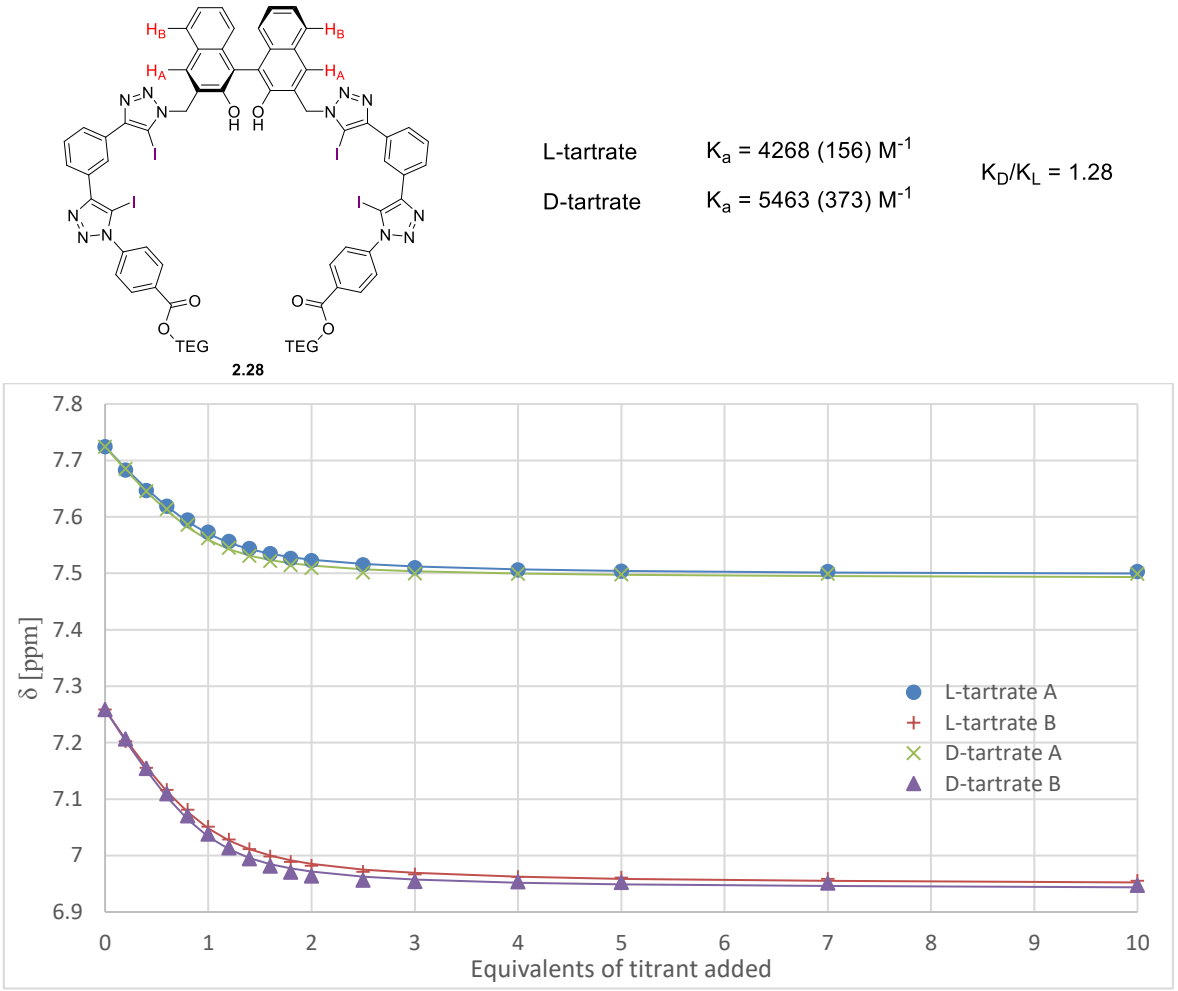

Figure 54 Top: protons chosen for monitoring in 2.28 and the resulting binding constants. Bottom: ^{1}H NMR titrations of 2.28 with (TBA)$_2$L-tartrate and (TBA)$_2$D-tartrate). Points: experimental data; lines: fitted binding isotherms (fitted simultaneously to H_A and H_B using Bindfit).

A reaction promoted by Cl^- abstraction (Scheme 8) was attempted with both **2.4b** and **2.28**. It was allowed to proceed at −78 °C (ensuring slow background reaction) for 2 days before warming to room temperature. However, only racemic products were obtained.

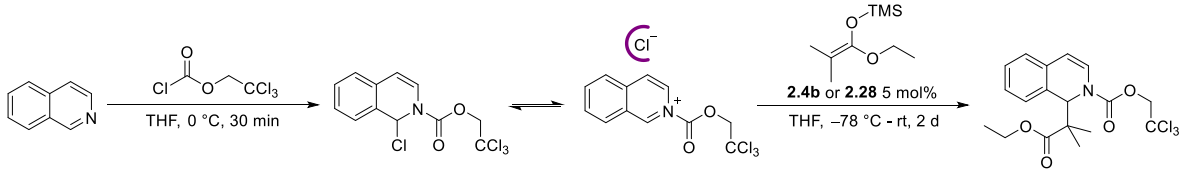

Scheme 8 Stereogenic addition to an acylisoquinolinium cation done in the presence of 2.4d and 2.28.

2.6 Conclusions

The XB receptor design based on four iodotriazoles connected by 1,3-phenylene units proved to be successful for the construction of anion binding molecules. Compared to their HB analogues **2.1a**–**2.4a**, the XB receptors showed enhanced anion affinities, with a general preference for binding heavier halides over oxoanions. The advantage of XB for anion binding was especially evident in **2.3b** and **2.4b** where the HB analogues **2.3a** and **2.4a** displayed very weak affinities due to the deletion of secondary HB donors, while the XB receptors **2.3b** and **2.4b** remained effective. Incorporation of anthracene and chiral binaphthol groups into the XB foldamer structure design enabled fluorescent anion sensing and modest chiral discrimination capabilities.

Improvement of chiral recognition ability is an interesting avenue for continuation of this project. Chiral XB or mixed XB/HB receptors with less conformational freedom compared to **2.4b** are particularly promising for this objective.

Chapter 3 Water-soluble XB and ChB receptors

3.1 Background

The basic triazole-phenylene anion receptor backbone introduced in Chapter 2 can be modified to introduce preorganisation, thus reducing the entropic cost of complex formation. This principle has been demonstrated in certain recent examples shown in Figure 55. In all these cases the backbone is preorganised by intramolecular HB interactions between the triazole nitrogen atoms and the OH or NH protons on substituents *ortho* to the triazoles.

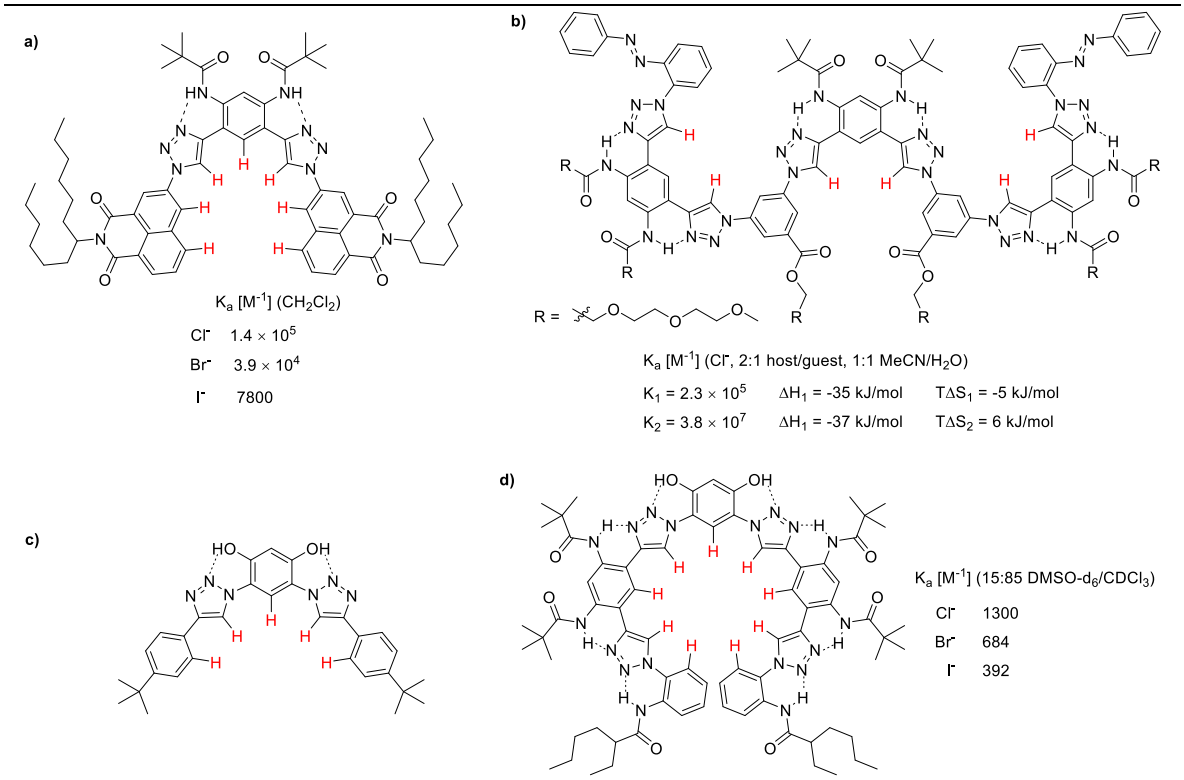

Figure 55 Examples of preorganised triazole-based anion receptors.

Preorganisation due to intramolecular HB from amide NH to triazole nitrogen was demonstrated by Amar Flood and co-workers in a bis(triazole) receptor assisted by naphthaleneimide units (Figure 55a).[96] This concept was taken further in a more complex, hexadentate foldamer (Figure 55b).[224] This compound was soluble in 1:1 MeCN/H_2O and strongly bound Cl^- in 2:1 host/guest stoichiometry. Two receptor molecules were able to fold into a double helical capsule with a central

cavity which contained several inward-facing C-H HB donors and was complementary in size to Cl^-. Stacking of the hydrophobic receptor surfaces in this structure efficiently masks them from solvent (ca. 80% of π-surfaces buried). As a result, 2:1 association is favoured by increased water content in the solvent. This strong hydrophobic effect allowed the thermodynamic cost of desolvating the Cl^- guest to be overcome, resulting in a very high affinity ($\beta_2 = 9 \times 10^{12}$). Importantly, the complexation is enthalpy-driven, which was thought to come from CH···Cl^- HB contacts as well as from additional water-water HB formed upon hydrophobic collapse of the receptor. An increase in entropy commonly associated with the hydrophobic effect was balanced by conformational restriction of the receptor, leading to little net effect.

Resorcinol units can be used to effect a similar preorganisation via intramolecular HB. A simple bidentate receptor (Figure 55c) proved to be a much stronger Cl^- binder than its analogue lacking the phenolic OH groups.[225] An extended, tetradentate receptor with the same resorcinol-derived core (Figure 55d) displayed anion binding that could be attenuated by treatment with a base.[226] Upon deprotonation of its phenolic OH groups (using DBU) this molecule switched to an unfolded state with CH···O intramolecular contacts between triazoles and phenolate anions. This state is unfavourable for anion binding, which was experimentally confirmed. The folded state could be restored upon treatment with picric acid, showing good reversibility in multiple base-acid cycles.

The aim of the work described in this chapter was to prepare water-soluble XB and ChB receptors on a preorganised triazole-based scaffold. Isophthalate diester or isophthalamide unit was chosen as the preorganising structure to be incorporated into receptor arms (Figure 56). Due to the steric bulk of iodine and methyltellanyl substituents on the triazole 5-position, any non-hydrogen groups placed *ortho* to the triazoles will restrict their rotation relatively to the bridging phenylene (Figure 56a). The σ-hole donors can therefore be directed towards the convergent conformation favourable for anion binding. The isophthalamide variant was also thought to enable preorganisation via intramolecular HB (Figure 56b). This is similar to the literature examples

discussed above, but appears more optimal for stabilising the structure where the triazoles are tilted relative to the phenylene (such a conformation was observed in a crystal structure of anion-bound XB receptor described in Chapter 2). In the end no evidence of this intramolecular HB was found, but the amide groups still effect preorganisation by steric repulsion.

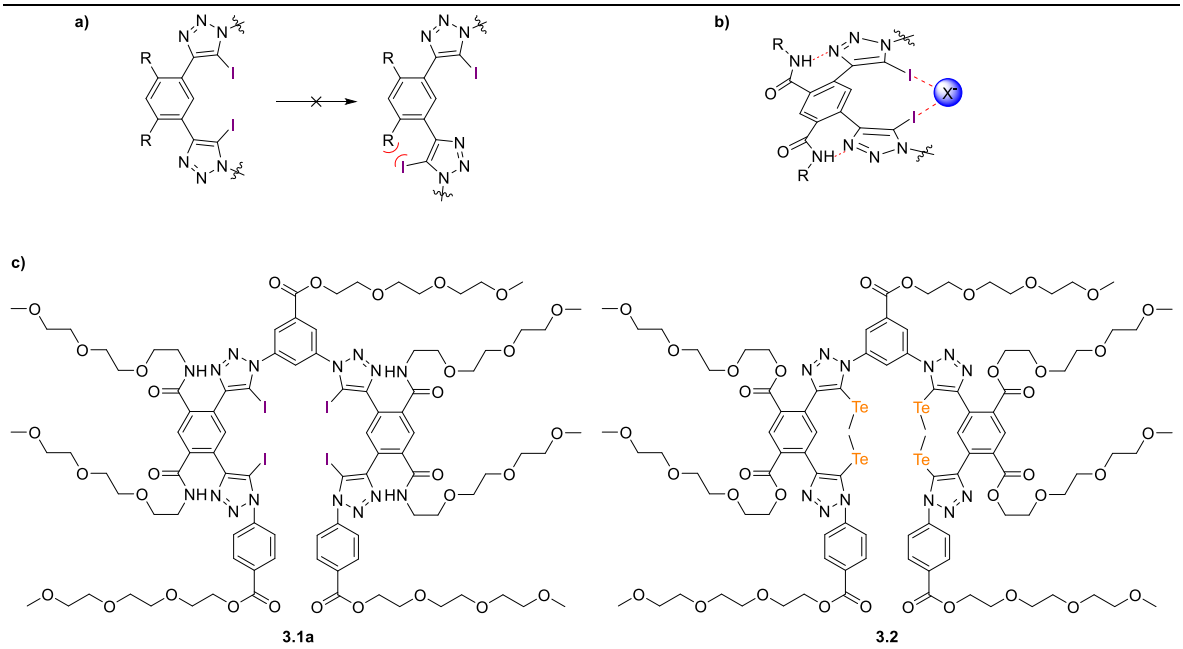

Figure 56 Design of water-soluble, preorganised XB and ChB receptors. a) Preorganisation by steric repulsion. b) Proposed preorganisation by intramolecular HB (not observed experimentally). c) Complete structures of water-soluble, preorganised XB and ChB anion receptors.

The preorganising groups chosen here are also electron-withdrawing which can be expected to increase the strength of σ-hole interactions. As was demonstrated in Chapter 2, the nature of substituents on the aromatic rings connected to the iodotriazoles has a large effect on anion affinity. Substituents introduced here should be therefore much more favourable compared to the acylamino or hydroxyl groups seen in the literature examples. The isophthalate/isophthalamide structure also provides additional attachment points for the placement of solubilising groups with the ultimate goal of water solubility. The receptors built in such a manner (Figure 56c) have clearly defined hydrophilic outer rims and hydrophobic inner rims, which together with the steric preorganisation was intended to favour folding of the molecule in an aqueous environment.

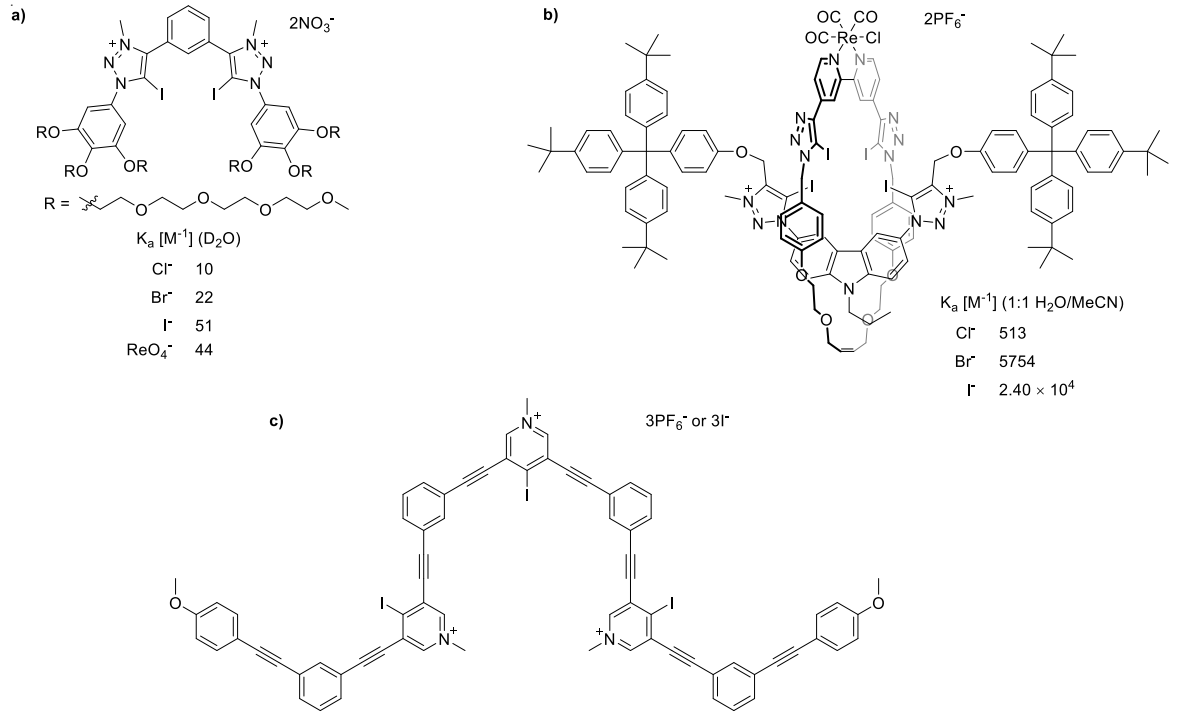

Figure 57 Examples of XB receptors that were studied in water or aqueous-organic mixtures.

XB receptors have been recently studied in partially aqueous mixtures and even neat water.[227] Rare examples of water-soluble systems include the bidentate cationic receptor (Figure 57a) solubilised by extensive oligo(ethylene glycol) substitution.[228] This receptor was selective for the weakly solvated I^- and ReO_4^- and proved a stronger complexing agent than its HB (prototriazole) analogue. A tetradentate all-XB rotaxane (Figure 57b) was not water-soluble but could still be studied in highly competitive 1:1 H_2O/MeCN mixture.[229] Similar to the previous case it was selective for I^- over lighter halides; this selectivity was also more pronounced with increasing water content in the solvent. Another example is the tris(iodopyridinium) chain (Figure 57c) that formed a triple helicate complex encapsulating two I^- ions in solution and in the solid state (3:2 host/guest stoichiometry).[230] While in absence of I^- the iodopyridinium units were readily hydrolysed, they could be protected inside the hydrophobic interior of the I^- complex. Indeed, with I^- counterion this compound was stable for several days in 1:1 H_2O/DMF, demonstrating the highly efficient complex formation.

Although recent advances cast some light on the properties of XB in the presence of water, so far there have been no examples of pure-XB, charge-neutral receptors that would be soluble and

effective in pure H_2O. In the case of ChB which is far less extensively studied than XB, no aqueous receptors are currently known. The novel anion hosts described herein are therefore interesting for elucidating the fundamental properties of the σ-hole and hydrophobic interactions, in addition to the applications of anion binding and recognition.

3.2 Synthesis

3.2.1 Initial attempts

The first synthesis plan followed the most intuitive disconnection analogous to the synthesis of receptors in Chapter 2 (Scheme 9). This approach required the 4,6-bis(iodoethynyl) isophthalamide precursor **A**. Synthesis of this compound started from bromination of *m*-xylene and oxidation to 4,6-dibromoisophthalic acid **3.7**. Tri(ethyleneglycol) isophthalamide **3.8** was then formed via acyl chloride and finally ethynyl groups were installed in a Sonogashira coupling. Desilylation of the intermediate TMS-alkyne **3.9** provided the terminal bis(alkyne) **3.10**.

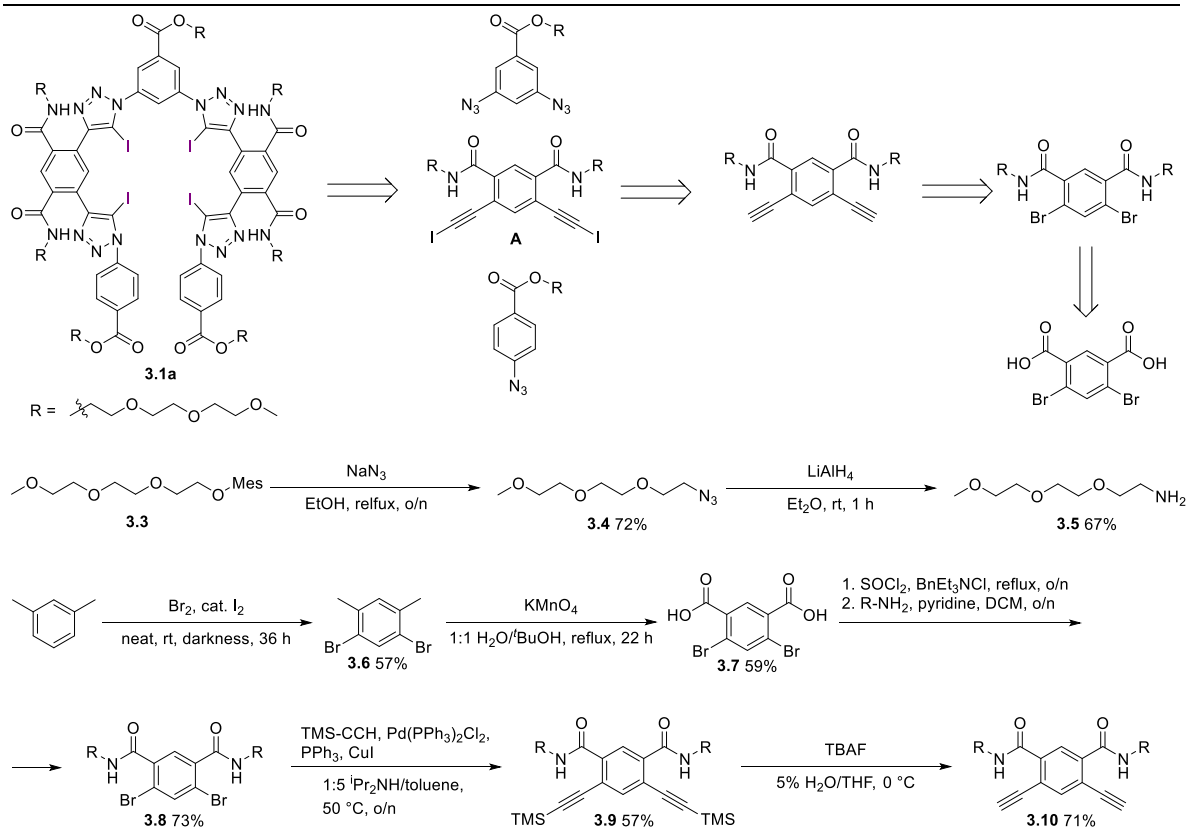

Scheme 9 Initial plan for the synthesis of preorganised receptors and the preparation of bis(ethynyl) isophthalamide precursor.

Attempts to prepare the bis(iodoalkyne) **A** were however unsuccessful. Instead of the desired terminal iodination cyclised iodoalkene products were formed (Scheme 10a). This is a literature-known reaction[231,232] that presumably occurs due to the nucleophilic character of the amide N atom allowing it to ring-open the iodonium intermediates formed in the presence of iodinating reagents (Scheme 10b). The resulting iodocyclisation product is an isomer of the desired bis(iodoalkyne) which was deceiving as the test reactions were monitored by mass spectrometry. In some attempts where an excess of iodinating reagent was used, triple and quadruple iodination was detected by MS. This indicates that the desired terminal iodination probably takes place but is followed by iodocyclisation of the resulting iodoalkyne.

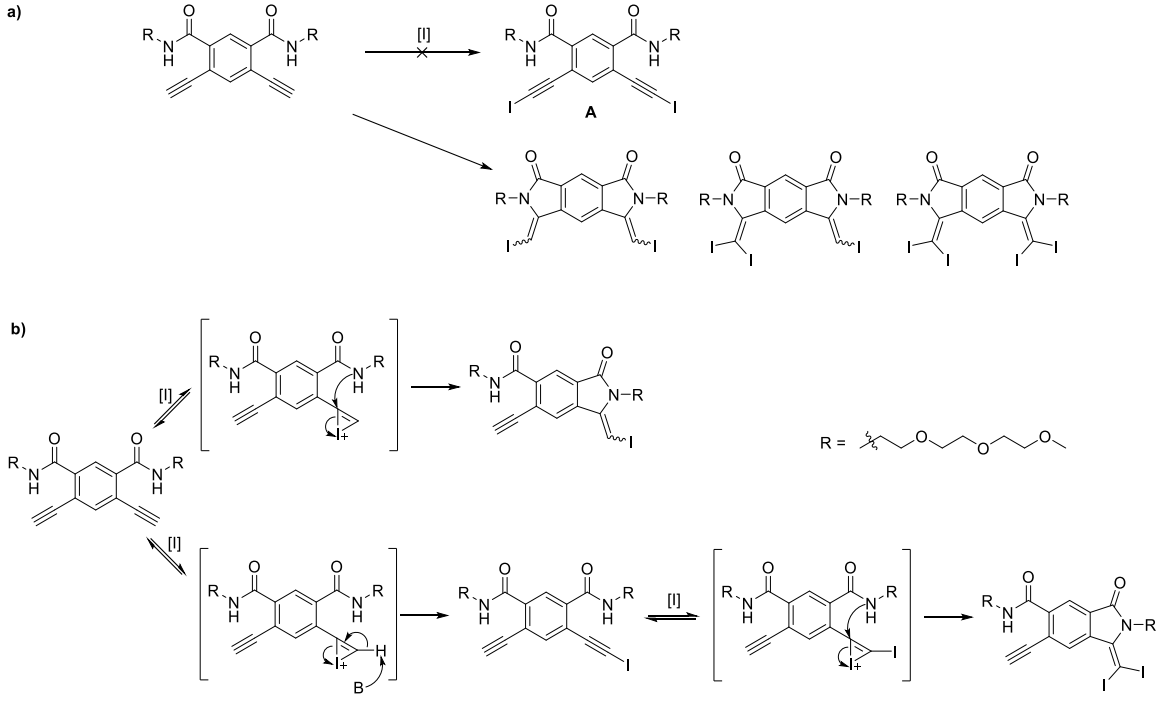

Scheme 10 a) Failed terminal iodination of bis(ethynyl)isophthalamide to provide A. b) Proposed processes that explain the observed products.

Approaches summarised in Scheme 11 were tried to circumvent this problem. One attempt was to Boc-protect the amides, rendering them inert towards iodocyclisation (Scheme 11a). However, Sonogashira coupling of the Boc-protected dibromoisophthalamide did not work, presumably due to steric hindrance. The coupling also failed in the presence of p-nitrophenyl esters introduced as

reactive groups that would be transformed into amides after the terminal iodination (Scheme 11b). In another approach, the desired iodoalkynes were successfully formed in the presence of methyl esters (Scheme 11c). However, hydrolysis of these esters intended to allow installation of TEG amides interfered with the electrophilic iodoalkynes, resulting in decomposition. Another attempt was to carry out terminal iodination in the presence of acyl chlorides and then react them with TEG-NH_2 to afford **A** (Scheme 11d). Formation of acyl chlorides in the vicinity of alkynes was however unsuccessful, leading to significant decomposition.

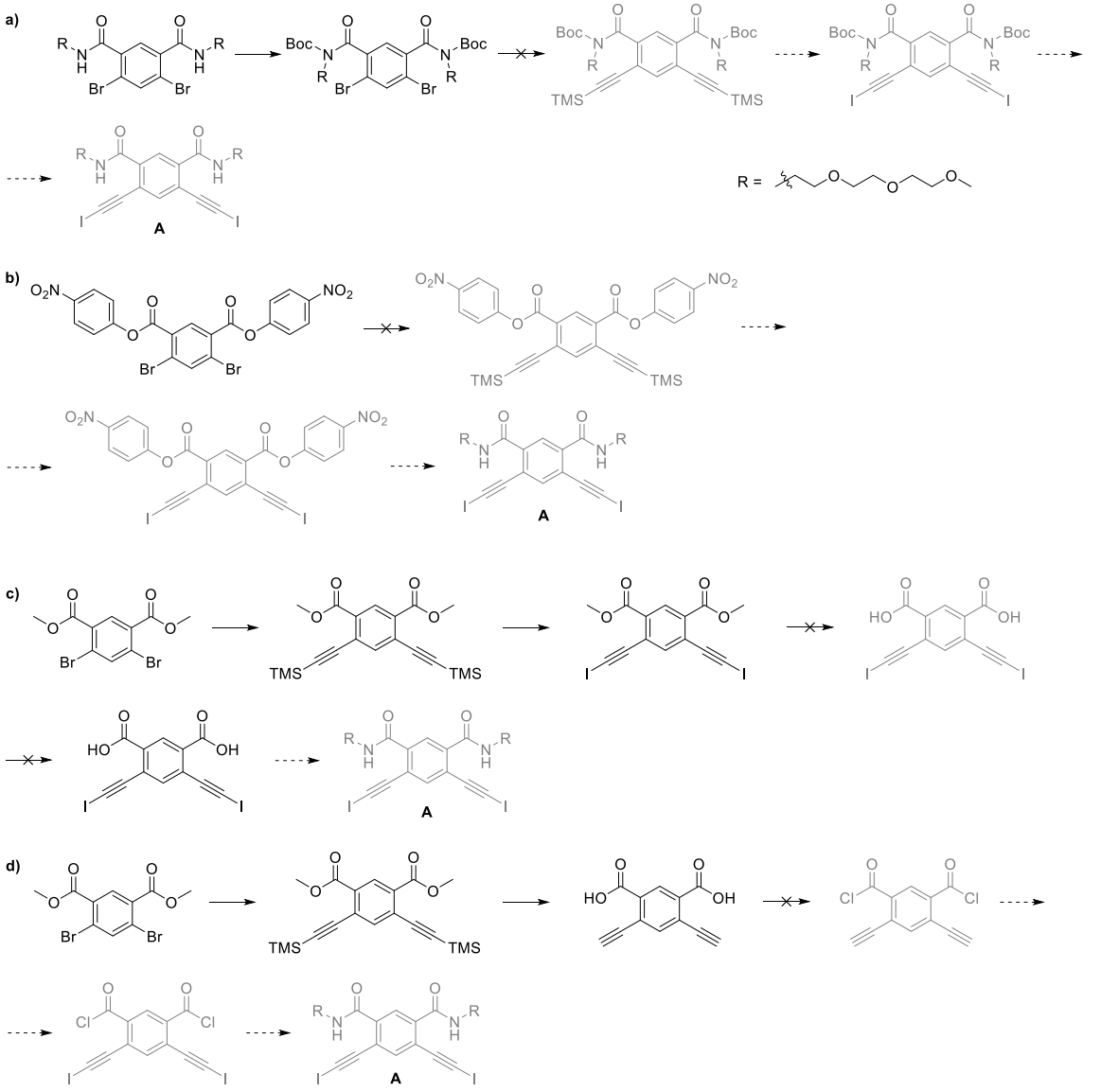

Scheme 11 Unsuccessful attempts at circumventing the terminal iodination of alkynes in the vicinity of amides.

3.2.2 Final synthesis of preorganised, solubilised XB receptors

A solution to the synthetic problems described above was to introduce ethyl *p*-hydroxybenzoate (ethylparaben) esters that would be inert in the terminal iodination step but could be transformed into amides afterwards (Scheme 12a). Reactivity of these esters is very well-tuned for this purpose. They do not interfere with Sonogashira coupling, terminal iodination, or azide-iodoalkyne cycloaddition. They are also stable under aqueous workup conditions, providing that bases are not used. However, upon treatment with a primary amine in DCM the ethylparaben esters undergo amidation at room temperature on a timescale of 1 – 2 days.

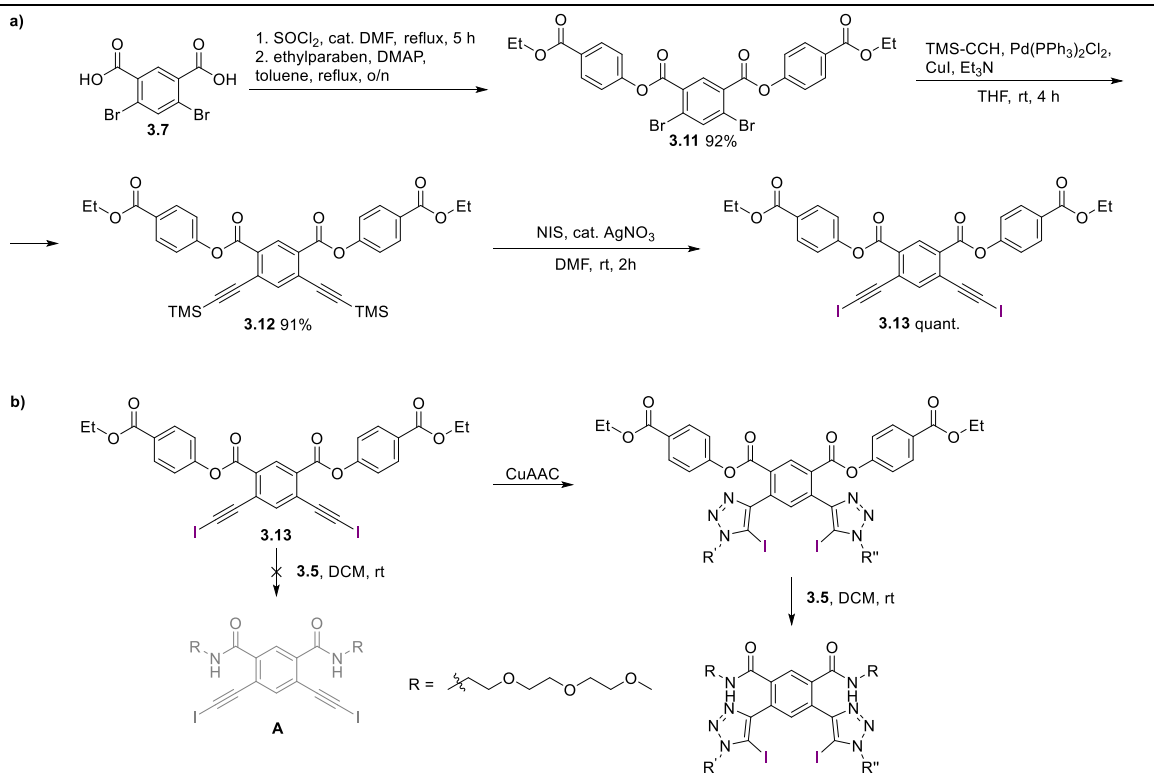

Scheme 12 a) Synthesis of bis(iodoalkyne) precursor 3.13. b) Amidation of reactive ethylparaben esters can be successfully performed after the CuAAC steps.

Amidation of **3.13** to provide **A** was not successful, indicating that decomposition of the electrophilic iodoalkynes occurs in the presence of the nucleophilic TEG-NH_2 **3.5** (Scheme 12b). However, iodotriazoles were stable under the same conditions. Therefore, carrying out amidation after the assembly of the receptor backbone in a sequence of two CuAAC reactions proved to be a

viable approach (Scheme 12b). Introduction of tri(ethylene glycol) amide groups in the last step has an additional benefit of alleviating the purification difficulties that are common for heavily PEG-substituted compounds.

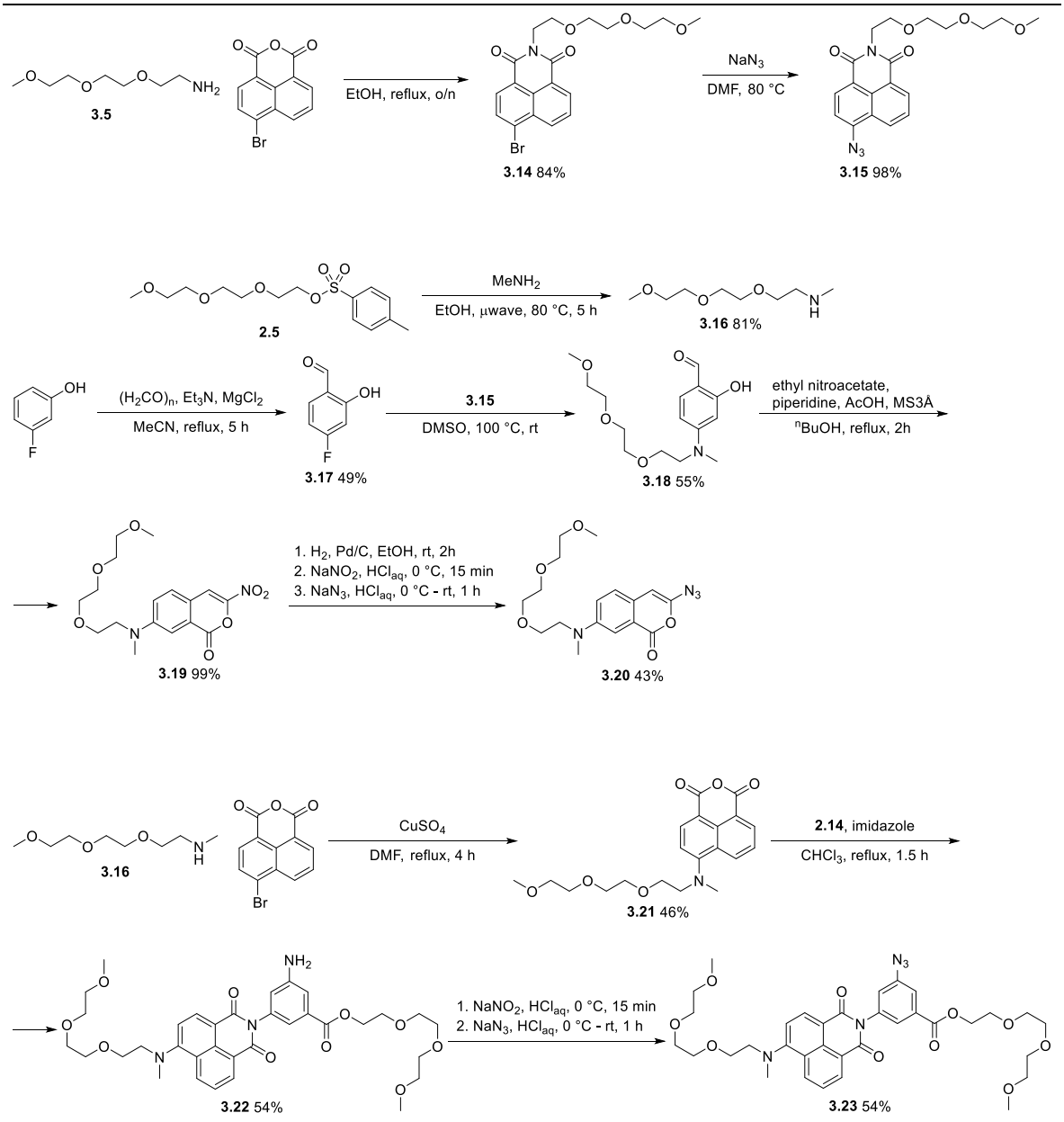

Scheme 13 Synthesis of the azide terminal precusors 3.15, 3.20, 3.23 that contain fluorophores.

Different terminal groups were incorporated into the XB anion receptor framework. Simple TEG-N_3 (**3.4**) was used as well as the two previously described azides **2.10** and **2.11**. In addition, a receptor capable of a fluorescent response in water was sought for. To this end, three different fluorescent

terminal units functionalised with water-solubilising chains were synthesised (Scheme 13). These contained naphthaleneimide (**3.15**), 4-aminonaphthaleneimide (**3.23**) and coumarin (**3.20**) fluorophores. In addition to solubility and fluorescent properties these were chosen for their relatively electron-withdrawing character which is favourable for the anion binding properties of the target receptors.

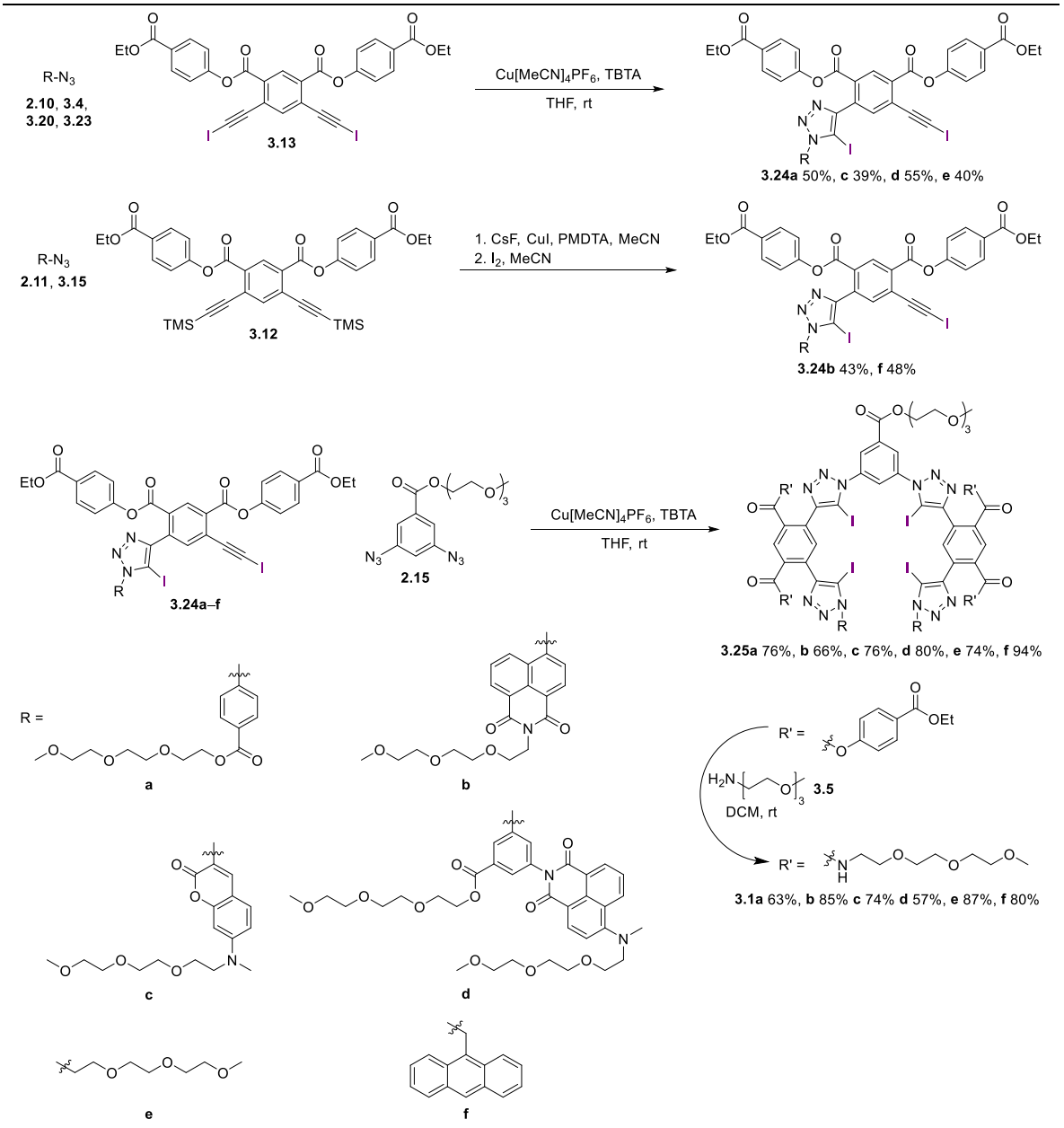

Scheme 14 CuAAC and amidation steps in the synthesis of preorganised receptors 3.1a-e.

Similar to the synthesis described in Chapter 2, the XB receptors **3.1a–f** were assembled in a sequence of two CuAAC reactions (Scheme 14). An arm fragment **3.24a–f** was first prepared in a statistical reaction of an azide with **3.13** or via the one-pot desilylation-cycloaddition-iodination protocol with **3.12** (see below). Typically 1.2 equivalents of **3.13** were used, leading to moderate yields (39–55%) of **3.24a–f**. Two equivalents of the resulting iodoalkyne-terminated compound were then reacted with the bis-azide **2.15**, leading to the active ester precursors **3.25a–f**. Finally, quadruple amidation of these intermediates was performed by treatment with **3.5**, providing the final products **3.1a–f**. Despite the need to transform four groups per molecule and the delicate nature of iodotriazole compounds, this reaction was overall successful, giving moderate to high yields (57–87%). It had to performed under anhydrous conditions, as traces of water could participate in amine-catalysed ester hydrolysis, leading to low yields.

While the azide precursors **2.10**, **3.4**, **3.20**, **3.23** successfully reacted with **3.13** under the usual azide-iodoalkyne cycloaddition conditions, **2.11** and **3.15** did not react. This can be attributed to steric hindrance preventing the assembly of a reactive complex where both azide and iodoalkyne are coordinated to Cu(I). Unlike the other azide precursors described here, **3.15** is effectively an *ortho*-substituted aryl azide. The anthryl group in **2.11** also has a significant steric bulk, even though it is separated from the azide by one carbon atom. Combined with the steric bulk of ethylparaben ester positioned *ortho* to the iodoalkyne in **3.13** and the size of its I atom, this results in prohibitive steric crowding in the CuAAC step.

To bypass this problem, a one-pot desillylation-cycloaddition-iodination protocol was devised (Scheme 15). In this process the bis(TMS-alkyne) **3.12** was stirred with the desired azide, CsF, CuI, and PMDTA in MeCN under thoroughly anhydrous conditions. CsF slowly dissolves into MeCN and desilylates **3.12**. The resulting alkynide forms a complex with Cu[PMDTA] which is highly reactive towards CuAAC. Steric hindrance is in this case alleviated by the lack of I atom on the alkyne. A Cu-bound triazolide is formed via CuAAC, which is relatively stable in the absence of proton donors

or electrophiles. When full consumption of the azide starting material was found by TLC, I_2 was added which immediately reacted with the Cu triazolides to form iodotriazoles. The mixture was then left stirring (typically overnight) to ensure complete transformation of any remaining TMS-alkynes into iodoalkynes. The yields obtained with this protocol are comparable to the standard CuAAC method used for non-bulky azides (in both cases 1.2 eq of **3.12** or **3.13** relatively to the azide was used).

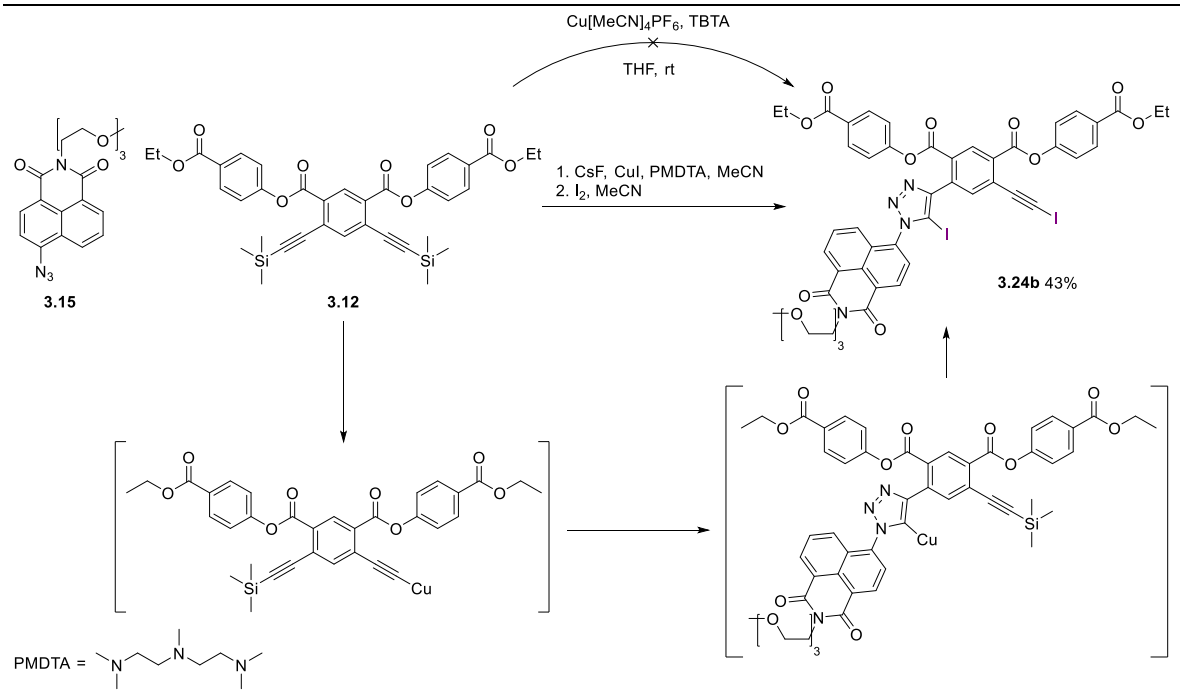

Scheme 15 Pathway of the one-pot desilylation-cycloaddition-iodination.

For a comparison between HB and XB in an aqueous environment, a HB analogue **3.1a$_H$** was also synthesised (Scheme 16). The required bis(alkyne) **3.13**$_H$ could not be obtained via the usual methods (hydrolysis with K_2CO_3 or cleavage with TBAF) due to the reactive nature of its ethylparaben esters. Instead, this deprotection was effected by the formation of Ag alkynide. This could be done by treatment with AgF in MeCN or $AgNO_3$ in MeOH. The latter method is preferred as AgF tends to activate MeCN which leads to oxidative coupling products.[233] Using AgF in MeOH is also not feasible, as its basicity causes methanolysis of ethylparaben esters. Treatment of the resulting silver alkynide with HCl afforded the deprotected product **3.13**$_H$. The HB receptor **3.1a$_H$**

was then assembled similarly to the XB analogues via two CuAAC steps and the final amidation of ethylparaben esters.

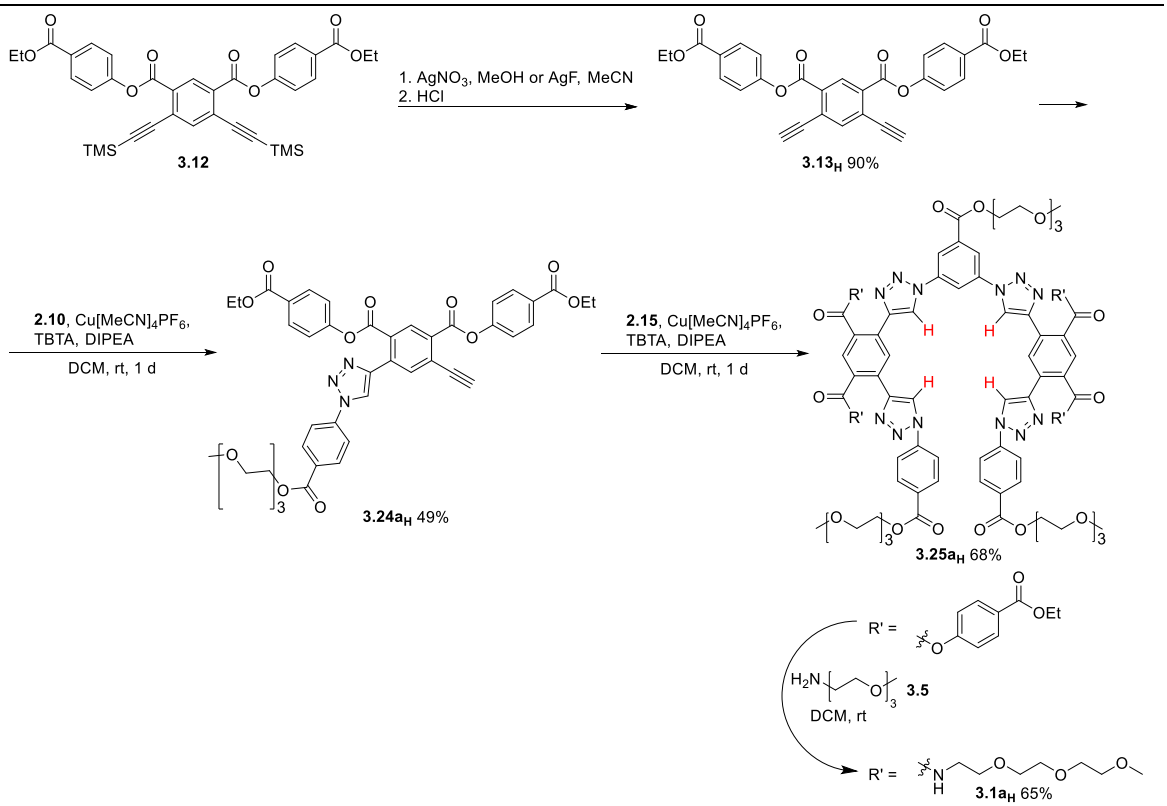

Scheme 16 Synthesis of the solubilised HB receptor 3.1a$_H$.

3.2.3 Synthesis of a Te-based ChB receptor

Preparation of ChB receptors is generally more difficult than of their XB counterparts. Especially in the case of Te-based compounds stable receptor structures are rare due to the weakness of the C-Te bond (ca. 200 kJ/mol).[131] For this reason electron-deficient organotellurium(II) compounds are especially vulnerable towards polar cleavage, to the point of being unstable in the presence of protic solvents. Methyltellanyltriazole units have been recently demonstrated as viable ChB donors.[135] Although less durable than iodotriazoles (for example, cationic iodotriazolium species are stable, while MeTe-triazolium analogues are not), they have proved to be synthetically feasible and effective for anion binding.

3.2 Synthesis

Previously reported synthetic approaches to 5-alkyltellanyl-1,2,3-triazoles include an S_NAr-type reaction of iodo- or fluorotriazoles (Scheme 17a).[135] In this process a strong Te nucleophile MeTeLi is formed in a reaction of MeLi with elemental Te. It then displaces a halide from the triazole scaffold, thus forming a methyltellanyltriazole. Alternatively, such compounds can be synthesised in a CuAAC reaction between an organic azide and an organotellanylalkyne (Scheme 17b).[234,235] The RTe-alkyne precursors have been commonly synthesised by treatment of elemental Te with lithium acetylide, followed by capping of lithium alkynyltelluride with an alkylating reagent.

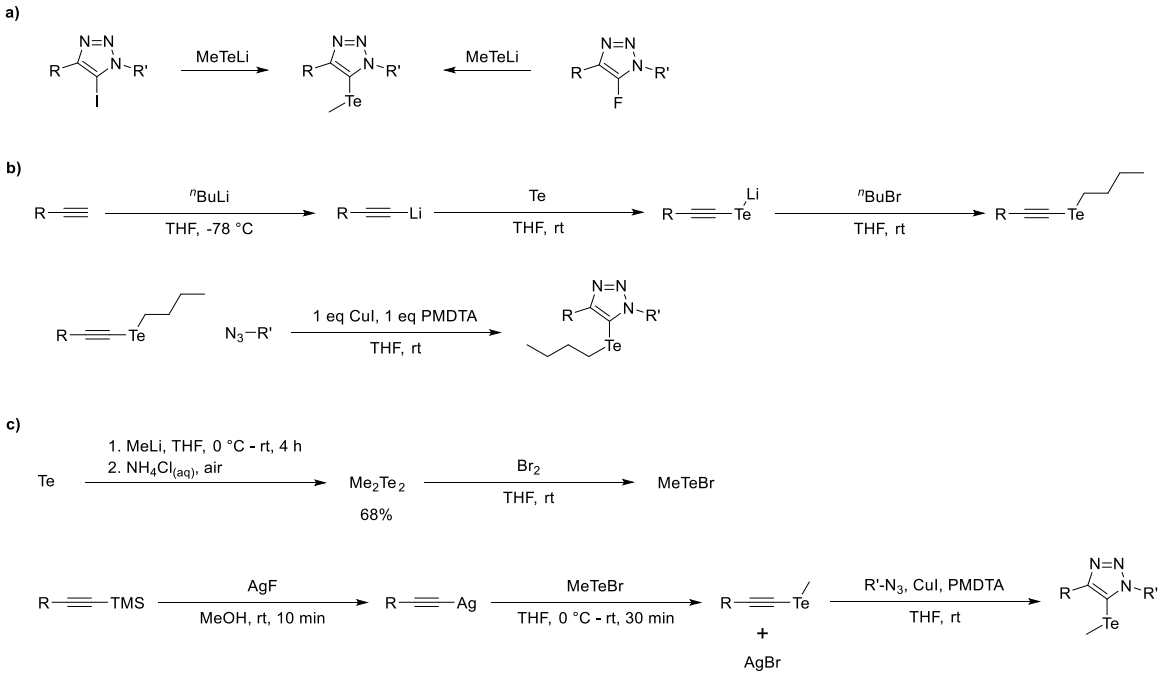

Scheme 17 a) S_NAr approach for MeTe-triazole synthesis. b) Synthesis of an organotellanylalkyne followed by CuAAC reaction. c) Synthetic approach in this work: synthesis of methyltellanylalkyne by Ag-Te transmetallation.

The CuAAC approach towards methyltellanyltriazoles was chosen in this work. However, synthesis of the required bis(methyltellanylalkynyl) precursors via the reaction of lithium alkynide with Te followed by methylation was considered unsuitable in this case. The highly nucleophilic species involved in this process were anticipated to be incompatible with the ester groups that would be present in the bis(alkyne) material. Instead, a transmetallation reaction between silver alkynide and MeTeBr was proposed (Scheme 17c). Transmetallations driven by the formation of a silver

halide are known in many variants, but no precedents were found for the synthesis of organotellanyl alkynes in this manner. As opposed to the nucleophilic RTeLi species, electrophilic MeTeBr was deemed compatible with organic scaffolds containing esters.

The necessary precursor MeTeBr was prepared as shown in Scheme 17c. First, Te was treated with MeLi to provide MeTeLi. Upon aqueous workup the thermodynamically unstable MeTeH was formed, which readily disproportionated to Me_2Te_2 at room temperature. Pure Me_2Te_2 was then obtained by extraction and vacuum distillation. It is a dark brown liquid notable for its intense smell of rotten garlic with an additional metallic flavour. When treated with Br_2 in THF it instantly reacted to form a dark solution of MeTeBr.[236] This reaction was used to prepare MeTeBr freshly as needed, thus avoiding the unpleasant isolation of this reagent.

First attempts at synthesising a bis(methyltellanylethynyl) precursor were made starting with **3.12** (Scheme 18) to eventually prepare a ChB receptor by the same pathway as the XB receptors **3.1a-f**. As was mentioned above, preparation of silver alkynide from this compound is challenging due to the reactivity of its ethylparaben esters. For example, methanolysis occurs when **3.12** is treated with AgF in MeOH. Using AgF in MeCN avoids this problem, but leads to formation of side products with precipitation of metallic Ag. Transmetallation of silver alkynide obtained in this manner resulted in characteristic orange MeTe-alkyne product $\mathbf{3.13_{Te}}$. However, a difficult purification was required, presumably due to the unclean nature of silver alkynide formation.

This method was not successful when attempted on the TEG isophthalamide substrate **3.7**. The amide groups clearly interfere in the silver alkynide formation step, resulting in a black material that did not provide the desired product when treated with MeTeBr.

When the TEG isophthalate **3.27** was used as starting material the process afforded very good results (Scheme 18). Because **3.27** only contains weakly reactive esters, its silver alkynide derivative could be easily prepared using AgF in MeOH. After switching the solvent to THF, the alkynide was treated with MeTeBr to provide the desired MeTe-alkyne **3.28** in high yield (93%). This shows that

this method is very amenable for the simultaneous formation of two methyltellanylalkynes per molecule and works very well providing that the substrate does not have interfering reactivity.

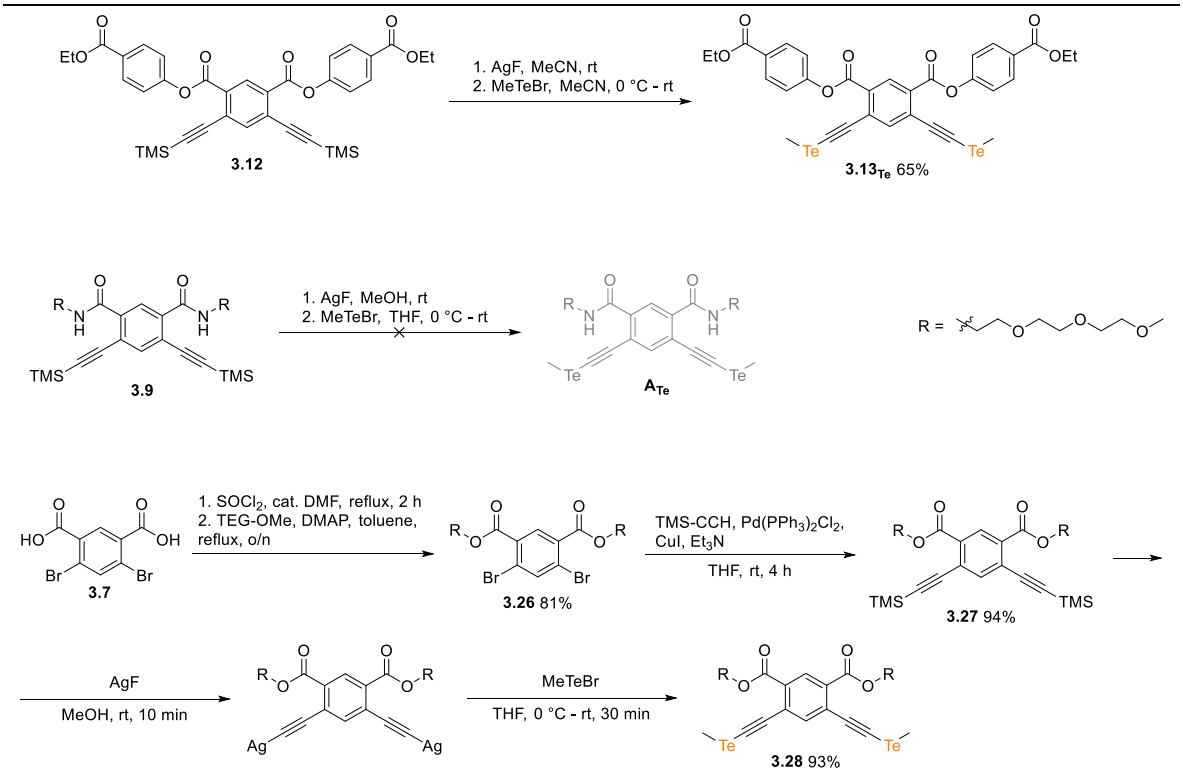

Scheme 18 Synthesis of bis(methyltellanylethynyl) precursors.

Compound **3.13$_{Te}$** was then used to assemble a reactive ester precursor to the planned ChB receptor **3.1a$_{Te}$** (Scheme 19). The CuAAC reactions proceeded successfully, but the synthesis failed in the reactive ester amidation step. ^{1}H NMR of the product obtained in this reaction showed that multiple impurities were present even though the material appeared as a single TLC spot. Although the exact origins of this outcome are unclear, the most likely explanation is the interference of the nucleophilic amine **3.5** with the MeTe groups.

Starting form **3.28** the amidation step was not needed and the assembly of a ChB receptor **3.2** was successful (Scheme 19). It was found that the all-ester scaffold was significantly less water-soluble than the structure containing four amide groups in XB receptors **3.1a**–**e**. Additionally, its solubility sharply decreased with increasing temperature: at 4 °C, a 1 mM concentration is attainable, while at 20 – 21 °C, the maximum concentration of a stable solution was close to 0.2 mM. At 25 °C this

decreased further to ca. 0.05 mM. This can be explained by the known transition of TEG chains from C–C *gauche* to *anti* conformation which is less hydrophilic and undergoes entropy-driven dehydration.[237] Introduction of strongly hydrated amide groups into PEG-solubilised molecules is also known to cancel this temperature dependency.[238]

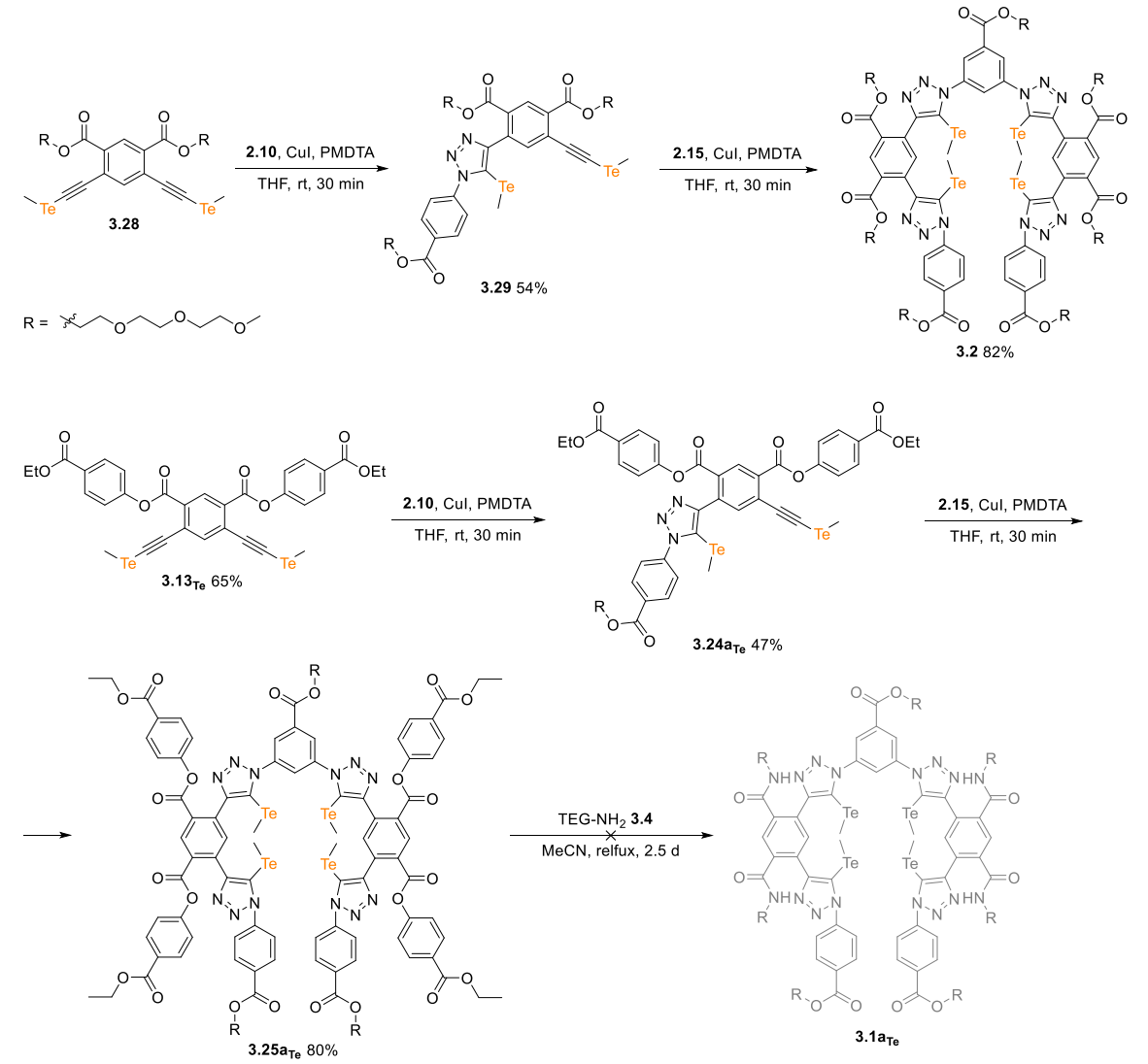

Scheme 19 Synthesis of the ChB receptor 3.2 and the attempted synthesis of a ChB receptor with amide-functionalised scaffold 3.1a$_{Te}$.

To attain a direct comparison between XB and ChB anion receptors, an XB analogue with an all-ester scaffold **3.2$_I$** was prepared (Scheme 20). Iodoalkynes in **3.28** were formed in a high-yielding iododesilylation reaction that was previously used to synthesise **3.13**. The standard sequence of two CuAAC reactions then provided the XB receptor **3.2$_I$**. Due to the all-ester scaffold its water

solubility was much lower than in **3.1a–e**. Interestingly, it is also somewhat lower than in **3.2**, confirming that solubility is indeed diminished by the lack of amide groups rather than the introduction of MeTe substituents.

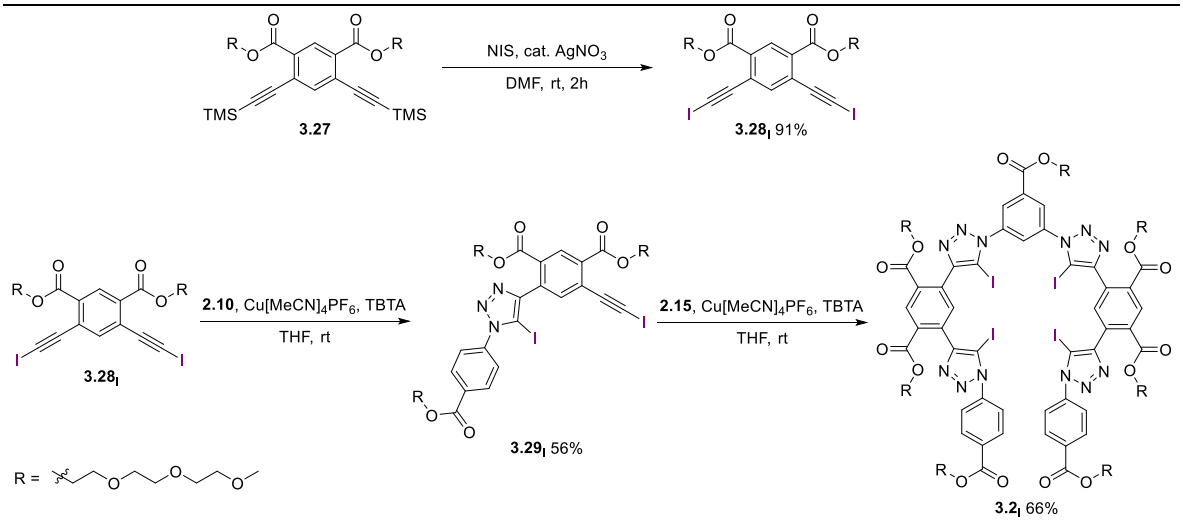

Scheme 20 Synthesis of the XB receptor with all-ester scaffold 3.2$_I$ for comparison with the ChB analogue 3.2.

3.3 Anion binding studies

3.3.1 ITC experiments

The XB and ChB anion receptors described herein were studied by isothermal titration calorimetry (ITC) in pure water, which was enabled by the good water solubility of **3.1a–e** and **3.1a$_H$** and much lower, but still practical solubility of **3.2** and **3.2$_I$**. In addition to binding affinities, this method conveniently provides the thermodynamic parameters of host-guest interactions, allowing a deep insight into the nature of binding equilibria.

ITC titrations were performed using a Malvern MicroCal PEAQ-ITC Automated calorimeter. In all experiments the sample cell was loaded with 0.2 ml of solution and stirred at 750 rpm. The cell solution was titrated over the course of 35 injections of titrant (1×0.4 µl, then 34×1 µl) with 150 s intervals. All experiments with anion receptors **3.1a–e** and **3.1a$_H$** were performed at 298 K. Experiments with **3.2** and **3.2$_I$** were performed at 293 K due to the strong negative dependence of the solubility of these compounds in water on temperature.

For all anions except I^-, a 0.2 mM receptor solution (0.05 mM in the case of **3.2$_I$**) was titrated with a solution of Na salt of the desired anion (usually 20 mM, reduced to 10, 5 or 1 mM where strong binding was present). For I^- with XB receptors, anion affinity was generally strong enough to perform an "reverse" titration where 0.025 or 0.05 mM NaI solution was titrated with 0.5, 0.75 or 1 mM receptor solution. ITC traces from these experiments are shown in Figure 58 – Figure 60. These titrations demonstrate the 2:1 binding mode, as can be judged from good fits obtained using the 2:1 sequential binding sites model. Further evidence of 2:1 binding was found in DOSY NMR experiments (see section 3.3.2). For all XB and ChB receptors, the resulting ITC traces were thus fitted using the sequential binding sites model with two binding sites. In the case of HB receptor **3.1a$_H$**, a 1:1 binding model was used. These conclusions about binding stoichiometry are once again supported by DOSY NMR as will be shown below.

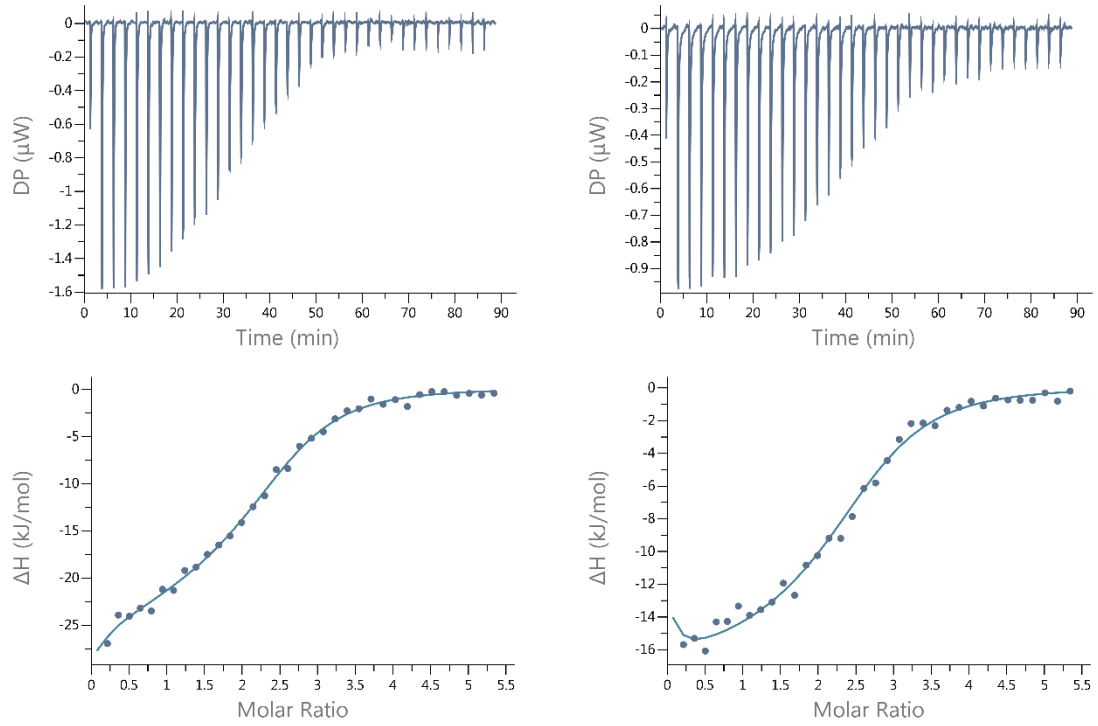

Figure 58 Left: NaI (0.025 mM) titrated with 3.1a (0.75 mM). Right: NaI (0.025 mM) titrated with 3.1b (0.75 mM).

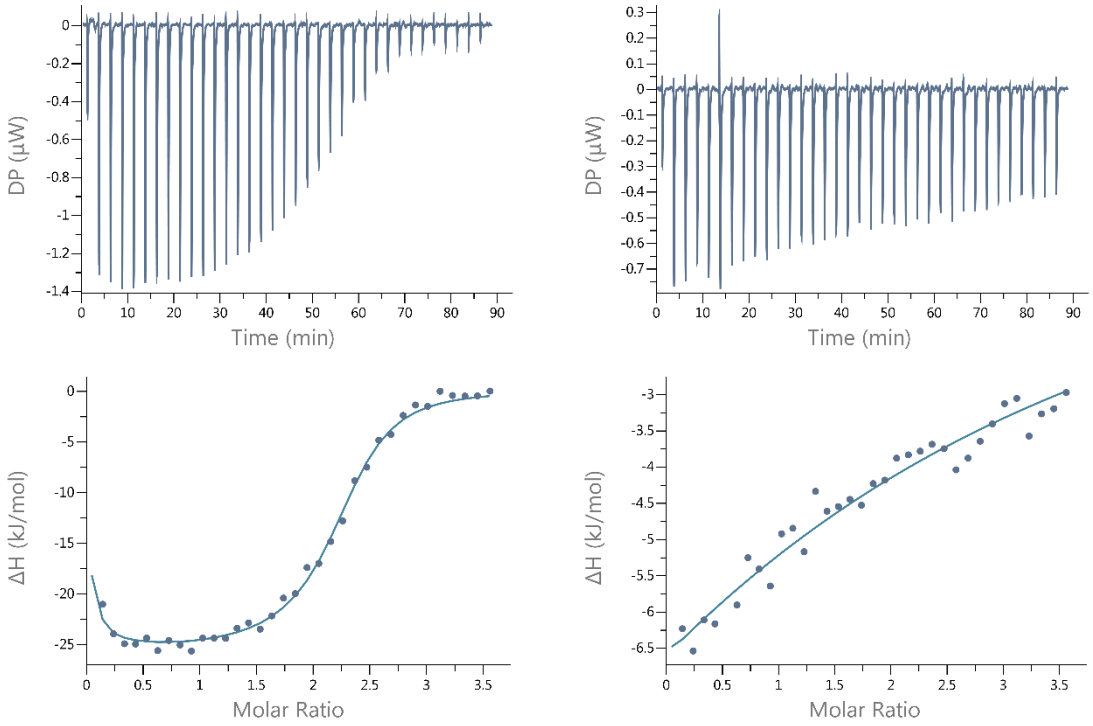

Figure 59 Left: NaI (0.025 mM) titrated with 3.1c (0.5 mM). Right: NaI (0.05 mM) titrated with 3.1d (1 mM).

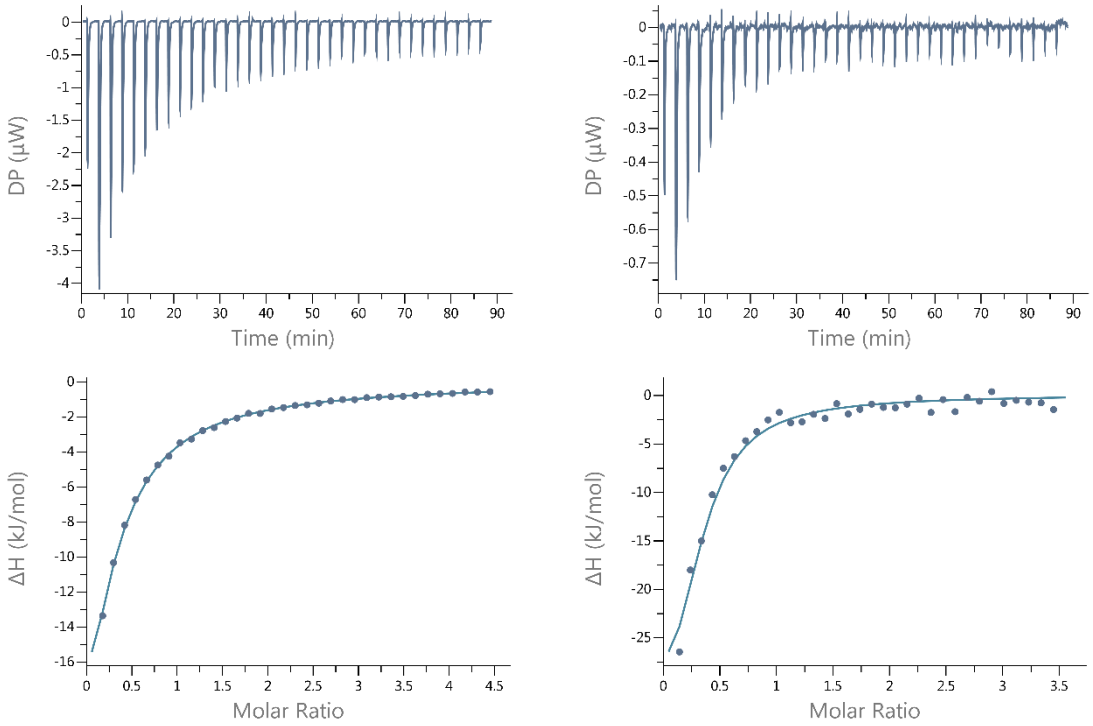

Figure 60 Left: 3.2 (0.2 mM) titrated with NaI (5 mM). Right: 3.2$_I$ (0.025 mM) titrated with NaI (0.5 mM).

3.3.2 Investigation of the binding mode by diffusion-ordered NMR

Diffusion-ordered ^{1}H NMR (DOSY) was used to study the anion binding mode of the receptors in water. To this end, diffusion coefficients D (D_2O, 298 K) were measured for all receptors **3.1a**–**e**, **3.1a$_H$**, **3.2** and **3.2$_I$** in absence and in presence of NaI (Table 3). Additionally, **3.1a**, **3.1a$_H$** and **3.2** were analysed in the presence of all anions for which a significant interaction was found by ITC (Table 4). Due to significant broadening of the receptor NMR signals in D_2O, D values were determined using a single integral over the major part of the aliphatic region (typically 3.8 – 2.9 ppm), containing most of the signals from tri(ethylene glycol) chains. Additionally, diffusion coefficients in D_2O were recorded for two different samples of poly(ethylene glycol) (weight-average molecular weight M_w = 2050 and M_w = 4600).

For PEG in water, a linear dependency between logD and logM_w has been demonstrated.[239] Parameters a and b in the equation $logD = a * logM_w + b$ can be determined using diffusion coefficients of two different PEGs of known M_w. Obtained parameters (a = −0.55, b = −8.02) were in agreement with the literature values.[239,240] Dependency determined in this way can then be used to calculate M_w corresponding to the diffusion coefficient of the investigated anion receptor. This quantity will be referred to as "PEG equivalent molecular weight" (M_{eq}). While this figure does not directly correspond to the molecular weight of an anion receptor or its complexes, changes in M_{eq} upon addition of guest species are indicative of the presence and extent of aggregation. Calculated values of M_{eq} for anion receptors in the presence of I^- and other guests are shown in Table 3 and Table 4.

The results clearly confirm the 2:1 host/guest binding mode in XB receptors. In receptors **3.1a**–**c** a close to 2-fold increase in M_{eq} was seen upon addition of NaI. In the case of **3.1e** a smaller increase was observed, while with **3.1d** the M_{eq} remained approximately constant. Taking into account the ITC results, this indicated that less pronounced 2:1 association occurs in these two receptors. In **3.1a$_H$** a decrease of M_{eq} was observed. This can be attributed to the conformational change upon I^-

binding and shows no evidence of binding stoichiometry higher than 1:1. The ChB receptor **3.2** displayed a M_{eq} of 5555 in the presence of 5 eq of NaI, which is consistent with the 2:1 stoichiometric complex.

Table 3 Diffusion coefficients and M_{eq} values for anion receptors in D_2O (1 mM for 3.1a–d and 3.1a$_H$, 0.5 mM for 3.2) in the presence of NaI.

	0 eq NaI		0.5 eq NaI		2 eq NaI	
	D [m²/s]	**M_{eq} [g/mol]**	**D [m²/s]**	**M_{eq} [g/mol]**	**D [m²/s]**	**M_{eq} [g/mol]**
3.1a	1.227×10^{-10}	2812	8.418×10^{-11}	5593	9.301×10^{-11}	4662
3.1b	1.276×10^{-10}	2618	1.073×10^{-10}	3592	8.796×10^{-11}	5163
3.1c	1.182×10^{-10}	3011	8.700×10^{-11}	5267	8.499×10^{-11}	5497
3.1d	1.174×10^{-10}	3048	1.219×10^{-10}	2846	1.201×10^{-10}	2924
3.1e	1.575×10^{-10}	1783	1.448×10^{-10}	2079	1.385×10^{-10}	2254
3.1a$_H$	1.303×10^{-10}	2520	1.483×10^{-10}	1990	1.529×10^{-10}	1882
3.2	---[a]	---[a]	---[a]	---[a]	8.450×10^{-11}	5555

[a]Could not be done due to the low solubility of 2_{Te}.

When anions other than I^- were added to **3.1a** and **3.2**, increases in M_{eq} not exceeding two times the M_{eq} of **3.1a** in absence of guest were observed. This confirms that the 2:1 binding mode occurs in all cases with these two receptors (the only exception was ClO_4^- binding by **3.1a** where 2:1 association likely occurs to a small extent). With **3.1a$_H$** the M_{eq} values recorded in the presence of anions never exceeded the base M_{eq} of the receptor which confirmed the 1:1 binding stoichiometry.

Receptor **3.1c** provided unexpected results. With ReO_4^- it displayed no trace of 2:1 complexation, while with Br^- very low diffusion coefficients were recorded which corresponded to M_{eq} of ca. 15000. This indicated that a binding stoichiometry higher than 2:1 was present, where the dominant species likely contains five molecules of **3.1c**. These maverick results highlight the importance of confirming the binding stoichiometry before analysing the binding information obtained from ITC.

Table 4 Diffusion coefficients and M_{eq} values for selected anion receptors in D_2O (1 mM for 3.1a, 3.1a$_H$, 0.5 mM for 3.2, 0.2 mM for 3.2$_I$) in the presence of anions that displayed significant binding as determined by ITC.

	Additive	D [m^2/s]	M_{eq} [g/mol]
3.1a	$NaReO_4$ 0.5 eq	1.088×10^{-10}	3502
	$NaReO_4$ 2 eq	1.009×10^{-10}	4019
	NaSCN 0.5 eq	1.277×10^{-10}	2614
	NaSCN 2 eq	1.188×10^{-10}	2983
	NaBr 0.5 eq	1.216×10^{-10}	2859
	NaBr 2 eq	1.101×10^{-10}	3427
	$NaClO_4$ 0.5 eq	1.280×10^{-10}	2603
	$NaClO_4$ 2 eq	1.257×10^{-10}	2691
3.1a$_H$	NaCl 0.5 eq	1.382×10^{-10}	2263
	NaCl 2 eq	1.382×10^{-10}	2263
	NaSCN 0.5 eq	1.341×10^{-10}	2391
	NaSCN 2 eq	1.432×10^{-10}	2121
	NaBr 0.5 eq	1.461×10^{-10}	2045
	NaBr 2 eq	1.368×10^{-10}	2306
	$NaClO_4$ 0.5 eq	1.408×10^{-10}	2188
	$NaClO_4$ 2 eq	1.536×10^{-10}	1866
	$NaNO_3$ 0.5 eq	1.369×10^{-10}	2303
	$NaNO_3$ 2 eq	1.425×10^{-10}	2140
	NaOAc 0.5 eq	1.306×10^{-10}	2509
	NaOAc 2 eq	1.355×10^{-10}	2346
3.2	$NaReO_4$ 5 eq	1.041×10^{-10}	3796
	NaSCN 5 eq	1.144×10^{-10}	3196
3.1c	$NaReO_4$ 0.5 eq	1.229×10^{-10}	2804
	$NaReO_4$ 2 eq	1.275×10^{-10}	2622
	NaSCN 0.5 eq	9.971×10^{-11}	4107
	NaSCN 2 eq	1.067×10^{-10}	3629
	NaBr 0.5 eq	4.852×10^{-11}	15290
	NaBr 2 eq	4.952×10^{-11}	14732

3.3.3 Results and discussion

ITC and DOSY experiments revealed 2:1 host-guest binding stoichiometry for **3.1a**–**d**, **3.2**$_I$, and **3.2** with I^-, the same was observed in titrations of **3.1a** and **3.2** with other binding anions. The HB receptor **3.1a**$_H$, on the other hand, was found to bind only in 1:1 stoichiometry. This can be explained by the highly different steric bulk of HB and σ-hole donor atoms. In the case of **3.1a**$_H$, the guest anion can be bound in the plane of the folded receptor backbone similarly to the known triazolophane[214,241] and foldamer[93,94] receptors. In XB and ChB receptors, the large size of convergent I or TeMe units results in a capped binding geometry, as was observed in the solid state in Chapter 2. This allows for coordination of a second receptor molecule to the guest anion. As this reduces the exposure of the phenylene-triazole receptor backbones to solvent, 2:1 binding can be expected to be favoured in water.

As shown in Figure 61 for **3.1a**, this stepwise binding consists of an enthalpy-driven formation of a 1:1 complex followed by entropy-driven coordination of another receptor molecule. In the first binding equilibrium four strong halogen bonds are formed while the open complex geometry allows I^- to remain partially hydrated, resulting in a strong exothermic effect. At the same time, an entropic penalty is incurred due to immobilisation of I^- and the conformational rigidification of **3.1a**.

In the second equilibrium, formation of new XB-anion interactions is likely less efficient due to the steric crowding and conformational restriction. It is thus offset by the enthalpic penalty which can be explained by the dehydration of I^-, leading to the net positive ΔH. This binding event is therefore driven by favourable entropy associated with the release of ordered H_2O molecules interacting with I^- and also partial dehydration of the receptor molecules.

A similar breakdown of thermodynamic signatures was observed for **3.2**$_I$ and **3.2** (Figure 61). Compared to **3.1a** a notably smaller exothermic effect and a smaller entropic penalty are observed in the first equilibrium. This may be explained by the less hydrophilic character of the outer rims of these molecules, which disfavours their folding into the 1:1 binding conformation.

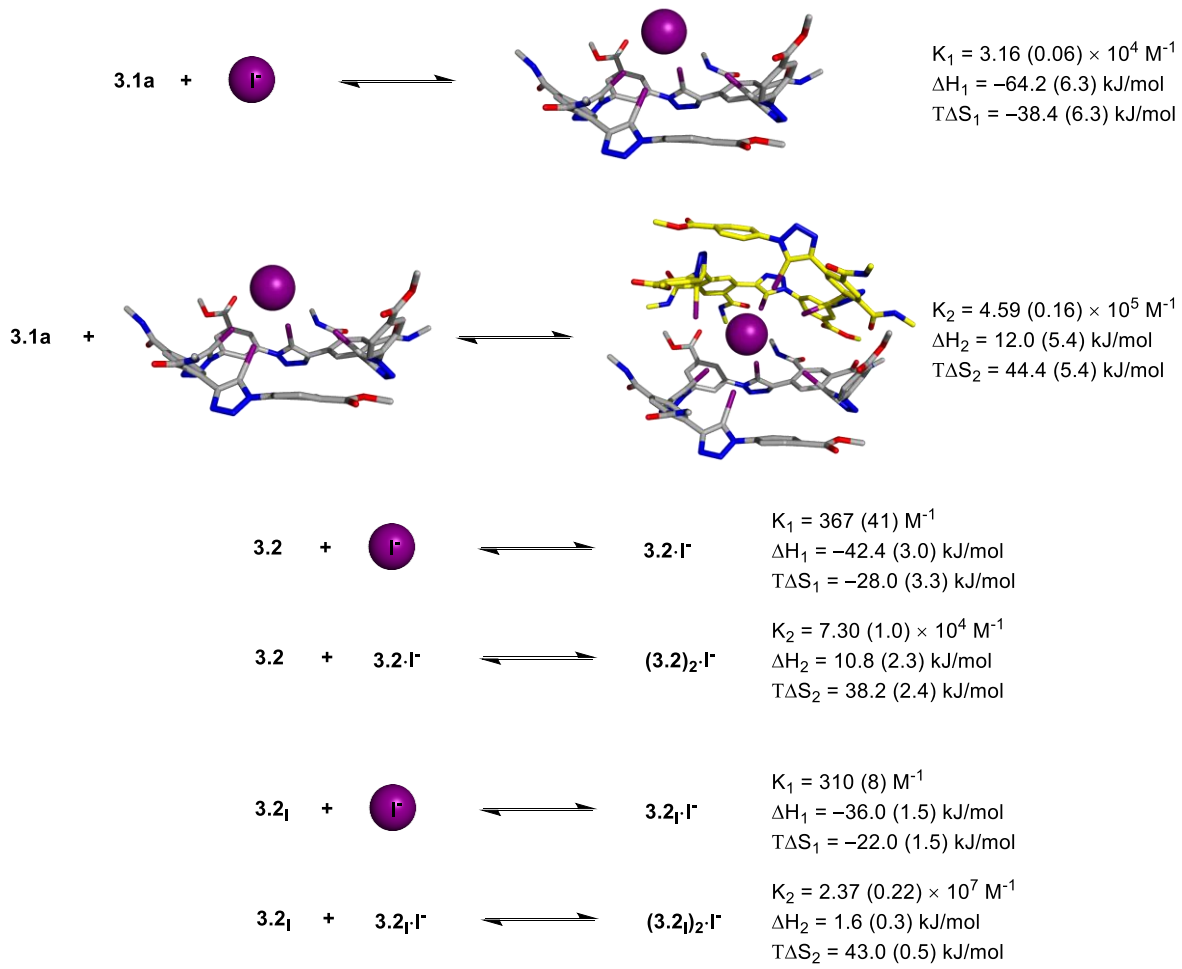

Figure 61 Equilibria and thermodynamic signatures of stepwise I^- binding in 2:1 host-guest stoichiometry shown for the receptors 3.1a, 3.2, and 3.2_I. For 3.1a the receptor model is shown with truncated solubilising chains.*

XB receptors **3.1a–d** displayed very high I^- affinity, with 2:1 complex formation constants (β_2) up to 1.68×10^{11} in the case of **3.1c** (Table 3). K_2 was 1-2 orders of magnitude higher than K_1 in **3.1a–c**, indicating a strong preference for 2:1 binding. In **3.1d** K_2 was exceptionally low, which is likely due to the large size of its termini sterically disfavouring the formation of 2:1 complex. The all-ester XB receptor $\mathbf{3.2_I}$ displayed a similar β_2 value to **3.1a**, however its binding was much more dominated by K_2. This may be attributed to the all-ester outer rim of $\mathbf{3.2_I}$ being less hydrophilic than the mixed ester-amide pattern of **3.1a**. This can be expected to disfavour the folding of $\mathbf{3.2_I}$ into a 1:1 binding

* The structure of 2:1 complex between **3.1a** and I^- shown here is the result of a preliminary MD simulation done by Igor Marques and Vitor Félix.

conformation but enhance the hydrophobic collapse into a 2:1 complex. Additionally, the higher entropic contribution in **3.2$_I$** and **3.2** can be explained by the release of water molecules weakly interacting with their ester groups.

In all XB and ChB receptors I^- binding was mainly enthalpy-driven with overall ΔH of 2:1 binding in the range of −30 to −55 kJ/mol. This indicates that there is little interaction between σ-hole donors and water, and the negative ΔH results from XB or ChB formation with weakly hydrated I^-. Additionally, further enthalpic contribution may arise from water-water HB upon formation of host-guest complexes. Unusually low enthalpic contribution in **3.1b** is an indication that the XB contacts from its outer iodotriazoles are disrupted by the steric bulk of its naphthaleneimide termini. At the same time, restricted rotation of these termini relative to the iodotriazoles is an explanation for a higher TΔS. In **3.1d** the naphthaleneimide units are separated from iodotriazoles, leading to similar ΔH as in **3.1a** and **3.1c**. Their larger size and additional degrees of freedom accounts for the negative TΔS observed for **3.1d**.

Table 5 ITC equilibria and thermodynamics of I^- binding by XB anion receptors 3.1a–d (298 K) and 3.2$_I$ (293 K), ChB receptor 3.2 (293 K), and HB receptor 3.1a$_H$ (298 K).

	β_2 [M]$^{-2}$	K_1 [M^{-1}]	K_2 [M^{-1}]	ΔH [kJ/mol]	TΔS [kJ/mol]
3.1a	1.45 (0.04) × 10^{10}	3.16 (0.06) × 10^4	4.59 (0.16) × 10^5	−52.2 (1.0)	5.9 (1.0)
3.1b	8.68 (2.18) × 10^9	1.60 (0.37) × 10^4	5.54 (1.32) × 10^5	−38.3 (2.1)	18.4 (2.7)
3.1c	1.68 (0.14) × 10^{11}	4.77 (0.40) × 10^4	3.53 (0.24) × 10^6	−55.3 (0.9)	8.8 (1.0)
3.1d	7.47 (0.57) × 10^6	4.87 (0.52) × 10^3	1.54 (0.11) × 10^3	−52.5 (1.8)	−13.3 (1.6)
3.2	2.64 (0.05) × 10^7	3.67 (0.41) × 10^2	7.30 (1.00) × 10^4	−31.6 (2.3)	10.1 (2.2)
3.2$_I$	7.33 (0.57) × 10^9	3.10 (0.08) × 10^2	2.37 (0.22) × 10^7	−34.5 (1.4)	21.0 (1.6)
3.1a$_H$	---[a]	3876 (21)	---[a]	−23.2 (0.1)	-2.7 (0.1)

Table 1. Uncertainties are given in parentheses Uncertainties are given in parentheses and correspond to the standard deviation of three experiments. [a]1:1 binding stoichiometry.

The ChB receptor **3.2** displayed a similar binding pattern to **3.2$_I$** albeit with much lower K_2. Formation of 2:1 complex by **3.2** is disfavoured by the additional steric bulk of Te-bound CH_3 groups. As the K_1 and ΔH values are similar in **3.2** and **3.2$_I$**, it follows that the XB and ChB interactions with

I^- must have a comparable strength and enthalpically driven character. The presence of ChB with I^- was confirmed by observing large downfield changes in ^{125}Te chemical shifts (Δδ) upon titration with TBAI in CD_3CN (Figure 62). A fit of binding isotherms based on this NMR titration revealed a low 1:1 stoichiometric K_a of 96.8 (0.6) M^{-1}. Combined with the low Δδ shifts of the outer Te atoms relatively to the inner Te, this implies that in CD_3CN there is no solvophobic effect to drive the folding and 2:1 association of **3.2**. In water however, hydrophobic collapse stabilises the 1:1 and especially 2:1 bound states, prevailing over the weak solvation of I^-.

Interestingly, the downfield movement of ^{125}Te signals observed here is in contrast to the upfield shifts observed in the previously reported ChB rotaxanes based on MeTe- and MeSe-triazoles.[135] In this literature example introduction of negative charge upon halide binding was proposed to account for the upfield shifts. The effect was the largest with Cl^- compared to Br^- and I^-, implying that anions with lower charge density have a reduced influence on the shielding of Te or Se nuclei. In the case of **3.2**, the downfield shifts observed indicate that with I^- in a tetradentate binding mode the additional negative charge is too diffuse to cause a significant increase of electron density around the Te atoms. Instead, this is evidence of a charge transfer contribution to I^- binding, which causes deshielding of the Te atoms by weakening the C-Te bonds opposite to the occupied σ-hole.

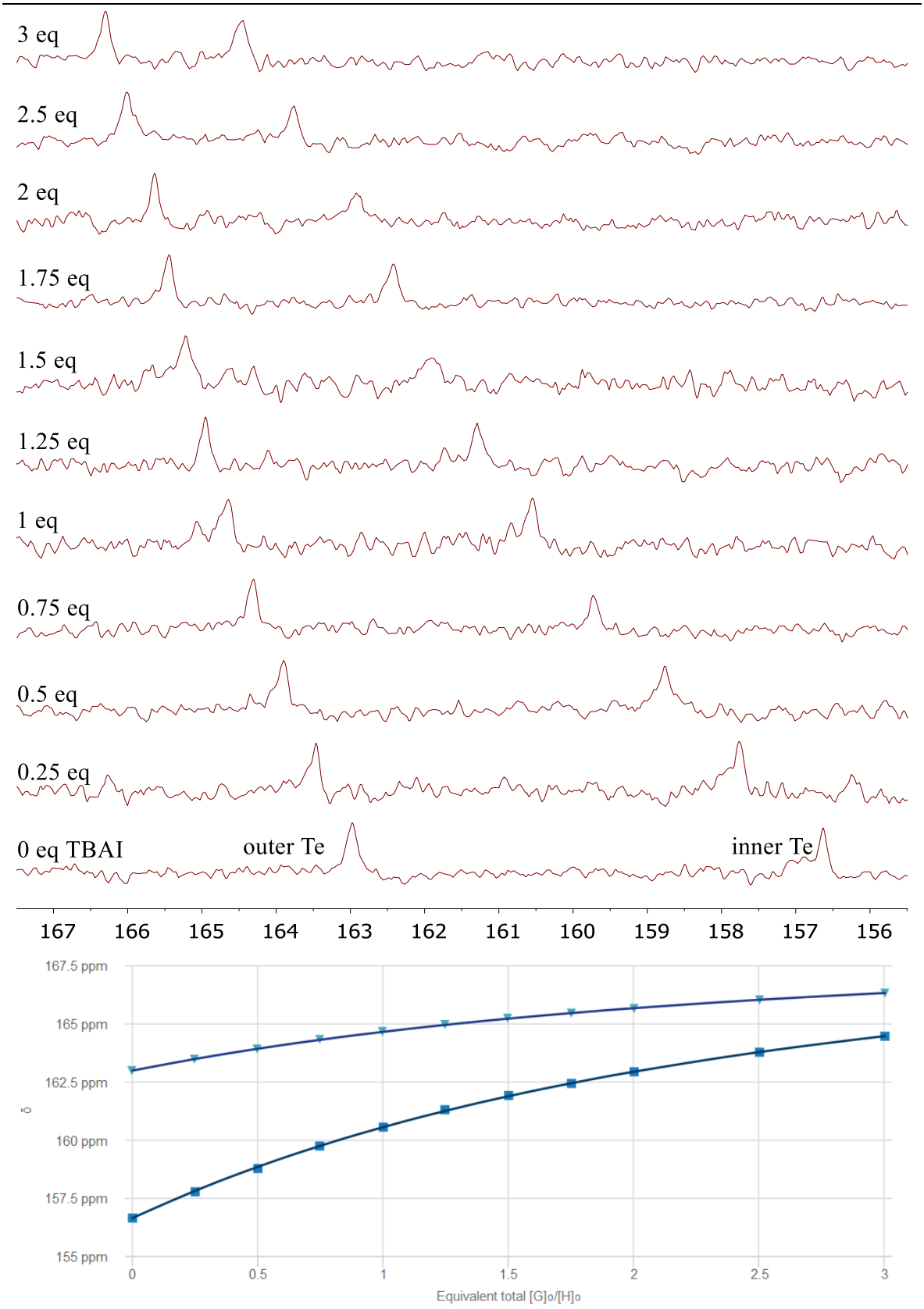

Figure 62 Changes of ^{125}Te chemical shifts of 3.2 (5 mM in CD_3CN, 298 K, 158 MHz) titrated with tetrabutylammonium iodide (TBAI) and the fit of binding isotherms for 1:1 association (Bindfit).

In the case of **3.1a$_H$** its 1:1 I^- association constant is lower than K_1 of **3.1a–d**, indicating a significantly weaker interaction than in XB receptors and a size mismatch with I^-. Due to its inability to form a 2:1 complex, **3.1a$_H$** exhibits a much lower overall I^- affinity than any of the XB or ChB analogues. Similarly to the σ-hole receptors, **3.1a$_H$** displays enthalpic binding. This indicates that the weakly acidic C-H HB donor units of **3.1a$_H$** have very little attractive interaction with water molecules.

Table 6 Affinities of 3.1a, 3.2 and 3.1a$_H$ for a range of anions.

Host	Guest	β_2 [M^{-2}]	K_1 [M^{-1}]	K_2 [M^{-1}]	ΔH [kJ/mol]	TΔS [kJ/mol]
3.1$_a$	NaI	1.45 (0.04) × 10^{10}	3.16 (0.06) × 10^4	4.59 (0.16) × 10^5	−52.2 (1.0)	5.9 (1.0)
	NaBr	3.43 (0.50) × 10^6	1.03 (0.13) × 10^3	3.34 (0.45) × 10^3	−25.6 (1.1)	11.7 (1.4)
	NaCl	nb	nb	nb	nb	nb
	$NaReO_4$	6.66 (0.67) × 10^8	4.91 (0.22) × 10^4	1.35 (0.08) × 10^4	−20.3 (0.5)	30.1 (0.3)
	NaSCN	3.40 (0.17) × 10^7	5.38 (0.22) × 10^3	6.33 (0.55) × 10^3	−31.0 (0.9)	12.1 (0.8)
	$NaClO_4$	1.21 (0.14) × 10^5	5.55 (0.74) × 10^1	2.19 (0.09) × 10^3	−29.4 (3.2)	−0.4 (3.4)
3.2	NaI	2.64 (0.05) × 10^7	3.67 (0.41) × 10^2	7.30 (1.00) × 10^4	−31.6 (2.3)	10.1 (2.2)
	NaBr	1.26 (0.70) × 10^3	1.69 (0.55) × 10^2	6.94 (1.56) × 10^0	−13.9 (6.0)	3.2 (6.8)
	NaCl	nb	nb	nb	nb	nb
	$NaReO_4$	1.58 (0.11) × 10^6	1.84 (0.18) × 10^2	8.67 (1.09) × 10^3	−25.4 (2.5)	9.4 (2.5)
	NaSCN	5.70 (0.25) × 10^6	4.92 (0.12) × 10^2	1.16 (0.05) × 10^4	−2.0 (0.5)	35.9 (0.5)
	$NaClO_4$	nb	nb	nb	nb	nb
3.1a$_H$	NaI		3876 (21)		−23.2 (0.1)	-2.7 (0.1)
	NaBr		---[c]		---[c]	---[c]
	NaCl		3367 (983)		−0.5 (0.1)	19.7 (0.7)
	$NaReO_4$		nd		nb	nb
	NaSCN		346 (14)		−21.7 (0.5)	-7.2 (0.6)
	$NaClO_4$		2000 (14)		−23.3 (0.1)	-4.5 (0.1)

nb – no binding (too weak to quantify). Uncertainties are given in parentheses and correspond to the standard deviation of three experiments. [a]Formation constants of 2:1 host-guest complex (β_2, M^{-2}). [b]Association constants of 1:1 host-guest complex (K_a, M^{-1}). [c]No satisfactory 1:1 fit obtained, possible complex binding equilibria.

Apart from strong I^- binding the σ-hole receptors **3.1a** and **3.2** showed a general preference for binding weakly hydrated anions such as SCN^- and ReO_4^- (Table 6). In **3.1a** high selectivity for I^- (ΔH_{hyd} = −325 kJ/mol) over SCN^- and ClO_4^- (ΔH_{hyd} = −310, −229 kJ/mol, respectively)[13] indicates that

shape and size complementarity effects are present. In **3.2** this selectivity is less pronounced and compared to **3.1a** it has a higher affinity for SCN^- relative to I^- and Br^-. Additionally, SCN^- binding by **3.2** is predominantly entropy-driven, which presumably results from formation of strong ChB contacts only with the S atom of SCN^-, leaving one receptor molecule bound only via hydrophobic interactions.

Compared to the σ-hole receptors, the HB analogue **3.1a$_H$** displayed a weaker and less selective anion binding ability. Being weakly selective for I^-, it also bound Cl^- as well as the more hydrophilic AcO^-. Interestingly, no ReO_4^- binding was observed, which is probably due to a strong size mismatch. Overall the anion recognition capability of **3.1a$_H$** was much lower than that of XB receptors **3.1a**–**d** as well as the ChB analogue **3.2**.

3.4 Fluorescent anion sensing

Compounds **3.1b**–**d** incorporate fluorophores in their termini, which were introduced in search for fluorescent output upon anion binding. These receptors were subjected to titrations with NaI monitored by fluorescence spectroscopy. In each case fluorescence spectra were recorded in the presence of 0 – 100 eq NaI. In all experiments the titrant contained the respective receptor at the same concentration as in the sample to avoid dilution. While **3.1b** and **3.1c** showed little to no response upon titration with NaI (Figure 63, Figure 64), **3.1d** displayed a nearly 2-fold enhancement of emission intensity (Figure 65). A small shift of emission maximum from 564 nm to 558 nm was also observed. Fluorescence enhancement most likely results from restriction of intramolecular motion[242] upon I^- complex formation. Specifically, slower rotation around the naphthalene – tertiary amine bonds of the 4-aminonaphthaleneimide units is likely to suppress non-radiative decay and increase emission intensity.

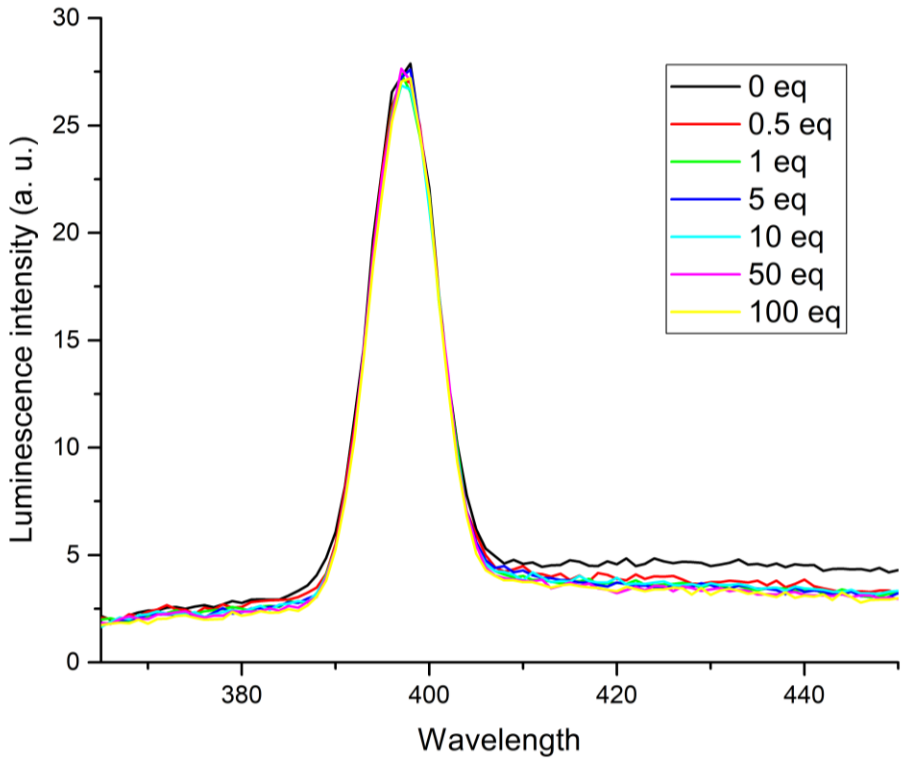

Figure 63 Receptor 3.1b (2 µM) titrated with 0 – 100 equivalents of NaI. λ_{ex} = 350 nm.

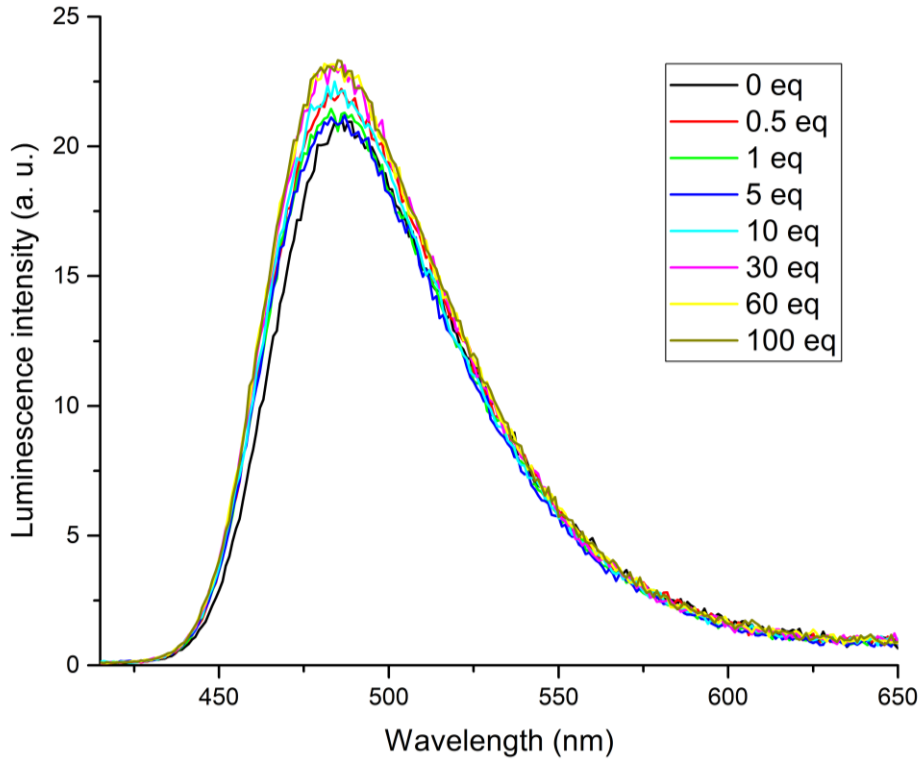

Figure 64 Receptor 3.1c (5 µM) titrated with 0 – 100 equivalents of NaI. λ_{ex} = 400 nm.

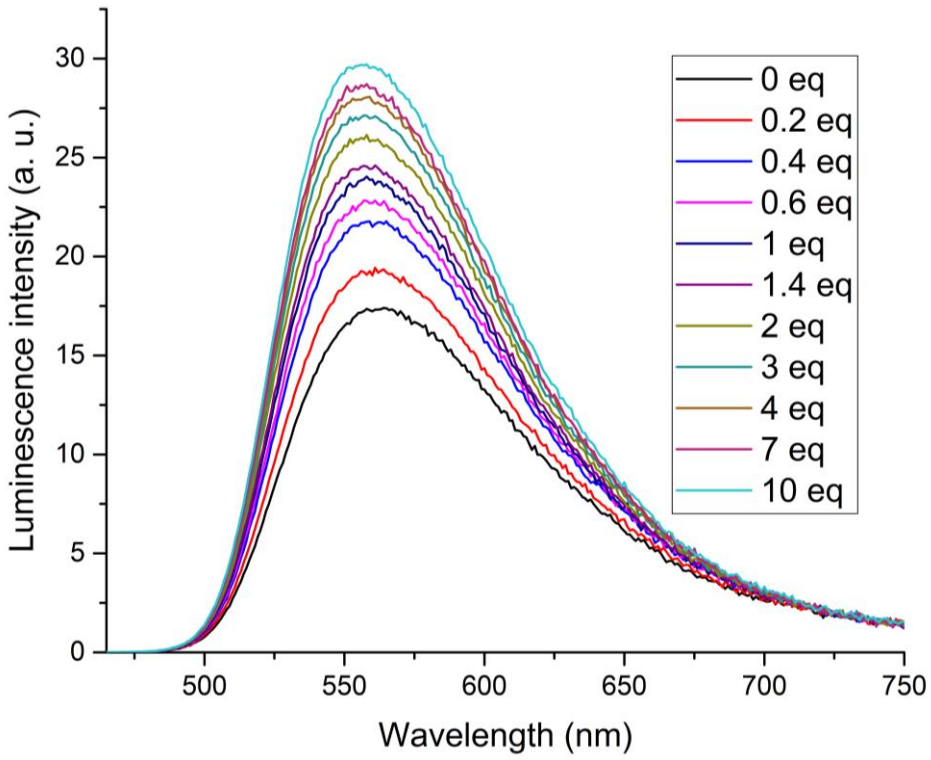

Figure 65 Receptor 3.1d (100 µM) titrated with 0 – 10 equivalents of NaI. λ_{ex} = 442 nm.

3.5 Electrochemical sensing*

The XB receptor structure developed in this work was applied to electrochemical anion sensing. To this end, electrode surface-bound XB receptor and a solution-phase redox-responsive analogue were investigated. In particular, the XB surface layers are unprecedented in sensing applications and present a possibility of reagentless sensing of anions in solution.

3.5.1 Synthesis

XB and HB anion receptors for electrode surface functionalisation were prepared using the same approach as the solution-based analogues (Scheme 21). Starting with the bis-azide core **3.32**, XB and HB receptors **3.34** and **3.34$_H$** with a free alcohol-terminated chain were obtained. These were then conjugated with lipoic acid to afford compounds **3.35** and **3.35$_H$** carrying a cyclic disulfide functionality suitable for attachment to a gold electrode surface.

*This work was done in cooperation with Robert Hein who contributed all electrochemical analysis work, the final synthetic step towards **3.35** and **3.35$_H$** (lipoic acid esterification), and the preparation of **3.36**.

The XB receptor **3.39** with ferrocene termini designed for voltammetric anion sensing was derived from the azide precursor **3.36** (Scheme 22). In the first CuAAC step the ester-bound solubilising group was displaced in a nucleophilic substitution reaction with MeOH during the chromatographic purification. The synthesis was continued regardless, leading to **3.39**.

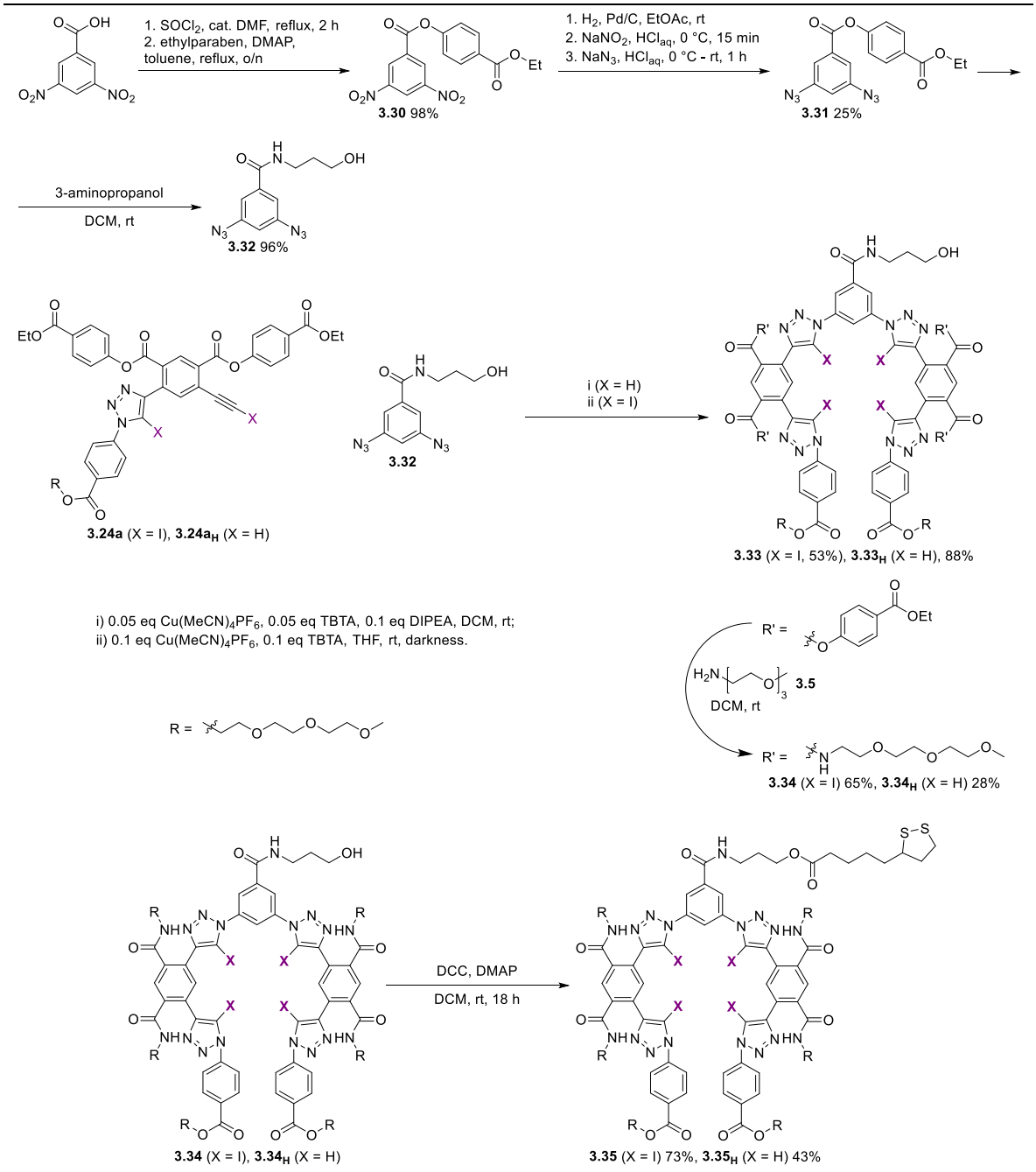

Scheme 21 Synthesis of XB and HB receptors for electrode surface functionalisation.

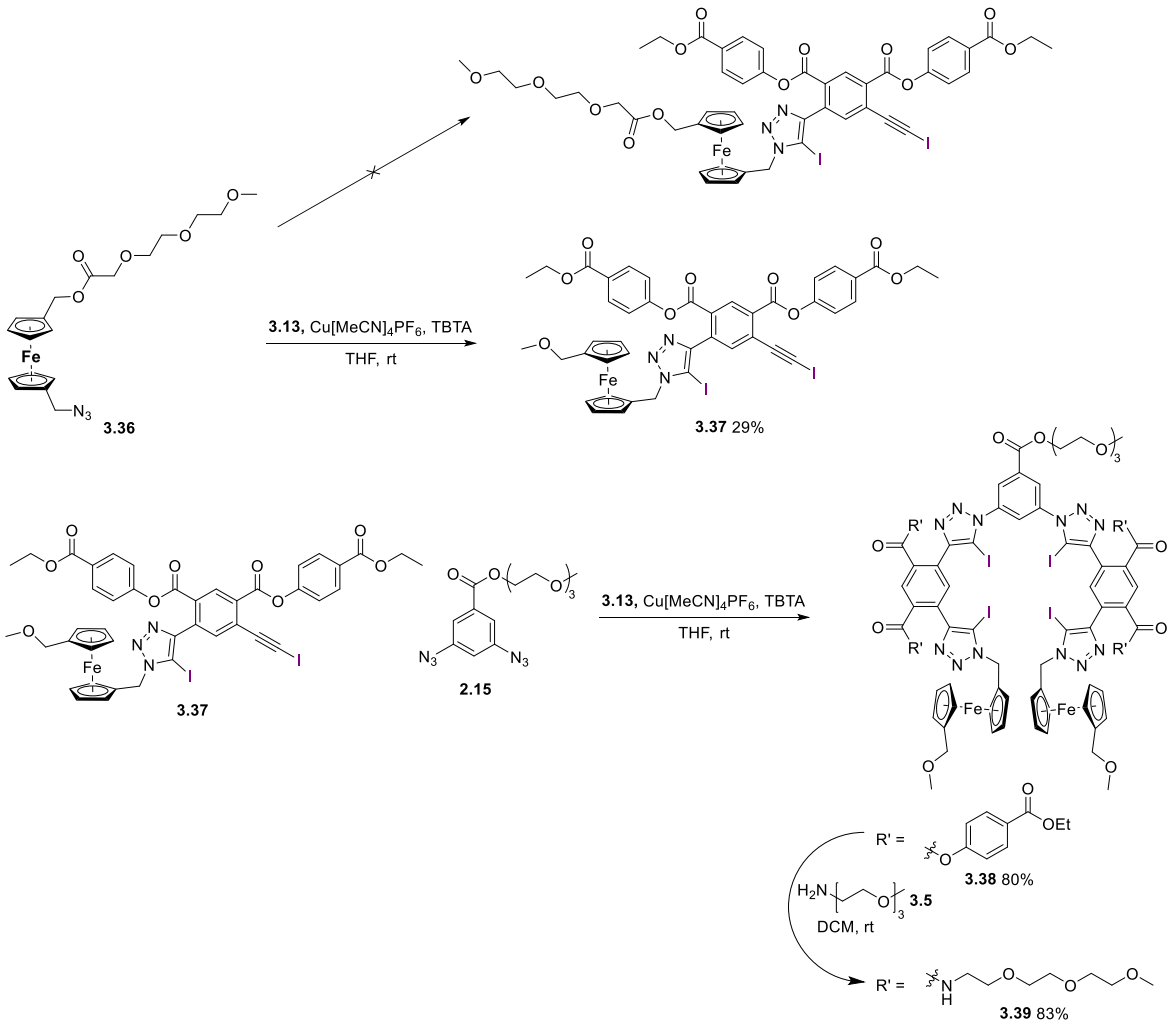

Scheme 22 Synthesis of the ferrocene-terminated XB receptor 3.39.

3.5.2 Capacitive anion sensing

Treatment of gold disk electrodes with a solution of **3.35** or **3.35$_H$** (1:1 MeCN/H_2O, rt, o/n) resulted in the formation of a self-assembled monolayer (SAM) on the gold surface. The thickness of the resulting layers measured by ellipsometry was 3.22 (0.21) nm for **3.35** and 3.51 (0.40) nm for **3.35$_H$**, which is in good agreement with monolayer formation. Analysis of the elemental composition of the SAMs by X-ray photoelectron spectroscopy (XPS) provided relative abundances of C, N, O, S, and I in very good agreement with the theoretical elemental composition of **3.35** and **3.35$_H$** (Table 7). In particular, XPS signals due to I 3d electrons were observed only in the SAM made using **3.35** (see Appendix C).

Table 7 Experimental and theoretical elemental composition of SAMs determined by XPS.

	3.35-SAM		**3.35_H-SAM**	
	Experimental[a]	Theoretical	Experimental	Theoretical
C	93.92 (8.69)	98	101.86 (5.17)	98
N	16.65 (3.42)	17	16.68 (1.25)	17
O	25.47 (2.48)	29	28.33 (1.02)	29
S	2 (0.46)	2	2 (0.39)	2
I	3.54 (0.24)	4	-	-

[a]Values were normalized to S = 2. Errors represent one standard deviation of triplicate measurements.

Further characterisation using reductive stripping voltammetry revealed a surface coverage of 8.85 (1.70) × 10^{-11} mol/cm^2 for **3.35**-SAM and 6.40 (1.60) × 10^{-11} mol/cm^2 for **3.35_H**-SAM. These values translate into a molecular footprint of ca. 2 nm^2 for each receptor molecule. Additionally, no Faradaic activity was observed in cyclic voltammetry of **3.35**-SAM in 100 mM NaCl or in the presence of 10 mM $Fe(CN)_6^{3-/4-}$ (see Appendix C). This proved that the respective SAM was densely packed and had a high resistance.

Response of the SAMs to the presence of anionic analytes was then sought using electrochemical impedance spectroscopy (EIS). In this technique, an alternating potential with a very small amplitude (normally 1 – 10 mV) and variable frequency is applied to the electrode. Impedance of the interface can then be measured. In this case impedance was not very sensitive to the presence of weakly hydrated anions expected to bind to the **3.35**-SAM. However, capacitive analysis provided a strong response to anionic analytes. This is done by processing the impedimetric data via $C''(\omega) = Z'/\omega Z^2$ and $C'(\omega) = Z''/\omega Z^2$ (Figure 66).

Using the resulting capacitive Nyquist plot, film capacitance can be obtained as the intercept of its hemispherical region (extrapolated by fitting to a semicircle) with the x axis. In **3.35**-SAM this parameter exhibited a significant increase in the presence of weakly hydrated anions in water containing 100 mM NaCl (Figure 67), thus mirroring the anion coordination ability of solution-based

receptors. Interestingly, ReO_4^- caused the highest increase in capacitance, reaching up to ca. 36%. This effect can be explained by an increase in dielectric constant of the film* upon binding of anions.

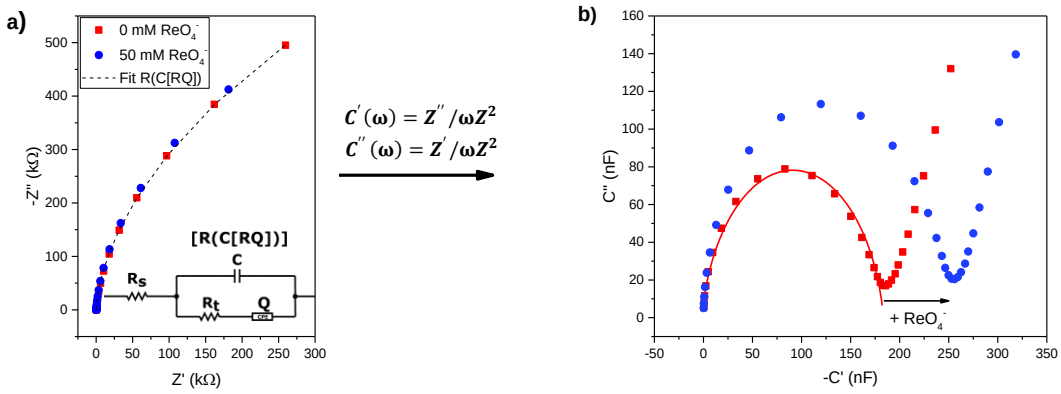

Figure 66 EIS/ECS response of 3.35-SAM on gold disk electrode in 100 mM NaCl at open-circuit potential (OCP, ≈ 0 V) in absence (red squares) and presence (blue circles) of 50 mM perrhenate. a) Impedimetric Nyquist plot and fitting to the equivalent circuit $R_S(C[R_TQ])$.† Transformation of impedimetric data via $C''(\omega) = Z'/\omega Z^2$ and $C'(\omega) = Z''/\omega Z^2$ to obtain capacitive data. b) Capacitive Nyquist plot and fitting to a semicircle to obtain C as the x-intersect.

While **3.35$_H$**-SAM displayed capacitive response of comparable magnitude, it was significantly less sensitive than its XB counterpart. Fitting of Langmuir adsorption isotherm‡ to capacitance response data revealed lower binding constants, especially in the case of ReO_4^- (Table 8). Likewise, the limit of detection (LOD)§ was significantly lower for **3.35$_H$**-SAM. These large differences in capacitive response obtained from structurally similar SAMs confirm that the observed increase in capacitance is indeed due to anion binding to XB and HB donor units of **3.35** and **3.35$_H$**. In contrast, SAMs that do not contain specific anion binding sites tend to exhibit very small changes in capacitance in the presence of salts.

*According to the Helmholtz plate capacitor model, $C = \frac{\varepsilon_0 * \varepsilon_r * A}{d}$ where A – electroactive area, d – separation between the capacitor plates.

† R_S – solution resistance; C – film capacitance; R_T – translational resistive term arising from ionic ingress;[283] Q – a constant phase element.

‡ $\theta = \frac{K*[Anion]}{1+K*[Anion]}$; θ – occupation of surface binding sites, K – 1:1 association constant.

§ $LOD = \frac{3*\sigma_{C_0}}{s}$; σ_{C_0} – standard deviation of capacitance in absence of guest anion, s – slope of adsorption isotherm at the origin.

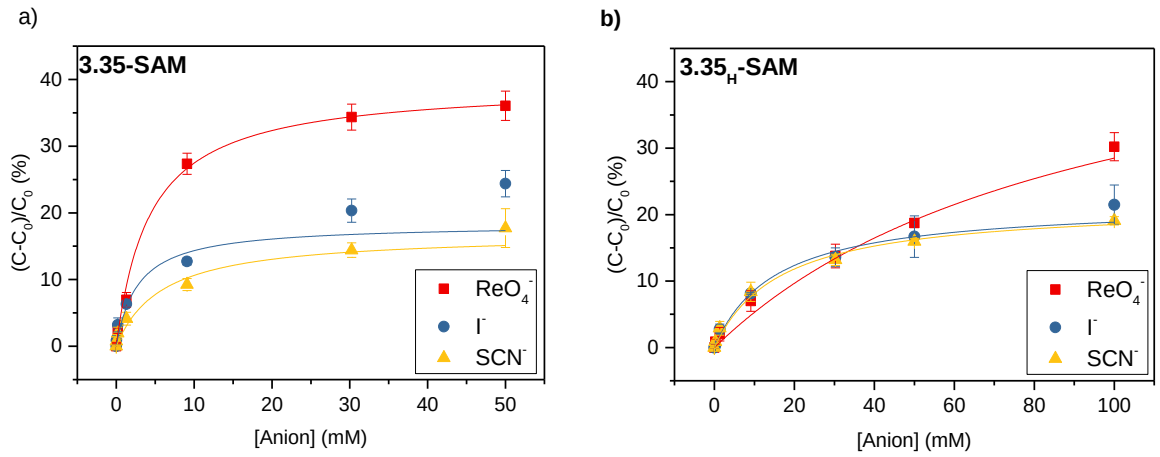

Figure 67 Normalized capacitance increase of 3.35-SAM (a) and 3.35$_H$-SAM (b) at OCP in the presence of increasing amounts of perrhenate (red squares), iodide (blue circles) and thiocyanate (yellow triangles). Fits were obtained according to a Langmuir adsorption model. Error bars represent one standard deviation across three separate electrodes. Note the difference concentration ranges for both graphs.

Binding affinities of the surface-anchored XB and HB receptors are much lower than of their solution-phase counterparts **3.1a** and **3.1a$_H$**. The most likely reason for this is the reduced ability of anion receptors to form multidentate binding sites as the molecules are conformationally restricted in the crowded SAM. In particular, formation of 2:1 complexes which accounts for the extremely high I^- affinity of **3.1**-type XB receptors is probably not possible in a SAM. A welcome effect of this relatively weak binding is the excellent selectivity for the best anionic guests. No significant response was observed upon addition of Br^-, ClO_4^-, and NO_3^-.

Table 8 Binding constants, limits of detection, and maximum increases in capacitance for relevant anions interacting with 3.35-SAM and 3.35$_H$-SAM.

	3.35-SAM			**3.35$_H$-SAM**		
Anion	K (M^{-1})	LOD (µM)	y_{max} (%)[a]	K (M^{-1})	LOD (µM)	y_{max} (%)[a]
ReO_4^-	231	28	39.3	11	80	55.6
I^-	362	14	18.3	66	47	21.7
SCN^-	170	42	16.9	61	113	21.5

[a]Maximum relative increase in SAM capacitance (adsorption isotherm extrapolated to [anion] = ∞).

3.5.3 Voltammetric sensing

Anion sensing via solution-phase voltammetry was investigated using the ferrocene-containing XB receptor **3.39** designed to provide a redox response in the presence of anions. Although **3.39** was soluble at 0.1 mM concentration in water containing 100 mM $NaPF_6$, strong adsorption onto glassy carbon as well as metal electrodes was observed. In MeCN no adsorption was seen, as shown by the linear dependence of anodic and cathodic peak currents on the square root of scan rate in cyclic voltammetry experiments (see Appendix C).

Cathodic shifts of the half-wave potential in the presence of Cl^- and Br^- were observed in MeCN (Figure 68) as determined by square wave voltammetry (SWV). Fitting a relationship between ΔE and anion affinity of the receptor* derived from the Nernst equation reveals an order of magnitude increase in binding affinity upon oxidation of the ferrocene termini of **3.39**.

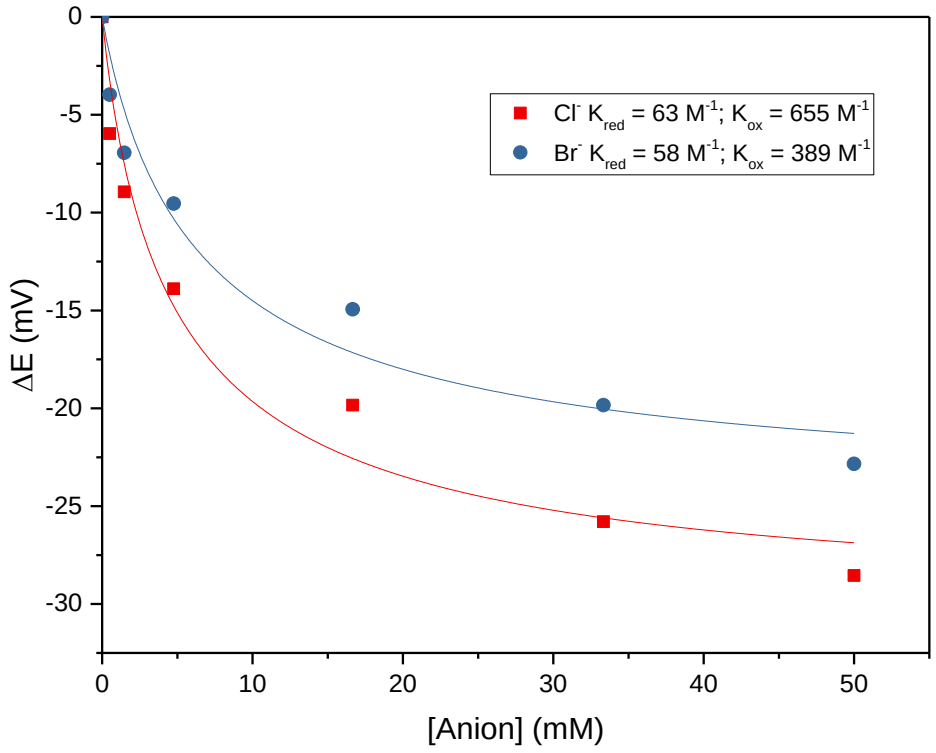

Figure 68 Changes of $E_{1/2}$ for 3.39 (0.1 mM) upon addition of Cl^- and Br^- (100 mM $TBAPF_6$/MeCN). Points: experimental data, lines: fitted equation for ΔE(K_{ox}, K_{red}).

* $\Delta E = -\frac{RT}{nF} * \ln\left(\frac{1+K_{Ox}*[Anion]}{1+K_{Red}*[Anion]}\right)$

3.6 Conclusions

A series of water-soluble, preorganised tetradentate XB receptors **3.1a–f** was prepared along with a ChB analogue **3.2**. An isostructural HB variant **3.1a$_H$** was also synthesised for comparison purposes. The σ-hole receptors were found to be highly selective for I^- in water. Predominantly enthalpic formation of a 2:1 stoichiometric host-guest complex occurred, driven by the XB or ChB interactions as well as hydrophobic collapse. Apart from I^-, the σ-hole receptors strongly bound the weakly hydrated ReO_4^- and SCN^-. Their selectivity for these guests was much more pronounced than in the case of the HB analogue. This work provides the first examples of charge-neutral anion receptors based exclusively on XB or ChB to be studied in pure water. The utility of these non-covalent interactions in the supramolecular toolbox for anion recognition in water is thus demonstrated.

Additionally, XB receptors with response capability were studied to show their applicability for anion sensing in water. A fluorescent host **3.1d** containing 4-aminonaphthaleneimide fluorophores displayed emission enhancement in the presence of I^-. A receptor anchored to gold electrode surface provided an anion-responsive SAM. The capacitance of such a modified electrode increased strongly in the presence of ReO_4^-; a less significant response was also observed with I^- and SCN^-. This provides a method of additive-free ReO_4^- sensing in water, which is likely to be applicable to TcO_4^-. The ferrocene-containing redox-active XB receptor **3.39** displayed a voltammetric response to halides in MeCN, although it could not be used for sensing in water.

A possibility for future work is the investigation of dimeric (octadentate) or extended (hexadentate) XB receptors that would exhibit anion binding assisted by hydrophobic collapse in 1:1 stoichiometry. Further studies of electrode surface-bound XB and ChB SAMs are also of interest.

Chapter 4 Biomimetic transesterification catalysis

4.1 Background

Carbonyl group substitution reactions of esters: hydrolysis, transesterification, and amidation are some of the simplest organic transformations. However, due to the low reactivity of most esters these processes tend to require harsh conditions such as the use of strong bases and elevated temperatures. Mild catalytic methods are highly desirable as they would open the access to finely chemoselective transformations of esters. Additionally, stereoselective reactions such as desymmetrising mono-hydrolysis of *meso*-diesters would be accessible.

Esterase and protease enzymes provide an excellent example of such mild transformation as they function under physiological temperature and pH conditions. These natural catalysts are often based on the Ser-His-Asp catalytic triad.[243] The activated Ser alcohol in this assembly undergoes a transesterification with a substrate ester (Scheme 23).[244] In the second step of the catalytic cycle, the acylated Ser residue is hydrolysed by an activated water molecule.[245]

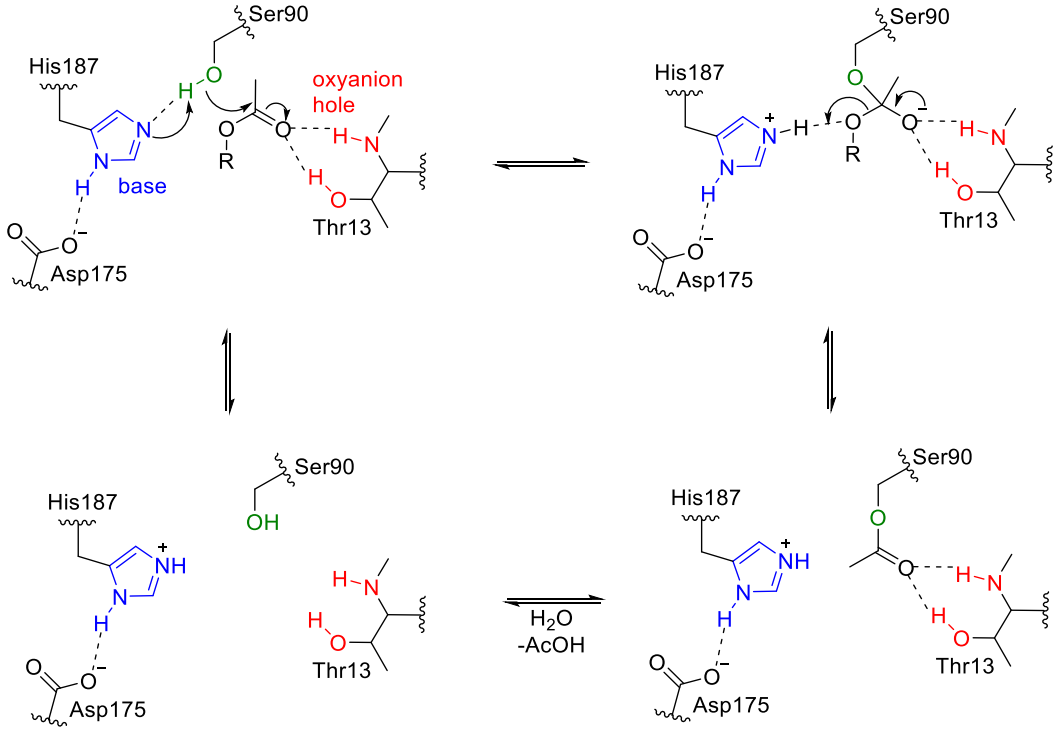

Scheme 23 Mechanism of the acetylxylan esterase of *Trichoderma reesei*.[244]

Enzymatic ester hydrolysis has proved synthetically useful. In particular, pig liver esterase has been applied to a wide range of desymmetrising hydrolysis reactions of diesters and kinetic resolutions of racemic esters, allowing highly enantioselective transformations in some cases.[246] To mimick the function of the Ser-His-Asp catalytic triad with a small-molecule organocatalyst and replicate the reactivity and stereoselectivity of esterases is a very ambitious objective with a high potential for synthetic applications.[247]

The two-step biomimetic mechanism has been demonstrated in certain synthetic organocatalysts (Scheme 24). However, the reported catalysts were limited to highly reactive ester substrates and their reactivity did not come close to that of esterase enzymes. Additionally, these literature precedents included only simple test reactions used for kinetic studies. No synthetic applications or stereoselective transformations have been demonstrated.

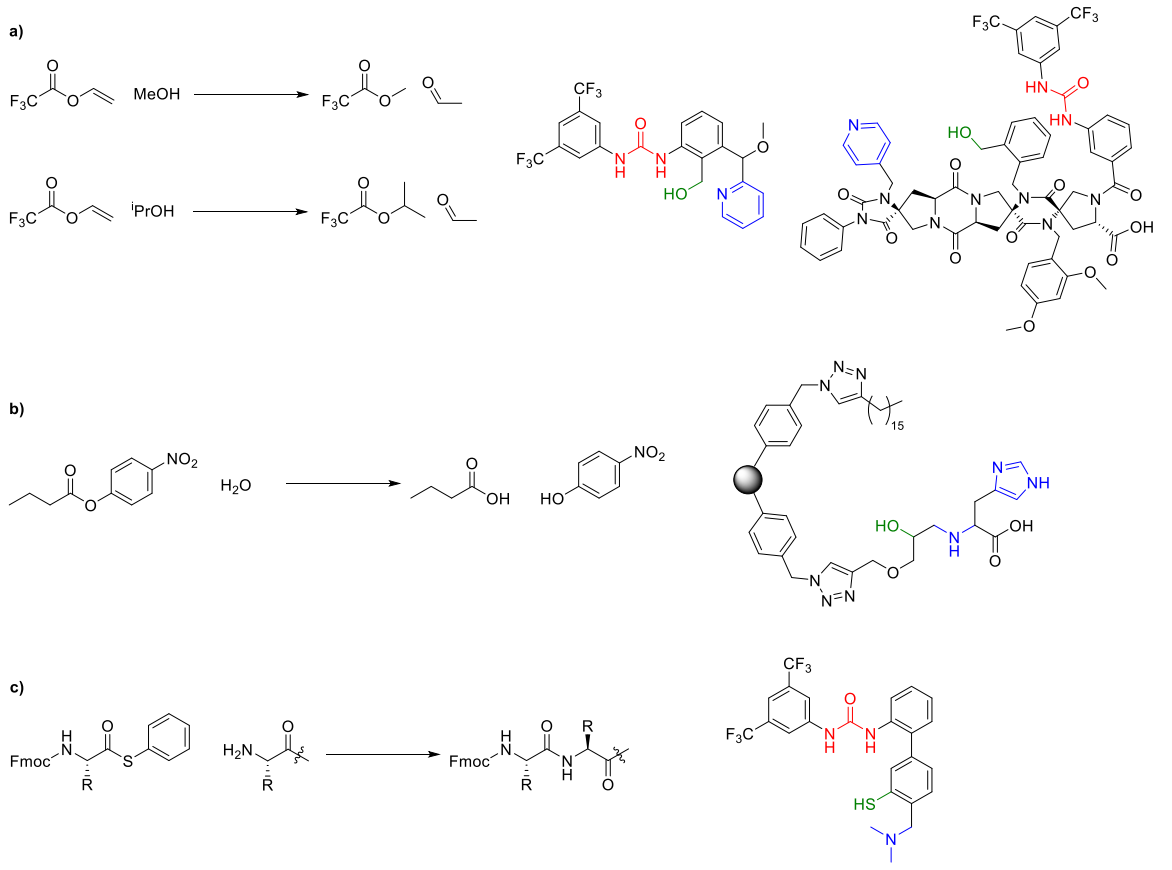

Scheme 24 Previously reported examples of biomimetic transesterifications.

Transesterification of vinyl trifluoroacetate with methanol and isopropanol was promoted by a trifunctional organocatalyst which contained an alcohol, a pyridine base, and a urea or thiourea oxyanion hole (Scheme 24a).[248] The two-step mechanism was confirmed and the kinetics of the first and second transesterification step were quantified. Although very significant rate enhancements over uncatalyzed reaction have been achieved, this catalyst could not promote the transesterification of less reactive substrates such as vinyl acetate. Reaction between vinyl trifluoroacetate and MeOH was also catalysed by a spiroligozyme scaffold carrying the same functions as in the previous example.[249]

A solid-supported catalyst consisting of a histidine unit located in the vicinity of a secondary alcohol could promote the hydrolysis of p-nitrophenyl butyrate in water (Scheme 24b).[250] Activity of this material was enhanced by the attachment of hydrophobic alkyl chains to the resin alongside the catalytic unit. An organocatalyst incorporating an oxyanion hole, a thiol, and a tertiary amine base was reported to catalyse the amide formation from amino acid thioesters (Scheme 24c).[251] Similarly to the previous examples, this occurred via a S-acylated intermediate where the carbonyl group of the thioester is positioned to accept HB from the urea. Together with the catalysts in Scheme 24a this highlights the role of oxyanion hole in catalytic transesterifications and supports the parallel with anion receptor chemistry.

Building on these replications of the biomimetic transesterification mechanism in small-molecule catalysts, the objective of this work was to find a new catalyst design by combining an oxyanion hole, an alcohol, and a base in various configurations. The primary goal was to achieve high catalytic activity in a modular, easily synthesised, and readily tunable structure. In addition to that, stereoselectivity in desymmetrisation and kinetic resolution reactions was sought for.

4.2 Initial advances towards higher reactivity

The starting point of this work was to investigate combinations of serine alcohol with various bases. As for the oxyanion hole, a urea-thiourea β-turn mimic (Scheme 25a) previously developed in the group[252] was selected. This structure was previously found to be highly effective in the asymmetric Mukaiyama-Mannich reaction (Scheme 25b), notably outperforming the analogue without the additional urea. A similar turn motif was reported in a catalyst for a different type of Mannich reaction,[253] corroborating the effectiveness of such oxyanion holes. Conformational rigidification via HB between the urea and thiourea units was proposed to reduce the entropic cost of transition state binding. Additionally, this HB was theorised to be strengthened upon binding, thus resulting in positive cooperativity. This effect is similar to the contraction of some protein structures due to the reinforcement of intramolecular HB which occurs upon ligand binding.[254–256]

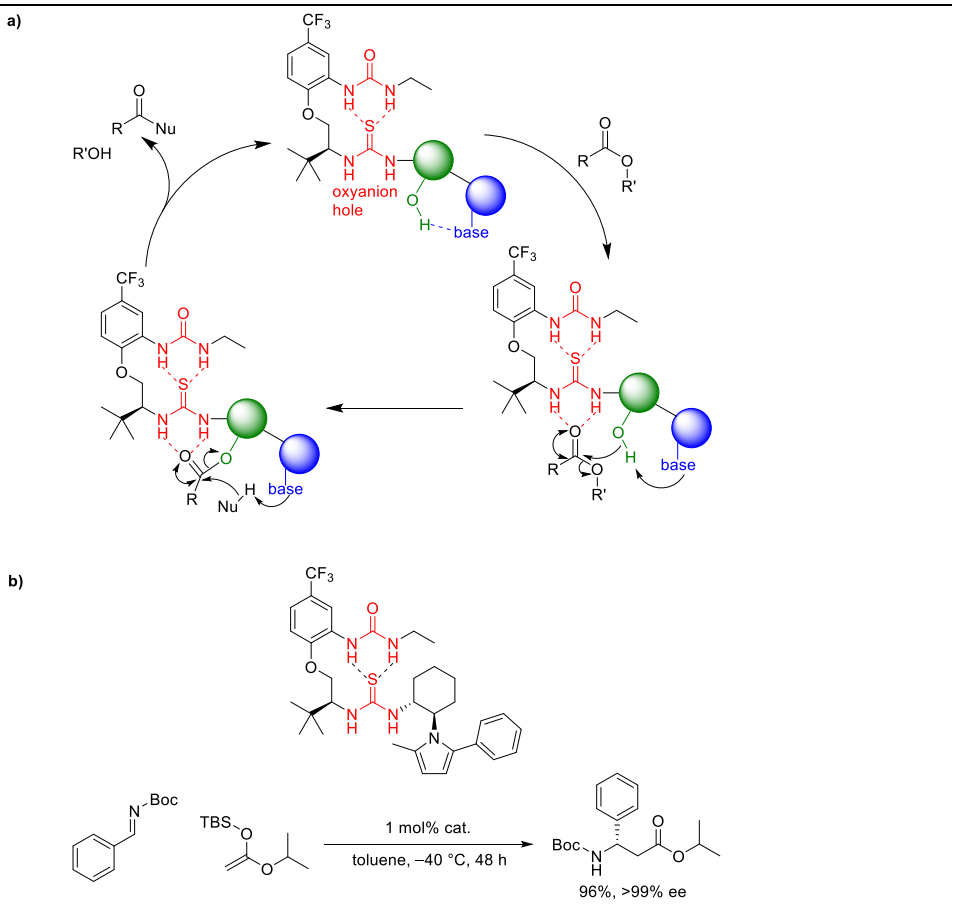

Scheme 25 a) Conceptual structure of the first-generation transesterification catalysts. b) Organocatalyst for the asymmetric Mukaiyama-Mannich reaction incorporating the urea-thiourea turn structure.

The first generation of transesterification catalysts is shown in Figure 69. In compounds **4.1**–**4.5** various bases (pyridine, tertiary amine, and imidazole) are appended to serine in order to enhance the nucleophilicity of its OH group. The N-terminus of serine is used to form a thiourea, thus introducing the oxyanion hole. Compound **4.2** is a cysteine analogue meant to determine whether the more acidic SH group could promote transesterifications via a thioester intermediate.[257] Catalysts **4.6**–**4.8** are based on a different, diaminocyclohexane-bridged architecture. This is a common design feature in thiourea organocatalysts,[258] and the amide NH in this structure may reinforce the oxyanion hole.[259] The base in these examples is a cyclic amidine or guanidine constructed using the amino group of serine. Two compounds missing the thiourea oxyanion hole were also evaluated: **4.9** which is the standalone alcohol-base chain of **4.1**, and the Boc-Ser-His-OMe dipeptide **4.10**.

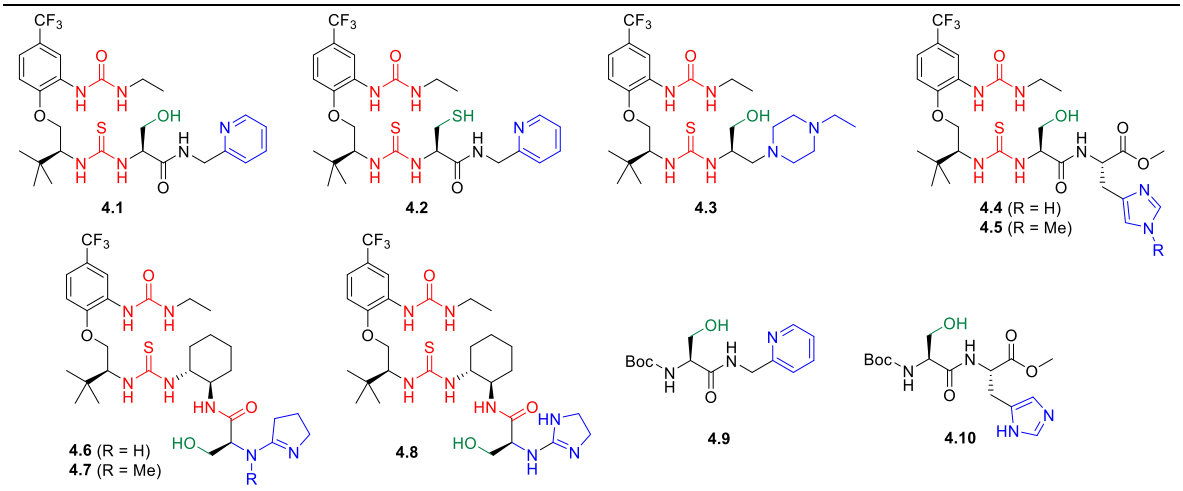

Figure 69 First generation catalysts incorporating various configurations of oxyanion hole, alcohol/thiol, and base.

4.2.1 Synthesis

Preparation of the urea-thiourea turn precursor **4.16** is shown in Scheme 26. First *L*-*tert*-leucine was reduced to an alcohol with *in situ* generated BH_3. The product was *N*-Boc-protected and subjected to an S_NAr reaction which provided **4.13**. The nitro group was reduced and the urea was constructed via reaction of the resulting aniline **4.14** with ethyl isocyanate. The amino group was

then Boc-deprotected and transformed into isothiocyanate upon treatment with thiophosgene, providing **4.16**. In practice **4.16** was prepared freshly as needed for the thiourea formation reactions.

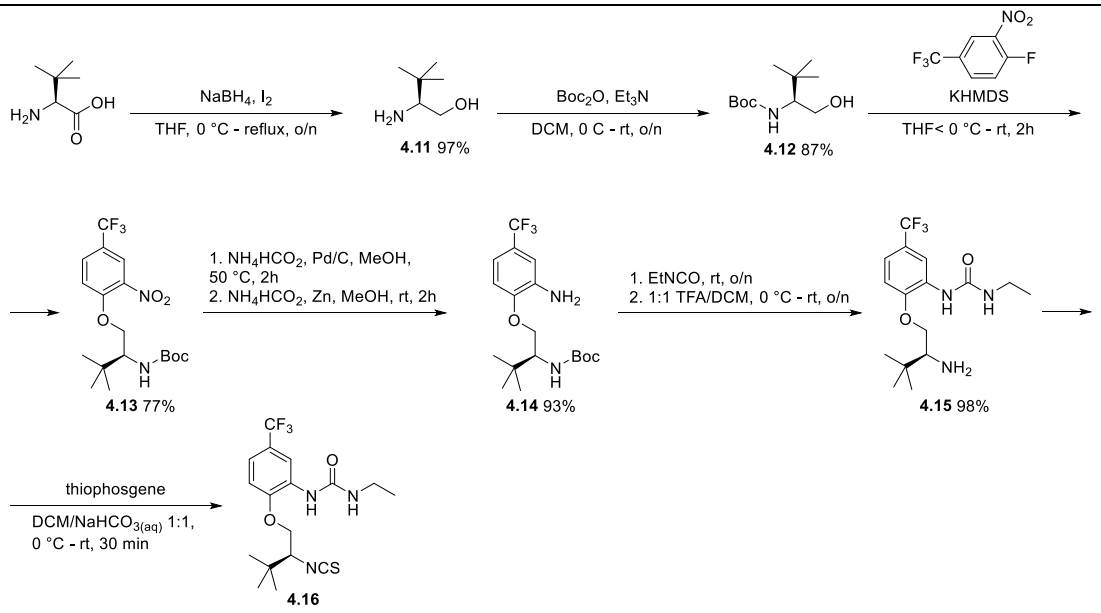

Scheme 26 Synthesis of the urea-thiourea turn precursor.

Most of the alcohol-base chains were assembled by amide formation reactions (Scheme 27). In particular, it was found that the mixed anhydride method where the carboxylic acid is activated with isobutyl chloroformate is suitable for serine with unprotected side chain. No significant epimerisation at the serine α carbon was observed, as shown by the NMR spectra of products with multiple stereocenters.

This method was however unsuitable for the use with unprotected histidine as amine coupling partner. In this case amide formation was performed using COMU as an activating reagent, providing the Ser-His dipeptides **4.10** and **4.18** in yields close to 50%. Serine OH was in these cases protected as benzyl ether, which was then removed by hydrogenation. The piperazine structure in **4.19** was installed via reductive amination following the reduction of Boc-Ser(OTIPS)-OMe to an aldehyde with DIBAL.

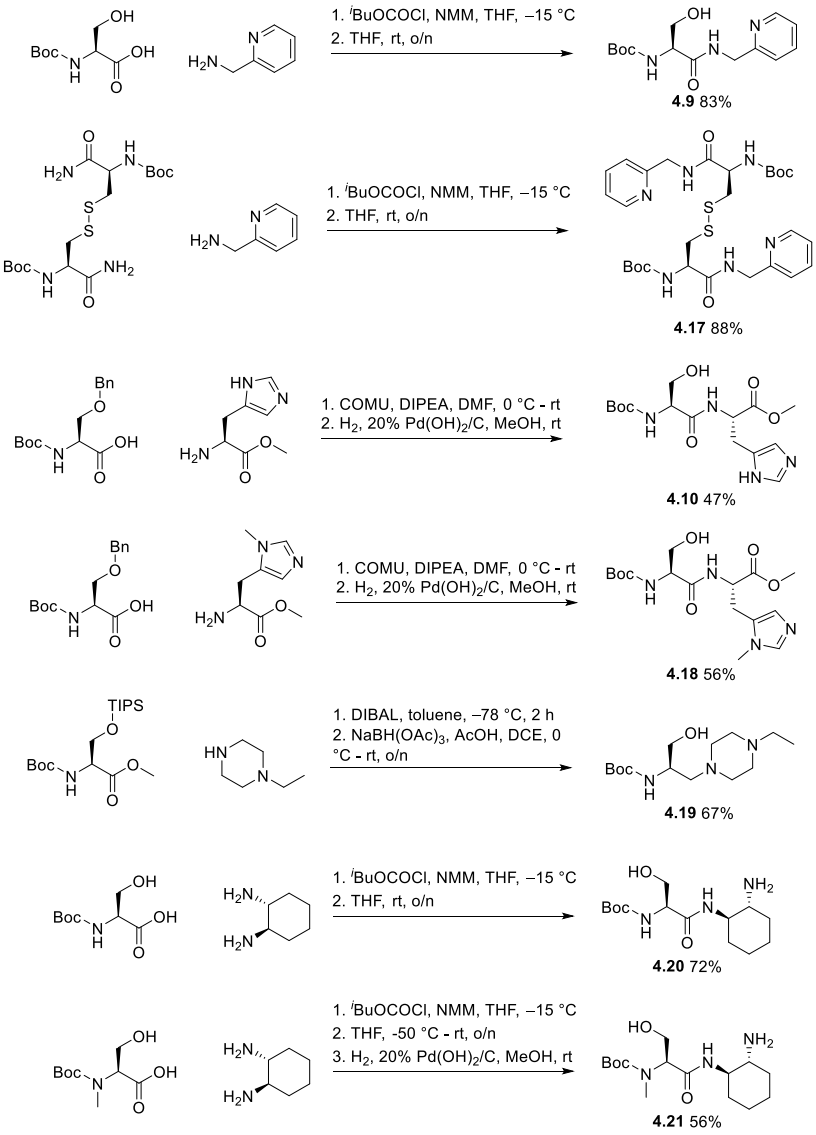

Scheme 27 Synthesis of alcohol/thiol – base motif precursors.

In final steps of the synthesis the alcohol-base precursors **4.9**, **4.10**, and **4.17**–**4.19** were Boc-deprotected by treatment with HCl in dioxane. The resulting amines (as hydrochloride salts) were then used in the thiourea formation reaction with **4.16**. This afforded the final catalyst structures in generally good yields. The cysteine analogue **4.2** was initially formed as disulfide. It was reduced to the final product using PBu_3 in the presence of water.

Thiourea formation from **4.20** and **4.21** followed by Boc-deprotection provided **4.23** and **4.24**. The free amine groups in these compounds were incorporated into a cyclic amidine or guanidine via treatment with isoamide or isothiourea reagents, respectively.

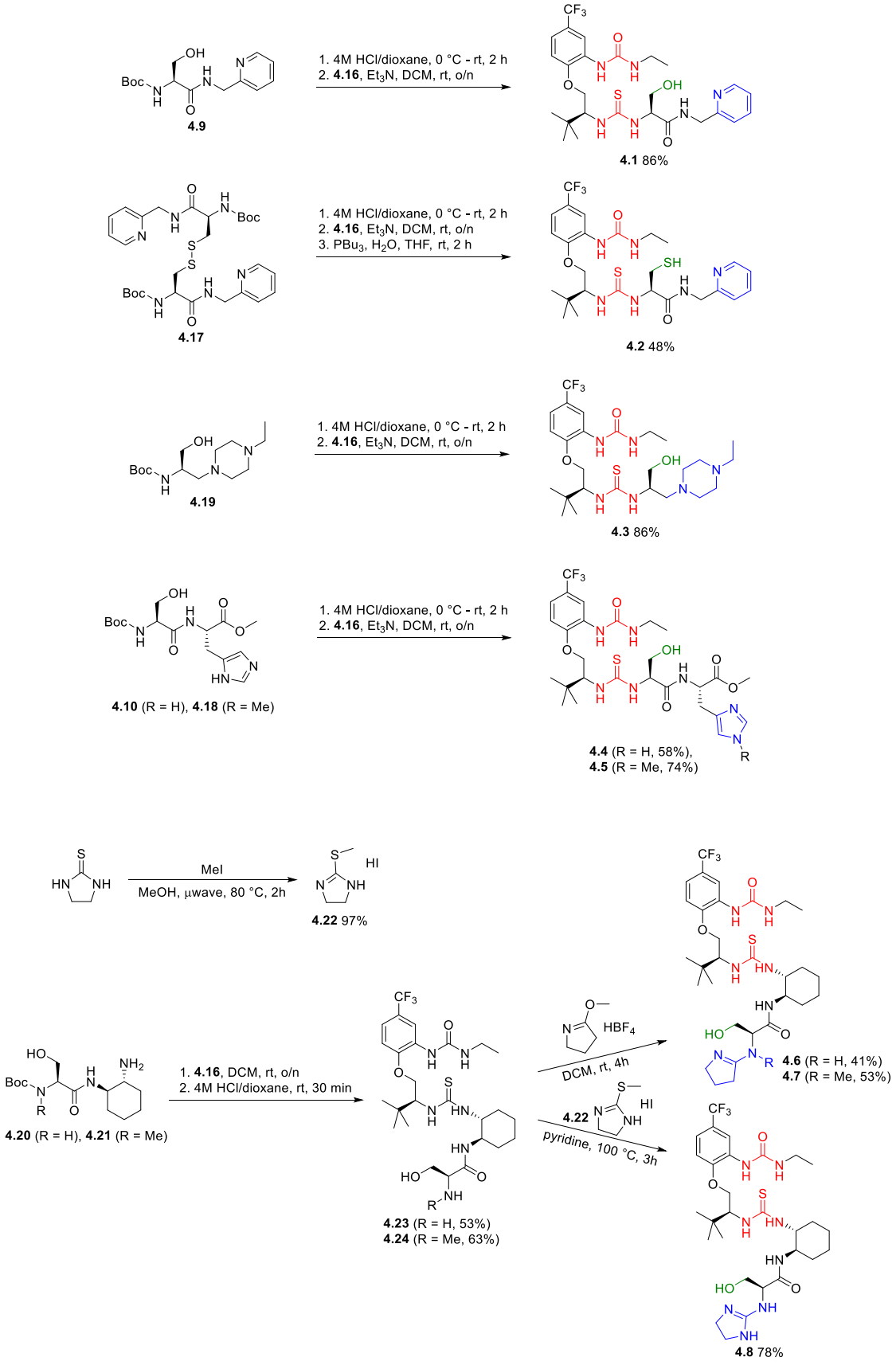

Scheme 28 Final steps in the synthesis of the first-generation catalysts.

4.2.2 Reactivity studies

The model reaction used to assess the catalytic activity of the obtained compounds was the transesterification between vinyl trifluoroacetate and methanol (Figure 70). This transformation can be conveniently monitored by ^{19}F NMR and the traces of conversion versus time used to compare different catalysts.

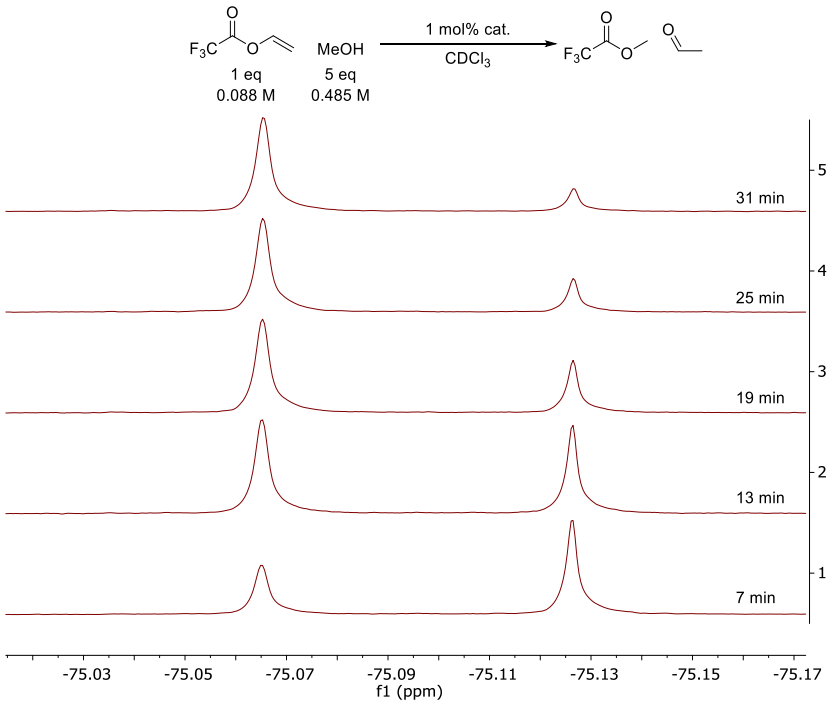

Figure 70 Top: model transesterification reaction used to study the reactivity of catalysts (reagent concentrations shown as used for the first-generation compounds). Bottom: ^{19}F NMR spectra showing the transformation of vinyl trifluoroacetate into methyl trifluoroacetate (traces for a third-generation compound 4.52 are shown here).

In a typical experiment,* a solution of the test compound was prepared (10 mM, $CDCl_3$). Separately, vinyl trifluoroacetate was dissolved in $CDCl_3$ to 0.1 M concentration and 0.5 ml of the resulting solution was loaded into an NMR tube. Immediately before starting the measurement, MeOH (11 µl, 5 eq wrt vinyl trifluoroacetate) was added to the NMR sample. Finally, solution of the test compound (50 µl, 0.01 eq wrt vinyl trifluoroacetate) was added and the conversion of vinyl trifluoroacetate (δ_F = −75.13 ppm) into methyl trifluoroacetate (δ_F = −75.07 ppm) was monitored

* This protocol is different from the one used to study second and third-generation catalysts.

by ^{19}F NMR (476 MHz) over 90 min in 5 min intervals at 298 K. Conversion was calculated using the sum of vinyl trifluoroacetate and methyl trifluoroacetate peaks as internal reference.

Reaction profiles obtained in this manner are shown in Figure 71. Compounds **4.1**, **4.4**, **4.5**, and **4.10** displayed moderate to high levels of activity. The most reactive of them (**4.4**) approached 70% conversion over 100 min, but the transformation slowed down over time. This can be explained by *N*-acylation of the histidine base which may occur via undesired reaction with vinyl trifluoroacetate or methyl trifluoroacetate, or via O to N acyl transfer within the acylated catalyst (Scheme 29). The methylated analogue **4.5** was aimed at making this process reversible, as the cationic acylimidazolium species resulting from its N-acylation should be labile towards deacylation by MeOH or the serine OH. However, **4.5** proved significantly less reactive compared to **4.4**.

The simple protected dipeptide **4.10** unexpectedly proved to be a fairly good catalyst, albeit still less active than **4.4**. Although it lacks the thiourea unit, its amide and carbamate NH protons may still function as a weaker oxyanion hole. The serine-picolylamine fragment **4.9** was similarly much less reactive than **4.1**. These observations are consistent with the involvement of the oxyanion hole in the binding of anionic transition state.

The cysteine analogue **4.2** showed very little reactivity, implying that the thiol is unable to undergo transesterification even with the highly reactive vinyl trifluoroacetate. Compound **4.3** displayed initial reaction rate similar to **4.1**, but it quickly decreased to background rate. Although deactivation of the catalyst via formation of stable acylammonium is unlikely, some other form of decomposition may occur.

In the cases of **4.6**–**4.8** an initial jump to 13-20% conversion within the first 5 min was followed by slow reaction at a rate comparable to the uncatalysed process. This shows that an initially fast reaction is rapidly stopped by N-acylation of the nucleophilic amidine or guanidine bases. With **4.7** the steady-state reaction is marginally faster than for **4.6** and **4.8**, which can be attributed to slow deacylation of the cationic N-acylated **4.7** which must be highly reactive towards nucleophiles.

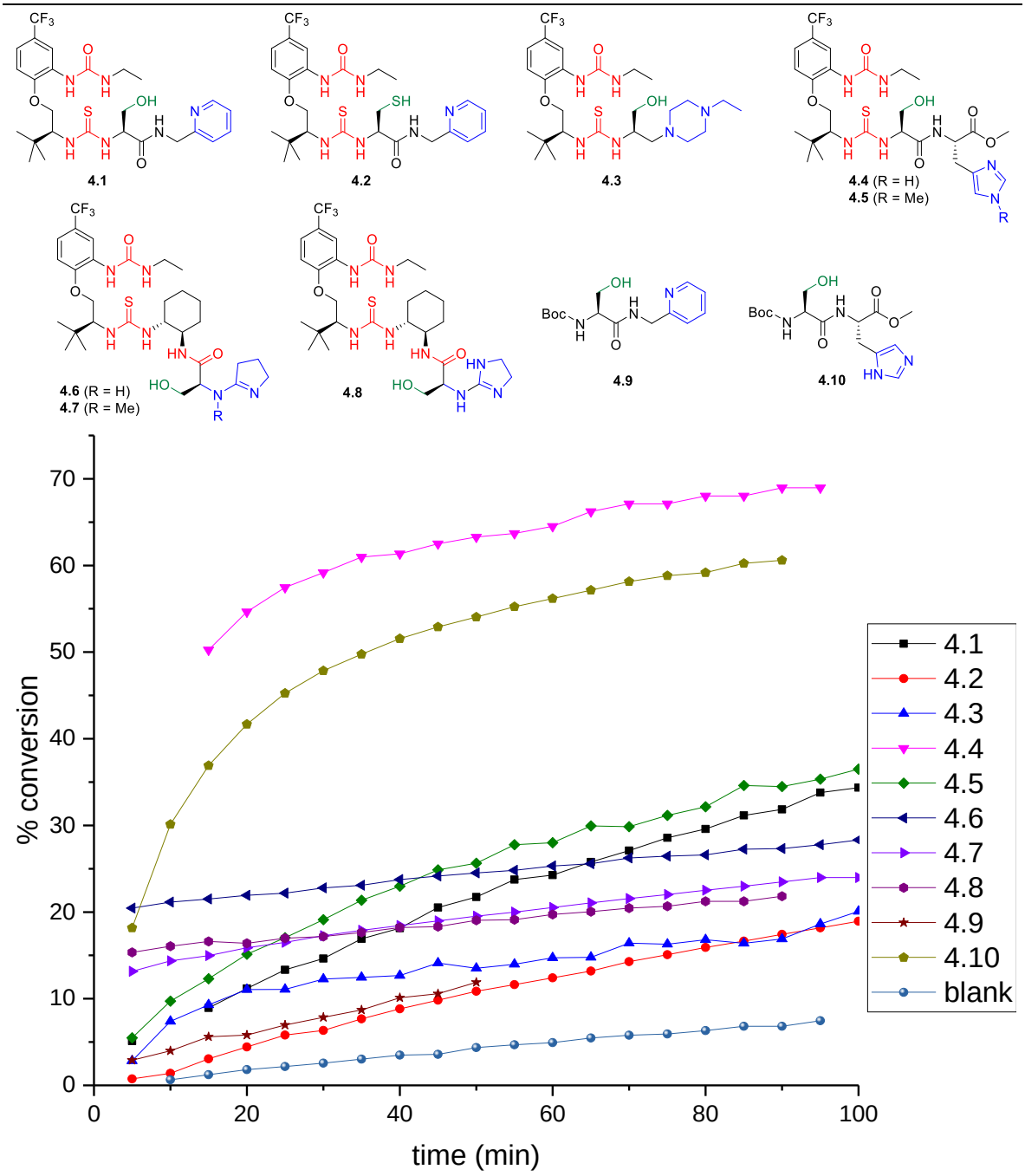

Figure 71 Conversion versus time plots for the transesterification of vinyl trifluoroacetate with MeOH catalysed by the first-generation compounds (0.088 M vinyl trifluoroacetate, 0.485 M MeOH, 0.00088 M catalyst, $CDCl_3$, 298 K).

In addition to the kinetic studies, stoichiometric reactivity tests with the less reactive vinyl acetate were conducted. With the diaminocyclohexane-serine-amidine/guanidine compounds **4.6**–**4.8** considerable conversions were observed where vinyl acetate was combined with 1 eq of test compound and 5 eq of MeOH (**4.6**: 25%, 12h; **4.7**: 77%, 14h; **4.8**: 16%, 1d). However, very little

MeOAc formed in all cases, implying that transesterification of the O-acylated catalyst with MeOH was very slow.

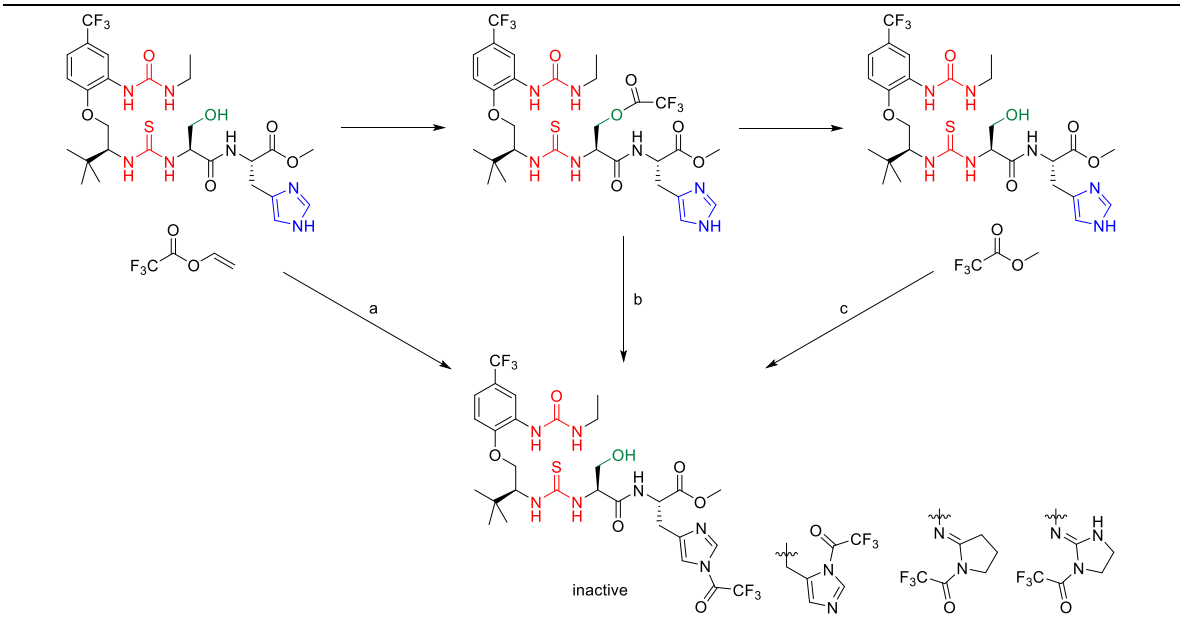

Scheme 29 Proposed pathways for deactivation of catalysts with nucleophilic bases.

4.3 Final tripeptide-based design

Following the demonstration of Ser-His dipeptide combined with an oxyanion hole (**4.4**) as the most successful first-generation compound, it was decided to introduce a more electron-deficient thiourea to further improve the reactivity. Compound **4.25** was initially prepared, where the thiourea carried the electron-withdrawing 3,5-bis(trifluoromethyl)phenyl group which is routinely used in thiourea organocatalysts.[203] It was connected to the Ser-His dipeptide via a *tert*-leucine linker which is frequently introduced adjacent to thiourea as a bulky chiral group[260,261] Analysed by the same protocol as the first-generation compounds, this catalyst proved superior to **4.4**, providing 79% conversion within the first 20 min (Figure 72).

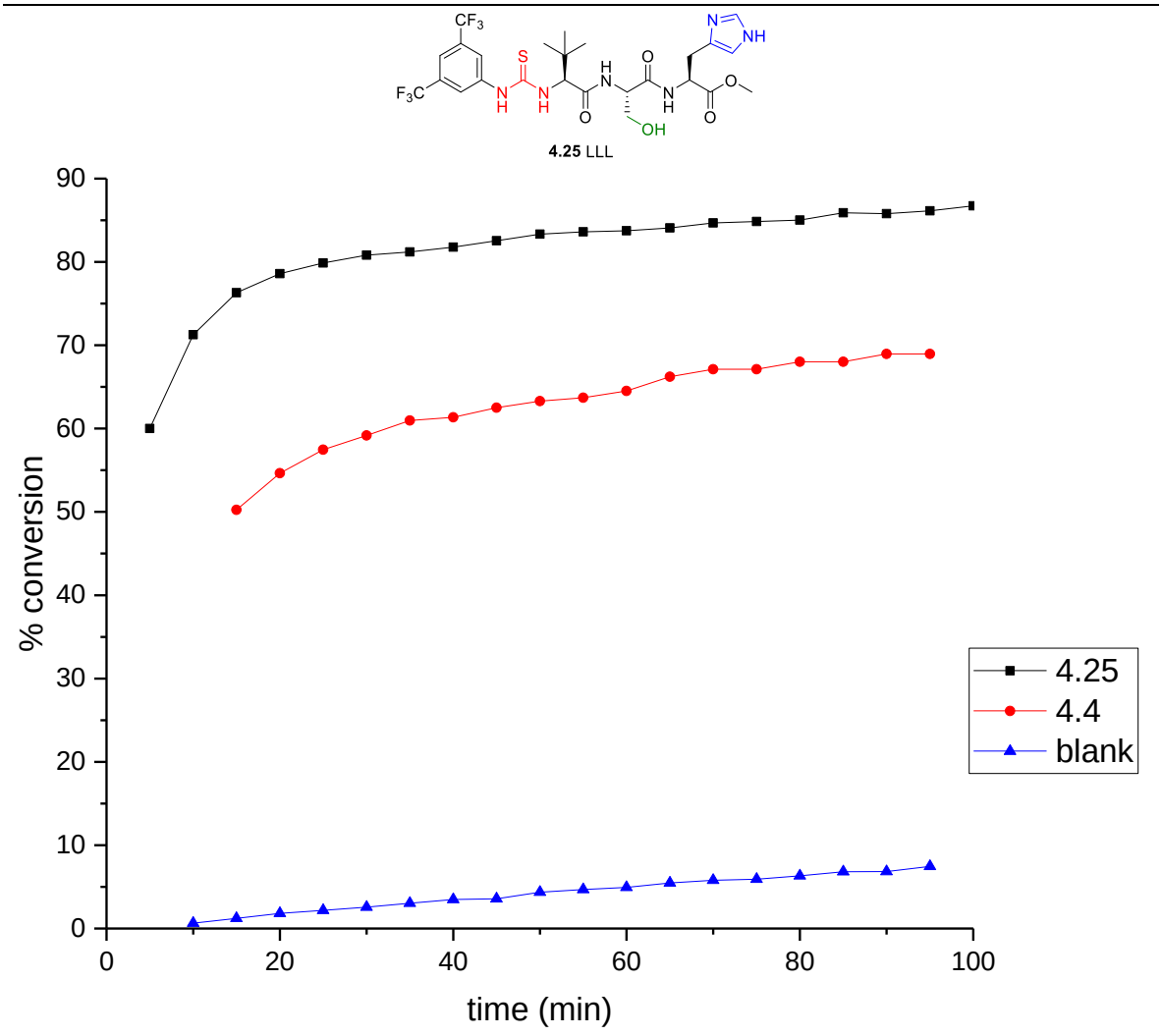

Figure 72 Conversion versus time profiles by transesterification of vinyl trifluroacetate with MeOH, comparing the activity of 4.4 and 4.25.

Compound **4.25** was thus chosen as a starting point for the second generation of catalysts shown in Figure 73. This series of compounds includes all four diastereoisomers of the tripeptide **4.25**–**4.28**, urea analogues, homoserine and cysteine analogues, and compounds **4.33**–**4.36** where certain functional elements have been deleted.

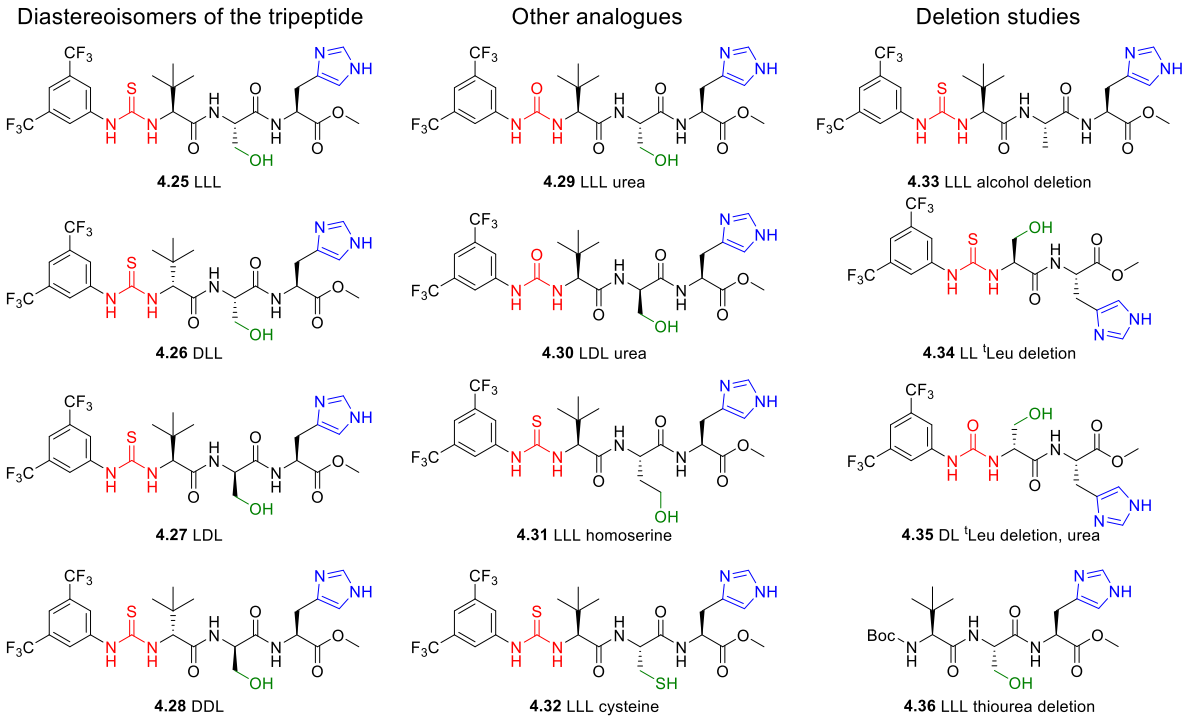

Figure 73 Second generation compounds based on the ^{t}Leu-Ser-His tripeptide.

4.3.1 Synthesis

The sequence of amide and thiourea formations used to prepare this series of catalysts is similar to the preparation of the first-generation compounds (especially **4.4**). However, a somewhat different approach was followed (Scheme 30). Amide and thiourea formations involving unprotected histidine imidazole were previously found to be inefficient. In this case N^{τ}-trityl-protected histidine was used which significantly improved the yields of such transformations. The protecting group was removed in the final step by treatment with 5% solution of pyridine hydrochloride in MeOH at 65 °C. It was conveniently possible for Boc-amine and Trt-imidazole to

be deprotected orthogonally: HCl in dioxane/MeOH did not remove the trityl group, whereas the pyridine hydrochloride solution did not cleave the Boc group.[262]

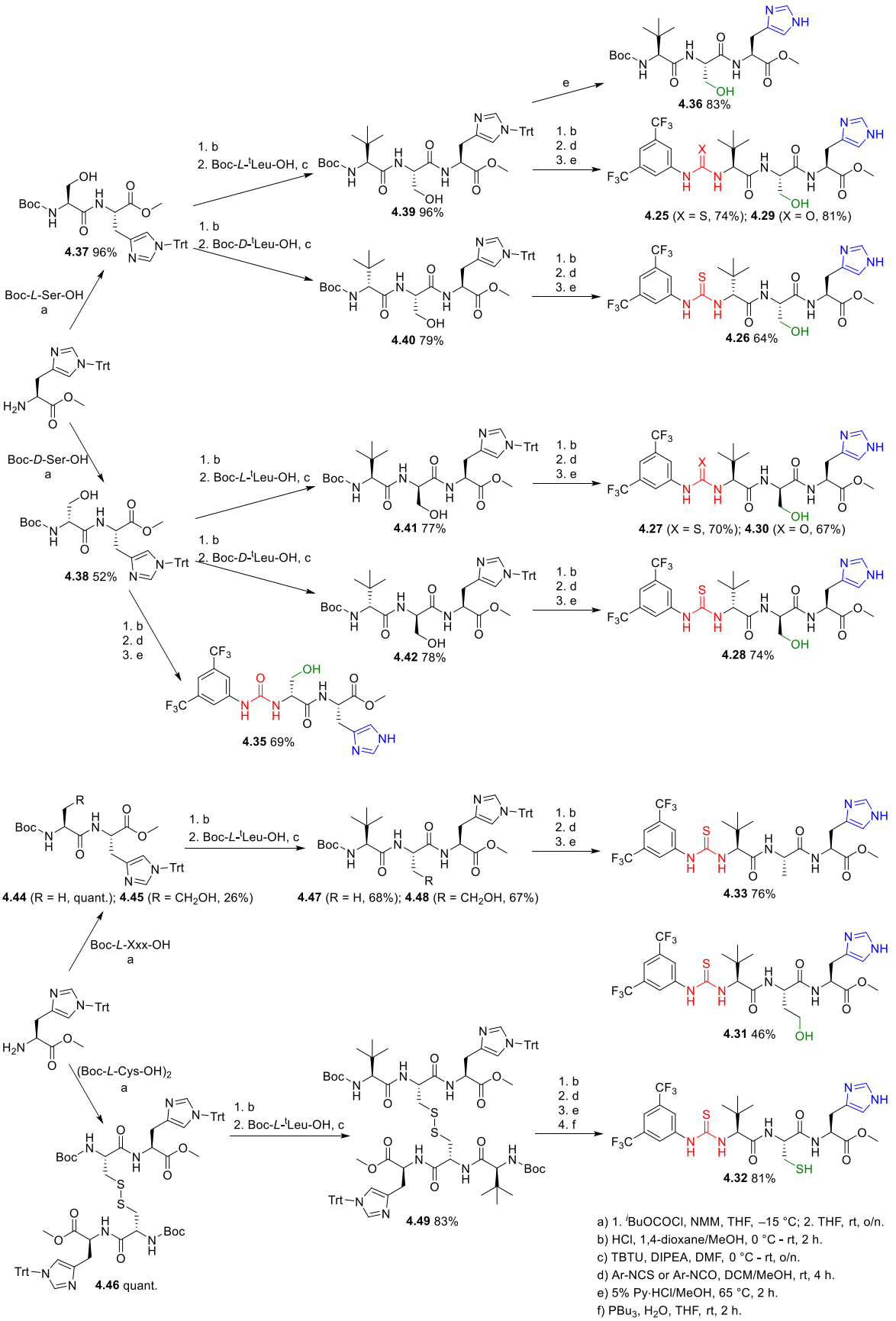

Scheme 30 Synthesis of the second-generation catalysts based on the tripeptide design.

4.3.2 Kinetic studies

To analyse the second-generation catalysts, a different protocol was used, improving upon the crude semi-quantitative approach applied to the first-generation compounds. In order to decrease the interference from N-acylation of the imidazole base a lower initial concentration of vinyl trifluoroacetate (0.01 M) and a higher concentration of MeOH (1 M) were used. Catalyst concentration was very low (0.00005 M or 0.5 mol% loading), allowing to monitor the reaction at low conversions, close to the initial rate conditions.

In a typical experiment, 50 µl of 0.1 M vinyl trifluoroacetate solution in $CDCl_3$ was added to a NMR tube containing 430 µl of $CDCl_3$. Immediately before the start of NMR monitoring 20.2 µl of catalyst solution (0.001236 M) in MeOH was added to the sample. Final sample volume was 500 µl and the concentrations of reagents were as stated above. During the reaction monitoring by ^{19}F NMR 5-10 spectra were taken with 3 min intervals with the sample kept at 298 K.

As the transesterification proceeds under pseudo-first order conditions ([A] ≫ [B]), the profile of conversion versus time can be described with the following kinetic equation: *

$$[B] = [B]_0(1 - c) = [B]_0 e^{-k_{obs}t}$$

$$\ln(1 - c) = -k_{obs}t$$

It follows that the plot of $\ln(1 - c)$ versus time should be a straight line with a slope of $-k_{obs}$. In practice these plots show a small deviation from linearity due to the catalyst deactivation via N-acylation. This can be corrected for in a straightforward manner. By assuming that the concentration of active catalyst decreases linearly with time ($k_{obs} = k_{in} - k_d t$) we get a modified equation describing conversion versus time:†

$$\ln(1 - c) = -(k_{in} - k_d t)t = k_d t^2 - k_{in} t$$

* A – MeOH; B – vinyl trifluoroacetate; c – conversion; k_{obs} – observed rate constant.
† k_{in} – observed rate constant with the initial catalyst concentration; k_d – catalyst deactivation rate constant.

Therefore, fitting a second degree polynomial to a plot of $\ln(1-c)$ provides $-k_{in}$ as the linear parameter (Figure 74). The quadratic parameter corresponds to k_d and can be used as a rough measure of the rate of catalyst N-acylation.

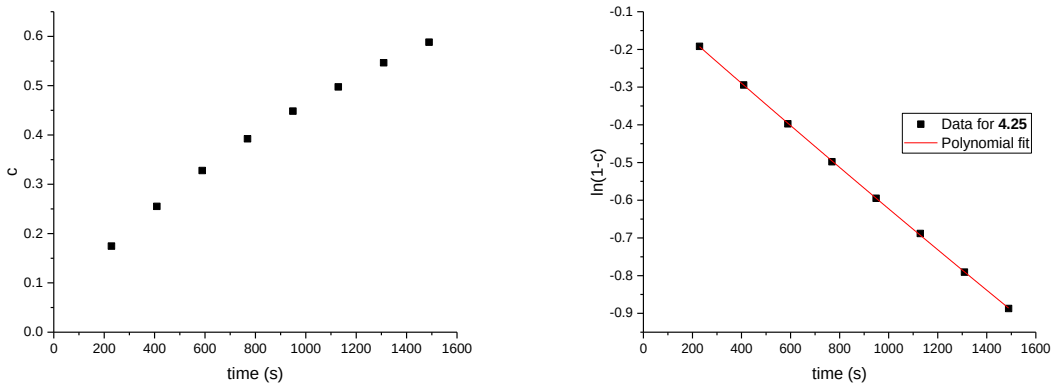

Figure 74 Left: conversion versus time for transesterification catalysed by 4.25 (0.01 M vinyl trifluoroacetate, 1 M MeOH, 0.00005 M catalyst, $CDCl_3$, 298 K). Right: plot of $\ln(1-c)$ versus time derived from the same data. Polynomial fit gives k_{in} = 5.76 × 10^{-4} s^{-1} and k_d = 1.50 × 10^{-8} s^{-1}.

Finally, the pseudo-first order rate constant for the background (uncatalyzed) reaction can be determined from a blank experiment (k_b = 6.02 × 10^{-5} s^{-1}) and subtracted from k_{in} to provide the rate constant due to the catalysed reaction (k_{cat}). The values of k_{cat} and k_d determined for all second-generation compounds are shown in Figure 75.

Significant differences in k_{cat} were observed for the diastereoisomers **4.25**–**4.28**, which implies that the placement of functional groups in space is important for reactivity. Of these compounds, the LDL variant **4.27** was the most active of the entire second-generation series, closely followed by **4.25**. Deletion of *tert*-leucine in **4.34** and **4.35**, and of the thiourea in **4.36** caused a decrease in k_{cat}, supporting the role of these functional elements.

Interestingly, significant reactivity was retained in **4.33**, indicating that without the alcohol function this compound is still capable of direct base catalysis of the model transesterification. This is to be expected, as the histidine base is meant to activate MeOH to effect the deacylation of the

O-acylated catalysts. In **4.33** the imidazole group is likely a much stronger MeOH activator than in the non-acylated forms of other compounds, as it cannot form HB with a nearby OH group.

The urea analogues **4.29** and **4.30** displayed lower k_{cat} values compared to the corresponding thioureas, showing that the stronger HB donor properties of the thioureas are beneficial. Additionally, the urea-containing compounds were deactivated faster, judging by the high k_d values.

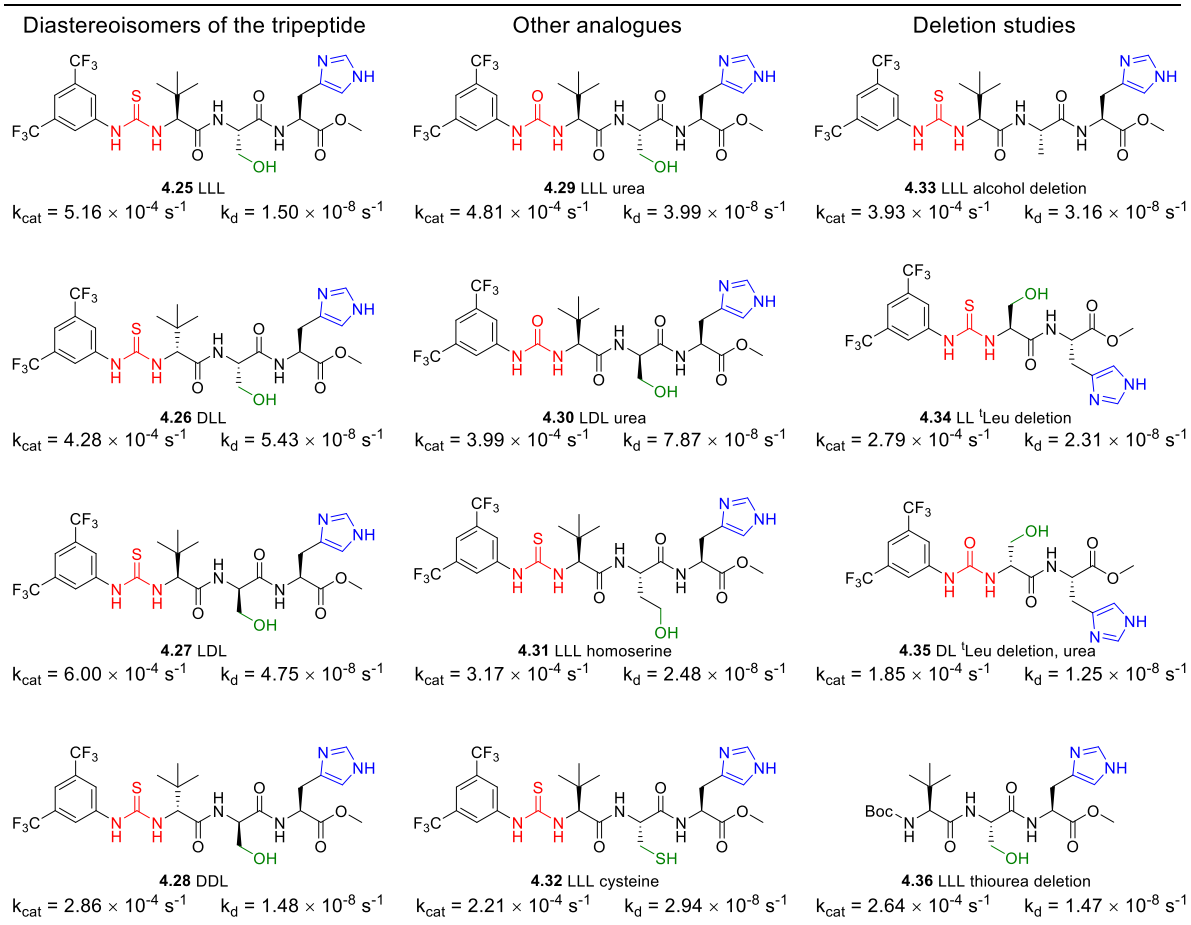

Figure 75 Values of k_{cat} and k_d for the second-generation catalysts.

4.4 Introduction of auxiliary base

For a further improvement of catalyst activity it was decided to introduce an auxiliary base on the C-end of the tripeptide. This addition was an attempt to activate the imidazole base, thus mimicking the role of carboxylate (Asp or Glu residue) in natural catalytic triads (Figure 76). To this end, two derivatives of the most active second-generation catalyst **4.27** were prepared. These compounds, **4.52** and **4.55** included an additional pyridine base in different connectivity variants. Additionally, diastereoisomers of **4.52** were made, as well as **4.56** in which the *tert*-leucine unit was absent.

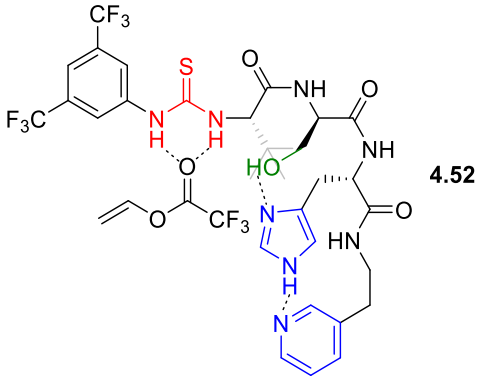

Figure 76 Proposed role of the auxiliary base.

4.4.1 Synthesis

The catalysts containing an auxiliary base were synthesised using the same general procedures as for the previously described second-generation tripeptide compounds. In this case the first step was the amide formation connecting Boc-His(Trt)-OH to the auxiliary pyridine base (Scheme 31).

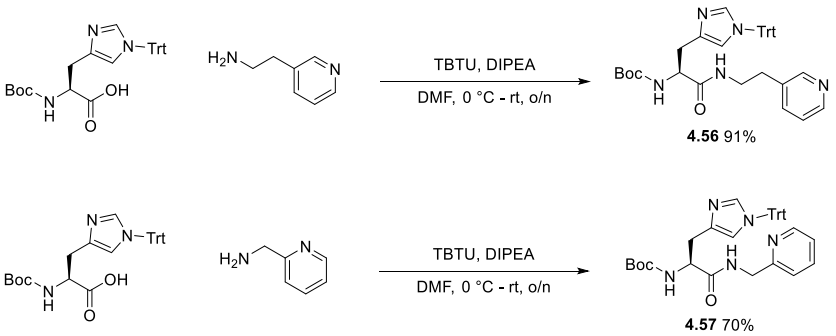

Scheme 31 a) Proposed role of the auxiliary base. b) Preparation of the precursors for 4.50–4.55.

4.4.2 Kinetic and mechanistic studies

Comparison of third-generation catalysts

The third-generation compounds **4.50**–**4.56** incorporating an auxiliary base are shown in Figure 77 along with the k_{cat} and k_d values determined by the same protocol as used for **4.25**–**4.36**. Differences between the four diastereoisomers show the DDL diastereoisomer **4.53** as the least active, which replicates the findings for second-generation compounds. The highest activity was observed in **4.50** (LLL) and **4.51** (DLL) diastereoisomers, with **4.52** (LDL) being not far behind. Deletion of the *tert*-leucine in **4.55** caused a strong decrease in activity, confirming the effectiveness of the chosen oxyanion hole design.

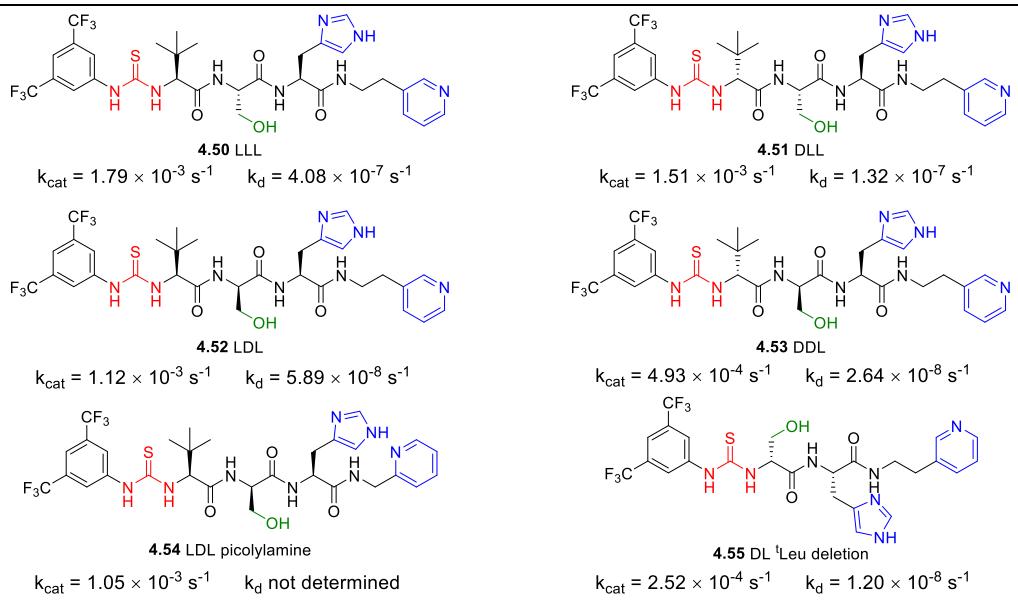

Figure 77 Compounds based on the tripeptide motif and including an auxiliary pyridine base.

Following these preliminary studies, further insights into the reaction mechanism and kinetics were sought. The variation of observed catalysed reaction rate with the catalyst concentration is shown in Figure 78 for **4.52**. The catalyst displays complex behaviour: at very low concentrations the increase in k_{cat} with its concentration is slow and non-linear. At concentrations above ca. 30 μM, however, a fast, linear increase is observed. This indicates that **4.52** undergoes intermolecular self-activation via formation of non-covalently bound aggregates.

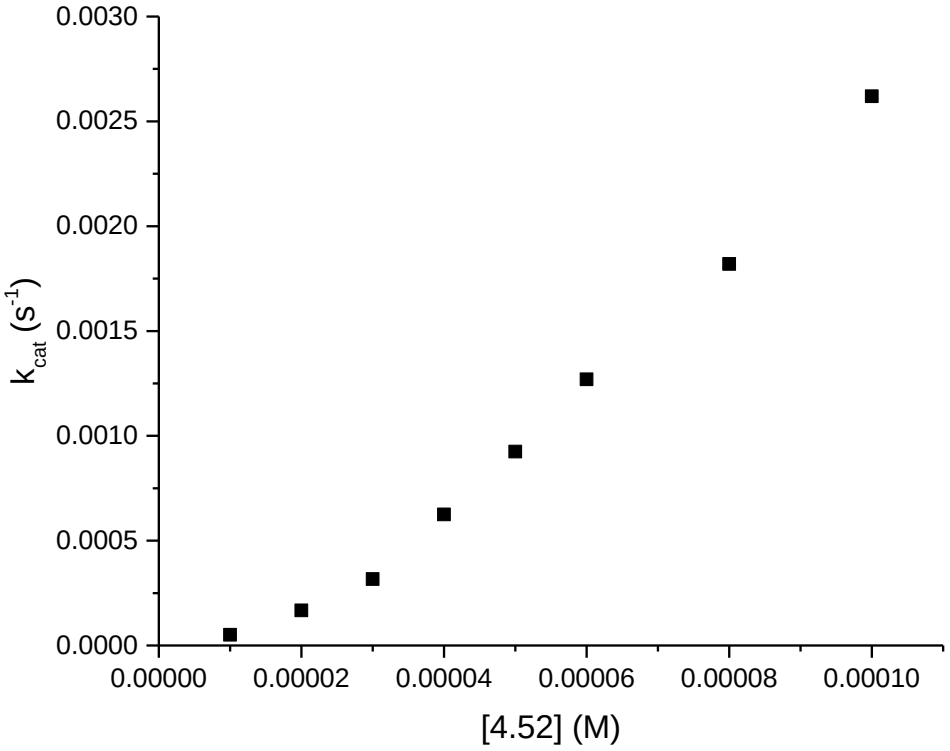

Figure 78 Values of k_{cat} in the presence of various concentrations of 4.52 (0.01 M vinyl trifluoroacetate, 1M MeOH, $CDCl_3$, 298 K).

Detection of O-acylation and N-acylation

In order to visualise the acylated catalyst species, compound **4.52** and vinyl trifluoroacetate were combined in absence of MeOH. A ^{19}F NMR peak at −74.73 ppm (downfield of vinyl trifluoroacetate, consistent with aliphatic trifluoroacetate esters) appears initially, indicating that O-acylation of the catalyst occurs and is too fast to be monitored by NMR (Figure 79). Over time, this signal decays and is replaced by a peak at −75.52 ppm, which is thought to correspond to the N-acylated **4.52**. The same transformation is also observed in the Ar-CF_3 region of the ^{19}F spectrum. The transition from O-acylated to N-acylated catalyst is accompanied by changes in chemical shifts of the signals for each species. This indicates that the non-covalent interactions between the molecules of **4.52** are affected by the change in acylation mode. This observation supports the intermolecular self-activation of **4.52** proposed above, although its exact nature is still unclear.

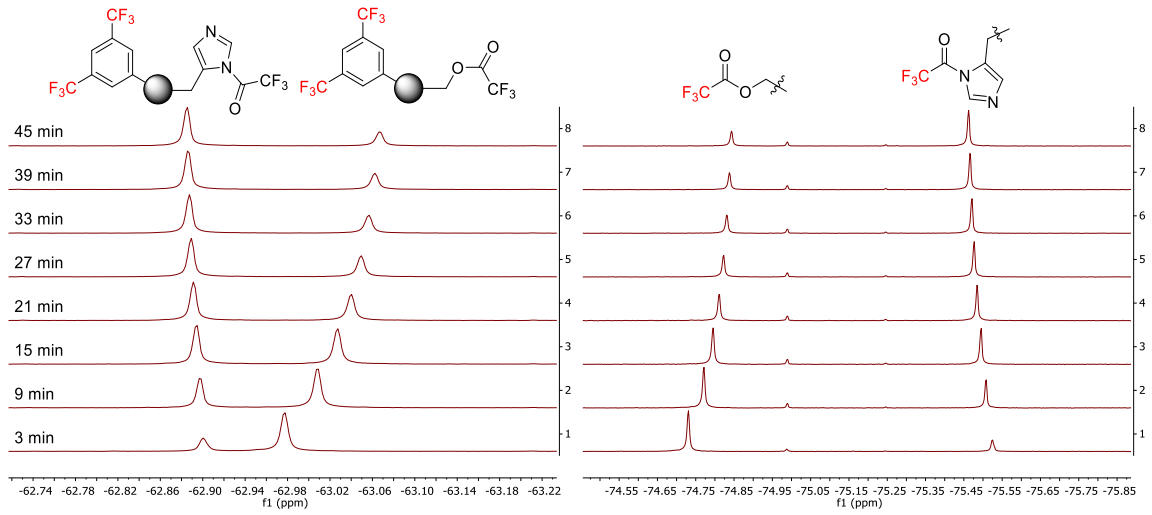

Figure 79 Partial ^{19}F NMR spectra (left: Ar-CF_3 signals; right: trifluoroacetate signals) for an experiment where 4.52 (0.01 M) and vinyl trifluoroacetate (0.01 M) were combined in absence of MeOH (5% DMSO-d_6/$CDCl_3$, 298 K).

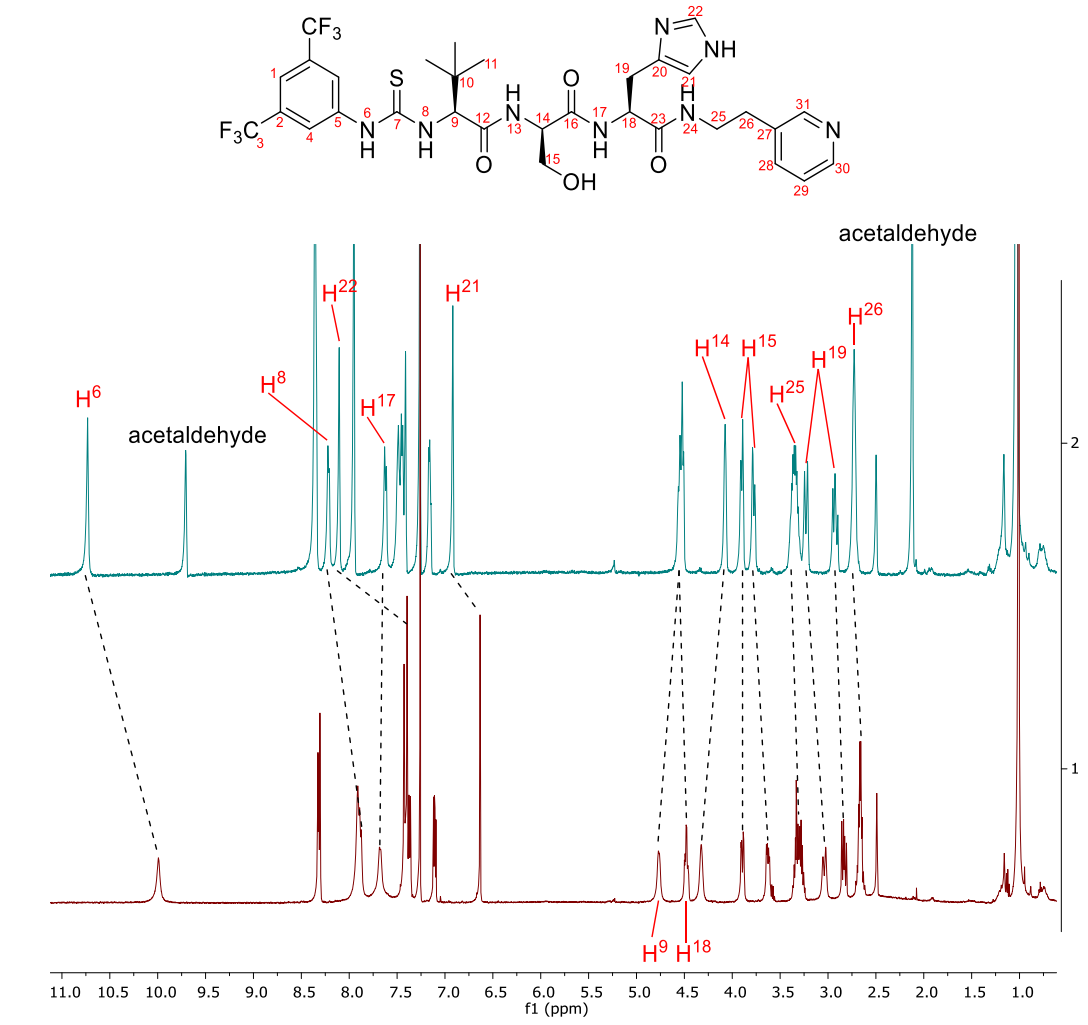

Figure 80 ^{1}H NMR spectra of 4.52 before (bottom) and after (top) treatment with 1 equivalent of vinyl trifluoroacetate for 1 day (5% DMSO-d_6/$CDCl_3$).

^{1}H NMR spectra before and after the treatment of **4.52** with 1 eq of vinyl trifluoroacetate are shown in Figure 80. Significant downfield shifts were observed for the imidazole protons, which is consistent with the formation of N-acylated derivative of **4.52**. The thiourea protons also move downfield, which may indicate their interaction with the imidazole-bound trifluoroacyl group. No significant shifts are observed elsewhere in the spectrum, including the serine C*H*$_2$OH protons, which rules out the possibility that the end product is the O-acylated **4.52**.

In order to observe the formation and alcoholysis of an O-acylated catalyst which is expected in a biomimetic transesterification mechanism, a less reactive ester substrate was needed. The chosen compound was 1-phenylvinyl 2,2-difluoro-2-phenylacetate **4.66** which is easily prepared in a regioselective manner via a Ru-catalysed addition of difluorophenylacetic acid to phenylacetylene (Scheme 32). It is much less reactive than vinyl trifluoroacetate and displays no observable uncatalysed reaction with MeOH in $CDCl_3$ solution over the course of hours at 25 °C.

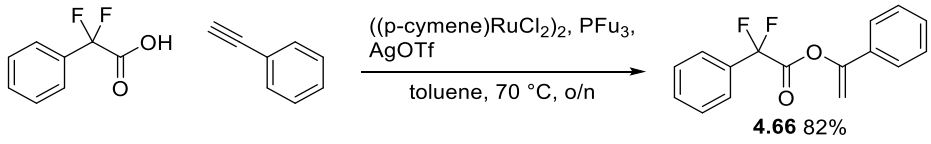

4.66 82%

Scheme 32 Preparation of 1-phenylvinyl 2,2-difluoro-2-phenylacetate.

A transesterification between **4.66** and **4.52** (10 mol%) was monitored by ^{19}F NMR (Figure 81). An additional Ar-CF_3 signal appeared at −62.92 ppm and increased in intensity over the course of reaction. Upon addition of MeOH this signal became gradually weaker while the peak due to the free **4.52** was partially restored. This was accompanied by the formation of methyl 2,2-difluoro-2-phenylacetate. As the N-acylated derivatives of the imidazole-based catalysts are known to be stable in the presence of MeOH, the signal at −62.92 ppm (−62.95 ppm in the presence of MeOH) must correspond to the O-acylated **4.52**. This observation confirms that the biomimetic two-step

transesterification mechanism is indeed displayed by **4.52**. Additionally, no evidence of N-acylation was observed in this case, showing that it is limited to the highly reactive trifluoroacetates.

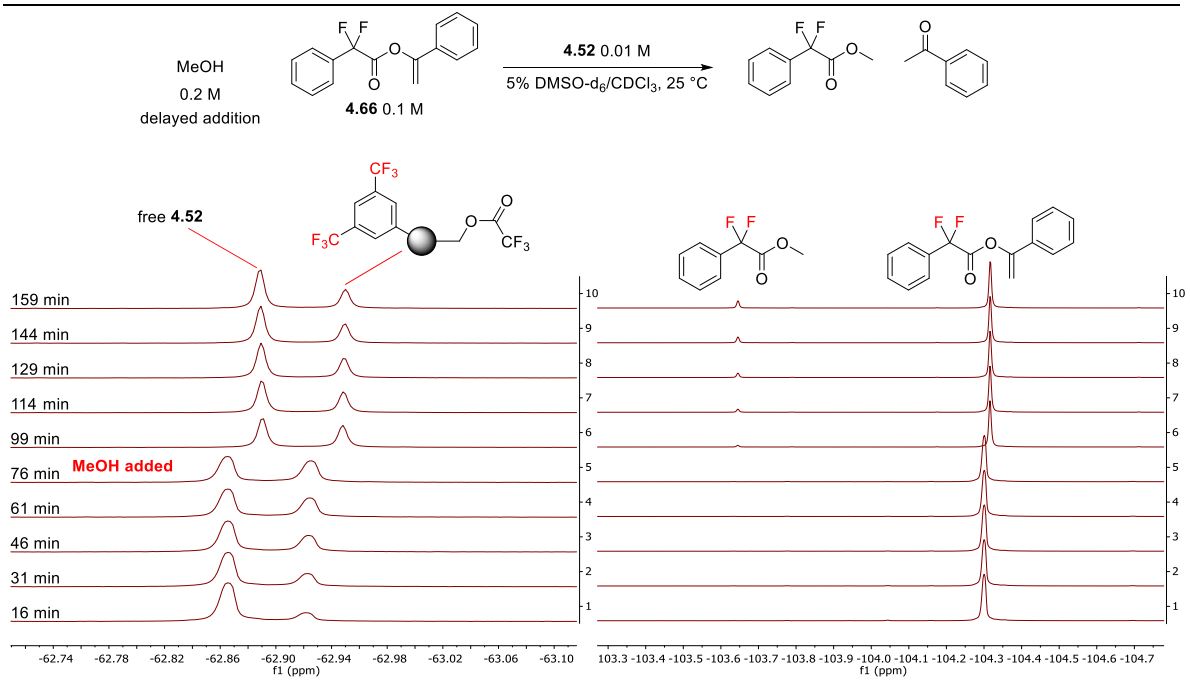

Figure 81 Observation of O-acylated catalyst in a transesterification of 1-phenylvinyl 2,2-difluoro-2-phenylacetate with MeOH. The 2,2-difluoro-2-phenylacetyl F atoms of the O-acylated 4.52 appear as two broad diastereotopic signals close to −100.60 ppm and are not shown here.

Detailed investigation of the catalysed reaction kinetics

Following the preliminary kinetic studies based on determination of the observed rate constant for the catalysed reaction (k_{cat}), further insight was sought by determining the rate constants for the first (k_1) and second (k_2) step of the biomimetic transesterification mechanism (Figure 82). According to a literature precedent,[248] k_{cat} can be deconvoluted into these consecutive rate constants by varying the initial concentration of vinyl trifluoroacetate.

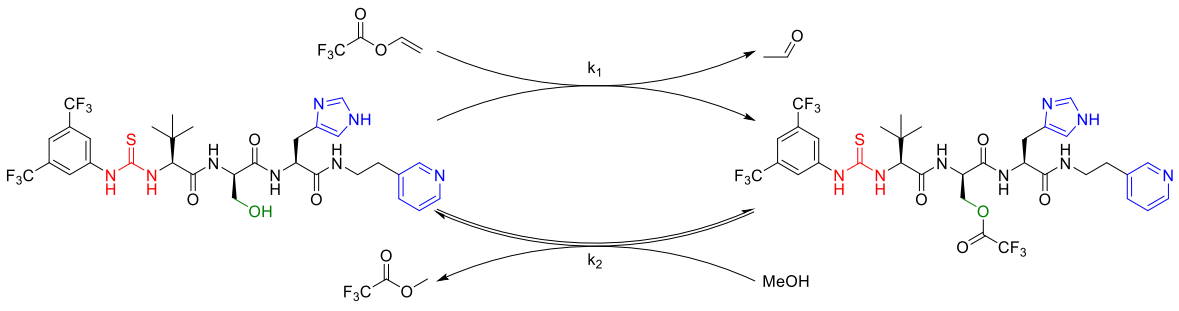

Figure 82 The two-step transesterification mechanism, quantified by the rate constants k_1 and k_2.

This method is based on a derivation which starts with the steady-state approximation for the acylated catalyst intermediate:*

$$\frac{d[C_{Ac}]}{dt} = k_1[B][C] - k_2[A][C_{Ac}] = 0$$

Substituting $[C]_0 - [C_{Ac}]$ for $[C]$ gives:

$$k_1[B][C]_0 - k_1[B][C_{Ac}] - k_2[A][C_{Ac}] = 0$$

$$[C_{Ac}] = \frac{k_1[B][C]_0}{k_1[B] + k_2[A]}$$

The expression for $[C_{Ac}]$ can now be substituted into the equation describing the rate of product formation (observed reaction rate):

$$v = k_2[A][C_{Ac}] + k_b[A][B] = \frac{k_1k_2[A][B][C]_0}{k_1[B] + k_2[A]} + k_b[A][B]$$

As the experiment is done under pseudo-first order conditions ($[A] \gg [B]$), it can be assumed that $v = k_{obs}[B]$. Substituting this into the above equation gives:

$$k_{obs}[B] = \frac{k_1k_2[A][B][C]_0}{k_1[B] + k_2[A]} + k_b[A][B]$$

* A – MeOH; B – vinyl trifluoroacetate; C – free catalyst; C_{Ac} – O-acylated catalyst, k_{obs} – observed rate constant; k_b – background/uncatalyzed rate constant; v – observed reaction rate.

$$k_{obs} - k_b[A] = \frac{k_1 k_2 [A][C]_0}{k_1[B] + k_2[A]}$$

$$\frac{1}{k_{obs} - k_b[A]} = \frac{k_1[B] + k_2[A]}{k_1 k_2 [A][C]_0}$$

$$\frac{1}{k_{obs} - k_b[A]} = \frac{[B]}{k_2[A][C]_0} + \frac{1}{k_1[C]_0}$$

With 1 M concentration of MeOH and under initial rate conditions this can be simplified to:

$$\frac{1}{k_{cat}} = \frac{[B]_0}{k_2[C]_0} + \frac{1}{k_1[C]_0}$$

It follows that plotting $1/k_{cat}$ versus $[B]_0$ should give a linear plot where k_1 can be derived from the intercept with the y-axis and k_2 from the slope of graph.

This plot for **4.52** is shown in Figure 83. The variation of $1/k_{cat}$ with increasing initial concentration of vinyl trifluoroacetate is initially linear, but deviates from linearity at $[B]_0 > 0.05$ M. This complex behaviour can be understood considering the observations of catalyst aggregation and intermolecular self-activation. The steady-state fraction of the O-acylated catalyst increases with the concentration of vinyl trifluoroacetate. When a significant proportion of the catalyst is acylated, the intermolecular activation may become disfavoured.

However, fitting a line to the observed linear regime at $[B]_0$ between 0.01 and 0.05 M allowed to determine k_1 and k_2 for this range of conditions (Figure 83). Values of $k_1 = 26.4$ M^{-1} s^{-1} and $k_2 = 1.11$ M^{-1} s^{-1} were obtained for **4.52**.

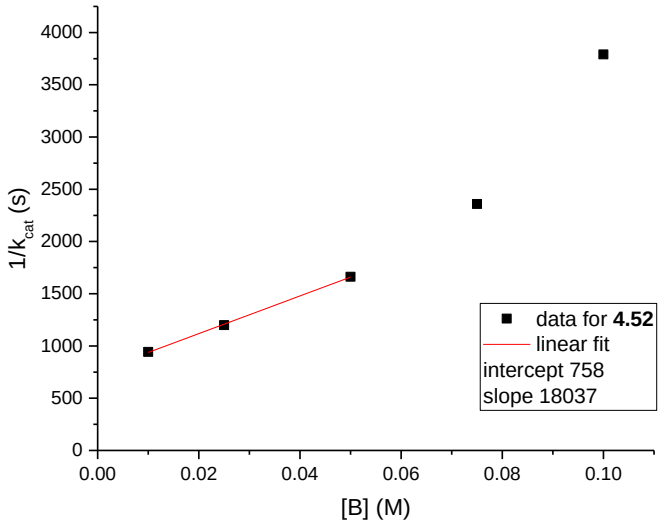

Figure 83 Determination of k_1 and k_2 for 4.52. k_1 = 26.4 M^{-1} s^{-1}; k_2 = 1.11 M^{-1} s^{-1}.

Other diastereoisomers of the third-generation design showed a much faster onset of non-linear behaviour, which in these cases was observed well below $[B]_0$ = 0.05 M. This is an indication of either high k_1/k_2 ratios or weaker intermolecular activation compared to **4.52**. In these cases a determination of k_1 and k_2 is still possible by fitting a line to data points in 0.005-0.03 M range of $[B]_0$ (Figure 84 – Figure 87).

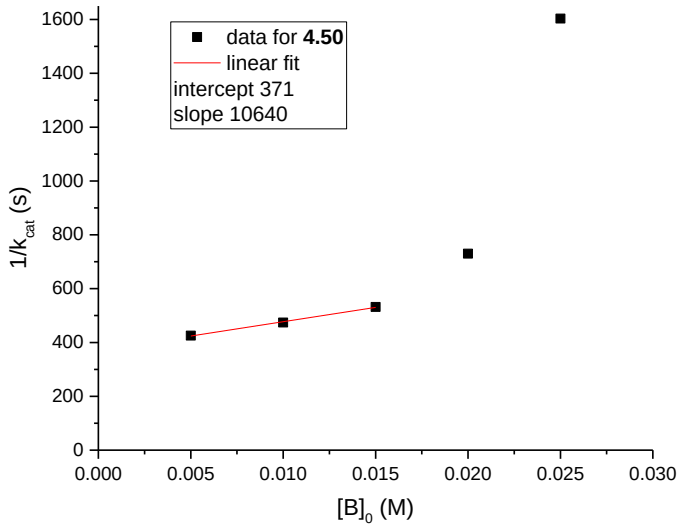

Figure 84 Determination of k_1 and k_2 for 4.50. k_1 = 53.9 M^{-1} s^{-1}; k_2 = 1.88 M^{-1} s^{-1}.

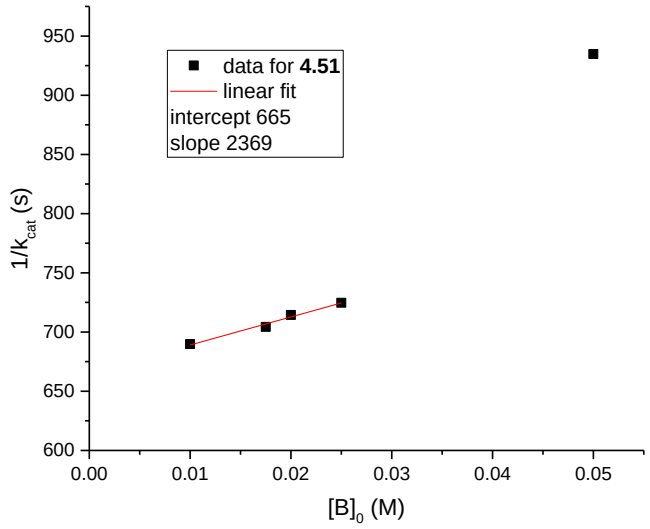

Figure 85 Determination of k_1 and k_2 for 4.51. k_1 = 30.1 M^{-1} s^{-1}; k_2 = 8.44 M^{-1} s^{-1}.

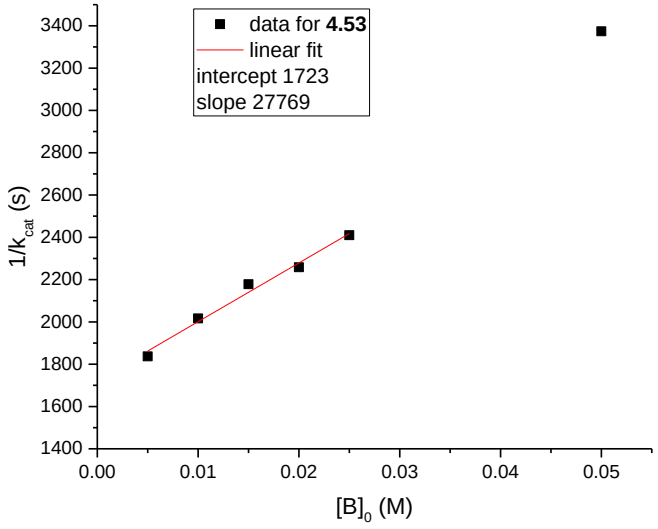

Figure 86 Determination of k_1 and k_2 for 4.53. k_1 = 11.6 M^{-1} s^{-1}; k_2 = 0.72 M^{-1} s^{-1}.

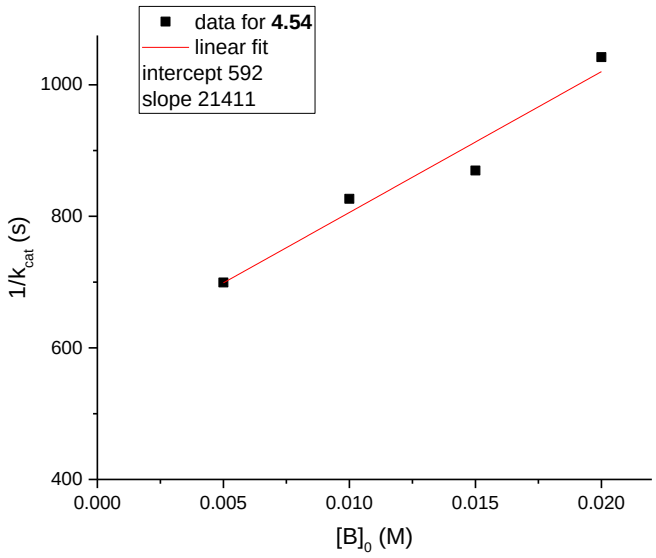

Figure 87 Determination of k_1 and k_2 for 4.54. k_1 = 33.8 M^{-1} s^{-1}; k_2 = 0.93 M^{-1} s^{-1}.

Significant differences in k_1 and k_2 between the diastereoisomeric catalysts were observed. In particular, the LLL diastereoisomer **4.50** is remarkable for a high k_1, while the DLL analogue **4.51** displays a very high k_2. Compounds **4.52** and **4.54** which are both based on a LDL tripeptide but differ by the connectivity of the auxiliary base provided very similar values of k_1 and k_2. While it was anticipated that the pyridine and imidazole in **4.54** will not be able to make an intramolecular contact, with the observed intermolecular activation mode this is no longer relevant. Compared to the literature precedents (Sakai's catalyst:[248] k_1 = 14.4 M^{-1} s^{-1}, k_2 = 0.63 M^{-1} s^{-1}; Schafmeister's spiroligozyme:[249] k_1 = 0.17 M^{-1} s^{-1}, k_2 = 0.01 M^{-1} s^{-1}) the five compounds discussed here represent a significant improvement.

4.4.3 Attempts at enantioselective transesterifications

Following the optimisation of the catalyst towards high reactivity, the final compounds **4.50**–**4.53** were tested in asymmetric transformations. The attempted reactions are shown in Scheme 33 and include an esterification (using O-acylated catalyst as a chiral acylating reagent) and a methanolysis (using free catalyst in the stereodetermining step). However, only racemic products were observed in all attempts. Although the catalysts are chiral, they were never designed with stereoselectivity

in mind. Achieving this goal would require an effective chiral space to be designed around the functional elements of the catalyst.

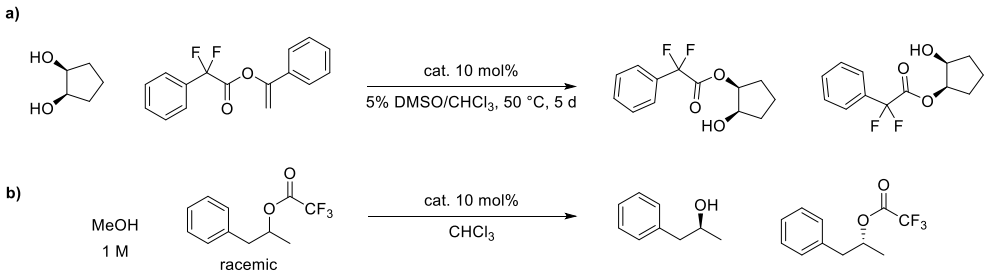

Scheme 33 Stereoselective reactions attempted with the third-generation catalysts.

4.5 Conclusions

Transesterification catalysts designed to follow the two-step biomimetic mechanism were optimised towards higher reactivity. The final design was highly reactive, significantly outperforming the literature precedents. Additionally, the compounds presented here are modular and easily synthesised. Kinetics of the catalysed reaction was analysed in detail, revealing the aggregation and intermolecular activation behaviour. Rate constants for the first and second transesterification steps were quantified for the final catalysts.

Stereoselective transesterifications were attempted but did not provide any enantioenriched products. However, due to the easily customised structure it should be possible to design a catalyst with a more effective chiral environment. In particular, the intermolecular activation observed in this work may be utilised by placing two catalytic peptide chains on a chiral scaffold. This provides an interesting lead for future work on transesterification catalysis.

Chapter 5 Summary

The work presented here was a tandem investigation of anion receptors for molecular recognition of anionic species in solution and of organocatalysts that rely on anionic transition state binding to promote chemical reactions.

In Chapter 2 a series of charge-neutral, tetradentate XB receptors were demonstrated to be effective for anion binding in organic solvents via convergent XB interactions. These anion hosts were selective for large halides, significantly outperforming their isostructural HB analogues. Introduction of fluorophores allowed to obtain a fluorescent response to anion binding. A chiral XB receptor showed a modest discrimination between enantiomers of tartrate and bulky amino acid anions.

In Chapter 3 this XB receptor design was enhanced by preorganisation and solubilisation in water. The resulting second-generation XB receptors displayed extremely strong and highly selective I^- binding in water, undergoing enthalpy-driven complex formation in 2:1 host-guest stoichiometry. A receptor containing Te σ-hole donor units on the same tetrakis(triazole) scaffold was also described. It displayed similar properties to the XB analogues, providing an unprecedented example of a ChB anion receptor effective in an aqueous environment. Further to these fundamental studies, applications in fluorescent and electrochemical anion sensing in water were successfully demonstrated using XB receptors.

In Chapter 4 transesterification catalysts designed to exhibit a mechanism reminiscent of serine esterase enzymes were iteratively designed towards higher reactivity. Eventually a tripeptide motif equipped with an electron-deficient thiourea oxyanion hole was established. Kinetic studies performed on the final compounds revealed their high reactivity compared to the literature precedents. Although the final catalysts were unable to effect stereoselective transesterifications, their modular, easily customisable character makes them a promising platform to accomplish this objective.

Chapter 6 Experimental

6.1 General information

Naming and numbering

Compounds were named according to the IUPAC convention or using common names. Numbering of atoms for NMR assignment does not follow the IUPAC convention.

Reaction conditions

Room temperature refers to 20-25 °C. For the temperature of 0 °C an ice/water bath was used. For temperatures between –78 °C and 0 °C a dry ice/acetone bath was used. Where anhydrous conditions were required, the reactions were done in flame-dried glassware and under an atmosphere of dry argon or nitrogen.

Solvents, reagents, and materials

All commercially available chemicals and solvents were used as received without further purification or purified using standard techniques. All dry solvents were thoroughly degassed with N_2, dried on a Mbraun MPSP-800 column and used immediately or following storage on 3 Å MS. Water used was deionized and where necessary passed through a Milli-Q® Millipore machine for microfiltration. Et_3N was distilled and stored over KOH. Silica column chromatography was done using silica gel 60 (40-63 μm). TBTA (tris(benzyltriazolemethyl)amine) was prepared according to the literature procedures.[263]

Analytical techniques

NMR spectra were recorded on Bruker AVIII HD Nanobay 400 MHz, Bruker AVIII 500 MHz and Bruker AVIII 500 MHz (with ^{13}C cryoprobe) spectrometers. Spectra were acquired at 298 K unless specified otherwise. Chemical shifts are quoted in parts per million and referenced using the residual solvent peak.

Electrospray ionisation mass spectrometry (ESI-MS) was performed using the Waters Micromass LCT and Bruker microTOF spectrometers.

Infrared spectra were recorded on a Bruker Tensor 27 FTIR spectrometer with ATR attachment with a diamond window.

Optical rotations were recorder on a Perkin-Elmer 241 polarimeter with 1 dm path length, using sodium D line (589 nm).

Melting points were measured on a Griffin melting point apparatus and are uncorrected.

Isothermal titration calorimetry (ITC) titrations were performed using a Malvern MicroCal PEAQ-ITC Automated calorimeter.

Luminescence spectroscopy was done using a HORIBA Fluorolog, and the data was processed using the FluorEssence software.

Chiral HPLC was done using a Dionex UltiMate 3000 with a Dionex LPG-3400A pump, WPS3000-SL autosampler, TCC3000SD column oven, DAD-3000 diode array detector, and a 0.46 cm ø × 25 cm Daicel Chiralpak column with a 0.4 cm ø × 1 cm guard column.

6.2 Compound data for Chapter 2

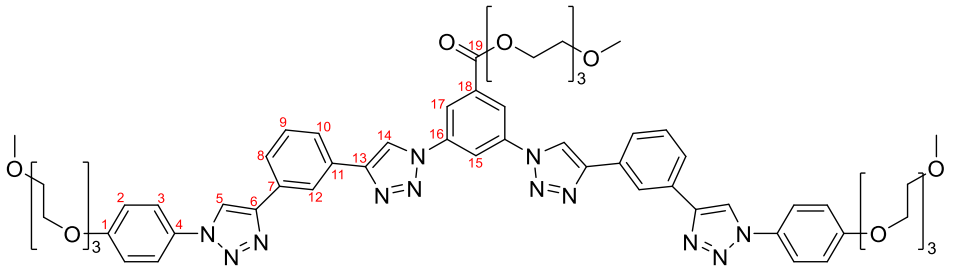

2.1a

General procedure for azide-alkyne cycloaddition was used to couple **2.15** (35 mg, 0.1 mmol) and **2.20a** (90 mg, 0.22 mmol). The product was separated by silica column chromatography (20% acetone/DCM then 3% MeOH/DCM) followed by PTLC (2.5→3% MeOH/DCM) to afford the product **2.1a** as a colorless amorphous solid (75 mg, 0.064 mmol, 64%).

δ_H (400 MHz, $CDCl_3$): 8.57 (s, 2H, H^{14}), 8.42 (s, 1H, H^{15}), 8.26 (s, 2H, H^{17}), 8.24 (s, 2H, H^{5}), 8.22 (s, 2H, H^{12}), 7.74 (m, 4H, H^{8}, H^{10}), 7.59 (d, J = 8.4 Hz, 4H, H^{3}), 7.30 (t, J = 8.0 Hz, 2H, H^{9}), 6.90 (d, J = 8.4 Hz, 4H, H^{2}), 4.41 (s, 2H, TEG-CH_2), 4.07 (t, J = 4.6 Hz, 4H, TEG-CH_2), 3.81 (m, 6H, TEG-CH_2), 3.75 – 3.56 (m, 18H, TEG-CH_2), 3.52 (m, 4H, TEG-CH_2), 3.45 (m, 2H, TEG-CH_2), 3.33 (s, 6H, ^{lateral}TEG-CH_3), 3.22 (s, 3H, ^{central}TEG-CH_3); δ_C (100 MHz, $CDCl_3$): 163.99 (C^{19}), 158.91 (C^{1}), 148.19 (C^{6}/C^{13}), 147.48 (C^{6}/C^{13}), 137.77 (C^{16}), 133.11 (C^{18}), 130.95 (C^{7}/C^{11}), 130.42 (C^{4}), 130.24 (C^{7}/C^{11}), 129.40 (C^{9}), 125.65 (C^{8}/C^{10}), 125.45 (C^{8}/C^{10}), 122.90 (C^{12}), 121.69 (C^{3}), 119.85 (C^{17}), 118.34 (C^{5}/C^{14}), 118.30 (C^{5}/C^{14}), 115.35 (C^{2}), 114.76 (C^{15}), 71.96 (TEG-CH$_2$), 71.88 (TEG-CH$_2$), 70.88 (TEG-CH$_2$), 70.73 (TEG-CH$_2$), 70.69 (TEG-CH$_2$), 70.64 (TEG-CH$_2$), 70.60 (TEG-CH$_2$), 70.54 (TEG-CH$_2$), 69.63 (TEG-CH$_2$), 68.90 (TEG-CH$_2$), 67.83 (TEG-CH$_2$), 65.11 (TEG-CH$_2$), 59.04 (^{lateral}TEG-CH$_3$), 58.90 (^{central}TEG-CH$_3$); LRMS m/z 1165.63 $[M+H]^+$; HRMS m/z calcd for $C_{60}H_{68}N_{12}O_{13}$ $[M+Na]^+$: 1165.51016, found: 1165.51083.

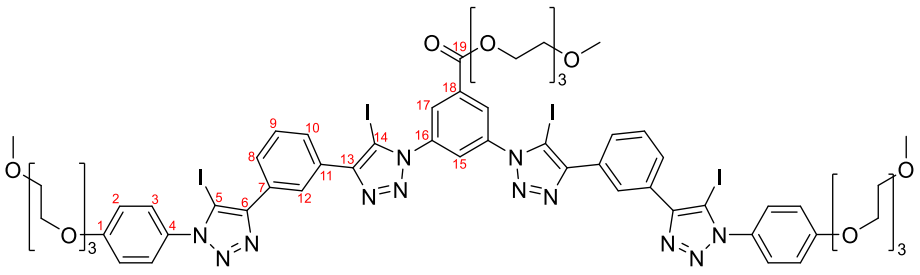

2.1b

General procedure for azide-iodoalkyne cycloaddition was used to couple **2.15** (35 mg, 0.1 mmol) and **2.20b** (145 mg, 0.22 mmol). The product was isolated by silica column chromatography (25-30% hexanes/acetone) to afford **2.1b** as a white solid foam (103 mg, 0.062 mmol, 62%).

δ_H (400 MHz, $CDCl_3$): δ 8.68 (t, J = 1.8 Hz, 2H, H^{12}), 8.55 (d, J = 2.0 Hz, 2H, H^{17}), 8.15 (t, J = 2.0 Hz, 1H, H^{15}), 8.11 (dt, J = 7.8, 1.4 Hz, 2H, H^{8}/H^{10}), 8.07 (dt, J = 7.9, 1.4 Hz, 2H, H^{8}/H^{10}), 7.64 (t, J = 7.8 Hz, 2H, H^{9}), 7.47 – 7.41 (m, 4H, H^{3}), 7.11 – 7.03 (m, 4H, H^{2}), 4.61 – 4.53 (m, 2H, TEG-CH_2), 4.21 (t, J = 4.8 Hz, 4H, TEG-CH_2), 3.88 (dt, J = 13.7, 4.8 Hz, 6H, TEG-CH_2), 3.78 – 3.58 (m, 18H, TEG-CH_2), 3.55 (dd, J = 5.8, 3.5 Hz, 4H, TEG-CH_2), 3.49 (dd, J = 5.7, 3.5 Hz, 2H, TEG-CH_2), 3.37 (s, 6H, TEG-CH_3), 3.31 (d, J = 4.0 Hz, 3H, TEG-CH_3); δ_C (100 MHz, $CDCl_3$): 163.82 (C^{19}), 160.18 (C^{1}), 150.91 (C^{6}/C^{13}), 149.66 (C^{6}/C^{13}), 137.94 (C^{16}), 133.06 (C^{18}), 130.86 (C^{7}/C^{11}), 130.11 (C^{4}/C^{7}/C^{11}), 130.06 (C^{4}/C^{7}/C^{11}), 129.24 (C^{9}), 128.87 (C^{17}), 128.41 (C^{8}/C^{10}), 128.34 (C^{15}), 128.14 (C^{8}/C^{10}), 127.97 (C^{3}), 126.69 (C^{12}), 115.20 (C^{2}), 79.14 (C^{5}/C^{14}), 78.03 (C^{5}/C^{14}), 72.04 (TEG-CH$_2$), 71.99 (TEG-CH$_2$), 71.00 (TEG-CH$_2$), 70.83 (TEG-CH$_2$), 70.78 (TEG-CH$_2$), 70.70 (TEG-CH$_2$), 69.69 (TEG-CH$_2$), 69.02 (TEG-CH$_2$), 67.99 (TEG-CH$_2$), 65.52 (TEG-CH$_2$), 59.16 (^{lateral}TEG-CH$_3$), 59.13 (^{central}TEG-CH$_3$); LRMS m/z 1669.32 $[M+H]^+$, 1691.31 $[M+Na]^+$; HRMS m/z calcd for $C_{60}H_{64}I_4N_{12}O_{13}$ $[M+Na]^+$: 1691.07977, found: 1691.08228.

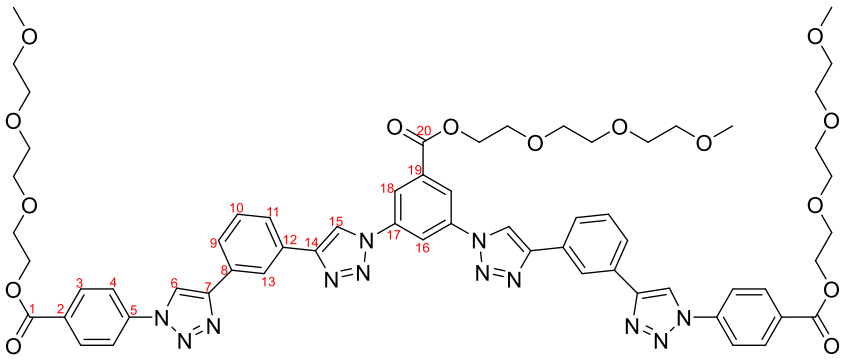

2.2a

General procedure for azide-alkyne cycloaddition was used to couple compounds **2.21a** (154 mg, 0.35 mmol) and **2.15** (56 mg, 0.16 mmol) using BTA (6.7 mg, 0.035 mmol) as catalyst instead of TBTA. The product was isolated by silica chromatography (2-3% MeOH/DCM followed by PTLC (2.5% MeOH/DCM) to afford **2.2a** (130 mg, 0.106 mmol, 67%) as a white solid.

δ_H (400 MHz, $CDCl_3$): 8.58 (s, 2H, H^{15}), 8.56 (s, 1H, H^{16}), 8.45 (s, 2H, H^{6}), 8.37 (s, 2H, H^{18}), 8.34 (s, 2H, H^{13}), 8.16 (d, J = 8.2 Hz, 4H, H^{3}), 7.87 (m, 8H, H^{4}, H^{9}, H^{11}), 7.44 (t, J = 7.8 Hz, 2H, H^{10}), 4.60 – 4.40 (m, 6H, TEG-CH_2), 3.87 (m, 6H, TEG-CH_2), 3.70 (m, 19H, TEG-CH_2), 3.51 (m, 7H, TEG-CH_2), 3.35 (s, 6H, TEG-CH_3), 3.26 (s, 3H, TEG-CH_3); δ_C (100 MHz, $CDCl_3$): 165.43 (C^{1}), 164.13 (C^{20}), 148.41 (C^{7}/C^{14}), 148.18 (C^{7}/C^{14}), 140.06 (C^{5}), 138.03 (C^{17}), 133.55 (C^{19}), 131.53 (C^{3}), 130.70 (C^{8}/C^{12}), 130.41 (C^{8}/C^{12}), 130.21 (C^{2}), 129.72 (C^{10}), 126.01 (C^{9}/C^{11}), 125.92 (C^{9}/C^{11}), 123.16 (C^{13}), 120.10 (C^{18}), 119.74 (C^{4}), 118.24 (C^{15}), 118.03 (C^{6}), 115.14 (C^{16}), 72.05 (TEG-CH$_2$), 72.00 (TEG-CH$_2$), 70.88 (TEG-CH$_2$), 70.83 (TEG-CH$_2$), 70.80 (TEG-CH$_2$), 70.74 (TEG-CH$_2$), 70.70 (TEG-CH$_2$), 69.26 (TEG-CH$_2$), 69.07 (TEG-CH$_2$), 65.33 (TEG-CH$_2$), 64.63 (TEG-CH$_2$), 59.16 (TEG-CH$_3$), 59.01 (TEG-CH$_3$); LRMS m/z 1243.4 $[M+Na]^+$ HRMS calcd. for $C_{62}H_{68}N_{12}O_{15}Na$ $[M+Na]^+$: 1243.48193, found: 1243.48171.

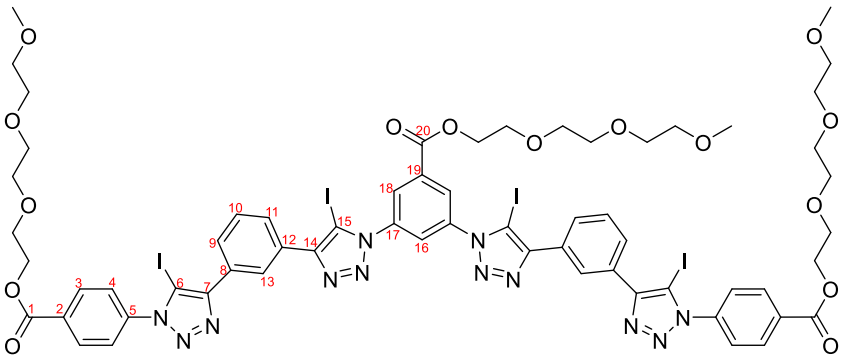

2.2b

General procedure for azide-iodoalkyne cycloaddition was used to couple compounds **2.21b** (136 mg, 0.20 mmol) and **2.15** (31 mg, 0.089 mmol). The product was isolated by silica column chromatography (1.5-2.5% MeOH/DCM) to afford **2.2b** (90 mg, 0.052 mmol, 58%) as a white foam.

δ_H (400 MHz, $CDCl_3$): 8.69 (t, J = 1.8 Hz, 2H, H^{13}), 8.59 – 8.53 (m, 2H, H^{18}), 8.29 (d, J = 8.3 Hz, 4H, H^{3}), 8.18 – 8.15 (m, 1H, H^{16}), 8.14 – 8.08 (m, 4H, H^{9}, H^{11}), 7.71 (d, J = 8.3 Hz, 4H, H^{4}), 7.67 (t, J = 7.9 Hz, 2H, H^{10}), 4.58 (m, 2H, TEG-CH_2), 4.54 (m, 4H, TEG-CH_2), 3.94 – 3.82 (m, 6H, TEG-CH_2), 3.77 – 3.58 (m, 18H, TEG-CH_2), 3.52 (m, 6H, TEG-CH_2), 3.36 (s, 6H, TEG-CH_3), 3.32 (s, 3H, TEG-CH_3); δ_C (100 MHz, $CDCl_3$): 165.41 (C^{1}), 163.83 (C^{20}), 150.87 (C^{7}/C^{14}), 150.51 (C^{7}/C^{14}), 140.42 (C^{5}), 137.96 (C^{17}), 133.10 (C^{19}), 131.88 (C^{2}), 131.01 (C^{3}), 130.55 (C^{8}/C^{12}), 130.21 (C^{8}/C^{12}), 129.33 (C^{10}), 128.90 (C^{18}), 128.56 (C^{9}/C^{11}), 128.36 (C^{9}/C^{11}), 128.34 (C^{16}), 126.88 (C^{13}), 126.49 (C^{4}), 77.93 (C^{6}/C^{15}), 77.63 (C^{6}/C^{15}), 72.06 (TEG-CH$_2$), 72.02 (TEG-CH$_2$), 70.86 (TEG-CH$_2$), 70.84 (TEG-CH$_2$), 70.81 (TEG-CH$_2$), 70.79 (TEG-CH$_2$), 70.75 (TEG-CH$_2$), 70.74 (TEG-CH$_2$), 69.24 (TEG-CH$_2$), 69.05 (TEG-CH$_2$), 65.57 (TEG-CH$_2$), 64.81 (TEG-CH$_2$), 59.20 (TEG-CH$_3$), 59.16 (TEG-CH$_3$); HRMS calcd. for $C_{62}H_{64}N_{12}O_{15}I_4Na$ $[M+Na]^+$: 1747.06850, found: 1747.06899.

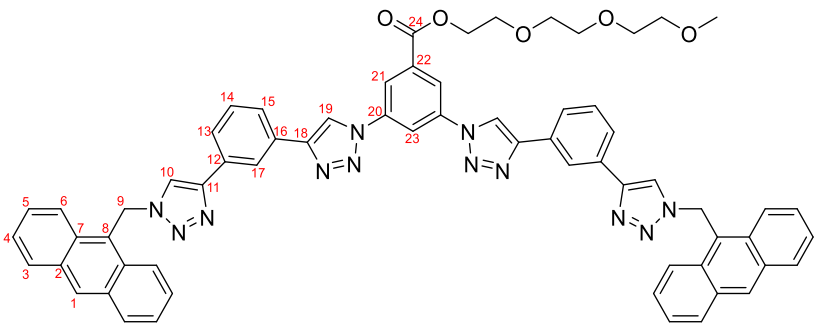

2.3a

General procedure for azide-alkyne cycloaddition was used to couple **2.22a** (79 mg, 0.22 mmol) and **2.15** (35 mg, 0.1 mmol). The product was isolated by silica column chromatography (1-1.5% MeOH/DCM) to provide **2.3a** (88 mg, 0.082 mmol 82%) as a yellowish solid.

δ_H (400 MHz, $CDCl_3$): 8.53 (s, 2H, H^1), 8.38 – 8.29 (m, 8H, H^6, H^{19}, H^{21}), 8.27 (t, J = 2.1 Hz, 1H, H^{23}), 8.07 (t, J = 1.7 Hz, 2H, H^{17}), 8.05 – 7.98 (d, J = 8.4 Hz, 4H, H^3), 7.77 (dt, J = 7.7, 1.4 Hz, 2H, H^{15}), 7.69 (dt, J = 7.8, 1.4 Hz, 2H, H^{13}), 7.54 (ddd, J = 8.7, 6.6, 1.4 Hz, 4H, H^5), 7.50 (s, 2H, H^{10}), 7.46 (ddd, J = 7.7, 6.6, 1.0 Hz, 4H, H^4), 7.33 (t, J = 7.8 Hz, 2H, H^{14}), 6.54 (s, 4H, H^9), 4.54 – 4.42 (m, 2H, TEG-CH_2), 3.87 – 3.78 (m, 2H, TEG-CH_2), 3.69 – 3.63 (m, 2H, TEG-CH_2), 3.63 – 3.58 (m, 2H, TEG-CH_2), 3.58 – 3.51 (m, 2H, TEG-CH_2), 3.45 – 3.39 (m, 2H, TEG-CH_2), 3.21 (s, 3H, TEG-CH_3); δ_C (100 MHz, $CDCl_3$): 164.17 (C^{24}), 148.52 (C^{18}), 147.38 (C^{11}), 138.01 (C^{20}), 133.47 (C^{22}), 131.53 (C^7), 131.30 (C^{12}), 130.92 (C^2), 130.16 (C^{16}), 130.05 (C^1), 129.60 (C^3), 129.49 (C^{14}), 127.85 (C^5), 125.89 (C^{13}), 125.54 (C^4), 125.50 (C^{15}), 123.75 (C^8), 123.03 (C^6), 122.98 (C^{17}), 120.26 (C^{21}), 119.83 (C^{10}), 118.02 (C^{19}), 115.28 (C^{23}), 71.93 (TEG-CH$_2$), 70.81 (TEG-CH$_2$), 70.69 (TEG-CH$_2$), 70.62 (TEG-CH$_2$), 68.99 (TEG-CH$_2$), 65.24 (TEG-CH$_2$), 58.96 (TEG-CH$_3$), 46.71 (C^9); LRMS m/z 1069.56 $[M+H]^+$; HRMS m/z calcd for $C_{64}H_{53}N_{12}O_5$ $[M+Na]^+$: 1091.40758, found: 1091.40832.

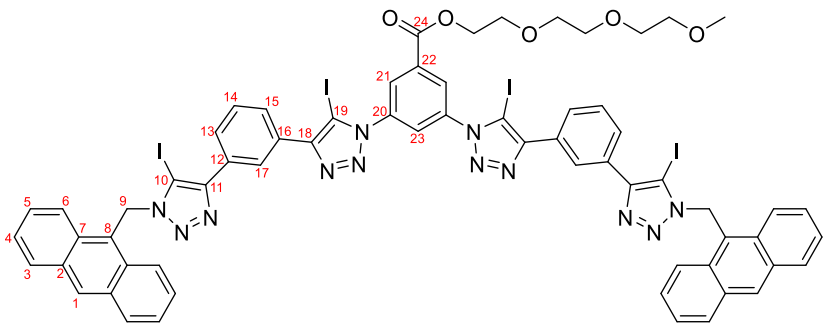

2.3b

General procedure for azide-iodoalkyne cycloaddition was used to couple **2.22b** (136 mg, 0.22 mmol) and **2.15** (35 mg, 0.1 mmol). The product was isolated by silica column chromatography (4-10% acetone/DCM) followed by PTLC (1% MeOH/DCM) to provide **2.3b** (84 mg, 0.053 mmol, 53%) as a yellow solid.

δ_H (400 MHz, $CDCl_3$): 8.59 (t, J = 1.8 Hz, 2H, H^{17}), 8.55 (s, 2H, H^1), 8.51 (d, J = 2.0 Hz, 2H, H^{21}), 8.32 – 8.23 (d, J = 8.8 Hz, 4H, H^6), 8.07 (t, J = 2.0 Hz, 1H, H^{23}), 8.03 (m, 8H, H^3, H^{13}, H^{15}), 7.63 – 7.52 (m, 6H, H^5, H^{14}), 7.48 (ddd, J = 7.7, 6.6, 1.0 Hz, 4H, H^4), 6.46 (s, 4H, H^9), 4.62 – 4.52 (m, 2H, TEG-CH_2), 3.91 – 3.81 (m, 2H, TEG-CH_2), 3.75 – 3.68 (m, 2H, TEG-CH_2), 3.67 – 3.62 (m, 2H, TEG-CH_2), 3.62 – 3.56 (m, 2H, TEG-CH_2), 3.53 – 3.44 (m, 2H, TEG-CH_2), 3.30 (s, 3H, TEG-CH_3); δ_C (125 MHz, $CDCl_3$): 163.84 (C^{24}), 150.90 (C^{11}/C^{18}), 149.36 (C^{11}/C^{18}), 137.91 (C^{20}), 133.06 (C^{22}), 131.56 (C^2/C^7), 131.43 (C^2/C^7), 130.94 (C^{12}/C^{16}), 130.02 (C^1), 129.54 (C^3), 129.19 (C^{14}), 128.87 (C^{21}), 128.30 (C^{13}/C^{15}, C^{23}), 128.04 (C^{13}/C^{15}), 127.29 (C^5), 126.59 (C^{17}), 125.29 (C^4), 123.89 (C^6), 123.86 (C^8), 77.97 (C^{19}), 76.54 (C^{10}), 72.01 (TEG-CH$_2$), 70.85 (TEG-CH$_2$), 70.80 (TEG-CH$_2$), 70.73 (TEG-CH$_2$), 69.04 (TEG-CH$_2$), 65.53 (TEG-CH$_2$), 59.15 (TEG-CH$_3$), 48.36 (C^9); HRMS m/z calcd for $C_{64}H_{49}I_4N_{12}O_5$ $[M+H]^+$: 1573.01221; found: 1573.01348.

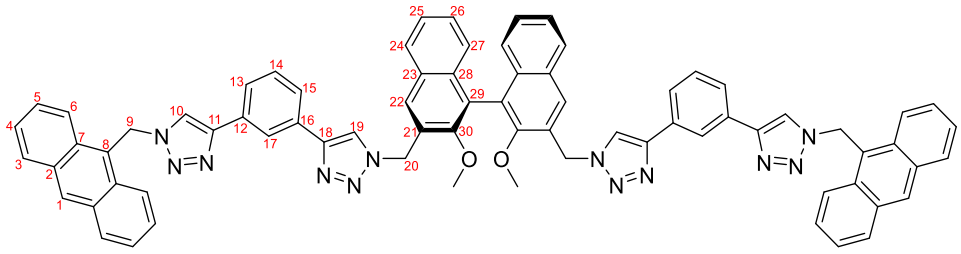

2.4a

General procedure for azide-iodoalkyne cycloaddition was used to couple **2.22a** (108 mg, 0.3 mmol) and **2.19** (57 mg, 0.135 mmol). The product was isolated by silica column chromatography (1-1.5% MeOH/DCM) to provide **2.4a** (136 mg, 0.119 mmol, 88%) as a yellowish solid.

δ_H (400 MHz, $CDCl_3$): 8.52 (s, 2H, H^1), 8.26 (d, J = 8.8 Hz, 4H, H^6), 8.04 – 7.97 (m, 6H, H^3, H^{17}), 7.91 (s, 2H, H^{19}), 7.78 (m, 4H, H^{22}, H^{27}), 7.65 (dt, J = 7.8, 1.4 Hz, 2H, H^{15}), 7.59 – 7.49 (m, 6H, H^5, H^{13}), 7.45 (ddd, J = 7.7, 6.6, 1.0 Hz, 4H, H^4), 7.36 (ddd, J = 8.1, 6.8, 1.2 Hz, 2H H^{25}), 7.32 (s, 2H, H^{10}), 7.29 – 7.20 (m, 4H, H^{14}, H^{26}), 7.17 – 7.11 (m, 2H, H^{24}), 6.49 (s, 4H, H^9), 5.88 – 5.69 (m, 4H, H^{20}), 3.06 (s, 6H, OCH_3); δ_C (100 MHz, $CDCl_3$): 154.43 (C^{30}), 147.69 (C^{18}), 147.53 (C^{11}), 134.48 (BINOL quat *C*), 131.56 (C^7), 131.14 (Ar quat *C*), 131.12 (Ar quat *C*), 130.92 (C^2), 130.41 (Ar quat *C*), 130.37 (C^{22}), 130.09 (C^1), 129.63 (C^3), 129.35 (C^{14}), 128.43 (C^{27}), 128.39 (BINOL quat *C*), 127.87 (C^5), 127.56 (C^{26}), 125.64 (C^{25}), 125.63 (C^{24}), 125.54 (C^4), 125.37 (C^{13}), 125.25 (C^{15}), 124.31 (BINOL quat *C*), 123.68 (C^8), 123.00 (C^6), 122.70 (C^{17}), 120.55 (C^{19}), 119.56 (C^{10}), 61.09 (OCH_3), 50.29 (C^{20}), 46.65 (C^9); LRMS m/z 1143.59 $[M+H]^+$; HRMS m/z calcd for $C_{74}H_{55}N_{12}O_2$ $[M+H]^+$: 1143.45655, found: 1143.45547; $[\alpha]_D^{25}$ 48.2° ($CHCl_3$).

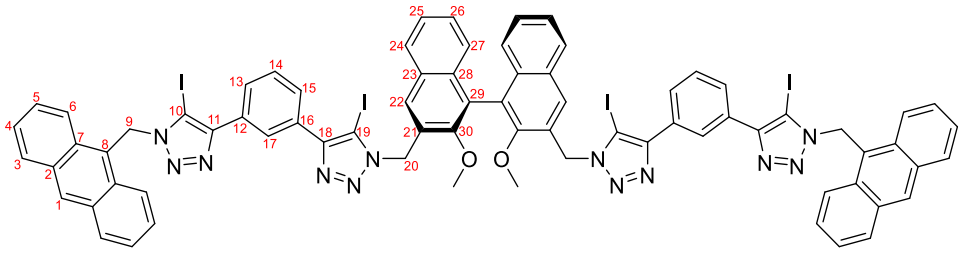

2.4b

General procedure for azide-iodoalkyne cycloaddition was used to couple **2.22b** (136 mg, 0.22 mmol) and **2.19** (42 mg, 0.1 mmol). The product was isolated by silica column chromatography (2% MeOH/DCM) followed by PTLC (1% MeOH/DCM) to provide **2.4b** (140 mg, 0.085 mmol, 85%) as a yellowish solid.

δ_H (500 MHz, $CDCl_3$): 8.61 (s, 2H, H^{17}), 8.55 (s, 2H, H^1), 8.27 (d, J = 8.9 Hz, 4H, H^6), 8.07 (d, J = 7.9 Hz, 2H, H^{13}/H^{15}), 8.04 (d, J = 8.4 Hz, 4H, H^3), 7.98 (d, J = 7.9 Hz, 2H, H^{13}/H^{15}), 7.76 (d, J = 8.2 Hz, 2H, H^{27}), 7.55 (m, 6H, H^5, H^{14}), 7.47 (t, J = 7.5 Hz, 4H, H^4), 7.40 (s, 2H, H^{22}), 7.36 (t, J = 7.5 Hz, 2H, H^{26}), 7.25 (t, J = 6.9, 5.8 Hz, 2H, H^{25}), 7.17 (d, J = 8.6 Hz, 2H, H^{24}), 6.45 (s, 4H, H^9), 5.93 (s, 4H, H^{20}), 3.28 (s, 6H, OCH_3); δ_C (125 MHz, $CDCl_3$): 153.93 (C^{30}), 149.94 (C^{11}/C^{18}), 149.52 (C^{11}/C^{18}), 134.25 (BINOL quat *C*), 131.55 (C^2/C^7), 131.41 (C^2/C^7), 130.82 (Ar quat *C*), 130.69 (Ar quat *C*), 130.39 (Ar quat *C*), 129.98 (C^1), 129.51 (C^3), 129.04 (C^{14}), 128.67 (C^{22}), 128.39 (C^{27}), 128.24 (BINOL quat *C*), 127.90 (C^{13}/C^{15}), 127.70 (C^{13}/C^{15}), 127.28 (C^{25}), 127.25 (C^5), 126.36 (C^{17}), 125.68 (C^{24}), 125.49 (C^{26}), 125.27 (C^4), 123.90 (C^8), 123.87 (C^6), 77.60 (C^{19}), 76.49 (C^{10}), 61.05 (OCH_3), 50.45 (C^{20}), 48.32 (C^9); HRMS m/z calcd for $C_{74}H_{51}I_4N_{12}O_2$ $[M+H]^+$: 1647.04312; found: 1647.04339; $[\alpha]_D^{25}$ 27.3° ($CHCl_3$).

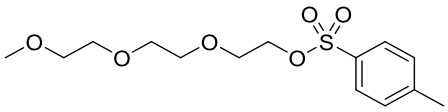

2.5

A literature procedure was used.[264] Triethylene glycol monomethyl ether (4.80 ml, 30 mmol) and dry triethylamine (6.27 ml, 45 mmol) were dissolved in dry DCM (60 ml) and *p*-toluenesulfonyl chloride (6.863 g, 36 mmol) was added. The reaction was stirred for 20 h at rt. The final mixture was washed with sat. aq. $NaHCO_3$, dried with anhydrous Na_2SO_4 and concentrated under vacuum. Crude material was purified by column chromatography (1.5% MeOH/DCM) to afford 8.870 g (27.86 mmol, 93%) of product **2.5** as a colourless oil.

δ_H (400 MHz, $CDCl_3$): 7.73 (d, J = 8.3 Hz, 2H, Ar*H*), 7.29 (d, J = 8.1 Hz, 2H, Ar*H*), 4.15 – 4.04 (m, 2H, TEG-CH_2), 3.67 – 3.56 (m, 2H, TEG-CH_2), 3.58 – 3.50 (m, 6H, TEG-CH_2), 3.47 (m, 2H, TEG-CH_2), 3.30 (s, 3H, TEG-CH_3), 2.39 (s, 3H, ArCH_3); δ_C (100 MHz, $CDCl_3$): 13C NMR (101 MHz, CDCl3) δ 144.75 (Ar*C*), 132.92 (Ar*C*), 129.77 (Ar*C*), 127.86 (Ar*C*), 71.81 (TEG-*C*H_2), 70.63 (TEG-*C*H_2), 70.45 (TEG-*C*H_2), 70.44 (TEG-*C*H_2), 69.23 (TEG-*C*H_2), 68.56 (TEG-*C*H_2), 58.91 (TEG-*C*H_3), 21.55 (Ar*C*H_3); LRMS m/z 341.1 $[M+Na]^+$.

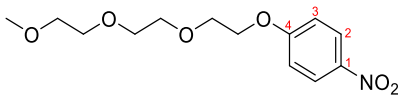

2.6

p-Nitrophenol (835 mg, 6 mmol) and **2.5** (1.592 g, 5 mmol) were added to dry MeCN (30 ml). K_2CO_3 (829 mg, 6 mmol) was added and the mixture was heated at reflux for 2.5 days. The solvent was then removed under vacuum and the residue suspended in water. The mixture was extracted with EtOAc and the combined organic phases were washed with water and brine, dried with anhydrous Na_2SO_4 and concentrated under vacuum. The crude product was purified by silica column chromatography (1.5% MeOH/DCM, R_f 0.37 in 2% MeOH/DCM) to afford 1.335 g (4.68 mmol, 94%) of **2.6** as a yellowish oil.

δ_H (400 MHz, $CDCl_3$): 8.16 (m, 2H, H^2), 6.95 (m, 2H, H^3), 4.21 (m, 2H, TEG-CH_2), 3.88 (m, 2H, TEG-CH_2), 3.80 – 3.58 (m, 6H, TEG-CH_2), 3.53 (m, 2H, TEG-CH_2), 3.35 (m, 3H, TEG-CH_3). δ_C (100 MHz, $CDCl_3$): 163.90 (C^1), 141.58 (C^4), 125.86 (C^2), 114.62 (C^3), 71.92 (TEG-*C*H_2), 70.91 (TEG-*C*H_2), 70.64 (TEG-*C*H_2), 70.57 (TEG-*C*H_2), 69.41 (TEG-*C*H_2), 68.23 (TEG-*C*H_2), 59.03 (TEG-*C*H_3); LRMS m/z 308.1 $[M+Na]^+$.

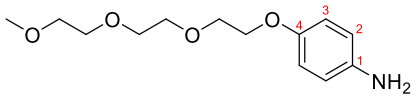

2.7

Compound **2.6** (1.300 g, 4.56 mmol) was dissolved in MeOH (50 ml). Hydrazine hydrate (2.2 ml, 45.6 mmol) and 10% Pd/C (60 mg) were added. The mixture was heated at reflux overnight. It was then filtered through Celite, concentrated under reduced pressure and dried under high vacuum. The crude product was purified by column chromatography on silica (1-5% MeOH/DCM) to afford 1.035 g (4.05 mmol, 89%) of **2.7** as a yellowish oil.

δ_H (400 MHz, $CDCl_3$): 6.70 – 6.62 (m, 2H, H^3), 6.57 – 6.51 (m, 2H, H^2), 3.96 (m, 2H, TEG-CH_2), 3.72 (m, 2H, TEG-CH_2), 3.67 – 3.61 (m, 2H, TEG-CH_2), 3.61 – 3.54 (m, 4H, TEG-CH_2), 3.50 – 3.44 (m, 2H, TEG-CH_2), 3.29 (s, 3H, TEG-CH_3), 3.19 (br s, 2H, NH_2). δ_C (100 MHz, $CDCl_3$): 151.70 (C^4), 140.27 (C^1), 116.19 (C^2), 115.77 (C^3), 71.81 (TEG-CH$_2$), 70.63 (TEG-CH$_2$), 70.51 (TEG-CH$_2$), 70.41 (TEG-CH$_2$), 69.79 (TEG-CH$_2$), 68.05 (TEG-CH$_2$), 58.90 (TEG-CH$_3$); LRMS m/z 256.2 $[M+H]^+$.

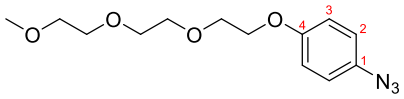

2.8

Compound **2.7** (1.005 g, 3.94 mmol) was dissolved in 17% aqueous HCl (26 ml) and the solution was cooled down to 0 °C. $NaNO_2$ (435 mg, 6.30 mmol) was added in small portions, causing the reaction mixture to become purple and then change colour to light brown. After strirring for 15 min at 0 °C, NaN_3 (410 mg, 6.30 mmol) was added in small portions, resulting in immediate evolution of gas. The reaction was stirred for 20 min at 0 °C and allowed to warm up to rt over 1 h. It was then diluted with water (25 ml) and neutralised with Na_2CO_3. The resulting solution was extracted with EtOAc, the organic fractions were dried with anhydrous Na_2SO_4 and concentrated under vacuum. The crude product was purified by silica column chromatography (1-1.5% MeOH/DCM), giving 776 mg (2.76 mmol, 67%) of **2.8** as a brown oil.

δ_H (400 MHz, $CDCl_3$): 6.97 – 6.83 (m, 4H, ArH), 4.09 (m, 2H, TEG-CH_2), 3.83 (m, 2H, TEG-CH_2), 3.75 – 3.69 (m, 2H, TEG-CH_2), 3.69 – 3.60 (m, 4H, TEG-CH_2), 3.56 – 3.51 (m, 2H, TEG-CH_2), 3.36 (s, 3H, TEG-CH_3). δ_C (100 MHz, $CDCl_3$): 156.29 (C^4), 132.58 (C^1), 120.02 (C^2), 116.02 (C^3), 72.02 (TEG-CH$_2$), 70.92 (TEG-CH$_2$), 70.74 (TEG-CH$_2$), 70.65 (TEG-CH$_2$), 69.80 (TEG-CH$_2$), 67.94 (TEG-CH$_2$), 59.10 (TEG-CH$_3$); LRMS m/z 304.1 $[M+H]^+$; HRMS calcd for $C_{13}H_{19}N_3NaO_4$ $[M+Na]^+$: 304.12678, found: 304.12669.

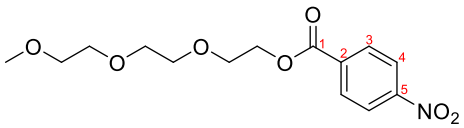

2.9

4-nitrobenzoic acid (1.671 g, 10 mmol) was added to $SOCl_2$ (20 ml). A few drops of DMF were then added and the mixture was heated at reflux for 2 h. It was then concentrated and dried under vacuum. The residue was dissolved in dry toluene (20 ml) and combined with tri(ethylene glycol) monomethyl ether (1.600 ml, 11 mmol) and DMAP (61 mg, 0.5 mmol). The reaction was heated at reflux overnight. The resulting mixture was concentrated under vacuum and separated by silica chromatography (0.5-1.5% MeOH/DCM) to provide **2.9** (2.350 g, 7.50 mmol, 75%) as a brown oil.

δ_H (400 MHz, $CDCl_3$) 8.31 – 8.26 (m, 2H, H^4), 8.25 – 8.20 (m, 2H, H^3), 4.56 – 4.49 (m, 2H, TEG-CH_2), 3.88 – 3.83 (m, 2H, TEG-CH_2), 3.75 – 3.69 (m, 2H, TEG-CH_2), 3.69 – 3.62 (m, 4H, TEG-CH_2), 3.56 – 3.51 (m, 2H, TEG-CH_2), 3.37 (s, 3H, TEG-CH_3); δ_C (100 MHz, $CDCl_3$) 164.82 (C^1), 150.68 (C^5), 135.63 (C^2), 130.98 (C^3), 123.65 (C^4), 72.05, 70.83, 70.79, 70.76, 69.12, 65.10, 59.21; ESI-MS m/z 336.1 $[M+Na]^+$.

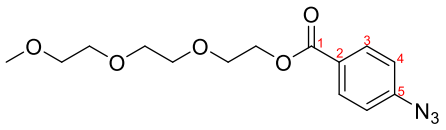

2.10

Compound **2.9** (2.350 g, 7.50 mmol) and 10% Pd/C (200 mg) were added to EtOAc (75 ml). The mixture was vigorously stirred under H_2 atmosphere for 24 h. It was then filtered through Celite and the filtrate concentrated under vacuum. The residue was dissolved in 1M HCl and the solution was cooled to 0 °C. $NaNO_2$ (543 mg, 7.88 mmol) in small amount of water was then added slowly. The resulting yellow solution was stirred for 10 min at 0 °C and NaN_3 (536 mg, 8.25 mmol) in small amount of water was added slowly. The mixture was stirred for 10 min at 0 °C and for 30 min at rt. It was then neutralised with sat. aq. $NaHCO_3$ and extracted with Et_2O. Combined organic phases were dried with anhydrous Na_2SO_4, decanted and concentrated under vacuum. The product was purified by silica chromatography (30-40% EtOAc/hexanes) to afford **2.10** (2.247 g, 7.26 mmol, 97%) as a yellow oil.

δ_H (400 MHz, $CDCl_3$): 8.11 – 7.98 (m, 2H, H^2), 7.12 – 6.99 (m, 2H, H^3), 4.53 – 4.36 (m, 2H, TEG-CH_2), 3.90 – 3.78 (m, 2H, TEG-CH_2), 3.78 – 3.61 (m, 6H, TEG-CH_2), 3.59 – 3.47 (m, 2H, TEG-CH_2), 3.37 (s, 3H, TEG-CH_3); δ_C (100 MHz, $CDCl_3$): 165.86 (C^1), 144.93 (C^2), 131.67 (C^3), 126.80 (C^5), 118.93 (C^4), 72.07 (TEG-CH$_2$), 70.84 (TEG-CH$_2$), 70.79 (TEG-CH$_2$), 70.74 (TEG-CH$_2$), 69.36 (TEG-CH$_2$), 64.34 (TEG-CH$_2$), 59.18; ESI-MS m/z calcd for $C_{14}H_{19}O_5N_3Na$ $[M+Na]^+$: 332.12169, found: 332.12151.

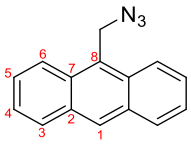

2.11

A literature procedure was used.[265] 9-Hydroxymethylanthracene (1.54 g, 7.40 mmol) was added to DCM (30 ml) and the solution was cooled to 0 °C. $SOCl_2$ (810 µl, 11.10 mmol) was then added slowly and the reaction was allowed to warm up to rt while being stirred for 1 h. Solvent was removed under vacuum and the residue redissolved in DMF (10 ml). NaN_3 (777 mg, 11.95 mmol) was added and the reaction was stirred at 50 °C for 1 h. It was then allowed to cool down, diluted with water and extracted with EtOAc. The combined organic phases were washed with brine, dried with anhydrous $MgSO_4$, filtered and concentrated under vacuum. The crude product was purified by silica column (1:19 EtOAc:petrol) to afford 980 mg (4.20 mmol, 57%) of **2.11** as a yellow crystalline solid.

δ_H (400 MHz, $CDCl_3$): 8.51 (s, 1H, H^1), 8.29 (dd, J = 8.9, 1.1 Hz, 2H, H^6), 8.05 (dd, J = 8.4, 1.2 Hz, 2H, H^3), 7.60 (ddd, J = 8.9, 6.5, 1.4 Hz, 2H, H^5), 7.52 (ddd, J = 7.8, 6.5, 1.0 Hz, 2H, H^4), 5.33 (s, 2H, CH_2). δ_C (100 MHz, $CDCl_3$): 131.50 (C^2), 130.83 (C^7), 129.42 (C^3), 129.12 (C^1), 126.97 (C^5), 125.90 (C^8), 125.33 (C^4), 123.64 (C^6), 46.49 (CH_2); EI-MS m/z 233.0949 $[M]^+$.

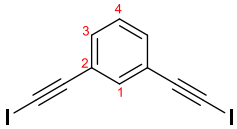

2.12

Method A: According to a literature procedure,[228] 1,3-diethynylbenzene (399 µl, 3 mmol) was added to dry THF (10 ml). The solution was cooled to −78 °C under N_2 atmosphere and 2.5M *n*-BuLi solution in THF (6 ml, 15 mmol) was added slowly, resulting in formation of a clumped precipitate. The reaction was strirred for 30 min at −78 °C. I_2 (3.807 g, 15 mmol) was separately dissolved in dry THF (12 ml) and the resulting solution was slowly added to the reaction mixture. The reaction was then allowed to warm to rt, diluted with water and extracted with $CHCl_3$. Sodium thiosulfate was added to the biphasic mixture during extraction to remove excess I_2. The organic layer was then washed with brine, dried with anhydrous $MgSO_4$, filtered and concentrated under vacuum. The residue was dry-loaded onto a silica column from DCM and eluted with petrol to afford **2.12** (1.078 g, 2.85 mmol, 95%) as a white crystalline solid.

Method B: According to a modified literature procedure,[266] 1,3-diethynylbenzene (864 µl, 6.50 mmol) was added to dry THF (26 ml). To this solution were added CuI (124 mg, 0.65 mmol), and N-iodomorpholine hydriodide (4.900 g, 14.37 mmol). The reaction was stirred at rt for 2 h. It was then filtered through Celite, concentrated under vacuum, diluted with DCM, washed with aqueous $Na_2S_2O_3$ solution, dried with anhydrous $MgSO_4$, filtered and concentrated under vacuum. The residue was dry-loaded onto a silica column from DCM and eluted with petrol to afford **2.12** (2.148 g, 5.68 mmol, 87%) as a white crystalline solid.

δ_H (400 MHz, $CDCl_3$): 7.42 (d, J = 1.8 Hz, 1H, H^1), 7.30 (dd, J = 7.8, 1.6 Hz, 2H, H^3), 7.18 (t, J = 7.7 Hz, 1H, H^4). δ_C (100 MHz, $CDCl_3$): δ 136.20 (C^1), 132.65 (C^3), 128.41 (C^4), 123.78 (C^2), 93.22 (*C*≡CI), 7.80 (C≡*C*I); EI-MS m/z 377.8398 $[M]^+$.

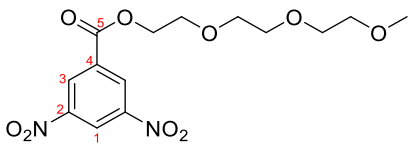

2.13

3,5-dinitrobenzoic acid (1.061 g, 5 mmol) was added to dry DCM (100 ml) and the solution was cooled to 0 °C. DCC (1.032 g, 5 mmol) and DMAP (61 mg, 0.5 mmol) were dissolved separately in small volumes of dry DCM and added to the reaction mixture, followed by triethylene glycol monomethyl ether (0.880 ml, 5.5 mmol). The reaction was allowed to warm up to rt overnight. The mixture was then filtered, concentrated under vacuum and separated by silica column chromatography (1-1.5% MeOH/DCM) to afford **2.13** as a clear oil (1.483 g, 4.14 mmol, 83%).

δ_H (400 MHz, $CDCl_3$): 9.20 (t, J = 2.2 Hz, 1H, H^1), 9.16 (d, J = 2.1 Hz, 2H, H^3), 4.63 – 4.55 (m, 2H, TEG-CH_2), 3.92 – 3.84 (m, 2H, TEG-CH_2), 3.75 – 3.69 (m, 2H, TEG-CH_2), 3.67 (dd, J = 6.2, 3.5 Hz, 2H, TEG-CH_2), 3.63 (dd, J = 5.7, 3.6 Hz, 2H, TEG-CH_2), 3.55 – 3.48 (m, 2H, TEG-CH_2), 3.33 (s, 3H, TEG-CH_3). δ_C (100 MHz, $CDCl_3$): 162.62 (C^5), 148.73 (C^2), 133.92 (C^4), 129.64 (C^3), 122.49 (C^1), 72.00 (TEG-CH$_2$), 70.77 (TEG-CH$_2$), 70.74 (TEG-CH$_2$), 70.70 (TEG-CH$_2$), 68.85 (TEG-CH$_2$), 65.89 (TEG-CH$_2$), 59.10 (TEG-CH$_2$). LRMS m/z 381.1 $[M+Na]^+$.

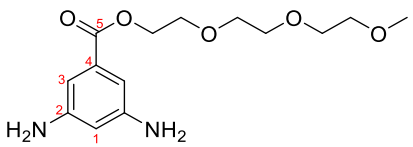

2.14

Compound **2.13** (1.250 g, 3.49 mmol) was dissolved in EtOAc (15 ml) and 10% Pd/C (100 mg) was added. The mixture was flushed with H_2 and stirred overnight under H_2 atmosphere at atmospheric pressure and rt. It was then filtered through Celite and concentrated to afford **2.14** as a brownish oil (1.044 g, 3.49 mmol, quant.).

δ_H (400 MHz, $CDCl_3$): 6.76 (d, J = 2.1 Hz, 2H, H^3), 6.15 (t, J = 2.1 Hz, 1H, H^1), 4.43 – 4.35 (m, 2H, TEG-CH_2), 3.78 (m, 2H, TEG-CH_2), 3.72 (br s, 4H, NH_2), 3.70 – 3.58 (m, 6H, TEG-CH_2), 3.52 (m, 2H, TEG-CH_2), 3.35 (s, 3H, TEG-CH_3); δ_C (100 MHz, $CDCl_3$): 166.96 (C^5), 147.66 (C^2), 131.98 (C^4), 106.99 (C^3), 105.79 (C^1), 71.98 (TEG-CH$_2$), 70.76 (TEG-CH$_2$), 70.66 (TEG-CH$_2$), 70.63 (TEG-CH$_2$), 69.32 (TEG-CH$_2$), 64.03 (TEG-CH$_2$), 59.06 (TEG-CH$_3$); LRMS m/z 299.2 $[M+H]^+$.

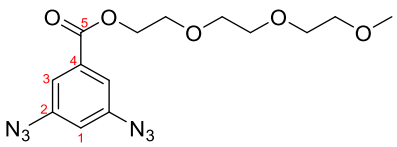

2.15

Compound **2.14** (994 mg, 3.33 mmol) was added to 37% aq HCl (50 ml) and the solution was cooled to 0 °C. $NaNO_2$ (781 mg, 11.33 mmol) was added in small portions and the mixture was stirred at 0 °C for 15 min. NaN_3 (737 mg, 11.33 mmol) was then added in small portions, resulting in release of gas. After stirring for another 15 min at 0 °C the reaction was allowed to warm to rt and stirred at rt for 20 min. It was then poured into cold water (150 ml) and extracted with EtOAc (4x). The extracts were washed with sat. aq. $NaHCO_3$ and brine, dried with anhydrous Na_2SO_4 and concentrated under vacuum. The crude product was purified by silica chromatography (1-2% MeOH/DCM) to afford **2.15** as a yellowish oil (785 mg, 2.24 mmol, 67%).

δ_H (400 MHz, $CDCl_3$): 7.48 (d, J = 2.2 Hz, 2H, H^3), 6.79 (t, J = 2.1 Hz, 1H, H^1), 4.55 – 4.43 (m, 2H, TEG-CH_2), 3.82 (m, 2H, TEG-CH_2), 3.75 – 3.59 (m, 6H, TEG-CH_2), 3.53 (m, 2H, TEG-CH_2), 3.36 (s, 3H, TEG-CH_3). δ_C (100 MHz, $CDCl_3$): 164.95 (C^5), 142.33 (C^2), 133.37 (C^4), 116.55 (C^3), 113.95 (C^1), 72.05 (TEG-CH$_2$), 70.82 (TEG-CH$_2$), 70.77 (TEG-CH$_2$), 70.73 (TEG-CH$_2$), 69.15 (TEG-CH$_2$), 64.88 (TEG-CH$_2$), 59.15 (TEG-CH$_2$); LRMS m/z 373.1 $[M+Na]^+$. HRMS m/z calcd for $C_{14}H_{18}N_6NaO_5$ $[M+Na]^+$: 373.12309, Found: 373.12336.

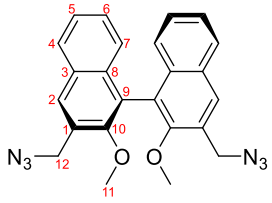

2.19

(S)-(2,2'-dimethoxy-[1,1'-binaphthalene]-3,3'-diyl)dimethanol (prepared according to literature procedures,[219] 112 mg, 0.300 mmol) was added to dry toluene (1.2 ml) and cooled to 0 °C. DPPA (155 µl, 0.720 mmol) and DBU (108 µl, 0.72 mmol) were then added slowly. The reaction was warmed to rt and stirred overnight under Ar atmosphere. It was then diluted with Et_2O, washed with water, dried with anhydrous Na_2SO_4, decanted, and concentrated under vacuum. The product was purified by silica chromatography (10–20% EtOAc/hexanes) to provide **2.19** (108 mg, 0.254 mmol, 85%) as a colourless oil.

δ_H (400 MHz, $CDCl_3$): 8.01 (s, 2H, H^2), 7.93 (dt, J = 8.2, 0.9 Hz, 2H, H^4), 7.44 (ddd, J = 8.2, 6.8, 1.3 Hz, 2H, H^5), 7.30 (ddd, J = 8.2, 6.7, 1.3 Hz, 2H, H^6), 7.21 (dd, J = 8.5, 1.1 Hz, 2H, H^7), 4.69 (d, J = 2.7 Hz, 4H, H^{12}), 3.32 (s, 6H, H^{11}); δ_C (101 MHz, $CDCl_3$): 154.76 (C^{10}), 134.42 (C^8), 130.38 (C^3), 130.13 (C^2), 129.02 (C^1), 128.24 (C^4), 127.08 (C^6), 125.73 (C^7), 125.36 (C^5), 124.30 (C^9), 61.12 (C^{11}), 50.99 (C^{12}); ESI-MS m/z 447.2 $[M+Na]^+$.

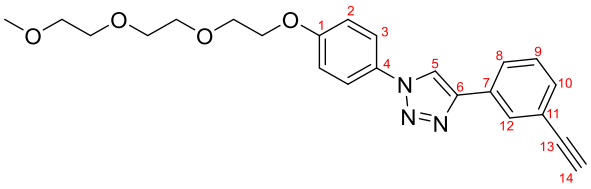

2.20a

General procedure for azide-alkyne cycloaddition

2.8 (281 mg, 1.00 mmol), diethynylbenzene (266 µl, 2.00 mmol) and DIPEA (17 µl, 0.10 mmol) were added to dry, degassed DCM (10 ml) under Ar atmosphere. Then $Cu(MeCN)_4PF_6$ (19 mg, 0.05 mmol) and TBTA (27 mg, 0.05 mmol) were added simultaneously. The mixture was stirred overnight at rt and under Ar. It was then diluted with DCM, washed with dilute aqueous NH_3, dried with anhydrous Na_2SO_4 and concentrated. The product was isolated by silica column chromatography (3-10% acetone/DCM) to provide **2.20a** as a white solid (280 mg, 0.69 mmol, 69%).

δ_H (400 MHz, $CDCl_3$): 8.12 (s, 1H, H^5), 7.97 (t, J = 1.7 Hz, 1H, H^{12}), 7.87 (dt, J = 7.7, 1.5 Hz, 1H, H^8), 7.67 – 7.57 (m, 2H, H^3), 7.43 (dt, J = 7.6, 1.4 Hz, 1H, H^{10}), 7.36 (t, J = 7.7 Hz, 1H, H^9), 7.03 – 6.95 (m, 2H, H^2), 4.14 (m, 2H, TEG-CH_2), 3.85 (m, 2H, TEG-CH_2), 3.72 (m, 2H, TEG-CH_2), 3.69 – 3.59 (m, 4H, TEG-CH_2), 3.52 (m, 2H, TEG-CH_2), 3.34 (s, 3H, TEG-CH_3), 3.11 (s, 1H, H^{14}); δ_C (100 MHz, $CDCl_3$): 159.13 (C^1), 147.21 (C^6), 131.81 (C^{10}), 130.69 (C^7), 130.48 (C^4), 129.36 (C^{12}), 128.98 (C^9), 126.15 (C^8), 122.78 (C^{11}), 122.05 (C^3), 118.19 (C^5), 115.51 (C^2), 83.29 (C^{13}), 77.81 (C^{14}), 71.94 (TEG-CH$_2$), 70.89 (TEG-CH$_2$), 70.67 (TEG-CH$_2$), 70.59 (TEG-CH$_2$), 69.63 (TEG-CH$_2$), 67.90 (TEG-CH$_2$), 59.04 (TEG-CH$_3$); LRMS m/z 408.2 $[M+H]^+$. HRMS m/z calcd for $C_{23}H_{26}N_3O_4$ $[M+Na]^+$: 408.19178, Found: 408.19153.

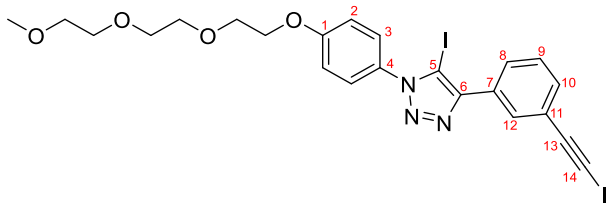

2.20b

General procedure for azide-iodoalkyne cycloaddition

2.8 (141 mg, 0.5 mmol) and **2.12** (227 mg, 0.6 mmol) were added to dry, degassed THF (5 ml) under Ar atmosphere. Then $Cu(MeCN)_4PF_6$ (19 mg, 0.05 mmol) and TBTA (27 mg, 0.05 mmol) were added simultaneously and the reaction was stirred for 4 h under Ar. The reaction mixture was diluted with DCM and washed with dilute aqueous NH_3. The DCM layer was dried with anhydrous Na_2SO_4, and concentrated. The product was isolated by silica column chromatography (5-10% acetone/DCM) to afford **2.20b** (152 mg, 0.23 mmol, 46%) as an off-white solid.

δ_H (400 MHz, $CDCl_3$): 8.08 (s, 1H, H^{12}), 7.97 (dt, J = 7.6, 1.7 Hz, 1H, H^8), 7.51 – 7.37 (m, 4H, H^3, H^9, H^{10}), 7.13 – 7.01 (m, 2H, H^2), 4.21 (t, J = 4.8 Hz, 2H, TEG-CH_2), 3.90 (t, J = 4.7 Hz, 2H, TEG-CH_2), 3.80 – 3.73 (m, 2H, TEG-CH_2), 3.73 – 3.63 (m, 4H, TEG-CH_2), 3.55 (m, 2H, TEG-CH_2), 3.38 (s, 3H, TEG-CH_3). δ_C (100 MHz, $CDCl_3$): δ 160.21 (C^1), 149.15 (C^6), 132.52 (C^{10}), 131.41 (C^{12}), 130.55 (C^{11}), 130.00 (C^4), 128.71 (C^9), 128.12 (C^8), 127.94 (C^3), 123.87 (C^7), 115.21 (C^2), 93.85 (C^{13}), 78.99 (C^5), 72.05 (TEG-CH_2), 71.02 (TEG-CH_2), 70.79 (TEG-CH_2), 70.71 (TEG-CH_2), 69.70 (TEG-CH_2), 68.01 (TEG-CH_2), 59.17 (TEG-CH_3), 7.39 (C^{14}). LRMS m/z 682.0 $[M+Na]^+$ HRMS m/z calcd for $C_{23}H_{24}I_2N_3O_4$ $[M+H]^+$: 659.98507, Found: 659.98486.

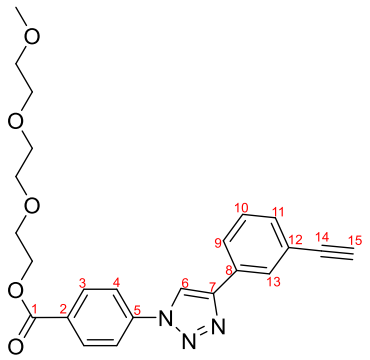

2.21a

General procedure for azide-alkyne cycloaddition was used to couple **2.10** (155 mg, 0.5 mmol) and 1,3-diethynylbenzene (133 µl, 1 mmol). The product was isolated by silica column (5-10% acetone/DCM) to afford **2.21a** (113 mg, 0.26 mmol, 69%) as a yellowish solid.

δ_H (400 MHz, $CDCl_3$): 8.30 (s, 1H, H^6), 8.24 – 8.17 (m, 2H, H^3), 7.99 (td, J = 1.7, 0.6 Hz, 1H, H^{13}), 7.93 – 7.84 (m, 3H, H^4, H^9), 7.46 (dt, J = 7.7, 1.4 Hz, 1H, H^{11}), 7.39 (td, J = 7.7, 0.6 Hz, 1H, H^{10}), 4.54 – 4.45 (m, 2H, TEG-CH_2), 3.90 – 3.80 (m, 2H, TEG-CH_2), 3.74 – 3.69 (m, 2H, TEG-CH_2), 3.69 – 3.61 (m, 4H, TEG-CH_2), 3.55 – 3.49 (m, 2H, TEG-CH_2), 3.34 (s, 3H, TEG-CH_3), 3.13 (s, 1H, H^{15}); δ_C (100 MHz, $CDCl_3$): 165.40 (C^1), 147.85 (C^7), 140.04 (C^5), 132.19 (C^{11}), 131.56 (C^3), 130.31 (C^2/C^8/C^{12}), 130.23 (C^2/C^8/C^{12}), 129.50 (C^{13}), 129.11 (C^{10}), 126.27 (C^9), 122.93 (C^8/C^{12}), 119.83 (C^4), 117.75 (C^6), 83.17 (C^{14}), 77.98 (C^{15}), 71.98 (TEG-CH_2), 70.76 (TEG-CH_2), 70.72 (TEG-CH_2), 70.67 (TEG-CH_2), 69.20 (TEG-CH_2), 64.61 (TEG-CH_2), 59.12 (TEG-CH_3); HRMS m/z calcd for $C_{24}H_{26}O_5N_3$ $[M+H]^+$: 436.18670, found: 436.18667.

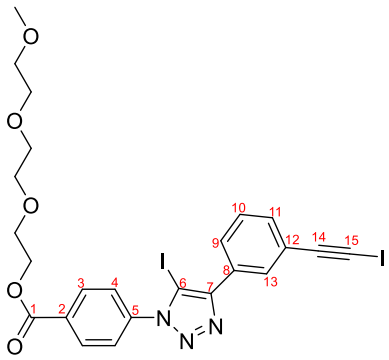

2.21b

General procedure for azide-iodoalkyne cycloaddition was used to couple compounds **2.10** (62 mg, 0.20 mmol) and **2.12** (83 mg, 0.22 mmol). The product was isolated by silica chromatography (25-50% acetone/hexanes) to afford **2.21b** (66 mg, 0.096 mmol, 53%) as a white solid.

δ_H (400 MHz, $CDCl_3$): 8.30 – 8.22 (m, 2H, H^3), 8.05 (m, 1H, H^{13}), 7.94 (dt, J = 7.5, 1.6 Hz, 1H, H^9), 7.69 – 7.61 (m, 2H, H^4), 7.50 – 7.36 (m, 2H, H^{10}, H^{11}), 4.58 – 4.45 (m, 2H, TEG-CH_2), 3.91 – 3.80 (m, 2H, TEG-CH_2), 3.74 – 3.69 (m, 2H, TEG-CH_2), 3.69 – 3.59 (m, 4H, TEG-CH_2), 3.56 – 3.46 (m, 2H, TEG-CH_2), 3.34 (s, 3H, TEG-CH_3); δ_C (100 MHz, $CDCl_3$): 165.29 (C^1), 149.86 (C^7), 140.24 (C^5), 132.66 (C^{11}), 131.77 (C^2), 131.44 (C^{13}), 130.92 (C^3), 130.11 (C^8/C^{12}), 128.72 (C^{10}), 128.14 (C^9), 126.37 (C^4), 123.87 (C^8/C^{12}), 93.65 (C^{14}), 77.61 (C^6), 71.95 (TEG-CH$_2$), 70.73 (TEG-CH$_2$), 70.68 (TEG-CH$_2$), 70.64 (TEG-CH$_2$), 69.14 (TEG-CH$_2$), 64.72 (TEG-CH$_2$), 59.11 (TEG-CH$_3$), 7.96 (C^{15}); LRMS m/z 682.0 probably $[M\text{-}N_2+Na]^+$ HRMS calcd. for $C_{24}H_{24}O_5N_3I_2$ $[M+H]^+$: 687.97998, found: 687.97973.

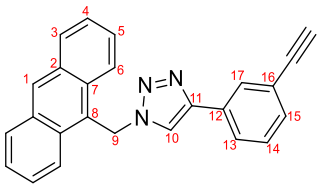

2.22a

General procedure for azide-alkyne cycloaddition was used to couple **2.11** (233 mg, 1 mmol) and 1,3-diethynylbenzene (266 µl, 2 mmol). The product was purified by silica column (20% EtOAc/hexanes) to afford **2.22a** (283 mg, 0.79 mmol, 79%) as a yellow solid.

δ_H (400 MHz, $CDCl_3$): 8.59 (s, 1H, H^1), 8.32 (d, J = 8.9, 2H, H^6), 8.09 (d, J = 8.4, 2H, H^3), 7.71 – 7.66 (m, 2H, H^{17}, H^{13}), 7.61 (ddd, J = 8.9, 6.6, 1.4 Hz, 2H, H^5), 7.54 (ddd, J = 7.8, 6.6, 1.1 Hz, 2H, H^4), 7.33 (dt, J = 7.7, 1.4 Hz, 1H, H^{15}), 7.28 (s, 1H, H^{10}), 7.27 – 7.22 (m, 1H, H^{14}), 6.56 (s, 2H, CH_2), 3.00 (s, 1H, C≡C*H*); δ_C (100 MHz, $CDCl_3$): 147.00 (C^{11}), 131.65 (C^{15}), 131.59 (C^2), 130.95 (C^7), 130.83 (C^{12}), 130.13 (C^1), 129.66 (C^3), 129.24 (C^{17}), 128.84 (C^{14}), 127.93 (C^5), 126.07 (C^{13}), 125.60 (C^4), 123.68 (C^8), 123.00 (C^6), 122.57 (C^{16}), 119.45 (C^{10}), 83.32 (*C*≡CH), 77.54 (C≡*C*H), 46.68 (CH_2); LRMS m/z 360.1 $[M+H]^+$; HRMS m/z calcd for $C_{25}H_{18}N_3$ $[M+H]^+$: 360.14952, found: 360.14965.

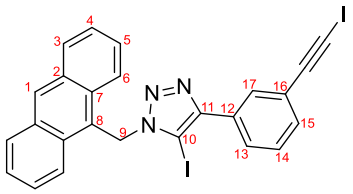

2.22b

General procedure for azide-iodoalkyne cycloaddition was used to couple **2.11** (233 mg, 1 mmol) and **2.12** (454 mg, 1.2 mmol). The product was isolated by silica column chromatography (1:1 DCM/hexanes) to provide **2.22b** (385 mg, 0.63 mmol, 63%) as a yellow solid.

δ_H (400 MHz, $CDCl_3$): 8.43 (s, 1H, H^1), 8.10 (d, J = 8.9 Hz, 2H, H^6), 7.92 (dd, J = 8.3, 1.5 Hz, 2H, H^3), 7.83 (t, J = 1.9 Hz, 1H, H^{17}), 7.72 (dt, J = 7.4, 1.8 Hz, 1H, H^{13}), 7.42 (m, 2H, H^5), 7.36 (m, 2H, H^4), 7.31 – 7.19 (m, 2H, H^{14}, H^{15}), 6.30 (d, J = 2.3 Hz, 2H, CH_2); δ_C (100 MHz, $CDCl_3$): 148.34 (C^{11}), 131.90 (C^{15}), 131.14 (Ar *C*), 130.97 (Ar *C*), 130.83 (Ar *C*), 130.41 (C^8), 129.52 (C^1), 129.14 (C^3), 128.30 (C^{14}), 127.58 (C^{13}), 126.93 (C^5), 124.96 (C^4), 123.6 (C^{12}), 123.46 (C^6), 93.13 (*C*≡CI), 77.36 (C^{10}), 47.86 (CH_2), 9.45 (C≡*C*I); LRMS m/z 633.9 $[M+Na]^+$; HRMS m/z calcd for $C_{25}H_{15}I_2N_3$ $[M+Na]^+$: 633.92475, found: 633.92458.

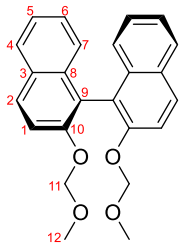

2.23

A literature procedure was used.[267] NaH (60% dispersion in mineral oil, 880 mg, 22 mmol) was added to dry THF (50 ml) and the mixture cooled to 0 °C. A solution of (S)-binaphthol (2.863 g, 10 mmol) in dry THF (17 ml) was then slowly added. The reaction was stirred at 0 °C for 1 h and at rt for 15 min. It was then cooled to 0 °C again and chloromethy methyl ether (1.655 ml, 22 mmol) was slowly added. The reaction was then stirred at rt for 5 h. Sat. aq. NH_4Cl was then added and THF was removed under vacuum. The aqueous phase was then extracted with DCM. The combined organic fractions were washed with brine, dried with anhydrous Na_2SO_4, decanted, and concentrated under vacuum. The crude product was purified by silica chromatography (10% EtOAc/hexanes) to provide **2.23** (3.074 g, 8.21 mmol, 82%) as a white solid.

δ_H (400 MHz, $CDCl_3$): 7.96 (d, J = 9.0 Hz, 2H, H^2), 7.91 – 7.84 (m, 2H, H^4), 7.58 (d, J = 9.0 Hz, 2H, H^1), 7.35 (ddd, J = 8.2, 6.6, 1.3 Hz, 2H, H^5), 7.23 (ddd, J = 8.1, 6.6, 1.3 Hz, 2H, H^6), 7.19 – 7.12 (m, 2H, H^7), 5.09 (d, J = 6.7 Hz, 2H, H^{11}), 4.98 (d, J = 6.8 Hz, 2H, H^{11}), 3.15 (d, J = 0.5 Hz, 6H, H^{12}); δ_C (101 MHz, $CDCl_3$): 152.79 (C^{10}), 134.16, 130.02, 129.52 (C^2), 128.00 (C^4), 126.42 (C^6), 125.69 (C^7), 124.19 (C^5), 121.45, 117.44 (C^1), 95.37 (C^{11}), 55.96 (C^{12}); ESI-MS m/z 397.2 $[M+Na]^+$.

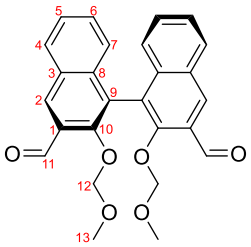

2.24

Compound **2.23** (1.498 g, 4 mmol) and TMEDA (2.399 ml, 16 mmol) were added to dry Et_2O under Ar atmosphere. The solution was cooled to 0 °C and ^{n}BuLi (2.5 M in hexanes, 4.4 ml) was added over 10 min. The reaction was stirred at 0 °C for 1 h. DMF (1.549 ml, 20 mmol) was then added and the reaction was stirred at 0 °C for 2 h. and at rt for 1 h. The mixture was then slowly acidified with 1 M HCl solution. Phases were separated and the aqueous phase wasfurther extracted with EtOAc. The combined organic fractions were washed with sat. aq. $NaHCO_3$ and brine, dried with anhydrous Na_2SO_4, decanted, and concentrated under vacuum. The crude product was purified by silica chromatography to provide **2.24** (310 mg, 0.78 mmol, 94%) as a white solid foam.

δ_H (400 MHz, $CDCl_3$): 10.55 (s, 2H, H^{11}), 8.61 (d, J = 0.7 Hz, 2H, H^{2}), 8.12 – 8.04 (m, 2H, H^{4}), 7.52 (ddd, J = 8.1, 6.8, 1.2 Hz, 2H, H^{5}), 7.42 (ddd, J = 8.3, 6.8, 1.4 Hz, 2H, H^{6}), 7.22 (dq, J = 8.5, 1.0 Hz, 2H, H^{7}), 4.73 (d, J = 6.2 Hz, 2H, H^{12}), 4.69 (d, J = 6.2 Hz, 2H, H^{12}), 2.87 (s, 6H, H^{13}); δ_C (101 MHz, $CDCl_3$): 190.78 (C^{11}), 154.19 (C^{10}), 136.85, 132.44 (C^{2}), 130.45 (C^{4}), 130.23, 129.77 (C^{6}), 129.05, 126.42 (C^{5}), 126.25 (C^{7}), 126.05, 100.75 (C^{12}), 57.16 (C^{13}); ESI-MS m/z 453.2 $[M+Na]^+$.

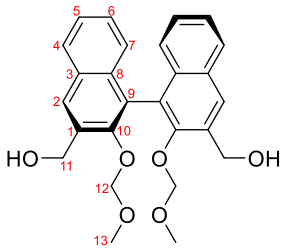

2.25

Compound **2.24** (1.360 g, 3.16 mmol) was added to 7:11 EtOH/Et_2O. The solution was cooled to 0 °C and $NaBH_4$ (135 mg, 3.57 mmol) was added. The mixture was stirred for 1 h at 0 °C and slowly acidified with 1 M HCl solution. Sat. aq. $NaHCO_3$ was then added and the organic solvents were removed under vacuum. The aqueous phase was extracted with EtOAc, the organic fractions were washed with water, dried with anhydrous Na_2SO_4, decanted, and concentrated under vacuum. The crude product was purified by silica chromatography (2% MeOH/DCM) to provide **2.25** (1120 mg, 2.58 mmol, 82%) as a white solid foam.

δ_H (400 MHz, $CDCl_3$): 8.02 (s, 2H, H^2), 7.91 (d, J = 8.1 Hz, 2H, H^4), 7.43 (ddt, J = 8.0, 6.8, 1.1 Hz, 2H, H^5), 7.31 – 7.24 (m, 2H, H^6), 7.15 (dd, J = 8.5, 1.1 Hz, 2H, H^7), 4.99 (dd, J = 12.5, 5.6 Hz, 2H, H^{11}), 4.84 (dd, J = 12.5, 7.3 Hz, 2H, H^{11}), 4.48 (d, J = 6.2 Hz, 2H, H^{12}), 4.45 (d, J = 6.2 Hz, 2H, H^{12}), 3.41 (t, J = 6.8 Hz, 2H, O*H*), 3.24 – 3.17 (m, 6H, H^{13}); δ_C (101 MHz, $CDCl_3$): 153.35 (C^{10}), 134.73, 133.94, 131.11, 129.96 (C^2), 128.37 (C^4), 127.03 (C^6), 125.92 (C^7), 125.61 (C^5), 125.34, 99.52 (C^{12}), 62.09 (C^{11}), 57.33 (C^{13}).

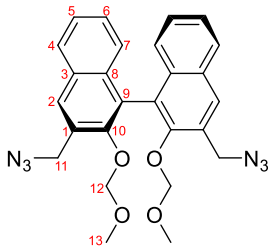

2.26

Compound **2.25** (434 mg, 1 mmol) was dissolved in dry toluene (4 ml) and the solution cooled to 0 °C under Ar atmosphere. DPPA (517 µl, 2.4 mmol) was then added slowly, followe by DBU (359 µl, 2.4 mmol). The reaction was allowed to warm to rt while stirring overnight. The mixture was then diluted with Et_2O and washed with water. The organic fraction was dried with anhydrous Na_2SO_4, decanted, and concentrated under vacuum. The crude product was purified by silica chromatography to provide **2.26** (407 mg, 0.840 mmol, 84%) as a colourless oil.

δ_H (400 MHz, $CDCl_3$): 8.02 (d, J = 0.8 Hz, 2H, H^2), 7.93 (ddd, J = 8.6, 1.2, 0.6 Hz, 2H, H^4), 7.45 (ddd, J = 8.1, 6.8, 1.2 Hz, 2H, H^5), 7.30 (ddd, J = 8.2, 6.8, 1.3 Hz, 2H, H^6), 7.18 (ddd, J = 8.6, 1.3, 0.7 Hz, 2H, H^7), 4.79 (dd, J = 14.2, 0.8 Hz, 2H, H^{11}), 4.68 (dd, J = 14.2, 0.8 Hz, 2H, H^{11}), 4.53 (d, J = 5.9 Hz, 2H, H^{12}), 4.48 (d, J = 6.0 Hz, 2H, H^{12}), 3.01 (s, 6H, H^{13}); δ_C (101 MHz, $CDCl_3$): 152.59 (C^{10}), 134.08, 130.71, 129.95 (C^2), 129.38, 128.29 (C^4), 127.26 (C^6), 126.06 (C^7), 125.72 (C^5), 125.47, 99.65 (C^{12}), 57.04 (C^{13}), 50.98 (C^{11}).

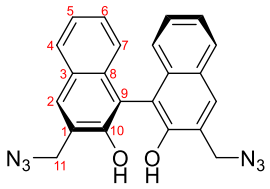

2.27

Compound **2.26** (400 mg, 0.83 mmol) was added to THF (4 ml) and cooled to 0 °C. Concentrated $HCl_{(aq)}$ was then added slowly and the reaction was stirred at rt for 3 h. The final mixture was diluted with water and extracted with EtOAc. The combined organic fractions were washed with sat. aq. $NaHCO_3$ and brine, dried with anhydrous Na_2SO_4, decanted, and concentrated under vacuum to provide **2.27** (310 mg, 0.78 mmol, 94%) as a light yellow solid.

δ_H (400 MHz, $CDCl_3$): 8.00 (s, 2H, H^2), 7.96 – 7.90 (m, 2H, H^4), 7.42 (ddd, J = 8.1, 6.8, 1.2 Hz, 2H, H^5), 7.34 (ddd, J = 8.3, 6.9, 1.4 Hz, 2H, H^6), 7.12 (dd, J = 8.4, 1.2 Hz, 2H, H^7), 5.29 (s, 2H, OH), 4.66 (s, 4H, H^{11}); δ_C (101 MHz, $CDCl_3$): 151.05 (C^{10}), 133.27 (C^8), 131.16 (C^2), 129.23 (C^3), 128.67 (C^4), 128.07 (C^6), 124.81 (C^5), 124.50 (C^1), 124.15 (C^7), 111.26 (C^9), 50.82 (C^{11}); ESI-MS m/z 395.1 $[M\text{-}H]^-$.

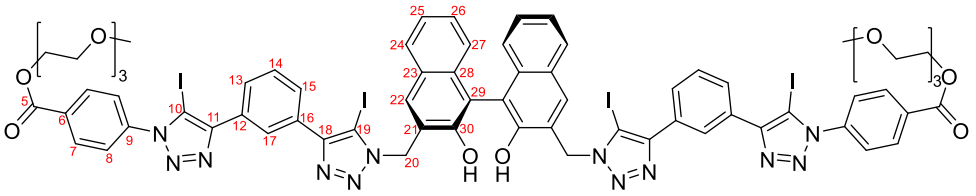

2.28

General procedure for azide-iodoalkyne cycloaddition was used to couple **2.21b** (137 mg, 0.2 mmol) and **2.27** (39.6 mg, 0.1 mmol). The product was isolated by silica column chromatography (2% MeOH/DCM) **2.28** (115 mg, 0.065 mmol, 65%) as a white solid.

δ_H (500 MHz, $CDCl_3$) 8.57 (s, 2H, H^{17}), 8.24 (dd, J = 8.4, 2.3 Hz, 4H, H^{7}), 8.00 (d, J = 7.8 Hz, 2H, H^{13}/H^{15}), 7.96 (d, J = 7.9 Hz, 2H, H^{13}/H^{15}), 7.70 (d, J = 8.3 Hz, 2H, H^{24}), 7.67 (dd, J = 8.6, 2.2 Hz, 4H, H^{8}), 7.56 (td, J = 7.8, 2.2 Hz, 2H, H^{14}), 7.36 (s, 2H, H^{22}), 7.32 – 7.24 (m, 2H, H^{25}), 7.21 (t, J = 7.7 Hz, 2H, H^{26}), 7.10 (d, J = 8.4 Hz, 2H, H^{27}), 6.74 (s, 2H, O*H*), 5.85 (d, J = 16.3 Hz, 2H, H^{20}), 5.79 (d, J = 16.2 Hz, 2H, H^{20}), 4.54 – 4.46 (m, 4H, TEG-CH_2), 3.87 – 3.80 (m, 4H, TEG-CH_2), 3.73 – 3.68 (m, 4H, TEG-CH_2), 3.68 – 3.64 (m, 4H, TEG-CH_2), 3.64 – 3.59 (m, 4H, TEG-CH_2), 3.53 – 3.48 (m, 4H, TEG-CH_2), 3.33 (s, 6H, TEG-CH_2); δ_C (126 MHz, $CDCl_3$): 165.37 (C^{5}), 150.70 (C^{30}), 150.54 (C^{11}/C^{18}), 149.51 (C^{11}/C^{18}), 140.36 (C^{9}), 133.55 (C^{28}), 131.74 (C^{6}), 130.95 (C^{7}), 130.66 (C^{12}/C^{16}), 130.25 (C^{12}/C^{16}), 129.39 (C^{22}), 129.11 (C^{14}), 128.97 (C^{23}), 128.43 (C^{24}), 128.10 (C^{13}/C^{15}), 128.07 (C^{13}/C^{15}), 127.70 (C^{26}), 126.56 (C^{17}), 126.43 (C^{8}), 124.50 (C^{25}), 124.39 (C^{27}), 124.04 (C^{21}), 112.57 (C^{29}), 78.11 (C^{19}), 77.90 (C^{10}), 71.99, 70.76, 70.72, 70.67, 69.18, 64.74, 59.14, 50.20 (C^{20}); HRMS m/z calcd for $C_{70}H_{63}I_4N_{12}O_{12}$ $[M+H]^+$: 1771.08726; found: 1771.08669; $[\alpha]_D^{25}$ -23.2° (c = 1.00, $CHCl_3$).

6.3 Compound data for Chapter 3

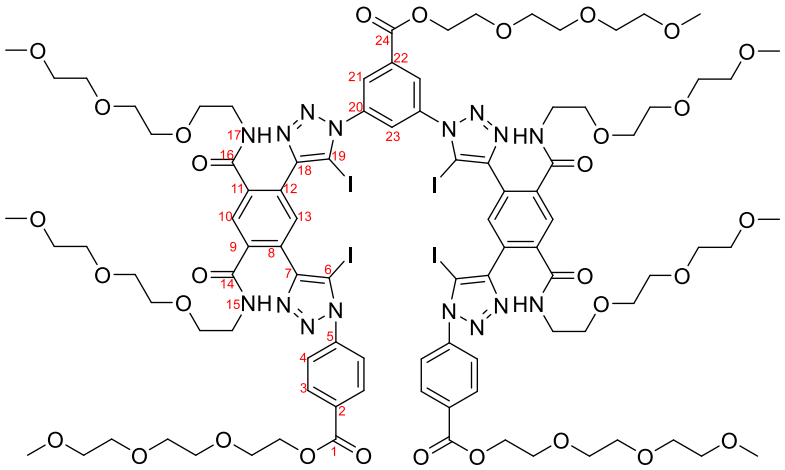

3.1a

General procedure for amidation of active ester precursors

Compound **3.5** (46 mg, 0.281 mmol) was dissolved in dry DCM (1 ml) and further dried on 3 Å MS. This solution was then added to **3.25a** (70 mg, 0.0281 mmol). The reaction was stirred under Ar atmosphere (to exclude moisture) and in darkness until completion (24 h). Reaction mixture was directly loaded onto a silica column and separated (MeOH/DCM) to provide **3.1a** (44 mg, 0.0177 mmol, 63%) as a yellowish amorphous solid.

δ_H (400 MHz, $CDCl_3$) 8.55 (d, J = 2.0 Hz, 2H, H^{21}), 8.29 – 8.23 (m, 4H, H^3), 8.22 (t, J = 2.1 Hz, 1H, H^{23}), 8.07 (s, 2H, H^{10}), 7.81 (s, 2H, H^{13}), 7.77 – 7.69 (m, 4H, H^4), 7.24 – 7.14 (m, 4H, H^{15}, H^{17}), 4.61 – 4.46 (m, 6H, TEG-CH_2), 3.89 – 3.82 (m, 6H, TEG-CH_2), 3.75 – 3.40 (m, 72H, TEG-CH_2), 3.35 (s, 6H, TEG-CH_3), 3.30 (s, 3H, TEG-CH_3), 3.24 (s, 6H, TEG-CH_3), 3.20 (s, 6H, TEG-CH_3); δ_C (101 MHz, $CDCl_3$) 167.59 (C^{14}, C^{16}), 165.39 (C^1), 163.82 (C^{24}), 150.84 (C^7/C^{18}), 150.51 (C^7/C^{18}), 140.32 (C^5), 137.87 (C^{20}), 137.64 (C^8/C^{12}), 137.57 (C^8/C^{12}), 134.25 (C^{13}), 132.96 (C^{22}), 131.69 (C^2), 130.95 (C^3), 130.06 (C^9/C^{11}), 129.95 (C^9/C^{11}), 129.13 (C^{10}), 128.57 (C^{21}), 127.90 (C^{23}), 126.19 (C^4), 81.48 (C^6/C^{19}), 80.96 (C^6/C^{19}), 71.98, 71.93, 71.85, 71.84, 70.75, 70.72, 70.68, 70.63, 70.54, 70.41, 70.38, 70.15, 70.11, 69.57, 69.52, 69.19, 68.97, 65.42, 64.73, 59.15, 59.10, 58.99, 58.97, 40.00; ESI-MS m/z calcd for $C_{94}H_{126}O_{31}N_{16}I_4$ $[M+2H]^{2+}$ 1241.24768, found: 1241.24584.

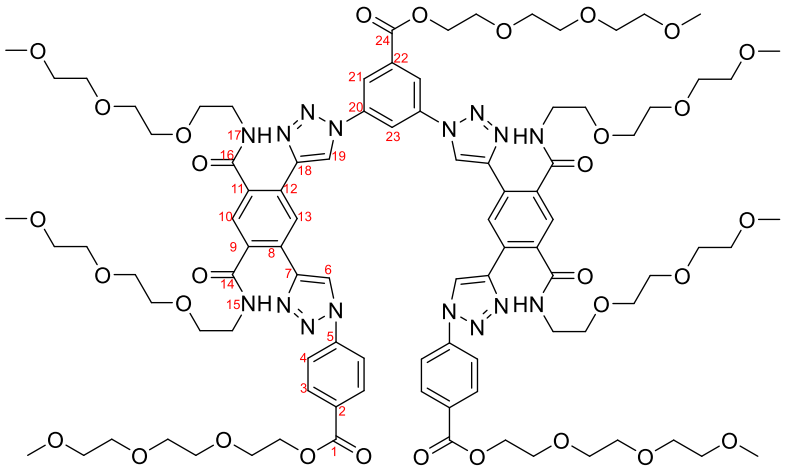

3.1a$_H$

General procedure for amidation of active ester precursors was used to react **3.25a$_H$** (68 mg, 0.0342 mmol) and **3.5** (56 mg, 0.342 mmol). The product was purified by silica chromatography (3-6% MeOH/DCM) to provide **3.1a$_H$** (44 mg, 0.0222 mmol, 65%) as an off-white solid.

δ_H (500 MHz, $CDCl_3$) 8.76 (s, 2H, H^{21}), 8.64 (s, 2H, H^{10}), 8.55 (s, 1H, H^{23}), 8.51 – 8.38 (m, 4H, H^6/H^{19}, H^{13}), 8.18 (d, J = 8.2 Hz, 4H, H^3), 7.91 (d, J = 8.2 Hz, 4H, H^4), 7.68 – 7.41 (m, 6H, H^{15}, H^{17}, H^6/H^{19}), 4.57 (t, J = 5.0 Hz, 2H, TEG-CH_2), 4.50 (t, J = 4.8 Hz, 4H, TEG-CH_2), 3.96 – 3.81 (m, 6H, TEG-CH_2), 3.80 – 3.47 (m, 54H, TEG-CH_2), 3.47 – 3.38 (m, 8H, TEG-CH_2), 3.35 (s, 6H, TEG-CH_2), 3.34 – 3.27 (m, 7H, TEG-CH_2, TEG-CH_3), 3.20 (s, 6H, TEG-CH_3), 3.11 (s, 6H, TEG-CH_3); δ_C (126 MHz, $CDCl_3$) 169.05 (C^{14}, C^{16}), 165.45 (C^1), 164.13 (C^{24}), 145.45 (C^7/C^{18}), 145.27 (C^7/C^{18}), 140.00 (C^5), 137.99, 134.91, 134.82, 133.50, 131.46 (C^3), 130.19, 129.16 (C^6/C^{19}), 128.90, 128.70, 128.35 (C^6/C^{19}), 121.30 (C^{10}, C^{21}), 120.39 (C^{13}), 119.86 (C^4), 115.41 (C^{23}), 72.00, 71.95, 71.84, 71.75, 70.76, 70.74, 70.71, 70.68, 70.62, 70.54, 70.40, 70.30, 70.09, 70.03, 69.43, 69.38, 69.22, 69.00, 65.21, 64.59, 59.13, 59.05, 58.92, 58.80, 39.94, 39.86; ESI-MS m/z calcd for $C_{94}H_{126}O_{31}N_{16}I_4$ $[M+2H]^{2+}$ 989.45440, found: 989.45269.

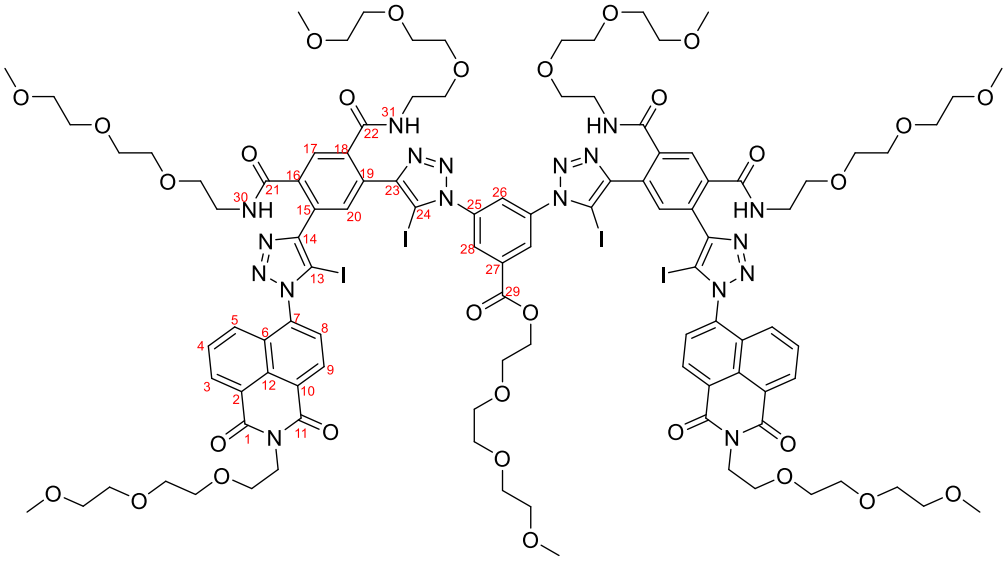

3.1b

General procedure for amidation of active ester precursors was used starting with **3.25b** (106 mg, 0.0401 mmol) and **3.5** (65 mg, 0.401 mmol). The product was purified by silica chromatography (5-9% MeOH, 15% acetone/DCM to provide **3.1b** (90 mg, 0.0342 mmol, 85%) as an off-white solid.

δ_H (500 MHz, $CDCl_3$) 8.75 (d, J = 7.7 Hz, 2H, H^9), 8.68 (dd, J = 7.2, 1.1 Hz, 2H, H^3), 8.57 (d, J = 2.0 Hz, 2H, H^{28}), 8.25 (t, J = 2.0 Hz, 1H, H^{26}), 8.11 (s, 2H, H^{17}), 7.94 – 7.90 (m, 4H, H^8, H^{20}), 7.83 (dd, J = 8.5, 7.2 Hz, 2H, H^4), 7.72 (dd, J = 8.5, 1.1 Hz, 2H, H^5), 7.25 (t, J = 5.5 Hz, 2H, H^{30}/H^{31}), 7.21 (t, J = 5.5 Hz, 2H, H^{30}/H^{31}), 4.59 – 4.54 (m, 2H, TEG-CH_2), 4.46 (t, J = 6.0 Hz, 4H, TEG-CH_2), 3.89 – 3.82 (m, 6H, TEG-CH_2), 3.74 – 3.69 (m, 6H, TEG-CH_2), 3.69 – 3.54 (m, 52H, TEG-CH_2), 3.50 – 3.47 (m, 2H, TEG-CH_2), 3.47 – 3.42 (m, 12H, TEG-CH_2), 3.31 (s, 9H, TEG-CH_3), 3.22 (s, 6H, TEG-CH_3), 3.20 (s, 6H, TEG-CH_3); δ_C (126 MHz, $CDCl_3$) 167.56 (C^{21}/C^{22}), 167.46 (C^{21}/C^{22}), 163.79 (C^{29}), 163.67 (C^1), 163.21 (C^{11}), 150.86 (C^{14}/C^{23}), 150.28 (C^{14}/C^{23}), 138.06 (C^7), 137.89 (C^{25}), 137.69 (C^{15}/C^{19}), 137.64 (C^{15}/C^{19}), 134.25 (C^{20}), 133.02 (C^{27}), 132.37 (C^3), 130.54 (C^9), 130.11 (C^{16}/C^{18}), 130.09 (C^{16}/C^{18}), 129.41 (C^5), 129.08 (C^{17}), 128.99 (C^4), 128.96 (C^{12}), 128.57 (C^{28}), 128.28 (C^6), 127.86 (C^{26}), 127.06 (C^8), 124.98 (C^{10}), 123.05 (C^2), 84.34 (C^{13}/C^{24}), 81.70 (C^{13}/C^{24}), 71.95, 71.87, 70.75, 70.73, 70.70, 70.64, 70.60, 70.59, 70.46, 70.41, 70.23, 70.13, 69.54, 69.41, 68.97, 67.93, 65.44, 59.09, 58.95, 40.16, 39.99, 39.47; ESI-MS m/z calcd for $C_{104}H_{128}O_{31}N_{18}I_4$ $[M+2H]^{2+}$ 1316.25803 found: 1316.25406.

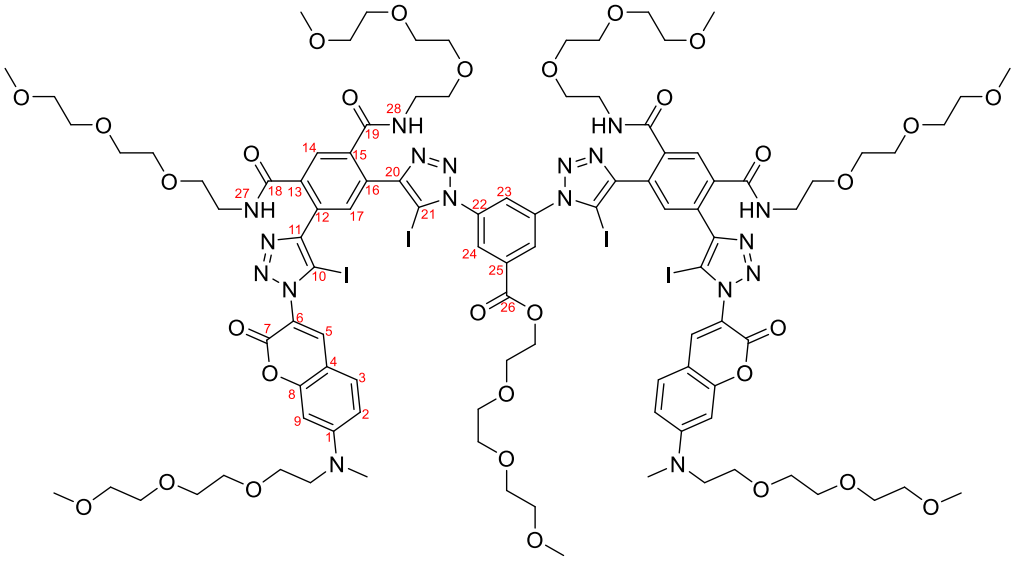

3.1c

General procedure for amidation of active ester precursors was used to react **3.25c** (87 mg, 0.0335 mmol) and **3.5** (55 mg, 0.335 mmol). The product was purified by silica chromatography (20% acetone, 4-10% MeOH/$CHCl_3$, then again with 8% MeOH/$CHCl_3$) to provide **3.1c** (64 mg, 0.0247 mmol, 74%) as a yellow solid.

δ_H (500 MHz, $CDCl_3$) 8.56 (d, J = 2.0 Hz, 2H, H^{24}), 8.24 (d, J = 2.1 Hz, 1H, H^{23}), 8.07 (s, 2H, H^{14}), 7.95 (s, 2H, H^{5}), 7.84 (s, 2H, H^{17}), 7.38 (d, J = 9.0 Hz, 2H, H^{3}), 7.09 (t, J = 5.5 Hz, 2H, H^{27}/H^{28}), 6.96 (t, J = 5.4 Hz, 2H, H^{27}/H^{28}), 6.73 (dd, J = 8.9, 2.4 Hz, 2H, H^{2}), 6.58 (d, J = 2.3 Hz, 2H, H^{9}), 4.61 – 4.50 (m, 2H, TEG-CH_2), 3.86 (t, J = 4.7 Hz, 2H, TEG-CH_2), 3.73 – 3.41 (m, 80H, TEG-CH_2), 3.35 (s, 6H, TEG-CH_3), 3.31 (s, 3H, TEG-CH_3), 3.26 (s, 6H, TEG-CH_3), 3.22 (s, 6, TEG-CH_3), 3.12 (s, 6H, NCH_3); δ_C (126 MHz, $CDCl_3$) 167.69 (C^{18}/C^{19}), 167.63 (C^{18}/C^{19}), 163.86 (C^{26}), 157.25 (C^{7}), 156.96 (C^{8}), 153.81 (C^{1}), 150.76 (C^{11}/C^{20}), 149.52 (C^{11}/C^{20}), 143.15 (C^{5}), 137.92 (C^{22}), 137.67 (C^{12}/C^{16}), 137.58 (C^{12}/C^{16}), 134.01 (C^{17}), 133.01 (C^{25}), 130.38 (C^{3}), 129.93 (C^{13}/C^{15}), 129.79 (C^{13}/C^{15}), 129.40 (C^{14}), 128.59 (C^{24}), 127.98 (C^{23}), 116.95 (C^{6}), 110.36 (C^{2}), 107.27 (C^{4}), 97.91 (C^{9}), 84.19 (C^{10}/C^{21}), 81.60 (C^{10}/C^{21}), 72.01, 71.97, 71.90, 70.94, 70.81, 70.77, 70.75, 70.69, 70.66, 70.57, 70.45, 70.45, 70.22, 70.17, 69.55, 69.39, 68.98, 68.52, 65.39, 59.15, 59.00, 52.41, 40.09, 39.96, 39.57 (NCH_3); ESI-MS m/z calcd for $C_{100}H_{132}O_{31}N_{18}I_4$ $[M+2H]^{2+}$ 1294.27368, found: 1294.27422.

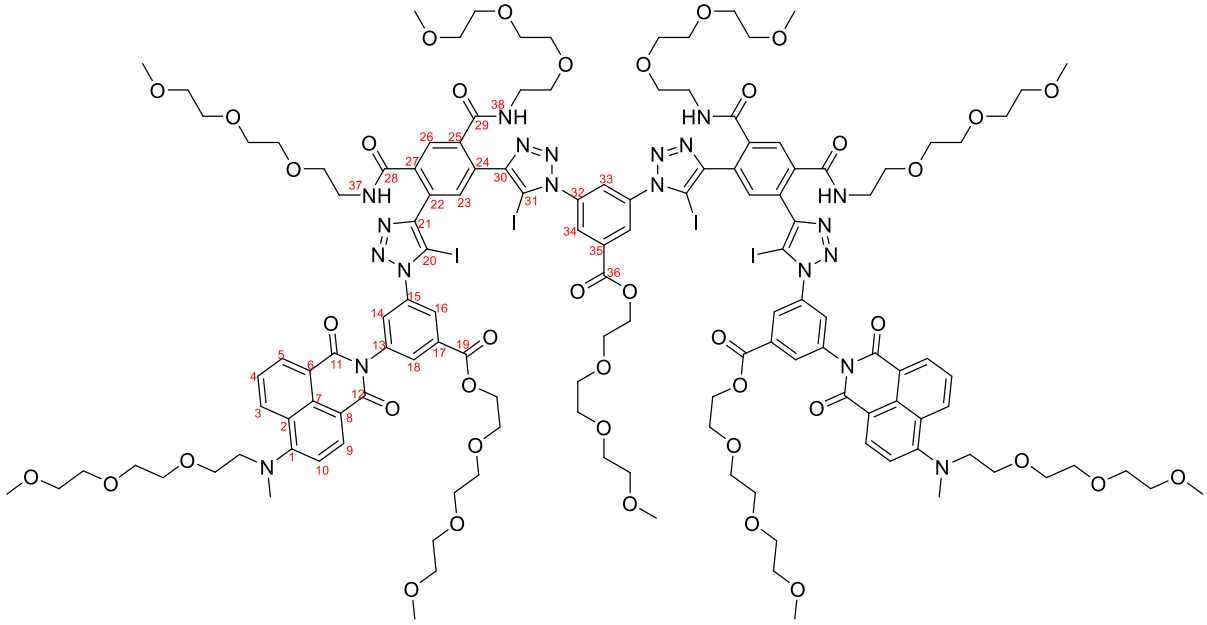

3.1d

General procedure for amidation of active ester precursors was used to react **3.25d** (97 mg, 0.0300 mmol) and **3.5** (100 mg, 0.613 mmol). The product was purified by silica chromatography (6-8% MeOH/$CHCl_3$, then again with 5-8% MeOH/DCM) to provide **3.1d** (55 mg, 0.0171 mmol, 57%) as a yellow solid.

δ_H (500 MHz, $CDCl_3$) 8.70 (dd, J = 8.5, 1.2 Hz, 2H, H^3), 8.59 (dd, J = 7.3, 1.2 Hz, 2H, H^5), 8.55 (d, J = 2.0 Hz, 2H, H^{34}), 8.49 (d, J = 8.2 Hz, 2H, H^9), 8.46 (t, J = 1.8 Hz, 2H, H^{16}/H^{18}), 8.24 (t, J = 2.0 Hz, 1H, H^{33}), 8.21 (t, J = 1.7 Hz, 2H, H^{16}/H^{18}), 8.08 (s, 2H, H^{26}), 7.87 (t, J = 2.0 Hz, 2H, H^{14}), 7.82 (s, 2H, H^{23}), 7.69 (dd, J = 8.5, 7.3 Hz, 2H, H^4), 7.23 (d, J = 8.3 Hz, 2H, H^{10}), 7.10 – 7.01 (m, 4H, H^{37}, H^{38}), 4.58 – 4.53 (m, 2H, TEG-CH_2), 4.52 – 4.46 (m, 4H, TEG-CH_2), 3.86 – 3.83 (m, 2H, TEG-CH_2), 3.83 – 3.79 (m, 8H, TEG-CH_2), 3.71 – 3.50 (m, 78H, TEG-CH_2), 3.49 – 3.45 (m, 6H, TEG-CH_2), 3.45 – 3.41 (m, 8H, TEG-CH_2), 3.35 (s, 6H, TEG-CH_3), 3.30 (s, 3H, TEG-CH_3), 3.29 (s, 6H, TEG-CH_3), 3.22 (s, 6H, TEG-CH_3), 3.21 (s, 6H, TEG-CH_3), 3.13 (s, 6H, NCH_3); δ_C (126 MHz, $CDCl_3$) 167.52 (C^{28}/C^{29}), 167.45 (C^{28}/C^{29}), 164.45 (C^{19}), 164.36 (C^{11}), 163.79 (C^{36}), 163.68 (C^{12}), 157.53 (C^1), 150.79 (C^{21}/C^{30}), 150.38 (C^{21}/C^{30}), 137.90 (C^{32}), 137.79 (C^{22}/C^{24}), 137.72 (C^{22}/C^{24}), 137.51 (C^{13}/C^{15}), 137.02 (C^{13}/C^{15}), 134.16 (C^{23}), 133.19 (C^9), 132.91 (C^{35}), 132.48 (C^{17}), 132.25 (C^3), 132.10 (C^{16}/C^{18}), 131.79 (C^5), 131.47 (C^{14}), 130.76 (C^7), 129.93 (C^{25}/C^{27}), 129.84 (C^{25}/C^{27}), 129.20 (C^{26}), 128.53 (C^{34}), 127.86 (C^{33}), 127.10 (C^{16}/C^{18}), 125.94 (C^2), 125.27 (C^4), 122.72 (C^6), 114.92 (C^{10}), 114.71 (C^8), 81.26 (C^{20}/C^{31}), 81.18 (C^{20}/C^{31}), 72.00, 71.93, 71.88, 71.87, 70.78, 70.76, 70.73, 70.69, 70.66, 70.63, 70.62, 70.58, 70.56, 70.41, 70.41, 70.17, 70.14, 69.53, 69.05, 68.94, 68.81, 65.38, 64.91, 57.13, 41.10 (NCH_3), 39.96, 39.94; ESI-MS m/z calcd for $C_{134}H_{170}O_{41}N_{20}I_4$ $[M+2H]^{2+}$ 1611.40000 found: 1611.40183.

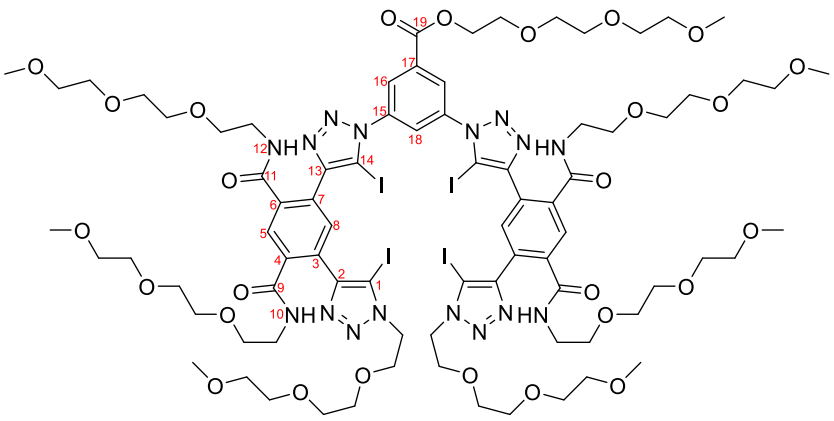

3.1e

General procedure for amidation of active ester precursors was used to react **3.25e** (75 mg, 0.0333 mmol) and **3.5** (54 mg, 0.333 mmol). The product was purified by silica chromatography (MeOH/DCM) to provide **3.1e** (65 mg, 0.0290 mmol, 87%) as a yellow solid.

δ_H (400 MHz, $CDCl_3$) 8.54 (d, J = 2.0 Hz, 2H, H^{16}), 8.20 (t, J = 2.0 Hz, 1H, H^{20}), 8.03 (s, 2H, H^5), 7.71 (s, 2H, H^8), 7.09 (t, J = 5.5 Hz, 2H, H^{10}/H^{12}), 7.02 (t, J = 5.5 Hz, 2H, H^{10}/H^{12}), 4.59 (t, J = 6.0 Hz, 4H, TEG-CH_2), 4.56 – 4.50 (m, 2H, TEG-CH_2), 3.96 (t, J = 6.0 Hz, 4H, TEG-CH_2), 3.88 – 3.81 (m, 2H, TEG-CH_2), 3.72 – 3.66 (m, 3H, TEG-CH_2), 3.66 – 3.45 (m, 70H, TEG-CH_2), 3.45 – 3.39 (m, 5H, TEG-CH_2), 3.31 (s, 6H, TEG-CH_3), 3.30 (s, 3H, TEG-CH_3), 3.26 (s, 6H, TEG-CH_3), 3.19 (s, 6H, TEG-CH_3); δ_C (101 MHz, $CDCl_3$) 167.53 (C^{10}/C^{11}), 167.51 (C^{10}/C^{11}), 163.79 (C^{19}), 150.86 (C^2/C^{13}), 149.20 (C^2/C^{13}), 137.85 (C^{15}), 137.54 (C^3/C^7), 137.35 (C^3/C^7), 134.05 (C^8), 132.93 (C^{17}), 130.35 (C^4/C^6), 129.81 (C^4/C^6), 129.11 (C^5), 128.52 (C^{16}), 127.83 (C^{18}), 81.48 (C^1/C^{14}), 81.31 (C^1/C^{14}), 71.92, 71.88, 71.84, 70.78, 70.71, 70.69, 70.62, 70.58, 70.53, 70.46, 70.39, 70.25, 70.10, 69.50, 69.44, 69.18, 68.92, 65.35, 59.09, 58.94, 50.55, 39.97; ESI-MS m/z calcd for $C_{80}H_{117}O_{27}N_{16}I_4$ $[M+H]^+$ 2241.44473, found: 2241.44015.

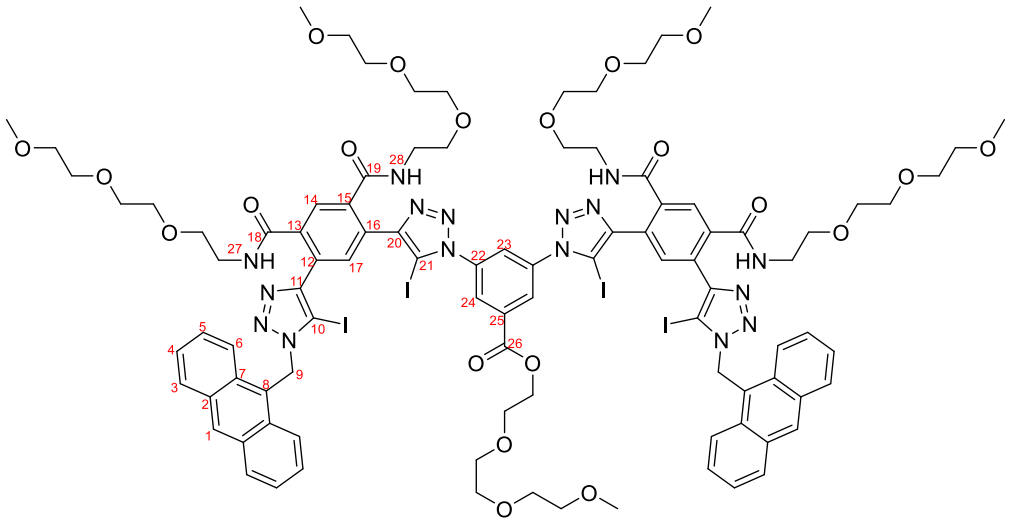

3.1f

General procedure for amidation of active ester precursors was used to react **3.25f** (75 mg, 0.0320 mmol) and **3.5** (52 mg, 0.320 mmol). The product was purified by silica chromatography (5-7.5% MeOH/ DCM) to provide **3.1f** (60 mg, 0.0258 mmol, 80%) as a yellow solid.

δ_H (500 MHz, $CDCl_3$) 8.52 (d, J = 1.8 Hz, 4H, H^1, H^{24}), 8.25 (d, J = 8.8 Hz, 4H, H^6), 8.05 (s, 3H, H^{14}, H^{23}), 8.00 (d, J = 8.4 Hz, 4H, H^3), 7.64 (s, 2H, H^{17}), 7.51 (ddd, J = 8.7, 6.6, 1.4 Hz, 4H, H^5), 7.47 – 7.42 (m, 4H, H^4), 7.03 (t, J = 5.6 Hz, 2H, H^{27}/H^{28}), 6.94 (t, J = 5.4 Hz, 2H, H^{27}/H^{28}), 6.42 (s, 4H, H^9), 4.57 – 4.51 (m, 2H, TEG-CH_2), 3.87 – 3.82 (m, 2H, TEG-CH_2), 3.69 (dd, J = 5.9, 3.5 Hz, 2H, TEG-CH_2), 3.66 – 3.58 (m, 12H, TEG-CH_2), 3.58 – 3.51 (m, 12H, TEG-CH_2), 3.51 – 3.45 (m, 6H, TEG-CH_2), 3.44 – 3.35 (m, 16H, TEG-CH_2), 3.35 – 3.29 (m, 11H, TEG-CH_2, TEG-CH_3), 3.21 (s, 6H, TEG-CH_3), 3.19 (s, 6H, TEG-CH_3); δ_C (126 MHz, $CDCl_3$) 167.59 (C^{26}), 167.49 (C^{18}/C^{19}), 163.82 (C^{18}/C^{19}), 150.73 (C^{11}/C^{20}), 149.35 (C^{11}/C^{20}), 137.81 (C^{22}), 137.63 (C^{12}/C^{16}), 137.55 (C^{12}/C^{16}), 134.04 (C^{17}), 132.98 (C^{25}), 131.47 (C^2), 131.34 (C^7), 130.02 (C^{13}/C^{15}), 129.98 (C^1), 129.81 (C^{13}/C^{15}), 129.47 (C^3), 129.35 (C^{14}), 128.50 (C^{24}), 127.87 (C^{23}), 127.24 (C^5), 125.25 (C^4), 123.91 (C^6), 123.85 (C^8), 81.78 (C^{21}), 80.41 (C^{10}), 71.96, 71.88, 71.85, 70.75, 70.73, 70.66, 70.58, 70.43, 70.39, 70.37, 70.17, 70.04, 69.52, 69.24, 68.95, 65.35, 59.10, 58.97, 48.23 (C^9), 39.97, 39.89; ESI-MS m/z calcd for $C_{96}H_{108}O_{21}N_{16}I_4Na_2$ $[M+2Na]^{2+}$ 1187.19246 found: 1187.19177.

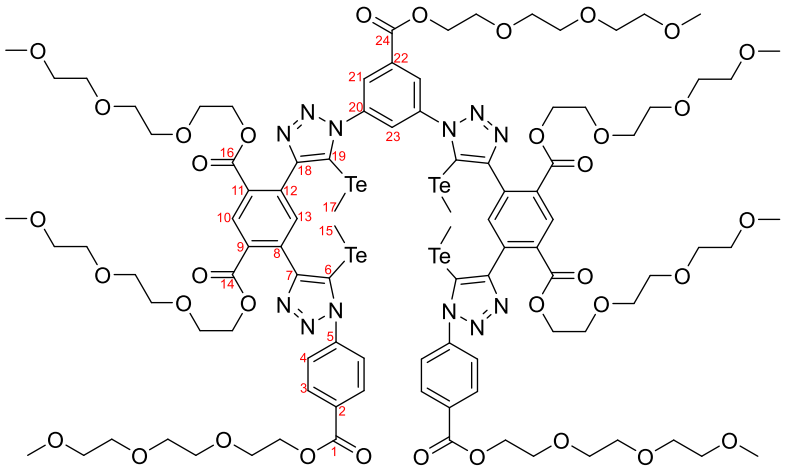

3.2

Compounds **3.29** (160 mg, 0.146 mmol) and **2.15** (24.3 mg, 0.0693 mmol) were added to dry THF (1.5 ml). PMDTA (29 µl, 0.139 mmol) and CuI (26.4 mg, 0.139 mmol) were then added. The reaction was stirred for 30 min at rt under Ar and in darkness. The mixture was then partitioned in DCM and aqueous Na_2EDTA. Aqueous layer was extracted with DCM, the organic fractions combined, dried with anhydrous Na_2SO_4, decanted and evaporated. The residue was separated by silica chromatography (3-4% MeOH, 10% acetone/DCM) to provide **3.2** (145 mg, 0.0569 mmol, 82%) as a nearly colorless oil.

δ_H (500 MHz, $CDCl_3$) 8.67 (s, 2H, H^{10}), 8.55 (d, J = 1.9 Hz, 2H, H^{21}), 8.31 (t, J = 2.1 Hz, 1H, H^{23}), 8.24 (d, J = 8.3 Hz, 4H, H^3), 7.90 (s, 2H, H^{13}), 7.75 (d, J = 8.3 Hz, 4H, H^4), 4.60 – 4.54 (m, 2H, TEG-CH_2), 4.54 – 4.47 (m, 4H, TEG-CH_2), 4.42 – 4.34 (m, 8H, TEG-CH_2), 3.90 – 3.81 (m, 6H, TEG-CH_2), 3.75 – 3.54 (m, 50H, TEG-CH_2), 3.54 – 3.44 (m, 14H, TEG-CH_2), 3.34 (s, 6H, TEG-CH_3), 3.32 (s, 6H, TEG-CH_3), 3.31 (s, 3H, TEG-CH_3), 3.30 (s, 6H, TEG-CH_3), 1.82 (s, 6H, H^{17}), 1.70 (s, 6H, H^{15}); δ_C (126 MHz, $CDCl_3$) 166.14 (C^{14}/C^{16}), 165.90 (C^{14}/C^{16}), 165.42 (C^1), 164.05 (C^{24}), 154.41 (C^7/C^{18}), 153.75 (C^7/C^{18}), 141.20 (C^5), 138.65 (C^{20}), 135.72 (C^{13}), 135.38 (C^8/C^{12}), 135.29 (C^8/C^{12}), 132.86 (C^{10}), 132.43 (C^{22}), 131.63 (C^9/C^{11}), 131.38 (C^9/C^{11}), 131.27 (C^2), 130.84 (C^3), 127.62 (C^{21}), 127.11 (C^{23}), 125.77 (C^4), 103.02 (C^{19}), 102.59 (C^6), 71.96, 71.92, 70.72, 70.70, 70.67, 70.65, 70.63, 70.58, 70.56, 70.54, 70.53, 69.16, 68.97, 68.90, 65.26, 64.76, 64.70, 64.66, 59.10, 59.05, 59.03, -12.71 (C^{15}/C^{17}), -13.38 (C^{15}/C^{17}); δ_{125Te} (158 MHz, $CDCl_3$) 164.23 (outer Te), 155.58 (inner Te); ESI-MS m/z calcd for $C_{98}H_{132}N_{12}O_{35}Te_4Na$ $[M+Na]^+$ 2579.50647 (with $^{130}Te_4$), found: 2579.50750.

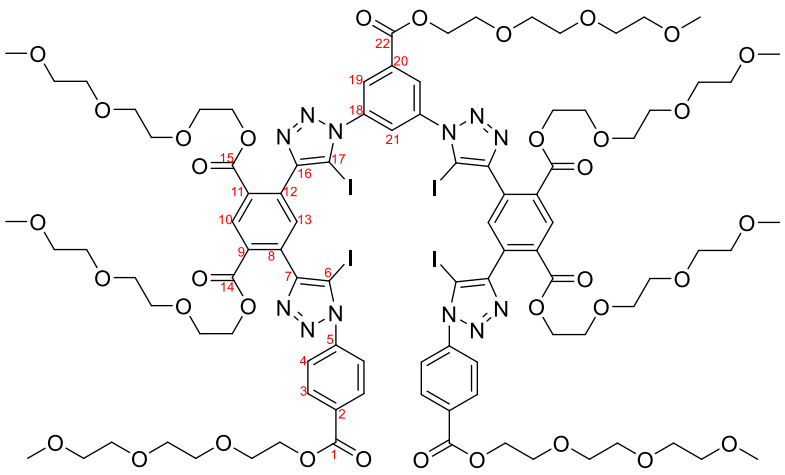

3.2$_I$

General procedure for azide-iodoalkyne cycloaddition

Compounds **3.29$_I$** (128 mg, 0.120 mmol) and **2.15** (21 mg, 0.0599 mmol) were added to dry THF (5 ml). Cu[MeCN]$_4$PF$_6$ (4.5 mg, 0.0120 mmol) and TBTA (6.4 mg, 0.0120 mmol) were then added simultaneously. The reaction was then stirred overnight at rt under Ar atmosphere and in darkness. The mixture was then partitioned in aqueous solution of Na_2EDTA and DCM. Organic fraction was dried with anhydrous Na_2SO_4, decanted and concentrated under vacuum. The residue was separated by silica chromatography (2.5-4% MeOH, 10% acetone/DCM) to provide **3.2$_I$** (98 mg, 0.0394 mmol, 66%) as a colourless oil.

δ_H (500 MHz, $CDCl_3$) 8.67 (s, 2H, H^{10}), 8.56 (d, J = 2.1 Hz, 2H, H^{19}), 8.28 – 8.24 (m, 4H, H^3), 8.23 (t, J = 2.0 Hz, 1H, H^{21}), 7.86 (s, 2H, H^{13}), 7.76 – 7.71 (m, 4H, H^4), 4.59 – 4.54 (m, 2H, TEG-CH_2), 4.54 – 4.47 (m, 4H, TEG-CH_2), 4.44 – 4.35 (m, 8H, TEG-CH_2), 3.90 – 3.81 (m, 6H, TEG-CH_2), 3.76 – 3.43 (m, 60H, TEG-CH_2), 3.34 (s, 6H, TEG-CH_3), 3.30 (s, 6H, TEG-CH_3), 3.30 (s, 3H, TEG-CH_3), 3.28 (s, 6H, TEG-CH_3); δ_C (126 MHz, $CDCl_3$) 165.84 (C^{14}/C^{15}), 165.64 (C^{14}/C^{15}), 165.31 (C^1), 163.73 (C^{22}), 151.20 (C^7/C^{16}), 150.83 (C^7/C^{16}), 140.25 (C^5), 137.85 (C^{18}), 135.11 (C^{13}), 133.93 (C^8/C^{12}), 133.76 (C^8/C^{12}), 133.07 (C^{10}), 133.04 (C^{20}), 131.88 (C^9/C^{11}), 131.70 (C^2), 131.68 (C^9/C^{11}), 130.93 (C^3), 128.35 (C^{19}), 127.56 (C^{21}), 126.07 (C^4), 81.35 (C^6/C^{17}), 80.71 (C^6/C^{17}), 71.95, 71.91, 71.89, 71.86, 70.73, 70.70, 70.69, 70.67, 70.64, 70.61, 70.54, 70.50, 69.14, 68.94, 68.85, 68.80, 65.42, 64.98, 64.95, 64.70, 59.10, 59.05, 59.02, 59.00; ESI-MS m/z calcd for $C_{94}H_{122}O_{35}N_{12}I_4$ $[M+2H]^{2+}$ 1243.21572 found: 1243.21825.

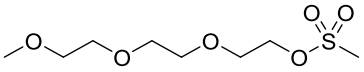

3.3

Triethylene glycol monomethyl ether (8 ml, 50 mmol) was added to DCM (125 ml) and combined with Et_3N (7.666 ml, 55 mmol). The mixture was cooled to 0 °C and methylsulfonyl chloride (4.257 ml, 55 mmol) was added. The mixture was stirred at 0 °C for 2 h and allowed to warm to rt. It was then washed with brine and concentrated under vacuum. The residue was partitioned in water and hexanes, the aqueous phase was separated, saturated with NaCl and extracted with DCM. The DCM extracts were dried with anhydrous Na_2SO_4 and concentrated under vacuum to provide 11.798 g (48.69 mmol, 97%) of **3.3** as a colourless oil.

δ_H (400 MHz, $CDCl_3$): 4.39 – 4.33 (m, 2H), 3.77 – 3.72 (m, 2H), 3.68 – 3.58 (m, 6H), 3.54 – 3.49 (m, 2H), 3.35 (s, 3H), 3.05 (s, 3H); δ_C (100 MHz, $CDCl_3$): 71.94, 70.66, 70.58, 69.41, 69.06, 59.08, 37.75;ESI-MS m/z 265.0 $[M+H]^+$.

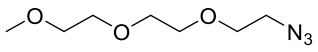

3.4

2-(2-(2-methoxyethoxy)ethoxy)ethyl methanesulfonate **3.3** (1.211 g, 5 mmol) was added to EtOH (10 ml). NaN_3 (390 mg, 6 mmol) was then added and the mixture was heated at reflux overnight. It was then evaporated, the residue redissolved in Et_2O, washed with brine, dried with anhydrous Na_2SO_4 and concentrated under vacuum. Crude material was purified by column chromatography (50% Et_2O/hexanes) to afford 683 mg (3.61 mmol, 72%) of **3.4** as a colourless oil.

δ_H (400 MHz, $CDCl_3$): 3.69 – 3.63 (m, 8H), 3.57 – 3.52 (m, 2H), 3.41 – 3.34 (m, 5H); δ_C (101 MHz, $CDCl_3$): 72.05, 70.83, 70.79, 70.74, 70.15, 59.15, 50.81; ESI-MS m/z 212.1 $[M+Na]^+$.

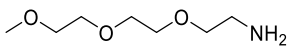

3.5

Compound **3.4** (517 mg, 2.73 mmol) was dissolved in dry Et_2O (6 ml). This solution was then slowly added to 2 M $LiAlH_4$ solution in THF (3 ml) and the mixture was stirred for 1 h at rt. It was then cooled to 0 °C and the excess $LiAlH_4$ was quenched with MeOH. The mixture was then partitioned in Et_2O and water containing Rochelle's salt and the aqueous phase further extracted with DCM. The organic phases were dried with anhydrous Na_2SO_4, filtered and concentrated under vacuum to provide **3.5** (300 mg, 1.84 mmol, 67%) as a colourless oil.

δ_H (400 MHz, $CDCl_3$): 3.69 – 3.58 (m, 6H, CH_2), 3.54 (m, 2H, CH_2), 3.49 (t, J = 5.2 Hz, 2H, CH_2), 3.37 (s, 3H, CH_3), 2.85 (t, J = 5.2 Hz, 2H, NH_2); δ_C (100 MHz, $CDCl_3$): 73.61 (*C*H_2), 72.05 (*C*H_2), 70.72 (*C*H_2), 70.65 (*C*H_2), 70.39 (*C*H_2), 59.15 (*C*H_3), 41.92 (*C*H_2NH_2); LRMS m/z 164.1 $[M+H]^+$.

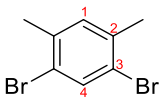

3.6

According to a literature procedure,[268] iodine (53 mg, 0.21 mmol) was added to *m*-xylene (3.68 ml, 30 mmol). The flask was darkened with aluminium foil and bromine (4.15 ml, 81 mmol) was added dropwise over 2 h. The reaction was stirred at rt in darkness for 36 h and quenched by stirring with 20% KOH solution until the red colour disappeared. The resulting mixture was cooled to 0 °C and the aqueous solution was decanted from the precipitated white solid. The residue was dissolved in DCM, washed with brine, dried with anhydrous Na_2SO_4, filtered and concentrated. The product was purified by short path distillation (132 °C at 16 mbar) to give **3.6** as a white solid (4.500 g, 17.05 mmol, 57%).

δ_H (400 MHz, $CDCl_3$): 7.68 (s, 1H, H^4), 7.10 (s, 1H, H^1), 2.31 (s, 6H, CH_3); δ_C (100 MHz, $CDCl_3$): 137.01 (C^2), 135.05 (C^4), 132.73 (C^1), 122.15 (C^3), 22.39 (*C*H_3), CI-MS 264.9057 $[M+H]^+$.

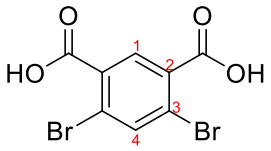

3.7

According to a literature procedure,[268] compound **3.6** (3.610 g, 13.68 mmol) was added to 1:1 ^{t}BuOH/H_2O (30 ml). $KMnO_4$ (4.755 g, 30.09 mmol) was added and the reaction was heated at reflux for 2 h. It was then brought to RT and another portion of $KMnO_4$ (4.755 g, 30.09 mmol) was added. The mixture was heated to reflux again for 20 h. It was then filtered on Celite and the filter washed with hot water. ^{t}BuOH was evaporated from the resulting clear solution, the resulting aqueous mixture was allowed to cool down to rt, washed with Et_2O and acidified with 1M HCl. The resulting white precipitate was filtered off and recrystallised in water to afford **3.7** (2.630 g, 8.12 mmol, 59%) as a white solid.

δ_H (400 MHz, $CDCl_3$ + 5% DMSO-d_6): 8.30 (s, 1H, *H*^{4}), 7.88 (s, 1H, *H*^{1}), 7.23 (br s, 2H, COO*H*); δ_C (100 MHz, $CDCl_3$): 166.31 (*C*OOH), 139.32 (*C*^{1}), 134.25 (*C*^{4}), 131.49 (*C*^{2}), 125.11 (*C*^{3}); ESI-MS m/z 322.9 $[M-H]^-$.

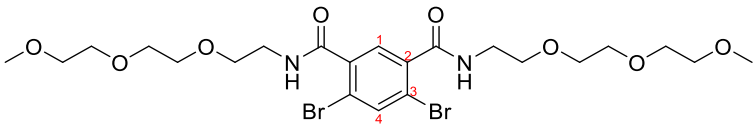

3.8

Compound **3.7** (1.335 g, 4.12 mmol) and benzyltriethylammonium chloride (23 mg, 0.10 mmol) were combined with $SOCl_2$ (16 ml) and heated at reflux for 12 h. The volatiles were then evaporated and the residual solid dried under vacuum. It was dissolved in DCM (16 ml) and the solution cooled to 0 °C. Pyridine (0.833 ml, 10.3 mmol) was then added followed by **3.5** (1.548 g, 9.48 mmol) and the reaction was allowed to warm up to rt overnight. The mixture was then combined with water and extracted with DCM. The extracts were dried with anhydrous Na_2SO_4, filtered and evaporated. The residue was purified by silica column chromatography (hexanes/acetone 7:3 – 1:1) to afford **3.8** (1.856 g, 3.02 mmol, 73%) as a clear oil.

δ_H (400 MHz, $CDCl_3$): 7.84 (s, 1H,), 7.65 – 7.62 (s, 1H), 6.86 (s, 2H, N*H*$_2$), 3.70 – 3.55 (m, 20H, C*H*$_2$), 3.49 – 3.42 (m, 4H, C*H*$_2$), 3.27 (d, J = 1.2 Hz, 6H, C*H*$_3$); δ_C (100 MHz, $CDCl_3$): 166.27 (*C*=O), 137.40, 137.34, 129.87, 121.47, 71.95 (*C*H_2), 70.61 (*C*H_2), 70.52 (*C*H_2), 70.41 (*C*H_2), 69.61 (*C*H_2), 59.03 (*C*H_2), 40.01 (*C*H_3); LRMS m/z 615.0 $[M+H]^+$; ESI-MS m/z calcd for $C_{22}H_{35}O_8N_2Br_2$ $[M+H]^+$: 615.07342, found: 615.07399.

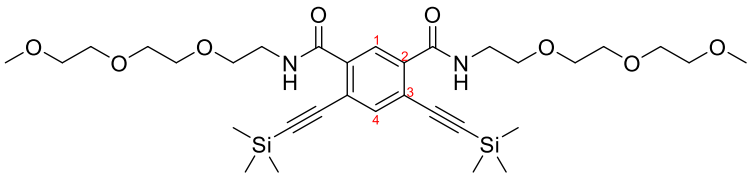

3.9

A modified literature procedure was used.[4] Compound **3.8** (1.229 g, 2 mmol) was added to degassed 5:1 toluene/$^{i}Pr_2NH$ (4 ml). PPh_3 (21 mg, 0.08 mmol, $Pd(PPh_3)_2Cl_2$ (28 mg, 0.04 mmol) and CuI (8 mg, 0.04 mmol) were then added. The mixture was stirred at rt under Ar for 5 min and ethynyltrimethylsilane (0.831 ml, 6 mmol) was added. The mixture was heated to 80 °C and stirred for 1h. Over the course of reaction the mixture turned black and a lump of diisopropylammonium bromide formed; it was then diluted with 4 ml of toluene. After reaction was determined to be complete by MS the mixture was allowed to cool and loaded directly onto a silica column. Dark impurities were eluted with 9:1 DCM/acetone, the product was then eluted with 7:3 – 1:1 hexanes/acetone to afford **3.9** (1.080 g, 1.66 mmol, 83%) as a yellow oil.

δ_H (400 MHz, $CDCl_3$): 8.41 (s, 1H, H^1), 7.67 (s, 1H, H^4), 7.47 (s, 2H, N*H*), 3.62 (m, 20H, TEG-CH_2), 3.48 (m, 4H, TEG-CH_2), 3.32 (s, 6H, TEG-CH_3); δ_C (100 MHz, $CDCl_3$): 165.41 (*C*=O), 138.87 (C^4), 136.63 (C^3), 130.85 (C^1), 121.81 (C^2), 103.80 (C≡*C*-TMS), 101.53 (Ar-*C*≡C), 72.01 (TEG-*C*H_2), 70.63 (TEG-*C*H_2), 70.48 (TEG-*C*H_2), 69.81 (TEG-*C*H_2), 59.12 (TEG-*C*H_3), 40.09 (TEG-*C*H_2), -0.18 (Si-*C*H_3); ESI-MS m/z calcd for $C_{32}H_{53}O_8N_2Si_2$ $[M+H]^+$: 649.33350, found: 649.33330.

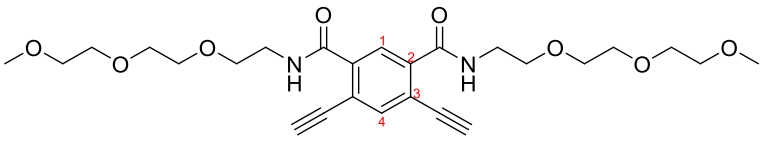

3.10

Compound **3.9** (1.080 g, 1.66 mmol) was added to 5% H_2O/THF (20 ml) and cooled to 0 °C. TBAF (1M in THF) was then added slowly. The resulting mixture was partitioned in H_2O/DCM, the organic phase was dried with anhydrous Na_2SO_4, decanted and concentrated under vacuum to provide **3.10** (595 mg, 1.18 mmol, 71%) as a yellow oil.

δ_H (400 MHz, $CDCl_3$): 8.46 (s, 1H, *H*^{1}), 7.73 (s, 1H, *H*^{4}), 7.66 (s, 2H, N*H*), 3.89 (s, 2H, C≡C*H*), 3.72 – 3.59 (m, 22H, TEG-C*H*$_2$), 3.51 (m, 4H, TEG-C*H*$_2$), 3.33 (s, 6H, TEG-C*H*$_3$); δ_C (100 MHz, $CDCl_3$): 165.07 (*C*=O), 139.19 (*C*^{4}), 137.23 (*C*^{3}), 130.78 (*C*^{1}), 121.29 (*C*^{2}), 86.89 (C≡*C*H), 80.39 (Ar-*C*≡CH), 71.94 (TEG-*C*H$_2$), 70.77 (TEG-*C*H$_2$), 70.59 (TEG-*C*H$_2$), 70.53 (TEG-*C*H$_2$), 69.87 (TEG-*C*H$_2$), 59.01 (TEG-*C*H$_3$), 40.10 (TEG-*C*H$_2$); ESI-MS m/z calcd for $C_{26}H_{37}O_8N_2$ $[M+H]^+$: 505.25444, found: 505.25439.

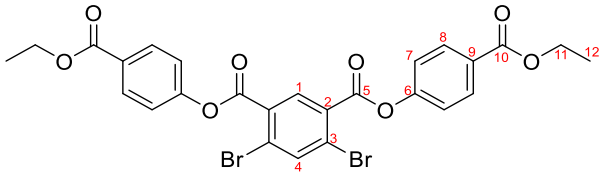

3.11

General procedure for esterification

Dibromoisophthalic acid **3.7** (3.239 g, 10 mmol) was combined with $SOCl_2$ (20 ml) and a few drops of DMF. The mixture was heated at reflux for 5 h, concentrated and dried under vacuum. The resulting acyl chloride was combined with toluene (20 ml), ethyl p-hydroxybenzoate (3.656 g, 22 mmol) and DMAP (61 mg, 0.5 mmol). The reaction was heated under reflux overnight and concentrated under vacuum. The product was purified by column chromatography (0-2% MeOH/DCM) to provide **3.11** (5.710 g, 9.2 mmol, 92%) as a white solid.

δ_H (400 MHz, $CDCl_3$) 8.60 (s, 1H, *H*^{1}), 8.06 (s, 1H, *H*^{4}), 8.05 – 8.01 (m, 4H, *H*^{8}), 7.27 – 7.21 (m, 4H, *H*^{7}), 4.29 (q, J = 7.1 Hz, 4H, *H*^{11}), 1.30 (t, J = 7.1 Hz, 6H, *H*^{12}); δ_C (101 MHz, $CDCl_3$) 165.59 (*C*^{10}), 162.19 (*C*^{5}), 153.73 (*C*^{6}), 140.61 (*C*^{4}), 134.92 (*C*^{1}), 131.28 (*C*^{8}), 129.90, 128.70 (*C*^{9}), 127.49, 121.48 (*C*^{7}), 61.23 (*C*^{11}), 14.36 (*C*^{12}); CI-MS m/z 620.9580 $[M+H]^+$.

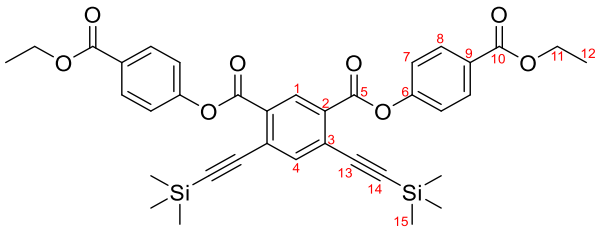

3.12

General procedure for Sonogashira coupling

Compound **3.11** (3.950 g, 6.37 mmol) was added to dry, degassed THF (42 ml) under Ar. $Pd(PPh_3)_2Cl_2$ (223 mg, 0.318 mmol) was then added followed by Et_3N (5.326 ml, 38.21 mmol). The mixture was stirred at rt for 10 min and trimethylsilylacetylene (3.529 ml, 25.47 mmol) and CuI (61 mg, 0.318 mmol) were added. The reaction was stirred at rt for 4 h when it was determined to be complete by TLC. Reaction mixture was partially evaporated under vacuum and partitioned in Et_2O and dilute aqueous solution of citric acid. Organic phase was dried with anhydrous Na_2SO_4, decanted and evaporated. Crude product was dry loaded onto silica and purified by silica chromatography (10-15% Et_2O/hexanes) to provide **3.12** (3.809 g, 5.82 mmol, 91%) as a white solid.

δ_H (400 MHz, $CDCl_3$) 8.81 (s, 1H, H^1), 8.20 – 8.10 (m, 4H, H^8), 7.93 (s, 1H, H^4), 7.40 – 7.30 (m, 4H, H^7), 4.39 (q, J = 7.1 Hz, 4H, H^{11}), 1.41 (t, J = 7.1 Hz, 6H, H^{12}), 0.21 (s, 18H, H^{15}); δ_C (101 MHz, $CDCl_3$) 165.91 (C^{10}), 162.87 (C^5), 154.19 (C^6), 141.13 (C^4), 133.88 (C^1), 131.35 (C^8), 130.26 (C^2), 128.52 (C^9), 128.06 (C^3), 121.69 (C^7), 106.10, 101.27, 61.29 (C^{11}), 14.48 (C^{12}), -0.22 (C^{15}); ESI-MS m/z calcd for $C_{36}H_{39}O_8Si_2$ $[M+H]^+$ 655.21780, found: 655.21777.

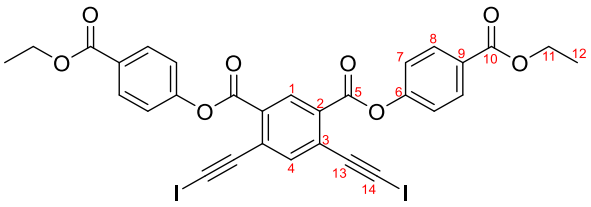

3.13

General procedure for iododesilylation

According to a modified literature procedure,[269] compound **3.12** (131 mg, 0.2 mmol) was dissolved in dry DMF (1.33 ml), combined with $AgNO_3$ (5 mg, 0.03 mmol) and cooled to 0 °C. NIS (94.5 mg, 0.42 mmol) was then added, the reaction was stirred in darkness at 0 °C for 10 min and at rt for 4 h. The reaction mixture was then combined with water (10 ml) and filtered. The collected solid was dissolved in DCM, the solution was washed with water, dried with anhydrous Na_2SO_4, filtered and evaporated, providing **3.13** (152 mg, 0.2 mmol, quant.) as an off-white solid.

δ_H (400 MHz, $CDCl_3$/DMSO-d_6) 8.89 (s, 1H, H^1), 8.19 – 8.09 (m, 4H, H^8), 7.89 (s, 1H, H^4), 7.41 – 7.32 (m, 4H, H^7), 4.40 (q, J = 7.1 Hz, 4H, H^{11}), 1.41 (t, J = 7.1 Hz, 6H, H^{12}); δ_C (101 MHz, $CDCl_3$/DMSO-d_6) 165.41 (C^{10}), 162.21 (C^5), 153.85 (C^6), 141.97 (C^4), 133.48 (C^1), 130.98 (C^8), 130.05 (C^2), 128.41 (C^9), 128.19 (C^3), 121.51 (C^7), 90.06 (C^{13}), 60.95 (C^{11}), 14.17 (C^{12}); ESI-MS m/z calcd for $C_{30}H_{21}I_2O_8$ $[M+H]^+$ 762.93203, found: 762.93197.

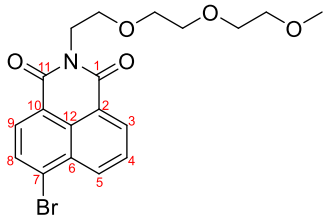

3.14

According to a literature procedure,[270] 4-bromonaphthalic anhydride (416 mg, 1.5 mmol) and TEG-NH_2 **3.5** (245 mg, 1.5 mmol) were added to EtOH (15 ml). The reaction was heated at reflux overnight. Solvent was then evaporated under vacuum and the residue was purified by silica chromatography (0.75 – 1.5% MeOH/DCM to afford **3.14** (531 mg, 1.26 mmol, 84%) as a yellowish solid.

δ_H (400 MHz, $CDCl_3$) 8.62 (dd, J = 7.3, 1.2 Hz, 1H, H^3/H^5), 8.54 (dd, J = 8.5, 1.1 Hz, 1H, H^3/H^5), 8.38 (d, J = 7.9 Hz, 1H, H^8/H^9), 8.01 (d, J = 7.9 Hz, 1H, H^8/H^9), 7.82 (dd, J = 8.5, 7.3 Hz, 1H, H^4), 4.41 (t, J = 6.1 Hz, 2H, TEG-CH_2), 3.81 (t, J = 6.1 Hz, 2H, TEG-CH_2), 3.72 – 3.67 (m, 2H, TEG-CH_2), 3.63 – 3.59 (m, 2H, TEG-CH_2), 3.59 – 3.54 (m, 2H, TEG-CH_2), 3.46 – 3.39 (m, 2H, TEG-CH_2), 3.30 (s, 3H, TEG-CH_3); δ_C (101 MHz, $CDCl_3$) 163.73 (C^1/C^{11}), 163.71 (C^1/C^{11}), 133.39, 132.18, 131.36, 131.18, 130.69, 130.39, 129.12, 128.17 (C^4), 123.13, 122.27, 71.97, 70.72, 70.61, 70.26, 67.96, 59.11, 39.35; ESI-MS m/z 444.0 $[M+Na]^+$.

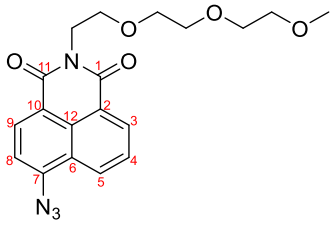

3.15

According to a modified literature procedure,[271] compound **3.14** (690 mg, 1.63 mmol) and NaN_3 (212 mg, 3.27 mmol) were added to dry DMF (8 ml) and stirred at 80 °C until determined complete by TLC. The mixture was then cooled to room temperature, diluted with water and extracted with Et_2O. The organic phases were dried with anhydrous Na_2SO_4, filtered and concentrated under vacuum. The residue was purified by silica chromatography (1.5 – 2% MeOH/DCM) to provide **3.15** (612 mg, 1.59 mmol, 98%) as a yellow solid.

δ_H (400 MHz, $CDCl_3$) 8.60 (d, J = 7.3 Hz, 1H, H^3/H^5), 8.54 (d, J = 8.0 Hz, 1H, H^8/H^9), 8.41 (d, J = 8.4 Hz, 1H, H^3/H^5), 7.72 (t, J = 7.8 Hz, 1H, H^4), 7.44 (d, J = 8.0 Hz, 1H, H^8/H^9), 4.41 (t, J = 6.1 Hz, 2H, TEG-CH_2), 3.81 (t, J = 6.1 Hz, 2H, TEG-CH_2), 3.70 (t, J = 4.8 Hz, 2H, TEG-CH_2), 3.61 (t, J = 4.8 Hz, 2H, TEG-CH_2), 3.58 (t, J = 4.8 Hz, 2H, TEG-CH_2), 3.44 (t, J = 4.7 Hz, 2H, TEG-CH_2), 3.31 (d, J = 1.1 Hz, 3H, TEG-CH_3); δ_C (101 MHz, $CDCl_3$) 164.10 (C^1/C^{11}), 163.66 (C^1/C^{11}), 143.56, 132.35, 131.84, 129.29, 128.91, 126.94 (C^4), 124.42, 122.65, 118.93, 114.76, 71.98, 70.72, 70.61, 70.24, 68.03, 59.11, 39.21; ESI-MS m/z calcd for $C_{19}H_{20}O_5N_4Na$ $[M+Na]^+$ 407.13259, found: 407.13237.

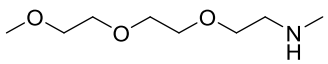

3.16

Compound **2.5** (955 mg, 3 mmol) was added to 33% $MeNH_2$ solution in EtOH (9 ml). The reaction was then conducted in a sealed vial under microwave heating at 80 °C for 5 h. The mixture was then concentrated under vacuum and the residue dissolved in Et_2O. The solution was then stirred with solid K_2CO_3 and Na_2SO_4, filtered and evaporated to provide **3.16** (430 mg, 2.43 mmol, 81%) as a yellowish oil.

δ_H (400 MHz, $CDCl_3$) δ 3.67 – 3.59 (m, 6H), 3.59 – 3.51 (m, 4H), 3.37 (s, 3H), 2.76 – 2.71 (m, 2H), 2.42 (s, 3H); δ_C (101 MHz, $CDCl_3$) 72.05, 70.74, 70.65, 70.49, 59.18, 51.42, 36.50; ESI-MS m/z 178.2 $[M+H]^+$.

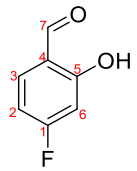

3.17

According to a literature procedure,[272] 3-Fluorophenol (905 µl, 10 mmol) was added to dry MeCN (50 ml). The solution was combined with $MgCl_2$ (2.856 g, 30mmol), Et_3N (4.878 ml, 35 mmol) and paraformaldehyde (2.100 g, 70 mmol). The reaction was stirred at reflux for 5 h and cooled to rt. It was then diluted with water, acidified with 1 M HCl and extracted with EtOAc. The organic fractions were washed with water, dried with anhydrous Na_2SO_4, decanted and concentrated under vacuum. The residue was separated by a short silica column (DCM) to provide **3.17** (680 mg, 4.85 mmol, 49%) as a white solid.

δ_H (400 MHz, $CDCl_3$) 11.37 (d, J = 1.7 Hz, 1H, O*H*), 9.83 (s, 1H, H^7), 7.56 (dd, J = 8.6, 6.3 Hz, 1H, H^3), 6.73 (td, J = 8.4, 2.4 Hz, 1H, H^2), 6.67 (dd, J = 10.4, 2.4 Hz, 1H, H^6); δ_C (101 MHz, $CDCl_3$, ^{19}F-coupled) 195.32, 169.48, 166.91, 164.35, 164.21, 141.09, 136.31, 136.18, 118.03, 108.52, 108.29, 104.95, 104.70.

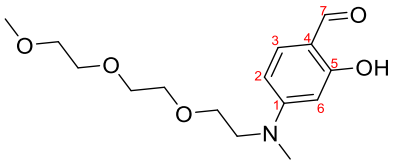

3.18

According to a modified literature procedure,[273] compound **3.17** (280 mg, 2 mmol) and **3.16** (354 mg, 2 mmol) were added to DMSO (2 ml). The mixture was stirred at 100 °C overnight and cooled to rt. It was then added to water and extracted with EtOAc. The organic fractions were dried with anhydrous Na_2SO_4, decanted and concentrated under vacuum. The residue was separated by silica chromatography (0-2% MeOH/DCM) to provide **3.18** (327 mg, 1.10 mmol, 55%) as a yellow oil.

δ_H (500 MHz, $CDCl_3$) 11.58 (s, 1H, O*H*), 9.51 (s, 1H, H^7), 7.27 (d, J = 8.9 Hz, 1H, H^3), 6.31 (dd, J = 8.9, 2.4 Hz, 1H, H^2), 6.09 (d, J = 2.4 Hz, 1H, H^6), 3.66 (td, J = 5.6, 1.1 Hz, 2H, TEG-CH_2), 3.61 (d, J = 4.8 Hz, 8H, TEG-CH_2), 3.54 – 3.51 (m, 2H, TEG-CH_2), 3.36 (s, 3H, TEG-CH_3), 3.08 (s, 3H, NCH_3); δ_C (126 MHz, $CDCl_3$) 192.44 (C^7), 164.27 (C^5), 155.59 (C^1), 135.32 (C^3), 111.90 (C^4), 104.78 (C^2), 97.42 (C^6), 72.05, 70.94, 70.81, 70.74, 68.60, 59.17, 52.18, 39.55 (NCH_3); ESI-MS m/z calcd for $C_{15}H_{24}O_5N$ $[M+H]^+$ 298.16490, found: 298.16504.

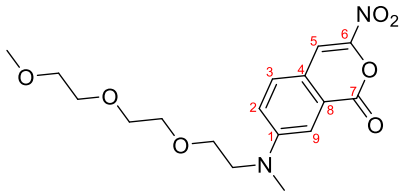

3.19

According to a modified literature procedure,[274] compound **3.18** (327 mg, 1.10 mmol) and ethyl nitroacetate (122 µl, 1.10 mmol) were added to n-BuOH, followed by addition of piperidine (27 µl, 0.275 mmol), AcOH (50 µl, 0.880 mmol) and MS3Å. The mixture was heated at reflux for 2h and cooled to rt. Molecular sieves were then separated and the mixture concentrated under vacuum. The residue was dissolved in EtOAc and washed with water. The organic fractions were dried with anhydrous Na_2SO_4, decanted and concentrated under vacuum. The residue was separated by silica chromatography (1.5% MeOH/DCM) to provide **3.19** (400 mg, 1.09 mmol, 99%) as an orange solid.

δ_H (500 MHz, $CDCl_3$) 8.70 (s, 1H, H^5), 7.43 (d, J = 9.1 Hz, 1H, H^3), 6.77 (dd, J = 9.1, 2.4 Hz, 1H, H^2), 6.52 (d, J = 2.4 Hz, 1H, H^9), 3.74 – 3.67 (m, J = 3.0 Hz, 4H, TEG-CH_2), 3.64 – 3.57 (m, 6H, TEG-CH_2), 3.54 – 3.49 (m, 2H, TEG-CH_2), 3.36 (s, 3H, TEG-CH_3), 3.18 (s, 3H, NCH_3); δ_C (126 MHz, $CDCl_3$) 158.54, 156.05, 153.47 (C^1), 143.54 (C^5), 132.34 (C^3), 127.43, 111.60 (C^2), 106.57, 97.46 (C^9), 72.03, 71.00, 70.79, 70.72, 68.53, 59.17, 52.74, 39.87 (NCH_3); ESI-MS m/z calcd for $C_{17}H_{22}O_7N_2Na$ $[M+Na]^+$ 389.13192, found: 389.13189.

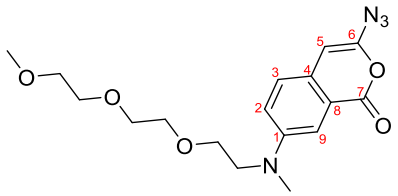

3.20

Compound **3.19** (386 mg, 1.05 mmol) and 10% Pd/C (40 mg) were added to EtOH (11 ml). The mixture was stirred under H_2 atmosphere for 2 h, filtered through Celite and concentrated under vacuum. Residue was dissolved in 17% HCl (11 ml) and cooled to 0 °C. A solution of $NaNO_2$ (87 mg, 1.26 mmol) in a small amount of water was then added slowly. The reaction was stirred at 0 °C for 10 min and NaN_3 (137 mg, 2.11 mmol) dissolved in a small amount of water was slowly added. The reaction was then stirred for 30 min at 0 °C and 1 h at rt. The mixture was diluted with water, neutralised with Na_2CO_3 (taking care to use minimum amount of base to avoid coumarin hydrolysis), And extracted with EtOAc. The organic fractions were dried with anhydrous Na_2SO_4, decanted and concentrated under vacuum. The residue was separated by silica chromatography (1% MeOH/DCM) to provide **3.20** (163 mg, 0.450 mmol, 43%) as a yellow solid.

δ_H (400 MHz, $CDCl_3$) 7.18 (d, J = 8.8 Hz, 1H, H^3), 7.08 (s, 1H, H^5), 6.63 (dd, J = 8.8, 2.4 Hz, 1H, H^2), 6.51 (d, J = 2.4 Hz, 1H, H^9), 3.68 – 3.55 (m, 10H, TEG-CH_2), 3.51 (dd, J = 5.9, 3.5 Hz, 2H, TEG-CH_2), 3.35 (d, J = 1.1 Hz, 3H, TEG-CH_3), 3.04 (s, 3H, NCH_3); δ_C (101 MHz, $CDCl_3$) 158.38 (C^7), 153.88 (C^1), 151.27 (C^8), 128.05 (C^3), 127.54 (C^5), 120.12 (C^6), 109.90 (C^2), 108.62 (C^4), 97.98 (C^9), 72.00, 70.88, 70.77, 70.69, 68.50, 59.13, 52.29, 39.30 (NCH$_3$).

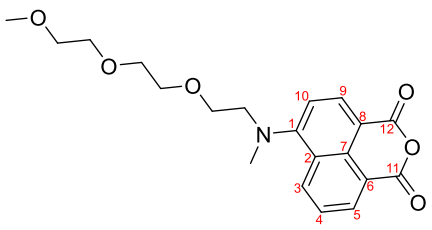

3.21

According to a modified literature procedure,[275] 4-Bromo-1,8-naphthalic anhydride (554 mg, 2 mmol) and **3.16** (390 mg, 2.2 mmol) were added to DMF (6 ml). $CuSO_4 \cdot 5H_2O$ (25 mg, 0.1 mmol) was added and the mixture was heated at reflux for 4 h. It was then cooled to rt, diluted with water and extracted with Et_2O. The combined organic phases were dried with anhydrous Na_2SO_4, decanted and evaporated. The residue was separated by silica chromatography (1-2% MeOH/DCM) to provide **3.21** (340 mg, 0.911 mmol, 46%) as an orange oil.

δ_H (400 MHz, $CDCl_3$) 8.74 – 8.67 (m, 1H, H^3), 8.58 – 8.51 (m, 1H, H^5), 8.48 – 8.42 (m, 1H, H^9), 7.74 – 7.63 (m, 1H, H^4), 7.21 (dd, J = 8.3, 1.9 Hz, 1H, H^{10}), 3.82 (t, J = 5.4 Hz, 2H, TEG-CH_2), 3.63 (qdd, J = 5.6, 4.6, 3.7, 1.8 Hz, 8H, TEG-CH_2), 3.55 – 3.50 (m, 2H, TEG-CH_2), 3.36 (d, J = 1.3 Hz, 3H, TEG-CH_3), 3.15 (s, 3H, NCH_3); δ_C (101 MHz, $CDCl_3$) 161.75 (C^{11}), 160.84 (C^{12}), 158.01 (C^1), 134.84 (C^9), 133.29 (C^5), 133.06 (C^3), 132.87 (C^7), 125.62 (C^2), 125.40 (C^4), 119.25 (C^6), 114.88 (C^{10}), 110.25 (C^8), 72.05, 70.83, 70.76, 68.69, 59.19, 57.03, 40.88 (NCH_3). ESI-MS m/z calcd for $C_{20}H_{24}O_6N$ $[M+H]^+$ 374.15981 found: 374.15982.

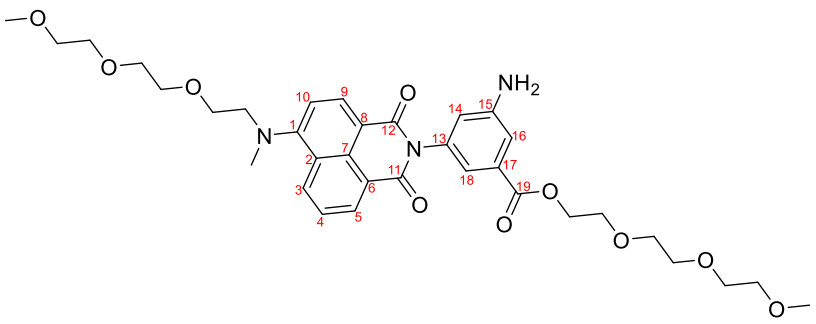

3.22

Compounds **3.21** (340 mg, 0.911 mmol) **2.14** (543 mg, 1.82 mmol) were added to dry $CHCl_3$ (6 ml) Imidazole (1.239 g, 18.2 mmol) was then added and the reaction was heated at reflux for 1.5 h. It was then cooled to rt, diluted with $CHCl_3$ and washed with dilute aqueous solution of AcOH. Aqueous phase was backextracted with DCM, the combined organic phases were dried with anhydrous Na_2SO_4, decanted and evaporated. The residue was separated by silica chromatography (2% MeOH/DCM) to provide **3.22** (320 mg, 0.489 mmol, 54%) as a yellow to orange oil.

δ_H (400 MHz, $CDCl_3$) 8.65 (dd, J = 8.5, 1.2 Hz, 1H, H^3), 8.54 (dd, J = 7.3, 1.2 Hz, 1H, H^5), 8.45 (d, J = 8.2 Hz, 1H, H^9), 7.64 (dd, J = 8.5, 7.3 Hz, 1H, H^4), 7.41 (dd, J = 2.3, 1.4 Hz, 1H, H^{16}/H^{18}), 7.32 (t, J = 1.6 Hz, 1H, H^{16}/H^{18}), 7.20 (d, J = 8.3 Hz, 1H, H^{10}), 6.76 (t, J = 2.1 Hz, 1H, H^{14}), 4.43 – 4.35 (m, 2H, TEG-CH_2), 4.01 (s, 2H, NH_2), 3.83 – 3.71 (m, 4H, TEG-CH_2), 3.66 – 3.57 (m, 12H, TEG-CH_2), 3.57 – 3.49 (m, 4H, TEG-CH_2), 3.49 – 3.45 (m, 2H, TEG-CH_2), 3.35 (s, 3H, TEG-CH_3), 3.29 (s, 3H, TEG-CH_3), 3.09 (s, 3H, NCH_3); δ_C (101 MHz, $CDCl_3$) 165.99 (C^{19}), 164.55 (C^{11}), 163.95 (C^{12}), 157.06 (C^1), 147.92 (C^{15}), 136.81 (C^{13}), 132.80 (C^9), 132.02 (C^{17}), 131.67 (C^3), 131.44 (C^5), 130.53 (C^7), 125.88 (C^2), 125.18 (C^4), 122.99 (C^6), 119.69 (C^{14}), 119.60 (C^{16}/C^{18}), 116.17 (C^{16}/C^{18}), 115.23 (C^8), 114.87 (C^{10}), 71.93, 71.87, 70.70, 70.65, 70.62, 70.55, 69.13, 68.76, 64.11, 59.06, 58.97, 57.06, 41.02 (NCH_3); ESI-MS m/z calcd for $C_{34}H_{44}O_{10}N_3$ $[M+H]^+$ 654.30212 found: 654.30178.

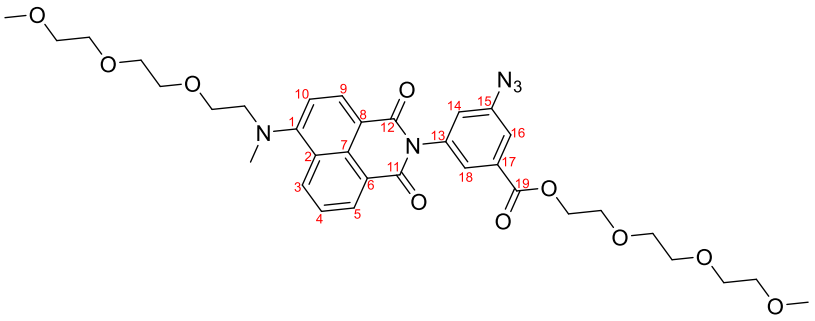

3.23

Compound **3.22** (320 mg, 0.489 mmol) was added to 17% aqueous HCl (5 ml) at 0 °C. Solution of $NaNO_2$ (41 mg, 0.587 mmol) in 1 ml of water was then added slowly. The reaction was stirred at 0 °C for 15 min and solution of NaN_3 (64 mg, 0.979 mmol) in 1 ml of water was added slowly. The reaction was stirred for 1 h at 0 °C and 1 h at rt. The mixture was then neutralised with solid Na_2CO_3, diluted with water and extracted with DCM. Organic fractions were dried with anhydrous Na_2SO_4, decanted and evaporated. The residue was separated by silica chromatography (1.5% MeOH/DCM) to provide **3.23** (211 mg, 0.310 mmol, 63%) as an orange oil.

δ_H (400 MHz, $CDCl_3$) 8.70 (dd, J = 8.5, 1.2 Hz, 1H, H^3), 8.58 (dd, J = 7.3, 1.2 Hz, 1H, H^5), 8.49 (d, J = 8.2 Hz, 1H, H^9), 7.80 (dd, J = 2.2, 1.4 Hz, 1H, H^{16}/H^{18}), 7.77 (t, J = 1.6 Hz, 1H, H^{16}/H^{18}), 7.68 (dd, J = 8.5, 7.3 Hz, 1H, H^4), 7.23 (d, J = 8.3 Hz, 1H, H^{10}), 7.17 (t, J = 2.0 Hz, 1H, H^{14}), 4.49 – 4.43 (m, 2H, TEG-CH_2), 3.84 – 3.76 (m, 4H, TEG-CH_2), 3.69 – 3.56 (m, 14H, TEG-CH_2), 3.55 – 3.51 (m, 2H, TEG-CH_2), 3.51 – 3.47 (m, 2H, TEG-CH_2), 3.36 (s, 3H, TEG-CH_3), 3.31 (s, 3H, TEG-CH_3), 3.13 (s, 3H, NCH_3); δ_C (101 MHz, $CDCl_3$) 164.97 (C^{11}/C^{19}), 164.54 (C^{11}/C^{19}), 163.88 (C^{12}), 157.43 (C^1), 141.62 (C^{15}), 137.49 (C^{13}), 133.10 (C^9), 132.85 (C^{17}), 132.12 (C^3), 131.70 (C^5), 130.70 (C^7), 126.88 (C^{16}/C^{18}), 125.91 (C^2), 125.24 (C^4), 124.30 (C^{14}), 122.77 (C^6), 120.42 (C^{16}/C^{18}), 114.89 (C^{10}), 114.82 (C^8), 71.99, 71.93, 70.77, 70.72, 70.69, 70.64, 70.62, 69.09, 68.78, 64.63, 59.13, 59.05, 57.14, 41.05 (NCH_3); ESI-MS m/z calcd for $C_{34}H_{42}O_{10}N_5$ $[M+H]^+$ 680.29262 found: 680.29242.

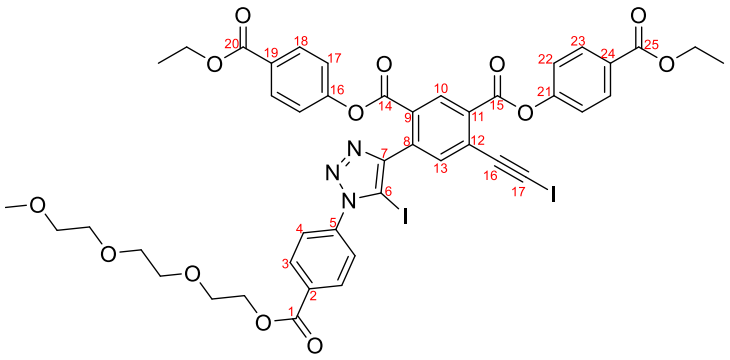

3.24a

General procedure for azide-iodoalkyne cycloaddition was used to couple compound **2.10** (155 mg, 0.5 mmol) and **3.13** (457 mg, 0.6 mmol) using 0.1 eq of $Cu[MeCN]_4PF_6$ and TBTA. The product was purified by silica chromatography(1-1.5% MeOH/DCM) to provide **3.24a** (270 mg, 0.252 mmol, 50%) as a yellow solid.

δ_H (400 MHz, $CDCl_3$) 8.93 (s, 1H, H^{10}), 8.28 – 8.21 (m, 2H, H^3), 8.17 – 8.09 (m, 2H, H^{18}/H^{23}), 8.09 – 8.03 (m, 2H, H^{18}/H^{23}), 7.92 (s, 1H, H^{13}), 7.68 – 7.60 (m, 2H, H^4), 7.40 – 7.34 (m, 2H, H^{17}/H^{22}), 7.25 – 7.19 (m, 2H, H^{17}/H^{22}), 4.54 – 4.47 (m, 2H, TEG-CH_2), 4.42 – 4.29 (m, 4H, OCH_2CH$_3$), 3.88 – 3.81 (m, 2H, TEG-CH_2), 3.73 – 3.68 (m, 2H, TEG-CH_2), 3.68 – 3.59 (m, 4H, TEG-CH_2), 3.55 – 3.47 (m, 2H, TEG-CH_2), 3.33 (s, 3H, TEG-CH_3), 1.41 – 1.32 (m, 6H, OCH$_2$CH_3); δ_C (101 MHz, $CDCl_3$) 165.70 (C^{20}/C^{25}), 165.62 (C^{20}/C^{25}), 165.17 (C^1), 163.40 (C^{14}/C^{15}), 162.48 (C^{14}/C^{15}), 154.07 (C^{16}/C^{21}), 153.92 (C^{16}/C^{21}), 149.93 (C^7), 139.93 (C^5), 138.69 (C^{13}), 134.94 (C^8), 133.71 (C^{10}), 131.99 (C^9/C^{11}), 131.86 (C^2), 131.30 (C^{18}/C^{23}), 131.22 (C^{18}/C^{23}), 130.96 (C^3), 129.80 (C^9/C^{11}), 128.52 (C^{19}/C^{24}), 128.50 (C^{19}/C^{24}), 128.41 (C^{12}), 125.96 (C^4), 121.63 (C^{17}/C^{22}), 121.38 (C^{17}/C^{22}), 91.31 (C^{16}), 80.40 (C^6), 71.92, 70.69, 70.65, 70.60, 69.08, 64.71, 61.19 (OCH$_2$CH$_3$), 61.16 (OCH$_2$CH$_3$), 59.05, 20.69 (C^{17}), 14.37 (OCH$_2$$CH_3$), 14.34 (OCH$_2$$CH_3$); ESI-MS m/z calcd for $C_{44}H_{40}O_{13}N_3I_2$ $[M+H]^+$ 1072.06450, found: 1072.06392.

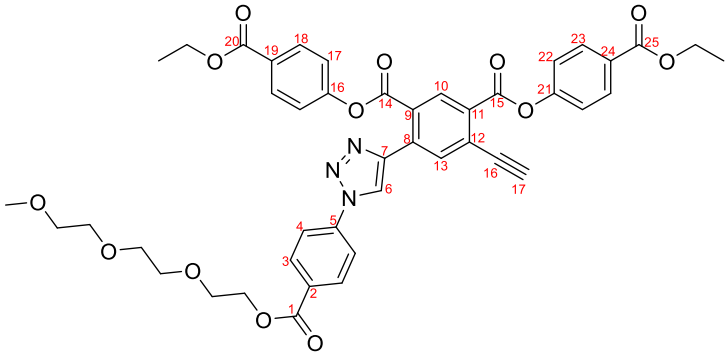

3.24a$_H$

Compound **3.12** (236 mg, 0.36 mmol) and AgF (109 mg, 0.86 mmol) were added to dry MeCN. Reaction was stirred for 8 h at rt, added to 1M HCl and stirred for 5 min. The aqueous suspension was then extracted with Et_2O, organic fractions washed with water (2x), dried with anhydrous Na_2SO_4, filtered and concentrated under vacuum. The residue was passed through a short silica column (DCM). This afforded deprotected alkyne (127 mg, 0.25 mmol) which was combined with **2.10** (64 mg, 0.21 mmol) in dry DCM. TBTA (11 mg, 0.021 mmol) and $Cu[MeCN]_4PF_6$ (7.7 mg, 0.021 mmol) were then added. The mixture was stirred at rt under Ar for 20 h and loaded directly onto a silica column (5-9% acetone/DCM) to provide **3.24a$_H$** (84 mg, 0.102 mmol, 49%) as a white solid.

δ_H (400 MHz, $CDCl_3$) 8.81 (s, 1H, H^{10}), 8.62 (s, 1H, H^{6}), 8.28 (s, 1H, H^{13}), 8.19 (d, J = 8.4 Hz, 2H, H^{3}), 8.10 (dd, J = 8.6, 6.9 Hz, 4H, H^{18}, H^{23}), 7.85 (d, J = 8.5 Hz, 2H, H^{4}), 7.33 (dd, J = 14.5, 8.5 Hz, 4H, H^{17}, H^{22}), 4.49 (t, J = 4.7 Hz, 2H, TEG-CH_2), 4.42 – 4.29 (m, 4H, OCH_2CH$_3$), 3.84 (t, J = 4.8 Hz, 2H, TEG-CH_2), 3.75 – 3.58 (m, 7H, TEG-CH_2, H^{17}), 3.52 (dd, J = 5.8, 3.5 Hz, 2H, TEG-CH_2), 3.33 (s, 3H, TEG-CH_3), 1.37 (q, J = 7.1 Hz, 6H, OCH$_2$CH_3); δ_C (101 MHz, $CDCl_3$) 165.75 (C^{20}/C^{25}), 165.67 (C^{20}/C^{25}), 165.27 (C^{14}/C^{15}), 164.65 (C^{14}/C^{15}), 162.53, 154.03 (C^{16}/C^{21}), 154.02 (C^{16}/C^{21}), 144.40 (C^{7}), 139.71 (C^{5}), 136.94 (C^{13}), 134.44 (C^{8}), 133.41 (C^{10}), 131.53 (C^{3}), 131.31 (C^{18}/C^{23}), 131.25 (C^{18}/C^{23}), 130.56, 128.63, 128.49, 127.31, 122.14 (C^{6}), 121.64 (C^{17}/C^{22}), 121.61 (C^{17}/C^{22}), 120.02 (C^{4}), 86.95 (C^{16}), 80.62 (C^{17}), 71.94, 70.71, 70.68, 70.63, 69.14, 64.62, 61.22 (OCH_2CH$_3$), 59.08, 14.37 (OCH$_2$$CH_3$); ESI-MS m/z calcd for $C_{44}H_{41}O_{13}N_3Na$ $[M+Na]^+$ 842.25316, found: 842.25292.

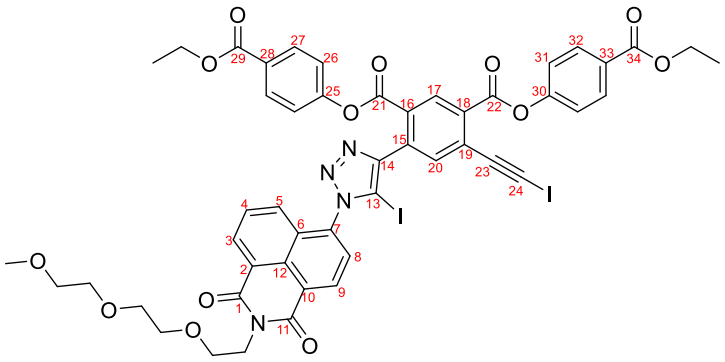

3.24b

General procedure for one-pot desilylation-cycloaddition-iodination

CsF (118 mg, 0.78 mmol) and CuI (171 mg, 0.9 mmol) were combined in a flask and dried under vacuum at 110 °C for 1 h. Compounds **3.12** (236 mg, 0.36 mmol) and **3.15** (115 mg, 0.3 mmol) were combined in another flask and dried under vacuum at rt. They were then dissolved in dry MeCN (15 ml) under Ar and added to the flask containing CsF and CuI. PMDETA (35 µl, 0.168 mmol) was then added and the reaction was stirred at rt under Ar for 2 h until the azide **3.15** was fully consumed. At this point I_2 (305 mg, 1.2 mmol) was added and the reaction was stirred overnight under Ar. The final mixture was added to a dilute aqueous solution of Na_2EDTA and extracted with DCM. The organic fractions were washed with aqueous solution of $Na_2S_2O_3$. The DCM solution was then dried with anhydrous Na_2SO_4, decanted and concentrated under vacuum. The residue was separated by silica chromatography (1 – 1.35% MeOH/DCM) to provide **3.24b** (148 mg, 0.129 mmol, 43%) as an off-white solid.

δ_H (400 MHz, $CDCl_3$) 8.99 (s, 1H, H^{17}), 8.74 (d, J = 7.9 Hz, 1H, H^{9}), 8.64 (d, J = 7.3 Hz, 1H, H^{3}), 8.17 (d, J = 8.7 Hz, 2H, H^{25}/H^{30}), 8.10 (d, J = 8.8 Hz, 2H, H^{25}/H^{30}), 8.02 (s, 1H, H^{20}), 7.82 (d, J = 7.7 Hz, 1H, H^{8}), 7.59 (dd, J = 8.5, 7.3 Hz, 1H, H^{4}), 7.46 (d, J = 8.5 Hz, 1H, H^{5}), 7.39 (d, J = 8.9 Hz, 2H, H^{24}/H^{29}), 7.29 (d, J = 8.8 Hz, 2H, H^{24}/H^{29}), 4.46 (t, J = 5.9 Hz, 2H, TEG-CH_2), 4.43 – 4.34 (m, 4H, OCH_2CH$_3$), 3.84 (t, J = 6.0 Hz, 2H, TEG-CH_2), 3.71 (dd, J = 6.1, 3.6 Hz, 2H, TEG-CH_2), 3.62 (dd, J = 5.7, 3.8 Hz, 2H, TEG-CH_2), 3.60 – 3.55 (m, 2H, TEG-CH_2), 3.45 (dd, J = 5.6, 3.8 Hz, 2H, TEG-CH_2), 3.31 (d, J = 1.2 Hz, 3H, TEG-CH_3), 1.44 – 1.36 (m, 6H, OCH$_2$CH_3); δ_C (101 MHz, $CDCl_3$) 165.82 (C^{29}/C^{34}), 165.72 (C^{29}/C^{34}), 163.57, 163.43, 163.12, 162.57, 154.11 (C^{25}/C^{30}), 153.96 (C^{25}/C^{30}), 149.80 (C^{14}), 138.77 (C^{20}), 137.59, 134.79 (C^{15}), 134.01 (C^{17}), 132.45 (C^{3}), 132.31, 131.43 (C^{27}/C^{32}), 131.39 (C^{27}/C^{32}), 130.43 (C^{9}), 129.83, 128.96 (C^{4}), 128.80 (C^{5}), 128.73, 128.70, 128.67, 128.15 (C^{6}), 126.89 (C^{8}), 125.21 (C^{10}), 123.13 (C^{2}), 121.70 (C^{26}/C^{31}), 121.57 (C^{26}/C^{31}), 91.39 (C^{23}), 83.66 (C^{13}), 71.95, 70.71, 70.60, 70.22, 67.92, 61.36 (OCH_2CH$_3$), 61.31 (OCH_2CH$_3$), 59.11, 39.50, 20.70 (C^{24}), 14.45 (OCH$_2$$CH_3$); ESI-MS m/z calcd for $C_{49}H_{40}O_{13}N_4I_2Na$ $[M+Na]^+$ 1169.05734, found: 1169.05775.

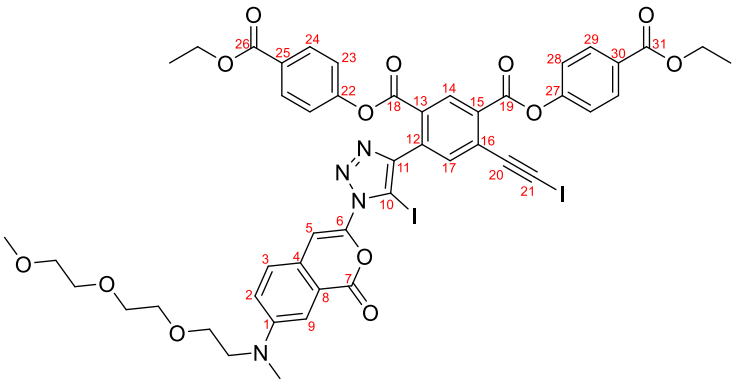

3.24c

General procedure for azide-iodoalkyne cycloaddition was used to couple compound **3.20** (91 mg, 0.251 mmol) and **3.13** (248 mg, 0.325 mmol) using 0.1 eq of $Cu[MeCN]_4PF_6$ and TBTA. The product was purified by silica chromatography to provide **3.24c** (110 mg, 0.0978 mmol, 39%) as a yellow solid.

δ_H (400 MHz, $CDCl_3$) 8.81 (s, 1H, H^{14}), 8.10 – 8.04 (m, 2H, H^{24}/H^{29}), 8.01 – 7.96 (m, 2H, H^{24}/H^{29}), 7.90 (s, 1H, H^{17}), 7.76 (s, 1H, H^{5}), 7.33 – 7.24 (m, 3H, H^{3}, H^{23}/H^{28}), 7.21 – 7.16 (m, 2H, H^{23}/H^{28}), 6.64 (dd, J = 8.9, 2.4 Hz, 1H, H^{2}), 6.52 (d, J = 2.3 Hz, 1H, H^{9}), 4.35 – 4.23 (m, 4H, OCH_2CH_3), 3.64 – 3.49 (m, 10H, TEG-CH_2), 3.46 – 3.40 (m, 2H, TEG-CH_2), 3.27 (s, 3H, TEG-CH_3), 3.04 (s, 3H, NCH_3), 1.36 – 1.24 (m, 6H, OCH_2CH_3); δ_C (101 MHz, $CDCl_3$) 165.78 (C^{31}, C^{36}), 163.89 (C^{18}/C^{19}), 162.56 (C^{18}/C^{19}), 157.08 (C^{7}), 156.93 (C^{8}), 154.12 (C^{22}/C^{27}), 154.01 (C^{22}/C^{27}), 153.86 (C^{1}), 149.02 (C^{11}), 142.85 (C^{5}), 138.56 (C^{17}), 134.76 (C^{11}), 133.71 (C^{14}), 131.68 (C^{13}/C^{15}), 131.32 (C^{24}/C^{29}), 131.17 (C^{24}/C^{29}), 130.28 (C^{3}), 130.02 (C^{13}/C^{15}), 128.48, 128.33, 128.28, 121.67 (C^{23}/C^{28}), 121.55 (C^{23}/C^{28}), 116.51 (C^{6}), 110.39 (C^{2}), 107.03 (C^{4}), 97.83 (C^{9}), 91.34 (C^{20}), 83.48 (C^{10}), 71.93, 70.86, 70.69, 70.62, 68.43, 61.21 (OCH_2CH_3), 61.12 (OCH_2CH_3), 59.08, 52.33, 39.50 (NCH_3), 20.29 (C^{21}), 14.38 (OCH_2CH_3), 14.37 (OCH_2CH_3); ESI-MS m/z calcd for $C_{47}H_{43}O_{13}N_4I_2$ $[M+H]^+$ 1125.09105, found: 1125.09125.

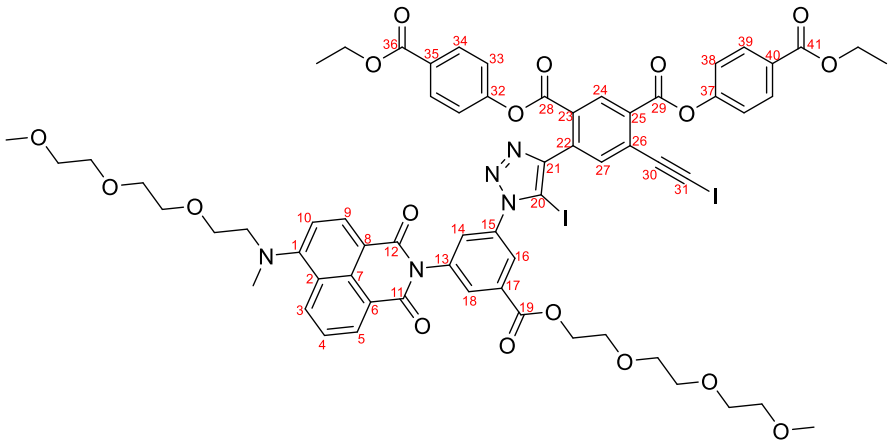

3.24d

General procedure for azide-iodoalkyne cycloaddition was used to couple compound **3.23** (102 mg, 0.150 mmol) and **3.13** (172 mg, 0.225 mmol) using 0.1 eq of $Cu[MeCN]_4PF_6$ and TBTA. The product was purified by silica chromatography (1.5-2% MeOH/DCM) to provide **3.24d** (120 mg, 0.0832 mmol, 55%) as a sticky orange solid.

δ_H (500 MHz, $CDCl_3$) 8.94 (s, 1H, H^{24}), 8.73 (dd, J = 8.6, 1.2 Hz, 1H, H^{3}), 8.62 (dd, J = 7.3, 1.2 Hz, 1H, H^{5}), 8.53 (d, J = 8.3 Hz, 1H, H^{9}), 8.43 (t, J = 1.7 Hz, 1H, H^{16}/H^{18}), 8.26 (t, J = 1.7 Hz, 1H, H^{16}/H^{18}), 8.20 – 8.15 (m, 2H, H^{34}/H^{39}), 8.10 – 8.05 (m, 2H, H^{34}/H^{39}), 7.99 (s, 1H, H^{27}), 7.84 (t, J = 2.0 Hz, 1H, H^{14}), 7.72 (dd, J = 8.5, 7.3 Hz, 1H, H^{4}), 7.42 – 7.38 (m, 2H, H^{33}/H^{38}), 7.29 – 7.23 (m, 3H, H^{10}, H^{33}/H^{38}), 4.56 – 4.52 (m, 2H, TEG-CH_2), 4.41 (q, J = 7.1 Hz, 2H, OCH_2CH$_3$), 4.34 (q, J = 7.1 Hz, 2H, OCH_2CH$_3$), 3.87 – 3.81 (m, 4H, TEG-CH_2), 3.73 – 3.59 (m, 14H, TEG-CH_2), 3.57 – 3.53 (m, 2H, TEG-CH_2), 3.53 – 3.48 (m, 2H, TEG-CH_2), 3.38 (s, 3H, TEG-CH_3), 3.33 (s, 3H, TEG-CH_3), 3.16 (s, 3H, NCH_3), 1.42 (t, J = 7.1 Hz, 3H, OCH$_2$CH_3), 1.36 (t, J = 7.1 Hz, 3H, OCH$_2$CH_3); δ_C (126 MHz, $CDCl_3$) 165.80 (C^{36}/C^{41}), 165.73 (C^{36}/C^{41}), 164.38 (C^{11}/C^{19}), 164.36 (C^{11}/C^{19}), 163.68 (C^{12}), 163.57 (C^{28}/C^{29}), 162.58 (C^{28}/C^{29}), 157.57 (C^{1}), 154.14 (C^{32}/C^{37}), 154.01 (C^{32}/C^{37}), 149.78 (C^{21}), 138.69 (C^{27}), 137.23 (C^{13}/C^{15}), 137.15 (C^{13}/C^{15}), 135.03 (C^{22}), 133.72 (C^{24}), 133.24 (C^{9}), 132.56 (C^{17}), 132.29 (C^{16}/C^{18}), 131.91 (C^{23}/C^{25}), 131.83 (C^{5}), 131.35 (C^{34}/C^{39}), 131.31 (C^{34}/C^{39}), 131.29 (C^{14}), 130.76 (C^{7}), 130.01 (C^{23}/C^{25}), 128.56 (C^{35}/C^{40}), 128.45 (C^{35}/C^{40}), 128.36 (C^{26}), 126.89 (C^{16}/C^{18}), 125.90 (C^{2}), 125.26 (C^{4}), 122.66 (C^{6}), 121.68 (C^{33}/C^{38}), 121.45 (C^{33}/C^{38}), 114.90 (C^{10}), 114.61 (C^{8}), 91.39 (C^{30}), 80.79 (C^{20}), 72.00, 70.77, 70.74, 70.72, 70.68, 70.62, 69.05, 68.79, 64.97, 61.23 (OCH$_2$CH$_3$), 61.09 (OCH$_2$CH$_3$), 59.11, 59.04, 57.13, 41.08 (NCH$_3$), 20.21 (C^{31}), 14.41 (OCH$_2$$CH_3$), 14.36 (OCH$_2$$CH_3$); ESI-MS m/z calcd for $C_{64}H_{62}O_{18}N_5I_2$ $[M+H]^+$ 1442.21737 found: 1442.21291.

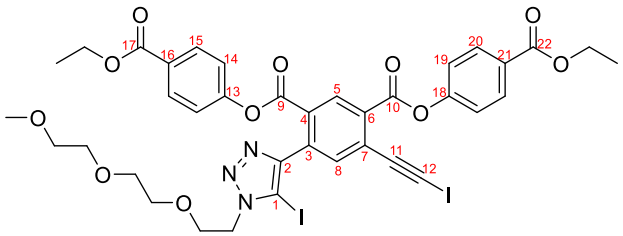

3.24e

General procedure for azide-iodoalkyne cycloaddition was used to couple compound **3.13** (229 mg, 0.3 mmol) and **3.4** (47 mg, 0.25 mmol) using 0.1 eq of $Cu[MeCN]_4PF_6$ and TBTA. The product was purified by silica chromatography to provide **3.24e** (96 mg, 0.101 mmol, 40%) as a yellow solid foam.

δ_H (400 MHz, $CDCl_3$) 8.81 (s, 1H, H^5), 8.14 – 8.04 (m, 2H, H^{15}/H^{20}), 8.03 – 7.94 (m, 2H, H^{15}/H^{20}), 7.81 (s, 1H, H^8), 7.33 – 7.28 (m, 2H, H^{14}/H^{19}), 7.17 – 7.11 (m, 2H, H^{14}/H^{19}), 4.54 (t, J = 5.7 Hz, 2H, TEG-CH_2), 4.36 – 4.25 (m, 4H, OCH_2CH$_3$), 3.88 (t, J = 5.7 Hz, 2H, TEG-CH_2), 3.54 – 3.37 (m, 8H, TEG-CH_2), 3.28 (s, 3H, TEG-CH_3), 1.36 – 1.27 (m, 6H, OCH$_2$CH_3); δ_C (101 MHz, $CDCl_3$) 165.74 (C^{17}/C^{22}), 165.68 (C^{17}/C^{22}), 163.68 (C^9/C^{10}), 162.54 (C^9/C^{10}), 154.07 (C^{13}/C^{18}), 153.97 (C^{13}/C^{18}), 148.52 (C^2), 138.38 (C^8), 135.30 (C^3), 133.56 (C^5), 131.58 (C^4/C^6), 131.30 (C^{15}/C^{20}), 131.12 (C^{15}/C^{20}), 129.88 (C^4/C^6), 128.48, 128.35, 128.19, 121.64 (C^{14}/C^{19}), 121.46 (C^{14}/C^{19}), 91.33 (C^{11}), 80.75 (C^1), 71.88, 70.76, 70.55, 70.50, 69.24, 61.19 (*C*H$_2$CH$_3$), 61.15 (*C*H$_2$CH$_3$), 59.06, 50.67, 20.14 (C^{12}), 14.36 (CH$_2$*C*H$_3$), 14.33 (CH$_2$*C*H$_3$).

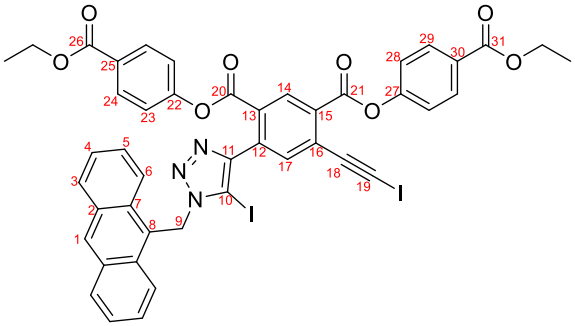

3.24f

General procedure for one-pot desilylation-cycloaddition-iodination was used to couple **2.11** (93 mg, 0.4 mmol) and **3.12** (314 mg, 0.48 mmol). Azide **2.11** was fully consumed after 1 h and I_2 was added immediately. The product was purified by silica chromatography (0.5-1% acetone/DCM) to provide **3.24f** (193 mg, 0.194 mmol, 48%) as a white solid.

δ_H (500 MHz, $CDCl_3$) 8.82 (s, 1H, H^{14}), 8.56 (s, 1H, H^{1}), 8.21 – 8.17 (m, 2H, H^{6}), 8.15 (d, J = 8.7 Hz, 3H, H^{24}/H^{29}), 8.07 – 8.00 (m, 2H, H^{3}), 7.89 (d, J = 8.6 Hz, 2H, H^{24}/H^{29}), 7.82 (s, 1H, H^{17}), 7.48 – 7.40 (m, 4H, H^{4}, H^{5}), 7.36 (d, J = 8.6 Hz, 2H, H^{23}/H^{28}), 6.95 (d, J = 8.5 Hz, 2H, H^{23}/H^{28}), 6.44 (s, 2H, H^{9}), 4.44 – 4.36 (m, 4H, OCH_2CH_3), 1.46 – 1.37 (m, 6H, OCH_2CH_3); δ_C (126 MHz, $CDCl_3$) 165.84 (C^{26}/C^{31}), 165.83 (C^{26}/C^{31}), 163.85 (C^{20}/C^{21}), 162.56 (C^{20}/C^{21}), 154.15 (C^{22}/C^{27}), 153.82 (C^{22}/C^{27}), 149.09 (C^{11}), 138.44 (C^{17}), 135.14 (C^{12}), 133.73 (C^{14}), 131.70 (C^{13}/C^{15}), 131.43 (C^{2}), 131.37 (C^{24}/C^{29}), 131.26 (C^{7}), 131.11 (C^{24}/C^{29}), 130.16 (C^{1}), 129.51 (C^{3}), 128.56 (C^{25}/C^{30}), 128.27 (C^{25}/C^{30}), 128.17 (C^{16}), 127.29 (C^{5}), 125.27 (C^{4}), 123.58 (C^{6}), 123.28 (C^{8}), 121.69 (C^{23}/C^{28}), 121.30 (C^{23}/C^{28}), 91.45 (C^{18}), 79.04 (C^{10}), 61.27 (OCH_2CH_3), 61.21 (OCH_2CH_3), 53.56, 48.47, 19.76 (C^{19}), 14.50 (OCH_2CH_3), 14.45 (OCH_2CH_3); ESI-MS m/z calcd for $C_{45}H_{32}O_8N_3I_2$ $[M+H]^{2+}$ 996.02733 found: 996.02730.

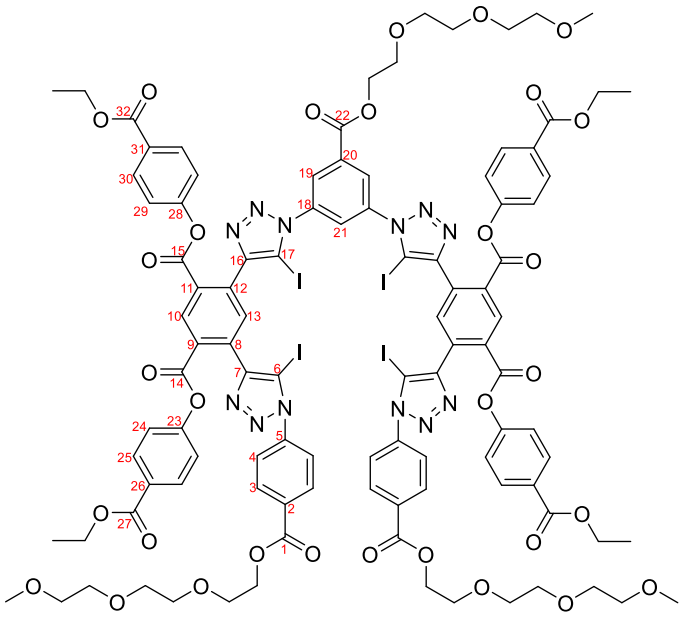

3.25a

General procedure for azide-iodoalkyne cycloaddition was used to couple compound **3.24a** (90 mg, 0.0840 mmol) and **2.15** (14.7 mg, 0.0420 mmol). The product was purified by silica chromatography (15-25% acetone/DCM) to provide **3.25a** (80 mg, 0.0321 mmol, 76%) as a yellow solid.

δ_H (400 MHz, $CDCl_3$) 9.00 (s, 2H, H^{10}), 8.54 (d, J = 2.0 Hz, 2H, H^{19}), 8.32 – 8.22 (m, 4H, H^3), 8.14 (t, J = 2.0 Hz, 1H, H^{21}), 8.13 – 8.07 (m, 8H, H^{25}, H^{30}), 8.05 (s, 2H, H^{13}), 7.73 – 7.62 (m, 4H, H^4), 7.33 – 7.27 (m, 8H, H^{24}, H^{29}), 4.60 – 4.47 (m, 6H, TEG-CH_2), 4.41 – 4.31 (m, 8H, OCH_2CH$_3$), 3.91 – 3.80 (m, 6H, TEG-CH_2), 3.75 – 3.61 (m, 16H, TEG-CH_2), 3.61 – 3.56 (m, 2H, TEG-CH_2), 3.55 – 3.51 (m, 4H, TEG-CH_2), 3.50 – 3.45 (m, 2H, TEG-CH_2), 3.35 (s, 6H, TEG-CH_3), 3.30 (s, 3H, TEG-CH_3), 1.43 – 1.32 (m, 12H, OCH$_2$CH_3) δ_C (101 MHz, $CDCl_3$) 165.77 (C^{27}/C^{32}), 165.75 (C^{27}/C^{32}), 165.30 (C^1), 163.85 (C^{14}/C^{15}), 163.66 (C^{14}/C^{15}), 163.62 (C^{22}), 154.08 (C^{23}, C^{28}), 150.68 (C^7/C^{16}), 150.24 (C^7/C^{16}), 140.05 (C^5), 137.72 (C^{18}), 135.06 (C^{13}), 135.01 (C^8/C^{12}), 134.73 (C^8/C^{12}), 133.73 (C^{10}), 133.20 (C^{20}), 131.98 (C^2/C^8/C^{12}), 131.49 (C^2/C^9/C^{11}), 131.40 (C^{25}/C^{30}), 131.37 (C^{25}/C^{30}), 131.14 (C^2/C^9/C^{11}), 131.07 (C^3), 128.67 (C^{26}, C^{31}), 128.39 (C^{19}), 127.33 (C^{21}), 126.09 (C^4), 121.54 (C^{24}/C^{29}), 121.51 (C^{24}/C^{29}), 80.88 (C^6/C^{17}), 80.50 (C^6/C^{17}), 72.02, 71.95, 70.79, 70.75, 70.70, 70.64, 69.20, 68.99, 65.58, 64.80, 61.27 (OCH$_2$CH$_3$), 59.16, 59.10, 14.42 (OCH$_2$$CH_3$); ESI-MS m/z calcd for $C_{102}H_{97}O_{31}N_{12}I_4$ $[M+H]^+$ 2493.25559, found: 2493.24848.

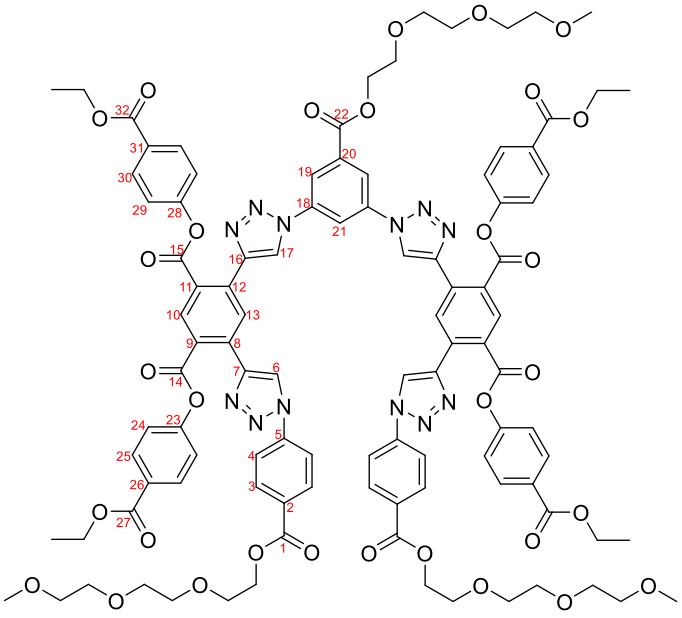

3.25a$_H$

General procedure for azide-protoalkyne cycloaddition was used to couple compound **3.24a$_H$** (84 mg, 0.102 mmol) and **2.15** (17.5 mg, 0.0500 mmol). The product was purified by silica chromatography (20-25% acetone/DCM) to provide **3.25a$_H$** (68 mg, 0.0342 mmol, 68%) as a white solid.

δ_H (500 MHz, $CDCl_3$) 8.94 – 8.78 (m, 2H), 8.73 (s, 2H), 8.61 (s, 2H), 8.43 (s, 4H), 8.07 (t, J = 8.0 Hz, 8H, H^3, H^{25}/H^{30}), 7.99 (d, J = 7.9 Hz, 4H, H^{25}/H^{30}), 7.81 (d, J = 8.2 Hz, 4H, H^4), 7.37 – 7.27 (m, 8H, H^{24}, H^{29}), 4.50 (d, J = 39.8 Hz, 6H, TEG-CH_2), 4.37 (q, J = 7.1 Hz, 4H, OCH_2CH$_3$), 4.30 (q, J = 7.1 Hz, 4H, OCH_2CH$_3$), 3.91 – 3.75 (m, 6H, TEG-CH_2), 3.65 (ddt, J = 36.5, 19.9, 4.5 Hz, 18H, TEG-CH_2), 3.56 – 3.43 (m, 6H, TEG-CH_2), 3.34 (s, 6H, TEG-CH_3), 3.27 (s, 3H, TEG-CH_3), 1.39 (t, J = 7.1 Hz, 6H, OCH$_2$CH_3), 1.33 (t, J = 7.1 Hz, 6H, OCH$_2$CH_3); δ_C (126 MHz, $CDCl_3$) 165.74 (C^{27}/C^{32}), 165.64 (C^{27}/C^{32}), 165.32, 164.99, 164.84 (C^{24}), 154.22 (C^{23}/C^{28}), 154.15 (C^{23}/C^{28}), 145.38 (C^7/C^{16}), 145.00 (C^7/C^{16}), 139.71 (C^5), 137.79, 133.95, 133.70, 133.12, 131.85, 131.42, 131.26 (C^{25}/C^{30}), 131.20 (C^{25}/C^{30}), 130.31, 128.59, 128.53, 128.45, 122.05, 121.72 (C^{24}/C^{29}), 121.64 (C^{24}/C^{29}), 120.59, 119.83 (C^4), 71.99, 71.92, 70.74, 70.67, 70.63, 70.53, 69.23, 65.22, 64.57, 61.21 (OCH$_2$CH$_3$), 61.17 (OCH$_2$CH$_3$), 59.13, 59.05, 14.41 (OCH$_2$$CH_3$), 14.36 (OCH$_2$$CH_3$); ESI-MS m/z calcd for $C_{102}H_{100}O_{31}N_{12}Na$ $[M+H]^+$ 2011.65096, found: 2011.65445.

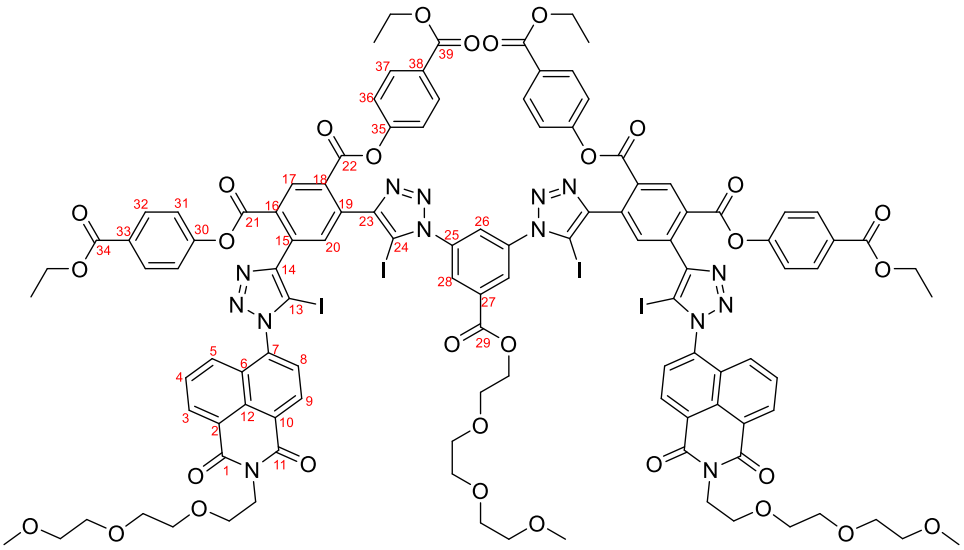

3.25b

General procedure for azide-iodoalkyne cycloaddition was used to couple compound **3.24b** (148 mg, 0.129 mmol) and **2.15** (22.6 mg, 0.0645 mmol). The product was purified by silica chromatography (0.25-0.8% MeOH, 15% acetone/DCM) to provide **3.25b** (113 mg, 0.0427 mmol, 66%) as a white solid.

δ_H (500 MHz, $CDCl_3$) 9.05 (s, 2H, H^{17}), 8.73 (d, J = 7.7 Hz, 2H, H^{9}), 8.63 (dd, J = 7.2, 1.1 Hz, 2H, H^{3}), 8.55 (d, J = 2.0 Hz, 2H, H^{28}), 8.16 – 8.11 (m, 7H, H^{26}, H^{32}/H^{37}, H^{20}), 8.11 – 8.07 (m, 4H, H^{32}/H^{37}), 7.84 (d, J = 7.7 Hz, 2H, H^{8}), 7.58 (dd, J = 8.5, 7.3 Hz, 2H, H^{4}), 7.47 (dd, J = 8.5, 1.1 Hz, 2H, H^{5}), 7.37 – 7.33 (m, 4H, H^{31}/H^{36}), 7.33 – 7.29 (m, 4H, H^{31}/H^{36}), 4.59 – 4.55 (m, 2H, TEG-CH_2), 4.46 (t, J = 5.9 Hz, 4H, TEG-CH_2), 4.39 (q, J = 7.1 Hz, 4H, OCH_2CH$_3$), 4.34 (q, J = 7.1 Hz, 4H, OCH_2CH$_3$), 3.85 (q, J = 6.1, 5.4 Hz, 6H, TEG-CH_2), 3.70 (dt, J = 5.3, 3.9 Hz, 6H, TEG-CH_2), 3.65 – 3.54 (m, 12H, TEG-CH_2), 3.50 – 3.43 (m, 6H, TEG-CH_2), 3.31 (s, 6H, TEG-CH_3), 3.29 (s, 3H, TEG-CH_3), 1.40 (t, J = 7.2 Hz, 6H, OCH$_2$CH_3), 1.35 (t, J = 7.1 Hz, 6H, OCH$_2$CH_3); δ_C (126 MHz, $CDCl_3$) 165.72 (C^{34}, C^{39}), 163.77 (C^{21}/C^{22}), 163.62 (C^{1}/C^{21}/C^{22}/C^{29}), 163.60 (C^{1}/C^{21}/C^{22}/C^{29}), 163.17 (C^{11}), 154.05 (C^{30}, C^{35}), 150.68 (C^{14}/C^{23}), 150.03 (C^{14}/C^{23}), 137.72 (C^{25}), 137.66 (C^{7}), 135.08 (C^{20}), 134.94 (C^{15}/C^{19}), 134.81 (C^{15}/C^{19}), 133.93 (C^{17}), 133.25 (C^{27}), 132.46 (C^{3}), 131.44 (C^{15}/C^{19}), 131.42 (C^{32}/C^{37}), 131.41 (C^{32}/C^{37}), 131.34 (C^{16}/C^{18}), 130.46 (C^{9}), 128.98 (C^{4}/C^{12}), 128.96 (C^{4}/C^{12}), 128.84 (C^{5}), 128.80 (C^{33}/C^{38}), 128.70 (C^{33}/C^{38}), 128.41 (C^{28}), 128.18 (C^{6}), 127.34 (C^{26}), 126.93 (C^{8}), 125.20 (C^{10}), 123.12 (C^{2}), 121.59 (C^{31}/C^{36}), 121.52 (C^{31}/C^{36}), 83.79 (C^{13}/C^{24}), 80.88 (C^{13}/C^{24}), 71.93, 71.91, 70.75, 70.74, 70.62, 70.53, 70.21, 68.98, 68.06, 65.60, 61.36 (OCH_2CH$_3$), 61.28 (OCH_2CH$_3$), 59.11, 59.08, 39.60, 14.44 (OCH$_2$$CH_3$); ESI-MS m/z calcd for $C_{112}H_{98}O_{31}N_{14}I_4Na_2$ $[M+2Na]^{2+}$ 1344.12428 found: 1344.12591.

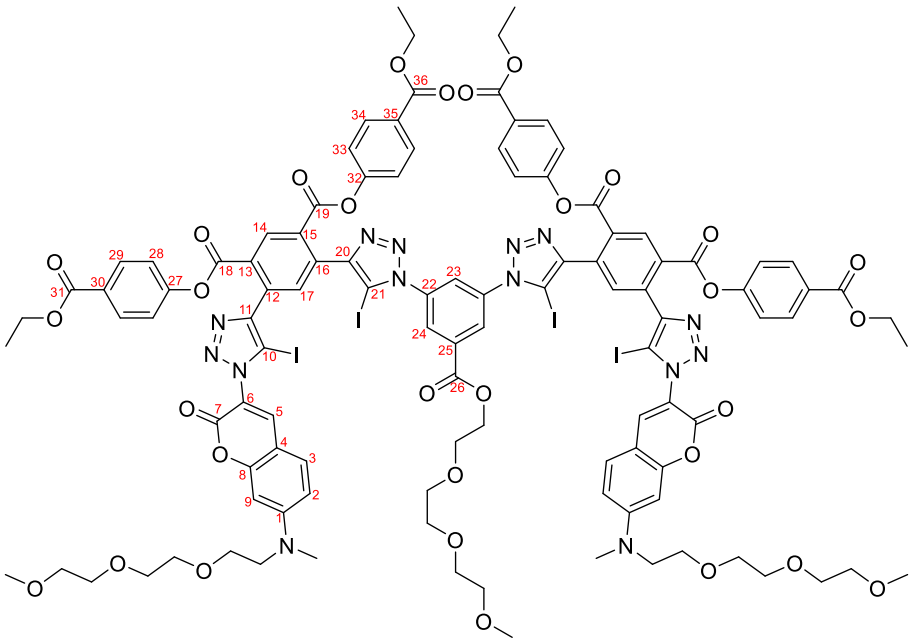

3.25c

General procedure for azide-iodoalkyne cycloaddition was used to couple compound **3.24c** (110 mg, 0.0978 mmol) and **2.15** (15.4 mg, 0.0440 mmol). The product was purified by silica chromatography to provide **3.25c** (87 mg, 0.0335 mmol, 76%) as a yellow solid.

δ_H (400 MHz, $CDCl_3$) 8.92 (s, 2H, H^{14}), 8.52 (s, 2H, H^{24}), 8.14 (s, 1H, H^{23}), 8.08 (d, J = 8.6 Hz, 10H, H^{29}, H^{34}, H^{17}), 7.85 (s, 2H, H^{5}), 7.39 – 7.27 (m, 10H, H^{3}, H^{28}, H^{33}), 6.71 (d, J = 8.9 Hz, 2H, H^{2}), 6.57 (s, 2H, H^{9}), 4.55 (t, J = 4.3 Hz, 2H, TEG-CH_2), 4.41 – 4.28 (m, 8H, OCH_2CH$_3$), 3.84 (t, J = 4.6 Hz, 2H, TEG-CH_2), 3.72 – 3.55 (m, 27H, TEG-CH_2), 3.54 – 3.44 (m, 6H, TEG-CH_2), 3.34 (s, 6H, TEG-CH_3), 3.29 (s, 3H, TEG-CH_3), 3.11 (s, 6H, NCH_3), 1.43 – 1.30 (m, 12H, OCH$_2$CH_3); δ_C (101 MHz, $CDCl_3$) 165.88 (C^{31}/C^{36}), 165.77 (C^{31}/C^{36}), 164.34 (C^{18}/C^{19}), 163.81 (C^{18}/C^{19}), 163.70 (C^{26}), 157.18 (C^{7}), 156.95 (C^{8}), 154.13 (C^{27}/C^{32}), 154.09 (C^{27}/C^{32}), 153.87 (C^{1}), 150.52 (C^{11}/C^{20}), 149.24 (C^{11}/C^{20}), 143.00 (C^{5}), 137.67 (C^{22}), 134.63 (C^{17}), 134.56 (C^{12}/C^{16}), 134.46 (C^{12}/C^{16}), 133.61 (C^{14}), 133.12 (C^{25}), 131.59 (C^{13}/C^{15}), 131.35 (C^{29}/C^{34}), 131.24 (C^{29}/C^{34}), 130.94 (C^{13}/C^{15}), 130.34 (C^{3}), 128.53 (C^{30}/C^{35}), 128.43 (C^{30}/C^{35}), 128.39 (C^{24}), 127.40 (C^{23}), 121.63 (C^{28}/C^{33}), 121.55 (C^{28}/C^{33}), 116.56 (C^{6}), 110.41 (C^{2}), 107.08 (C^{4}), 97.84 (C^{9}), 71.95, 71.85, 70.88, 70.70, 70.63, 70.53, 68.99, 68.45, 65.47, 61.22 (OCH_2CH$_3$), 59.12, 52.34, 39.53 (NCH_3), 14.40 (OCH$_2$CH_3); ESI-MS m/z calcd for $C_{108}H_{103}O_{31}N_{14}I_4$ $[M+H]^+$ 2599.30869, found: 2599.30677.

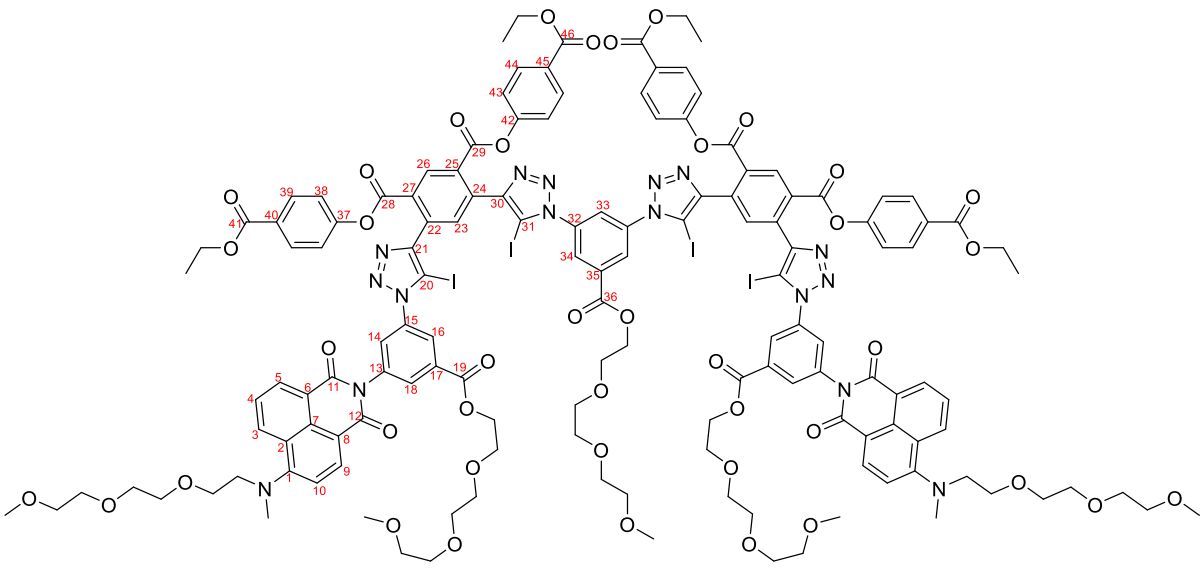

3.25d

General procedure for azide-iodoalkyne cycloaddition was used to couple compound **3.24d** (120 mg, 0.0832 mmol) and **2.15** (13.1 mg, 0.0374 mmol). The product was purified by silica chromatography to provide **3.25d** (97 mg, 0.0300 mmol, 80%) as a yellow solid.

δ_H (500 MHz, $CDCl_3$) 8.96 (s, 2H, H^{26}), 8.71 (dd, J = 8.5, 1.2 Hz, 2H, H^3), 8.60 (dd, J = 7.2, 1.2 Hz, 2H, H^5), 8.54 (d, J = 2.0 Hz, 2H, H^{34}), 8.50 (d, J = 8.2 Hz, 2H, H^9), 8.44 – 8.41 (m, 2H, H^{16}/H^{18}), 8.23 (t, J = 1.7 Hz, 2H, H^{16}/H^{18}), 8.15 (t, J = 2.0 Hz, 1H, H^{33}), 8.12 – 8.05 (m, 10H, H^{23}, H^{39}, H^{44}), 7.83 (t, J = 2.0 Hz, 2H, H^{14}), 7.70 (dd, J = 8.5, 7.3 Hz, 2H, H^4), 7.31 – 7.27 (m, 8H, H^{38}, H^{43}), 7.24 (d, J = 8.4 Hz, 2H, H^{10}), 4.59 – 4.54 (m, 2H, TEG-CH_2), 4.54 – 4.47 (m, 4H, TEG-CH_2), 4.37 – 4.29 (m, 8H, OCH_2CH$_3$), 3.88 – 3.78 (m, 10H, TEG-CH_2), 3.70 – 3.56 (m, 34H, TEG-CH_2), 3.55 – 3.51 (m, 4H, TEG-CH_2), 3.49 – 3.45 (m, 6H, TEG-CH_2), 3.36 (s, 6H, TEG-CH_3), 3.30 – 3.28 (m, 9H, TEG-CH_3), 3.14 (s, 6H, NCH_3), 1.39 – 1.30 (m, 12H, OCH$_2$CH_3); δ_C (126 MHz, $CDCl_3$) 165.79 (C^{41}/C^{46}), 165.73 (C^{41}/C^{46}), 164.41 (C^{11}), 164.38 (C^{19}), 163.97 (C^{28}/C^{29}), 163.77 (C^{28}/C^{29}), 163.72 (C^{12}), 163.60 (C^{36}), 157.60 (C^1), 154.10 (C^{37}/C^{42}), 154.08 (C^{37}/C^{42}), 150.57 (C^{21}/C^{30}), 150.04 (C^{21}/C^{30}), 137.71 (C^{32}), 137.27 (C^{13}/C^{15}), 137.18 (C^{13}/C^{15}), 134.92 (C^{22}/C^{24}), 134.80 (C^{23}), 134.52 (C^{22}/C^{24}), 133.64 (C^{26}), 133.26 (C^9), 133.15 (C^{35}), 132.57 (C^{17}), 132.31 (C^3/C^{16}/C^{18}), 132.30 (C^3/C^{16}/C^{18}), 131.84 (C^5), 131.56 (C^{25}/C^{27}), 131.38 (C^{39}/C^{44}), 131.37 (C^{39}/C^{44}), 131.32 (C^{14}), 131.15 (C^{25}/C^{27}), 130.78 (C^7), 128.60 (C^{40}/C^{45}), 128.53 (C^{40}/C^{45}), 128.40 (C^{34}), 127.34 (C^{33}), 126.92 (C^{16}/C^{18}), 125.93 (C^2), 125.28 (C^4), 122.68 (C^6), 121.52 (C^{38}, C^{43}), 114.92 (C^{10}), 114.63 (C^8), 80.80 (C^{20}/C^{31}), 80.60 (C^{20}/C^{31}), 72.01, 71.93, 70.79, 70.77, 70.74, 70.70, 70.67, 70.62, 69.06, 68.94, 68.81, 65.52, 64.99, 61.23 (OCH_2CH$_3$), 61.13 (OCH_2CH$_3$), 59.13, 59.05, 57.15, 41.10 (NCH_3), 14.39 (OCH$_2$CH_3); ESI-MS m/z calcd for $C_{134}H_{170}O_{41}N_{20}I_4$ $[M+2H]^{2+}$ 1617.28431 found: 1617.28209.

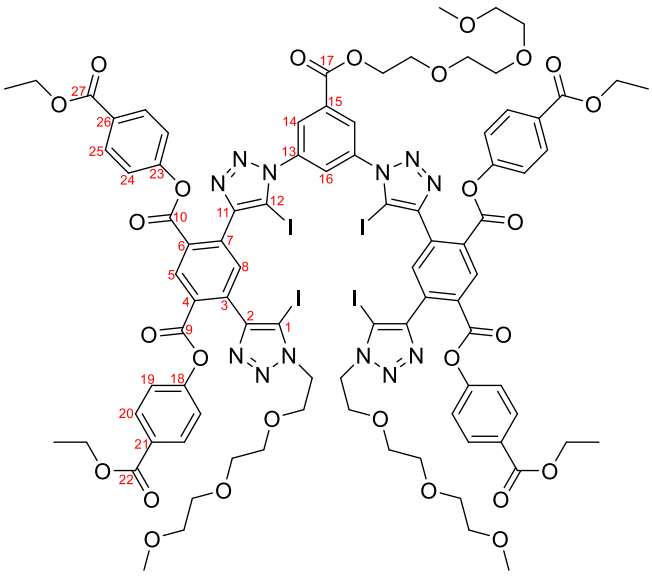

3.25e

General procedure for azide-iodoalkyne cycloaddition was used to couple compound **3.24e** (96 mg, 0.100 mmol) and **2.15** (15.7 mg, 0.0450 mmol). The product was purified by silica chromatography to provide **3.25e** (75 mg, 0.0333 mmol, 74%) as a yellow solid foam.

δ_H (500 MHz, $CDCl_3$) 8.92 (s, 2H, H^5), 8.52 (d, J = 2.0 Hz, 2H, H^{14}), 8.14 (t, J = 2.0 Hz, 1H, H^{16}), 8.08 (dd, J = 8.7, 3.2 Hz, 8H, H^{20}, H^{25}), 7.98 (s, 2H, H^8), 7.33 – 7.20 (m, 8H, H^{19}, H^{24}), 4.62 (t, J = 5.7 Hz, 4H, TEG-CH_2), 4.58 – 4.53 (m, 2H, TEG-CH_2), 4.40 – 4.31 (m, 8H, OCH_2CH$_3$), 3.96 (t, J = 5.7 Hz, 4H, TEG-CH_2), 3.87 – 3.82 (m, 2H, TEG-CH_2), 3.70 – 3.67 (m, 2H, TEG-CH_2), 3.64 – 3.61 (m, 2H, TEG-CH_2), 3.60 – 3.57 (m, 2H, TEG-CH_2), 3.56 – 3.44 (m, 18H, TEG-CH_2), 3.31 (s, 6H, TEG-CH_3), 3.30 (s, 3H, TEG-CH_3), 1.41 – 1.33 (m, 12H, OCH$_2$CH_3); δ_C (126 MHz, $CDCl_3$) 165.77 (C^{22}/C^{27}), 165.73 (C^{22}/C^{27}), 164.17 (C^9/C^{10}), 163.68 (C^9/C^{10}), 163.61 (C^{17}), 154.14 (C^{18}/C^{23}), 154.07 (C^{18}/C^{23}), 150.70 (C^2/C^{11}), 148.81 (C^2/C^{11}), 137.71 (C^{13}), 135.26, 134.67, 134.49, 133.53 (C^5), 133.18, 131.54, 131.36 (C^{20}/C^{25}), 131.23 (C^{20}/C^{25}), 130.74, 128.59 (C^{21}/C^{26}), 128.49 (C^{21}/C^{26}), 128.35 (C^{14}), 127.32 (C^{16}), 121.56 (C^{19}/C^{24}), 121.53 (C^{19}/C^{24}), 81.02 (C^1/C^{12}), 80.95 (C^1/C^{12}), 71.94, 70.83, 70.75, 70.74, 70.63, 70.61, 70.58, 69.31, 68.93, 65.52, 61.22 (OCH$_2$CH$_3$), 59.10, 59.07, 50.77, 14.40 (OCH$_2$$CH_3$); ESI-MS m/z calcd. for $C_{88}H_{89}O_{27}N_{12}I_4$ 2253.21333, found: 2253.20722.

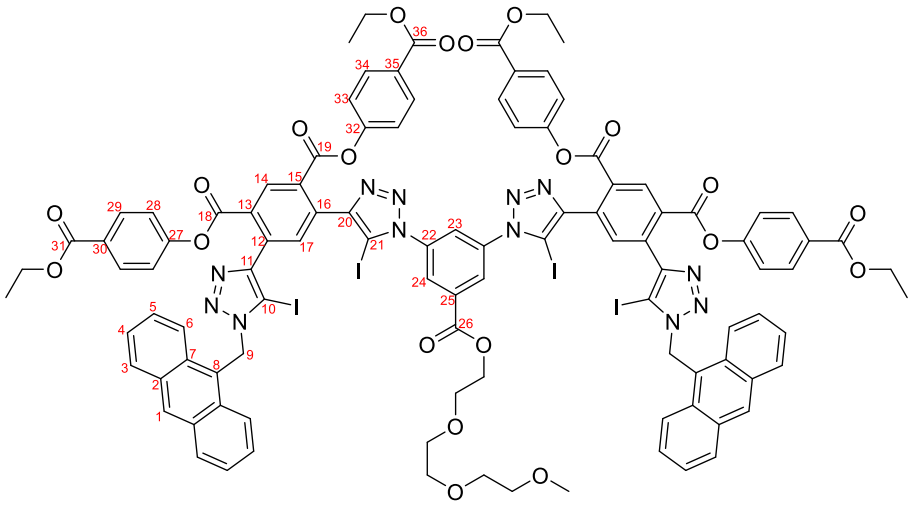

3.25f

General procedure for azide-iodoalkyne cycloaddition was used to couple compound **3.24f** (193 mg, 0.194 mmol) and **2.15** (34 mg, 0.0969 mmol). The product was purified by silica chromatography to provide **3.25f** (213 mg, 0.0910 mmol, 94%) as a yellow solid.

δ_H (400 MHz, $CDCl_3$) 8.91 (d, J = 1.8 Hz, 2H, H^{14}), 8.56 (s, 2H, H^{1}), 8.55 – 8.52 (m, 2H, H^{24}), 8.26 – 8.15 (m, 4H, H^{6}), 8.15 – 8.07 (m, 5H, H^{23}, H^{29}/H^{33}), 8.07 – 7.99 (m, 4H, H^{3}), 7.95 (s, 2H, H^{17}), 7.91 (d, J = 8.7 Hz, 4H, H^{29}/H^{33}), 7.50 – 7.36 (m, 8H, H^{4}, H^{5}), 7.34 – 7.23 (m, 4H, H^{28}/H^{32}), 7.08 – 6.95 (m, 4H, H^{28}/H^{32}), 6.47 (s, 4H, H^{9}), 4.62 – 4.51 (m, 2H, TEG-CH_2), 4.43 (q, J = 7.1 Hz, 4H, OCH_2CH$_3$), 4.36 (q, J = 7.1 Hz, 4H, OCH_2CH$_3$), 3.90 – 3.83 (m, 2H, TEG-CH_2), 3.74 – 3.67 (m, 2H, TEG-CH_2), 3.67 – 3.56 (m, 4H, TEG-CH_2), 3.52 – 3.46 (m, 2H, TEG-CH_2), 3.31 (s, 3H, TEG-CH_3), 1.46 (t, J = 7.1 Hz, 6H, OCH$_2$CH_3), 1.37 (t, J = 7.1 Hz, 6H, OCH$_2$CH_3); δ_C (101 MHz, $CDCl_3$) 165.82 (C^{31}/C^{36}), 165.73 (C^{31}/C^{36}), 164.24 (C^{18}/C^{19}), 163.63 (C^{18}/C^{19}), 163.60 (C^{26}), 154.04 (C^{27}/C^{32}), 153.85 (C^{27}/C^{32}), 150.69 (C^{11}/C^{20}), 149.22 (C^{11}/C^{20}), 137.65 (C^{22}), 135.06 (C^{12}/C^{16}), 134.67 (C^{17}), 134.43 (C^{12}/C^{16}), 133.67 (C^{14}), 133.13 (C^{25}), 131.67 (C^{13}/C^{15}), 131.41 (C^{2}), 131.35 (C^{29}/C^{34}), 131.23 (C^{7}), 131.12 (C^{29}/C^{34}), 130.73 (C^{13}/C^{15}), 130.13 (C^{1}), 129.48 (C^{3}), 128.55 (C^{30}/C^{35}), 128.35 (C^{24}), 128.28 (C^{30}/C^{35}), 127.27 (C^{5}, C^{23}), 125.25 (C^{4}), 123.54 (C^{6}), 123.31 (C^{8}), 121.52 (C^{28}/C^{33}), 121.33 (C^{28}/C^{33}), 80.85 (C^{10}/C^{21}), 79.38 (C^{10}/C^{21}), 71.91, 70.73, 70.61, 68.91, 65.52, 61.23 (OCH$_2$CH$_3$), 61.21 (OCH$_2$CH$_3$), 59.07, 48.46 (C^{9}), 14.49 (OCH$_2$CH$_3$), 14.40 (OCH$_2$CH$_3$); ESI-MS m/z calcd for $C_{104}H_{81}O_{21}N_{12}I_4$ $[M+H]^+$ 2341.18125 found: 2341.18037.

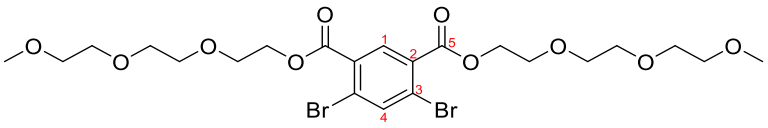

3.26

General procedure for esterification was used starting with **3.7** (648 mg, 2 mmol) and triethylene glycol monomethyl ether (722 mg, 4.4 mmol). The product was purified by column chromatography (6-11% acetone/DCM) to provide **3.26** (995 mg, 1.61 mmol, 81%) as a colorless oil.

δ_H (400 MHz, $CDCl_3$) 8.26 (s, 1H, H^1), 8.00 (s, 1H, H^4), 4.52 – 4.46 (m, 4H, TEG-CH_2), 3.85 – 3.80 (m, 4H, TEG-CH_2), 3.71 – 3.60 (m, 12H, TEG-CH_2), 3.55 – 3.49 (m, 4H, TEG-CH_2), 3.35 (s, 6H, TEG-CH_3); δ_C (101 MHz, $CDCl_3$) 164.67 (C^5), 139.75 (C^4), 134.12 (C^1), 131.14 (C^2), 125.84 (C^3), 72.03, 70.76, 70.71, 68.95, 65.16, 59.15; ESI-MS m/z calcd for $C_{22}H_{33}O_{10}Br_2$ $[M+H]^+$ 615.04350, found: 615.04374.

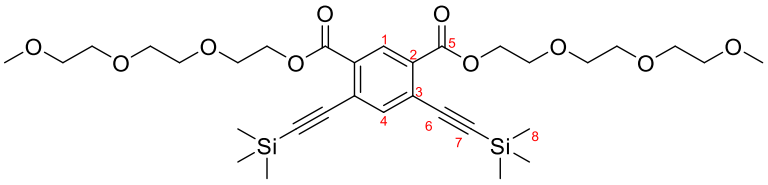

3.27

General procedure for Sonogashira coupling was used starting with **3.26** (660 mg, 1.07 mmol). The product was purified by silica chromatography (2% MeOH/DCM) to provide **3.27** (660 mg, 1.01 mmol, 94%) as a brownish oil.

δ_H (400 MHz, $CDCl_3$) 8.43 (s, 1H, H^1), 7.76 (s, 1H, H^4), 4.52 – 4.44 (m, 4H, TEG-CH_2), 3.87 – 3.78 (m, 4H, TEG-CH_2), 3.73 – 3.59 (m, 12H, TEG-CH_2), 3.55 – 3.48 (m, 4H, TEG-CH_2), 3.35 (s, 6H, TEG-CH_3), 0.27 (s, 18H, H^8); δ_C (101 MHz, $CDCl_3$) 164.87 (C^5), 140.77 (C^4), 132.54 (C^1), 131.31 (C^2), 126.71 (C^3), 104.04, 101.77, 72.04, 70.83, 70.73, 69.04, 64.62, 59.15, -0.12 (C^8); ESI-MS m/z calcd for $C_{32}H_{51}O_{10}Si_2$ $[M+H]^+$ 651.30153, found: 651.30151.

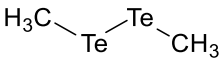

Me_2Te_2

According to a literature procedure,[276] Te powder (3.828 g, 30 mmol) was added to dry THF (30 ml). The suspension was cooled to 0 °C under Ar atmosphere and 1.6 M MeLi (22.5 ml, 36 mmol) was added over 10 min. The reaction was then stirred at 0 °C for 30 min and at then at rt for 4 h with brief sonication. Excess MeLi was then quenched by slow addition of MeOH. To the resulting mixture was added sat. aq. NH_4Cl, resulting in formation of brown Me_2Te_2 (MeTeH is thermodynamically unstable at rt). The mixture was stirred in air for 15 min, diluted with water and extracted with Et_2O. Combined extracts were dried with anhydrous Na_2SO_4, decanted and concentrated under vacuum. The residue was distilled (100 °C, 13 mbar) to provide Me_2Te_2 (2.9 g, 10.2 mmol, 68%) as a dark brown liquid with extremely foul odour.

δ_H (500 MHz, $CDCl_3$) 2.66 (s, 6H); δ_C (126 MHz, $CDCl_3$) -20.27; δ_{125Te} (158 MHz, $CDCl_3$) 49.10.

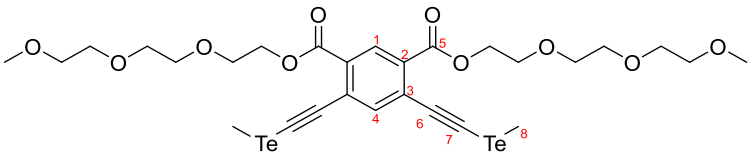

3.28

Compound **3.27** (328 mg, 0.504 mmol) was dissolved in MeOH (3 ml). Separately, AgF (131 mg, 1.033 mmol) was dissolved in MeOH (7 ml). AgF solution was then added to the solution of **3.27**, the mixture was stirred for 10 min, evaporated and dried under vacuum. The resulting silver alkynide was then suspended in dry THF (10 ml). Separately, Me_2Te_2 (144 mg, 0.504 mmol) was added to dry THF (3 ml). The solution was cooled to 0 °C and 1M Br_2 in dry DCM (0.504 ml, 0.504 mmol) was added, immediately forming a dark solution of MeTeBr. This solution was warmed to rt and added to the silver alkynide suspension. The reaction was briefly sonicated and stirred for 30 min at rt. The mixture was then filtered through Celite and concentrated under vacuum. The product was purified by silica chromatography (2% MeOH/DCM) to provide **3.28** (370 mg, 0.468 mmol, 93%) as a yellow oil.

δ_H (400 MHz, $CDCl_3$) 8.48 (d, J = 0.5 Hz, 1H, H^1), 7.56 (d, J = 0.5 Hz, 1H, H^4), 4.48 – 4.39 (m, 4H, TEG-CH_2), 3.82 – 3.76 (m, 4H, TEG-CH_2), 3.69 – 3.65 (m, 4H, TEG-CH_2), 3.64 – 3.58 (m, 8H, TEG-CH_2), 3.51 – 3.46 (m, 4H, TEG-CH_2), 3.32 (s, 6H, TEG-CH_2), 2.22 (s, 6H, H^8); δ_C (101 MHz, $CDCl_3$) 164.56 (C^5), 139.18 (C^4), 132.81 (C^1), 129.06 (C^2), 127.04 (C^3), 109.07 (C^6), 71.92, 70.70, 70.63, 70.58, 68.99, 64.45, 59.02, 58.10 (C^7), -13.92 (C^8); δ_{125Te} (158 MHz, $CDCl_3$) 178.30; ESI-MS m/z calcd for $C_{28}H_{38}O_{10}Te_2Na$ $[M+Na]^+$ 817.04929 (with $^{130}Te_2$), found: 817.04986.

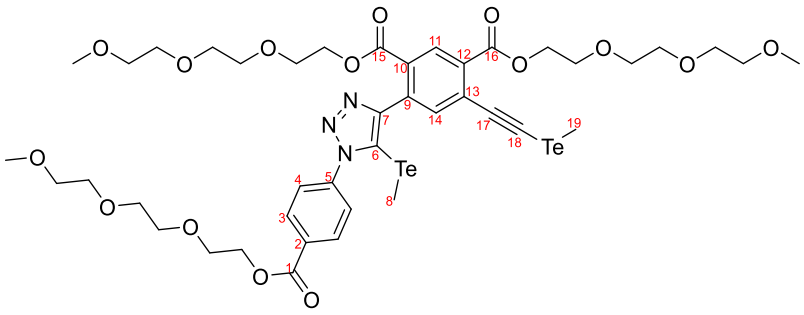

3.29

Compound **2.10** (114 mg, 0.369 mmol) and **3.28** (350 mg, 0.443 mmol) were added to dry THF (4 ml). PMDTA (77 µl, 0.369 mmol) and CuI (70 mg, 0.369 mmol) were then added. The reaction was stirred for 30 min at rt under Ar and in darkness. The mixture was then partitioned in DCM and aqueous Na_2EDTA. Aqueous layer was extracted with DCM, the organic fractions combined, dried with anhydrous Na_2SO_4, decanted and evaporated. The residue was separated by silica chromatography (2.5% MeOH/DCM) to provide **3.29** (220 mg, 0.200 mmol, 54%) as a yellow oil.

δ_H (500 MHz, $CDCl_3$) 8.57 (s, 1H, H^{11}), 8.25 – 8.20 (m, 2H, H^3), 7.75 – 7.71 (m, 2H, H^4), 7.70 (s, 1H, H^{12}), 4.52 – 4.45 (m, 4H, TEG-CH_2), 4.30 – 4.26 (m, 2H, TEG-CH_2), 3.85 – 3.80 (m, 4H, TEG-CH_2), 3.71 – 3.67 (m, 4H, TEG-CH_2), 3.67 – 3.59 (m, 10H, TEG-CH_2), 3.57 – 3.52 (m, 6H, TEG-CH_2), 3.52 – 3.47 (m, 4H, TEG-CH_2), 3.47 – 3.43 (m, 2H, TEG-CH_2), 3.33 (s, 3H, TEG-CH_3), 3.32 (s, 3H, TEG-CH_3), 3.29 (s, 3, TEG-CH_3), 2.22 (s, 3H, H^{19}), 1.61 (s, 3H, H^8); δ_C (126 MHz, $CDCl_3$) 165.77 (C^{15}/C^{17}), 165.37 (C^1), 164.76 (C^{15}/C^{17}), 153.63 (C^7), 141.15 (C^5), 137.46 (C^{14}), 135.39 (C^9), 132.87 (C^{11}), 131.21 (C^2), 130.87 (C^{10}/C^{12}), 130.77 (C^3), 129.48 (C^{10}/C^{12}), 127.11 (C^{13}), 125.71 (C^4), 109.40 (C^{17}), 102.59 (C^6), 71.92, 71.86, 70.71, 70.68, 70.65, 70.61, 70.59, 70.57, 70.50, 70.46, 69.12, 69.02, 68.82, 64.62, 64.57, 64.53, 59.06, 59.03, 58.99, 58.34 (C^{18}), -13.76 (C^8/C^{19}), -13.88 (C^8/C^{19}); δ_{125Te} (158 MHz, $CDCl_3$) 178.29 (alkynyl-Te), 164.13 (triazolyl-Te); ESI-MS m/z calcd for $C_{42}H_{58}N_3O_{15}Te_2$ $[M+H]^+$ 1104.19924 (with $^{130}Te_2$), found: 1104.19897.

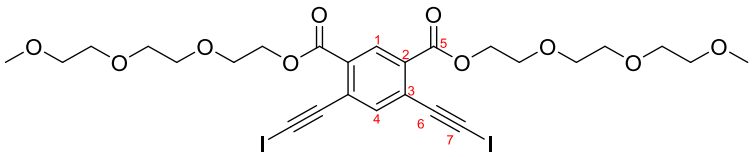

3.28$_I$

General procedure for iododesilylation was used starting with **3.27** (956 mg, 1.46 mmol). Final reaction mixture was partitioned in water and DCM and further extracted with DCM. Combined organic fractions were dried with anhydrous Na_2SO_4, decanted and evaporated. The product was purified by silica chromatography (2% MeOH/DCM) to provide **11$_I$** (1.004 g, 1.324 mmol, 91%) as a yellow oil.

δ_H (400 MHz, $CDCl_3$) 8.52 (s, 1H, H^1), 7.73 (s, 1H, H^4), 4.53 – 4.43 (m, 4H, TEG-CH_2), 3.88 – 3.79 (m, 4H, TEG-CH_2), 3.74 – 3.69 (m, 4H, TEG-CH_2), 3.69 – 3.60 (m, 8H, TEG-CH_2), 3.56 – 3.49 (m, 4H, TEG-CH_2), 3.35 (s, 6H, TEG-CH_3); δ_C (101 MHz, $CDCl_3$) 164.58 (C^5), 141.96 (C^4), 133.00 (C^1), 131.76, (C^2) 127.04 (C^3), 91.35 (C^6), 72.02, 70.82, 70.72, 70.68, 69.03, 64.89, 59.13, 17.89 (C^7); ESI-MS m/z calcd for $C_{26}H_{33}O_{10}I_2$ $[M+H]^+$ 759.01576, found: 759.01587.

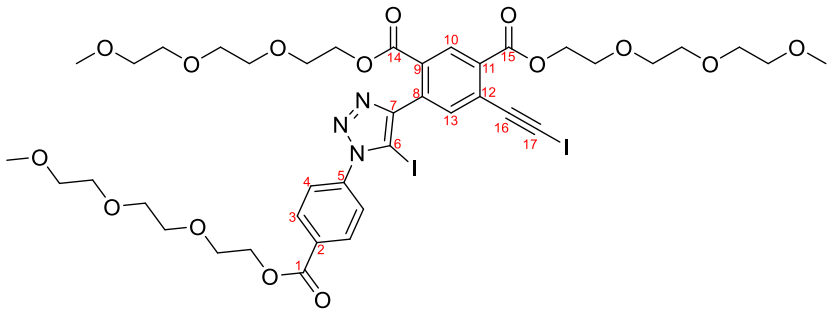

3.29$_I$

General procedure for azide-iodoalkyne cycloaddition was used to couple compound **2.10** (66 mg, 0.213 mmol) and **3.28$_I$** (210 mg, 0.277 mmol) using 0.1 eq of Cu[MeCN]$_4$PF$_6$ and TBTA. The product was purified by silica chromatography (2-2.5% MeOH/DCM) to provide **3.29$_I$** (128 mg, 0.120 mmol, 56%) as a colorless oil.

δ_H (400 MHz, $CDCl_3$) 8.58 (s, 1H, H^{10}), 8.28 – 8.22 (m, 2H, H^3), 7.75 (s, 1H, H^{13}), 7.74 – 7.68 (m, 2H, H^4), 4.54 – 4.46 (m, 4H, TEG-CH_2), 4.35 – 4.29 (m, 2H, TEG-CH_2), 3.88 – 3.81 (m, 4H, TEG-CH_2), 3.74 – 3.68 (m, 4H, TEG-CH_2), 3.68 – 3.59 (m, 10H, TEG-CH_2), 3.56 – 3.48 (m, 10H, TEG-CH_2), 3.47 – 3.42 (m, 2H, TEG-CH_2), 3.33 (s, 3H, TEG-CH_3), 3.32 (s, 3H, TEG-CH_3), 3.28 (s, 3H, TEG-CH_3); δ_C (101 MHz, $CDCl_3$) 165.48 (C^{14}/C^{15}), 165.28 (C^1), 164.67 (C^{14}/C^{15}), 150.58 (C^7), 140.21 (C^5), 138.52 (C^{13}), 133.81 (C^8), 132.99 (C^{10}/C^{14}/C^{15}), 132.86 (C^{10}/C^{14}/C^{15}), 131.68 (C^2), 130.91 (C^3), 130.55 (C^9/C^{11}), 127.09 (C^{12}), 126.02 (C^4), 91.63 (C^{16}), 80.63 (C^6), 71.94, 71.85, 70.75, 70.71, 70.67, 70.64, 70.62, 70.60, 70.49, 70.45, 69.12, 68.97, 68.73, 64.84, 64.69, 59.07, 59.05, 58.98, 18.10 (C^{17}); ESI-MS m/z calcd for $C_{40}H_{52}O_{15}N_3I_2$ $[M+H]^+$ 1068.14823, found: 1068.14795.

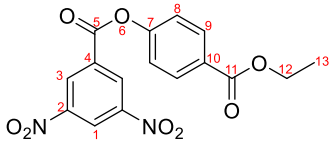

3.30

General procedure for esterification was used starting with 3,5-dinitrobenzoic acid (1060 mg, 5 mmol) and ethylparaben (914 mg, 5.5 mmol). The product was purified by column chromatography (DCM) to provide **3.30** (1.761 mg, 4.89 mmol, 98%) as an off-white solid.

δ_H (400 MHz, $CDCl_3$) 9.36 – 9.28 (m, 3H, H^1, H^3), 8.22 – 8.12 (m, 2H, H^9), 7.42 – 7.31 (m, 2H, H^8), 4.40 (q, J = 7.1 Hz, 2H, H^{12}), 1.41 (t, J = 7.1 Hz, 3H, H^{13}); δ_C (101 MHz, $CDCl_3$) 165.60 (C^{11}), 160.86 (C^5), 153.51 (C^7), 148.94 (C^2/C^4), 132.98 (C^2/C^4), 131.58 (C^9), 130.05 (C^3), 129.26 (C^{10}), 123.27 (C^1), 121.37 (C^8), 61.46 (C^{12}), 14.45 (C^{13}); ESI-MS m/z calcd for $C_{16}H_{13}O_8N_2$ $[M+H]^+$: 361.06664, found: 361.06653.

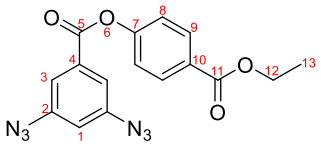

3.31

Compound **3.30** (1.735 g, 4.816 mmol) and 10% Pd/C (170 mg) were added to EtOAc (50 ml). The mixture was stirred in H_2 atmosphere until completion. It was then filtered on Celite and concentrated under vacuum. The residue was dissolved in water (50 ml) with conc. HCl (4 ml) and the solution cooled to 0 °C. $NaNO_2$ (731 mg, 10.59 mmol) in small amount of water was then added slowly, followed after 15 min by NaN_3 (751 mg, 11.56 mmol) in small amount of water. The reaction was stirred at 15 min at 0 °C and for 1 h at rt. It was then extracted with EtOAc, the organic phase was washed with brine, dried with anhydrous Na_2SO_4, decanted and concentrated under vacuum. The residue was separated by silica chromatography (15% Et_2O/hexanes) and the isolated product was recrystallised ($CHCl_3$/hexane) to provide **3.31** (426 mg, 1.209 mmol, 25%) as a white solid.

δ_H (400 MHz, $CDCl_3$) 8.14 (d, J = 8.7 Hz, 2H, H^9), 7.62 (t, J = 1.6 Hz, 2H, H^3), 7.29 (d, J = 8.9 Hz, 2H, H^8), 6.88 (t, J = 2.0 Hz, 1H, H^1), 4.40 (q, J = 7.1 Hz, 2H, H^{13}), 1.41 (t, J = 7.1 Hz, 3H, H^{13}); δ_C (101 MHz, $CDCl_3$) 165.84 (C^{11}), 163.13 (C^5), 154.14 (C^7), 142.74 (C^2), 132.35 (C^4), 131.40 (C^9), 128.65 (C^{10}), 121.65 (C^8), 116.91 (C^3), 114.70 (C^1), 61.32 (C^{12}), 14.47 (C^{13}), ESI-MS m/z 375.0 $[M+Na]^+$.

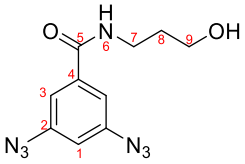

3.32

General procedure for amidation of reactive esters was used starting with **3.31** (70 mg, 0.200 mmol) and 3-aminopropan-1-ol (30 µl, 0.400 mmol). The product was purified by silica chromatography to provide **3.32** (50 mg, 0.191 mmol, 96%) as a white solid.

δ_H (400 MHz, $CDCl_3$/MeOD) 7.22 – 7.14 (m, 2H, H^3), 6.70 – 6.62 (m, 1H, H^1), 3.66 – 3.57 (m, 2H, H^9), 3.51 – 3.41 (m, 2H, H^7), 1.83 – 1.65 (m, 2H, H^8); δ_C (101 MHz, $CDCl_3$/MeOD) 166.59 (C^5), 142.26 (C^2), 137.44 (C^4), 114.11 (C^3), 112.23 (C^1), 59.78 (C^9), 37.43 (C^7), 31.48 (C^8); ESI-MS m/z calcd for $C_{10}H_{11}O_2N_7Na$ $[M+Na]^+$ 284.08664, found: 284.08673.

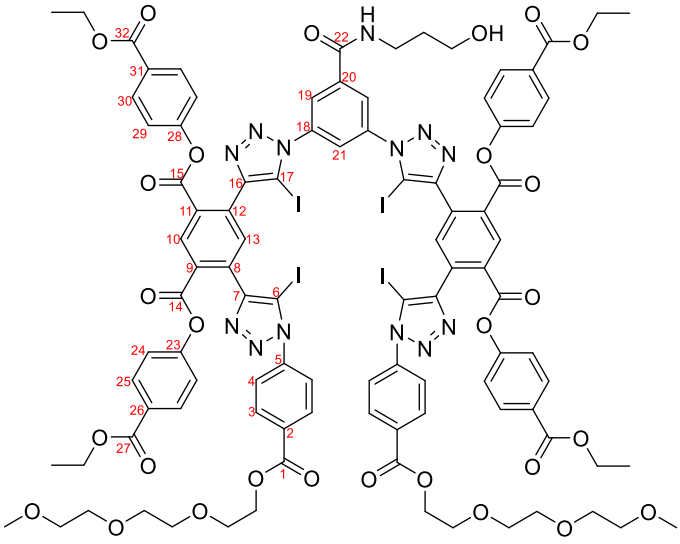

3.33

General procedure for azide-iodoalkyne cycloaddition was used to couple compound **3.24a** (84 mg, 0.102 mmol) and **3.32** (17.5 mg, 0.0500 mmol). The product was purified by silica chromatography (20-25% acetone/DCM) to provide **3.33** (68 mg, 0.0342 mmol, 68%) as a white solid.

δ_H (500 MHz, $CDCl_3$) 8.94 – 8.78 (m, 2H, H^{10}), 8.73 (s, 2H), 8.61 (s, 2H), 8.43 (s, 4H), 8.07 (t, J = 8.0 Hz, 8H, H^3, H^{25}/H^{30}), 7.99 (d, J = 7.9 Hz, 4H, H^{25}/H^{30}), 7.81 (d, J = 8.2 Hz, 4H, H^4), 7.37 – 7.27 (m, 8H, H^{24}, H^{29}), 4.50 (d, J = 39.8 Hz, 6H, TEG-CH_2), 4.37 (q, J = 7.1 Hz, 4H, OCH_2CH$_3$), 4.30 (q, J = 7.1 Hz, 4H, OCH_2CH$_3$), 3.91 – 3.75 (m, 6H, TEG-CH_2), 3.65 (ddt, J = 36.5, 19.9, 4.5 Hz, 18H, TEG-CH_2), 3.56 – 3.43 (m, 6H, TEG-CH_2), 3.34 (s, 6H, TEG-CH_3), 3.27 (s, 3H, TEG-CH_3), 1.39 (t, J = 7.1 Hz, 6H, OCH$_2$CH_3), 1.33 (t, J = 7.1 Hz, 6H, OCH$_2$CH_3); δ_C (126 MHz, $CDCl_3$) 165.74 (C^{27}/C^{32}), 165.64 (C^{27}/C^{32}), 165.32, 164.99, 164.84 (C^{24}), 154.22 (C^{23}/C^{28}), 154.15 (C^{23}/C^{28}), 145.38 (C^7/C^{18}), 145.00 (C^7/C^{18}), 139.71, 137.79, 133.95, 133.70, 133.12, 131.85, 131.42, 131.26 (C^{25}/C^{30}), 131.20 (C^{25}/C^{30}), 130.31, 128.59, 128.53, 128.45, 122.05, 121.72 (C^{24}/C^{29}), 121.64 (C^{24}/C^{29}), 120.59, 119.83 (C^4), 71.99, 71.92, 70.74, 70.67, 70.63, 70.53, 69.23, 65.22, 64.57, 61.21 (OCH$_2$CH$_3$), 61.17 (OCH$_2$CH$_3$), 59.13, 59.05, 14.41 (OCH$_2$CH$_3$), 14.36 (OCH$_2$CH$_3$); ESI-MS m/z calcd for $C_{102}H_{100}O_{31}N_{12}Na$ $[M+H]^+$ 2011.65096, found: 2011.65445.

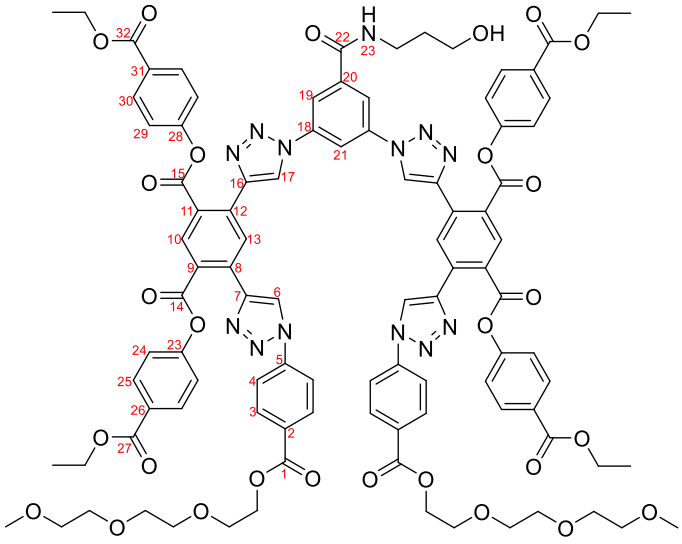

3.33$_H$

Compound **3.24a$_H$** (172 mg, 0.210 mmol) and **3.32** (26 mg, 0.100 mmol) were added to dry DCM. $Cu(MeCN)_4PF_6$ (7.5 mg, 0.02 mmol), TBTA (10.6 mg, 0.02 mmol) and DIPEA (7 µL, 0.04 mmol). The reaction was stirred under Ar atmosphere for 1 d. It was then diluted with DCM, washed with aqueous Na_2EDTA solution, dried with anhydrous Na_2SO_4, decanted and concentrated under vacuum. The product was purified by silica chromatography (3–4.5% MeOH/DCM) to provide **3.33$_H$** (168 mg, 0.0884 mmol, 88%) as an off-white solid.

δ_H (500 MHz, $CDCl_3$) 8.88 – 8.67 (m, 4H), 8.53 (s, 2H), 8.36 (s, 2H), 8.23 (s, 1H, H^{21}), 8.11 (s, 2H), 8.04 (d, J = 8.1 Hz, 8H, H^3, H^{25}/H^{30}), 7.94 (d, J = 8.1 Hz, 4H, H^{25}/H^{30}), 7.84 (s, 1H, H^{23}), 7.74 (d, J = 8.2 Hz, 4H, H^4), 7.29 (d, J = 8.2 Hz, 4H, H^{24}/H^{29}), 7.26 – 7.18 (m, 4H, H^{24}/H^{29}), 4.45 (t, J = 4.7 Hz, 4H, TEG-CH_2), 4.37 (q, J = 7.1 Hz, 4H, OCH_2CH$_3$), 4.28 (q, J = 7.1 Hz, 4H, OCH_2CH$_3$), 3.82 (t, J = 4.8 Hz, 4H, TEG-CH_2), 3.79 – 3.54 (m, 18H, TEG-CH_2), 3.51 (dd, J = 5.8, 3.6 Hz, 4H, TEG-CH_2), 3.32 (s, 6H, TEG-CH_3), 1.39 (t, J = 7.1 Hz, 6H, OCH$_2$CH_3), 1.31 (t, J = 7.1 Hz, 6H, OCH$_2$CH_3); δ_C (126 MHz, $CDCl_3$) 165.75 (C^{14}/C^{16}), 165.65 (C^{14}/C^{16}), 165.26, 164.89 164.86, 154.15 (C^{23}/C^{28}), 154.04 (C^{23}/C^{28}), 145.24 (C^7/C^{16}), 144.73 (C^7/C^{16}), 139.58 (C^5), 138.17, 137.45, 133.97, 133.51, 133.25, 131.44, 131.31, 131.23, 130.40, 128.64, 128.55, 128.26, 127.97, 122.46, 122.22, 121.72, 121.62, 119.76, 118.04, 72.01, 70.78, 70.75, 70.69, 69.20, 64.64, 61.29, 60.72, 59.13, 31.57, 14.45 (OCH$_2$CH$_3$), 14.39 (OCH$_2$CH$_3$). ESI-MS m/z calcd for $C_{98}H_{94}N_{13}NaO_{28}$ $[M+H+Na]^{2+}$ 961.81145, found: 961.81183.

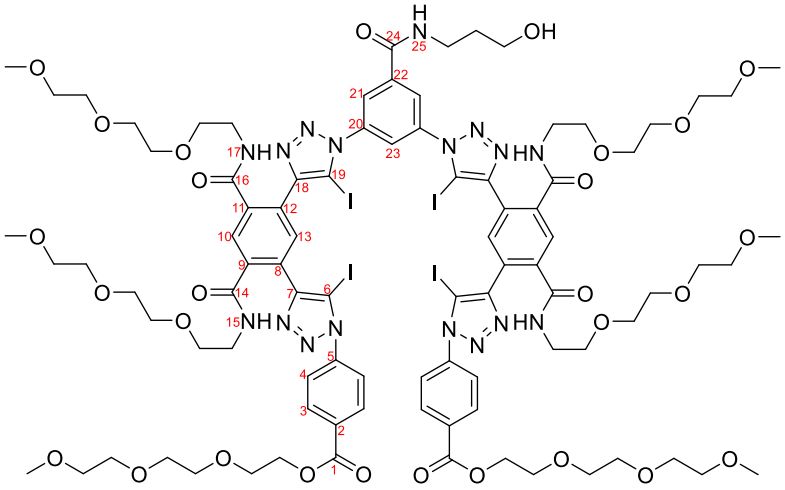

3.34

General procedure for amidation of active ester precursors was used to react **3.33** (68 mg, 0.0342 mmol) and **3.5** (56 mg, 0.342 mmol). The product was purified by silica chromatography (3-6% MeOH/DCM) to provide **3.34** (44 mg, 0.0222 mmol, 65%) as an off-white solid.

δ_H (500 MHz, $CDCl_3$) 8.29 (s, 3H, H^{21}, H^{25}), 8.22 (d, J = 8.2 Hz, 4H, H^3), 8.01 – 7.94 (m, 3H, H^{10}, H^{23}), 7.74 (s, 2H, H^{13}), 7.71 (d, J = 8.1 Hz, 4H, H^4), 7.41 (s, 2H, H^{15}/H^{17}), 7.28 (s, 2H, H^{15}/H^{17}), 4.52 – 4.48 (m, 4H, TEG-CH_2), 3.84 (t, J = 4.8 Hz, 4H, TEG-CH_2), 3.75 – 3.37 (m, 70H, TEG-CH_2), 3.34 (s, 6H, TEG-CH_3), 3.23 (s, 6H, TEG-CH_3), 3.18 (s, 6H, TEG-CH_3); δ_C (126 MHz, $CDCl_3$) 167.84 (C^{14}/C^{16}), 167.75 (C^{14}/C^{16}), 165.38 (C^1), 165.06 (C^{24}), 150.34 (C^7, C^{18}), 140.35 (C^5), 137.58 (C^8/C^{12}), 137.42 (C^{20}), 137.22 (C^8/C^{12}), 133.94 (C^{13}), 131.62 (C^2), 130.90 (C^3), 130.08 (C^9/C^{11}), 129.78 (C^9/C^{11}), 129.13 (C^{10}), 126.65 (C^{21}), 126.22 (C^4), 125.92 (C^{23}), 82.46 (C^6/C^{19}), 81.53 (C^6/C^{19}), 71.97, 71.86, 71.76, 70.74, 70.71, 70.66, 70.56, 70.42, 70.36, 70.15, 70.09, 69.46, 69.40, 69.16, 64.70, 60.11, 59.12, 58.96, 58.89, 39.99; ESI-MS m/z calcd for $C_{90}H_{119}O_{28}N_{17}I_4$ $[M+2H]^{2+}$ (first isotope peak) 1197.23260, found: 1197.23133.

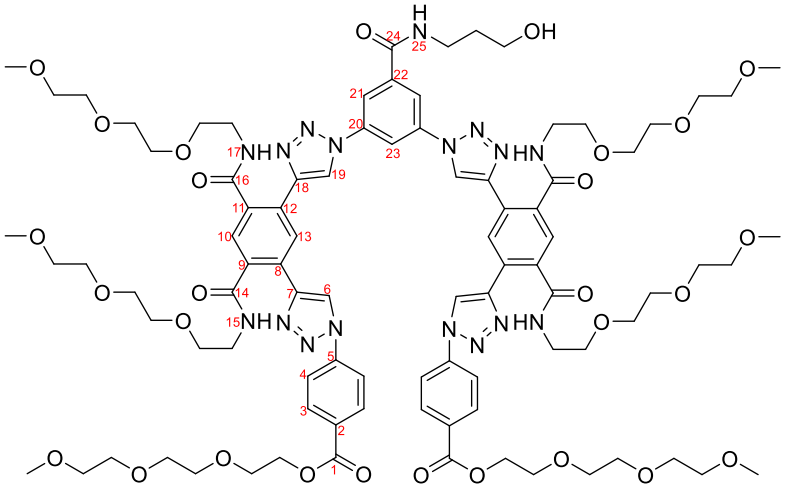

3.34$_H$

General procedure for amidation of active ester precursors was used to react **3.33$_H$** (161 mg, 0.0848 mmol) and **3.5** (111 mg, 0.678 mmol). The product was purified by silica chromatography (5-8% MeOH/DCM) followed by PTLC (7% MeOH/$CHCl_3$) to provide **3.34$_H$** (44 mg, 0.0238 mmol, 28%) as a white solid.

δ_H (500 MHz, $CDCl_3$) 8.81 – 8.38 (m, 4H), 8.38 – 7.63 (m, 17H), 7.62 – 7.30 (m, 3H), 4.49 (s, 4H), 4.01 – 2.90 (m, 87H), 2.72 (s, 3H), 1.35 – 1.11 (m, 2H); δ_C (126 MHz, $CDCl_3$) 169.47, 169.18, 165.46, 145.14, 139.90, 137.73, 137.30, 134.62, 134.25, 133.17, 131.38, 130.11, 128.49, 128.27, 121.21, 120.62, 119.71, 117.44, 72.02, 71.88, 71.72, 70.77, 70.69, 70.57, 70.45, 70.29, 70.07, 69.89, 69.32, 69.22, 64.59, 59.84, 59.14, 58.97, 58.78, 39.80, 37.65, 32.00, 29.78; ESI-MS m/z calcd for $C_{90}H_{123}N_{17}O_{28}$ $[M+2H]^{2+}$ 944.93562, found: 944.93554.

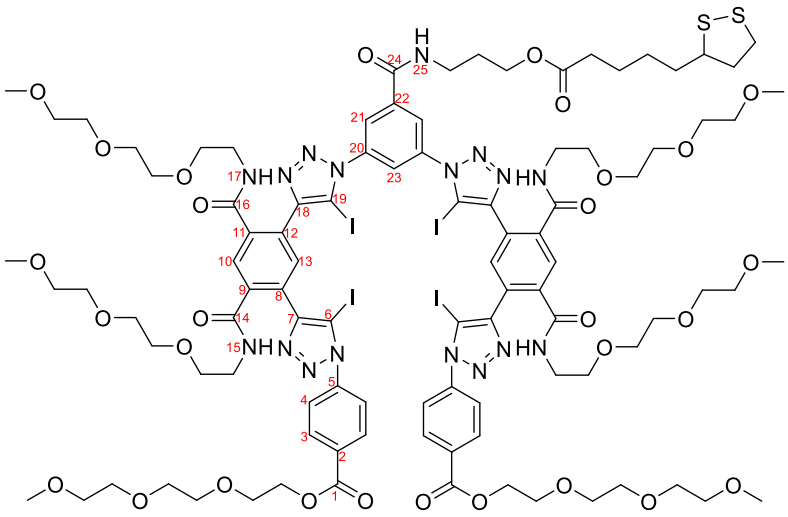

3.35

Compound **3.34** (30 mg, 0.0125 mmol), lipoic acid (7.8 mg, 0.0375 mmol), N,N'-dicyclohexylcarbodiimide (7.8 mg, 0.0375 mmol) and a catalytic amount of 4-dimethylaminopyridine were dissolved in 8 mL dry DCM. After stirring under N_2 in the dark for 18 h the product was isolated by preparative TLC (DCM/MeOH/acetone 8:1:1) as an off-white solid (14 mg, 43%).

δ_H (500 MHz, $CDCl_3$) 8.40 (d, *J* = 2.0 Hz, 2H), 8.26 (d, *J* = 8.3 Hz, 4H), 8.09 (m, 3H), 7.82 (s, 2H, H^{13}), 7.74 (d, *J* = 8.3 Hz, 4H, H^4), 7.16 (m, 2H), 7.10 (m, 2H), 4.53 (t, *J* = 4.8 Hz, 4H), 4.21 (t, *J* = 6.1 Hz, 2H), 3.87 (t, *J* = 4.8 Hz, 4H), 3.76 – 3.71 (m, 4H), 3.70 – 3.67 (m, 4H), 3.67 – 3.51 (m, 52H), 3.47 (m, 20H), 3.37 (s, 6H), 3.26 (s, 6H), 3.22 (s, 6H), 3.20 – 3.04 (m, 2H), 2.44 (m, 1H), 2.33 (t, *J* = 7.4 Hz, 2H), 1.99 (q, *J* = 6.5 Hz, 1H), 1.94 – 1.85 (m, 1H), 1.74 – 1.55 (m, 4H), 1.46 (m, 2H). δ_C (126 MHz, $CDCl_3$) 173.71, 167.52, 165.32, 164.51, 150.56, 150.37, 140.26, 137.66, 137.62, 137.27, 134.14, 131.65, 130.88, 130.10, 129.75, 129.23, 126.71, 126.13, 71.93, 71.82, 71.71, 70.70, 70.67, 70.62, 70.54, 70.50, 70.38, 70.36, 70.11, 70.01, 69.44, 69.13, 64.66, 61.89, 59.08, 58.92, 58.84, 56.43, 56.37, 50.86, 40.27, 40.24, 39.95, 39.82, 38.54, 37.32, 34.58, 34.05, 33.50, 28.77, 28.73, 28.62, 24.68, 24.54. ESI-MS m/z calcd for $C_{98}H_{131}O_{29}N_{17}I_4S_2$ $[M+2H]^{2+}$ 1290.74539, found: 1290.74512.

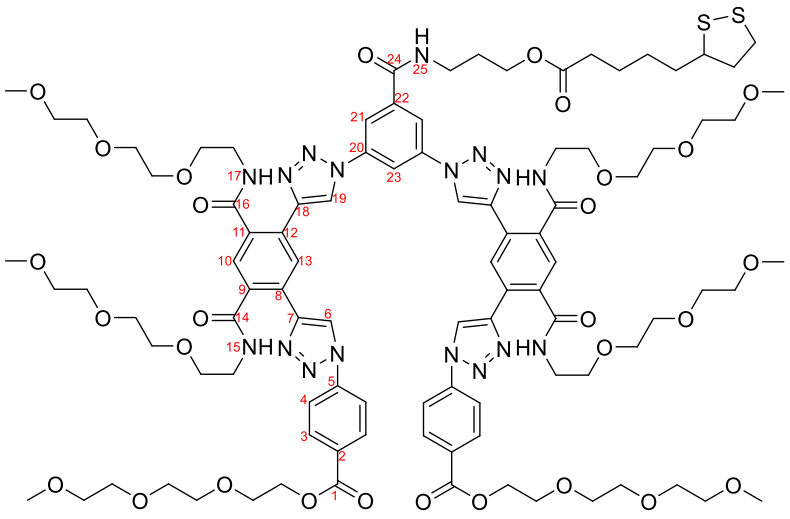

3.35$_H$

Compound **3.34$_H$** (20 mg, 0.0106 mmol), lipoic acid (6.6 mg, 0.0318 mmol), N,N'-dicyclohexylcarbodiimide (6.6 mg, 0.0318 mmol) and a catalytic amount of 4-dimethylaminopyridine were dissolved in 7 mL dry DCM. After stirring under N_2 in the dark for 18 h the product was isolated by preparative TLC (DCM/MeOH/acetone 11:1:1) as a white solid (16 mg, 73 %).

δ_H (500 MHz, $CDCl_3$) 8.67 (d, *J* = 15.8 Hz, 4H), 8.42 (s, 3H), 8.30 – 8.13 (m, 6H), 8.04 (s,1H), 7.94 (d, *J* = 8.2 Hz, 4H), 7.82 (s,1H), 7.57 (s,4H), 4.52 (t, *J* = 4.7 Hz, 4H), 4.27 (t, *J* = 6.4 Hz, 2H) 3.88 (t, *J* = 4.8 Hz, 4H), 3.82 (s, 4H), 3.77 – 3.49 (m, 60H), 3.48 – 3.40 (m, 10H), 3.38 (s, 6H), 3.32 (m, 4H), 3.23 (s, 6H), 3.18 – 3.04 (m, 10H), 2.49 – 2.3 (m, 4H), 2.09 (m, 2H), 1.88 (m, 10H), 1.67 (m, 4H), 1.48 (m, 2H). δ_C (101 MHz, $CDCl_3$) 173.64, 169.21, 168.99, 165.40, 145.15, 144.95, 139.91, 137.57, 134.70, 134.46, 131.39, 130.14, 128.68, 128.37, 121.26, 120.92, 119.82, 117.88, 71.94, 71.79, 71.63, 70.70, 70.68, 70.62, 70.53, 70.47, 70.34, 70.23, 70.03, 69.79, 69.30, 69.20, 69.15, 64.53, 62.21, 59.06, 58.86, 58.68, 56.36, 40.25, 40.22, 39.78, 39.69, 38.49, 37.48, 34.61, 34.07, 33.20, 28.79, 28.73, 28.71, 24.70, 24.51. ESI-MS m/z calcd for $C_{98}H_{131}O_{29}N_{17}I_4S_2$ $[M+2H]^{2+}$ 1038.95210, found: 1038.94983.

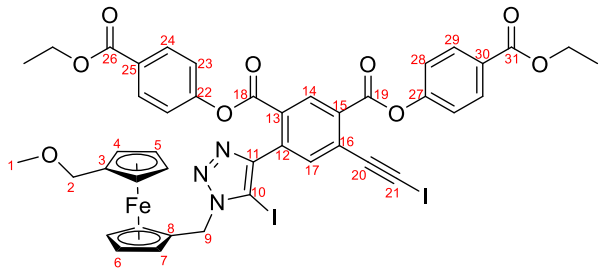

3.37

General procedure for azide-iodoalkyne cycloaddition was used to couple compound **3.36** (72 mg, 0.167 mmol) and **3.13** (255 mg, 0.334 mmol) using 0.1 eq of $Cu[MeCN]_4PF_6$ and TBTA. The product was purified by silica chromatography (0.5-0.7% MeOH/DCM). Compound **3.37** (51 mg, 0.0487 mmol, 29%) was inadvertently obtained in a nucleophilic substitution reaction of the CuAAC product with MeOH under the chromatographic conditions.

δ_H (500 MHz, $CDCl_3$) 8.85 (s, 1H, H^{14}), 8.15 (d, J = 8.8 Hz, 2H, H^{24}/H^{29}), 8.01 (d, J = 8.7 Hz, 2H, H^{24}/H^{29}), 7.84 (s, 1H, H^{17}), 7.37 (d, J = 8.8 Hz, 2H, H^{23}/H^{28}), 7.06 (d, J = 8.7 Hz, 2H, H^{23}/H^{28}), 5.40 (s, 2H, H^{9}), 4.42 – 4.34 (m, 4H, OCH_2CH_3), 4.34 (t, J = 1.9 Hz, 2H, H^{7}), 4.25 (t, J = 1.9 Hz, 2H, H^{4}), 4.20 (s, 2H, H^{2}), 4.19 – 4.17 (m, 2H, H^{5}), 4.13 (t, J = 1.9 Hz, 2H, H^{6}), 3.36 (s, 3H, H^{1}), 1.44 – 1.36 (m, 6H, OCH_2CH_3); δ_C (126 MHz, $CDCl_3$) 165.85 (C^{26}/C^{31}), 165.84 (C^{26}/C^{31}), 163.82 (C^{18}/C^{19}), 162.61 (C^{18}/C^{19}), 154.17 (C^{22}/C^{27}), 153.93 (C^{22}/C^{27}), 148.93 (C^{11}), 138.50 (C^{17}), 135.23 (C^{12}), 133.74 (C^{14}), 131.72 (C^{13}/C^{15}), 131.40 (C^{24}/C^{29}), 131.21 (C^{24}/C^{29}), 130.07 (C^{13}/C^{15}), 128.59 (C^{25}/C^{30}), 128.31 (C^{25}/C^{30}), 128.26 (C^{16}), 121.71 (C^{23}/C^{28}), 121.36 (C^{23}/C^{28}), 91.44 (C^{20}), 84.83 (C^{3}), 81.29 (C^{8}), 78.81 (C^{10}), 70.47 (C^{2}), 69.94 (C^{4}), 69.83 (C^{7}), 69.49 (C^{6}), 69.44 (C^{5}), 61.28 (OCH_2CH_3), 61.23 (OCH_2CH_3), 58.22 (C^{1}), 50.93 (C^{9}), 19.84 (C^{21}), 14.45 (OCH_2CH_3); ESI-MS m/z calcd for $C_{43}H_{35}FeI_2N_3O_9Na$ $[M+Na]^+$ 1069.97098 found: 1069.96853.

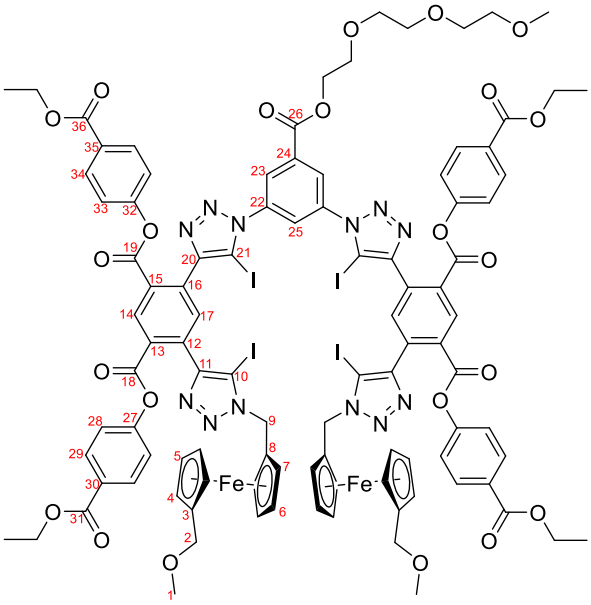

3.38

General procedure for azide-iodoalkyne cycloaddition was used to couple compound **3.37** (50 mg, 0.0419 mmol) and **2.15** (7.3 mg, 0.0209 mmol). The product was purified by silica chromatography (1-1.75% MeOH/DCM) to provide **3.38** (46 mg, 0.0168 mmol, 80%) as a yellow solid.

δ_H (500 MHz, $CDCl_3$) 8.91 (s, 2H, H^{14}), 8.51 (d, J = 2.0 Hz, 2H, H^{23}), 8.11 (t, J = 2.1 Hz, 1H, H^{25}), 8.11 – 8.07 (m, 4H, H^{29}/H^{34}), 8.06 – 8.01 (m, 4H, H^{29}/H^{34}), 7.94 (s, 2H, H^{17}), 7.31 – 7.27 (m, 4H, H^{28}/H^{33}), 7.15 – 7.10 (m, 4H, H^{28}/H^{33}), 5.42 (s, 4H, H^{9}), 4.59 – 4.52 (m, 2H, TEG-CH_2), 4.43 – 4.30 (m, 12H, H^{7}, OCH_2CH$_3$), 4.25 (t, J = 1.8 Hz, 4H, H^{4}), 4.21 – 4.16 (m, 8H, H^{2}, H^{5}), 4.15 – 4.10 (m, 4H, H^{6}), 3.88 – 3.80 (m, 2H, TEG-CH_2), 3.72 – 3.65 (m, 2H, TEG-CH_2), 3.65 – 3.60 (m, 2H, TEG-CH_2), 3.60 – 3.56 (m, 2H, TEG-CH_2), 3.51 – 3.45 (m, 2H, TEG-CH_2), 3.35 (s, 6H, H^{1}), 3.30 (s, 3H, TEG-CH_3), 1.44 – 1.32 (m, 12H, OCH$_2$CH_3); δ_C (126 MHz, $CDCl_3$) 165.87 (C^{31}/C^{36}), 165.77 (C^{31}/C^{36}), 164.20 (C^{18}/C^{19}), 163.64 (C^{18}/C^{19}, C^{26}), 154.09 (C^{27}/C^{32}), 154.01 (C^{27}/C^{32}), 150.74 (C^{11}/C^{20}), 149.10 (C^{11}/C^{20}), 137.71 (C^{22}), 135.19 (C^{12}/C^{16}), 134.73 (C^{17}), 134.53 (C^{12}/C^{16}), 133.67 (C^{14}), 133.18 (C^{24}), 131.61 (C^{13}/C^{15}), 131.40 (C^{29}/C^{34}), 131.26 (C^{29}/C^{34}), 130.75 (C^{13}/C^{15}), 128.62 (C^{30}/C^{35}), 128.38 (C^{23}, C^{30}/C^{35}), 127.34 (C^{25}), 121.55 (C^{28}/C^{33}), 121.42 (C^{28}/C^{33}), 84.83 (C^{3}), 81.41 (C^{8}), 80.73 (C^{21}), 78.95 (C^{10}), 71.97 (TEG-CH_2), 70.78 (TEG-CH_2), 70.77 (TEG-CH_2), 70.66 (TEG-CH_2), 70.47 (C^{2}), 69.97 (C^{4}), 69.85 (C^{7}), 69.49 (C^{6}), 69.47 (C^{5}), 68.96 (TEG-CH_2), 65.55 (TEG-CH_2), 61.25 (OCH_2CH$_3$), 59.10 (TEG-CH_3), 58.23 (C^{1}), 50.92 (C^{9}), 14.46 (OCH$_2$CH_3), 14.44 (OCH$_2$CH_3); ESI-MS m/z calcd for $C_{100}H_{88}Fe_2I_4N_{12}O_{23}Na$ $[M+Na]^+$ 2467.08605 found: 2467.08924.

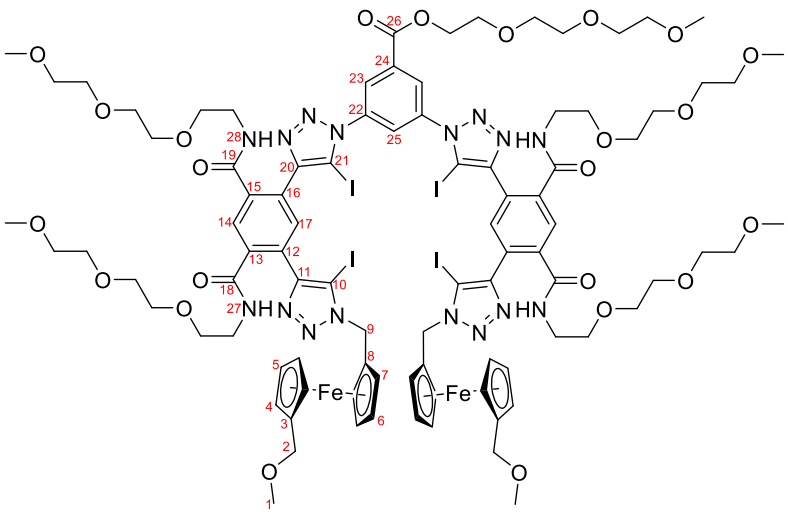

3.39

General procedure for amidation of active ester precursors was used to react **3.38** (46 mg, 0.0188 mmol) and **3.5** (25 mg, 0.151 mmol). The product was purified by silica chromatography (4-7% MeOH/DCM) to provide **3.39** (38 mg, 0.0156 mmol, 83%) as a yellow solid.

δ_H (500 MHz, $CDCl_3$) 8.53 (d, J = 2.0 Hz, 2H, H^{23}), 8.17 (t, J = 2.0 Hz, 1H, H^{25}), 8.04 (s, 2H, H^{14}), 7.68 (s, 2H, H^{17}), 7.08 (t, J = 5.5 Hz, 2H, H^{27}/H^{28}), 6.95 (t, J = 5.2 Hz, 2H, H^{27}/H^{28}), 5.37 (s, 4H, H^{9}), 4.60 – 4.50 (m, 2H, TEG-CH_2), 4.37 (t, J = 1.9 Hz, 4H, H^{7}), 4.25 (t, J = 1.9 Hz, 4H, H^{4}), 4.21 – 4.17 (m, 8H, H^{2}, H^{5}), 4.13 (t, J = 1.8 Hz, 4H, H^{6}), 3.88 – 3.82 (m, 2H, TEG-CH_2), 3.70 (dd, J = 5.8, 3.4 Hz, 2H, TEG-CH_2), 3.67 – 3.52 (m, 36H, TEG-CH_2), 3.52 – 3.41 (m, 20H, TEG-CH_2), 3.34 (s, 6H, H^{1}), 3.31 (s, 3H, TEG-CH_3), 3.28 (s, 6H, TEG-CH_3), 3.21 (s, 6H, TEG-CH_3); δ_C (126 MHz, $CDCl_3$) 167.60 (C^{18}/C^{19}), 167.55 (C^{18}/C^{19}), 163.84 (C^{26}), 150.86 (C^{11}/C^{20}), 149.31 (C^{11}/C^{20}), 137.88 (C^{22}), 137.61 (C^{12}/C^{16}), 137.46 (C^{12}/C^{16}), 134.05 (C^{17}), 133.00 (C^{24}), 130.31 (C^{13}/C^{15}), 129.85 (C^{13}/C^{15}), 129.20 (C^{14}), 128.56 (C^{23}), 127.90 (C^{25}), 84.71 (C^{3}), 81.66 (C^{8}), 81.52 (C^{21}), 79.75 (C^{10}), 71.98, 71.95, 71.90, 70.78, 70.75, 70.67, 70.58, 70.51, 70.50, 70.44, 70.31, 70.17, 69.99, 69.93, 69.57, 69.48, 69.43, 69.38, 68.97, 65.38, 59.12, 59.05, 58.99, 58.19 (C^{1}), 50.76 (C^{9}), 40.06, 39.98; ESI-MS m/z calcd for $C_{92}H_{115}Fe_2I_4N_{16}O_{23}$ $[M-H]^-$ 2431.31986 found: 2431.31664.

6.4 Compound data for Chapter 4

6.4.1 First generation compounds

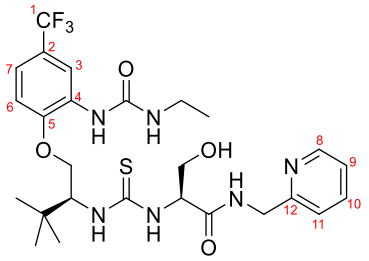

4.1

General procedure for thiourea formation

4.15 (174 mg, 0.5 mmol) was dissolved in 1:1 DCM : sat. $NaHCO_{3(aq)}$ (10 ml). The mixture was cooled to 0 °C and thiophosgene (42.2 µl, 0.55 mmol) was added to the DCM layer without stirring. The mixture was stirred for 30 min at 0 °C and allowed to warm to rt. Organic phase was separated and the aqueous phase was extracted with DCM. The combined organic fractions were dried with anhydrous Na_2SO_4, filtered and evaporated to give the isothiocyanate **4.16** as a yellowish solid. Compound **4.9** was Boc-deprotected by treating with 4M HCl in dioxane followed by evaporation of solvent and vacuum drying. The resulting dihydrochloride salt (134 mg, 0.5 mmol) was dissolved in DCM (3 ml) with triethylamine (209 µl, 1.5 mmol). This solution was combined with **4.16** and stirred at rt for 16 h. Reaction mixture was diluted with DCM, washed with pH 7 buffer and brine, dried with anhydrous Na_2SO_4, filtered and evaporated. The product was purified by silica chromatography (3-5% MeOH/DCM) to afford **4.1** (252 mg, 0.431 mmol, 86%) as a white solid.

Mp 118 °C; δ_H (500 MHz, $CDCl_3$): 8.36 (d, *J* = 2.2 Hz, 1H, H^3), 8.29 (s, 1H, H^8), 7.91 (s, 1H, N*H*CS) 7.79 (s, 1H, ArN*H*CO), 7.69 (s, 1H, N*H*CS) 7.63 (s, 1H, SerCON*H*), 7.52 (d, *J* = 8.5 Hz, 1H, H^{10}), 7.08 (m, 1H, H^{11}) 7.07 – 6.98 (m, 2H, H^7 & H^9), 6.64 (d, *J* = 8.4 Hz, 1H, H^6), 6.00 (s, 1H, CON*H*Et), 5.19 (s, 1H, SerC*H*), 4.95 (d, *J* = 10.3 Hz, 1H, C*H*NHCS), 4.41 (m, 2H, CH_2Pyr), 4.26 (dd, *J* = 8.9, 3.0 Hz, 1H, CH_2OAr), 4.01 (d, *J* = 11.0 Hz, 1H, SerCH_2), 3.82 (t, *J* = 9.4 Hz, 1H, CH_2OAr), 3.64 (s, 1H, SerCH_2), 3.29 – 3.08 (m, 2H, CH_2CH_3), 1.08 (t, *J* = 7.2 Hz, 3H, CH_2CH_3), 1.03 (s, 9H, $C(CH_3)_3$); δ_C (126 MHz, $CDCl_3$): 184.14 (*C*S), 171.84 (Ser*C*ONH), 155.63 (NH*C*ONH), 155.45 (C^{12}), 148.70 (C^5) 148.38 (C^8), 137.66 (C^{10}), 129.93 (C^4), 124.49 (q, $J_{C\text{-}F}$ 272.2 Hz, C^1), 123.2 (q, $J_{C\text{-}F}$ 34.0 Hz, C^2), 122.89 (C^{11}), 122.18 (C^9), 118.18 (C^7), 114.58 (C^3), 109.31 (C^6), 68.77 (CH_2OAr), 62.74 (SerCH_2), 62.39 (*C*HNHCS) 59.51 (SerC*H*), 44.18 (CH_2Pyr), 34.90 (CH_2CH_3), 33.64 ($C(CH_3)_3$), 27.04 ($C(CH_3)_3$), 15.41 (CH_2CH_3); δ_F (377 MHz, $CDCl_3$) -61.47. υ_{max} (neat) cm^{-1}: 3309 (w), 2966 (w), 1666 (m), 1548 (s), 1115 (s); ESI-MS m/z 585.3 $[M+H]^+$; high resolution ESI-MS calcd for $C_{26}H_{35}F_3N_6O_4S$ $[M+Na]^+$: 607.22903 Found: 607.26915.

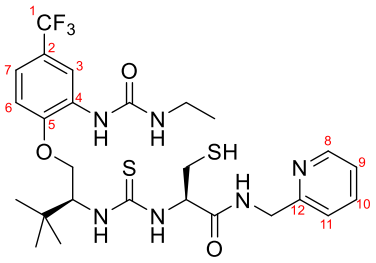

4.2

General procedure for thiourea formation was used to couple **4.15** (174 mg, 0.5 mmol) and Boc-deprotected **4.17** (283 mg, 0.5 mmol). The crude product was dissolved in THF containing a few drops of water. Tributylphosphine (408 µl, 1.65 mmol) was added to reduce disulphides and the reaction was stirred at rt for 2 h. The mixture was then concentrated under reduced pressure, redissolved in DCM, washed with pH 7 buffer and brine, dried with anhydrous Na_2SO_4, filtered and evaporated. The crude product was purified by column chromatography (3-5% MeOH/DCM, R_f 0.38 with 5% MeOH/DCM) to afford **4.2** contaminated with tributylphosphine oxide. The product was further purified by washing with 3x15 ml of hexane to afford **4.2** (145 mg, 0.24 mmol, 48%) as an oily semisolid.

δ_H (500 MHz, $CDCl_3$): 8.57 – 8.48 (m, 1H, H^3), 8.41 (d, *J* = 5.0 Hz, 1H, H^8), 8.24 (d, *J* = 9.9 Hz, 2H, N*H*CSN*H*), 7.92 (s, 1H, ArN*H*CO), 7.67 (d, *J* = 5.5 Hz, 1H, CysCON*H*), 7.59 (td, *J* = 7.7, 1.8 Hz, 1H, H^{10}), 7.18 (d, *J* = 7.9 Hz, 1H, H^{11}), 7.13 (dd, *J* = 7.4, 5.0 Hz, 1H, H^9), 7.05 (dd, *J* = 8.5, 2.2 Hz, 1H, H^7), 6.68 (d, *J* = 8.4 Hz, 1H, H^6), 6.01 (t, *J* = 5.4 Hz, 1H, CON*H*Et), 5.40 (s, 1H, CysC*H*), 4.99 (td, *J* = 11.0, 6.1 Hz, 1H, C*H*NHCS), 4.52 (qd, *J* = 16.4, 5.3 Hz, 2H, C*H*$_2$Pyr), 4.30 (dd, *J* = 8.9, 2.7 Hz, 1H, C*H*$_2$OAr), 3.77 (t, *J* = 9.6 Hz, 1H, C*H*$_2$OAr), 3.28 – 3.16 (m, 2H, C*H*$_2$CH$_3$), 3.06 – 2.94 (m, 1H, CysC*H*$_2$), 2.92 – 2.62 (m, 2H, CysC*H*$_2$), 1.11 (t, *J* = 7.2 Hz, 3H, CH$_2$C*H*$_3$), 1.03 (s, 9H, C(C*H*$_3$)$_3$); δ_C (126 MHz, $CDCl_3$): 184.45 (*C*S), 170.40 (Cys*C*ONH), 156.04 (Cys*C*ONH), 155.66 (NH*C*ONH), 148.93 (C^8), 148.81(C^5), 136.92 (C^{10}), 130.30 (C^4), 124.50 (q, $J_{C\text{-}F}$ 272 Hz, C^1), 123.43 (q, $J_{C\text{-}F}$ 31.5 Hz, C^2) 122.49 (C^9), 121.66 (C^{11}), 117.93 (C^7), 114.61 (C^3), 109.19 (C^6), 68.99 (C*H*$_2$OAr), 62.57 (*C*HNHCS), 59.81 (CysC*H*), 44.64 (C*H*$_2$Pyr), 34.94 (*C*H$_2$CH$_3$), 33.62 (*C*(CH$_3$)$_3$), 26.98 (C(*C*H$_3$)$_3$), 26.68 (Cys*C*H$_2$) 15.45 (CH$_2$*C*H$_3$); δ_F (471 MHz, $CDCl_3$) -61.58. υ_{max} (neat) cm^{-1}: 3292 (w), 2961 (w), 1672 (m), 1544 (s), 1114 (s) ; ESI-MS m/z 601.2 $[M+H]^+$; high resolution ESI-MS calcd for $C_{26}H_{35}F_3N_6O_3S_2$ $[M-H]^-$: 599.20914 Found: 599.20915.

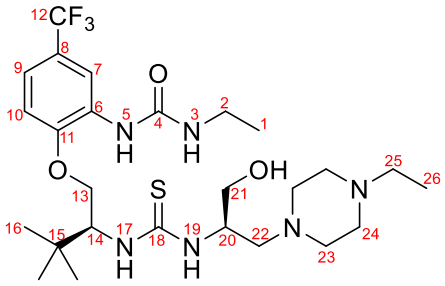

4.3

General procedure for thiourea formation was used to couple **4.15** (174 mg, 0.5 mmol) and Boc-deprotected **4.19** (149 mg, 0.5 mmol). The product was purified by silica column chromatography (2-5% MeOH/DCM) to afford **4.3** (190 mg, 0.33 mmol, 66%) as a white solid.

Mp 74-80 °C; δ_H (400 MHz, $CDCl_3$): 8.59 (s, 1H, H^{17}/H^{19}), 8.47 (d, J = 2.2 Hz, 1H, H^7), 8.07 (s, 1H, H^4), 7.05 (dd, J = 8.5, 2.1 Hz, 1H, H^9), 6.87 (s, 1H, H^{17}/H^{19}), 6.71 (d, J = 8.4 Hz, 1H, H^{10}), 6.33 (s, 1H, H^3), 4.98 (d, J = 11.0 Hz, 1H, H^{14}), 4.34 (dd, J = 9.1, 3.0 Hz, 1H, H^{13}), 3.80 (s, 1H, H^{13}), 3.70 – 3.34 (m, 2H, H^{21}), 3.17 (m, 2H, H^2), 2.65 – 1.99 (m, 13H, H^{20}, H^{22}, H^{23}, H^{24}, H^{25}), 1.08 (t, J = 7.2 Hz, 3H, H^1), 1.04 (s, 9H, H^{16}), 0.99 (t, J = 7.2 Hz, 3H, H^{26}); δ_C (101 MHz, $CDCl_3$): 183.95 (C^{18}), 155.89 (C^4), 148.84 (C^{11}), 130.31 (C^6), 124.49 (q, $J_{C\text{-}F}$ = 269.9 Hz, C^{12}), 123.47 (q, $J_{C\text{-}F}$ = 32.3 Hz, C^8), 118.03 (C^9), 114.44 (C^7), 109.69 (C^{10}), 69.36 (C^{13}), 65.20 (C^{21}), 64.14 (C^{14}), 59.93 ($C^{22}/C^{23}/C^{24}$), 53.47 ($C^{22}/C^{23}/C^{24}$), 52.31 ($C^{22}/C^{23}/C^{24}$, C^{25}), 34.89 (C^2), 33.47 (C^{15}), 27.10 (C^{16}), 15.32 (C^1), 11.89 (C^{26}); δ_F (376 MHz, $CDCl_3$): -61.45; υ_{max} (neat) cm^{-1}: 3306 (w), 2971 (m), 1673 (w), 1549 (s), 1444 (m), 1241 (m), 1116 (s); high resolution ESI-MS calcd. for $C_{26}H_{44}O_3N_6F_3S$ $[M+H]^+$ 660.27856, found 660.27814; $[\alpha]_D^{25}$ -42.3° (c 1.00, $CHCl_3$).

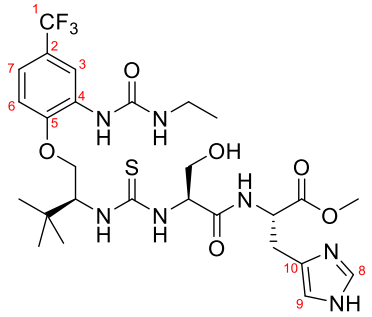

4.4

General procedure for thiourea formation was used to couple **4.15** (139 mg, 0.4 mmol) and Boc-deprotected **4.10** (165 mg, 0.5 mmol). The resulting crude product was purified by column chromatography (4-8% MeOH/DCM, R_f 0.33 with 10% MeOH/DCM) to afford **4.4** (149 mg, 0.231 mmol, 58%) as an off-white amorphous solid.

Mp 140-152 °C; δ_H (500 MHz, $CDCl_3$): ^{1}H NMR (500 MHz, Chloroform-*d*) δ 8.46 (d, *J* = 2.2 Hz, 1H, H^3), 8.06 (s, 1H, N*H*CSN*H*), 7.84 (s, 1H, N*H*CSN*H*), 7.80 (d, *J* = 10.1 Hz, 1H, ArN*H*CO), 7.31 (d, *J* = 1.2 Hz, 1H, SerCON*H*), 7.11 (m, 1H), 7.03 – 6.93 (m, 1H, H^7), 6.64 (d, *J* = 8.4 Hz, 1H, H^6), 6.62 (s, 1H, H^9), 6.03 (m, 1H, CON*H*Et), 4.83 (td, *J* = 9.9, 2.7 Hz, 1H, C*H*NHCS), 4.69 (s, 2H), 4.66 – 4.59 (m, 1H), 4.22 (dd, *J* = 8.8, 2.9 Hz, 1H, CH_2OAr), 3.98 (dd, *J* = 9.6, 6.0 Hz, 1H, SerCH_2), 3.67 (t, *J* = 9.5 Hz, 1H, CH_2OAr), 3.57 (s, 4H, OCH_3 & SerCH_2), 3.25 – 3.08 (m, 3H, CH_2CH$_3$ & HisCH_2), 2.81 (dd, *J* = 14.7, 6.6 Hz, 1H, HisCH_2), 1.05 (t, *J* = 7.2 Hz, 3H, CH$_2$CH_3), 0.93 (s, 9H, C(CH_3)$_3$). δ_C (126 MHz, $CDCl_3$): 184.16 (*C*S), 171.34 (Ser*C*ONH), 170.62 (His*C*O$_2$Me), 155.31 (NH*C*ONH), 148.64 (C^5), 135.03 (C^8), 130.33 (C^4), 124.37 (q, $J_{C\text{-}F}$ 270.9 Hz, C^1), 122.90 (q, $J_{C\text{-}F}$ 31.5 Hz, C^2) 117.45 (C^7), 114.06 (C^3), 109.18 (C^6), 68.96 (CH_2OAr), 62.65 (Ser*C*H$_2$), 61.94 (*C*HNHCS), 60.95 (Ser*C*H), 53.39, 53.10 (His*C*H), 52.25 (O*C*H$_3$), 34.49 (*C*H$_2$CH$_3$), 33.32 (*C*(CH$_3$)$_3$), 28.82 (His*C*H$_2$), 26.75 (C(*C*H$_3$)$_3$), 15.28 (CH$_2$*C*H$_3$). δ_F (377 MHz, $CDCl_3$) -61.45. υ_{max} (neat) cm^{-1}: 3306 (w), 2966 (w), 1671 (m), 1553 (s), 1243 (m), 1116 (s) ; ESI-MS m/z 646.3 $[M+H]^+$; high resolution ESI-MS calcd for $C_{27}H_{38}F_3N_7O_6S$ $[M+H]^+$: 646.26291 Found: 646.26296.

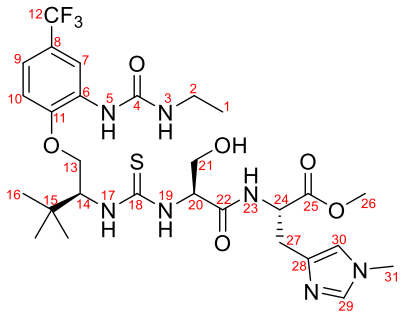

4.5

General procedure for thiourea formation was used to couple **4.15** (174 mg, 0.5 mmol) and Boc-deprotected **4.18** (172 mg, 0.5 mmol). The product was purified by silica column chromatography (2-5% MeOH/DCM) to afford **4.5** (244 mg, 0.37 mmol, 74%) as a white solid.

Mp 110-118 °C; δ_H (400 MHz, $CDCl_3$): 8.38 (s, 1H, H^7), 7.98 (s, 1H, H^{17}/H^{19}), 7.83 (s, 1H, H^5), 7.55 (s, 1H, H^{17}/H^{19}) 7.52 (d, J = 7.9 Hz, 1H, H^{23}), 7.17 (s, 1H, H^{29}), 6.96 (d, J = 7.6 Hz, 1H, H^9), 6.59 (d, J = 8.2 Hz, 1H, H^{10}), 6.56 (s, 1H, H^{30}), 5.96 (s, 1H, H^3), 4.96 (m, 2H, H^{14}, H^{20}), 4.75 (s, 1H, H^{24}), 4.22 (dd, J = 9.0, 2.9 Hz, 1H, H^{13}), 4.13 (d, J = 11.5 Hz, 1H, H^{21}), 3.87 – 3.74 (m, 2H, H^{13}, H^{21}), 3.61 (s, 3H, H^{26}), 3.51 (s, 3H, H^{31}), 3.27 – 3.16 (m, 2H, H^2), 3.04 (d, J = 14.8 Hz, 1H, H^{27}), 2.94 – 2.77 (m, 1H, H^{27}), 1.11 (t, J = 7.2 Hz, 3H, H^1), 1.00 (s, 9H, H^{16}); δ_C (101 MHz, $CDCl_3$): 184.20 (C^{18}), 171.38 (C^{25}), 170.57 (C^{22}), 155.43 (C^4), 148.44 (C^{11}), 137.52 (C^{29}), 136.82 (C^{28}), 130.02 (C^6), 124.47 (q, $J_{C\text{-}F}$ = 270 Hz, C^{12}), 118.20 (C^{30}), 117.66 (C^9), 114.19 (C^7), 109.09 (C^{10}), 68.62 (C^{13}), 62.51 (C^{21}), 62.30 (C^{14}), 60.36 (C^{20}), 52.93 (C^{24}), 52.41 (C^{26}), 34.71 (C^2), 33.40 (C^{31}), 33.38 (C^{15}) 28.90 (C^{27}), 26.85 (C^{16}), 15.33 (C^1); δ_F (376 MHz, $CDCl_3$): -61.38; υ_{max} (neat) cm^{-1}: 3317 (w), 2959 (w), 1671 (m), 1548 (s), 1115 (m); high resolution ESI-MS calcd. for $C_{28}H_{41}O_6N_7F_3S$ $[M+H]^+$ 660.27856, found 660.27814; $[\alpha]_D^{25}$ -25.2° (c 1.00, $CHCl_3$).

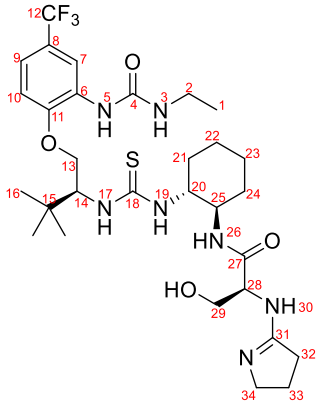

4.6

Pyrrolidinone (170.22 mg, 2 mmol) was added to dry DCM (10 ml). Trimethyloxonium tetrafluoroborate (325.4 mg, 2.2 mmol) was then added and the mixture was stirred at rt for 16 h to form amidination reagent in solution. **4.23** (100 mg, 0.169 mmol) was added to the resulting mixture. After stirring for 4 h at rt the solution was washed with 1M NaOH and the product was isolated by column chromatography (3-5% MeOH/DCM, R_f 0.29 in 5% MeOH/DCM). **4.6** was obtained as an amorphous white solid (45 mg, 0.068 mmol, 41%).

Mp 133-144 °C, decomp.; δ_H (500 MHz, $CDCl_3$): 8.53 (s, 1H, H^7), 8.22 (s, 1H, H^5), 7.50 (s, 2H, H^{19}, H^{26}), 7.11 (m, 1H, H^{17}), 7.08 (d, J = 8.4 Hz, 1H, H^9) 6.75 (s, 1H, H^3), 6.70 (d, J = 8.4 Hz, 1H, H^{10}), 5.04 (t, J = 10.0 Hz, 1H, H^{14}), 4.31 (dd, J = 8.7, 2.7 Hz, 1H, H^{13}), 4.18 (s, 1H, H^{28}), 3.87 (d, J = 10.1 Hz, 1H, H^{Cy}), 3.72 (t, J = 9.7 Hz, 1H, H^{13}), 3.47 (s, 1H, OH), 3.36 (m, 3H, H^2, H^{Cy}), 2.95-2.60 (m, 2H, H^{29}), 2.57–2.36 (m, 1H, H^{Cy}), 1.94 (dt, J = 12.9, 6.6 Hz, 3H, H^{Cy}, $H^{amidine}$), 1.81 (d, J = 14.4 Hz, 2H, $H^{amidine}$), 1.43 – 1.08 (m, 7H, H^1, H^{Cy}), 1.00 (s, 9H, H^{16}). δ_C (126 MHz, $CDCl_3$): 183.64 (C^{18}), 174.85 (C^{18}), 167.54 (C^{31}), 156.69 (C^4), 148.62 (C^{11}), 130.47 (C^6), 123.52 (q, $J_{C\text{-}F}$ = 272.2 Hz, C^{12}), 121.80 (q, $J_{C\text{-}F}$ = 34.0 Hz, C^8) 117.96 (C^9), 113.80 (C^7), 109.41 (C^{10}), 69.23 (C^{13}), 65.20 (C^{29}), 61.76 (C^{14}), 58.64 (C^{28}), 51.46, 35.01 (C^2), 33.41, 33.06, 29.84, 27.15 (C^{16}), 25.48, 24.84, 22.08, 16.10 (C^1), 1.16; δ_F (471 MHz, $CDCl_3$): -61.53; υ_{max} (neat) cm^{-1}: 3303 (w), 2938 (w), 1670 (m), 1552 (s), 1117 (m) ; ESI-MS m/z 658.3 $[M+H]^+$; high resolution ESI-MS calcd for $C_{30}H_{46}F_3N_7O_4S$ $[M-H]^-$: 656.32113 Found: 656.32147.

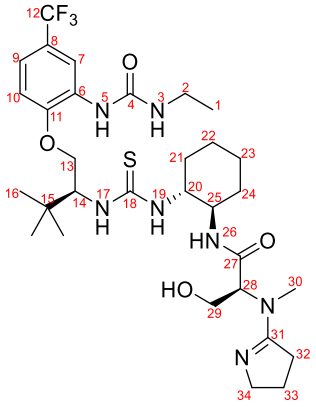

4.7

Amidination reagent was prepared by combining pyrrolidinone (102 mg, 1.2 mmol) and Me_3OBF_4 (148 mg, 1 mmol) in dry DCM (10 ml) under Ar. The mixture was stirred overnight, washed with sat. aq. $NaHCO_3$, dried with anhydrous Na_2SO_4 and concentrated to ca. 2 cm^3. The resulting solution was added to **4.24** (120 mg, 0.2 mmol) with a few drops of AcOH. The reaction was stirred for 2 d at rt. The solution was then diluted with DCM, washed with sat. aq. Na_2CO_3, dried with anhydrous Na_2SO_4 and evaporated. The crude product was purified by silica chromatography (3-8% MeOH w. 7N NH_3/DCM) followed by PTLC (10% MeOH w. 7N NH_3/DCM) to afford **4.7** (74 mg, 0.11 mmol, 53%) as a white solid.

Mp 68-74 °C; δ_H (400 MHz, $CDCl_3$) (rotamers): 8.57 (s, 1H, H^7), 8.03 (s, 1H, H^5), 7.19 – 6.98 (m, 2H, H^9, H^{26}), 6.75 (m, 1H, H^{10}), 6.34 (s, 1H, H^3) 5.04 (s, 1H, H^{14}), 4.37 (m, 1H, H^{13}), 3.77 (m, 5H, H^{13}), 3.57 (s, 1H), 3.52 – 3.18 (m, 4H, H^2, H^{29}), 2.61 (m, 3H, H^{28}), 2.16 (d, J = 13.6 Hz, 1H), 2.08 – 1.55 (m, 8H, H^{30}), 1.49 – 1.09 (m, 6H, H^1), 1.04 (d, J = 6.5 Hz, 10H, H^{16}), 0.86 (d, J = 17.4 Hz, 2H, H^{Cy}); δ_C (101 MHz, $CDCl_3$) (rotamers): 183.58 (C^{18}), 172.05 (C^{18}), 169.65 (C^{31}), 156.03 (C^4), 155.09, 149.02 (C^{11}), 130.30 (C^6), 125.83, 123.13, 118.25 (C^9), 114.66 (C^7), 109.71 (C^{10}), 69.28 (C^{13}), 64.14, 61.67 (C^{14}), 60.98, 60.42, 55.86, 55.33, 53.99, 52.17, 49.20, 47.28, 41.35, 36.07 (C^{28}), 34.97 (C^2), 33.64, 32.64, 32.04, 31.92, 30.92, 30.66, 29.39, 28.30, 27.07 (C^{16}), 24.68, 23.41, 23.06, 15.64 (C^1); δ_F (376 MHz, $CDCl_3$): -61.59; υ_{max} (neat) cm^{-1}: 3299 (w), 2980 (s), 1668 (w), 1606 (m), 1549 (s), 1241 (m), 1118 (s); high resolution ESI-MS calcd. for $C_{31}H_{49}O_4N_7F_3S$ $[M+H]^+$ 672.35133, found 672.35039; $[\alpha]_D^{25}$ -29.2° (c 1.00, $CHCl_3$).

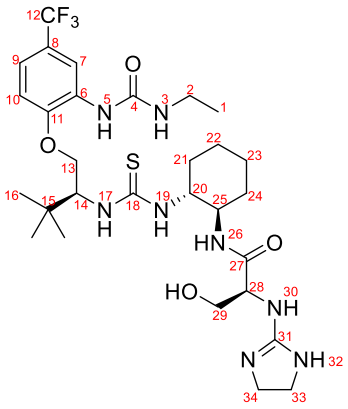

4.8

4.23 (70 mg, 0.12 mmol) and **4.22** (146 mg, 0.6 mmol) were added to pyridine (1 ml) and the solution was stirred for 3 h at 100 °C. It was then diluted with DCM, washed with 1M NaOH and the aqueous phase was backextracted with DCM. The product was isolated by column chromatography (5% MeOH/DCM – 5% $NH_4OH_{(aq)}$, 30% MeOH/DCM). Compound **4.8** was obtained as a white amorphous solid (61 mg, 0.093 mmol, 78%).

Mp 130-141 °C, decomp; δ_H (500 MHz, $CDCl_3$): 8.48 (s, 1H, H^7), 7.12 – 7.06 (m, 1H, H^9), 6.71 (d, J = 8.4 Hz, 1H, H^{10}), 5.14 – 4.81 (m, 1H, H^{14}), 4.29 (dd, J = 8.9, 2.8 Hz, 1H, H^{13}), 4.19 (s, 1H, H^{28}), 3.76 (m, 2H, H^{13}, H^{Cy}), 3.50 – 3.19 (m, 7H, H^{Cy}, $H^{guanidine}$), 2.96 (s, 1H, H^{29}), 2.81 (s, 1H, H^{29}), 2.51 – 2.38 (m, 1H, H^{Cy}), 1.91 (s, 1H, H^{Cy}), 1.79 (d, J = 14.2 Hz, 3H, H^{Cy}, $H^{guanidine}$), 1.44 – 1.07 (m, 9H, H^1, H^{Cy}, $H^{guanidine}$), 0.98 (s, 12H, H^{16}, H^{Cy}, $H^{guanidine}$); δ_C (126 MHz, $CDCl_3$): 183.54 (C^{18}), 174.24 (C^{27}), 159.95 (C^{31}), 156.69 (C^4), 148.71 (C^{11}), 130.26 (C^6), 124.66 (q, $J_{C\text{-}F}$ = 272.2 Hz, C^{12}), 122.93 (q, $J_{C\text{-}F}$ = 32.8 Hz, C^8), 118.06 (C^9), 113.72 (C^7), 109.38 (C^{10}), 77.41, 69.04 (C^{13}), 64.35 (C^{29}), 61.70 (C^{14}), 58.72 (C^{28}), 51.41, 34.93 (C^2), 33.40, 33.04 (C^{Cy}), 27.11 (C^{16}), 25.38 (C^{Cy}), 24.81 C^{Cy}), 16.00 (C^1), 1.13; δ_F (471 MHz, $CDCl_3$): -61.39; υ_{max} (neat) cm^{-1}: 3299 (w), 2940 (w), 1672 (m), 1553 (s) 1118 (m); ESI-MS m/z 659.3 $[M+H]^+$; high resolution ESI-MS calcd for $C_{29}H_{45}F_3N_8O_4S$ $[M-H]^-$: 657.31638 Found: 657.31671.

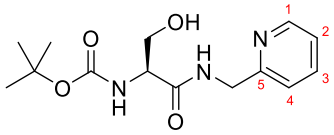

4.9

General procedure for mixed anhydride amide formation

Boc-Ser-OH (205 mg, 1 mmol) and NMM (132 µl, 1.2 mmol) were added to dry THF (2 ml). Separately, isobutyl chloroformate (143 µl, 1.1 mmol) was added to dry THF (1 ml). The chloroformate solution was cooled to −15 °C and the solution of Boc-Ser-OH and NMM was added dropwise over 15 min at −15 °C. The mixture was stirred at −15 °C for 15 min and 2-picolylamine (124 µl, 1.2 mmol) was added. The reaction was then stirred at rt for 16 h. The solvent was evaporated under reduced pressure, the residue was dissolved in DCM and subjected to column chromatography (3-5% MeOH/DCM, R_f 0.10 with 5% MeOH/DCM) to afford **4.9** as an off-white solid (246 mg, 0.831 mmol, 83%).

Mp 105 °C; δ_H (500 MHz, $CDCl_3$): 8.47 – 8.42 (m, 1H, H^1), 7.65 (td, J = 7.7, 1.8 Hz, 1H, H^3), 7.39 (s, 1H, CON$H$$CH_2$), 7.24 (d, J = 7.8 Hz, 1H, H^4), 7.20 – 7.13 (m, 1H, H^2), 5.67 (d, J = 7.5 Hz, 1H, NHBoc), 4.92 (s, 1H, OH), 4.61 (qd, J = 16.6, 5.4 Hz, 2H, CH_2Pyr), 4.27 (s, 1H, CHNHBoc), 4.12 – 3.98 (m, 1H, CH_2OH), 3.66 (dd, J = 11.4, 5.9 Hz, 1H, CH_2OH), 1.43 (s, 9H, C(CH_3)$_3$); δ_C (126 MHz, $CDCl_3$): 171.73 (*C*ONH), 156.31 (C^5), 155.73 (*C*O^{t}Bu), 148.82 (C^1), 137.10 (C^3), 122.48 (C^2), 121.86 (C^4), 80.21 (*C*(CH$_3$)$_3$), 63.21 (*C*H$_2$OH), 55.92 (*C*HNHBoc), 44.23 (CH_2Pyr), 28.31 (C(*C*H$_3$)$_3$). υ_{max} (neat) cm^{-1}: 3303 (w), 2977 (w), 1660 (s), 1524 (m), 1166 (s); ESI-MS m/z 296.1 $[M+H]^+$; high resolution ESI-MS calcd for $C_{14}H_{21}N_3O_4$ $[M-H]^-$: 294.14593 Found: 294.14566.

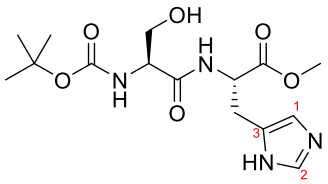

4.10

General procedure for amide formation with COMU

Boc-Ser(Bzl)-OH (295 mg, 1 mmol), H-His-OMe (242 mg, 1 mmol) and DIPEA (697 µl, 4 mmol) were added to dry DMF (7 ml). The mixture was cooled to 0 °C and COMU (428 mg, 1 mmol) was added. The mixture was stirred at 0 °C for 1 h and at rt for 1 h. It was then diluted with EtOAc, washed with sat $NaHCO_{3(aq)}$ and brine, dried with anhydrous Na_2SO_4, filtered and evaporated. The residue was purified by column chromatography (3-5% MeOH/DCM, R_f 0.31 in 5% MeOH/DCM) to give Boc-Ser(Bzl)-His-OMe as a white foam (257 mg, 0.576 mmol, 58%). It was dissolved in MeOH (40 ml), 20% $Pd(OH)_2/C$ (170 mg) was added and the mixture was stirred under H_2 atmosphere for 24 h. It was then filtered through Celite with MeOH washing, concentrated under reduced pressure, redissolved in DCM with MeOH and purified by column chromatography (5% MeOH/DCM) to give **4.10** (168 mg, 0.471 mmol, 47% over 2 steps) as a white foamy solid.

Mp 63-75 °C; δ_H (500 MHz, $CDCl_3$): ^{1}H NMR (500 MHz, Chloroform-*d*) δ 7.42 (d, *J* = 3.4 Hz, 1H, *H*^{2}), 7.31 (d, *J* = 7.7 Hz, 1H, CON*H*CH), 6.70 (d, *J* = 3.0 Hz, 1H, *H*^{1}), 5.86 (d, *J* = 7.1 Hz, 1H, N*H*Boc), 5.46 (s, 2H, O*H* & N$H_{imidazole}$), 4.72 (s, 1H, HisC*H*), 4.14 – 3.87 (m, 2H, SerCH_2 & Ser*CH*), 3.67 (m, 4H, OCH_3 & SerCH_2), 3.20 (dt, *J* = 14.9, 4.4 Hz, 1H, HisCH_2), 2.99 – 2.86 (m, 1H, HisCH_2), 1.39 (d, *J* = 3.4 Hz, 9H, C(CH_3)$_3$); δ_C (126 MHz, $CDCl_3$): 171.47 (*C*O_2CH_3), 171.08 (*C*ONH), 155.61 (*C*O^{t}Bu), 135.36 (*C*^{2}), 133.15 (C^3), 116.71 (*C*^{1}), 80.11 (*C*$(CH_3)_3$), 62.84 (Ser*C*H_2), 57.12 (Ser*C*H), 53.15 (His*C*H), 52.53 (O*C*H_3), 28.72 (His*C*H_2), 28.32 (C(*C*H_3)$_3$). υ_{max} (neat) cm^{-1}: 3390 (m), 1664 (m), 1024 (s), 996 (s); ESI-MS m/z 357.2 [M+H]$^+$.

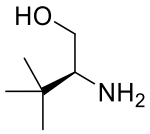

4.11

(*S*)-*tert*-leucine (1.312 g, 10 mmol) was dissolved in dry THF (25 ml) and $NaBH_4$ (908 mg, 24 mmol) was added. Separately, I_2 (2.538 g, 10 mmol) was dissolved in dry THF (8 ml) and the resulting solution was added to the reaction mixture over 30 min at 0 °C. The reaction was then heated at reflux for 16 h. After cooling down to room temperature MeOH was carefully added until the solution became clear. It was then stirred at rt for 30 min and evaporated under reduced pressure. The white semisolid residue was dissolved in 20% KOH (20 ml), stirred at rt for 4h and extracted with DCM. The extracts were dried with anhydrous Na_2SO_4, filtered and evaporated to give **4.11** as a white crystalline solid (1.134 g, 9.677 mmol, 97%).

Mp 28 °C; δ_H (500 MHz, $CDCl_3$): 3.70 (dd, *J* 10.4, 3.8 Hz, 1H, C*H*$_2$), 3.22 (t, *J* 10.2 Hz, 1H, C*H*), 2.52 (dd, *J* 10.1, 3.8 Hz, 1H, C*H*$_2$), 2.25 (s, 3H, O*H*, N*H*$_2$), 0.88 (s, 9H, C*H*$_3$); δ_C (126 MHz, $CDCl_3$): 62.33 (*C*H), 61.91 (*C*H_2), 33.31 (*C*), 26.39 (C*H*$_3$); υ_{max} (neat) cm^{-1}: 2594, 1047 ; ESI-MS m/z 118.2 $[M+H]^+$; $[\alpha]_D^{25}$ +38.3° (c = 1, $CHCl_3$).

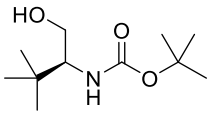

4.12

(*S*)-*tert*-leucinol **4.11** (882 mg, 7.53 mmol) and triethylamine (1.252 ml, 9.03 mmol) were added to DCM (25 ml). Separately, Boc_2O was dissolved in DCM (5 ml) and added to the reaction mixture dropwise at 0 °C. The reaction mixture was stirred at 0 °C for 1 h and at rt for 16h. The resulting mixture was washed with brine, dried with anhydrous Na_2SO_4, filtered and evaporated. The crude product was purified by column chromatography (4:1 hexanes:EtOAc) and recrystallized from hexane to afford **4.12** as a white crystalline solid (1.427 g, 6.567 mmol, 87%)

Mp 88 °C; δ_H (500 MHz, $CDCl_3$): 4.63 (s, 1H, N*H*), 3.84 (m, 1H, C*H*$_2$OH), 3.48 (m, 2H, C*H*$_2$OH & C*H*NHBoc), 2.24 (s, 1H, O*H*), 1.45 (s, 9H, $CO_2C(CH_3)_3$), 0.93 (s, 9H, $C(CH_3)_3$); δ_C (126 MHz, $CDCl_3$): 157.37 (C=O), 79.95 ($CO_2C(CH_3)_3$), 63.44 (*C*H_2), 61.18 (*C*H), 33.77 ($C(CH_3)_3$), 28.52 ($CO_2C(CH_3)_3$) 26.95 ($C(CH_3)_3$); υ_{max} (neat) cm^{-1}: 3250 (w), 3701 (m), 1678 (s); ESI-MS m/z 240.1 $[M+Na]^+$; $[\alpha]_D^{25}$ -4.0° (c = 1, $CHCl_3$).

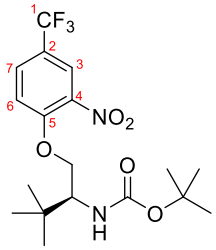

4.13

N-Boc-(*S*)-*tert*-leucinol **4.12** (1.620 g, 7.45 mmol) and 4-fluoro-3-nitrobenzotrifluoride (3.13 ml, 22.36 mmol) was added to dry THF (50 ml). The mixture was cooled to 0 °C and 0.5 M KHMDS in THF (14.9 ml, 7.45 mmol) was added over 1 h at 0 °C. The resulting solution was diluted with DCM, washed with sat. $NH_4Cl_{(aq)}$, dried with anhydrous Na_2SO_4, filtered and evaporated. The crude material was purified by column chromatography (8:1 hexanes:EtOAc) and the isolated product was refined by recrystallization from hexane. Additional product was obtained from mother liquor by repeating the sequence of chromatography and recrystallization. Product **4.13** was obtained as a white crystalline solid (2.345 g, 5.770 mmol, 77%).

Mp 120 °C; δ_H (500 MHz, $CDCl_3$): 8.15 (d, *J* 2.3 Hz, 1H, Ar-*H*^{3}), 7.79 (dd, *J* 8.8, 2.3 Hz, 1H, Ar-H^7), 7.20 (d, *J* 8.8 Hz, 1H, Ar-H^6), 5.03 (d, *J* 10.0 Hz, 1H, N*H*), 4.33 (dd, *J* 9.8, 3.5 Hz, 1H, C*H*$_2$OAr), 4.23 (dd, *J* 9.7, 4.3 Hz, 1H, C*H*$_2$OAr), 3.82 (dt, *J* 10.1, 3.9 Hz, 1H, C*H*NHBoc), 1.43 (s, 9H, $CO_2C(CH_3)_3$), 1.01 (s, 9H, $C(CH_3)_3$); δ_C (126 MHz, $CDCl_3$): 155.96 ($CO_2C(CH_3)_3$), 154.62 (*C*^{5}), 139.33(*C*^{4}), 131.31 (q, $J_{C\text{-}F}$ 3.7 Hz, C^7), 123.70 (q, $J_{C\text{-}F}$ 3.7 Hz, C^3), 123.25 (q, $J_{C\text{-}F}$ 33.8 Hz, C^2) 123.15 (q, $J_{C\text{-}F}$ 270 Hz, C^1) 114.83 (C^6), 79.79 ($CO_2C(CH_3)_3$), 69.77 (CH_2OAr), 56.96 (*C*HNHBoc), 34.56 ($C(CH_3)_3$), 28.47 ($CO_2C(CH_3)_3$), 27.26 $C(CH_3)_3$); δ_F (471 MHz, $CDCl_3$) -62.07; υ_{max} (neat) cm^{-1}: 3340 (w), 2969 (m), 1695 (m), 1584 (m), 1328 (s); ESI-MS m/z 429.2 $[M+Na]^+$.

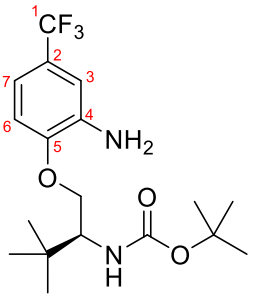

4.14

4.13 (1.844 g, 4.54 mmol), 10% Pd/C (184 mg) and NH_4HCO_2 (858 mg, 13.61 mmol) were added to 9:1 MeOH : EtOAc (45 ml) and stirred at 50 °C for 2 h. The mixture was filtered through Celite and the filter pad was washed with MeOH. The solvent was removed under reduced pressure to afford crude product as a greenish oily foam. It was redissolved in MeOH and Zn dust (500 mg) and NH_4HCO_2 (1 g) were added. The mixture was stirred at rt for 2h, filtered through Celite with a MeOH washing and the solvent was removed under reduced pressure. The residue was dissolved in DCM, washed with brine, dried with anhydrous Na_2SO_4, filtered and evaporated to give pure product **4.14** (1.583 g, 4.205 mmol, 93%) as a white solid.

Mp 110 °C; δ_H (500 MHz, $CDCl_3$): 6.93 (dd, *J* = 8.3, 2.1 Hz, 1H, Ar-H^7), 6.90 (s, 1H, Ar-*H*^{3}), 6.74 (d, *J* = 8.3 Hz, 1H, Ar-H^6), 4.69 – 4.62 (m, 1H, CHN*H*Boc), 4.25 – 4.15 (m, 1H, C*H*$_2$OAr), 3.94 (br s, 2H, N*H*$_2$), 3.93 – 3.85 (m, 2H, C*H*$_2$OAr & C*H*NHBoc), 1.44 (s, 9H, $CO_2C(CH_3)_3$), 1.02 (s, 9H, $C(CH_3)_3$); δ_C (126 MHz, $CDCl_3$): 156.44 ($CO_2C(CH_3)_3$), 148.69 (C^5), 136.98 (C^4), 124.62 (q, $J_{C\text{-}F}$ 270 Hz, C^1), 123.62 (q, $J_{C\text{-}F}$ 32.4 Hz, C^2), 115.19 (q, $J_{C\text{-}F}$ 4.0 Hz, C^7), 111.08 (q, $J_{C\text{-}F}$ 3.3 Hz, C^3), 110.46 (C^6), 79.57 ($CO_2C(CH_3)_3$), 68.93 (CH_2OAr), 58.19 (*C*HNHBoc), 33.72 ($C(CH_3)_3$), 28.53 ($CO_2C(CH_3)_3$), 27.08 ($C(CH_3)_3$); δ_F (377 MHz, $CDCl_3$) -61.72. υ_{max} (neat) cm^{-1}: 3357 (w), 2268 (w), 1695 (m), 1332 (s), 1220 (s), 1163 (s), 1114 (s); ESI-MS m/z 377.2 $[M+H]^+$.

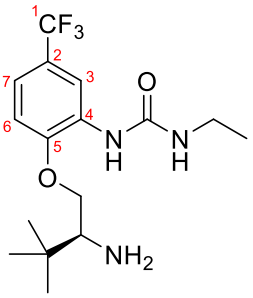

4.15

4.14 (2.130 g, 5.66 mmol) and ethyl isocyanate (8 ml) were combined and stirred at rt for 16 h. The resulting mixture was diluted with DCM, washed with pH 7 buffer and brine, dried with anhydrous Na_2SO_4, filtered and evaporated. The resulting material was dissolved in 1:1 TFA : DCM at 0 °C, allowed to slowly warm up to rt and stirred for 12 h. The solvents were removed under vacuum, the oily residue was dissolved in DCM and washed with sat. $NaHCO_{3(aq)}$. Aqueous phase was backextracted with DCM, the combined organic phases were dried with anhydrous Na_2SO_4, filtered and evaporated to give pure **4.15** (1.921 g, 5.531 mmol, 98%) as an off-white solid.

Mp 155 °C; δ_H (500 MHz, $CDCl_3$): 8.51 (d, *J* 2.2 Hz, 1H, Ar-*H*^{3}), 8.00 (s, 1H, ArN*H*CO), 7.15 (dd, *J* 8.5, 2.2 Hz, 1H, Ar-H^7), 6.90 (d, *J* 8.4 Hz, 1H, Ar-H^6), 5.35 (t, *J* 5.5 Hz, 1H, CON*H*Et), 4.21 (dd, *J* 9.6, 2.9 Hz, 1H, C*H*$_2$OAr), 3.72 (t, *J* 9.5 Hz, 1H, C*H*$_2$OAr), 3.27 (qd, *J* 7.2, 5.5 Hz, 2H, C*H*$_2$CH$_3$), 2.88 (dd, *J* 9.4, 2.9 Hz, 1H, C*H*NH$_2$), 1.95 (s, 2H, N*H*$_2$), 1.14 (t, *J* 7.2 Hz, 3H, CH$_2$C*H*$_3$), 0.96 (s, 9H, C(C*H*$_3$)$_3$); δ_C (126 MHz, $CDCl_3$): 155.54 (NH*C*ONH), 149.44 (C^5), 130.88 (C^4), 124.43 (q, $J_{C\text{-}F}$ 272 Hz, C^1), 124.39 (q, $J_{C\text{-}F}$ 32.6 Hz, C^2), 118.91 (q, $J_{C\text{-}F}$ 4.1 Hz, C^7), 116.23 (q, $J_{C\text{-}F}$ 3.9 Hz, C^3), 113.05 (C^6), 72.39 (*C*H$_2$OAr), 59.45 (*C*HNH$_2$), 35.15 (*C*H$_2$CH$_3$), 33.52 (*C*(CH$_3$)$_3$), 26.46 (C(*C*H$_3$)$_3$), 15.45 (CH$_2$*C*H$_3$); δ_F (377 MHz, $CDCl_3$) -61.69. υ_{max} (neat) cm^{-1}: 3344 (w), 2965 (w), 1657 (w), 1558 (m), 1115 (s); ESI-MS m/z 348.2 $[M+H]^+$; $[\alpha]_D^{25}$ 42.3° (c = 1, $CHCl_3$).

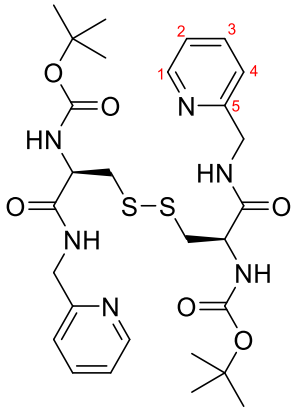

4.17

General procedure for mixed anhydride amide formation was used to couple $(Boc\text{-}Cys)_2$ (468 mg, 1 mmol) and picolylamine (247 µl, 2.4 mmol). Column chromatography (3-5% MeOH/DCM, R_f 0.31 with 5% MeOH/DCM) gave **4.17** (548 mg, 0.883 mmol, 88%) as a white solid.

Mp 145 °C; δ_H (500 MHz, $CDCl_3$): 8.51 (dt, *J* = 4.9, 1.2 Hz, 2H, H^1), 8.31 (t, *J* = 6.0 Hz, 2H, CON*H*CH_2), 7.63 (td, *J* = 7.7, 1.8 Hz, 2H, H^3), 7.29 – 7.24 (m, 2H, H^4), 7.16 (ddd, *J* = 7.5, 4.9, 1.1 Hz, 2H, H^2), 5.61 (d, *J* = 9.3 Hz, 2H, N*H*Boc), 4.94 (td, *J* = 9.8, 4.4 Hz, 2H, C*H*NHBoc), 4.67 (dd, *J* = 15.8, 6.2 Hz, 2H, CH_2Pyr), 4.52 (dd, *J* = 15.8, 5.6 Hz, 2H, CH_2Pyr), 3.07 (dd, *J* = 14.5, 4.4 Hz, 2H, CH_2S), 2.97 (dd, *J* = 14.5, 9.9 Hz, 2H, CH_2S), 1.28 (s, 18H, C(CH_3)$_3$); δ_C (126 MHz, $CDCl_3$): 170.60 (*C*ONH), 157.39 (C^5), 155.81 (*C*O^{t}Bu), 149.28 (C^1), 136.74 (C^3), 122.30 (C^2), 121.53 (C^4), 80.20 (*C*(CH$_3$)$_3$), 54.57 (*C*HNHBoc), 46.62 (*C*H$_2$S), 45.04 (*C*H$_2$Pyr), 28.22 (C(*C*H$_3$)$_3$). υ_{max} (neat) cm^{-1}: 3301 (w), 2979 (w), 1663 (s) 1521 (m) 1166 (s); ESI-MS m/z 621.3 $[M+H]^+$; high resolution ESI-MS calcd for $C_{14}H_{21}N_3O_4$ $[M-H]^-$: 619.23780 Found: 619.23767.

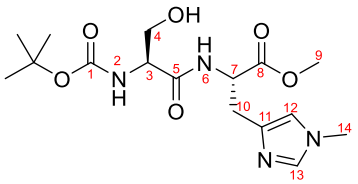

4.18

General procedure for amide formation with COMU was used to couple Boc-Ser(Bzl)-OH (295 mg, 1 mmol) and N$^{\tau}$-methylhistidine methyl ester dihydrochloride (256 mg, 1 mmol). The benzyl-deprotected product was purified by silica chromatography (5% MeOH/DCM) to afford **4.18** as a white solid foam (208 mg, 0.562 mmol, 56%).

δ_H (400 MHz, $CDCl_3$): 7.32 (d, J = 1.4 Hz, 1H, H^{13}), 7.25-7.17 (m, 1H, H^6) 6.64 (d, J = 1.3 Hz, 1H, H^{12}), 5.69 (s, 1H, H^2), 4.80 (m, 2H, H^7, OH), 4.09 (d, J = 11.8 Hz, 2H, H^3, H^4), 3.73 (s, 3H, H^9), 3.72 – 3.66 (m, 1H, H^4), 3.61 (s, 3H, H^{14}), 3.27 – 3.16 (m, 1H, H^{10}), 2.87 (dd, J = 14.6, 6.6 Hz, 1H, H^{10}), 1.44 (s, 9H, C(CH_3)$_3$); δ_C (101 MHz, $CDCl_3$): 171.69 (C^8), 171.09 (C^5), 155.53 (C^1), 137.75 (C^{13}), 137.04 (C^{11}), 118.30 (C^{12}), 80.18 (C(CH$_3$)$_3$), 63.15 (C^4), 57.26 (C^3), 53.17 (C^7), 52.64 (C^9), 33.69 (C^{14}), 29.43 (C^{10}), 28.42 (C(CH$_3$)$_3$); υ_{max} (neat) cm^{-1}: 3308 (w), 2980 (w), 1669 (m), 1509 (m), 1167 (s); ESI-MS m/z 371.2 [M+H]$^+$ high resolution ESI-MS calcd. for $C_{16}H_{27}N_4O_6$ [M+H]$^+$ 371.19251, found: 371.19188; $[\alpha]_D^{25}$ 20.2° (c 1.00, $CHCl_3$).

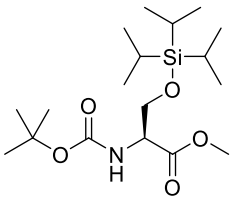

Boc-Ser(OTIPS)-OMe

Boc-Ser-OMe (3288 mg, 15 mmol) was added to dry DCM (17 ml) and cooled to 0 °C. Imidazole (2.519 mg, 37 mmol) was then added, followed by triisopropylsilyl chloride (3.51 ml, 16.5 mmol). The reaction was allowed to warm to rt and stirred for 24 h. The resulting mixture was washed with water, dried with anhydrous Na_2SO_4, filtered and evaporated. The product was purified by silica column chromatography to provide Boc-Ser(OTIPS)-OMe (5.500 g, 14.64 mmol, 98%) as a colourless oil.

δ_H (400 MHz, $CDCl_3$): 5.38 (d, J = 8.8 Hz, 1H, N*H*), 4.36 (dt, J = 8.9, 2.9 Hz, 1H, C*H*), 4.13 (dd, J = 9.8, 2.7 Hz, 1H, CH_2), 3.92 (dd, J = 9.8, 3.0 Hz, 1H, CH_2), 3.73 (s, 3H, OCH_3), 1.44 (s, 9H, OC(CH_3)$_3$), 1.15 – 0.94 (m, 21H, TIPS-*H*); δ_C (101 MHz, $CDCl_3$): 171.40 (*C*O_2CH_3), 155.55 (NH*C*O^{t}Bu), 79.94 (O*C*(CH$_3$)$_3$), 64.39 (*C*H_2), 55.84 (*C*H), 52.36 (O*C*H_3), 28.46 (OC(*C*H_3)$_3$), 17.94 (TIPS-*C*), 17.92 (TIPS-*C*), 11.95 (TIPS-*C*); υ_{max} (neat) cm^{-1}: 2944 (m), 2868 (m), 1751 (m), 1719 (s), 1499 (m), 1167 (m); ESI-MS m/z 398.2 [M+Na]$^+$; $[\alpha]_D^{25}$ 25.9° (c 1.00, $CHCl_3$).

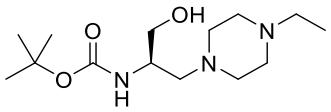

4.19

Boc-Ser(OTIPS)-OMe (1127 mg, 3 mmol) was added to dry toluene (20 ml) under Ar. The solution was cooled to −78 °C and DIBAL-H (1M in hexanes, 6.6 ml, 6.6 mmol) was added over 30 min. The reaction was then kept at −78 °C for 2 h after which time MeOH (6 ml) was added over 30 min. Saturated Rochelle's salt solution was then added and the mixture allowed to warm up to rt with vigorous stirring. It was then diluted with water and Et_2O, phases were separated and the aqueous phase was extracted with Et_2O. The combined organic phases were dried on anhydrous Na_2SO_4, filtered and evaporated to provide the crude aldehyde intermediate. It was then dissolved in DCE (10 ml) under Ar, cooled to 0 °C and combined with AcOH (429 µl, 7.5 mmol) followed by N-ethylpiperazine (343 mg, 3 mmol) and $NaBH(OAc)_3$ (954 mg, 4.5 mmol). The reaction was allowed to warm up to rt while stirring overnight. It was then combined with 1M NaOH and extracted with DCM. Combined organic fractions were washed with brine, dried on anhydrous Na_2SO_4, filtered and evaporated. Crude TIPS-protected product was combined with TBAF (1 M in THF, 3.1 ml, 3.1 mmol) at 0 °C, stirred for 1 h at 0 °C and for 1 h at rt. The mixture was combined with 1M NaOH and extracted with DCM, the organic extracts were dried on anhydrous Na_2SO_4, filtered and evaporated. The crude product was purified by column chromatography on silica (5-10% MeOH/DCM) to provide **4.19** (580 mg, 2.02 mmol, 67%) as a clear oil.

δ_H (400 MHz, $CDCl_3$): 4.95 (s, 1H, N*H*), 4.76 (s, 1H, O*H*), 3.83 – 3.68 (m, 2H, C*H*C*H*$_2$OH), 3.60 (q, J = 5.6 Hz, 1H, C*H*$_2$OH), 2.87 – 2.12 (m, 12H, NC*H*$_2$), 1.43 (s, 9H, C(C*H*$_3$)$_3$), 1.06 (t, J = 7.2 Hz, 3H, C*H*$_3$); δ_C (101 MHz, $CDCl_3$): 156.10 (*C*O), 79.76 (*C*(CH$_3$)$_3$), 66.51 (*C*H$_2$OH), 60.63, 53.62, 52.72, 52.20 (*C*H$_2$CH$_3$), 48.73 (*C*H), 28.37 (C(*C*H$_3$)$_3$), 11.91 (CH$_2$*C*H$_3$); υ_{max} (neat) cm^{-1}: 2972 (m), 2817 (m), 1697 (s), 1365 (m), 1168 (s); high-resolution ESI-MS calcd. for $C_{14}H_{30}N_3O_3$ $[M+H]^+$ 288.22817, found: 288.22815; $[\alpha]_D^{25}$ -5.0° (c 1.00, $CHCl_3$).

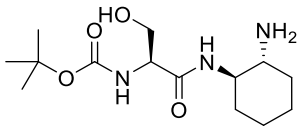

4.20

General procedure for mixed anhydride amide coupling was used to couple Boc-Ser-OH (616 mg, 3 mmol) and (*R*,*R*)-1,2-diaminocyclohexane (1713 mg, 15 mmol) The crude material was purified by column chromatography on silica (5-10% MeOH/DCM) to afford **4.20** as a white solid (647 mg, 2.14 mmol, 72%).

Mp 170 °C, decomp.; δ_H (400 MHz, D_2O): δ 4.05 (t, *J* = 5.3 Hz, 1H, SerC*H*), 3.78 (d, *J* = 5.2 Hz, 2H, SerCH_2), 3.45 (td, *J* = 10.2, 4.3 Hz, 1H, SerNHC*H*), 2.54 (td, *J* = 10.4, 4.0 Hz, 1H, C*H*NH_2), 1.95 – 1.85 (m, 1H, Cy-*H*), 1.79 (s, 1H, Cy-*H*), 1.73 – 1.63 (m, 2H, Cy-*H*), 1.41 (s, 9H, $C(CH_3)_3$); 1.30-1.15 (m, 4H, Cy-*H*); δ_C (100 MHz, D_2O): 172.75 (*C*ONH), 157.35 ($CO_2{}^tBu$), 81.69 ($C(CH_3)_3$), 61.05 (SerCH_2), 57.12 (SerCH_2), 55.59 (SerNH*C*H), 53.38 (*C*HNH_2), 32.86 (Cy-*C*), 31.30 (Cy-*C*), 27.52 ($C(CH_3)_3$), 24.43 (Cy-*C*), 24.20 (Cy-*C*); υ_{max} (neat) cm^{-1}: 3278 (w), 2933 (w), 1656 (m), 1536 (m) 1167 (m); ESI-MS m/z 302.2 $[M+H]^+$; high resolution ESI-MS calcd for $C_{14}H_{26}N_3O_4$ $[M-H]^-$: 300.19288 Found: 300.19244.

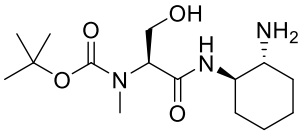

4.21

Isobutyl chloroformate (0.571 ml, 4.4 mmol) was added to dry THF (6 ml) and cooled to −15 °C. Separately, *O*-benzyl-*N*-(*tert*-butoxycarbonyl)-*N*-methyl-*L*-serine (1.181 g, 4 mmol) was dissolved in dry THF together with N-methylmorpholine (0.528 ml, 4.8 mmol). This solution was then added to the cooled chloroformate solution over 15 min. The reaction was stirred at −15 °C for 15 min. It was then cooled to −50 °C and (*R*,*R*)-1,2-diaminocyclohexane (1.028 g, 9 mmol) was added. The reaction was allowed to reach rt and stirred at rt for 2 h. It was then concentrated under vacuum and partitioned in EtOAc and sat. aq. Na_2CO_3. Organic extracts were then dried on anhydrous Na_2SO_4, filtered and evaporated. The crude material was purified by column chromatography on silica (5-10% MeOH/DCM) to afford *O*-benzyl protected product. It was then dissolved in MeOH (20 ml), combined with $Pd(OH)_2/C$ (60 mg) and stirred under H_2 atmosphere for 2 d. The mixture was then filtered through Celite with a MeOH washing and evaporated to provide **4.21** (530 mg, 1.68 mmol, 56%) as white foam.

Mp 146 °C; δ_H (400 MHz, CD_3OD): (rotamers) 8.20-7.73 (m, 1H), 4.19 (s, 1H), 4.10-3.98 (m, 1H), 3.95-3.74 (m, 2H), 3.36 (s, 2H), 3.10-2.89 (m, 3H), 2.11 (d, J = 12.5 Hz, 1H), 1.97 – 1.77 (m, 3H), 1.50 (s, 9H), 1.39 (m, 2H); δ_C (101 MHz, CD_3OD): (rotamers) 171.56, 157.09, 80.86, 63.73, 62.52, 59.66, 55.58, 53.23, 51.14, 50.38, 48.45, 42.54, 33.59, 31.15, 31.06, 30.56, 29.42, 27.32, 24.16, 24.03, 23.48; υ_{max} (neat) cm^{-1}: 3362 (w), 2980 (s), 1657 (s), 1392 (m), 1368 (m), 1155 (s); high resolution ESI-MS calcd. for $C_{15}H_{30}O_4N_3$ $[M+H]^+$ 316.22308, found: 316.22303; $[\alpha]_D^{25}$-16.5° (c 1.00, MeOH).

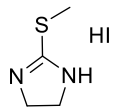

4.22

Imidazolidinethione (511 mg, 5 mmol) and MeI (342 µl, 5.5 mmol) were added to MeOH (1.25 ml). The resulting mixture was heated under microwave irradiation for 2 h at 80 °C. The solution was added to Et_2O, causing a white solid to precipitate. The suspension was filtered and the solid product washed with Et_2O. **4.22** (1.189 g, 4.871 mmol, 97%) was obtained as a white solid.

Mp 135 °C; δ_H (500 MHz, $CDCl_3$): 9.72 (s, 2H, N*H*), 3.94, (m, 4H, CH_2), 2.73 (m, 3H, CH_3); δ_C (126 MHz, $CDCl_3$): 171.29 (N*C*=N), 45.33 (*C*H_2), 15.14 (CH_3); υ_{max} (neat) cm^{-1}: 3387 (w), 992 (m); ESI-MS m/z 107.1 $[M+H]^+$.

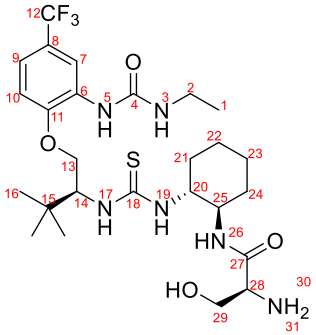

4.23

General procedure for thiourea formation was used to couple **4.15** (278 mg, 0.8 mmol) and **4.21** (338 mg, 1.12 mmol). Boc-protected product was purified by column chromatography (2-5% MeOH/DCM, R_f 0.35 with 5% MeOH/DCM) and obtained as a white solid (486 mg, 0.703 mmol, 72%). It was then treated with 4M HCl in dioxane (3 ml) for 30 min, the mixture was evaporated and the residue redissolved in DCM and sat. $NaHCO_{3(aq)}$. Organic phase was separated and the aqueous phase was extracted with DCM. Combined organic extracts were dried with anhydrous Na_2SO_4, filtered and evaporated. The crude product was purified by column chromatography (2-5% MeOH/DCM, R_f 0.27 with 5% MeOH/DCM) to afford **4.23** (302 mg, 0.51 mmol, 73%, 53% over 2 steps) as a white solid.

Mp 175 °C; δ_H (500 MHz, $CDCl_3$): δ 8.53 (d, *J* = 2.2 Hz, 1H, H^7), 8.09 (s, 1H, H^5), 7.37 (d, *J* = 8.6 Hz, 1H, H^{26}), 7.31 (d, *J* = 8.0 Hz, 1H, H^{19}), 7.12 (ddd, *J* = 8.4, 2.2, 0.9 Hz, 1H, H^9), 7.06 (d, *J* = 10.2 Hz, 1H, $H1^7$), 6.71 (d, *J* = 8.4 Hz, 1H, H^{10}), 6.43 (t, *J* = 5.6 Hz, 1H, H^3), 5.16 – 4.93 (m, 1H, H^{14}), 4.29 (dt, *J* = 14.7, 7.3 Hz, 2H, H^{13}, H^{28}), 3.76 (dd, *J* = 10.6, 8.8 Hz, 1H, H^{13}), 3.72 – 3.58 (m, 1H, H^{25}), 3.33 (qt, *J* = 7.3, 5.8 Hz, 2H, H^2), 3.11 (s, 1H, H^{29}), 2.93 (s, 2H, H^{29}, H^{20}), 2.42 (d, *J* = 12.4 Hz, 1H, H^{Cy}), 2.01 (d, *J* = 8.9 Hz, 1H, H^{Cy}), 1.82 (d, *J* = 14.1 Hz, 2H, H^{Cy}), 1.26 (t, *J* = 7.2 Hz, 3H, H^1), 1.45-1.1 (m 4H, H^{Cy}) 0.98 (s, 9H, H^{16}); δ_C (126 MHz, $CDCl_3$) 183.77 (C^{18}), 174.82 (C^{27}), 155.98 (C^4), 148.77 (C^{11}), 130.04 (C^6), 124.35 (q, J_{C-F} = 271.2 Hz, C^{12}), 123.33 (q, J_{C-F} = 31.5 Hz, C^8) 118.23 (C^9), 114.13 (C^7), 109.62 (C^{10}), 69.20 (C^{13}), 64.76 (C^{29}), 61.78 (C^{14}), 58.33 (C^{28}), 55.68 (C^{Cy}), 52.51 (C^{Cy}), 34.92 (C^2), 33.45 (C^{15}), 33.09 (C^{Cy}), 32.87 (C^{Cy}), 26.90 (C^{16}), 25.12 (C^{Cy}), 24.61 (C^{Cy}), 15.65 (C^1); δ_F (377 MHz, $CDCl_3$): -61.51; υ_{max} (neat) cm^{-1}: 3304 (w), 2939 (w), 1669 (w), 1550 (s), 1444 (m), 1116 (m); ESI-MS m/z 591.3 $[M+H]^+$; high resolution ESI-MS calcd for $C_{26}H_{41}F_3N_6O_4S$ $[M-H]^-$: 589.27893 Found: 589.27893.

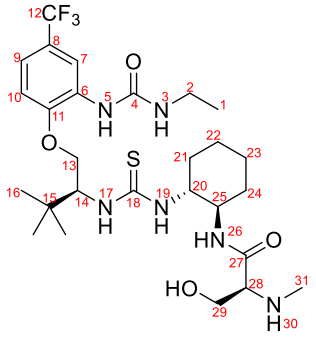

4.24

General procedure for thiourea formation was used to couple **4.15** (347 mg, 1 mmol) and **4.22** (379 mg, 1.2 mmol) in the presence of trimethylamine (0.150 ml, 2 mmol). The Boc-protected product was purified by silica column chromatography (1-2% MeOH/DCM). It was then dissolved in MeOH (5 ml), cooled to 0 °C and 4M HCl in dioxane (5 ml) was added. The mixture was then stirred at rt for 4 h. It was then evaporated under a stream of nitrogen and the residue partitioned in sat. aq. Na_2CO_3 and DCM. The solution was extracted with DCM, the extracts were dried on anhydrous Na_2SO_4, filtered and evaporated. The product was purified by silica column chromatography (2-5% MeOH/DCM) to afford **4.24** as a white solid (370 mg, 0.63 mmol, 63%).

Mp 188 °C, decomposition; δ_H (400 MHz, $CDCl_3$): 8.55 (s, 1H, H^7), 8.08 (s, 1H, H^5), 7.40 (d, J = 9.2 Hz, 1H, H^{19}), 7.26 (s, 1H, H^{26}), 7.12 (d, J = 8.3 Hz, 1H, H^9), 7.00 (s, 1H, H^{17}), 6.70 (d, J = 8.4 Hz, 1H, H^{10}), 6.40 (s, 1H, H^3), 5.04 (d, J = 10.8 Hz, 1H, H^{14}), 4.36 – 4.14 (m, 2H, H^{13}, H^{25}), 3.71 (t, J = 9.6 Hz, 2H, H^{13}, H^{20}), 3.35 (m, 2H, H^2), 3.05 (d, J = 22.9 Hz, 2H, H^{29}), 2.66 (s, 1H, H^{28}), 2.38 (s, 1H, H^{Cy}), 2.06 – 1.97 (m, 1H, H^{Cy}), 1.91 (s, 3H, H^{31}) 1.88 – 1.53 (m, 3H, H^{Cy}), 1.46 – 1.12 (m, 6H, H^1, H^{Cy}), 1.01 (s, 9H, H^{16}), 0.93 – 0.75 (m, 2H, H^{Cy}); δ_C (101 MHz, $CDCl_3$): 183.94 (C^{18}), 173.98 (C^{27}), 156.15 (C^4), 148.77 (C^{11}), 130.11 (C^6), 124.51 (q, $J_{C\text{-}F}$ = 270.0 Hz, C^{12}), 123.46 (q, $J_{C\text{-}F}$ = 32.0 Hz, C^8), 118.43 (C^9), 114.03 (C^7), 109.53 (C^{10}), 69.08 (C^{13}), 66.34 (C^{28}), 62.72 (C^{29}), 62.00 (C^{14}), 58.11 (C^{25}), 52.42 (C^{20}), 35.03 (C^2), 34.61 (C^{31}), 33.58 (C^{15}), 33.22 (C^{Cy}), 27.08 (C^{16}), 25.27 (C^{Cy}), 24.80 (C^{Cy}), 15.73 (C^1); δ_F (376 MHz, $CDCl_3$): -61.52; υ_{max} (neat) cm^{-1}: 3303 (w), 2980 (s), 1550 (s), 1444 (m), 1352 (m), 1240 (m), 1117 (m); high resolution ESI-MS calcd. for $C_{27}H_{44}O_4N_6F_3S$ $[M+H]^+$ 605.30914, found: 605.30941; $[\alpha]_D^{25}$ -22.0° (c 1.00, $CHCl_3$).

6.4.2 Second and third generation compounds

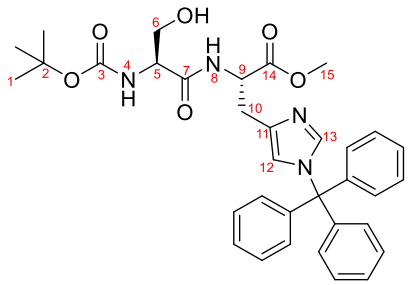

4.37

General procedure A for amide formation

Boc-Ser-OH (103 mg, 0.5 mmol) and NMM (60 µl, 0.55 mmol) were added to dry THF (2.5 ml) under argon. Separately, isobutyl chloroformate (68 µl, 0.525 mmol) was added to dry THF (2.5 ml). The chloroformate solution was cooled to −15 °C and the solution of Boc-Ser-OH and NMM was added dropwise over 15 min at −15 °C. The mixture was stirred at −15 °C for 15 min and H-His(Trt)-OMe (206 mg, 0.5 mmol) was added. The reaction was stirred for 10 min at −15 °C and for 2h at rt. The solvent was evaporated and the residue partitioned in DCM and sat. aq. $NaHCO_3$. The aqueous phase was further extracted with DCM, the extracts dried with anhydrous Na_2SO_4, filtered and evaporated. The product was purified by silica column chromatography (2-3% MeOH/DCM) to afford **4.37** as a white solid foam (286 mg, 0.48 mmol, 96%).

Mp 77 °C; δ_H (400 MHz, $CDCl_3$); 7.45 – 7.28 (m, 10H, H^{Trt}, H^{13}), 7.19 (d, J = 7.4 Hz, 1H, H^8), 7.08 (m, 6H, H^{Trt}), 6.50 (s, 1H, H^{12}), 6.32 (br s, 1H) 5.71 (d, J = 6.4 Hz, 1H, H^4), 4.79 (q, J = 5.7, 5.1 Hz, 1H, H^9), 4.09 (m, 2H, H^5, H^6), 3.68 (dd, J = 11.8, 4.5 Hz, 1H, H^6), 3.57 (s, 3H, H^{15}), 3.32 (dd, J = 14.6, 3.8 Hz, 1H, H^{10}), 2.83 (dd, J = 14.6, 5.6 Hz, 1H, H^{10}), 1.44 (s, 9H, H^1); δ_C (101MHz, $CDCl_3$); 171.48 (C^{14}), 171.17 (C^7), 155.48 (C^3), 142.09 (C^{Trt}), 138.85 (C^{13}), 135.96 (C^{11}), 129.85 (C^{Trt}), 128.28 (C^{Trt}), 128.26 (C^{Trt}), 120.09 (C^{12}), 80.16 (C^2), 75.58 (C^{Trt}), 63.17 (C^6), 57.45 (C^5), 53.43 (C^9), 52.46 (C^{15}), 29.15 (C^{10}), 28.43 (C^1); υ_{max} (neat) cm^{-1}: 3308, 2975, 1716, 1673, 1492, 1166, 749, 702; high resolution ESI-MS calcd. for $C_{34}H_{39}O_6N_4$ $[M+H]^+$: 599.28641, found: 599.28580; $[\alpha]_D^{25}$ −2.0° (c 1.00, MeOH).

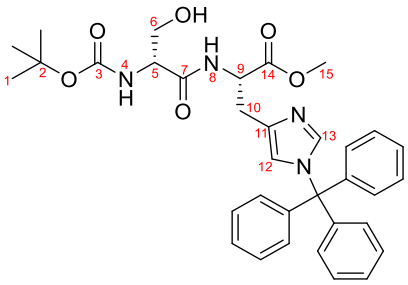

4.38

General procedure A was used to couple Boc-*D*-Ser-OH (103 mg, 0.5 mmol) and H-His(Trt)-OMe (206 mg, 0.5 mmol), the product was purified by silica column chromatography (2.5% MeOH/DCM) to afford **4.38** (155 mg, 0.259 mmol, 52%) as a white solid foam.

Mp 72–77 °C; δ_H (400 MHz, $CDCl_3$) 7.37 (d, J = 1.4 Hz, 1H, H^{13}), 7.36 – 7.30 (m, 9H, H^{Trt}), 7.12 – 7.03 (m, 6H, H^{Trt}), 6.89 (d, J = 7.8 Hz, 1H, H^{8}), 6.60 – 6.47 (m, 1H, H^{12}), 5.56 (d, J = 7.5 Hz, 1H, H^{4}), 4.86 (ddd, J = 7.8, 5.3, 3.8 Hz, 1H, H^{9}), 4.25 (td, J = 7.3, 3.8 Hz, 1H, H^{5}), 3.90 (dd, J = 11.7, 3.9 Hz, 1H, H^{6}), 3.63 (dd, J = 11.6, 7.1 Hz, 1H, H^{6}), 3.56 (s, 3H, H^{15}), 3.23 (dd, J = 14.6, 3.8 Hz, 1H, H^{10}), 2.88 (dd, J = 14.6, 5.3 Hz, 1H, H^{10}), 1.43 (s, 9H, H^{1}); δ_C (101 MHz, $CDCl_3$) 171.17 (C^{14}), 170.01 (C^{7}), 155.42 (C^{3}), 142.05 (C^{Trt}), 138.95 (C^{13}), 135.91 (C^{11}), 129.82 (C^{Trt}), 128.32 (C^{Trt}), 128.28 (C^{Trt}), 120.11 (C^{12}), 79.69 (C^{2}), 75.60 (C^{Trt}), 63.60 (C^{6}), 56.15 (C^{5}), 53.46 (C^{9}), 52.49 (C^{15}), 29.47 (C^{10}), 28.47 (C^{1}); υ_{max} (neat) cm^{-1}: 3310, 2980, 1742, 1716, 1671, 1490, 1166, 749, 701; high resolution ESI-MS calcd. for $C_{34}H_{39}O_6N_4$ $[M+H]^+$: 599.28641, found: 599.28603; $[\alpha]_D^{25}$ +15.9° (c 1.00, MeOH).

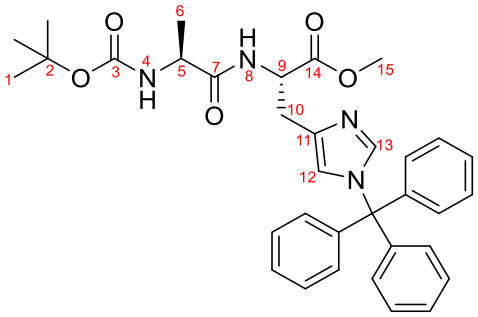

4.44

Boc-Ala-OH (47.3 mg, 0.250 mmol) and H-His(Trt)-OMe (103 mg, 0.250 mmol) were coupled according to the general procedure A. The product was purified by silica chromatography (2-3% MeOH/DCM) to provide **4.44** (145 mg, 0.249 mmol, quant.) as a white solid foam.

Mp 60–63 °C; δ_H (400 MHz, $CDCl_3$) 7.61 (d, J = 7.9 Hz, 1H, H^8), 7.36 (d, J = 1.4 Hz, 1H, H^{13}), 7.35 – 7.30 (m, 9H, H^{Trt}), 7.12 – 7.06 (m, 6H, H^{Trt}), 6.54 (d, J = 1.3 Hz, 1H, H^{12}), 5.29 (s, 1H, H^4), 4.77 (dt, J = 7.9, 4.8 Hz, 1H, H^9), 4.29 – 4.15 (m, 1H, H^5), 3.58 (s, 3H, H^{15}), 3.08 − 2.94 (m, 2H, H^{10}), 1.40 (s, 9H, H^1), 1.35 (d, J = 7.0 Hz, 3H, H^6); δ_C (101 MHz, $CDCl_3$) 172.54 (C^7/C^{14}), 171.58 (C^7/C^{14}), 155.24 (C^3), 142.34 (C^{Trt}), 138.79 (C^{13}), 136.48 (C^{11}), 129.85 (C^{Trt}), 128.20 (C^{Trt}), 119.76 (C^{12}), 79.64 (C^2), 52.58 (C^9), 52.25 (C^{15}), 50.13 (C^5), 29.75 (C^{10}), 28.46 (C^1), 19.21 (C^6); υ_{max} (neat) cm^{-1}: 2979, 1747, 1715, 1673, 1492, 1366, 1168, 749, 701; high resolution ESI-MS calcd. for $C_{34}H_{39}O_5N_4$ $[M+H]^+$: 583.29150, found: 583.29137; $[\alpha]_D^{25}$ −6.4° (c 1.00, MeOH).

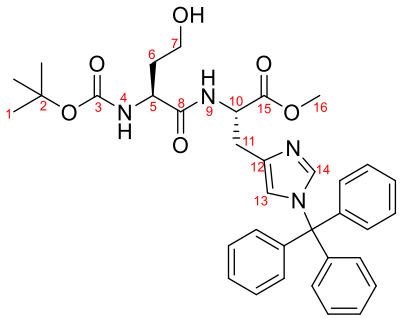

4.45

General procedure A was used to couple Boc-hSer-OH (110 mg, 0.5 mmol) and H-His(Trt)-OMe (206 mg, 0.5 mmol), the product was purified by silica column chromatography (3% MeOH/DCM) to afford **4.45** (80 mg, 0.131 mmol, 26%) as a white solid foam.

Mp 82 °C; δ_H (400 MHz, $CDCl_3$) 7.49 (d, J = 7.8 Hz, 1H, H^9), 7.42 (d, J = 1.4 Hz, 1H, H^{14}), 7.37 – 7.30 (m, 9H, H^{Trt}), 7.15 – 7.04 (m, 6H, H^{Trt}), 6.49 (d, J = 1.4 Hz, 1H, H^{13}), 6.17 (d, J = 7.7 Hz, 1H, H^4), 4.89 (dt, J = 8.1, 4.1 Hz, 1H, H^{10}), 4.53 – 4.37 (m, 1H, H^5), 3.89 – 3.74 (m, 1H, H^7), 3.74 – 3.63 (m, 1H, H^7), 3.50 (s, 3H, H^{16}), 3.15 – 2.90 (m, 2H, H^{11}), 2.08 (br s, 1H, O*H*) 2.07 – 1.98 (m, 2H, H^6), 1.43 (s, 9H, H^1); δ_C (101 MHz, $CDCl_3$) 171.27 (C^{15}), 171.00 (C^8), 155.87 (C^3), 142.07 (C^{Trt}), 138.96 (C^{14}), 135.94 (C^{12}), 129.82 (C^{Trt}), 128.30 (C^{Trt}), 128.26 (C^{Trt}), 120.23 (C^{13}), 79.95 (C^2), 75.58 (C^{Trt}), 58.05 (C^7), 53.50 (C^5), 52.75 (C^{10}), 52.20 (C^{16}), 34.59 (C^6), 30.24 (C^{11}), 28.47 (C^1); υ_{max} (neat) cm^{-1}: 3305, 2975, 1745, 1714, 1673, 1493, 1445, 1366, 1170, 1035, 749, 702, 661; high resolution ESI-MS calcd. for C35H41O6N4 $[M+H]^+$: 613.30206, found: 613.30160; $[\alpha]_D^{25}$ −7.8° (c 1.00, MeOH).

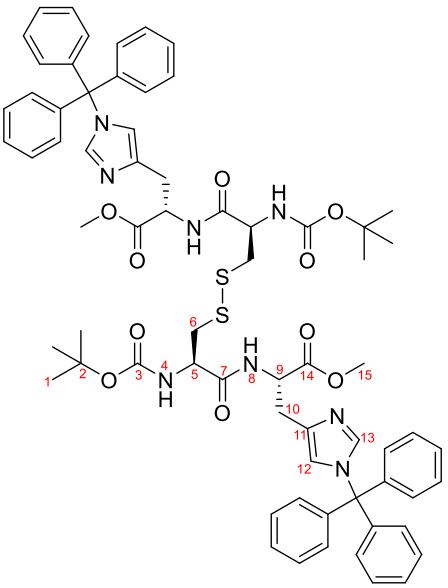

4.46

(Boc-Cys-OH)$_2$ (88 mg, 0.200 mmol) and H-His(Trt)-OMe (181 mg, 0.440 mmol) were coupled according to the general procedure A. The product was purified by silica chromatography to provide **4.46** (246 mg, 0.200 mmol, quant.) as a white solid foam.

Mp 88 °C; δ_H (400 MHz, $CDCl_3$); 7.94 (d, J = 7.9 Hz, 1H, H^8), 7.35 (d, J = 1.4 Hz, 1H, H^{13}), 7.34 – 7.28 (m, 9H, H^{Trt}), 7.09 (ddd, J = 6.2, 2.6, 1.3 Hz, 6H, H^{Trt}), 6.54 (d, J = 1.4 Hz, 1H, H^{12}), 5.90 (d, J = 8.3 Hz, 1H, H^4), 4.76 (dt, J = 7.8, 5.2 Hz, 1H, H^9), 4.53 (s, 1H, H^5), 3.57 (s, 3H, H^{15}), 3.21 – 3.04 (m, 2H, H^6), 3.01 (d, J = 5.3 Hz, 2H, H^{10}), 1.37 (s, 9H, H^1); δ_C (101 MHz, $CDCl_3$) 171.56 (C^{14}), 170.19 (C^7), 155.45 (C^3), 142.40 (C^{Trt}), 138.84 (C^{13}), 136.38 (C^{11}), 129.87 (C^{Trt}), 128.18 (C^{Trt}), 119.59 (C^{12}), 80.04 (C^2), 75.33 (C^{Trt}), 54.05 (C^5), 52.92 (C^9), 52.27 (C^{15}), 42.57 (C^6), 29.99 (C^{10}), 28.47 (C^1); υ_{max} (neat) cm^{-1}: 1683, 1490, 1167, 749, 669; high resolution ESI-MS calcd. for $C_{68}H_{75}O_{10}N_8S_2$ $[M+H]^+$: 1227.50421, found: 1227.50471; $[\alpha]_D^{25}$ −43.3° (c 1.00, MeOH).

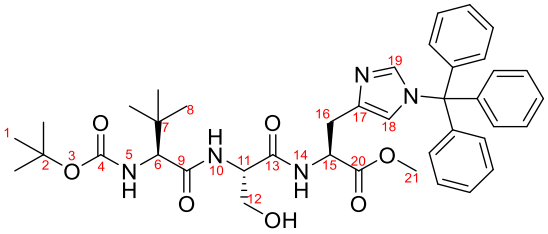

4.39

General procedure B for N-Boc deprotection

Compound **4.37** was dissolved in 2:1 4M HCl in 1,4-dioxane/MeOH at 0 °C, the resulting solution was stirred at rt for 2 h. It was then evaporated and the residue was partitioned in EtOAc and sat. aq. $NaHCO_3$. The aqueous phase was further extracted with EtOAc, the extracts dried with anhydrous Na_2SO_4, filtered and evaporated. The deprotected amine was used directly in the subsequent step.

General procedure C for amide formation

Boc-*tert*-leucine (108 mg, 0.468 mmol) and DIPEA (148 µl, 0.850 mmol) were added to dry DMF (5 ml). The solution was cooled to 0 °C and TBTU (164 mg, 0.510 mmol) was added. The mixture was stirred for 5 min at 0 °C and added to a fine suspension of Boc-deprotected **4.37** (212 mg, 0.425 mmol) in dry DMF at 0 °C. The reaction was stirred at 0 °C for 15 min and at rt for 16 h. The mixture was then diluted with water and extracted with Et_2O. The combined extracts were dried with anhydrous Na_2SO_4, filtered and evaporated. The product was purified by silica column chromatography (2-3% MeOH/DCM) to afford **4.39** as a white solid foam (290 mg, 0.407 mmol, 96%).

Mp 89–94 °C; δ_H (400 MHz, $CDCl_3$) 7.39 (d, J = 1.4 Hz, 1H, H^{19}), 7.35 (tt, J = 4.1, 2.1 Hz, 9H, H^{Trt}), 7.30 (d, J = 8.0 Hz, 1H, H^{14}), 7.15 – 7.05 (m, 6H, H^{Trt}), 6.95 (d, J = 6.7 Hz, 1H, H^{10}), 6.53 (d, J = 1.3 Hz, 1H, H^{18}), 5.31 (s, 1H, H^{5}), 4.81 (ddd, J = 7.9, 5.6, 3.8 Hz, 1H, H^{15}), 4.41 (ddd, J = 7.0, 4.6, 2.2 Hz, 1H, H^{11}), 4.09 (dd, J = 11.9, 2.3 Hz, 1H, H^{12}), 3.93 (d, J = 8.9 Hz, 1H, H^{6}), 3.71 (dd, J = 11.9, 4.8 Hz, 1H, H^{12}), 3.57 (s, 3H, H^{21}), 3.22 (dd, J = 14.6, 3.9 Hz, 1H, H^{16}), 2.90 (dd, J = 14.1, 6.2 Hz, 1H, H^{16}), 1.43 (s, 9H, H^{1}), 1.02 (s, 9H, H^{8}); δ_C (101 MHz, $CDCl_3$) 171.37 (C^{9}/C^{20}), 171.19 (C^{9}/C^{20}), 170.40 (C^{13}), 155.82 (C^{4}), 142.08 (C^{Trt}), 138.89 (C^{19}), 135.95 (C^{17}), 129.79 (C^{Trt}), 128.26 (C^{Trt}), 128.23 (C^{Trt}), 119.98 (C^{18}), 79.80 (C^{2}), 75.53 (C^{Trt}), 62.90 (C^{12}), 62.51 (C^{6}), 56.17 (C^{11}), 53.38 (C^{15}), 52.43 (C^{21}), 34.69 (C^{7}), 29.18 (C^{16}), 28.42 (C^{1}), 26.74 (C^{8}); υ_{max} (neat) cm^{-1}: 3311, 2954, 1654, 1495, 1392, 1171, 749, 702, 669; high resolution ESI-MS calcd. for $C_{40}H_{50}O_7N_5$ $[M+H]^+$ 712.37048, found: 712.36983; $[\alpha]_D^{25}$ -3.8° (c 1.00, MeOH).

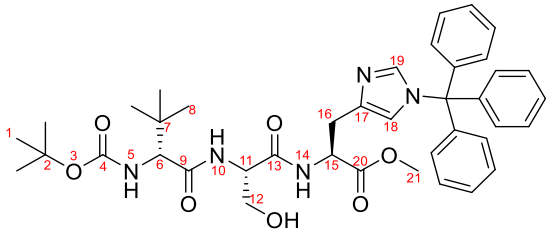

4.40

Boc-Ser-His(Trt)-OMe **4.37** was N-Boc deprotected according to the general procedure B. The resulting amine (270 mg, 0.54 mmol) was coupled with Boc-*D*-^{t}Leu-OH (137 mg, 0.59 mmol) according to the general procedure C. The product was purified by silica chromatography (2-3% MeOH/DCM) to afford **4.40** (305 mg, 0.428 mmol, 79%) as a white solid foam.

Mp 95 °C; δ_H (400 MHz, $CDCl_3$) 7.37 (s, 1H, H^{19}), 7.36 – 7.29 (m, 10H, H^{14}, H^{Trt}), 7.12 – 7.05 (m, 6H, H^{Trt}), 6.98 (d, J = 7.0 Hz, 1H, H^{10}), 6.51 (s, 1H, H^{18}), 5.30 (d, J = 8.3 Hz, 1H, H^{5}), 4.76 (ddd, J = 7.9, 5.9, 3.8 Hz, 1H, H^{15}), 4.41 (ddd, J = 7.1, 4.7, 2.2 Hz, 1H, H^{11}), 4.09 (dd, J = 11.8, 2.3 Hz, 1H, H^{12}), 3.92 (d, J = 8.9 Hz, 1H, H^{6}), 3.66 (dd, J = 11.8, 4.9 Hz, 1H, H^{12}), 3.56 (s, 3H, H^{21}), 3.22 (dd, J = 14.6, 3.8 Hz, 1H, H^{16}), 2.89 (dd, J = 14.5, 6.0 Hz, 1H, H^{16}), 2.13 (s, 1H, O*H*), 1.42 (s, 9H, H^{1}), 0.99 (s, 9H, H^{8}); δ_C (101 MHz, $CDCl_3$) 171.37 (C^{9}/C^{13}/C^{20}), 171.14 (C^{9}/C^{13}/C^{20}), 170.40 (C^{9}/C^{13}/C^{20}), 155.91 (C^{4}), 142.13 (C^{Trt}), 138.94 (C^{19}), 136.09 (C^{17}), 129.86 (C^{Trt}), 128.27 (C^{Trt}), 120.03 (C^{18}), 79.81 (C^{2}), 75.58 (C^{Trt}), 63.11 (C^{12}), 62.68 (C^{6}), 55.96 (C^{11}), 53.48 (C^{15}), 52.47 (C^{21}), 34.65 (C^{7}), 29.04 (C^{16}), 28.44 (C^{1}), 26.77 (C^{8}); υ_{max} (neat) cm^{-1}: 3324, 2971, 1669, 1495, 1446, 1367, 1240, 1172, 749, 702, 669; high resolution ESI-MS calcd. for $C_{40}H_{50}O_7N_5$ $[M+H]^+$: 712.37048, found: 712.37008; $[\alpha]_D^{25}$ -1.96° (c 1.00, MeOH).

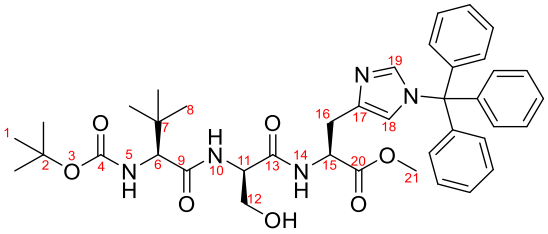

4.41

Boc-*D*-Ser-His(Trt)-OMe **4.38** was N-Boc deprotected according to the general procedure B. The resulting amine (70 mg, 0.140 mmol) was coupled with Boc-^{t}Leu-OH (29.5 mg, 0128 mmol) according to the general procedure C. The product was purified by silica chromatography (2.5-3% MeOH/DCM) to afford **4.41** (70 mg, 0.0983 mmol, 77%) as a white solid foam.

Mp 108 °C; δ_H (400 MHz, $CDCl_3$) 7.37 (d, J = 1.4 Hz, 1H, H^{19}), 7.35 – 7.30 (m, 9H, H^{Trt}), 7.12 – 7.01 (m, 6H, H^{Trt}), 6.92 (d, J = 7.5 Hz, 1H, H^{14}), 6.73 (d, J = 6.8 Hz, 1H, H^{10}), 6.49 (d, J = 1.4 Hz, 1H, H^{18}), 5.40 (d, J = 9.1 Hz, 1H, H^{5}), 4.85 (ddd, J = 7.5, 5.1, 3.8 Hz, 1H, H^{15}), 4.57 (td, J = 6.7, 3.6 Hz, 1H, H^{11}), 3.98 – 3.86 (m, 2H, H^{6}, H^{12}), 3.65 (dd, J = 11.7, 6.6 Hz, 1H, H^{12}), 3.56 (s, 3H, H^{21}), 3.26 (dd, J = 14.6, 3.8 Hz, 1H, H^{16}), 2.93 – 2.83 (m, 1H, H^{16}), 1.40 (s, 9H, H^{1}), 0.98 (s, 9H, H^{8}); δ_C (101 MHz, $CDCl_3$) 170.98 (C^{9}/C^{13}/C^{20}), 170.03 (C^{9}/C^{13}/C^{20}), 169.09 (C^{9}/C^{13}/C^{20}), 155.59 (C^{4}), 141.90 (C^{Trt}), 138.85 (C^{19}), 135.63 (C^{17}), 129.70 (C^{Trt}), 128.22 (C^{Trt}), 128.17 (C^{Trt}), 120.05 (C^{18}), 79.42 (C^{2}), 75.51 (C^{Trt}), 62.72 (C^{12}), 62.27 (C^{6}), 55.22 (C^{11}), 53.45 (C^{15}), 52.45 (C^{21}), 34.82 (C^{7}), 29.22 (C^{16}), 28.36 (C^{1}), 26.67 (C^{8}); υ_{max} (neat) cm^{-1}: 2981, 2888, 1653, 1492, 1391, 1250, 1163, 1071, 955, 702, 669; high resolution ESI-MS calcd. for $C_{40}H_{50}O_7N_5$ $[M+H]^+$: 712.37048, found: 712.36977; $[\alpha]_D^{25}$ +9.6° (c 1.00, MeOH).

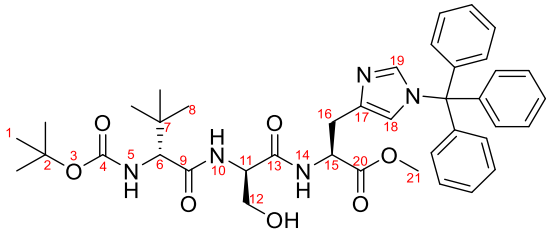

4.42

Boc-*D*-Ser-His(Trt)-OMe **4.38** was N-Boc deprotected according to the general procedure B. The resulting amine (160 mg, 0.32 mmol) was coupled with Boc-*D*-^{t}Leu-OH (74 mg, 0.32 mmol) according to the general procedure C. The product was purified by silica chromatography (2-3% MeOH/DCM) to afford **4.42** (177 mg, 0.249 mmol, 78%) as a white crystalline solid.

Mp 201 °C; δ_H (400 MHz, $CDCl_3$) 7.37 (s, 1H, H^{19}), 7.36 – 7.28 (m, 9H, H^{Trt}), 7.13 – 7.01 (m, 6H, H^{Trt}), 6.86 (d, J = 7.7 Hz, 1H, H^{14}), 6.74 (d, J = 7.3 Hz, 1H, H^{10}), 6.50 (s, 1H, H^{18}), 5.33 (d, J = 9.1 Hz, 1H, H^{5}), 4.86 (dt, J = 8.2, 4.5 Hz, 1H, H^{15}), 4.55 (td, J = 7.0, 3.8 Hz, 1H, H^{11}), 3.95 – 3.85 (m, 2H, H^{6}, H^{12}), 3.63 (dd, J = 11.7, 7.0 Hz, 1H, H^{12}), 3.55 (s, 3H, H^{21}), 3.23 (dd, J = 14.7, 3.8 Hz, 1H, H^{16}), 2.87 (dd, J = 14.6, 5.3 Hz, 1H, H^{16}), 2.15 (s, 1H, O*H*), 1.42 (s, 9H, H^{1}), 0.98 (s, 9H, H^{8}); δ_C (101 MHz, $CDCl_3$) 171.06 (C^{9}/C^{13}/C^{20}), 170.41 (C^{9}/C^{13}/C^{20}), 169.29 (C^{9}/C^{13}/C^{20}), 155.78 (C^{4}), 142.01 (C^{Trt}), 138.94 (C^{19}), 135.77 (C^{17}), 129.79 (C^{Trt}), 128.31 (C^{Trt}), 128.27 (C^{Trt}), 120.16 (C^{18}), 79.63 (C^{2}), 75.61 (C^{Trt}), 62.89 (C^{12}), 62.57 (C^{6}), 54.95 (C^{11}), 53.51 (C^{15}), 52.49 (C^{21}), 34.89 (C^{7}), 29.50 (C^{16}), 28.44 (C^{1}), 26.74 (C^{8}); υ_{max} (neat) cm^{-1}: 3308, 2969, 1743, 1650, 1494, 1445, 1366, 1238, 1172, 749, 702, 660, 638; high resolution ESI-MS calcd. for $C_{40}H_{50}O_7N_5$ $[M+H]^+$: 712.37048, found: 712.36998; $[\alpha]_D^{25}$ +26.5° (c 1.00, MeOH).

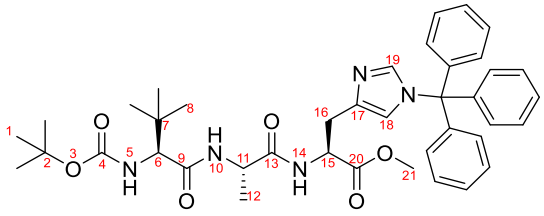

4.47

Boc-Ala-His(Trt)-OMe **4.44** was N-Boc deprotected according to the general procedure B. The resulting amine (96.5 mg, 0.200 mmol) was coupled with Boc-^{t}Leu-OH (46 mg, 0.200 mmol) according to the general procedure A. The product was purified by silica chromatography to afford **4.47** (95 mg, 0.136 mmol, 68%) as a white solid foam.

Mp 80–84 °C; δ_H (400 MHz, $CDCl_3$) 7.62 (d, J = 7.9 Hz, 1H, H^{14}), 7.31 (d, J = 1.4 Hz, 1H, H^{19}), 7.32 – 7.20 (m, 9H, H^{Trt}), 7.10 – 6.95 (m, 6H, H^{Trt}), 6.66 (d, J = 7.4 Hz, 1H, H^{10}), 6.48 (d, J = 1.3 Hz, 1H, H^{18}), 5.24 (d, J = 9.3 Hz, 1H, H^{5}), 4.71 (dt, J = 7.8, 4.7 Hz, 1H, H^{15}), 4.47 (p, J = 7.0 Hz, 1H, H^{11}), 3.78 (d, J = 9.4 Hz, 1H, H^{6}), 3.50 (s, 3H, H^{21}), 2.98 (dd, J = 14.7, 5.0 Hz, 1H, H^{16}), 2.88 (dd, J = 14.5, 4.7 Hz, 1H, H^{16}), 1.35 (s, 9H, H^{1}), 1.33 (d, J = 7.0 Hz, 3H, H^{12}), 0.88 (s, 9H, H^{8}); δ_C (100 MHz, $CDCl_3$) 171.76 (C^{9}/C^{13}/C^{20}), 171.30 (C^{9}/C^{13}/C^{20}), 170.28 (C^{9}/C^{13}/C^{20}), 155.69 (C^{4}), 142.17 (C^{Trt}), 138.77 (C^{19}), 136.24 (C^{17}), 129.73 (C^{Trt}), 129.13 (C^{Trt}), 128.10 (C^{Trt}), 119.69 (C^{18}), 79.51 (C^{2}), 75.32 (C^{Trt}), 62.27 (C^{6}), 52.63 (C^{15}), 52.15 (C^{21}), 48.72 (C^{11}), 34.77 (C^{7}), 29.47 (C^{16}), 28.34 (C^{1}), 26.61 (C^{8}), 18.84 (C^{12}); υ_{max} (neat) cm^{-1}: 2975, 1748, 1650, 1494, 1173, 748, 702, 659; high resolution ESI-MS calcd. for C40H50O6N5 $[M+H]^+$: 696.37556, found: 696.37503; $[\alpha]_D^{25}$ −14.8° (c 1.00, MeOH).

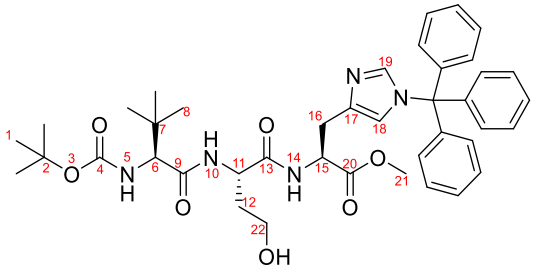

4.48

Boc-hSer-His(Trt)-OMe **4.45** was N-Boc deprotected according to the general procedure B. The resulting amine (65 mg, 0.127 mmol) was coupled with Boc-^{t}Leu-OH (29 mg, 0.127 mmol) according to the general procedure C. The product was purified by silica chromatography to afford **4.48** (62 mg, 0.0854 mmol, 67%) as an oily semisolid.

δ_H (400 MHz, $CDCl_3$) 7.43 (s, 1H), 7.43 – 7.39 (m, 1H), 7.38 (d, J = 1.4 Hz, 1H, H^{19}), 7.36 – 7.31 (m, 9H, H^{Trt}), 7.14 – 7.01 (m, 6H, H^{Trt}), 6.50 (d, J = 1.4 Hz, 1H, H^{18}), 5.29 (d, J = 9.1 Hz, 1H, H^{5}), 4.93 (dt, J = 8.3, 4.1 Hz, 1H, H^{15}), 4.70 (td, J = 7.2, 3.6 Hz, 1H, H^{11}), 3.87 (d, J = 9.2 Hz, 1H, H^{6}), 3.83 – 3.65 (m, 2H, H^{22}), 3.51 (s, 3H, H^{21}), 3.08 – 2.93 (m, 2H, H^{16}), 2.16 – 1.93 (m, 2H, H^{12}), 1.42 (s, 9H, H^{1}), 0.96 (s, 9H, H^{8}); δ_C (101 MHz, $CDCl_3$) 171.48 (C^{9}/C^{13}/C^{20}), 170.89 (C^{9}/C^{13}/C^{20}), 170.56 (C^{9}/C^{13}/C^{20}), 155.83 (C^{4}), 142.02 (C^{Trt}), 138.92 (C^{19}), 135.75 (C^{17}), 129.79 (C^{Trt}), 128.37 (C^{Trt}), 128.29 (C^{Trt}), 120.15 (C^{18}), 79.74 (C^{2}), 75.60 (C^{Trt}), 62.73 (C^{6}), 58.06 (C^{22}), 52.74 (C^{15}), 52.24 (C^{11}), 34.71 (C^{12}), 30.32 (C^{16}), 28.44 (C^{1}), 26.79 (C^{8}); υ_{max} (neat) cm^{-1}: 3323, 2954, 1654, 1494, 1171, 749, 702, 669; high resolution ESI-MS calcd. for $C_{41}H_{52}O_7N_5$ $[M+H]^+$: 726.38613, found: 726.38541; $[\alpha]_D^{25}$ −12.3° (c 1.00, MeOH).

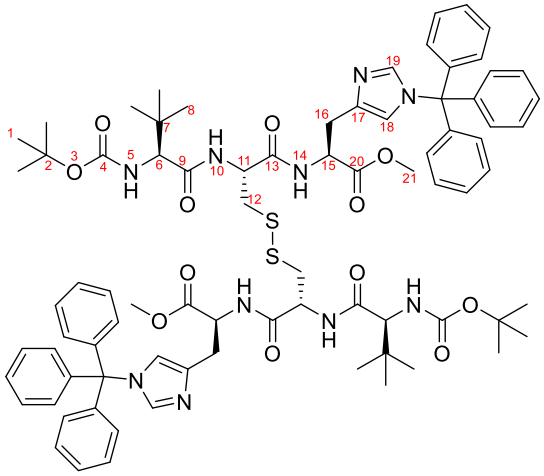

4.49

(Boc-Cys-His(Trt)-OMe)$_2$ **4.46** was N-Boc deprotected according to the general procedure B. The resulting amine (195 mg, 0.190 mmol) was coupled with Boc-^{t}Leu-OH (97 mg, 0.418 mmol) according to the general procedure C. The product was purified by silica chromatography to afford **4.49** (228 mg, 0.157 mmol, 83%) as a white solid foam.

Mp 126–130°C; δ_H (400 MHz, $CDCl_3$) 8.31 (d, J = 7.4 Hz, 1H, H^{10}), 7.40 (d, J = 1.5 Hz, 1H, H^{19}), 7.35 – 7.27 (m, 9H, H^{Trt}), 7.13 – 7.05 (m, 6H, H^{Trt}), 7.03 (d, J = 8.1 Hz, 1H, H^{14}), 6.56 (s, 1H, H^{18}), 6.05 (d, J = 9.5 Hz, 1H, H^5), 5.33 – 5.18 (m, 1H, H^{11}), 4.73 (q, J = 6.4 Hz, 1H, H^{15}), 3.99 (d, J = 9.5 Hz, 1H, H^6), 3.56 (s, 3H, H^{21}), 3.11 – 2.93 (m, 3H, H^{12}, H^{16}), 2.93 – 2.81 (m, 1H, H^{12}), 1.33 (s, 9H, H^1), 0.93 (s, 9H, H^8); δ_C (101 MHz, $CDCl_3$) 171.89 (C^9/C^{13}/C^{20}), 171.48 (C^9/C^{13}/C^{20}), 169.75 (C^9/C^{13}/C^{20}), 156.21 (C^4), 142.43 (C^{Trt}), 139.00 (C^{19}), 136.13 (C^{17}), 129.84 (C^{Trt}), 128.14 (C^{Trt}), 119.47 (C^{18}), 79.54 (C^2), 75.28 (C^{Trt}), 62.80 (C^6), 53.34 (C^{15}), 52.72 (C^{11}), 52.21 (C^{21}), 44.08 (C^{12}), 34.70 (C^7), 30.73 (C^{16}), 28.46 (C^1), 26.83 (C^8); υ_{max} (neat) cm^{-1}: 2980, 1653, 1495, 1367, 1170, 749, 702 669; high resolution ESI-MS calcd. for $C_{80}H_{97}O_{12}N_{10}S_2$ $[M+H]^+$ 1453.67234, found: 1453.67366; $[\alpha]_D^{25}$ −21.7° (c 1.00, MeOH).

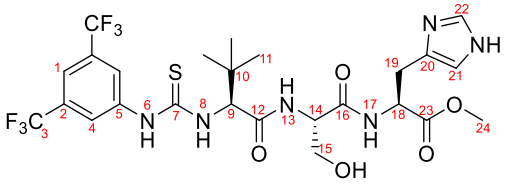

4.25

General procedure D for thiourea or urea formation

Boc-^{t}Leu-Ser-His(Trt)-OMe **4.39** was N-Boc deprotected according to the general procedure B. The resulting amine (91 mg, 0.149 mmol) was dissolved in 9:1 DCM/MeOH (1.5 ml) and 3,5-bis(trifluoromethyl)phenyl isothiocyanate (33 µl, 0.179 mmol) was added. The mixture was stirred at rt for 4 h, evaporated and dried under high vacuum. The resulting material was used directly in the subsequent step.

General procedure E for imidazolyl-Trt deprotection

Trityl-protected product obtained as described above was dissolved in 5% solution of pyridinium hydrochloride in MeOH (1.5 ml). The solution was stirred for 2 h at 65 °C and cooled to rt. It was then partitioned in EtOAc and sat. aq. $NaHCO_3$. The aqueous phase was further extracted with EtOAc, the extracts dried with anhydrous Na_2SO_4, filtered and evaporated. The product was purified by silica column chromatography (10% MeOH/DCM) to provide **4.25** as a white solid foam (71 mg, 0.111 mmol, 74%).

Mp 129–133 °C; δ_H (400 MHz, 5% methanol-d_4/$CDCl_3$) 9.91 (s, 1H, H^6), 8.06 (d, J = 1.5 Hz, 2H, H^4), 7.82 (d, J = 7.2 Hz, 1H, H^{13}), 7.69 (d, J = 8.2 Hz, 1H, H^8), 7.62 (d, J = 8.1 Hz, 1H, H^{17}), 7.53 (s, 1H, H^1), 7.48 (d, J = 1.2 Hz, 1H, H^{22}), 6.72 (d, J = 1.1 Hz, 1H, H^{21}), 4.80 (s, 1H, H^9), 4.70 (dt, J = 7.3, 4.7 Hz, 1H, H^{18}), 4.46 (dd, J = 5.9, 3.5 Hz, 1H, H^{14}), 3.89 (dd, J = 11.6, 4.4 Hz, 1H, H^{15}), 3.73 (dd, J = 11.6, 4.9 Hz, 1H, H^{15}), 3.64 (s, 3H, H^{24}), 3.10 (dd, J = 15.0, 4.3 Hz, 1H, H^{19}), 2.95 (dd, J = 14.9, 7.3 Hz, 1H, H^{19}), 1.03 (s, 9H, H^{11}); δ_C (100 MHz, 5% methanol-d_4/$CDCl_3$) 181.96 (C^7), 171.88 (C^{12}), 171.43 (C^{23}), 170.63 (C^{16}), 140.81 (C^5), 135.39 (C^{22}), 132.28 (C^{20}), 131.67 (q, J = 33.23 Hz, C^2) 123.20 (q, J = 270.94 Hz, C^3) 123.00 (C^4), 117.79 (C^1, C^{21}), 66.19 (C^9), 62.28 (C^{15}), 55.83 (C^{14}), 53.05 (C^{18}), 52.67 (C^{24}), 34.60 (C^{10}), 28.68 (C^{19}), 26.92 (C^{11}); δ_F (376 MHz, $CDCl_3$ + 5% methanol-d_4) -63.08; υ_{max} (neat) cm^{-1}: 3301, 2962, 1742, 1653, 1531, 1384, 1278, 1178, 1134; high resolution ESI-MS calcd. for $C_{25}H_{30}F_6N_6O_5S$ $[M+H]^+$: 641.19753, found 641.19642; $[\alpha]_D^{25}$ -41.0° (c 1.00, MeOH).

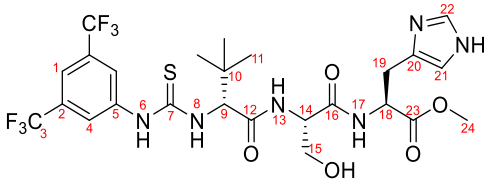

4.26

Compound **4.40** was N-Boc deprotected according to the general procedure B. The resulting amine (60 mg, 0.098 mmol) was treated according to the general procedures D and E. The product was purified by silica chromatography (8-10% MeOH/DCM) to afford **4.26** (40 mg, 0.0624 mmol, 64%) as a white semisolid.

δ_H (500 MHz, $CDCl_3$/DMSO-d_6) 10.00 (s, 1H, H^6), 8.02 (s, 2H, H^4), 7.86 (d, J = 8.6 Hz, 1H, H^8), 7.73 (d, J = 7.3 Hz, 1H, H^{13}), 7.49 (d, J = 8.4 Hz, 1H, H^{17}), 7.36 (s, 1H, H^1), 7.32 (s, 1H, H^{22}), 6.60 (s, 1H, H^{21}), 4.72 (d, J = 8.3 Hz, 1H, H^9), 4.54 (td, J = 8.4, 3.5 Hz, 1H, H^{18}), 4.21 (dt, J = 7.3, 3.4 Hz, 1H, H^{14}), 3.90 – 3.84 (m, 1H, H^{15}), 3.57 (dd, J = 11.6, 4.3 Hz, 1H, H^{15}), 3.38 (s, 3H, H^{24}), 2.98 (dd, J = 14.9, 3.6 Hz, 1H, H^{19}), 2.81 (dd, J = 14.8, 8.2 Hz, 1H, H^{19}), 0.94 (s, 9H, H^{11}); δ_C (126 MHz, $CDCl_3$/DMSO-d_6) 181.39 (C^7), 171.02 (C^{23}), 170.75 (C^{12}), 170.18 (C^{16}), 141.24 (C^5), 135.12 (C^{22}), 133.02 (C^{20}), 130.91 (q, $J_{C\text{-}F}$ = 33.2 Hz, C^2), 123.00 (q, $J_{C\text{-}F}$ = 272.6 Hz, C^3), 122.06 (C^4), 116.69 (C^{21}), 116.54 (C^1), 65.04 (C^9), 62.09 (C^{15}), 55.84 (C^{14}), 52.67 (C^{18}), 51.80 (C^{24}), 34.15 (C^{10}), 28.65 (C^{19}), 26.62 (C^{11}); δ_F (471 MHz, $CDCl_3$/DMSO-d_6) -62.90; υ_{max} (neat) cm^{-1}: 3293, 2960, 1746, 1655, 1537, 1474, 1386, 1277, 1175, 1132, 963, 681; high resolution ESI-MS calcd. for $C_{25}H_{31}F_6N_6O_5S$ $[M+H]^+$: 641.19753, found: 641.19734; $[\alpha]_D^{25}$ +46.2° (c 1.00, MeOH).

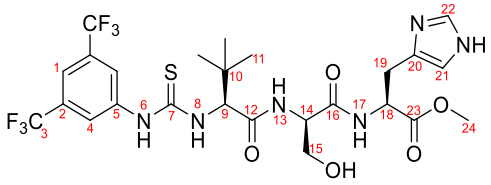

4.27

Boc-^{t}Leu-*D*-Ser-His(Trt)-OMe **4.41** was N-Boc deprotected according to the general procedure B. The resulting amine (87 mg, 0.142 mmol) was treated according to the general procedures D and E. The product was purified by silica column chromatography to provide **4.27** (64 mg, 0.0999 mmol, 70%) as a white solid foam.

Mp 132–135 °C; δ_H (500 MHz, $CDCl_3$/DMSO-d_6) 9.75 (s, 1H, H^6), 7.80 – 7.65 (m, 2H, H^4), 7.56 (s, 1H, H^8), 7.54 (s, 1H, H^{13}), 7.30 (d, J = 8.1 Hz, 1H, H^{17}), 7.04 (s, 1H, H^1), 7.01 (d, J = 1.1 Hz, 1H, H^{22}), 6.29 (s, 1H, H^{21}), 4.43 (d, J = 8.5 Hz, 1H, H^9), 4.26 (td, J = 7.9, 4.2 Hz, 1H, H^{18}), 3.99 (dt, J = 7.2, 5.1 Hz, 1H, H^{14}), 3.43 (dd, J = 11.3, 4.7 Hz, 1H, H^{15}), 3.27 – 3.15 (m, 4H, H^{15}, H^{24}), 2.66 (dd, J = 14.7, 4.3 Hz, 1H, H^{19}), 2.52 (dd, J = 14.7, 7.7 Hz, 1H, H^{19}), 0.62 (s, 9H, H^{11}); δ_C (126 MHz, $CDCl_3$/DMSO-d_6) 180.32 (C^7), 170.41 (C^{23}), 169.75 (C^{12}), 168.70 (C^{16}), 140.71 (C^5), 134.19 (C^{22}), 130.06 (q, J = 33.3 Hz, C^2), 122.31 (q, J = 272.4 Hz, C^3) 121.08 (C^4), 115.53 (C^1), 64.12 (C^9), 61.32 (C^{15}), 54.75 (C^{14}), 51.96 (C^{18}), 51.23 (C^{24}), 33.88 (C^{10}), 27.97 (C^{19}), 26.07 (C^{11}); δ_F (471 MHz, $CDCl_3$/DMSO-d_6) -62.61; υ_{max} (neat) cm^{-1}: 3293, 2962, 1741, 1653, 1533, 1384, 1278, 1177, 1133; high resolution ESI-MS calcd. for $C_{25}H_{31}O_5N_6F_6S$ $[M+H]^+$ 641.19753, found: 641.19701; $[\alpha]_D^{25}$ -32.3° (c 1.00, MeOH).

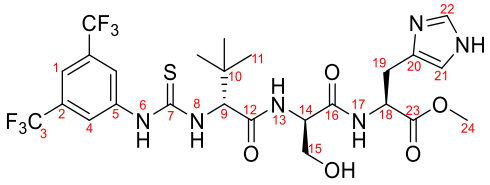

4.28

Compound **4.42** was N-Boc deprotected according to the general procedure B. The resulting amine (71mg, 0.116 mmol) was treated according to the general procedures D and E. The product was purified by silica chromatography (5-9% MeOH/DCM) to afford **4.28** (55 mg, 0.0859 mmol, 74%) as a white solid foam.

Mp 118 °C; δ_H (500 MHz, $CDCl_3$/DMSO-d_6) 9.99 (s, 1H, H^6), 8.14 (s, 2H, H^4), 7.91 (d, J = 8.5 Hz, 1H, H^8), 7.49 (s, 1H, H^1), 7.47 (s, 1H, H^{22}), 7.33 – 7.27 (m, 1H, H^{13}), 7.25 (d, J = 8.0 Hz, 1H, H^{17}), 6.73 (s, 1H, H^{21}), 4.86 (d, J = 8.6 Hz, 1H, H^9), 4.78 (q, J = 7.1, 6.2 Hz, 1H, H^{18}), 4.52 (q, J = 6.3 Hz, 1H, H^{14}), 3.94 – 3.83 (m, 1H, H^{15}), 3.74 – 3.58 (m, 4H, H^{15}, H^{24}), 3.24 – 3.13 (m, 1H, H^{19}), 3.00 – 2.88 (m, 1H, H^{19}), 1.02 (s, 9H, H^{11}); δ_C (126 MHz, $CDCl_3$/DMSO-d_6) 181.58 (C^7), 171.31 (C^{23}), 170.57 (C^{12}), 169.59 (C^{16}), 141.34 (C^5), 135.41 (C^{22}), 132.94 (C^{20}), 131.32 (q, $J_{C\text{-}F}$ = 33.3 Hz, C^2), 123.23 (q, $J_{C\text{-}F}$ = 272.5 Hz, C^3), 122.39 (C^4), 117.01 (C^1), 116.70 (C^{21}), 65.61 (C^9), 62.53 (C^{15}), 55.14 (C^{14}), 53.17 (C^{18}), 52.46 (C^{24}), 34.96 (C^{10}), 28.90 (C^{19}), 26.99 (C^{11}); δ_F (471 MHz, $CDCl_3$/DMSO-d_6) -62.90; υ_{max} (neat) cm^{-1}: 3297, 2969, 1736, 1653, 1534, 1473, 1385, 1279, 1178, 1135, 963, 887, 681; high resolution ESI-MS calcd. for $C_{25}H_{31}F_6N_6O_5S$ $[M+H]^+$: 641.19753, found: 641.19740; $[\alpha]_D^{25}$ +73.3° (c 1.00, MeOH).

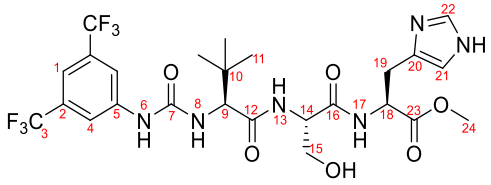

4.29

Boc-^{t}Leu-Ser-His(Trt)-OMe **4.39** was N-Boc deprotected according to the general procedure B. The resulting amine (91 mg, 0.149 mmol) was treated according to the general procedures D and E. The product was purified by silica column chromatography to provide **4.29** (75 mg, 0.120 mmol, 81%) as a white solid foam.

Mp 169 °C; δ_H (500 MHz, $CDCl_3$/DMSO-d_6) 8.77 (s, 1H, H^6), 7.63 (d, J = 7.5 Hz, 1H, H^{13}), 7.56 (s, 2H, H^4), 7.35 (d, J = 8.0 Hz, 1H, H^{17}), 7.11 (d, J = 1.1 Hz, 1H, H^{22}), 6.99 (s, 1H, H^1), 6.41 (s, 1H, H^{21}), 6.24 (d, J = 9.1 Hz, 1H, H^8), 4.36 (td, J = 7.4, 4.1 Hz, 1H, H^{18}), 4.08 (dt, J = 7.9, 4.2 Hz, 1H, H^{14}), 3.89 (d, J = 9.0 Hz, 1H, H^9), 3.57 (dd, J = 11.5, 3.8 Hz, 1H, H^{15}), 3.37 – 3.32 (m, 1H, H^{15}), 3.32 (s, 3H, H^{24}), 2.79 (dd, J = 14.8, 4.2 Hz, 1H, H^{19}), 2.62 (dd, J = 14.7, 7.0 Hz, 1H, H^{19}), 0.67 (s, 9H, H^{11}); δ_C (126 MHz, $CDCl_3$/DMSO-d_6) 170.62 (C^{12}/C^{23}), 170.60 (C^{12}/C^{23}), 169.53 (C^{16}), 154.23 (C^7), 141.39 (C^5), 134.50 (C^{22}), 130.81 (q, J = 32.8 Hz, C^2), 122.68 (q, J = 272.5 Hz, C^3), 116.69 (C^4), 113.25 (C^1), 61.90 (C^{15}), 60.19 (C^9), 55.25 (C^{14}), 52.26 (C^{18}), 51.48 (C^{24}), 34.04 (C^{10}), 28.12 (C^{19}), 26.01 (C^{11}); δ_F (470 MHz, $CDCl_3$/DMSO-d_6) -63.05; υ_{max} (neat) cm^{-1}: 3304, 2981, 2888, 1647, 1588, 1388, 1280, 1177, 1134; high resolution ESI-MS calcd. for $C_{25}H_{31}O_6N_6F_6$ $[M+H]^+$: 625.22038, found: 625.21957; $[\alpha]_D^{25}$ −23.2° (c 1.00, MeOH).

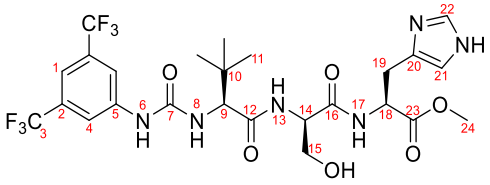

4.30

Compound **4.41** was Boc-deprotected according to the general procedure B. The resulting amine (125 mg, 0.204 mmol) was then treated according to the general procedures D (using 3,5-bis(trifluoromethyl)phenyl isocyanate) and E. The product was purified by silica chromatography (10% MeOH/DCM) to provide **4.30** (85 mg, 0.136 mmol, 67%) as a white solid.

Mp 139-147 °C; δ_H (500 MHz, $CDCl_3$/DMSO-d_6) 8.94 (s, 1H, H^6), 7.78 (s, 2H, H^4), 7.40 (s, 2H, H^{13}, H^{22}), 7.34 (d, J = 8.0 Hz, 1H, H^{17}), 7.28 (s, 1H, H^1), 6.64 (s, 1H, H^{21}), 6.52 (d, J = 8.3 Hz, 1H, H^8), 4.70 (tt, J = 6.1, 2.7 Hz, 1H, H^{18}), 4.43 (td, J = 8.5, 6.6, 4.0 Hz, 1H, H^{14}), 4.09 (dd, J = 8.5, 2.0 Hz, 1H, H^9), 3.95 – 3.84 (m, 1H, H^{15}), 3.67 – 3.54 (m, 4H, H^{15}, H^{24}), 3.07 (dd, J = 15.0, 3.7 Hz, 1H, H^{19}), 2.86 (ddd, J = 14.8, 7.4, 2.0 Hz, 1H, H^{19}), 0.97 (s, 9H, H^{11}); δ_C (126 MHz, $CDCl_3$/DMSO-d_6) 171.45, 171.25, 169.56, 155.25 (C^7), 141.59 (C^5), 135.30 (C^{22}), 131.59 (q, J = 33.1 Hz, C^2), 123.24 (q, J = 272.5 Hz, C^3), 117.56 (C^4), 114.35 (C^1), 62.32 (C^{15}), 61.65 (C^9), 55.40 (C^{14}), 52.97 (C^{18}), 52.31 (C^{24}), 34.21 (C^{10}), 28.52 (C^{19}), 26.68 (C^{11}); δ_F (471 MHz, $CDCl_3$/DMSO-d_6) -63.03; υ_{max} (neat) cm^{-1}: 3337, 2981, 2889, 1743, 1650, 1547, 1474, 1388, 1279, 1250, 1176, 1132, 1071, 953; high resolution ESI-MS calcd. for $C_{25}H_{31}F_6N_6O_6$ $[M+H]^+$: 625.22038, found: 625.21974; $[\alpha]_D^{25}$ +12.9° (c 1.00, MeOH).

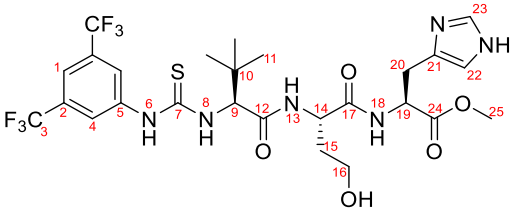

4.31

Boc-^{t}Leu-hSer-His(Trt)-OMe **4.48** was deprotected according to the general procedure B. The resulting H-^{t}Leu-hSer-His(Trt)-OMe (52 mg, 0.0831 mmol) was treated according to the general procedures D and E. The product was purified by silica column chromatography (10% MeOH/DCM) to provide **4.31** (25 mg, 0.0382 mmol, 46%) as an oily semisolid.

δ_H (500 MHz, $CDCl_3$/DMSO-d_6) 10.26 (s, 1H, H^6), 8.12 (s, 2H, H^4), 7.87 (d, J = 8.5 Hz, 1H, H^8), 7.77 (d, J = 7.1 Hz, 1H, H^{13}), 7.69 (d, J = 8.0 Hz, 1H, H^{18}), 7.51 (s, 1H, H^{23}), 7.49 (s, 1H, H^1), 6.72 (s, 1H, H^{22}), 4.83 (d, J = 8.3 Hz, 1H, H^9), 4.78 (dt, J = 8.0, 5.5 Hz, 1H, H^{19}), 4.61 (td, J = 7.2, 4.9 Hz, 1H, H^{14}), 3.70 – 3.59 (m, 2H, H^{16}), 3.62 (s, 3H, H^{25}), 3.13 – 2.96 (m, 2H, H^{20}), 2.00 (ddt, J = 14.1, 9.6, 5.0 Hz, 1H, H^{15}), 1.88 (ddt, J = 14.0, 7.5, 3.9 Hz, 1H, H^{15}), 0.99 (s, 9H, H^{11}); δ_C (126 MHz, $CDCl_3$/DMSO-d_6) 181.82 (C^7), 171.41 (C^{12}), 171.38 (C^{17}), 171.29 (C^{24}), 141.32 (C^5), 135.49 (C^{23}), 132.24 (C^{21}), 131.42 (q, J = 33.4 Hz C^2), 123.25 (q, J = 272.7 Hz C^3), 122.44 (C^4), 118.19 (C^{22}), 117.18 (C^1), 65.65 (C^9), 58.32 (C^{16}), 52.78 (C^{19}), 52.44 (C^{25}), 51.92 (C^{14}), 34.86 (C^{10}), 34.51 (C^{15}), 28.76 (C^{20}), 26.97 (C^{11}); δ_F (471 MHz, $CDCl_3$/DMSO-d_6) -62.92; υ_{max} (neat) cm^{-1}: 3288, 2959, 1744, 1651, 1534, 1385, 1277, 1175, 1131; high resolution ESI-MS calcd. for $C_{26}H_{33}O_5N_6F_6S_1$ $[M+H]^+$ 655.21318, found: 655.21359; $[\alpha]_D^{25}$ -48.9° (c 1.00, MeOH).

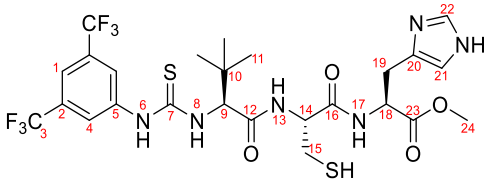

4.32

(H-^{t}Leu-Cys-His(Trt)-OMe)$_2$ **4.49** was deprotected according to the general procedure B. The resulting (H-^{t}Leu-Cys-His(Trt)-OMe)$_2$ (145 mg, 0.116 mmol) was treated according to the general procedures D and E. Crude disulfide was then dissolved in THF (2 ml) with a few drops of water. PBu_3 (87 µl, 0.347 mmol) was then added and the mixture was stirred for 2 h at rt. It was then evaporated, the residue redissolved in DCM and separated by silica chromatography to provide **4.32** (123 mg, 0.187 mmol, 81%) as a white solid foam.

Mp 75-80 °C; δ_H (500 MHz, $CDCl_3$/DMSO-d_6) 10.02 (s, 1H, H^6), 8.06 (s, 2H, H^4), 7.81 (dd, J = 14.6, 8.2 Hz, 2H, H^8, H^{13}), 7.69 (d, J = 7.8 Hz, 1H, H^{17}), 7.45 (s, 1H, H^{22}), 7.41 (s, 1H, H^1), 6.66 (s, 1H, H^{21}), 4.79 (d, J = 8.5 Hz, 1H, H^9), 4.72 – 4.61 (m, 1H, H^{18}), 4.55 (q, J = 6.1 Hz, 1H, H^{14}), 3.56 (s, 3H, H^{24}), 3.04 – 2.90 (m, 2H, H^{19}), 2.85 (dd, J = 14.0, 5.4 Hz, 1H, H^{15}), 2.76 (dd, J = 14.0, 5.5 Hz, 1H, H^{15}), 1.79 (s, 1H, S*H*), 0.96 (s, 9H, H^{11}); δ_C (126 MHz, $CDCl_3$/DMSO-d_6) 181.41 (C^7), 171.13 (C^{23}), 170.77 (C^{12}), 169.30 (C^{16}), 141.23 (C^5), 135.25 (C^{22}),132.29 (C^{20}), 131.16 (q, J = 33.2 Hz, C^2), 123.08 (q, J = 272.8 Hz, C^3), 121.99 (C^4), 117.84 (C^{21}), 116.78 (C^1), 65.24 (C^9), 55.04 (C^{14}), 52.69 (C^{18}), 52.18 (C^{24}), 34.62 (C^{10}), 28.56 (C^{19}), 26.81 (C^{11}), 26.44 (C^{15}); δ_F (471 MHz, $CDCl_3$/DMSO-d_6) -62.92; υ_{max} (neat) cm^{-1}: 3296, 2980, 1744, 1651, 1385, 1277, 1175, 1132; high resolution ESI-MS calcd. for $C_{25}H_{31}O_4N_6F_6S_2$ $[M+H]^+$ 657.17469, found: 657.17488; $[\alpha]_D^{25}$ -76.6° (c 1.00, MeOH).

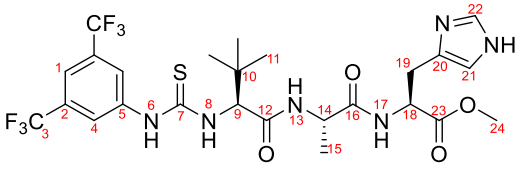

4.33

(H-^{t}Leu-Ala-His(Trt)-OMe)$_2$ **4.47** was N-Boc deprotected according to the general procedure B. The resulting amine (145 mg, 0.116 mmol) was treated according to the general procedures D and E. The product was purified by silica chromatography to afford **4.33** (60 mg, 0.0961 mmol, 76%) as a white solid.

Mp 125-130 °C; δ_H (500 MHz, $CDCl_3$/DMSO-d_6) 11.42 (s, 1H, H^6), 8.24 (s, 1H, H^8), 8.14 (s, 2H, H^4), 7.72 (s, 1H, H^{22}), 7.55 (s, 1H, H^1), 6.79 (s, 3H, H^{13}, H^{17}, H^{21}), 4.99 (d, J = 8.8 Hz, 1H, H^9), 4.80 (d, J = 4.0 Hz, 1H, H^{18}), 4.16 (s, 1H, H^{14}), 3.70 (s, 3H, H^{24}), 3.28 (dd, J = 15.3, 4.4 Hz, 1H, H^{19}), 3.23 – 3.10 (m, 1H, H^{19}), 1.44 (d, J = 7.0 Hz, 3H, H^{15}), 0.96 (s, 9H, H^{11}); δ_C (126 MHz, $CDCl_3$/DMSO-d_6) 182.50 (C^7), 172.26 (C^{12}), 171.56 (C^{16}), 170.56 (C^{23}), 141.33 (C^5), 135.80 (C^{22}), 131.62 (q, J = 33.3 Hz, C^2), 123.33 (q, J = 272.7 Hz, C^3), 122.65 (C^4), 117.55 (C^1), 64.83 (C^9), 53.28 (C^{18}), 52.85 (C^{24}), 51.11 (C^{14}), 35.01 (C^{10}), 26.74 (C^{11}, C^{19}), 17.10 (C^{15}); δ_F (471 MHz, $CDCl_3$/DMSO-d_6) -62.91; υ_{max} (neat) cm^{-1}: 3303, 1743, 1651, 1532, 1385, 1278, 1178, 1134; high resolution ESI-MS calcd. for $C_{25}H_{31}O_4N_6F_6S$ $[M+H]^+$: 625.20262, found: 625.20221; $[\alpha]_D^{25}$ −57.2° (c 1.00, MeOH).

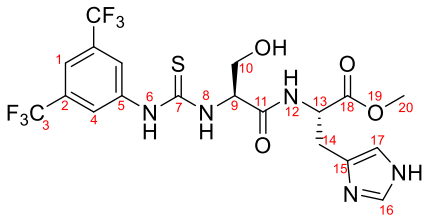

4.34

Boc-deprotected **4.10** (H-Ser-His-OMe·2HCl, 66 mg, 0.200 mmol) was added to DCM (2 ml) and combined with 3,5-bis(trifluoromethyl)phenyl isothiocyanate (40 µl, 0.220 mmol) followed by Et_3N (84 µl, 0.600 mmol). The mixture was stirred for 2h at rt, partitioned in sat. aq. $NaHCO_3$ and DCM and further extracted with DCM. The organic fractions were dried with anhydrous Na_2SO_4, filtered and evaporated. The product was purified by silica chromatography (8-10% MeOH/DCM) to provide **4.34** (48 mg, 0.0910 mmol, 46%) as a white solid foam.

Mp 110-120 °C; δ_H (400 MHz, $CDCl_3$/methanol-d_4) 8.05 (s, 2H, H^4), 7.82 (d, J = 10.7 Hz, 1H, H^{12}), 7.49 (s, 1H, H^1), 7.40 (s, 1H, H^{16}), 6.73 (s, 1H, H^{17}), 4.97 (s, 1H, H^9), 4.66 (dd, J = 7.0, 4.4 Hz, 1H, H^{13}), 4.03 (m, 1H, H^{10}), 3.77 (m, 1H, H^{10}), 3.63 (s, 3H, H^{20}), 3.10 (dd, J = 14.8, 4.5 Hz, 1H, H^{14}), 2.99 (dd, J = 14.8, 7.0 Hz, 1H, H^{14}); δ_C (101 MHz, $CDCl_3$ + 5% methanol-d_4) 181.61 (C^7), 171.75 (C^{11}/C^{18}), 171.25 (C^{11}/C^{18}), 140.85 (C^5), 135.21 (C^{16}), 131.50 (q, $J_{C\text{-}F}$ = 33.33 Hz, C^2), 133.14 (C^{15}), 123.16 (q, $J_{C\text{-}F}$ = 273.71 Hz, C^3) 122.89 (C^4), 117.65 (C^1), 116.60 (C^{17}), 62.16 (C^{10}), 59.36 (C^9), 53.12 (C^{13}), 52.59 (C^{20}), 28.66 (C^{14}); δ_F (377 MHz, $CDCl_3$ + 5% methanol-d_4) −63.20; υ_{max} (neat) cm^{-1}: 3308, 2981, 1734, 1655, 1540, 1384, 1278, 1177, 1128; high resolution ESI-MS calcd. for $C_{19}H_{20}O_4N_5F_6S$ $[M+H]^+$ 528.11347, found: 528.11289; $[\alpha]_D^{25}$ −4.5° (c 1.00, MeOH).

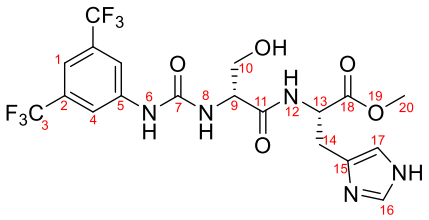

4.35

Compound Boc-D-Ser-His-OMe **4.38** was Boc-deprotected according to the general procedure B. The resulting amine (145 mg, 0.291 mmol) was then theated according to the general procedures D (using 3,5-bis(trifluoromethyl)phenyl isocyanate) and E. The product was purified by silica chromatography to provide **4.35** (103 mg, 0.201 mmol, 69%) as a white solid.

Mp 173-177 °C (decomp.); δ_H (500 MHz, $CDCl_3$/DMSO-d_6) 9.27 (s, 1H, H^6), 7.87 (s, 2H, H^4), 7.70 (d, J = 7.7 Hz, 1H, H^{12}), 7.37 (s, 1H, H^{16}), 7.28 (s, 1H, H^1), 6.69 (s, 1H, H^{17}), 6.64 (d, J = 7.2 Hz, 1H, H^8), 4.71 (td, J = 6.9, 4.1 Hz, 1H, H^{13}), 4.38 (td, J = 6.4, 3.8 Hz, 1H, H^9), 3.90 (dd, J = 11.3, 3.9 Hz, 1H, H^{10}), 3.64 (s, 3H, H^{20}), 3.60 (dd, J = 11.3, 6.0 Hz, 1H, H^{10}), 3.12 (dd, J = 14.7, 4.2 Hz, 1H, H^{14}), 2.94 (dd, J = 14.7, 6.5 Hz, 1H, H^{14}); δ_C (126 MHz, $CDCl_3$/DMSO-d_6) 170.74 (C^{18}), 169.68 (C^{11}), 154.17 (C^7), 141.39 (C^5), 134.49 (C^{16}), 130.81 (q, J = 32.8 Hz, C^2), 122.69 (q, J = 272.5 Hz, C^3), 116.75 (C^4), 113.32 (C^1), 62.46 (C^{10}), 54.75 (C^9), 52.38 (C^{13}), 51.60 (C^{20}), 28.17 (C^{14}); δ_F (126 MHz, $CDCl_3$/DMSO-d_6) -62.76; υ_{max} (neat) cm^{-1}: 3339, 2980, 2889, 1740, 1653, 1568, 1475, 1388, 1280, 1177, 1126; high resolution ESI-MS calcd. for $C_{19}H_{20}F_6N_5O_5$ $[M+H]^+$: 512.13631, found: 512.13582; $[\alpha]_D^{25}$ +9.0° (c 1.00, MeOH).

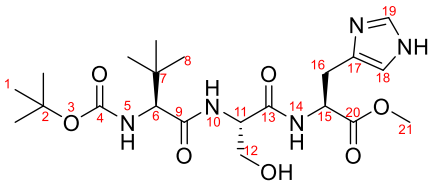

4.36

Boc-^{t}Leu-Ser-His(Trt)-OMe **4.39** (70 mg, 0.0980 mmol) was deprotected according to the general procedure E. The product was purified by silica chromatography to afford **4.36** (38 mg, 0.0809 mmol, 83%) as a white solid.

Mp 105 °C; δ_H (400 MHz, $CDCl_3$) 7.62 (d, J = 8.0 Hz, 1H, H^{14}), 7.56 (d, J = 6.7 Hz, 1H, H^{10}), 7.43 (s, 1H, H^{19}), 6.75 (s, 1H, H^{18}), 5.48 (d, J = 8.6 Hz, 1H, H^{5}), 4.78 (td, J = 7.4, 4.1 Hz, 1H, H^{15}), 4.42 (dt, J = 7.7, 4.1 Hz, 1H, H^{11}), 4.04 – 3.89 (m, 2H, H^{6}, H^{12}), 3.70 (m, 1H, H^{12}), 3.68 (s, 3H, H^{21}), 3.17 (dd, J = 14.7, 4.0 Hz, 1H, H^{16}), 2.97 (dd, J = 14.8, 7.1 Hz, 1H, H^{16}), 1.40 (s, 9H, H^{1}), 0.98 (s, 9H, H^{8}); δ_C (100 MHz, $CDCl_3$) 171.75 (C^{9}/C^{20}), 171.54 (C^{9}/C^{20}), 170.60 (C^{13}), 156.15 (C^{4}), 135.68 (C^{19}), 80.17 (C^{2}), 62.64 (C^{6}), 62.41 (C^{12}), 55.96 (C^{11}), 53.23 (C^{15}), 52.69 (C^{21}), 34.57 (C^{7}), 28.91 (C^{16}), 28.46 (C^{1}), 26.76 (C^{8}); υ_{max} (neat) cm^{-1}: 3295, 2969, 1651, 1508, 1367, 1170; high resolution ESI-MS calcd. for $C_{21}H_{36}O_7N_5$ $[M+H]^+$: 470.26092, found: 470.26015; $[\alpha]_D^{25}$ −13.5° (c 1.00, MeOH).

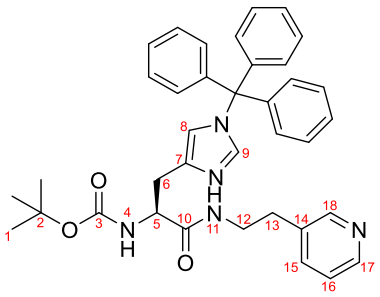

4.56

General procedure C for amide formation was used to couple Boc-His(Trt)-OH (995 mg, 2 mmol) and 3-(2-aminoethyl)pyridine (0.258 ml, 2.2 mmol). The product was purified by silica chromatography (2.5-6% MeOH/DCM) to provide **4.56** (1.093 g, 1.816 mmol, 91%) as a white solid foam.

Mp 79 °C; δ_H (500 MHz, $CDCl_3$) 8.48 – 8.35 (m, 2H, H^{17}, H^{18}), 7.47 (dt, J = 7.8, 1.9 Hz, 1H, H^{15}), 7.33 – 7.27 (m, 10H, H^{9}, H^{Trt}), 7.17 (dd, J = 7.8, 4.8 Hz, 2H, H^{11}, H^{16}), 7.11 – 7.04 (m, 6H, H^{Trt}), 6.64 (s, 1H, H^{8}), 6.33 (s, 1H, H^{4}), 4.38 (s, 1H, H^{5}), 3.46 (dq, J = 13.6, 6.9 Hz, 1H, H^{12}), 3.37 (dq, J = 13.4, 6.8 Hz, 1H, H^{12}), 3.06 (d, J = 16.7 Hz, 1H, H^{6}), 2.87 (dd, J = 14.8, 6.2 Hz, 1H, H^{6}), 2.73 (td, J = 7.1, 3.7 Hz, 2H, H^{13}), 1.41 (s, 9H, H^{1}); δ_C (126 MHz, $CDCl_3$) 171.92 (C^{10}), 155.81 (C^{3}), 150.21 (C^{18}), 148.01 (C^{17}), 142.36 (C^{Trt}), 138.45 (C^{9}), 136.99 (C^{7}), 136.39 (C^{15}), 134.50 (C^{14}), 129.80 (C^{Trt}), 128.21 (C^{Trt}), 128.16 (C^{Trt}), 123.51 (C^{16}), 119.67 (C^{8}), 79.91 (C^{2}), 75.41 (C^{Trt}), 54.79 (C^{5}), 40.52 (C^{12}), 33.11 (C^{13}), 30.49 (C^{6}), 28.48 (C^{1}); υ_{max} (neat) cm^{-1}: 3285, 2980, 1701, 1670, 1491, 1446, 1365, 1247, 1167, 1026, 749, 702, 669; high resolution ESI-MS calcd. for $C_{37}H_{40}N_5O_3$ $[M+H]^+$: 602.31257, found: 602.31284; $[\alpha]_D^{25}$ +4.5° (c 1.00, MeOH).

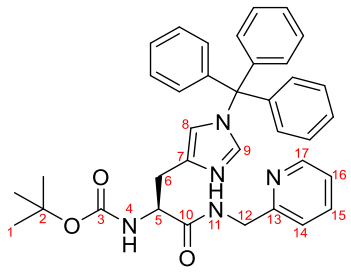

4.57

General procedure C for amide formation was used to couple Boc-His(Trt)-OH (249 mg, 0.5 mmol) and picolylamine (0.057 ml, 0.55 mmol). The product was purified by silica chromatography (2.5-4% MeOH/DCM) to provide **4.57** (207 mg, 0.352 mmol, 70%) as a white solid foam.

Mp 63 °C; δ_H (400 MHz, $CDCl_3$) 8.40 (d, J = 4.8 Hz, 1H, H^{17}), 7.56 – 7.44 (m, 2H, H^{11}, H^{15}), 7.28 (s, 1H, H^{9}), 7.22 (d, J = 6.6 Hz, 9H, H^{Trt}), 7.14 (d, J = 7.9 Hz, 1H, H^{14}), 7.07 (dd, J = 7.4, 5.2 Hz, 1H, H^{16}), 7.04 – 6.96 (m, 6H, H^{Trt}), 6.57 (s, 1H, H^{8}), 6.33 (d, J = 7.1 Hz, 1H, H^{4}), 4.52 (dd, J = 16.4, 5.8 Hz, 1H, H^{12}), 4.42 (d, J = 6.7 Hz, 1H, H^{5}), 4.32 (dd, J = 16.5, 4.9 Hz, 1H, H^{12}), 3.14 – 3.00 (m, 1H, H^{6}), 2.88 (dd, J = 14.7, 5.9 Hz, 1H, H^{6}), 1.36 (s, 9H, H^{1}); δ_C (101 MHz, $CDCl_3$) 171.89 (C^{10}), 156.91, 149.09 (C^{17}), 142.40 (C^{Trt}), 138.65 (C^{9}), 136.95 (C^{7}), 136.82 (C^{15}), 129.84 (C^{Trt}), 128.17 (C^{Trt}), 128.14 (C^{Trt}), 122.30 (C^{16}), 121.64 (C^{14}), 119.80 (C^{8}), 79.91 (C^{2}), 75.38 (C^{Trt}), 55.15 (C^{5}), 44.54 (C^{12}), 30.39 (C^{6}), 28.47 (C^{1}); υ_{max} (neat) cm^{-1}: 3297, 2975, 1706, 1666, 1493, 1445, 1366, 1246, 1167, 1020, 749, 701, 671; high resolution ESI-MS calcd. for $C_{36}H_{38}N_5O_3$ $[M+H]^+$: 588.29692, found: 588.29646; $[\alpha]_D^{25}$ +5.2° (c 1.00, MeOH).

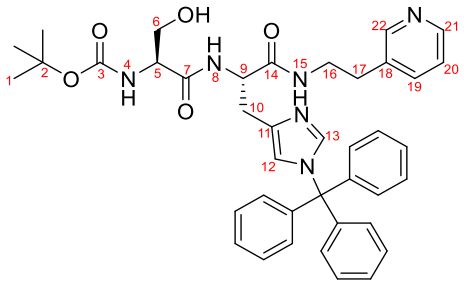

4.58

Compound **4.56** was N-Boc deprotected according to the general procedure B. The resulting amine (441 mg, 0.879 mmol) was coupled with Boc-*L*-Ser-OH (180 mg, 0.879 mmol) according to the general procedure A. The product was purified by silica chromatography (4-7% MeOH/DCM) to afford **4.58** (580 mg, 0.842 mmol, 96%) as a white solid foam.

Mp 95 °C; δ_H (500 MHz, $CDCl_3$) 8.41 – 8.33 (m, 2H, H^{21}, H^{22}), 8.03 (d, J = 8.4 Hz, 1H, H^{8}), 7.55 – 7.45 (m, 2H, H^{15}, H^{19}), 7.35 – 7.22 (m, 10H, H^{13}, H^{Trt}), 7.15 (dd, J = 7.8, 4.8 Hz, 1H, H^{20}), 7.09 – 6.97 (m, 6H, H^{Trt}), 6.58 (d, J = 1.3 Hz, 1H, H^{12}), 6.08 (d, J = 5.4 Hz, 1H, H^{4}), 4.76 – 4.64 (m, 1H, H^{9}), 4.07 (q, J = 4.6 Hz, 1H, H^{5}), 3.95 (dd, J = 11.6, 3.6 Hz, 1H, H^{6}), 3.74 – 3.63 (m, 1H, H^{6}), 3.51 – 3.41 (m, 1H, H^{16}), 3.27 – 3.16 (m, 1H, H^{16}), 3.01 (dd, J = 14.8, 4.3 Hz, 1H, H^{10}), 2.89 (dd, J = 14.7, 7.0 Hz, 1H, H^{10}), 2.71 (t, J = 7.6 Hz, 2H, H^{17}), 1.34 (s, 9H, H^{1}); δ_C (126 MHz, $CDCl_3$) 171.06 (C^{7}/C^{14}), 170.89 (C^{7}/C^{14}), 156.25 (C^{3}), 149.89 (C^{22}), 147.57 (C^{21}), 142.05 (C^{Trt}), 138.36 (C^{13}), 136.82 (C^{11}), 136.54 (C^{19}), 134.58 (C^{18}), 129.68 (C^{Trt}), 128.14 (C^{Trt}), 128.07 (C^{Trt}), 123.46 (C^{20}), 119.84 (C^{12}), 79.95 (C^{2}), 75.39 (C^{Trt}), 62.12 (C^{6}), 57.74 (C^{5}), 53.65 (C^{9}), 40.62 (C^{16}), 32.81 (C^{17}), 29.23 (C^{10}), 28.33 (C^{1}); υ_{max} (neat) cm^{-1}: 3304, 2975, 2931, 1655, 1523, 1492, 1446, 1366, 1246, 1163, 749, 702; high resolution ESI-MS calcd. for $C_{40}H_{45}N_6O_5$ $[M+H]^+$ 689.34459, found: 689.34461; $[\alpha]_D^{25}$ -3.8° (c 1.00, MeOH).

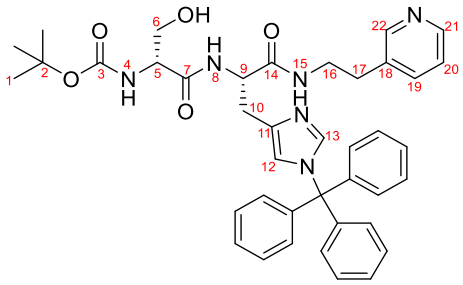

4.59

Compound **4.56** was N-Boc deprotected according to the general procedure B. The resulting amine (870 mg, 1.73 mmol) was coupled with Boc-*D*-Ser-OH (356 mg, 1.73 mmol) according to the general procedure A. The product was purified by silica chromatography (3-4.5% MeOH/$CHCl_3$) to afford **4.59** (1.096 g, 1.59 mmol, 92%) as a white solid foam.

Mp 70 °C; δ_H (500 MHz, $CDCl_3$) 8.38 (dd, J = 4.8, 1.7 Hz, 1H, H^{21}), 8.35 (d, J = 2.2 Hz, 1H, H^{22}), 7.75 (d, J = 7.9 Hz, 1H, H^{8}), 7.45 (dt, J = 7.9, 2.0 Hz, 1H, H^{19}), 7.29 (dt, J = 5.5, 3.0 Hz, 10H, H^{13}, H^{Trt}), 7.18 – 7.13 (m, 2H, H^{15}, H^{20}), 7.08 – 7.01 (m, 6H, H^{Trt}), 6.58 (s, 1H, H^{12}), 5.66 (d, J = 7.0 Hz, 1H, H^{4}), 4.62 – 4.53 (m, 1H, H^{9}), 4.12 (q, J = 6.8, 6.3 Hz, 1H, H^{5}), 3.90 (dd, J = 11.4, 3.8 Hz, 1H, H^{6}), 3.62 (dd, J = 11.3, 6.5 Hz, 1H, H^{6}), 3.44 – 3.31 (m, 2H, H^{16}), 3.04 (dd, J = 14.9, 4.2 Hz, 1H, H^{10}), 2.90 (dd, J = 14.9, 7.3 Hz, 1H, H^{10}), 2.72 (td, J = 7.1, 2.1 Hz, 2H, H^{17}), 1.38 (s, 9H, H^{1}); δ_C (126 MHz, $CDCl_3$) 171.34 (C^{7}/C^{14}), 170.73 (C^{7}/C^{14}), 155.73 (C^{3}), 150.10 (C^{22}), 147.83 (C^{21}), 142.15 (C^{Trt}), 138.49 (C^{13}), 136.83 (C^{11}), 136.51 (C^{19}), 134.53 (C^{18}), 129.79 (C^{Trt}), 128.24 (C^{Trt}), 128.19 (C^{Trt}), 123.54 (C^{20}), 119.88 (C^{12}), 80.02 (C^{2}), 75.52 (C^{Trt}), 62.74 (C^{6}), 56.44 (C^{5}), 54.31 (C^{9}), 40.59 (C^{16}), 32.88 (C^{17}), 29.30 (C^{10}), 28.41 (C^{1}); υ_{max} (neat) cm^{-1}: 3295, 2980, 1653, 1490, 1446, 1366, 1248, 1163, 749, 702, 669; high resolution ESI-MS calcd. for $C_{40}H_{45}N_6O_5$ $[M+H]^+$: 689.34459, found: 689.34457; $[\alpha]_D^{25}$ +9.8° (c 1.00, MeOH).

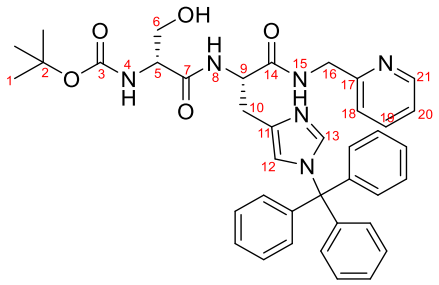

4.60

Compound **4.57** was N-Boc deprotected according to the general procedure B. The resulting amine (155 mg, 0.318 mmol) was coupled with Boc-*D*-Ser-OH (66 mg, 0.318 mmol) according to the general procedure A. The product was purified by silica chromatography (4-7% MeOH/DCM) to afford **x** (161 mg, 0.239 mmol, 75%) as a white solid foam.

Mp 93 °C; δ_H (400 MHz, $CDCl_3$) 8.42 (d, J = 4.8 Hz, 1H, H^{21}), 8.00 (d, J = 7.8 Hz, 1H, H^{8}), 7.75 (d, J = 5.6 Hz, 1H, H^{15}), 7.57 (t, J = 7.7 Hz, 1H, H^{19}), 7.39 – 7.26 (m, 10H, H^{13}, H^{Trt}), 7.19 (d, J = 7.9 Hz, 1H, H^{18}), 7.12 (dd, J = 7.5, 5.1 Hz, 1H, H^{20}), 7.10 – 7.02 (m, 6H, H^{Trt}), 6.60 (s, 1H, H^{12}), 5.82 (d, J = 7.1 Hz, 1H, H^{4}), 4.76 (q, J = 6.1 Hz, 1H, H^{9}), 4.52 (dd, J = 16.2, 5.8 Hz, 1H, H^{16}), 4.38 (dd, J = 16.2, 4.9 Hz, 1H, H^{16}), 4.28 – 4.16 (m, 1H, H^{5}), 3.99 (dd, J = 11.5, 3.6 Hz, 1H, H^{6}), 3.65 (dd, J = 11.4, 6.1 Hz, 1H, H^{6}), 3.18 – 3.05 (m, 1H, H^{10}), 2.98 (dd, J = 14.8, 6.9 Hz, 1H, H^{10}), 1.36 (s, 9H, H^{1}); δ_C (101 MHz, $CDCl_3$) 171.24, 170.71, 156.75 (C^{17}), 155.59 (C^{3}), 148.95 (C^{21}), 142.14 (C^{Trt}), 138.47 (C^{13}), 137.00 (C^{19}), 136.70 (C^{11}), 129.78 (C^{Trt}), 128.17 (C^{Trt}), 128.14 (C^{Trt}), 122.35 (C^{20}), 121.92 (C^{18}), 119.96 (C^{12}), 79.80 (C^{2}), 75.45 (C^{Trt}), 63.06 (C^{6}), 56.57 (C^{5}), 54.32 (C^{9}), 44.36 (C^{16}), 29.51 (C^{10}), 28.35 (C^{1}); υ_{max} (neat) cm^{-1}: 3314, 2980, 1658, 1524, 1493, 1445, 1366, 1248, 1164, 1057, 750, 702, 667; high resolution ESI-MS calcd. for $C_{39}H_{43}N_6O_5$ $[M+H]^+$: 675.32894, found: 675.32879; $[\alpha]_D^{25}$ +12.4° (c 1.00, MeOH).

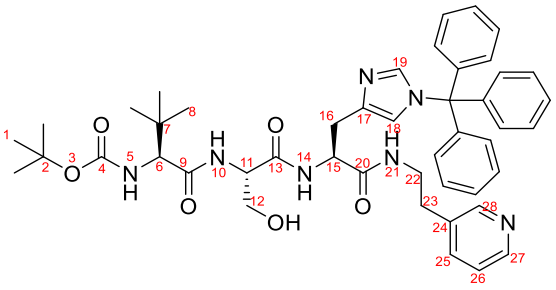

4.61

Compound **4.58** was N-Boc deprotected according to the general procedure B. The resulting amine (190 mg, 0.323 mmol) was coupled with Boc-^{t}Leu-OH (82 mg, 0.355 mmol) according to the general procedure C. The product was purified by silica chromatography (3-4% MeOH/$CHCl_3$) to afford **4.61** (200 mg, 0.249 mmol, 77%) as a white solid foam.

Mp 114 °C; δ_H (400 MHz, $CDCl_3$) 8.45 (d, J = 2.2 Hz, 1H, H^{28}), 8.41 (dd, J = 4.8, 1.6 Hz, 1H, H^{27}), 7.66 (d, J = 9.3 Hz, 1H, H^{14}), 7.55 (dt, J = 7.9, 2.0 Hz, 1H, H^{25}), 7.31 (p, J = 3.6 Hz, 9H, H^{Trt}), 7.28 – 7.22 (m, 3H, H^{10}, H^{19}, H^{21}), 7.17 (ddd, J = 7.8, 4.9, 0.8 Hz, 1H, H^{26}), 7.08 – 7.02 (m, 6H, H^{Trt}), 6.64 (d, J = 1.4 Hz, 1H, H^{18}), 5.15 (d, J = 3.8 Hz, 1H, H^{5}), 4.66 (ddd, J = 11.4, 9.3, 2.5 Hz, 1H, H^{15}), 4.06 (t, J = 4.8 Hz, 1H, H^{11}), 4.00 (dd, J = 12.2, 1.5 Hz, 1H, H^{12}), 3.66 (dd, J = 12.1, 4.2 Hz, 1H, H^{12}), 3.59 – 3.50 (m, 1H, H^{22}), 3.48 (d, J = 3.8 Hz, 1H, H^{6}), 3.45 – 3.37 (m, 1H, H^{22}), 3.34 (dd, J = 14.9, 2.4 Hz, 1H, H^{16}), 2.94 – 2.78 (m, 2H, H^{23}), 2.67 (dd, J = 14.9, 11.0 Hz, 1H, H^{16}), 1.39 (s, 9H, H^{1}), 1.03 (s, 9H, H^{8}); δ_C (101 MHz, $CDCl_3$) 171.91 (C^{9}), 171.01 (C^{20}), 170.58 (C^{13}), 156.85 (C^{4}), 150.18 (C^{28}), 147.58 (C^{27}), 142.17 (C^{Trt}), 138.53 (C^{19}), 137.76 (C^{17}), 136.52 (C^{25}), 134.96 (C^{24}), 129.78 (C^{Trt}), 128.21 (C^{Trt}), 128.18 (C^{Trt}), 123.44 (C^{26}), 119.75 (C^{18}), 81.30 (C^{2}), 75.48 (C^{Trt}), 65.33 (C^{6}), 61.70 (C^{12}), 57.31 (C^{11}), 53.93 (C^{15}), 40.75 (C^{22}), 33.06 (C^{7}), 32.68 (C^{23}), 28.93 (C^{16}), 28.47 (C^{1}), 27.18 (C^{8}); υ_{max} (neat) cm^{-1}: 3302, 2981, 2888, 1653, 1507, 1384, 1251, 1157, 1072, 954, 702, 669; high resolution ESI-MS calcd. for $C_{46}H_{56}N_7O_6$ $[M+H]^+$ 802.42866, found: 802.42829; $[\alpha]_D^{25}$ (c 1.00, MeOH).

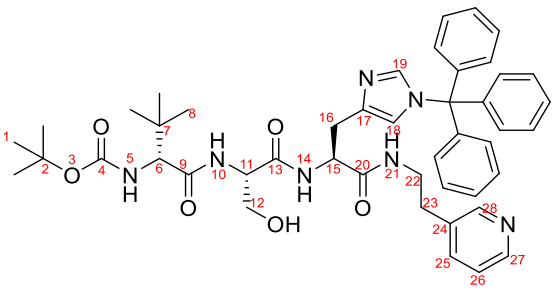

4.62

Compound **4.58** was N-Boc deprotected according to the general procedure B. The resulting amine (213 mg, 0.362 mmol) was coupled with Boc-D-^{t}Leu-OH (92 mg, 0.398 mmol) according to the general procedure C. The product was purified by silica chromatography (3-4% MeOH/$CHCl_3$) to afford **4.62** (254 mg, 0.317 mmol, 87%) as a white solid foam.

Mp 194 °C; δ_H (400 MHz, $CDCl_3$) 8.46 – 8.38 (m, 2H, H^{27}, H^{28}), 7.59 – 7.50 (m, 2H, H^{14}, H^{25}), 7.36 – 7.28 (m, 11H, H^{10}, H^{19}, H^{Trt}), 7.28 – 7.22 (m, 1H, H^{21}), 7.19 (dd, J = 7.8, 4.8 Hz, 1H, H^{26}), 7.12 – 7.01 (m, 6H, H^{Trt}), 6.62 (d, J = 1.4 Hz, 1H, H^{18}), 5.21 (d, J = 6.6 Hz, 1H, H^{5}), 4.65 (td, J = 9.6, 3.0 Hz, 1H, H^{15}), 4.18 (t, J = 5.0 Hz, 1H, H^{11}), 4.05 (d, J = 11.9 Hz, 1H, H^{12}), 3.79 (d, J = 6.8 Hz, 1H, H^{6}), 3.70 (dd, J = 11.9, 4.5 Hz, 1H, H^{12}), 3.54 – 3.38 (m, 1H, H^{22}), 3.37 – 3.17 (m, 2H, H^{16}, H^{22}), 2.91 – 2.74 (m, 2H, H^{23}), 2.74 – 2.63 (m, 1H, H^{16}), 1.34 (s, 9H, H^{1}), 1.01 (s, 9H, H^{8}); δ_C (101 MHz, $CDCl_3$) 172.91 (C^{9}), 170.78 (C^{20}), 170.56 (C^{13}), 156.29 (C^{4}), 150.03 (C^{28}), 147.65 (C^{27}), 142.14 (C^{Trt}), 138.57 (C^{19}), 137.65 (C^{17}), 136.60 (C^{25}), 134.81 (C^{24}), 129.81 (C^{Trt}), 128.24 (C^{Trt}), 128.21 (C^{Trt}), 123.57 (C^{26}), 119.75 (C^{18}), 80.45 (C^{2}), 75.57 (C^{Trt}), 63.35 (C^{6}), 61.96 (C^{12}), 57.15 (C^{11}), 53.97 (C^{15}), 40.94 (C^{22}), 33.83 (C^{7}), 32.71 (C^{23}), 28.93 (C^{16}), 28.48 (C^{1}), 26.74 (C^{8}); υ_{max} (neat) cm^{-1}: 3303, 2980, 2888, 1653, 1491, 1392, 1250, 1161, 1070, 954, 749, 702, 669; high resolution ESI-MS calcd. for $C_{46}H_{56}N_7O_6$ $[M+H]^+$ 802.42866, found: 802.42868; $[\alpha]_D^{25}$ -6.5° (c 1.00, MeOH).

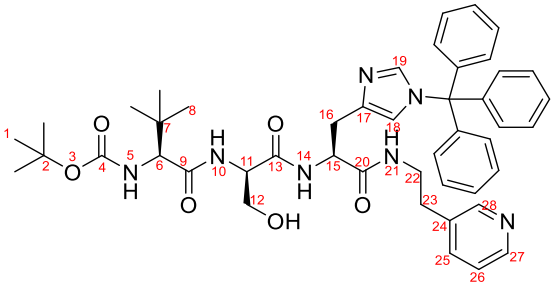

4.63

Compound **4.59** was N-Boc deprotected according to the general procedure B. The resulting amine (683 mg, 1.16 mmol) was coupled with Boc-^{t}Leu-OH (295 mg, 1.28 mmol) according to the general procedure C. The product was purified by silica chromatography (4-4.5% MeOH/$CHCl_3$) to afford **4.63** (802 mg, 1.00 mmol, 86%) as a white solid foam.

Mp 91 °C; δ_H (400 MHz, $CDCl_3$) 8.41 – 8.37 (m, 2H, H^{27}, H^{28}), 7.68 (d, J = 7.9 Hz, 1H, H^{14}), 7.46 (dt, J = 7.8, 2.0 Hz, 1H, H^{25}), 7.34 – 7.28 (m, 10H, H^{19}, H^{Trt}), 7.19 – 7.12 (m, 3H, H^{10}, H^{21}, H^{26}), 7.10 – 7.02 (m, 6H, H^{Trt}), 6.60 (d, J = 1.3 Hz, 1H, H^{18}), 5.44 (d, J = 8.6 Hz, 1H, H^{5}), 4.49 (td, J = 8.1, 3.8 Hz, 1H, H^{15}), 4.39 (td, J = 6.5, 3.8 Hz, 1H, H^{11}), 4.01 – 3.87 (m, 2H, H^{6}, H^{12}), 3.61 (dd, J = 11.4, 6.5 Hz, 1H, H^{12}), 3.48 – 3.33 (m, 2H, H^{22}), 3.08 (dd, J = 15.0, 3.9 Hz, 1H, H^{16}), 2.93 (dd, J = 15.0, 8.4 Hz, 1H, H^{16}), 2.74 (t, J = 7.1 Hz, 2H, H^{23}), 1.34 (s, 9H, H^{1}), 0.98 (s, 9H, H^{8}); δ_C (101 MHz, $CDCl_3$) 171.26 (C^{13}/C^{20}), 170.76 (C^{9}/C^{13}/C^{20}), 170.72 (C^{9}/C^{13}/C^{20}), 155.97 (C^{4}), 150.20 (C^{28}), 147.88 (C^{27}), 142.19 (C^{Trt}), 138.65 (C^{19}), 136.96 (C^{17}), 136.54 (C^{25}), 134.58 (C^{24}), 129.85 (C^{Trt}), 128.27 (C^{Trt}), 128.23 (C^{Trt}), 123.59 (C^{26}), 119.86 (C^{18}), 79.77 (C^{2}), 75.59 (C^{Trt}), 62.59 (C^{6}), 62.27 (C^{12}), 55.83 (C^{11}), 54.81 (C^{15}), 40.61 (C^{22}), 34.56 (C^{7}), 32.90 (C^{23}), 28.96 (C^{16}), 28.44 (C^{1}), 26.83 (C^{8}); υ_{max} (neat) cm^{-1}: 3310, 2980, 1653, 1507, 1366, 1246, 1166, 1060, 749, 702, 669; high resolution ESI-MS calcd. for $C_{46}H_{56}N_7O_6$ $[M+H]^+$ 802.42866, found: 802.42837; $[\alpha]_D^{25}$ +3.6° (c 1.00, MeOH).

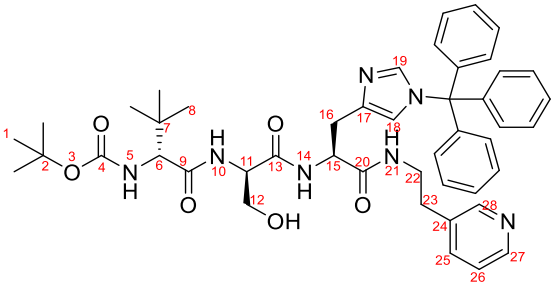

4.64

Compound **4.59** was N-Boc deprotected according to the general procedure B. The resulting amine (260 mg, 0.442 mmol) was coupled with Boc-D-^{t}Leu-OH (112 mg, 0.486 mmol) according to the general procedure C. The product was purified by silica chromatography to afford **4.64** (281 mg, 0.350 mmol, 79%) as a white solid.

Mp 218 °C; δ_H (500 MHz, $CDCl_3$) 8.42 (d, J = 4.7 Hz, 1H, H^{27}), 8.38 (s, 1H, H^{28}), 8.36 (d, J = 11.0 Hz, 1H, H^{10}), 7.87 (t, J = 5.9 Hz, 1H, H^{21}), 7.48 (d, J = 7.8 Hz, 1H, H^{25}), 7.33 – 7.22 (m, 9H, H^{Trt}), 7.20 – 7.13 (m, 2H, H^{14}, H^{26}), 7.10 (s, 1H, H^{19}), 7.04 (d, J = 7.5 Hz, 6H, H^{Trt}), 6.43 (s, 1H, H^{18}), 5.75 (d, J = 9.2 Hz, 1H, H^{5}), 5.10 (t, J = 9.3 Hz, 1H, H^{15}), 4.62 (q, J = 7.1 Hz, 1H, H^{11}), 4.32 (d, J = 9.2 Hz, 1H, H^{6}), 3.62 – 3.53 (m, 1H, H^{12}), 3.46 – 3.32 (m, J = 6.9 Hz, 2H, H^{22}), 3.23 (t, J = 10.0 Hz, 1H, H^{12}), 2.90 – 2.59 (m, 4H, H^{16}, H^{23}), 1.23 (s, 9H, H^{1}), 0.90 (s, 9H, H^{8}); δ_C (126 MHz, $CDCl_3$) 171.41 (C^{20}), 169.84 (C^{9}), 169.37 (C^{13}), 155.89 (C^{5}), 149.95 (C^{28}), 147.80 (C^{27}), 141.90 (C^{Trt}), 137.93 (C^{19}), 137.02 (C^{17}), 136.25 (C^{25}), 134.37 (C^{24}), 129.63 (C^{Trt}), 128.24 (C^{Trt}), 128.16 (C^{Trt}), 123.44 (C^{26}), 120.00 (C^{18}), 79.26 (C^{2}), 75.46 (C^{Trt}), 63.06 (C^{12}), 61.43 (C^{6}), 55.13 (C^{11}), 53.37 (C^{15}), 40.46 (C^{22}), 35.39 (C^{7}), 33.09 (C^{23}), 31.67 (C^{16}), 28.25 (C^{1}), 26.67 (C^{8}); υ_{max} (neat) cm^{-1}: 3304, 2980, 2887, 1652, 1496, 1392, 1250, 1162, 1060, 954, 749, 702, 669; high resolution ESI-MS calcd. for $C_{46}H_{56}N_7O_6$ $[M+H]^+$ 802.42866, found: 802.42895; $[\alpha]_D^{25}$ +16.4° (c 1.00, MeOH).

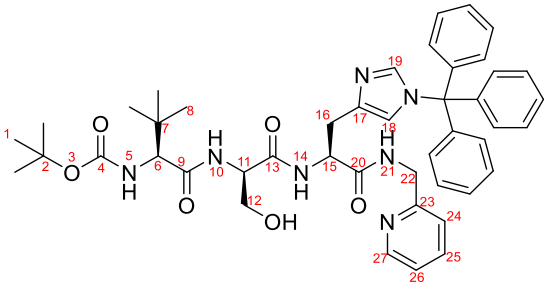

4.65

Compound **4.60** was N-Boc deprotected according to the general procedure B. The resulting amine (128mg, 0.223 mmol) was coupled with Boc-^{t}Leu-OH (52 mg, 0.223 mmol) according to the general procedure C. The product was purified by silica chromatography (4-6% MeOH/DCM) to afford **4.65** (103 mg, 0.131 mmol, 59%) as a white solid foam.

Mp 95 °C; δ_H (400 MHz, $CDCl_3$) 8.43 (d, J = 4.8 Hz, 1H, H^{27}), 7.84 – 7.68 (m, 2H, H^{14}, H^{21}), 7.56 (t, J = 7.8 Hz, 1H, H^{25}), 7.36 (s, 1H, H^{19}), 7.34 – 7.26 (m, 9H, H^{Trt}), 7.20 (d, J = 7.9 Hz, 1H, H^{24}), 7.16 (d, J = 6.7 Hz, 1H, H^{10}), 7.13 – 7.10 (m, 1H, H^{26}), 7.10 – 7.02 (m, 6H, H^{Trt}), 6.60 (s, 1H, H^{18}), 5.54 (d, J = 8.9 Hz, 1H, H^{5}), 4.85 – 4.69 (m, 1H, H^{15}), 4.61 – 4.44 (m, 3H, H^{11}, H^{22}), 3.98 (d, J = 9.5 Hz, 2H, H^{6}, H^{12}), 3.64 (dd, J = 11.5, 6.4 Hz, 1H, H^{12}), 3.17 (dd, J = 15.0, 3.7 Hz, 1H, H^{16}), 2.96 (dd, J = 14.9, 7.7 Hz, 1H, H^{16}), 1.35 (s, 9H, H^{1}), 0.97 (s, 9H, H^{8}); δ_C (101 MHz, $CDCl_3$) 170.77, 170.52, 170.32, 156.77 (C^{23}), 155.81 (C^{4}), 148.99 (C^{27}), 142.14 (C^{Trt}), 138.64 (C^{19}), 136.95 (C^{25}), 136.57, 129.81 (C^{Trt}), 128.19 (C^{Trt}), 128.15 (C^{Trt}), 122.35 (C^{26}), 121.95 (C^{24}), 119.99 (C^{18}), 79.51 (C^{2}), 75.50 (C^{Trt}), 62.55 (C^{12}), 62.23 (C^{6}), 55.68 (C^{11}), 54.50 (C^{15}), 44.48 (C^{22}), 34.80 (C^{7}), 29.57 (C^{16}), 28.38 (C^{1}), 26.75 (C^{8}); υ_{max} (neat) cm^{-1}: 3315, 2970, 1655, 1495, 1445, 1367, 1243, 1168, 1003, 750, 702, 661; high resolution ESI-MS calcd. for $C_{45}H_{54}N_7O_6$ $[M+H]^+$: 788.41301, found: 788.41282; $[\alpha]_D^{25}$ +6.0° (c 1.00, MeOH).

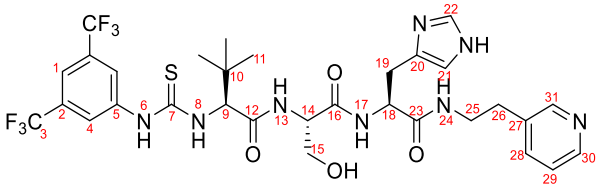

4.50

Compound **4.61** was N-Boc deprotected according to the general procedure B. The resulting amine (150 mg, 0.214 mmol) was treated according to the general procedures D and E. The product was purified by silica chromatography (10-13% MeOH/$CHCl_3$) to afford **4.50** (119 mg, 0.163 mmol, 76%) as a white solid foam.

Mp 140 °C; δ_H (500 MHz, $CDCl_3$/DMSO-d_6) 10.16 (s, 1H, H^6), 8.36 – 8.28 (m, 2H, H^{30}, H^{31}), 8.04 (s, 2H, H^4), 7.92 (d, J = 7.3 Hz, 1H, H^8), 7.78 – 7.65 (m, 2H, H^{13}, H^{17}), 7.50 – 7.32 (m, 4H, H^1, H^{22}, H^{24}, H^{28}), 7.10 (dd, J = 7.8, 4.8 Hz, 1H, H^{29}), 6.66 (s, 1H, H^{21}), 4.56 (d, J = 7.2 Hz, 1H, H^9), 4.51 (td, J = 9.2, 3.5 Hz, 1H, H^{18}), 4.21 – 4.13 (m, 1H, H^{14}), 3.84 (dd, J = 11.9, 3.1 Hz, 1H, H^{15}), 3.63 (dd, J = 11.9, 4.4 Hz, 1H, H^{15}), 3.42 – 3.33 (m, 1H, H^{25}), 3.33 – 3.24 (m, 1H, H^{25}), 3.12 (dd, J = 15.0, 3.6 Hz, 1H, H^{19}), 2.80 – 2.68 (m, 3H, H^{19}, H^{26}), 1.00 (s, 9H, H^{11}); δ_C (126 MHz, $CDCl_3$/DMSO-d_6) 181.93 (C^7), 171.63 (C^{12}), 170.62 (C^{23}), 170.51 (C^{16}), 149.86 (C^{31}), 147.40 (C^{30}), 141.06 (C^5), 136.33 (C^{28}), 134.61 (C^{27}), 134.46 (C^{22}), 133.88 (C^{20}), 131.23 (q, J = 33.4 Hz, C^2), 123.35 (C^{29}), 123.00 (q, J = 272.9 Hz, C^3), 122.50 (C^4), 117.17 (C^1), 116.26 (C^{21}), 66.88 (C^9), 61.73 (C^{15}), 56.60 (C^{14}), 53.46 (C^{18}), 40.45 (C^{25}), 34.25 (C^{10}), 32.46 (C^{26}), 28.18 (C^{19}), 27.11 (C^{11}); δ_F (471 MHz, $CDCl_3$/DMSO-d_6) -62.97; υ_{max} (neat) cm^{-1}: 3290, 2980, 1652, 1540, 1474, 1385, 1278, 1175, 1135, 963, 681; high resolution ESI-MS calcd. for $C_{31}H_{37}F_6N_8O_4S$ $[M+H]^+$: 731.25572, found: 731.25583; $[\alpha]_D^{25}$ -54.5° (c 1.00, MeOH).

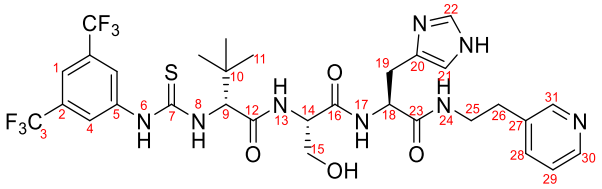

4.51

Compound **4.62** was N-Boc deprotected according to the general procedure B. The resulting amine (183 mg, 0.261 mmol) was treated according to the general procedures D and E. The product was purified by silica chromatography (10-13% MeOH/$CHCl_3$) to afford **4.51** (152 mg, 0.208 mmol, 80%) as a white solid foam.

Mp 140 °C; δ_H (500 MHz, $CDCl_3$/DMSO-d_6) 10.25 (s, 1H, H^6), 8.33 (dd, J = 4.9, 1.7 Hz, 1H, H^{30}), 8.29 (d, J = 2.1 Hz, 1H, H^{31}), 8.00 (s, 2H, H^4), 7.97 (s, 1H, H^{13}), 7.83 – 7.72 (m, 2H, H^8, H^{17}), 7.47 (s, 1H, H^1), 7.43 (s, 1H, H^{22}), 7.39 (dt, J = 7.8, 1.9 Hz, 1H, H^{28}), 7.30 – 7.25 (m, 1H, H^{24}), 7.12 (dd, J = 7.8, 4.9 Hz, 1H, H^{29}), 6.71 (s, 1H, H^{21}), 4.63 (d, J = 7.1 Hz, 1H, H^9), 4.54 (td, J = 9.3, 3.5 Hz, 1H, H^{18}), 4.15 (q, J = 4.2 Hz, 1H, H^{14}), 3.95 (dd, J = 11.6, 3.0 Hz, 1H, H^{15}), 3.72 (dd, J = 11.7, 4.2 Hz, 1H, H^{15}), 3.31 – 3.13 (m, 3H, H^{19}, H^{25}), 2.89 (dd, J = 15.1, 9.6 Hz, 1H, H^{19}), 2.74 – 2.57 (m, 2H, H^{26}), 1.02 (s, 9H, H^{11}); δ_C (126 MHz, $CDCl_3$/DMSO-d_6) 181.62 (C^7), 172.65 (C^{12}), 170.89 (C^{23}), 170.70 (C^{16}), 149.78 (C^{31}), 147.38 (C^{30}), 140.99 (C^5), 136.56 (C^{28}), 135.17 (C^{27}), 134.98 (C^{22}), 134.34 (C^{20}), 131.53 (q, J = 33.4 Hz, C^2), 123.57 (C^{29}), 123.13 (q, J = 272.9 Hz, C^3), 122.18 (C^4), 117.32 (C^1), 66.05 (C^9), 61.63 (C^{15}), 57.41 (C^{14}), 53.70 (C^{18}), 40.61 (C^{25}), 34.17 (C^{10}), 32.57 (C^{26}), 28.04 (C^{19}), 26.98 (C^{11}); δ_F (471 MHz, $CDCl_3$/DMSO-d_6) -62.87; υ_{max} (neat) cm^{-1}: 3290, 2981, 1653, 1540, 1385, 1278, 1175, 1135, 681; high resolution ESI-MS calcd. for $C_{31}H_{37}F_6N_8O_4S$ $[M+H]^+$: 731.25572, found: 731.25575; $[\alpha]_D^{25}$ +29.9° (c 1.00, MeOH).

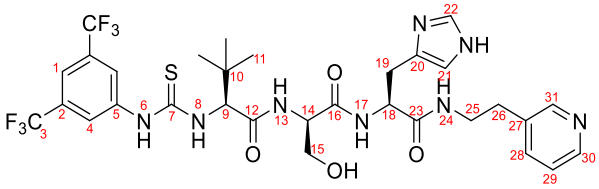

4.52

Compound **4.63** was N-Boc deprotected according to the general procedure B. The resulting amine (620 mg, 0.883 mmol) was treated according to the general procedures D and E. The product was purified by silica chromatography (10-12% MeOH/$CHCl_3$) to afford **4.52** (471 mg, 0.645 mmol, 73%) as a white solid foam.

Mp 134 °C; δ_H (500 MHz, $CDCl_3$/DMSO-d_6) 10.12 (s, 1H, H^6), 8.31 (d, J = 4.6 Hz, 1H, H^{30}), 8.27 (s, 1H, H^{31}), 8.21 (s, 1H, H^{13}/H^{17}), 8.12 – 8.03 (m, 1H, H^8), 7.98 (s, 2H, H^4), 7.92 (s, 1H, H^{13}/H^{17}), 7.47 (s, 1H, H^1), 7.40 (s, 1H, H^{22}), 7.32 (d, J = 7.7 Hz, 1H, H^{28}), 7.09 (t, J = 6.3 Hz, 1H, H^{29}), 6.67 (s, 1H, H^{21}), 4.95 (s, 1H, H^9), 4.69 (s, 2H, H^{14}, H^{18}), 3.82 (s, 1H, H^{15}), 3.66 (d, J = 9.7 Hz, 1H, H^{15}), 3.32 (s, 2H, H^{25}), 3.01 (d, J = 14.1 Hz, 1H, H^{19}), 2.86 (t, J = 12.0 Hz, 1H, H^{19}), 2.65 (t, J = 7.5 Hz, 2H, H^{26}), 1.03 (s, 9H, H^{11}); δ_C (126 MHz, $CDCl_3$/DMSO-d_6) 181.86 (C^7), 171.52 (C^{12}/C^{16}/C^{23}), 170.23 (C^{12}/C^{16}/C^{23}), 149.73 (C^{31}), 147.44 (C^{30}), 141.06 (C^5), 136.49 (C^{28}), 135.27 (C^{22}), 134.40 (C^{27}), 131.31 (q, J = 33.5 Hz, C^2), 123.60 (C^{29}), 123.25 (C^4), 123.13 (q, J = 272.8 Hz, C^3), 117.48 (C^1), 65.31 (C^9), 62.59 (C^{15}), 56.15 (C^{14}), 53.74 (C^{18}), 40.36 (C^{25}), 34.87 (C^{10}), 32.25 (C^{26}), 26.93 (C^{11}); δ_F (471 MHz, $CDCl_3$/DMSO-d_6) -62.89; υ_{max} (neat) cm^{-1}: 3657, 3298, 2981, 2888, 1652, 1539, 1473, 1384, 1277, 1137, 1073, 957; high resolution ESI-MS calcd. for $C_{31}H_{37}F_6N_8O_4S$ $[M+H]^+$: 731.25572, found: 731.25615; $[\alpha]_D^{25}$ -35.1° (c 1.00, MeOH).

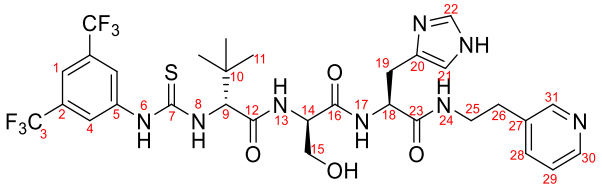

4.53

Compound **4.64** was N-Boc deprotected according to the general procedure B. The resulting amine (183 mg, 0.261 mmol) was treated according to the general procedures D and E. The product was purified by silica chromatography (10-12% MeOH/$CHCl_3$) to afford **4.53** (137 mg, 0.187 mmol, 72%) as a white solid foam.

Mp 138 °C; δ_H (500 MHz, $CDCl_3$/DMSO-d_6) 10.25 (s, 1H, H^6), 8.37 – 8.26 (m, 2H, H^{30}, H^{31}), 8.11 (s, 2H, H^4), 7.81 (dd, J = 12.5, 6.8 Hz, 3H, H^8, H^{13}, H^{17}), 7.58 (t, J = 5.5 Hz, 1H, H^{24}), 7.47 (s, 2H, H^1, H^{22}), 7.35 (d, J = 7.8 Hz, 1H, H^{28}), 7.12 (dd, J = 7.8, 4.9 Hz, 1H, H^{29}), 6.73 (s, 1H, H^{21}), 4.78 (d, J = 7.9 Hz, 1H, H^9), 4.58 (td, J = 8.0, 4.6 Hz, 1H, H^{18}), 4.33 (q, J = 5.6 Hz, 1H, H^{14}), 3.86 – 3.74 (m, 1H, H^{15}), 3.70 – 3.58 (m, 1H, H^{15}), 3.49 – 3.35 (m, 1H, H^{25}), 3.32 – 3.19 (m, 1H, H^{25}), 3.01 (dd, J = 15.1, 4.5 Hz, 1H, H^{19}), 2.92 (dd, J = 15.0, 8.0 Hz, 1H, H^{19}), 2.72 – 2.56 (m, 2H, H^{26}), 0.99 (s, 9H, H^{11}); δ_C (126 MHz, $CDCl_3$/DMSO-d_6) 181.66 (C^7), 171.28 (C^{12}), 171.04 (C^{23}), 170.60 (C^{16}), 149.75 (C^{31}), 147.32 (C^{30}), 141.29 (C^5), 136.87 (C^{28}), 134.93 (C^{27}), 134.89 (C^{22}), 131.41 (q, J = 33.4 Hz, C^2), 123.65 (C^{29}), 123.21 (q, J = 273.0 Hz, C^3), 122.41 (C^4), 117.18 (C^1), 65.78 (C^9), 62.18 (C^{15}), 56.14 (C^{14}), 53.86 (C^{18}), 40.32 (C^{25}), 34.92 (C^{10}), 32.65 (C^{26}), 28.79 (C^{19}), 27.06 (C^{11}); δ_F (471 MHz, $CDCl_3$/DMSO-d_6) -62.87; υ_{max} (neat) cm^{-1}: 3290, 2981, 1653, 1540, 1385, 1278, 1175, 1135, 681; high resolution ESI-MS calcd. for $C_{31}H_{37}F_6N_8O_4S$ $[M+H]^+$: 731.25572, found: 731.25574; $[\alpha]_D^{25}$ +56.4° (c 1.00, MeOH).

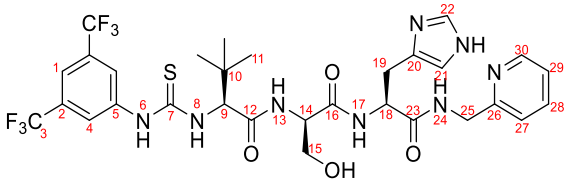

4.54

Compound **4.65** was N-Boc deprotected according to the general procedure B. The resulting amine (620 mg, 0.883 mmol) was treated according to the general procedures D and E. The product was purified by silica chromatography (10% MeOH/$CHCl_3$) to afford **4.54** (59 mg, 0.0823 mmol, 66%) as a white solid foam.

Mp 120-125 °C; δ_H (500 MHz, $CDCl_3$/DMSO-d_6) 10.03 (s, 1H, H^6), 8.57 – 8.22 (m, 3H, H^{17}, H^{24}, H^{30}), 8.11 (s, 1H, H^8), 7.95 (s, 2H, H^4), 7.76 (s, 1H, H^{13}), 7.50 (t, J = 7.7 Hz, 1H, H^{28}), 7.47 (s, 1H, H^1), 7.41 (s, 1H, H^{22}), 7.13 – 6.97 (m, 2H, H^{27}, H^{29}), 6.69 (s, 1H, H^{21}), 5.02 – 4.89 (m, 1H, H^9), 4.84 (s, 1H, H^{18}), 4.73 (s, 1H, H^{14}), 4.51 – 4.24 (m, 2H, H^{25}), 3.86 (d, J = 10.3 Hz, 1H, H^{15}), 3.67 (dd, J = 11.5, 5.5 Hz, 1H, H^{15}), 3.10 (d, J = 13.1 Hz, 1H, H^{19}), 2.92 (dd, J = 14.9, 9.4 Hz, 1H, H^{19}), 0.99 (s, 9H, H^{11}); δ_C (126 MHz, $CDCl_3$/DMSO-d_6) 182.01 (C^7), 171.72, 171.63, 170.39, 156.36 (C^{26}), 148.78 (C^{30}), 141.11 (C^5), 137.14 (C^{28}), 135.40 (C^{22}), 131.30 (q, J = 33.3 Hz, C^2), 123.63 (C^4), 123.18 (q, J = 272.8 Hz, C^3) 122.54 (C^{29}), 121.78 (C^{27}), 117.61 (C^1), 65.29 (C^9), 62.76 (C^{15}), 56.17 (C^{14}), 53.80 (C^{18}), 44.71 (C^{25}), 35.00 (C^{10}), 29.26 (C^{19}), 26.91 (C^{11}); δ_F (471 MHz, $CDCl_3$/DMSO-d_6) -62.87; υ_{max} (neat) cm^{-1}: 3293, 2965, 1651, 1535, 1474, 1385, 1277, 1176, 1132, 757, 701; high resolution ESI-MS calcd. for $C_{30}H_{35}F_6N_8O_4S$ $[M+H]^+$: 717.24007, found: 717.23982; $[\alpha]_D^{25}$ -23.3° (c 1.00, MeOH).

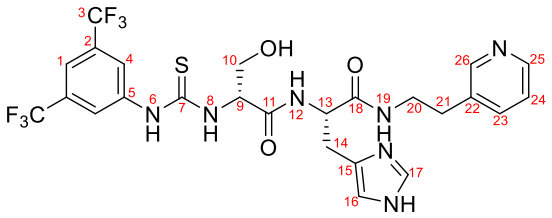

4.55

Compound **4.59** was N-Boc deprotected according to the general procedure B. The resulting amine (120 mg, 0.204 mmol) was treated according to the general procedures D and E. The product was purified by silica chromatography (10–15% MeOH/$CHCl_3$) to afford **4.55** (70 mg, 0.113 mmol, 56%) as a white solid foam.

Mp 145 °C; δ_H (400 MHz, $CDCl_3$/DMSO-d_6) 10.41 (s, 1H, H^6), 8.34 (dd, J = 5.0, 1.8 Hz, 2H, H^{25}, H^{26}), 8.21 (s, 2H, H^4), 8.16 (d, J = 8.3 Hz, 1H, H^{12}), 8.10 (d, J = 6.9 Hz, 1H, H^8), 7.72 (t, J = 5.8 Hz, 1H, H^{19}), 7.50 – 7.37 (m, 3H, H^1, H^{17}, H^{23}), 7.17 (dd, J = 7.8, 4.8 Hz, 1H, H^{24}), 6.72 (s, 1H, H^{16}), 4.85 (td, J = 6.2, 3.9 Hz, 1H, H^9), 4.47 (td, J = 8.2, 3.9 Hz, 1H, H^{13}), 3.95 (dd, J = 11.0, 3.9 Hz, 1H, H^{10}), 3.62 (dd, J = 11.1, 5.9 Hz, 1H, H^{10}), 3.42 – 3.24 (m, 2H, H^{20}), 3.02 (dd, J = 14.7, 4.0 Hz, 1H, H^{14}), 2.84 (dd, J = 14.8, 8.3 Hz, 1H, H^{14}), 2.70 (t, J = 7.1 Hz, 2H, H^{21}), 2.54 – 2.46 (m, 1H); δ_C (101 MHz, $CDCl_3$/DMSO-d_6) 179.39 (C^7), 169.81 (C^{18}), 168.86 (C^{11}), 148.82 (C^{26}), 146.35 (C^{25}), 140.69 (C^5), 135.18 (C^{23}), 133.64 (C^{17}/C^{22}), 133.60 (C^{17}/C^{22}), 129.79 (q, J = 33.1 Hz, C^2), 122.24 (C^{24}), 122.12 (q, J = 272.7 Hz, C^3), 120.59, 115.06 (C^1), 114.76 (C^{16}), 61.00 (C^{10}), 58.47 (C^9), 52.97 (C^{13}), 31.41 (C^{21}), 27.98 (C^{14}); δ_F (376 MHz, $CDCl_3$/DMSO-d_6) -62.51; υ_{max} (neat) cm^{-1}: 3275, 2981, 2888, 1653, 1540, 1473, 1383, 1277, 1176, 1129, 966, 886, 681; high resolution ESI-MS calcd. for $C_{25}H_{26}F_6N_7O_3S$ $[M+H]^+$ 618.17165, found: 618.17142; $[\alpha]_D^{25}$ +25.7° (c 1.00, MeOH).

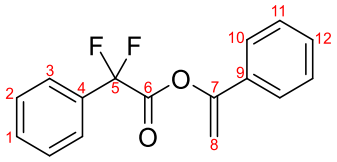

4.66

α,α-Difluorophenylacetic acid (1.721 g, 10 mmol) and phenylacetylene (2.2 ml, 20 mmol) were added to dry toluene (20 ml). Separately, ((*p*-cymene)$RuCl_2)_2$ (31 mg, 0.05 mmol) and tri(2-furyl)phosphine (23 mg, 0.1 mmol) were dissolved in dry toluene (20 ml). The two solutions were then combined and AgOTf (26 mg, 0.1 mmol) was added. The mixture was stirred overnight at 70 °C, filtered, and concentrated under vacuum. The residue was separated by silica chromatography (2-3% Et_2O/hexanes) to provide **4.66** (2.238 g, 8.16 mmol, 82%) as a light brown oil.

δ_H (400 MHz, $CDCl_3$/DMSO-d_6) 7.67 – 7.58 (m, 2H, H^3), 7.51 – 7.40 (m, 3H, H^1, H^2), 7.26 – 7.14 (m, 5H, H^{10}, H^{11}, H^{12}), 5.44 (d, J = 2.8 Hz, 1H, H^8), 5.00 (d, J = 2.8 Hz, 1H, H^8); δ_C (101 MHz, $CDCl_3$/DMSO-d_6) 162.26 (t, J = 36.9 Hz, C^6), 152.37 (C^7), 132.98 (C^9), 132.46 (t, J = 25.5 Hz, C^4), 131.44 (C^1), 129.49 (C^{12}), 128.98 (C^2), 128.73 (C^8/C^{11}), 125.72 (t, J = 6.0 Hz, C^3), 124.81 (C^8/C^{11}), 113.59 (t, J = 253.8 Hz, C^5), 102.65 (C^8); δ_F (376 MHz, $CDCl_3$/DMSO-d_6) -104.32.

Appendix A Host-host competition binding

Uncertainty analysis

Uncertainties of K_A values were estimated by assuming certain errors of sample preparation and propagating them through equations (3) – (9) in section 2.3.2. Errors were not propagated onto δ_{RX} for simplicity.

Assumptions:

- Relative uncertainty of a weighing: $\xi_1 = 0.004$ (weighing 5 mg with ± 0.02 mg accuracy)
- Relative uncertainty of solvent volume measurement: $\xi_2 = 0.005$ (dispensing 1 ml with ± 5 µl accuracy); this applies to addition of solvent to weighings of test compound, reference and titrant as well as to the transfer of test compound solution into NMR tube.
- Uncertainties in volume of reference solution and titrant added to the sample are neglected as relatively dilute (0.0015-0.015 M) solutions are added via a precision microsyringe, making these additions highly accurate.
- Uncertainty in chemical shift measurement is neglected as well; all spectra are referenced to residual solvent peak to ensure the accuracy of observed chemical shifts.

Error propagation was done as follows:

ΔY absolute uncertainty of value Y

$\frac{\Delta Y}{Y}$ relative uncertainty of value Y

$$\frac{\Delta C_A}{C_A} = \sqrt{{\xi_1}^2 + {\xi_2}^2}$$

$$\frac{\Delta[R]}{[R]} = \frac{\Delta C_X}{C_X} = \frac{\Delta C_R}{C_R} = \sqrt{{\xi_1}^2 + 2{\xi_2}^2}$$

$$\Delta[RX] = \sqrt{{\Delta C_R}^2 + \Delta[R]^2}$$

$$\frac{\Delta[X]}{[X]} = \sqrt{\left(\frac{\Delta[R]}{[R]}\right)^2 + \left(\frac{\Delta[RX]}{[RX]}\right)^2}$$

$$\Delta[AX] = \sqrt{\Delta C_X{}^2 + \Delta[X]^2 + \Delta[RX]^2}$$

$$\Delta[A] = \sqrt{\Delta C_A{}^2 + \Delta[AX]^2}$$

$$\Delta K_A = K_A \sqrt{\left(\frac{\Delta[AX]}{[AX]}\right)^2 + \left(\frac{\Delta[A]}{[A]}\right)^2 + \left(\frac{\Delta[X]}{[X]}\right)^2}$$

Plots of $K_A(K_R)$ used to determine anion affinities for 2.1b–2.3b

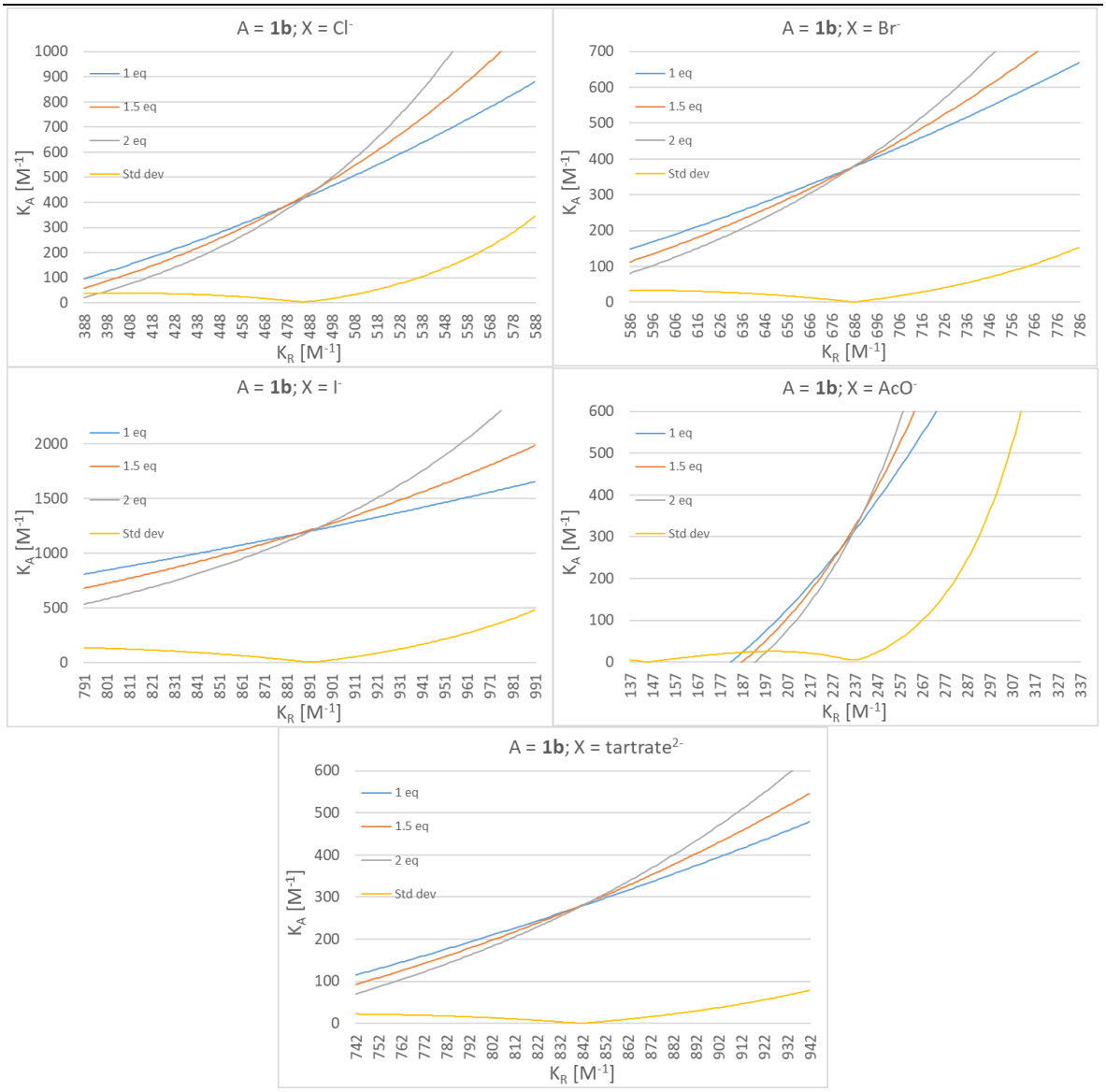

Figure 88 $K_A(K_R)$ plots for 2.1b titrated with various anions, 2.2a used as reference.

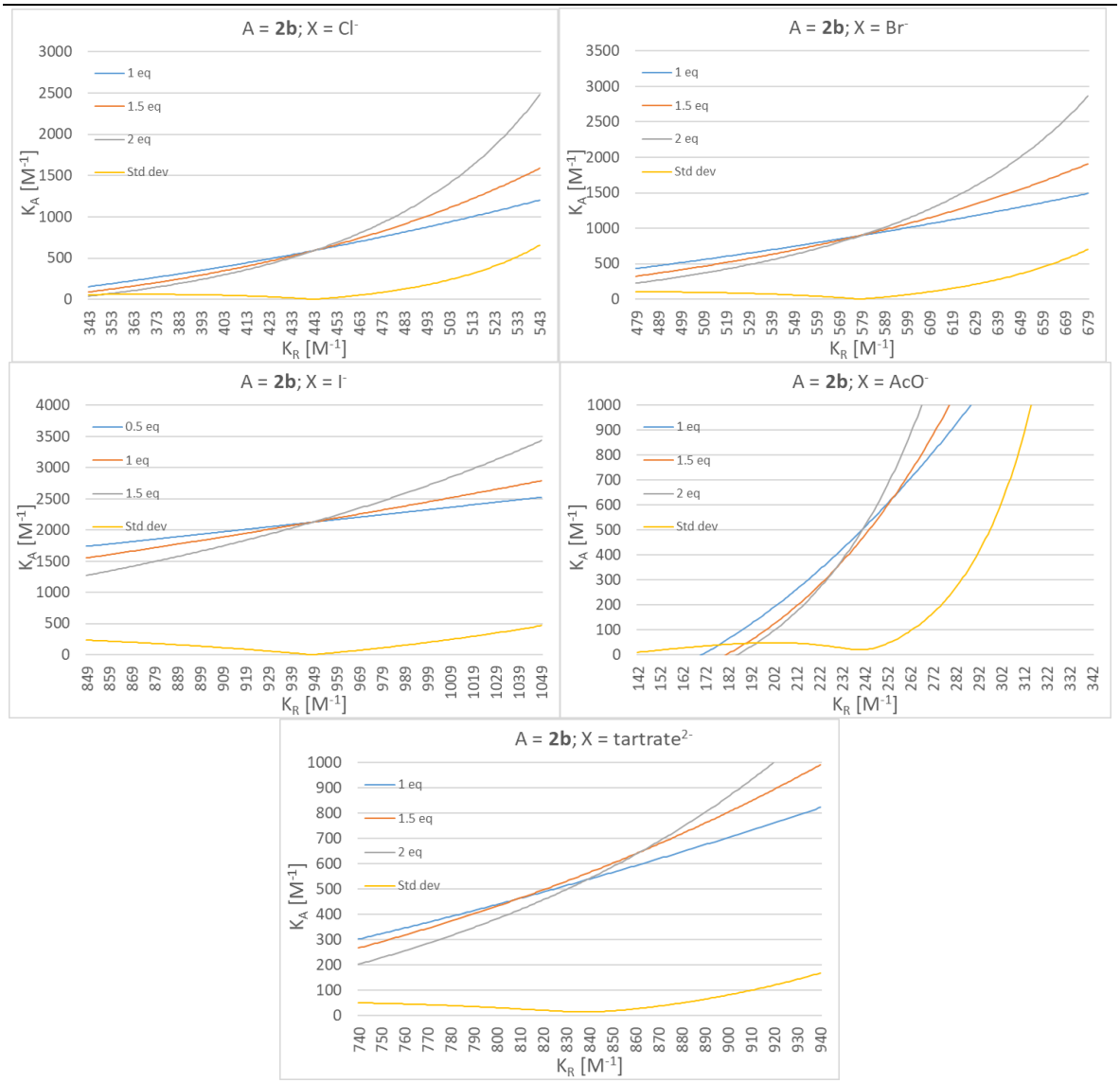

Figure 89 $K_A(K_R)$ plots for 2.2b titrated with various anions, 2.2a used as reference.

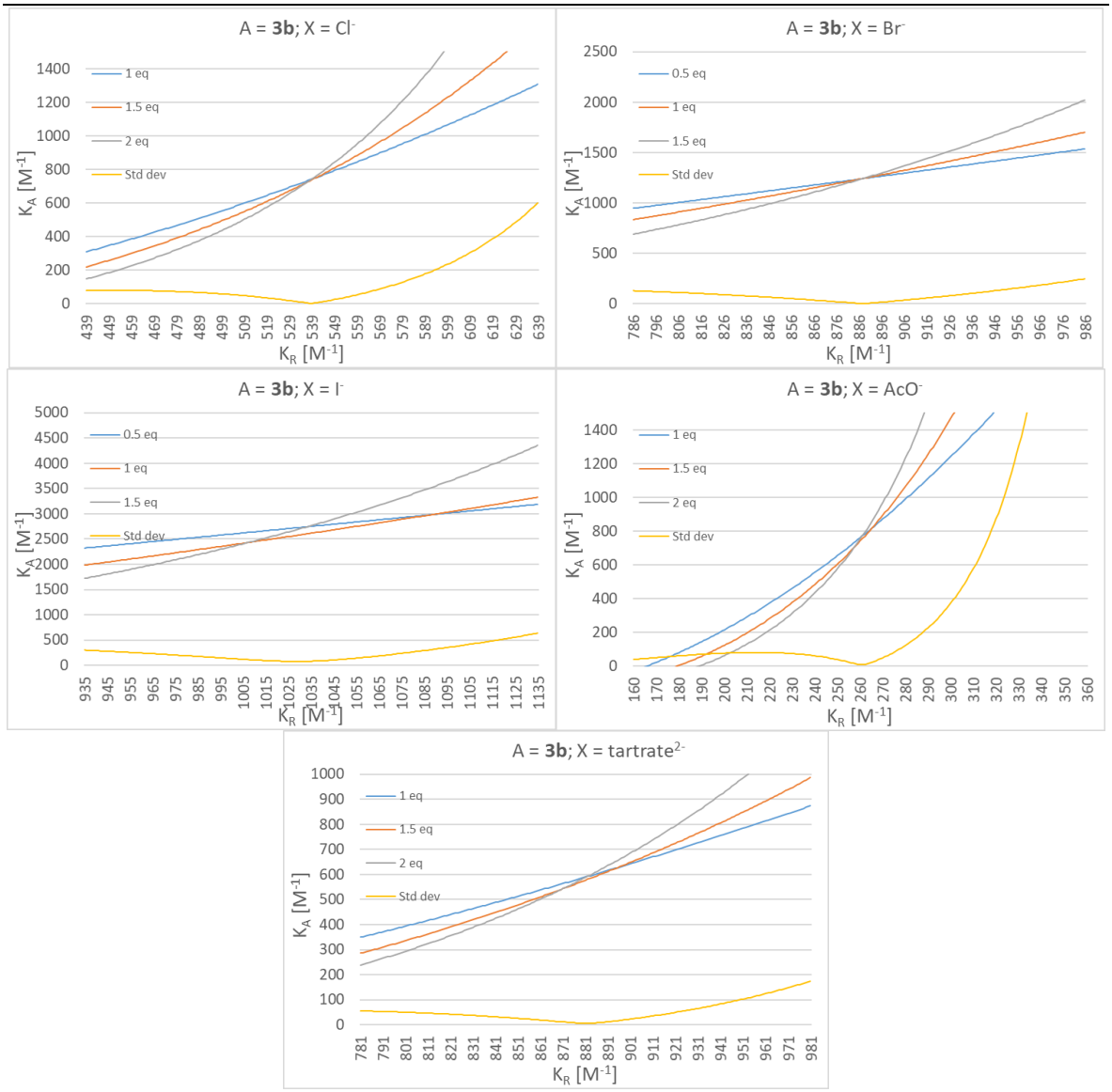

Figure 90 $K_A(K_R)$ plots for 2.3b titrated with various anions, 2.2a used as reference.

Appendix B Crystallographic data for **2.3b**·NaI*

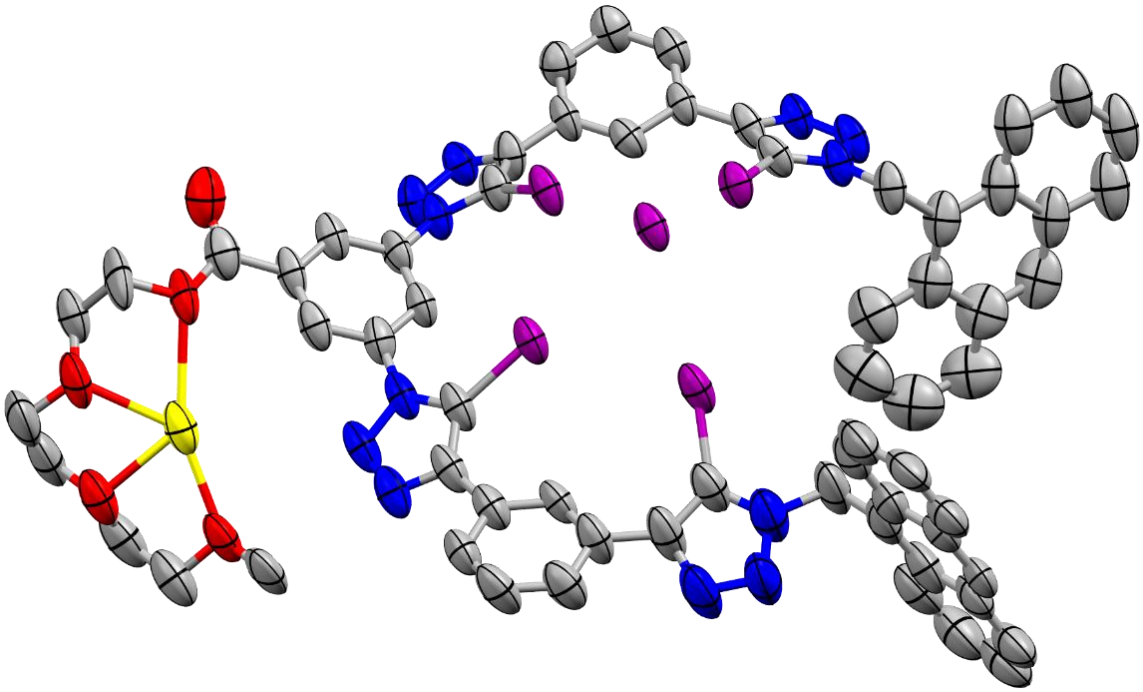

Empirical formula	$C_{76}H_{72}I_5N_{12}NaO_9$	
Formula weight	1954.99 g/mol	
Temperature	100 K	
Wavelength	0.68890 Å	
Crystal system	Triclinic	
Space group	P -1	
Unit cell dimensions	a = 14.3220(4)	α = 113.335(2)
	b = 17.7665(5)	β = 100.303(2)
	c = 17.7815(5)	γ = 93.903(2)
Volume	4038.8(2) $Å^3$	
Z	2	
Density	1.607 g/cm^3	

* X-ray diffraction data was collected and processed with contributions from Asha Brown, Jason Y. C. Lim, Amber L. Thompson, and Kirsten E. Christensen.

Absorption coefficient	1.991 mm^{-1}
F(000)	1920
Crystal size	0.1 × 0.3 × 0.6 mm
Theta range for data collection	1.661° to 36.434°
Reflections collected	88130
Independent reflections	37810
Absorption correction	Multi-scan
Refinement method	Full-matrix least-squares on F^2
Goodness-of-fit on F^2	0.9962
R indices (2σ cutoff)	R^1 = 0.0996, wR^2 = 0.2809
R indices (all data)	R^1 = 0.1180, wR^2 = 0.2929

Single crystals of compound **2.3b·NaI** were grown by combining **2.3b** and excess NaI in 6:4 $CHCl_3$/acetone. Crystal growth was initiated by vapour diffusion of acetone into the resulting supersaturated solution of **2.3b·NaI**. Diffraction data were collected at 100(2) K using a custom-built Crystal Logic diffractometer with synchrotron radiation (λ = 0.6889 Å) at Diamond Light Source, beamline I19.[277] Unit cell parameter determination and data reduction were carried out using CrysAlisPro. The structures were solved by charge-flipping using SUPERFLIP[278] and refined by full matrix least squares on F^2 using the CRYSTALS[279] suite. All non-hydrogen atoms were refined with anisotropic displacement parameters. Hydrogen atoms were initially positioned geometrically and their positions and displacement parameters refined using restraints prior to their inclusion in the final model using riding constraints.[280]

The crystals were small and weakly diffracting and, despite the use of synchrotron radiation, the diffraction was still weak and the data which were obtained were of relatively low quality. Where appropriate, restraints to bond lengths and angles were therefore applied to ensure a physically reasonable model, and thermal and vibrational restraints were applied to maintain sensible

displacement ellipsoids. Enlarged displacement ellipsoids suggested the presence of disorder in the non-coordinating acetone solvent molecules; however, attempts to model this disorder using two sites did not produce a satisfactory model. An area of residual electron density, presumably arising from diffuse disordered solvent molecules, was also present and since this electron density could not be modelled sensibly it was included in refinement by treating the discrete Fourier transform of the void region as contributions to the calculated structure factors with PLATON/SQUEEZE[281,282] (125 Å containing 51 electrons). Full refinement details are given in the CIF. Crystallographic data have been deposited with the Cambridge Crystallographic Data Centre (CCDC 1529410).

Appendix C Data for electrochemical sensing*

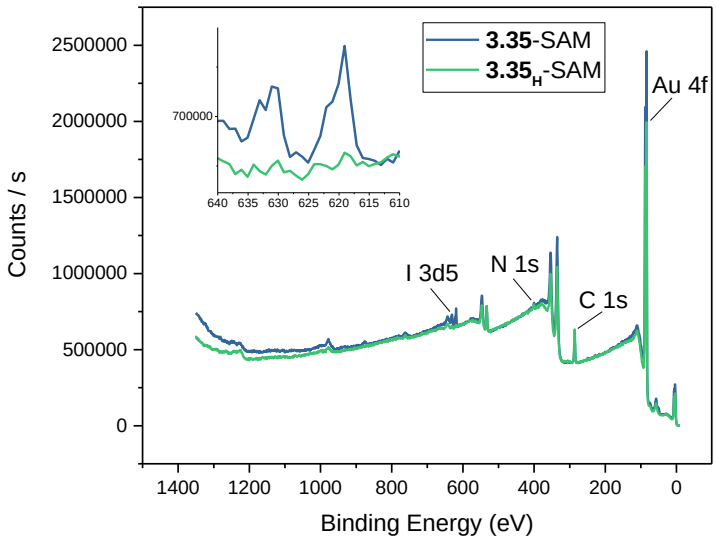

Figure 91 Low resolution survey XPS spectra of 3.35-SAM and 3.35_H-SAM. Inset: Magnification of I 3d region.

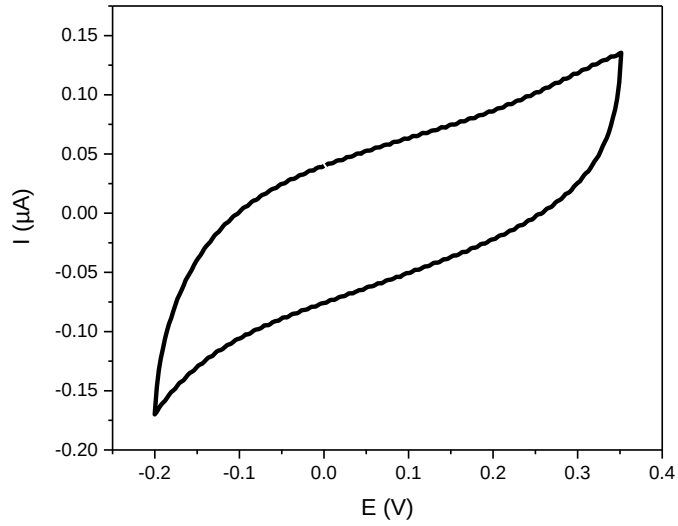

Figure 92 CV of 3.35-SAM in 100 mM NaCl at a scan rate of 0.1 V/s.

* The data shown here was collected by Robert Hein.

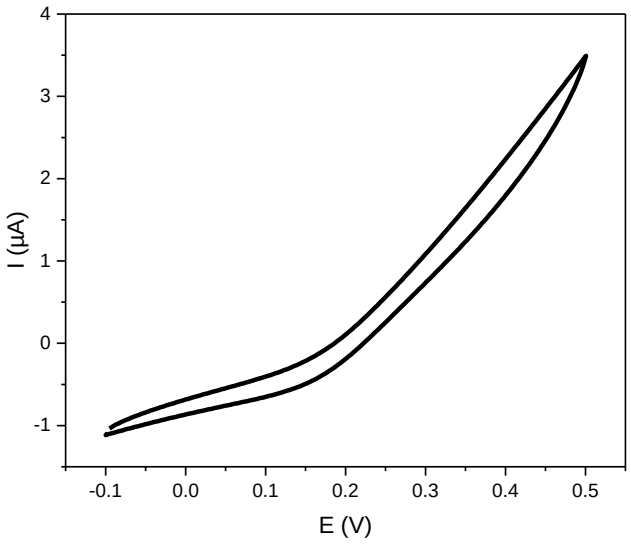

Figure 93 CV of 3.35-SAM in 10 mM $Fe(CN)_6^{3-/4-}$ and 100 mM NaCl at a scan rate of 0.1 V/s.

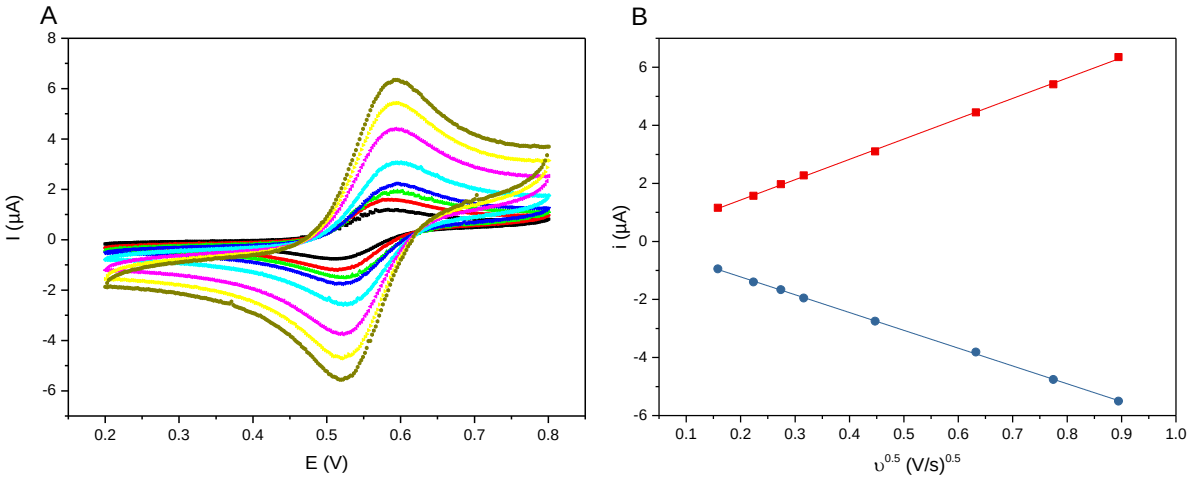

Figure 94 CVs (A) and anodic and cathodic peak currents (B) of 0.1 mM 3.39 in MeCN with 100 mM $TBAPF_6$ at varying scan rates.

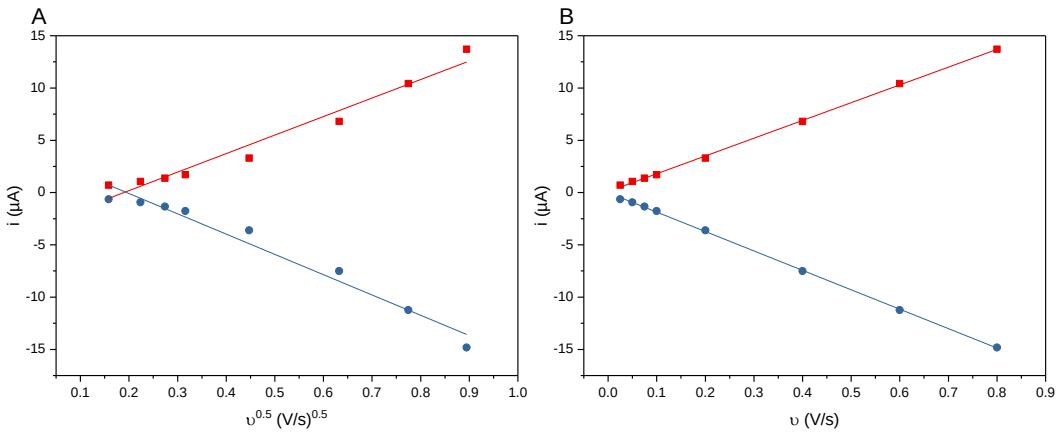

Figure 95 Anodic and cathodic peak currents of 0.1 mM 3.39 in H_2O with 100 mM $NaPF_6$ vs. square-root of scan rate (A) and scan rate (B).

References

1 D. Rossetto, N. Avvakumov and J. Côté, *Epigenetics*, 2012, **7**, 1098–1108.

2 G. Morrison, in *Clinical Methods: The History, Physical, and Laboratory Examinations*, 1990, pp. 890–894.

3 D. C. Gadsby, P. Vergani and L. Csanády, *Nature*, 2006, **440**, 477–483.

4 P. M. Quinton, *Nature*, 1983, **301**, 421–422.

5 A. N. Mayeno, A. J. Curran, R. L. Roberts and C. S. Foote, *J. Biol. Chem.*, 1989, **264**, 5660–5668.

6 A. S. McCall, C. F. Cummings, G. Bhave, R. Vanacore, A. Page-Mccaw and B. G. Hudson, *Cell*, 2014, **157**, 1380–1392.

7 O. Dohán, A. De La Vieja, V. Paroder, C. Riedel, M. Artani, M. Reed, C. S. Ginter and N. Carrasco, *Endocr. Rev.*, 2003, **24**, 48–77.

8 R. W. Howarth, G. Billen, D. Swaney, A. Townsend, N. Jaworski, K. Lajtha, J. A. Downing, R. Elmgren, N. Caraco, T. Jordan, F. Berendse, J. Freney, V. Kudeyarov, P. Murdoch and Z. L. Zhu, *Biogeochemistry*, 1996, **35**, 75–139.

9 S. G. Chang, D. Littlejohn and K. Y. Hu, *Science*, 1987, **237**, 756–758.

10 Z. Liu, M. Frasconi, J. Lei, Z. J. Brown, Z. Zhu, D. Cao, J. Iehl, G. Liu, A. C. Fahrenbach, Y. Y. Botros, O. K. Farha, J. T. Hupp, C. A. Mirkin and J. F. Stoddart, *Nat. Commun.*, 2013, **4**, 1–9.

11 N. N. Popova, I. G. Tananaev, S. I. Rovnyi and B. F. Myasoedov, *Russ. Chem. Rev.*, 2003, **72**, 101–121.

12 D. R. Rosseinsky, *Chem. Rev.*, 1965, **65**, 467–490.

13 D. W. Smith, *J. Chem. Educ.*, 1977, **54**, 540.

14 Y. Zhang and P. S. Cremer, *Curr. Opin. Chem. Biol.*, 2006, **10**, 658–663.

15 A. M. Hyde, S. L. Zultanski, J. H. Waldman, Y. L. Zhong, M. Shevlin and F. Peng, *Org. Process Res. Dev.*, 2017, **21**, 1355–1370.

16 F. Hofmeister, *Arch. für Exp. Pathol. und Pharmakologie*, 1888, **25**, 1–30.

17 W. Kunz, J. Henle and B. W. Ninham, *Curr. Opin. Colloid Interface Sci.*, 2004, **9**, 19–37.

18 T. Morita, P. Westh, K. Nishikawa and Y. Koga, *J. Phys. Chem. B*, 2014, **118**, 8744–8749.

19 N. H. Evans and P. D. Beer, *Angew. Chemie Int. Ed.*, 2014, **53**, 11716–11754.

20 Y. Marcus, *Biophys. Chem.*, 1994, **51**, 111–127.

21 D. F. Shriver and M. J. Biallas, *J. Am. Chem. Soc.*, 1967, **89**, 1078–1081.

22 C. H. Park and H. E. Simmons, *J. Am. Chem. Soc.*, 1968, **90**, 2431–2432.

23 C. J. Pedersen, *J. Am. Chem. Soc.*, 1967, **89**, 7017–7036.

24 J. Cullinane, R. I. Gelb, T. N. Margulis and L. J. Zompa, *J. Am. Chem. Soc.*, 1982, **104**, 3048–3053.

25 R. I. Gelb, B. T. Lee and L. J. Zompa, *J. Am. Chem. Soc.*, 1985, **107**, 909–916.

26 R. I. Gelb, L. M. Schwartz and L. J. Zompa, *Inorg. Chem.*, 1986, **25**, 1527–1535.

27 J.-M. Lehn, *Pure Appl. Chem.*, 1978, **50**, 871–892.

28 M. W. Hosseini and J.-M. Lehn, *Helv. Chim. Acta*, 1988, **71**, 749–756.

29 M. E. Jung and H. Xia, *Tetrahedron Lett.*, 1988, **29**, 297–300.

30 M. Newcomb, J. H. Horner, M. T. Blanda and P. J. Squattrito, *J. Am. Chem. Soc.*, 1989, **111**, 6294–6301.

31 N. H. Evans and P. D. Beer, *Angew. Chem. Int. Ed.*, 2014, **53**, 11716–11754.

32 P. A. Gale, *Coord. Chem. Rev.*, 2000, **199**, 181–233.

33 P. a. Gale, *Coord. Chem. Rev.*, 2003, **240**, 191–221.

34 P. A. Gale and R. Quesada, *Coord. Chem. Rev.*, 2006, **250**, 3219–3244.

35 P. A. Gale, S. E. García-Garrido and J. Garric, *Chem. Soc. Rev.*, 2008, **37**, 151–190.

36 P. A. Gale, *Chem. Soc. Rev.*, 2010, **39**, 3746–3771.

37 M. Wenzel, J. R. Hiscock and P. A. Gale, *Chem. Soc. Rev.*, 2012, **41**, 480–520.

38 P. A. Gale, N. Busschaert, C. J. E. Haynes, L. E. Karagiannidis and I. L. Kirby, *Chem. Soc. Rev.*, 2014, **43**, 205–241.

39 P. A. Gale, E. N. W. Howe and X. Wu, *Chem*, 2016, **1**, 351–422.

40 A. Brown and P. D. Beer, *Chem. Commun.*, 2016, **52**, 8645–8658.

41 J. Y. C. Lim and P. D. Beer, *Chem*, 2018, **4**, 731–783.

42 B. L. Schottel, H. T. Chifotides and K. R. Dunbar, *Chem. Soc. Rev.*, 2008, **37**, 68–83.

43 S. Kubik, *Chem. Soc. Rev.*, 2010, **39**, 3648–3663.

44 M. J. Langton, C. J. Serpell and P. D. Beer, *Angew. Chem. Int. Ed.*, 2016, **55**, 1974–1987.

45 R. Vilar, *Angew. Chem. Int. Ed.*, 2003, **42**, 1460–1477.

46 M. Bru, I. Alfonso, M. I. Burguete and S. V. Luis, *Angew. Chem. Int. Ed.*, 2006, **45**, 6155–6159.

47 M. S. Vickers and P. D. Beer, *Chem. Soc. Rev.*, 2007, **36**, 211–225.

48 P. A. Gale, *Acc. Chem. Res.*, 2011, **44**, 216–226.

49 S. K. Mc Kim and J. L. Sessler, *Chem. Soc. Rev.*, 2010, **39**, 3784–3809.

50 A. J. McConnell and P. D. Beer, *Angew. Chem. Int. Ed.*, 2012, **51**, 5052–5061.

51 M. Brune, J. L. Hunter, S. A. Howell, S. R. Martin, T. L. Hazlett, J. E. T. Corrie and M. R. Webb, *Biochemistry*, 1998, **37**, 10370–10380.

52 M. Hirshberg, K. Henrick, L. L. Haire, N. Vasisht, M. Brune, J. E. T. Corrie and M. R. Webb, *Biochemistry*, 1998, **37**, 10381–10385.

53 M. Brune, J. L. Hunter, J. E. Corrie and M. R. Webb, *Biochemistry*, 1994, **33**, 8262–8271.

54 J. J. He and F. A. Quiocho, *Protein Sci.*, 1993, **2**, 1643–1647.

55 L. W. Hung, I. X. Wang, K. Nikaido, P. Q. Liu, G. F. L. Ames and S. H. Kim, *Nature*, 1998, **396**,

703–707.

56 C. F. Higgins and K. J. Linton, *Nat. Struct. Mol. Biol.*, 2004, **11**, 918–926.

57 R. Dutzler, E. B. Campbell and R. MacKinnon, *Science*, 2003, **300**, 108–112.

58 R. Dutzler, E. B. Campbel, M. Cadene, B. T. Chait and R. MacKinnon, *Nature*, 2002, **415**, 287–294.

59 A. Accardi and A. Picollo, *Biochim. Biophys. Acta - Biomembr.*, 2010, **1798**, 1457–1464.

60 J. W. Larson and T. B. Mcmahon, *Inorg. Chem.*, 1984, **23**, 2029–2033.

61 P. A. Wood, F. H. Allen and E. Pidcock, *CrystEngComm*, 2009, **11**, 1563.

62 A. C. Legon and D. J. Millen, *Chem. Soc. Rev.*, 1987, **16**, 467–498.

63 B. Dietrich, D. L. Fyles, T. M. Fyles and J.-M. Lehn, *Helv. Chim. Acta*, 1979, **62**, 2763–2787.

64 A. Metzger, V. M. Lynch and E. V. Anslyn, *Angew. Chem. Int. Ed.*, 1997, **36**, 862–865.

65 A. Metzger and E. V. Anslyn, *Angew. Chem. Int. Ed.*, 1998, **37**, 649–652.

66 J. S. Mendy, M. L. Pilate, T. Horne, V. W. Day and M. A. Hossain, *Chem. Commun.*, 2010, **46**, 6084–6086.

67 I. Alfonso, B. Dietrich, F. Rebolledo, V. Gotor and J.-M. Lehn, *Helv. Chim. Acta*, 2001, **84**, 280–295.

68 K. Kavallieratos, S. R. De Gala, D. J. Austin and R. H. Crabtree, *J. Am. Chem. Soc.*, 1997, **119**, 2325–2326.

69 K. Kavallieratos, C. M. Bertao and R. H. Crabtree, *J. Org. Chem.*, 1999, **64**, 1675–1683.

70 S. I. Kondo, Y. Hiraoka, N. Kurumatani and Y. Yano, *Chem. Commun.*, 2005, 1720–1722.

71 S. Kubik, R. Goddard, R. Kirchner, D. Nolting and J. Seidel, *Angew. Chem. Int. Ed.*, 2001, **40**, 2648–2651.

72 S. Kubik, R. Kirchner, D. Nolting and J. Seidel, *J. Am. Chem. Soc.*, 2002, **124**, 12752–12760.

73 T. Fiehn, R. Goddard, R. W. Seidel and S. Kubik, *Chem. Eur. J.*, 2010, **16**, 7241–7255.

74 A. Schaly, R. Belda, E. García-España and S. Kubik, *Org. Lett.*, 2013, **15**, 6238–6241.

75 P. Bühlmann, S. Nishizawa, K. P. Xiao and Y. Umezawa, *Tetrahedron*, 1997, **53**, 1647–1654.

76 C. Raposo, M. Almaraz, M. Martín, V. Weinrich, M. L. Mussóns, V. Alcázar, M. C. Caballero and J. R. Morán, *Chem. Lett.*, 1995, **24**, 759–760.

77 A. Frontera, J. Morey, A. Oliver, M. N. Piña, D. Quiñonero, A. Costa, P. Ballester, P. M. Deyà and E. V. Anslyn, *J. Org. Chem.*, 2006, **71**, 7185–7195.

78 S. ichi Sasaki, M. Mizuno, K. Naemura and Y. Tobe, *J. Org. Chem.*, 2000, **65**, 275–283.

79 D. Meshcheryakov, V. Böhmer, M. Bolte, V. Hubscher-Bruder, F. Arnaud-Neu, H. Herschbach, A. Van Dorsselaer, I. Thondorf and W. Mögelin, *Angew. Chem. Int. Ed.*, 2006, **45**, 1648–1652.

80 J. Scheerder, M. Fochi, J. F. J. Engbersen and D. N. Reinhoudt, *J. Org. Chem.*, 1994, **59**, 7815–7820.

81 A. Baeyer, *Ber. Dtsch. Chem. Ges.*, 1886, **19**, 2184–2185.

82 C. H. Lee, H. Miyaji, D. W. Yoon and J. L. Sessler, *Chem. Commun.*, 2008, 24–34.

83 P. Anzenbacher, K. Jursíková, V. M. Lynch, P. A. Gale and J. L. Sessler, *J. Am. Chem. Soc.*, 1999, **121**, 11020–11021.

84 D. W. Yoon, D. E. Gross, V. M. Lynch, J. L. Sessler, B. P. Hay and C. H. Lee, *Angew. Chem. Int. Ed.*, 2008, **47**, 5038–5042.

85 M. Buda, A. Iordache, C. Bucher, J. C. Moutet, G. Royal, E. Saint-Aman and J. L. Sessler, *Chem. Eur. J.*, 2010, **16**, 6810–6819.

86 E. A. Kataev, P. Pantos, E. Karnas, G. V. Kolesnikov, I. G. Tananaev, V. M. Lynch and J. L. Sessler, *Supramol. Chem.*, 2015, **27**, 346–356.

87 K. J. Chang, D. Moon, S. L. Myoung and K. S. Jeong, *Angew. Chem. Int. Ed.*, 2005, **44**, 7926–7929.

88 N. K. Kim, K. J. Chang, D. Moon, M. S. Lah and K. S. Jeong, *Chem. Commun.*, 2007, 3401–3403.

89 J. Il Kim, H. Juwarker, X. Liu, M. S. Lah and K. S. Jeong, *Chem. Commun.*, 2010, **46**, 764–766.

90 J. M. Suk, D. A. Kim and K. S. Jeong, *Org. Lett.*, 2012, **14**, 5018–5021.

91 V. Haridas, S. Sahu, P. P. Praveen Kumar and A. R. Sapala, *RSC Adv.*, 2012, **2**, 12594–12605.

92 Y. Bourne, H. C. Kolb, Z. Radic, K. B. Sharpless, P. Taylor and P. Marchot, *Proc. Natl. Acad. Sci.*, 2004, **101**, 1449–1454.

93 H. Juwarker, J. M. Lenhardt, D. M. Pham and S. L. Craig, *Angew. Chem. Int. Ed.*, 2008, **47**, 3740–3743.

94 H. Juwarker, J. M. Lenhardt, J. C. Castillo, E. Zhao, S. Krishnamurthy, R. M. Jamiolkowski, K. H. Kim and S. L. Craig, *J. Org. Chem.*, 2009, **74**, 8924–8934.

95 Y. Li and A. H. Flood, *J. Am. Chem. Soc.*, 2008, **130**, 12111–12122.

96 K. P. McDonald, R. O. Ramabhadran, S. Lee, K. Raghavachari and A. H. Flood, *Org. Lett.*, 2011, **13**, 6260–6263.

97 K. Chellappan, N. J. Singh, I. C. Hwang, W. L. Jung and K. S. Kim, *Angew. Chem. Int. Ed.*, 2005, **44**, 2899–2903.

98 S. Lee, C. H. Chen and A. H. Flood, *Nat. Chem.*, 2013, **5**, 704–710.

99 E. M. Fatila, M. Pink, E. B. Twum, J. A. Karty and A. H. Flood, *Chem. Sci.*, 2018, **9**, 2863–2872.

100 M. Lisbjerg, B. M. Jessen, B. Rasmussen, B. E. Nielsen, A. Madsen and M. Pittelkow, *Chem. Sci.*, 2014, **5**, 2647–2650.

101 J. Svec, M. Necas and V. Sindelar, *Angew. Chemie Int. Ed.*, 2010, **49**, 2378–2381.

102 V. Havel, J. Svec, M. Wimmerova, M. Dusek, M. Pojarova and V. Sindelar, *Org. Lett.*, 2011, **13**, 4000–4003.

103 M. A. Yawer, V. Havel and V. Sindelar, *Angew. Chem. Int. Ed.*, 2015, **54**, 276–279.

104 H. J. Buschmann, E. Cleve and E. Schollmeyer, *Inorg. Chem. Commun.*, 2005, **8**, 125–127.

105 T. Fiala, K. Sleziakova, K. Marsalek, K. Salvadori and V. Sindelar, *J. Org. Chem.*, 2018, **83**, 1903–1912.

106 T. Clark, M. Hennemann, J. S. Murray and P. Politzer, *J. Mol. Model.*, 2007, **13**, 291–296.

107 S. Scheiner, *Faraday Discuss.*, 2017, **203**, 213–226.

108 F. Zapata, A. Caballero, P. Molina, I. Alkorta and J. Elguero, *J. Org. Chem.*, 2014, **79**, 6959–6969.

109 D. J. Pascoe, K. B. Ling and S. L. Cockroft, *J. Am. Chem. Soc.*, 2017, **139**, 15160–15167.

110 C. C. Robertson, R. N. Perutz, L. Brammer and C. A. Hunter, *Chem. Sci.*, 2014, **5**, 4179–4183.

111 Y. Liu, A. Sengupta, K. Raghavachari and A. H. Flood, *Chem*, 2017, **3**, 411–427.

112 H. Wang, W. Wang and W. J. Jin, *Chem. Rev.*, 2016, **116**, 5072–5104.

113 A. Bauzá and A. Frontera, *Angew. Chem. Int. Ed.*, 2015, **54**, 7340–7343.

114 P. Politzer, J. S. Murray and T. Clark, *Phys. Chem. Chem. Phys.*, 2013, **15**, 11178.

115 H. A. Bent, *Chem. Rev.*, 1968, **68**, 587–648.

116 G. Cavallo, P. Metrangolo, R. Milani, T. Pilati, A. Priimagi, G. Resnati and G. Terraneo, *Chem. Rev.*, 2016, **116**, 2478–2601.

117 A. Mukherjee, S. Tothadi and G. R. Desiraju, *Acc. Chem. Res.*, 2014, **47**, 2514–2524.

118 B. K. Saha, A. Nangia and M. Jaskólski, *CrystEngComm*, 2005, **7**, 355–358.

119 N. Guo, R. Maurice, D. Teze, J. Graton, J. Champion, G. Montavon and N. Galland, *Nat. Chem.*, 2018, **10**, 1–7.

120 M. G. Sarwar, B. Dragisic, S. Sagoo and M. S. Taylor, *Angew. Chem. Int. Ed.*, 2010, **49**, 1674–1677.

121 S. H. Jungbauer, S. Schindler, E. Herdtweck, S. Keller and S. M. Huber, *Chem. Eur. J.*, 2015, **21**, 13625–13636.

122 V. Amendola, G. Bergamaschi, M. Boiocchi, N. Fusco, M. V. La Rocca, L. Linati, E. Lo Presti, M. Mella, P. Metrangolo and A. Miljkovic, *RSC Adv.*, 2016, **6**, 67540–67549.

123 S. M. Walter, F. Kniep, L. Rout, F. P. Schmidtchen, E. Herdtweck and S. M. Huber, *J. Am. Chem. Soc.*, 2012, **134**, 8507–8512.

124 S. H. Jungbauer and S. M. Huber, *J. Am. Chem. Soc.*, 2015, **137**, 12110–12120.

125 A. Caballero, F. Zapata, N. G. White, P. J. Costa, V. Félix and P. D. Beer, *Angew. Chem. Int. Ed.*, 2012, **51**, 1876–1880.

126 A. Dreger, E. Engelage, B. Mallick, P. D. Beer and S. M. Huber, *Chem. Commun.*, 2018, **54**, 4013–4016.

127 M. J. Langton, S. W. Robinson, I. Marques, V. Félix and P. D. Beer, *Nat. Chem.*, 2014, **6**, 1039–1043.

128 D. Mungalpara, S. Stegmüller and S. Kubik, *Chem. Commun.*, 2017, **53**, 5095–5098.

129 J. Y. C. Lim, T. Bunchuay and P. D. Beer, *Chem. Eur. J.*, 2017, **23**, 4700–4707.

130 K. T. Mahmudov, M. N. Kopylovich, M. F. C. Guedes Da Silva and A. J. L. Pombeiro, *Dalt.*

Trans., 2017, **46**, 10121–10138.

131 T. Chivers and R. S. Laitinen, *Chem. Soc. Rev.*, 2015, **44**, 1725–1739.

132 N. A. Semenov, A. V. Lonchakov, N. A. Pushkarevsky, E. A. Suturina, V. V. Korolev, E. Lork, V. G. Vasiliev, S. N. Konchenko, J. Beckmann, N. P. Gritsan and A. V. Zibarev, *Organometallics*, 2014, **33**, 4302–4314.

133 G. E. Garrett, G. L. Gibson, R. N. Straus, D. S. Seferos and M. S. Taylor, *J. Am. Chem. Soc.*, 2015, **137**, 4126–4133.

134 G. E. Garrett, E. I. Carrera, D. S. Seferos and M. S. Taylor, *Chem. Commun.*, 2016, **52**, 9881–9884.

135 J. Y. C. Lim, I. Marques, A. L. Thompson, K. E. Christensen, V. Félix and P. D. Beer, *J. Am. Chem. Soc.*, 2017, **139**, 3122–3133.

136 G. Müller, J. Brand and S. E. Jetter, *Z. Naturforsch. B Chem. Sci.*, 2001, **56**, 1163–1171.

137 D. Setiawan, E. Kraka and D. Cremer, *J. Phys. Chem. A*, 2015, **119**, 1642–1656.

138 S. Scheiner, *Acc. Chem. Res.*, 2013, **46**, 280–288.

139 Y. S. Chen, L. F. Yao and X. F. Lin, *Comput. Theor. Chem.*, 2014, **1036**, 44–50.

140 J. Qiu, D. K. Unruh and A. F. Cozzolino, *J. Phys. Chem. A*, 2016, **120**, 9257–9269.

141 S. Benz, A. I. Poblador-Bahamonde, N. Low-Ders and S. Matile, *Angew. Chem. Int. Ed.*, 2018, **57**, 5408–5412.

142 M. Newcomb, J. H. Horner and M. T. Blanda, *J. Am. Chem. Soc.*, 1987, **109**, 7878–7879.

143 M. Newcomb, A. M. Madonik, M. T. Blanda and J. K. Judice, *Organometallics*, 1987, **6**, 145–150.

144 A. R. Bassindale, H. Chen, Z. Liu, I. A. MacKinnon, D. J. Parker, P. G. Taylor, Y. Yang, M. E. Light, P. N. Horton and M. B. Hursthouse, *J. Organomet. Chem.*, 2004, **689**, 3287–3300.

145 A. R. Bassindale, D. J. Parker, M. Pourny, P. G. Taylor, P. N. Horton and M. B. Hursthouse, *Organometallics*, 2004, **23**, 4400–4405.

146 P. G. Taylor, A. R. Bassindale, Y. El Aziz, M. Pourny, R. Stevenson, M. B. Hursthouse and S. J. Coles, *Dalt. Trans.*, 2012, **41**, 2048–2059.

147 L. A. Villaescusa, P. Lightfoot and R. E. Morris, *Chem. Commun.*, 2002, **2**, 2220–2221.

148 D. X. Wang, Q. Y. Zheng, Q. Q. Wang and M. X. Wang, *Angew. Chem. Int. Ed.*, 2008, **47**, 7485–7488.

149 D. X. Wang and M. X. Wang, *J. Am. Chem. Soc.*, 2013, **135**, 892–897.

150 P. De Hoog, P. Gamez, I. Mutikainen, U. Turpeinen and J. Reedijk, *Angew. Chem. Int. Ed.*, 2004, **43**, 5815–5817.

151 J. Luo, Y.-F. Ao, C. Malm, J. Hunger, Q.-Q. Wang and D.-X. Wang, *Dalt. Trans.*, 2018, **47**, 7883–7887.

152 Y. Chen, D. X. Wang, Z. T. Huang and M. X. Wang, *Chem. Commun.*, 2011, **47**, 8112–8114.

153 O. B. Berryman, A. C. Sather, B. P. Hay, J. S. Meisner and D. W. Johnson, *J. Am. Chem. Soc.*, 2008, **130**, 10895–10897.

154 S. T. Schneebeli, M. Frasconi, Z. Liu, Y. Wu, D. M. Gardner, N. L. Strutt, C. Cheng, R. Carmieli, M. R. Wasielewski and J. F. Stoddart, *Angew. Chem. Int. Ed.*, 2013, **52**, 13100–13104.

155 S. Guha and S. Saha, *J. Am. Chem. Soc.*, 2010, **132**, 17674–17677.

156 N. Busschaert, C. Caltagirone, W. Van Rossom and P. A. Gale, *Chem. Rev.*, 2015, **115**, 8038–8155.

157 A. Ojida, Y. Mito-Oka, M. A. Inoue and I. Hamachi, *J. Am. Chem. Soc.*, 2002, **124**, 6256–6258.

158 A. Ojida, Y. Mito-Oka, K. Sada and I. Hamachi, *J. Am. Chem. Soc.*, 2004, **126**, 2454–2463.

159 Z. Zeng, A. A. J. Torriero, A. M. Bond and L. Spiccia, *Chem. Eur. J.*, 2010, **16**, 9154–9163.

160 D. G. Smith, G. L. Law, B. S. Murray, R. Pal, D. Parker and K. L. Wong, *Chem. Commun.*, 2011, **47**, 7347–7349.

161 R. Mailhot, T. Traviss-Pollard, R. Pal and S. J. Butler, *Chem. Eur. J.*, 2018, 10745–10755.

162 H. E. Katz, *J. Org. Chem.*, 1985, **50**, 5027–5032.

163 S. Solé and F. P. Gabbaï, *Chem. Commun.*, 2004, **4**, 1284–1285.

164 C. W. Chiu and F. P. Gabbaï, *J. Am. Chem. Soc.*, 2006, **128**, 14248–14249.

165 A. Kawachi, A. Tani, J. Shimada and Y. Yamamoto, *J. Am. Chem. Soc.*, 2008, **130**, 4222–4223.

166 M. Melaimi and F. P. Gabbaï, *J. Am. Chem. Soc.*, 2005, **127**, 9680–9681.

167 N. Ahmed, B. Shirinfar, I. Geronimo and K. S. Kim, *Org. Lett.*, 2011, **13**, 5476–5479.

168 M. Zhang, W. J. Ma, C. T. He, L. Jiang and T. B. Lu, *Inorg. Chem.*, 2013, **52**, 4873–4879.

169 I. Suzuki, M. Ui and A. Yamauchi, *J. Am. Chem. Soc.*, 2006, **128**, 4498–4499.

170 S. Y. Kim and J. I. Hong, *Org. Lett.*, 2007, **9**, 3109–3112.

171 S. Y. Kim, J. Park, M. Koh, S. B. Park and J. I. Hong, *Chem. Commun.*, 2009, 4735–4737.

172 T. Liu, A. Nonat, M. Beyler, M. Regueiro-Figueroa, K. Nchiminono, O. Jeannin, F. Camerel, F. Debaene, S. Cianférani-Sanglier, R. Tripier, C. Platas-Iglesias and L. J. Charbonnière, *Angew. Chem. Int. Ed.*, 2014, **53**, 7259–7263.

173 S. Jayaraman and A. S. Verkman, *Biophys. Chem.*, 2000, **85**, 49–57.

174 R. Krapf, N. P. Illsley, H. C. Tseng and A. S. Verkman, *Anal. Biochem.*, 1988, **169**, 142–150.

175 J. Biwersi, B. Tulk and A. S. Verkman, *Anal. Biochem.*, 1994, **219**, 139–143.

176 S. Nabavi and N. Alizadeh, *Sensors Actuators, B Chem.*, 2014, **200**, 76–82.

177 T. Sato, H. Konno, Y. Tanaka, T. Kataoka, K. Nagai, H. H. Wasserman and S. Ohkuma, *J. Biol. Chem.*, 1998, **273**, 21455–21462.

178 S. Rastogi, E. Marchal, I. Uddin, B. Groves, J. Colpitts, S. A. McFarland, J. T. Davis and A. Thompson, *Org. Biomol. Chem.*, 2013, **11**, 3834–3845.

179 E. Hernando, V. Capurro, C. Cossu, M. Fiore, M. García-Valverde, V. Soto-Cerrato, R. Pérez-Tomás, O. Moran, O. Zegarra-Moran and R. Quesada, *Sci. Rep.*, 2018, **8**, Article number: 2608.

180 V. Soto-Cerrato, P. Manuel-Manresa, E. Hernando, S. Calabuig-Fariñas, A. Martínez-Romero,

V. Fernández-Dueñas, K. Sahlholm, T. Knöpfel, M. García-Valverde, A. M. Rodilla, E. Jantus-Lewintre, R. Farràs, F. Ciruela, R. Pérez-Tomás and R. Quesada, *J. Am. Chem. Soc.*, 2015, **137**, 15892–15898.

181 N. Busschaert, I. L. Kirby, S. Young, S. J. Coles, P. N. Horton, M. E. Light and P. A. Gale, *Angew. Chem. Int. Ed.*, 2012, **51**, 4426–4430.

182 C. M. Dias, H. Valkenier and A. P. Davis, *Chem. Eur. J.*, 2018, **24**, 6262–6268.

183 P. V. Santacroce, J. T. Davis, M. E. Light, P. A. Gale, J. C. Iglesias-Sánchez, P. Prados and R. Quesada, *J. Am. Chem. Soc.*, 2007, **129**, 1886–1887.

184 S. K. Ko, S. K. Kim, A. Share, V. M. Lynch, J. Park, W. Namkung, W. Van Rossom, N. Busschaert, P. A. Gale, J. L. Sessler and I. Shin, *Nat. Chem.*, 2014, **6**, 885–892.

185 A. V. Jentzsch, D. Emery, J. Mareda, S. K. Nayak, P. Metrangolo, G. Resnati, N. Sakai and S. Matile, *Nat. Commun.*, 2012, **3**, Article number: 905.

186 C. Ren, X. Ding, A. Roy, J. Shen, S. Zhou, F. Chen, S. F. Yau Li, H. Ren, Y. Y. Yang and H. Zeng, *Chem. Sci.*, 2018, **9**, 4044–4051.

187 S. Benz, M. Macchione, Q. Verolet, J. Mareda, N. Sakai and S. Matile, *J. Am. Chem. Soc.*, 2016, **138**, 9093–9096.

188 V. Gorteau, G. Bollot, J. Mareda, A. Perez-Velasco and S. Matile, *J. Am. Chem. Soc.*, 2006, **128**, 14788–14789.

189 J. Mareda and S. Matile, *Chem. Eur. J.*, 2009, **15**, 28–37.

190 A. Perez-Velasco, V. Gorteau and S. Matile, *Angew. Chem. Int. Ed.*, 2008, **47**, 921–923.

191 A. Vargas Jentzsch and S. Matile, *J. Am. Chem. Soc.*, 2013, **135**, 5302–5303.

192 M. Macchione, M. Tsemperouli, A. Goujon, A. R. Mallia, N. Sakai, K. Sugihara and S. Matile, *Helv. Chim. Acta*, 2018, **101**, e1800014.

193 S. M. Walter, F. Kniep, E. Herdtweck and S. M. Huber, *Angew. Chem. Int. Ed.*, 2011, **50**, 7187–7191.

194 P. Wonner, L. Vogel, M. Düser, L. Gomes, F. Kniep, B. Mallick, D. B. Werz and S. M. Huber, *Angew. Chem. Int. Ed.*, 2017, **56**, 12009–12012.

195 S. E. Reisman, A. G. Doyle and E. N. Jacobsen, *J. Am. Chem. Soc.*, 2008, **130**, 7198–7199.

196 Y. Park, K. C. Harper, N. Kuhl, E. E. Kwan, R. Y. Liu and E. N. Jacobsen, *Science*, 2017, **355**, 162–166.

197 F. Kniep, S. H. Jungbauer, Q. Zhang, S. M. Walter, S. Schindler, I. Schnapperelle, E. Herdtweck and S. M. Huber, *Angew. Chem. Int. Ed.*, 2013, **52**, 7028–7032.

198 M. S. Taylor, N. Tokunaga and E. N. Jacobsen, *Angew. Chem. Int. Ed.*, 2005, **44**, 6700–6704.

199 M. Zurro, S. Asmus, J. Bamberger, S. Beckendorf and O. García Mancheño, *Chem. Eur. J.*, 2016, **22**, 3785–3793.

200 Z. Zhang and P. R. Schreiner, *Chem. Soc. Rev.*, 2009, **38**, 1187–98.

201 Y. Nishikawa, *Tetrahedron Lett.*, 2018, **59**, 216–223.

202 S. H. Jungbauer, S. M. Walter, S. Schindler, L. Rout, F. Kniep and S. M. Huber, *Chem.*

Commun., 2014, **50**, 6281–6284.

203 P. R. Schreiner and A. Wittkopp, *Org. Lett.*, 2002, **4**, 217–220.

204 Y. Takeda, D. Hisakuni, C. H. Lin and S. Minakata, *Org. Lett.*, 2015, **17**, 318–321.

205 A. Bruckmann, M. A. Pena and C. Bolm, *Synlett*, 2008, 900–902.

206 V. Mugnaini, C. Punta, R. Liantonio, P. Metrangolo, F. Recupero, G. Resnati, G. F. Pedulli and M. Lucarini, *Tetrahedron Lett.*, 2006, **47**, 3265–3269.

207 S. Jew and H. Park, *Chem. Commun.*, 2009, 7090–7103.

208 U. H. Dolling, P. Davis and E. J. J. Grabowski, *J. Am. Chem. Soc.*, 1984, **106**, 446–447.

209 J. D. Jolliffe, R. J. Armstrong and M. D. Smith, *Nat. Chem.*, 2017, **9**, 558–562.

210 G. Pupo, F. Ibba, D. M. H. Ascough, A. C. Vicini, P. Ricci, K. E. Christensen, L. Pfeifer, J. R. Morphy, J. M. Brown, R. S. Paton and V. Gouverneur, *Science*, 2018, **360**, 638–642.

211 J. Shang, W. Zhao, X. Li, Y. Wang and H. Jiang, *Chem. Commun.*, 2016, **52**, 4505–4508.

212 L. Yang, Y. Wang, Y. Che and H. Jiang, *Org. Biomol. Chem.*, 2017, **15**, 7747–7752.

213 W. Zhao, F. Huang, Y. Wang, Q. Li, J. Shang, Y. Che and H. Jiang, *Tetrahedron Lett.*, 2016, **57**, 1691–1694.

214 Y. Li and A. H. Flood, *Angew. Chem. Int. Ed.*, 2008, **47**, 2649–2652.

215 S. Lee, B. E. Hirsch, Y. Liu, J. R. Dobscha, D. W. Burke, S. L. Tait and A. H. Flood, *Chem. Eur. J.*, 2016, **22**, 560–569.

216 S. Jin, S. Kato and Y. Nakamura, *Chem. Lett.*, 2016, 869–871.

217 Y. Wang, W. Zhao, F. Bie, L. Wu, X. Li and H. Jiang, *Chem. Eur. J.*, 2016, **22**, 5233–5242.

218 C. T. Li, Q. Y. Cao, J. J. Li, Z. W. Wang and B. N. Dai, *Inorganica Chim. Acta*, 2016, **449**, 31–37.

219 J. Y. C. Lim, I. Marques, L. Ferreira, V. Félix and P. D. Beer, *Chem. Commun.*, 2016, **52**, 5527–5530.

220 T. R. Chan, R. Hilgraf, K. B. Sharpless and V. V Fokin, *Org. Lett.*, 2004, **6**, 2853–2855.

221 M. J. Hynes, *J. Chem. Soc. Dalt. Trans.*, 1993, 311–312.

222 J. M. Daniel, S. D. Friess, S. Rajagopalan, S. Wendt and R. Zenobi, *Int. J. Mass Spectrom.*, 2002, **216**, 1–27.

223 A. Bondi, *J. Phys. Chem.*, 1964, **68**, 441–451.

224 Y. Hua, Y. Liu, C. H. Chen and A. H. Flood, *J. Am. Chem. Soc.*, 2013, **135**, 14401–14412.

225 S. Lee, Y. Hua, H. Park and A. H. Flood, *Org. Lett.*, 2010, **12**, 2100–2102.

226 W. Zhao, Y. Wang, J. Shang, Y. Che and H. Jiang, *Chem. Eur. J.*, 2015, **21**, 7731–7735.

227 R. Tepper and U. S. Schubert, *Angew. Chem. Int. Ed.*, 2018, **57**, 6004–6016.

228 J. Y. C. Lim and P. D. Beer, *Chem. Commun.*, 2015, **51**, 3686–3688.

229 B. R. Mullaney, A. L. Thompson and P. D. Beer, *Angew. Chem. Int. Ed.*, 2014, **53**, 11458–11462.

230 C. J. Massena, N. B. Wageling, D. A. Decato, E. Martin Rodriguez, A. M. Rose and O. B. Berryman, *Angew. Chem. Int. Ed.*, 2016, **55**, 12398–12402.

231 T. Yao and R. C. Larock, *J. Org. Chem.*, 2005, **70**, 1432–1437.

232 A. Bubar, P. Estey, M. Lawson and S. Eisler, *J. Org. Chem.*, 2012, **77**, 1572–1578.

233 T. Wu, X. Mu and G. Liu, *Angew. Chem. Int. Ed.*, 2011, **50**, 12578–12581.

234 H. A. Stefani, N. C. S. Silva, S. N. S. Vasconcelos, F. Manarin and F. B. Souza, *Tetrahedron Lett.*, 2013, **54**, 2809–2812.

235 H. A. Stefani, S. N. S. Vasconcelos, F. Manarin, D. M. Leal, F. B. Souza, L. S. Madureira, J. Zukerman-Schpector, M. N. Eberlin, M. N. Godoi and R. De Souza Galaverna, *Eur. J. Org. Chem.*, 2013, 3780–3785.

236 V. A. Potapov, S. V Amosova, A. V Khangurov and P. A. Petrov, *Phosphorus, Sulfur, and Silicon*, 1993, **79**, 273–275.

237 M. J. Hey, S. M. Ilett and G. Davidson, *J. Chem. Soc. Faraday Trans.*, 1995, **91**, 3897–3900.

238 S. Aroua, E. G. V. Tiu, T. Ishikawa and Y. Yamakoshi, *Helv. Chim. Acta*, 2016, **99**, 805–813.

239 A. Chen, D. Wu and C. S. Johnson, *J. Am. Chem. Soc.*, 1995, **117**, 7965–7970.

240 W. Brown, P. Stilbs and R. M. Johnsen, *J. Polym. Sci. Part A-2, Polym. Phys.*, 1983, **21**, 1029–1039.

241 Y. Hua, R. O. Ramabhadran, J. a Karty, K. Raghavachari and A. H. Flood, *Chem. Commun.*, 2011, **47**, 5979–5981.

242 J. Mei, N. L. C. Leung, R. T. K. Kwok, J. W. Y. Lam and B. Z. Tang, *Chem. Rev.*, 2015, **115**, 11718–11940.

243 A. Rauwerdink and R. J. Kazlauskas, *ACS Catal.*, 2015, 5, 6153–6176.

244 N. Hakulinen, M. Tenkanen and J. Rouvinen, *J. Struct. Biol.*, 2000, **132**, 180–190.

245 Y. Sun, S. Yin, Y. Feng, J. Li, J. Zhou, C. Liu, G. Zhu and Z. Guo, *J. Biol. Chem.*, 2014, **289**, 15867–15879.

246 G. M. Whitesides and C. H. Wong, *Angew. Chemie Int. Ed.*, 1985, **24**, 617–718.

247 L. Bernardi, M. Fochi, M. Comes Franchini and A. Ricci, *Org. Biomol. Chem.*, 2012, **10**, 2911.

248 T. Ema, D. Tanida, T. Matsukawa and T. Sakai, *Chem. Commun.*, 2008, 957–9.

249 M. Kheirabadi, N. Çelebi-Ölçüm, M. F. L. Parker, Q. Zhao, G. Kiss, K. N. Houk and C. E. Schafmeister, *J. Am. Chem. Soc.*, 2012, **134**, 18345–18353.

250 M. D. Nothling, A. Ganesan, K. Condic-Jurkic, E. Pressly, A. Davalos, M. R. Gotrik, Z. Xiao, E. Khoshdel, C. J. Hawker, M. L. O'Mara, M. L. Coote and L. A. Connal, *Chem*, 2017, **2**, 732–745.

251 H. Wu, Handoko, M. Raj and P. S. Arora, *Org. Lett.*, 2017, **19**, 5122–5125.

252 C. R. Jones, G. Dan Panto, A. J. Morrison and M. D. Smith, *Angew. Chem. Int. Ed.*, 2009, **48**, 7391–7394.

253 A. J. Neuvonen and P. M. Pihko, *Org. Lett.*, 2014, **16**, 5152–5155.

254 D. H. Williams, E. Stephens and M. Zhou, *J. Mol. Biol.*, 2003, **329**, 389–399.

255 D. H. Williams, M. Zhou and E. Stephens, *J. Mol. Biol.*, 2006, **355**, 760–767.

256 D. H. Williams, E. Stephens, D. P. O'Brien and M. Zhou, *Angew. Chem. Int. Ed.*, 2004, **43**, 6596–6616.

257 F. Richter, R. Blomberg, S. D. Khare, G. Kiss, A. P. Kuzin, A. J. T. Smith, J. Gallaher, Z. Pianowski, R. C. Helgeson, A. Grjasnow, R. Xiao, J. Seetharaman, M. Su, S. Vorobiev, S. Lew, F. Forouhar, G. J. Kornhaber, J. F. Hunt, G. T. Montelione, L. Tong, K. N. Houk, D. Hilvert and D. Baker, *J. Am. Chem. Soc.*, 2012, **134**, 16197–16206.

258 D. W. C. MacMillan, *Nature*, 2008, 455, 304–308.

259 C. L. Jarvis, J. S. Hirschi, M. J. Vetticatt and D. Seidel, *Angew. Chem. Int. Ed.*, 2017, **56**, 2670–2674.

260 M. S. Sigman and E. N. Jacobsen, *J. Am. Chem. Soc.*, 1998, **120**, 4901–4902.

261 M. S. Sigman, P. Vachal and E. N. Jacobsen, *Angew. Chem. Int. Ed.*, 2000, **39**, 1279–1281.

262 P. Sieber and B. Riniker, *Tetrahedron Lett.*, 1987, **28**, 6031–6034.

263 B. Y. Lee, S. R. Park, H. B. Jeon and K. S. Kim, *Tetrahedron Lett.*, 2006, **47**, 5105–5109.

264 S. Kohmoto, E. Mori and K. Kishikawa, *J. Am. Chem. Soc.*, 2007, **129**, 13364–13365.

265 D. Lu, J. Lei, Z. Tian, L. Wang and J. Zhang, *Dye. Pigment.*, 2012, **94**, 239–246.

266 F. Kniep, L. Rout, S. M. Walter, H. K. V. Bensch, S. H. Jungbauer, E. Herdtweck and S. M. Huber, *Chem. Commun.*, 2012, **48**, 9299–9301.

267 T. R. Wu, L. Shen and J. M. Chong, *Org. Lett.*, 2004, **6**, 2701–2704.

268 Y. Shi, T. Suguri, C. Dohi, H. Yamada, S. Kojima and Y. Yamamoto, *Chem. Eur. J.*, 2013, **19**, 10672–10689.

269 M. J. Langton, Y. Xiong and P. D. Beer, *Chem. Eur. J.*, 2015, **21**, 18910–18914.

270 S. Trupp, A. Schweitzer and G. J. Mohr, *Org. Biomol. Chem.*, 2006, **4**, 2965.

271 B. Gao, L. Cui, Y. Pan, G. Zhang, Y. Zhou, C. Zhang, S. Shuang and C. Dong, *RSC Adv.*, 2016, **6**, 43028–43033.

272 WO2004087686 (A2), 2004.

273 M. G. Woll, H. Qi, A. Turpoff, N. Zhang, X. Zhang, G. Chen, C. Li, S. Huang, T. Yang, Y. C. Moon, C. S. Lee, S. Choi, N. G. Almstead, N. A. Naryshkin, A. Dakka, J. Narasimhan, V. Gabbeta, E. Welch, X. Zhao, N. Risher, J. Sheedy, M. Weetall and G. M. Karp, *J. Med. Chem.*, 2016, **59**, 6070–6085.

274 C.-S. Tsai, P.-Y. Liu, H.-Y. Yen, T.-L. Hsu and C.-H. Wong, *Chem. Commun.*, 2010, **46**, 5575–5577.

275 K. J. Kilpin, C. M. Clavel, F. Edafe and P. J. Dyson, *Organometallics*, 2012, **31**, 7031–7039.

276 EP1767539 (A1), 2007.

277 H. Nowell, S. A. Barnett, K. E. Christensen, S. J. Teat and D. R. Allan, *J. Synchrotron Radiat.*, 2012, **19**, 435–441.

278 L. Palatinus and G. Chapuis, *J. Appl. Crystallogr.*, 2007, **40**, 786–790.

279 P. W. Betteridge, J. R. Carruthers, R. I. Cooper, K. Prout and D. J. Watkin, *J. Appl. Crystallogr.*, 2003, **36**, 1487–1487.

280 R. I. Cooper, A. L. Thompson and D. J. Watkin, *J. Appl. Crystallogr.*, 2010, **43**, 1100–1107.

281 P. Van Der Sluis and A. L. Spek, *Acta Crystallogr. Sect. A*, 1990, **46**, 194–201.

282 A. L. Spek, *J. Appl. Crystallogr.*, 2003, **36**, 7–13.

283 J. Lehr, J. R. Weeks, A. Santos, G. T. Feliciano, M. I. G. Nicholson, J. J. Davis and P. R. Bueno, *Phys. Chem. Chem. Phys.*, 2017, **19**, 15098–15109.